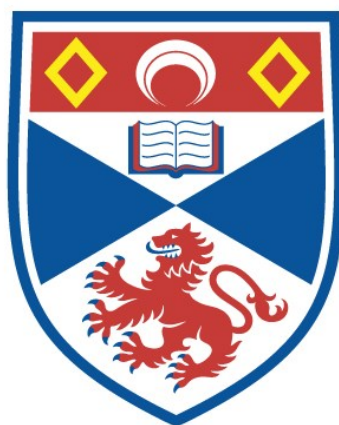


ASPECTS OF LIPID PEROXIDATION

Emanuele Bascetta

A Thesis Submitted for the Degree of PhD
at the
University of St Andrews



1983

Full metadata for this item is available in
St Andrews Research Repository
at:

<http://research-repository.st-andrews.ac.uk/>

Please use this identifier to cite or link to this item:

<http://hdl.handle.net/10023/14181>

This item is protected by original copyright

summary.

The photosensitised oxidation of the conjugated diene ester methyl octadeca-9E,11E-dienoate gives an unsaturated cyclic peroxide (epidioxide) in high yield. This has been characterised spectroscopically. The 9,12-peroxide undergoes facile rearrangement to the 9,12-furanoid ester under a variety of reaction conditions. Catalytic reduction of the unsaturated peroxide cleaves the O-O bond. Bromination and epoxidation give dibromo and epoxy esters in high yield with the peroxide group still intact.

Methyl 9(10)-hydroperoxyoctadec-10(8)E-enoates (1a,b), produced by photosensitised oxidation of methyl oleate are suitable substrates for the synthesis of substituted dioxolanes. Peroxymercuration of (1) affords on hydrogenodemercuration methyl 8,10- and 9,11-epdioxyoctadecanoates (2a,b) in good yield (45-70%). Bromodemercuration yields the corresponding bromo substituted cyclic peroxides (3a,b) in higher yield (95%). Direct bromination of the allylic hydroperoxides (1a,b) also affords the bromo substituted cyclic peroxides (3a,b) in almost quantitative yield, presumably via a bromonium ion intermediate.

The photosensitised oxidation of methyl vernolate, ricinoleate, 12-oxooctadec-9Z-enoate and 12-bromooctadec-9Z-enoate leads to allylic hydroperoxides with a shifted double bond as required by the ene-mechanism. The products are thermally sensitive and sample lifetimes are short.

ProQuest Number: 10167338

All rights reserved

INFORMATION TO ALL USERS

The quality of this reproduction is dependent upon the quality of the copy submitted.

In the unlikely event that the author did not send a complete manuscript and there are missing pages, these will be noted. Also, if material had to be removed, a note will indicate the deletion.



ProQuest 10167338

Published by ProQuest LLC (2017). Copyright of the Dissertation is held by the Author.

All rights reserved.

This work is protected against unauthorized copying under Title 17, United States Code
Microform Edition © ProQuest LLC.

ProQuest LLC.
789 East Eisenhower Parkway
P.O. Box 1346
Ann Arbor, MI 48106 – 1346

The silver trifluoroacetate assisted reaction of alkyl halides with hydrogen peroxide has been investigated. Reaction with methyl 12-bromostearate has furnished for the first time methyl 12-hydroperoxystearate in 34% isolated yield. Reaction with methyl 12-bromooleate, however, is more complicated and leads to the formation of cyclopropane hydroperoxides via a homoallylic cation rearrangement, and to hydroperoxy-epidioxides presumably via methyl 12-hydroperoxyoleate which we were unable to isolate. Methyl 12-*t*-butylperoxyoleate has been produced by reaction of methyl 12-bromooleate with *t*-butylhydroperoxide in the presence of silver trifluoroacetate. None of these transformations occur if the silver salt is replaced by silver acetate.

¹³C nmr chemical shifts are reported for a number of oxygenated long chain aliphatic compounds, including, epoxides alcohols, hydroperoxides and cyclic peroxides. The influence of the oxygenated functional groups on the chemical shifts of neighbouring carbons have been determined and a comprehensive set of chemical shift parameters derived. Results are discussed where applicable in terms of steric and electric field effects. The empirical equation $\Delta\delta_{AB} = A e^{-\zeta(2\eta+1)}$ is proposed to describe the non-equivalence of functionalised carbons.

The development of preparative high pressure liquid chromatography as a technique for the purification of lipids is described and compared with existing methodologies such as

preparative thin layer chromatography, column chromatography and low temperature crystallisation. Effective procedures for obtaining methyl oleate, linoleate, α and γ -linolenate and ricinoleate are described.

The radicals generated from unsaturated fatty acid esters by hydrogen abstraction with photochemically formed t-butoxy radicals have been investigated by e.s.r. spectroscopy. The substituted allyl and pentadienyl radicals generated from monoenoic and dienoic esters were conformationally stable under the conditions of the experiments. The main species observed on H-abstraction from monoenic esters were substituted propynyl radicals, and the same radical type was generated from dienoic esters with more than one methylene unit separating the triple bonds. Substituted penta-1,4-diynyl and penta-1,3-diynyl radicals were identified on H-abstraction from methylene-interrupted and conjugated dienoic esters. Hydrogen abstraction from triacylglycerols containing one or more double bonds was also examined. Most of the unsaturated esters also gave rise to secondary radicals produced by H-abstraction from the chain methylene groups. From the measured concentrations of the secondary and delocalised radicals the following relative rates of H-abstraction by t-butoxy radicals from the different sites were obtained; secondary : propynylic : allylic : bisallylic = 1 : 18 : 36 : 116 at 293 K.

The radicals generated from saturated fatty acids and their derivatives by hydrogen abstraction with photochemically formed t-butoxyl radicals have been investigated by e.s.r. spectroscopy. The main species observed from propionic and butyric acids arose from hydrogen abstraction α to the carboxyl group. The proportion of radicals arising from hydrogen abstraction from in chain secondary radicals increases concomitantly with chain length. Radicals arising from hydrogen abstraction of the ω -1 methylene were observed for all the acids investigated. From the measured concentrations of the α -carboxyl : in chain secondary : ω -1 radicals the following approximate rates of hydrogen abstraction by t-butoxyl radicals from the different sites were obtained 2.3 : 1 : 2.3.

Hydrogen abstraction by t-butoxyl radicals from propyl chloride and butyryl nitrile also occurs predominantly α to the head group.

The neutral α -tocopheroxyl radicals, generated in monolayers on silica gel containing α -tocopherol and partly autoxidised methyl linoleate at 90°C, were detected and identified by E.S.R. spectroscopy. Addition of ascorbic acid to the monolayer resulted in the complete quenching of the α -tocopheroxyl radical spectrum. This lends support to the view that ascorbate transfers hydrogen to α -tocopheroxyl radicals thus regenerating α -tocopherol.

Autoxidation rates of polyunsaturated fatty acid methyl ester monolayers deposited on a silica gel surface at 70°C have been

determined. First-order kinetics were observed for all the esters investigated, both as pure compounds or as mixtures of esters differing in degree of unsaturation. The relative rates of autoxidation of methyl oleate : linoleate : linolenate : arachidonate as pure compounds were 1 : 380 : 1140 : 1500. When examined as mixtures the relative rates were 1 : 5.6 : 10.3 : 17.3. The autoxidation rates on silica gel are compared with autoxidation rates of the methyl esters in dodecane at 70°C, for which autocatalytic kinetic profiles are observed. The kinetics of hydrogen abstraction from unsaturated fatty acid methyl esters by photochemically generated t-butoxyl radicals has also been investigated, both for pure compounds and mixtures. First-order kinetics were observed, with relative rates for hydrogen abstraction from oleate : linoleate : linolenate : arachidonate of 1 : 2.4 : 3.7 : 5.3.

Molecular structures and energies have been calculated in the MINDO/3 approximation for dioxirane, dioxetane, dioxolane, dioxane and their methyl derivatives. Potential surfaces have been calculated for dioxirane, dioxetane and dioxolane. The calculations predict planar geometries for dioxetane and dioxolane. Ab-initio calculations on the parent cyclic peroxides have been performed with STO-3G and 3-21G basis sets. Agreement between the semi-empirical and ab-initio approaches is good in all cases. Attempted calculations on the O-O bond cleavage of 2,3-dioxobicyclo[2.2.1]-heptane were however unsatisfactory, even with the inclusion of configurational interaction (CI) in the calculations.

Aspects of Lipid Peroxidation.

A Thesis

Presented for the degree of

DOCTOR OF PHILOSOPHY

in the Faculty of Science of the

University of St.Andrews

by

Emanuele Bascetta, B.Sc.

United College of St.Salvator

and St.Leonard, St.Andrews.

February 1983



Th 9835

DECLARATION

I declare that this thesis is my own composition, that the work of which it is a record has been carried out by me, and that it has not been submitted in any previous application for a Higher Degree.

This thesis describes results of research carried out at the Department of Chemistry, United College of St.Salvator and St.Leonard, University of St.Andrews, under the supervision of Prof. F.D.Gunstone since the 1st October, 1979.

Emanuele Bascetta.

CERTIFICATE

I hereby certify that Emanuele Bascetta has spent twelve terms of research under my supervision, has fulfilled the conditions of Ordinance No. 12 and Resolution of the University Court 1967, No. 1, and is qualified to submit the accompanying thesis in application for the degree of Doctor of Philosophy.

Prof. F.D.Gunstone.

Acknowledgements.

The author is deeply indebted to Prof. F.D. Gunstone for advice, guidance and encouragement throughout the course of this work and during the preparation of the thesis.

Sincere gratitude is extended to Dr. J.C. Walton for invaluable assistance in the E.S.R. experiments (Chapter 4) and for initiating the authors interest in free radical research.

Thanks are also due to Dr. J.R. Ball for collaboration and useful discussions on theoretical calculations (Chapter 6). To Dr. C. M. Scrimgeour for many useful suggestions and generally sharing the benefit of his expertise and experience during the early stages of the project.

Financial support from the Science and Engineering Research Council and from Unilever for a CASE studentship (1979-1982) is deeply appreciated. Gratitude is also extended to Dr. F.B. Padly of Unilever Research, the authors Industrial supervisor, for useful discussions.

The services of all the teaching and technical staff of the University of St. Andrews Chemistry Department, especially Mrs. M. Smith (n.m.r), Mr. C. Miller (mass spec.), Mr. J. Rennie (workshop), and Mr. C. Smith (glassblowing) is gratefully acknowledged.

Also, the assistance of Mr. L.R. Dunley, Mrs. J. Paye, Mrs. S. Johnson, Mr. C. Tuchel, Mr. A. Speght and Mr. W. Ayton was much appreciated.

My deepest and sincere thanks are also due to my father, mother, sisters and Gill, for their loyalty, encouragement and support during my entire University education.

Finally, I would like to thank Professors Lord Tedder and P.A. Wyatt for providing the research facilities throughout this work.

Volume 1

contents

VOLUME 1

	Page
General Introduction	1
CHAPTER 1. <u>SYNTHESIS OF LIPID PEROXIDES.</u>	
Introduction.	15
Section 1. Synthesis, characterisation and transformations of an unsaturated lipid peroxide.	40
1 Introduction.	42
2 Results and discussion.	43
3 Experimental.	60
References.	81
Section 2. Synthesis of cyclic peroxides from methyl oleate.	85
1 Introduction.	87
2 Results and discussion.	89
3 Experimental.	113
References.	129
Section 3. Photosensitised oxidation of oxygenated fatty acid esters.	133
1 Introduction.	134
2 Results and discussion.	135
3 Experimental.	148
References.	161
Section 4. On the attempted synthesis of methyl 12-hydroperoxy oleate and stearate.	163
1 Introduction.	164
2 Results and discussion.	165
3 Experimental.	174
References.	182

Section 5.	Synthesis of long-chain primary hydroperoxides.	184
1	Introduction.	185
2	Results and discussion.	187
3	Experimental.	189
	References.	193
CHAPTER 2.	<u>A ¹³C CHEMICAL SHIFT STUDY OF OXYGENATED LONG CHAIN MOLECULES.</u>	195
1	Introduction.	196
2	Results and discussion.	206
3	Experimental.	250
	References.	251
CHAPTER 3.	<u>IMPROVED PROCEDURES FOR THE ISOLATION OF FATTY ACIDS.</u>	254
1	Introduction.	255
2	Experimental parameters & procedures.	258
3	Results and discussion.	265
	References.	281

VOLUME 2

CHAPTER 4.	<u>E.S.R. STUDIES ON FATTY ACIDS</u> <u>AND THE ROLE OF VITAMINS E AND</u> <u>C IN LIPID PEROXIDATION.</u>	1
Section 1.	An E.S.R. study of fatty acids. Part 1. Hydrogen abstraction from unsaturated long chain esters.	21
	1 Introduction.	22
	2 Results and discussion.	24
	3 Experimental.	53
	References.	59
Section 2.	An E.S.R. study of fatty acids. Part II. Hydrogen abstraction from saturated acids and related derivatives.	65
	1 Introduction.	66
	2 Results and discussion.	68
	3 Discussion.	90
	4 Experimental.	98
	References.	105
Section 3.	An E.S.R. study of the role of vitamins C and E in the inhibition of fatty acid oxidation in a model membrane.	108
	Results and discussion.	109
	References.	113
CHAPTER 5.	<u>A KINETIC STUDY OF THE OXIDATION OF</u> <u>FATTY ACIDS IN A MODEL MEMBRANE AND</u> <u>IN SOLUTION.</u>	114
Section 1.	Introduction.	115
Section 2.	Autoxidation of unsaturated fatty acid esters in a model membrane.	121
	2.1 Introduction.	121
	2.2 Results and discussion.	126
	2.3 Experimental.	150

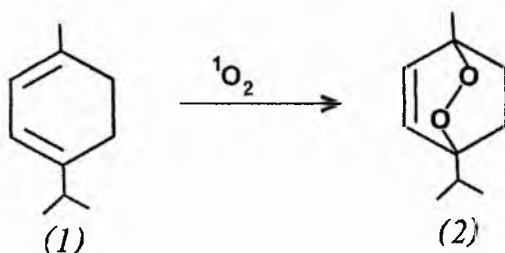
Section 3.	Autoxidation of unsaturated fatty acid esters in dilute solution.	152
3.1	Introduction.	152
3.2	Results and discussion.	153
3.3	Experimental.	156
Section 4.	The reactivity of t-butoxyl radicals towards fatty acid methyl esters.	157
4.1	Introduction.	157
4.2	Results and discussion.	158
4.3	Experimental.	167
Section 5.	Conclusions.	168
	References.	173
CHAPTER 6.	<u>A THEORETICAL INVESTIGATION OF THE CONFORMATIONS OF CYCLIC PEROXIDES.</u>	179
1	Introduction.	180
2.1	Dioxirane.	182
2.2	Dioxetane.	197
2.3	Dioxolane.	209
2.4	Dioxane.	225
2.5	The decomposition of 2,3-dioxobicyclo-[2.2.1]heptane and derivatives.	236
	Theoretical procedures.	245
	References.	246

General Introduction.

The majority of organic compounds are thermodynamically unstable in the presence of oxygen but fortunately for life as we know it a vast percentage of these reactions are kinetically slow. The interaction of organic compounds with molecular oxygen or its derivatives such as hydrogen peroxide, superoxide ion and ozone may lead to peroxidic products. Organic peroxides play an important and diverse role in biological systems. Some are key regulators in biosynthetic pathways while others show deleterious effects and are associated with a host of pathological changes^[1,2].

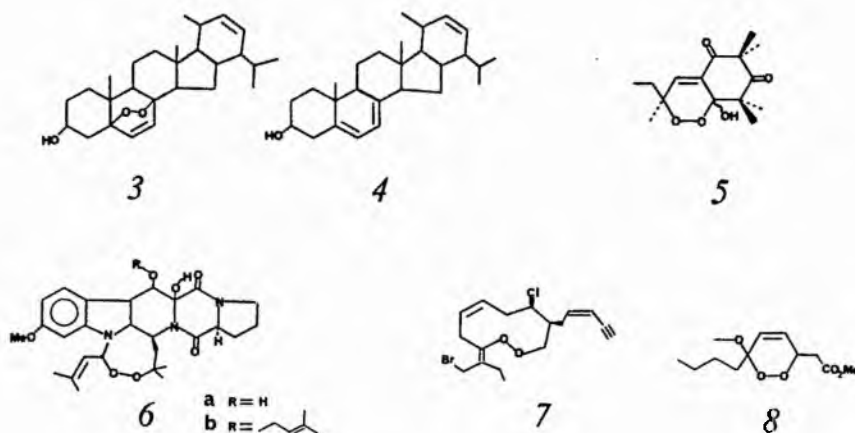
The natural occurrence of bio-peroxides and their metabolites.

Ascaridole (2), the first naturally occurring peroxide to be isolated, is produced in the leaves of the plant by photosensitised oxidation of α -terpinene (1).



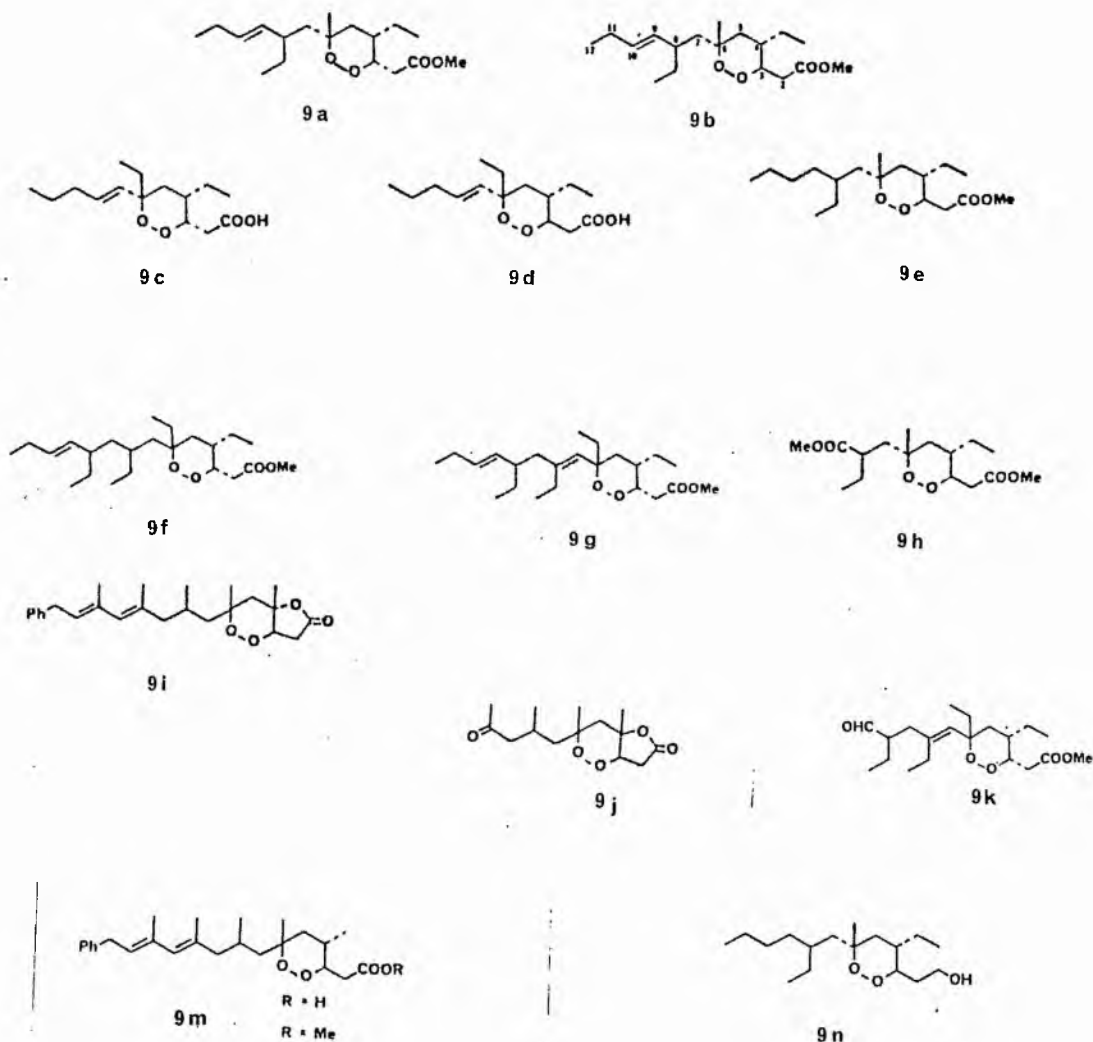
Windaus^[3] later discovered ergosterol endoperoxide (3) while investigating vitamin D. Wieland and Prelog (1947)^[4] claimed the

peroxide was naturally occurring after isolating it from the mycelium Asperigillus fumigatus, which had been cultured in the absence of sunlight. Other workers^[5,6] however, claimed that (3) was the product of fortuitous photosensitised oxidation of ergosterol (4). Although the full biological details are not fully understood Bates et al^[7] have established that the endoperoxide is a product of a controlled enzymatic oxygenation. Photosensitised oxidation is believed to be responsible for the formation of (5) in the leaves of Eucalyptus grandis^[8] whereas the biosynthetic origin of the two fungal peroxides verruculogen (6a) and fumitremorgin A (6b) is not fully known.^[9,10]



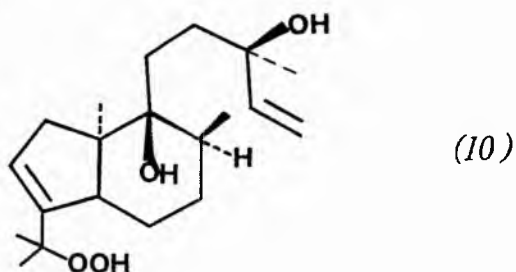
The marine world has provided a variety of examples of naturally occurring peroxides. Rhodophytin^[11] (7) was isolated from the marine algae of the genus Laurencia rhodophyta and is the only known example of a stable vinyl peroxide, although Adam et al^[12] suggest that more structural confirmation is required. The stable natural peroxide (8) containing a peroxy ketal moiety was isolated from the sponge of the genus Chondrilla.^[13]

A wide variety of stable and unstable bioperoxides have been obtained. (9a-g,i) from Caribbean sponges of the genus Plakortis and Chondrosia^[14a-c].

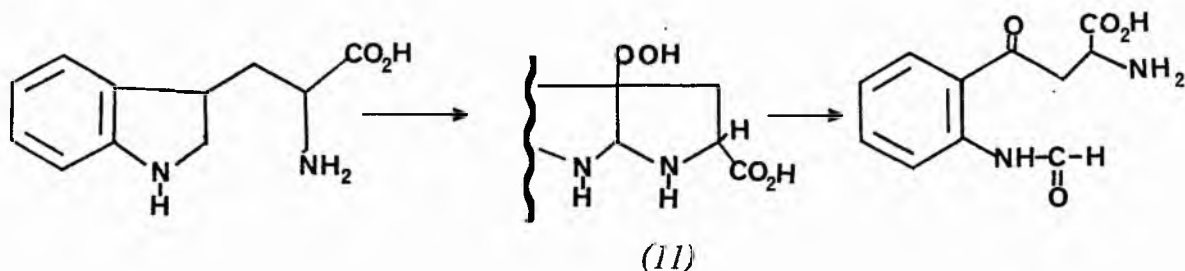


The peroxides 9h and 9n were isolated from 9a and 9e after ozonolysis and lithium tri-*t*-butoxy aluminium hydride reduction respectively. Similarly the intriguing peroxy-lactone 9j and the peroxide 9k were obtained by ozonolysis and oxidation with Jones

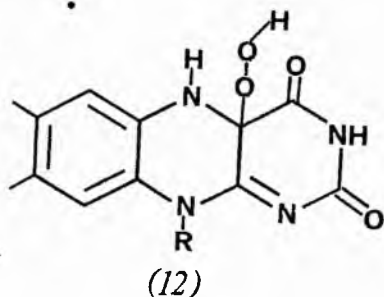
reagent and ozonolysis followed by reduction with dimethyl sulphide respectively from 9i and 9g respectively. Despite spectroscopic data for the reported products these transformations seem unlikely. The neoconcinndiol hydroperoxide^[15] (10) has been isolated from the red seaweed Laurencia sugderiae. Although it is not certain whether this hydroperoxide (10) is the product of a dioxygenase biogenic pathway or an artifact of photosensitised oxidation, the two sponge peroxides (7) and (9a) appear to be formed from an enzymatic pathway since both are formed stereospecifically.



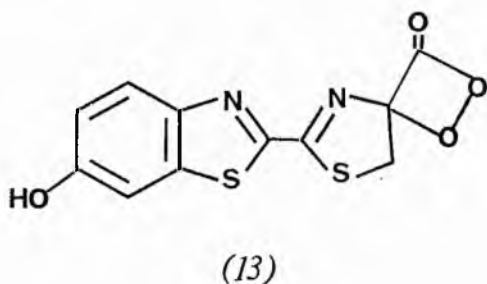
Numerous biochemical pathways are believed to proceed with the intervention of peroxides at some stage. Tryptophan hydroperoxide (11) is reported to be the precursor to formylkynurenine^[16] in the metabolism of tryptophan. The hydroperoxide is formed by a 2,3-dioxygenase enzyme. Model studies on other indole derivatives support the enzymatic pathway^[17].



Hydroxylation of aromatic rings by molecular oxygen with the help of flavine monooxygenase has been the subject of mechanistic controversy. Although numerous intermediates, all capable of transferring a single oxygen atom to an aromatic substrate, have been proposed^[18,19], recent evidence indicates the participation of the hydroperoxide(12)^[20-22].

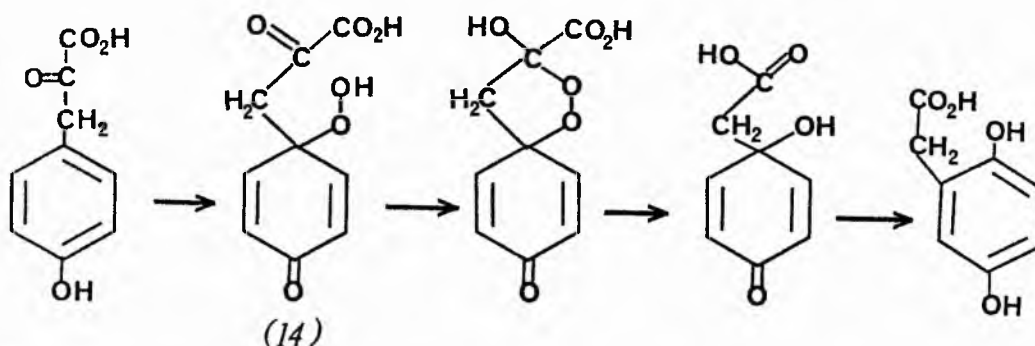


The α -peroxy lactones are active intermediates in bioluminescence^[23,24]. The intervention of α -peroxy lactone (13) was postulated for firefly luciferin^[25,26] and established some 10 years later by isotopic labelling^[27,28]. These compounds have eluded isolation because of their extreme lability but Adam *et al.*^[29] have prepared several model compounds which emit light on thermal decomposition^[30].



The enzymatic oxygenation of 4-hydroxyphenylpyruvic acid to furnish homogentisic acid is considered to proceed via the quinol hydroperoxide (14) on the basis of ¹⁸O labelling experiments^[31] and, although challenged^[32], the evidence of model systems supports its

intervention^[33].

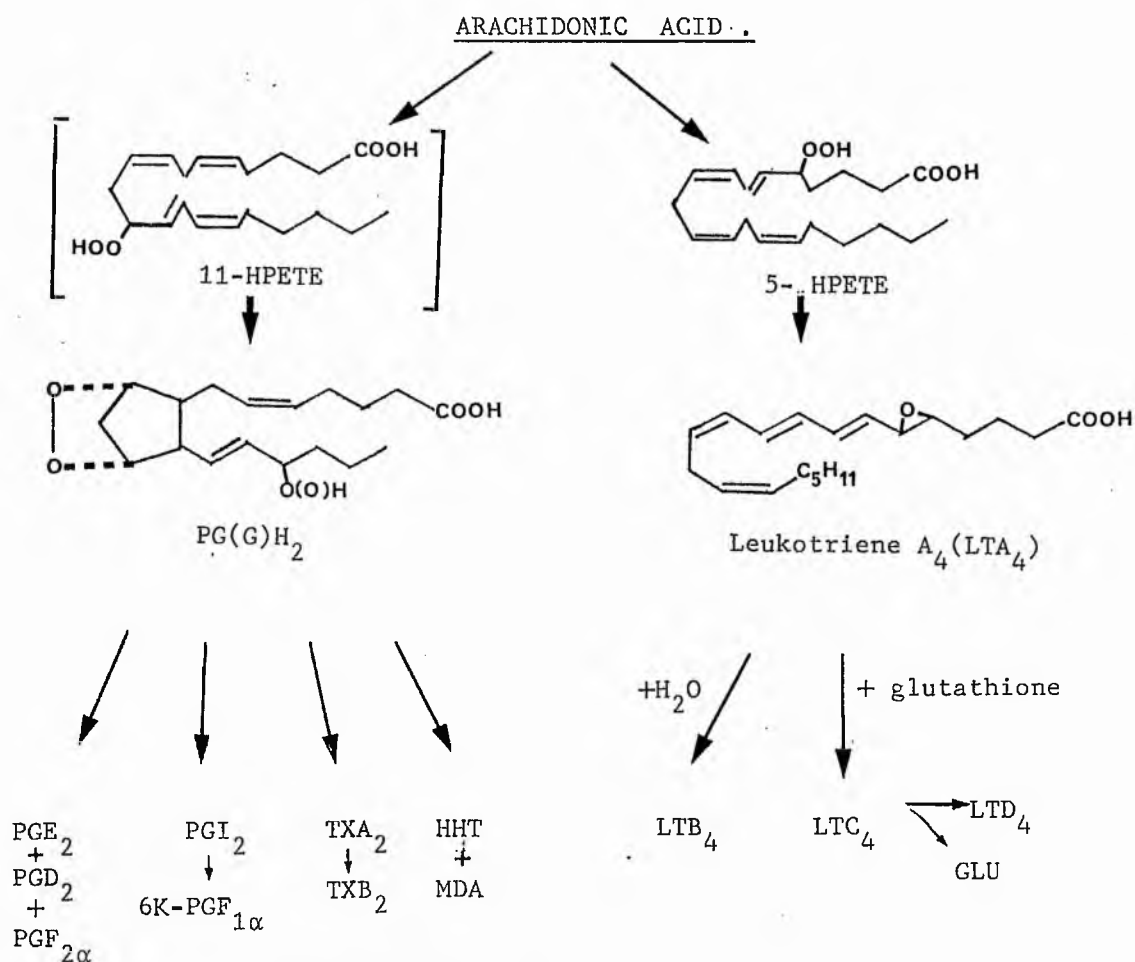


Although many of the biological pathways described have been questioned the involvement of lipid peroxides in the metabolism of arachidonic acid is for the most part undisputed. The biogenesis of the prostaglandins PGE, PGD, PGF, PGI and thromboxanes TXA, and TXB proceed via the prostaglandin endoperoxides PGG and PGH produced from arachidonic acid by an endoperoxide synthetase^[34-37]. The alternative oxidation of arachidonic acid via lipoxygenase gives rise to hydroperoxy eicosatetraenoic acids which are precursors of the leukotrienes (Scheme 1). The prostaglandins and thromboxanes constitute important regulators and mediators of various cellular functions whereas the leukotrienes are of importance in relation to the slow reacting substances of anaphylaxis (SRS-A), which is considered to be an important mediator in immediate hypersensitivity reactions.

PG's are widely distributed in mammals and van Dorp *et al.*^[38-40] have reported the comparative aspects of PG biosynthesis in different animals. In lower animals prostaglandins have been detected in the urinary bladder^[40] and in the intestine^[41] of the frog, in the testis and semen of Teleosts^[42], and in the gastrointestinal tract of the shark^[43]. A marine coral *Plexaura homomalla* contains large amounts of PGA and PGE^[44]. In higher mammals prostaglandins have

been found in a variety of organs, tissues and fluids including the iris of the eye, the pancreas, the intestine, adrenal glands, stomach, kidneys, lungs, thymus, brain, nervous tissues, seminal plasma, seminal fluid, the ovary and the uterus^[45].

Scheme 1 Formation of prostaglandins, thromboxanes and leukotrienes from arachidonic acid.

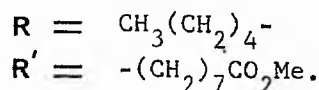
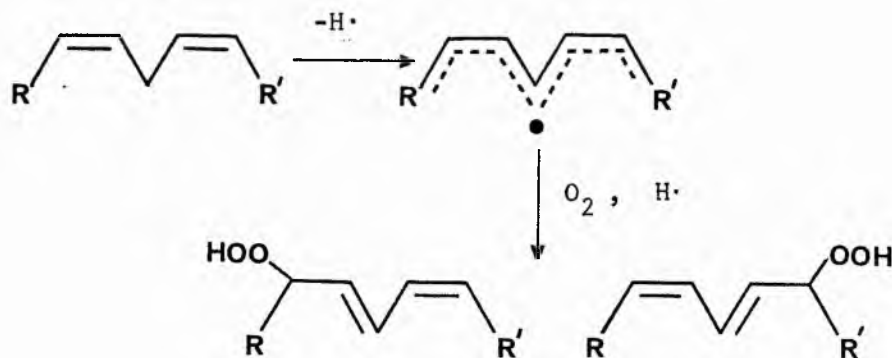


The potent pharmacological effects of the prostaglandins have been lucidly reviewed^[46]. They act on many different systems including cardiovascular, respiratory, gastrointestinal, nervous and female and male reproductive system. They have a wide and varied

regulatory role on the blood system. A more recent and exciting development in prostaglandin pharmacology is its association with cancer^[47]. Apparently malignant tumours form more prostaglandins than the normal tissues in which they arise. Several prostaglandin inhibitors such as aspirin and indomethacin have shown some success in cancer therapy. Bennet^[48] has reviewed the evidence for and against the concept of prostaglandin involvement in tumour growth.

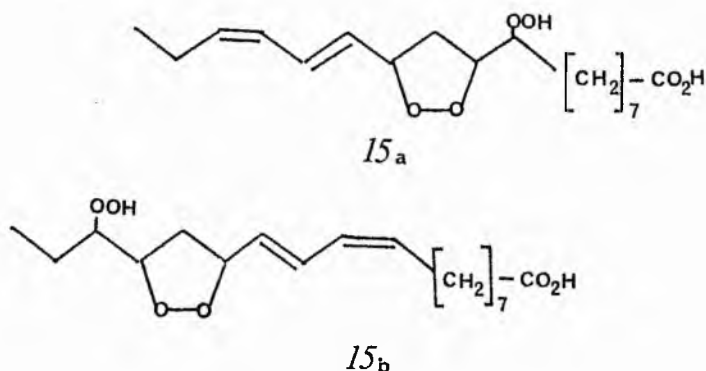
Plant lipoxygenases are widely distributed in nature. The lipoxygenases catalyse the oxidation of PUFA containing a 1,4-pentadiene system to hydroperoxides (Scheme 2). In general the enzymes show considerable stereospecificity^[49-55].

Despite extensive study the physiological role of lipoxygenases is not fully understood. Recent reviews^[51,53] have discussed the current theories regarding the biological significance of this dioxygenase. The primary stable products, the hydroperoxides are unlikely to be the ultimate goal although some of their metabolites may be. Veldink^[49] has postulated that the enzyme may be important at various stages of ripening and/or germination.



SCHEME 2

Cyclic peroxides have been isolated from soybean lipoxygenase oxidations of polyunsaturates containing three or more methylene interrupted double bonds. Roza and Francke^[56] have isolated and characterised cyclic peroxides (15a and b) from soybean lipoxygenase oxidation of methyl linolenate.



Prostaglandin analogues have also been tentatively identified from a flaxseed extract oxidation of linolenic acid^[57]. More recently cyclic peroxides of similar structure to 15a,b have been identified in thermally treated methyl linolenate^[58] and as secondary oxidation products from polyene esters from both triplet^[59,60,61] and singlet oxidations^[62].

References.

1. A.A. Barber and F. Bernheim, Advan. Gerontological Res., 1967, 2, 355.
2. J. Bland, J. Chem. Edn., 1978, 55, 151.
3. A Windaus and J. Brunken, J. Liebig. Ann. Chem., 1928, 460, 225.
4. P. Wieland and V. Prelog, Helv. Chem. Acta. 1947, 30, 3272.
5. K. Gollnick and G.O. Schenck in "1,4-Cycloaddition Reactions",
ed. J. Hamer, Academic Press 1967, Ch 10, pp
6. J. Arditti, R. Ernest, M.H. Fisch and B.H. Flick, J.C.S. Chem. Comm., 1972, 1217.
7. M.L. Bates, W.W. Reid and J.D. White, J.C.S. Chem. Comm., 1976, 44.
8. W.D. Crow, W. Nicholls, and M. Sterns, Tetrahedron Lett., 1971, 1353.
9. J. Fayos, D. Lokensgard, J. Clardy, R.J. Cole and J.W. Kirksey, J. Amer. Chem. Soc., 1974, 96, 6785.
10. N. Eickman, J. Clardy, R.J. Cole and J.W. Kirksey, Tetrahedron Lett., 1975, 1051.
11. W. Fenical, J. Amer. Chem. Soc., 1974, 96, 5580.
12. W. Adam and A.J. Bloodworth, Annual Reports B, 1978, 342
13. R.J. Wells, Tetrahedron Lett., 1976, 2637.
14. a) M.D. Higgs and D.J. Faulkner, J. Org. Chem., 1978, 43, 3454.
b) D.B. Stierle and D.J. Faulkner, J. Org. Chem., 1979, 44, 964.
c) D.B. Stierle and D.J. Faulkner, J. Org. Chem., 1980, 45, 3396.
15. B.M. Howard, W. Fenical, J. Finer, K. Hirotsu and J. Clardy, J. Amer. Chem. Soc., 1977, 99, 6446.
16. M. Nakagawa, H. Watanabe, S. Kodato, H. Okaziura, T. Hino, J.L. Flippen and B. Witkop, Proc. Nat. Acad. Sci. U.S.A. 1977, 74, 4730.

17. I. Scuto, T. Matsuura, M. Nakagawa and T. Hino, Accounts Chem. Res., 1977, 10, 346.
18. G.I. Dmitrienko, V. Snieckus and T. Viswanatha, Biorg. Chem., 1977, 6, 421.
19. H.W. Orf and D. Dolphin, Proc. Nat. Acad. Sci. U.S.A. 1974, 71, 2646.
20. C. Kemal, T.W. Chan and T.C. Bruice, J. Amer. Chem. Soc., 7272.
21. C. Kemal and T.C. Bruice, J. Amer. Chem. Soc., 1977, 99, 7064.
22. J.W. Hastings and K.H. Nealson, Ann. Rev. Microbiol., 1977, 31, 549.
23. J.W. Hastings and T. Wilson, Photochem. Photobiol., 1976, 23, 461.
24. W. Adam, J. Chem. Ed., 1975, 51, 138.
25. T.A. Hopkins, H.H. Siliger, E.H. White and M.W. Cass, J. Amer. Chem. Soc., 1967, 89, 7148.
26. F. McCapra, Y.C. Chang and V.P. Francois, J.C.S. Chem. Comm., 1968, 22.
27. O. Shimomura, T. Goto and F.H. Johnson, Proc. Nat. Acad. Sci. U.S.A. 1977, 74, 2799.
28. J. Wannlund, M. DeLuca, K. Stempel and P.D. Boyer, Biochem. Biophys. Res. Comm., 1978, 81, 987.
29. W. Adam, A. Alzérreca, J.C. Liu and F. Yony, J. Amer. Chem. Soc., 1977, 99, 5768.
30. W. Adam, O. Cueto, and F. Yony, J. Amer. Chem. Soc., 1978, 100, 2587.
31. B. Lindblad, G. Linstedt and S. Linstedt, J. Amer. Chem. Soc., 1970, 92, 7446.

32. A.S. Widman, A.H. Solaway, R.L. Stern and M.M. Bursey,
Biorg. Chem., 1973, 2, 176.
33. I. Scuto, Y. Chiyo, H. Shimazu, M. Yamane, T. Mutsuura and
H.J. Cahnmann, J. Amer. Chem. Soc., 1975, 97, 5272.
34. K.C. Nicolaou, G.P. Gasic and W.E. Barnett, Angew. Chem. Int.
Ed., 1978, 17, 293.
35. K.H. Gibson, Chem. Soc. Revs., 1977, 6, 489.
36. P. Crabbé (Ed) "Prostaglandin Research", Academic Press,
New York, 1977.
37. R.T. Holman (Ed) "Progress in Lipid Research" Vol 20
Essential Fatty Acids and Prostaglandins, Pergamon Press,
Oxford, 1981.
38. D.A. van Dorp, Proc. K. Ned. Akad. Wet., 1975, 84, 34.
39. D.A. van Dorp, Proc. Nutr. Soc., 1975, 34, 279.
40. E.J. Crist and D.A. van Dorp, Biochim. Biophys. Acta. 1972,
270, 537.
41. T. Suzuki and W. Vogt, Naunyn-Schmiedebergs Arch. Exp. Pathol.
Pharmakol., 1965, 252, 68.
42. T. Nomura, H. Ogata, and M. Itoh, Tohuka J. Agric. Res., 1973,
24, 138.
43. H. Ogata and T. Nomura, Biochim. Biophys. Acta. 1975, 84, 388.
44. a) W.P. Schneider, R.D. Hamilton and L.E. Rhuland, J. Amer.
Chem. Soc., 1972, 94, 2122.
b) R.L. Spraggins, Tetr. Lett., 1972, 4343
c) A. Prince, F.S. Alvarez and J. Young, Prostaglandins. 1973,
3, 531.
45. P. Crabbé in "Prostaglandin Research", Org. Chem., 1977, 36, 1.

46. a) See Progress in Lipid Research 1982, 20.
b) B. Samuelsson in Ref 45 pp 17.
c) R.L. Jones ibid pp 65.
d) "Biochemical Aspects of Prostaglandins and Thromboxones"
Ed. N. Kharasch and J. Friend, Academic Press,
New York, 1977.
47. a) Ref 46a pp 667 - 705.
b) Ref 46d pp 95 - 102.
48. A.Bennet in "Practical Applications of Prostaglandins and their
Synthesis Inhibitors" pp 149-188 Ed. S.M.M. Karim,
MTP Press, Lancaster, 1979.
49. G.A. Veldink, J.F.G. Vliegenthart and J. Boldingh, Prog. Chem.
Fats other Lipids. 1977, 15, 131.
50. A.L. Tappel in "The Enzymes", Second edition, pp 275. Ed. P.D.
Boyer, H. Lardy and K. Myrbäck, Academic Press, New York,
1963.
51. B. Axelrod, Adv. Chem. Ser., 1974, 324.
52. R. Drapron and A. Uzzan, Ann. Nutr. Alim., 1968, 22, B393.
53. T. Galliard in "Recent Advances in the Chemistry and Biochemistry
of Plant Lipids", Ed. T. Galliard and E.I. Mercer,
Academic Press, London, 1975.
54. H.W. Gardner, J. Agr. Food Chem., 1975, 23, 129.
55. Strictly speaking lipoxygenases also show appreciable
regioselectivity. See R.T. Holman, P.O. Egwin, and
W.W. Christie, J. Biol. Chem., 1969, 244, 1149.
56. M. Roza and A. Francke, Biochim. Biophys. Acta. 1978, 528, 119.
57. D.C. Zimmerman and P. Feng, Lipids. 1978, 13, 313.

58. H. W.-S. Chan, J.A. Matthew and D.T. Coxon,
J.C.S. Chem. Comm., 1980, 235.
59. D.T. Coxon, K.R. Price and H.W.-S. Chan, Chem. Phys. Lipids,
1981, 28, 365.
60. W.E. Neff, E.N. Frankel and D. Weisleder, Lipids, 1981, 16, 439.
61. D.E. O'Connor, E.D. Mihelich and M.C. Coleman, J. Amer. Chem. Soc.,
1981, 103, 223
62. a) E.D. Mihelich, J. Amer. Chem. Soc., 1980, 102, 7141.
b) E.N. Frankel, W.E. Neff, E. Selke and D. Weisleder,
Lipids, 1982, 17, 11

CHAPTER 1

SYNTHESIS of LIPID PEROXIDES

Introduction and survey of synthetic methods.

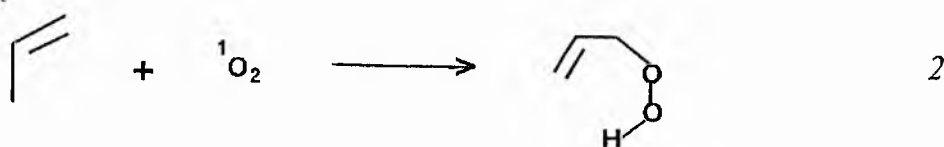
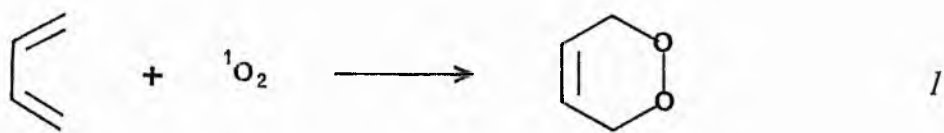
The synthesis of labile compounds susceptible to thermal, base catalysed and numerous other modes of decomposition presents a considerable synthetic challenge. The classical approach to the synthesis of peroxides or cyclic peroxides, required extremes of temperature and /or pH resulting generally in poor yields. For the synthesis of larger molecules of biological significance such harsh conditions would be unacceptable and result in rapid decomposition of the desired product. Following the discovery of prostaglandin endoperoxides the last decade or so has seen an upsurge in the development of milder techniques for the synthesis of peroxides. In this introduction we will review these more recent methods of synthesising hydroperoxides, dialkyl peroxides and cyclic peroxides. Polyperoxides^[1], ozonides^[2], acyl peroxides^[3], organometallic peroxides^[4] and peracids^[5] are considered outwith the scope of this brief survey.

Singlet oxidation.

Undoubtedly an area of peroxide synthesis which has flourished in the past 15 or so years is that of singlet oxidation. Biochemists and biologists have become increasingly interested in singlet oxygen following the realisation that it may be implicated in numerous biological processes^[6]. Among these are the reactions involved in the destruction of cells and tissues (in the presence of light, oxygen and a suitable sensitiser) such as phagocytosis^[7], red blood cell damage^[8], and certain cancer-inducing processes^[9]. The chemistry of singlet oxygen has been the subject of a large number of reviews^[10] and texts^[11].

Ground state oxygen has its outermost pair of electrons in different orbitals with their spins parallel making the ground state a 'triplet' state ($^3\Sigma_g^-$)^[12]. Two other arrangements of these two electrons are possible resulting in the presence of two low lying 'singlet' states ($^1\Delta_g$ and $^1\Sigma_g^+$)^[13]. The two spin states were identified spectroscopically by Herzberg (1934)^[14] and Childs and Mecke (1931)^[15] with potential energies of 22.54 and 37.51 kcal above the ground state. The theoretical status of excited oxygen is the subject of a number of comprehensive discussions^[16].

Reaction of singlet oxygen (1O_2) with unsaturated substrates may be categorised into three classes (equations 1-3 which indicate only the minimum functional requirement for each process).



Reaction 1 requires a cisoid conjugated diene unit and despite a few dissenters the general consensus of opinion is that the reaction proceeds through a six-membered ring transition state formally analogous to the Diels-Alder $2 + 4\pi$ cycloaddition reaction. Reactions of type 2 require the presence of at least one allylic hydrogen and the mechanism of the reaction is still uncertain with the postulation of radical, ionic, dioxetane, peroxirane, or concerted "ene" type mechanisms. Of these five only the latter two are still serious contenders (several excellent reviews^[10,11] have appeared on the question of mechanism of singlet oxygen reactions with olefins so the topic will not be discussed here). Whatever the outcome of the debate the formation of allylic hydroperoxides always results in a shifted double bond and is, therefore, clearly distinguishable from the well-known autoxidation reaction. The latter proceeds by a primary dehydrogenation of the olefin and subsequent addition of ground state oxygen (${}^3\Sigma_g^-$) to the allylic radical.

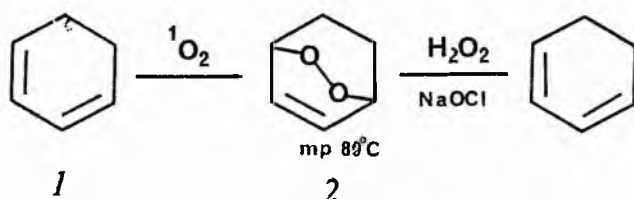
Reaction 3 leads to the formation of dioxetanes via a concerted $2 + 2\pi$ cycloaddition reaction.

A wide variety of techniques are used for generating singlet oxygen but the most common is via dye-sensitisation. The dye or sensitiser (typically Rose Bengal, tetraphenyl porphorine or methylene blue) absorbs incident light to become electronically excited. The excited sensitiser can then undergo energy transfer to oxygen in the ground state to produce the excited singlet state. The process is described by equations 4-6.

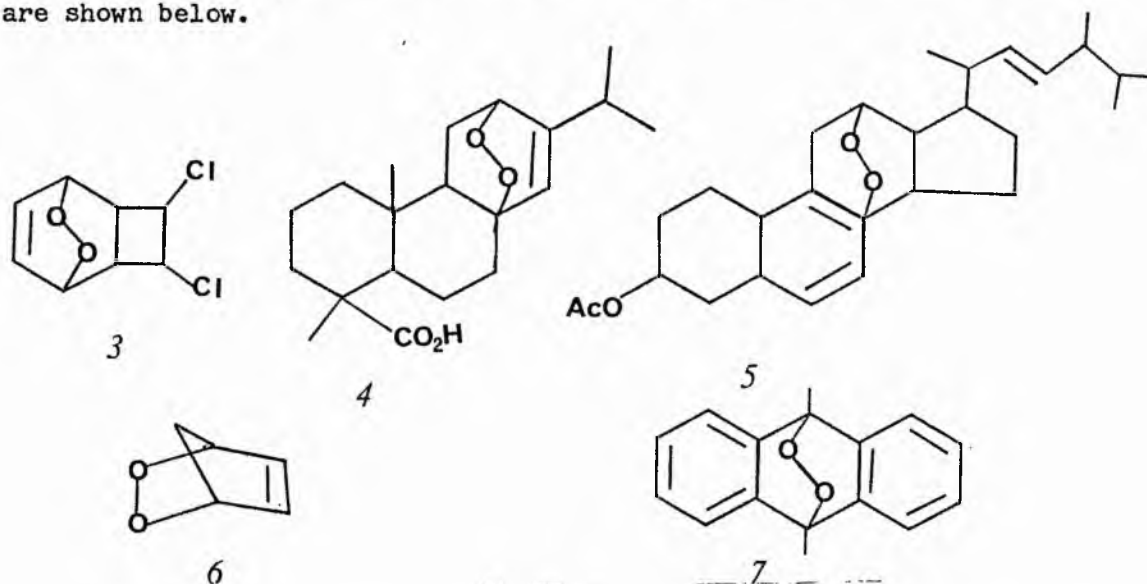


Singlet oxygen reacts with cyclic and acyclic conjugated dienes as well as with aromatic substrates by reaction 1 to give cyclic peroxides consisting of a six-membered ring with unsaturation in the 3,4 position.

Irradiation of 1,3 cyclohexadiene (1), in the presence of oxygen and sensitiser leads to norascaridole (2)^[17], which is reported to explode at 100°C. The same compound has been prepared by Foote using $H_2O_2/NaOCl$ as source of singlet oxygen^[18].



A wide variety of cyclic 1,3-dienes have been used as substrates for $^1\text{O}_2$ to give the corresponding (cyclic) peroxides. Some examples are shown below.



Polycyclic aromatics such as rubrene, 9,10-disubstituted anthracenes and activated naphthalenes give 1,4 adducts that release singlet oxygen on thermolysis^[19].

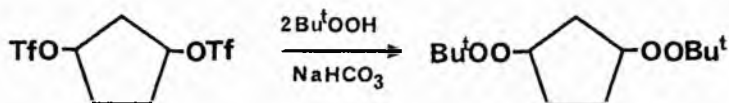
Peroxides produced from acyclic 1,3-dienes are less well known. Indeed it was reported in a popular review article^[10b] that cycloperoxides were not obtained from aliphatic conjugated dienes. This observation was shown to be incorrect by Kondo and Matsumoto^[20] who obtained cyclic peroxides from butadiene derivatives.

Nucleophilic displacement by hydrogen peroxide and related derivatives.

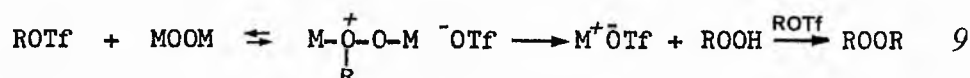
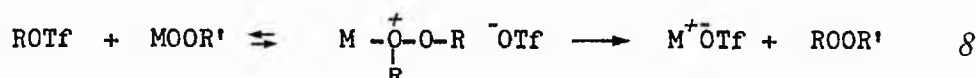
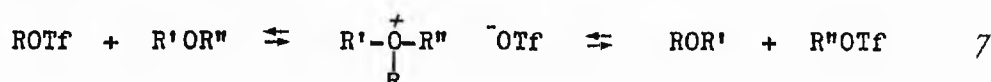
Alkyl hydroperoxides and dialkyl peroxides can be obtained at tertiary, secondary, or primary centres by nucleophilic displacement. Pre 1970 methodology of nucleophilic displacement by hydrogen peroxide and related species invariably involved harsh conditions causing extensive decomposition of the desired product. Milder reaction conditions require the use of either more powerful alkylating agents or more reactive nucleophilic sources such as superoxide anion.

Alkylation by alkyl trifluoromethanesulphonates.

Alkylation by alkyl methanesulphonates requires alkaline conditions^[21]. Salomon *et al.*^[22] described a milder procedure using alkyl trifluoromethanesulphonates (triflates) which are sufficiently powerful alkylating agents to react with *t*-butyl hydroperoxide under non-alkaline conditions giving fair yields (33-56%) of secondary alkyl peroxides.



The same group^[23,24] modified their original procedure by reacting alkyl triflates with bis-(tri-n-butyltin) peroxide in a so called peroxide transfer reaction. The transfer reaction is based upon the transalkylation of alkyl ethers with triflates^[25] (equation 7). Analogous transalkylation of dialkyl peroxides yields new peroxides. Organometallic peroxides react with alkyl triflates to afford alkyl peroxides; decomposition of the intermediate metalloxonium ion yielding the desired alkyl peroxide by expulsion of a stable cation (equation 8).



Good yields of mixed dialkyl peroxides (equation 9) were obtained from bis(trialkyltin) or bis(trialkyl germanium) peroxides, but not the corresponding silyl peroxides. Symmetrical dialkyl peroxides and cyclic peroxides (equation 10) can also be formed.



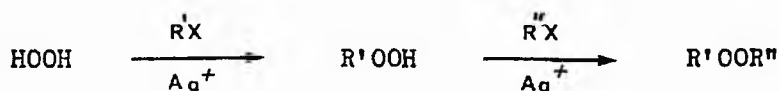
The reactions are generally accompanied by minor yields of the corresponding dialkyl ethers.

Yields of cyclic peroxides for simple compounds are in the range 23-68 %.

The reaction was applied in the first synthesis of 2,3-dioxabicyclo[2.2.1]heptane (8)^[26] the nucleus of prostaglandin endoperoxides.

Alkylation by alkyl halides.

The silver trifluoroacetate assisted intermolecular reaction of an alkyl halide with an alkyl hydroperoxide or hydrogen peroxide (Scheme 1) provides a facile route to alkyl hydroperoxides and to symmetric and mixed dialkyl peroxides^[27].



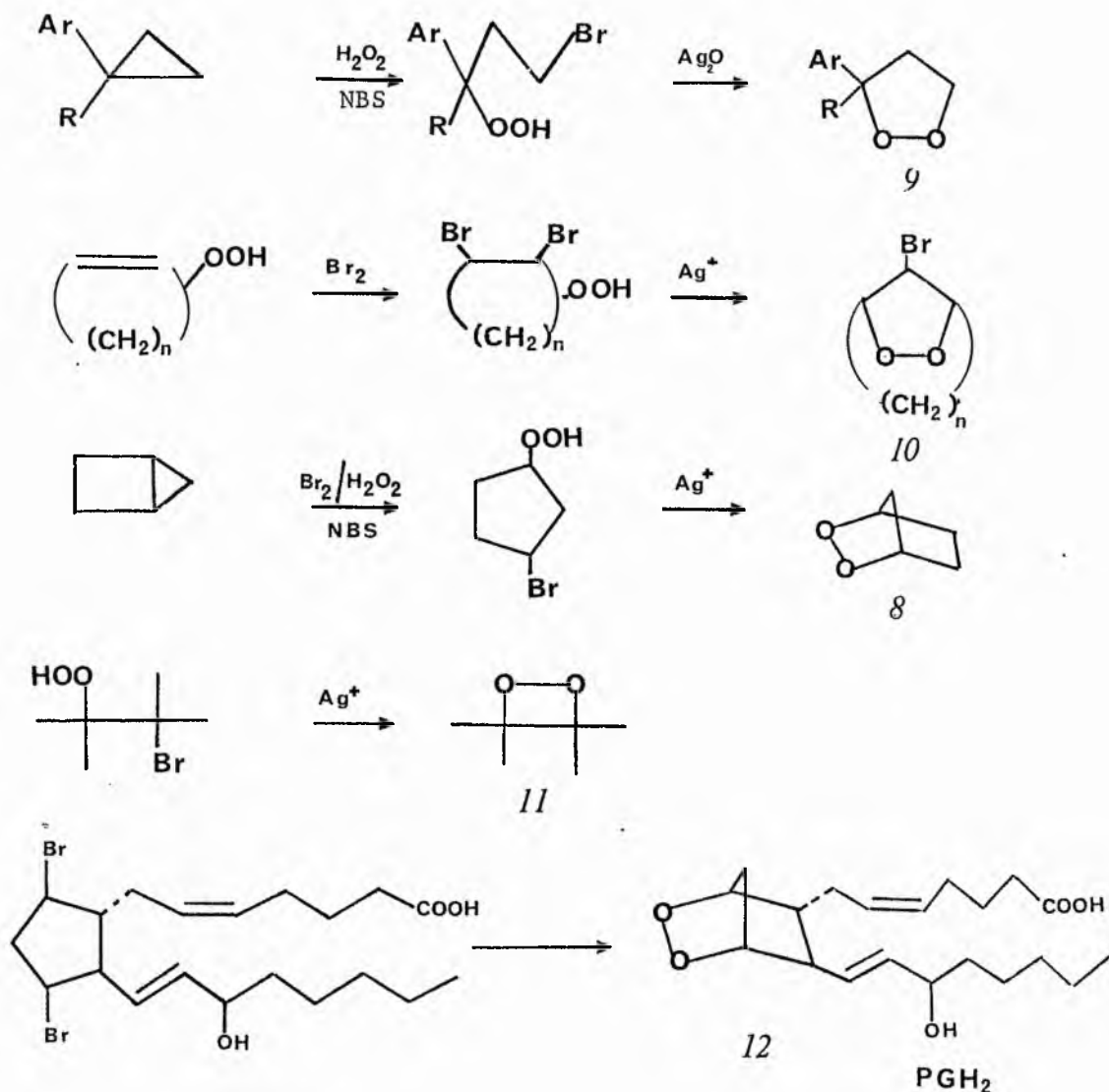
SCHEME 1

These alkylations also proceed via oxonium ion intermediates



Alkyl bromides are sufficiently reactive for making tertiary and secondary derivatives, but iodides are required for the preparation of primary peroxides. The intramolecular reaction has been extended to γ -bromo alkyl hydroperoxides thereby providing synthesis of 1,2-dioxabicyclopentanes (9)^[28], bicyclic peroxides (10)^[29],

including 2,3-dioxabicyclo[2.2.1]heptane (8)^[30] and dioxetanes (11)^[31] (Scheme 2).

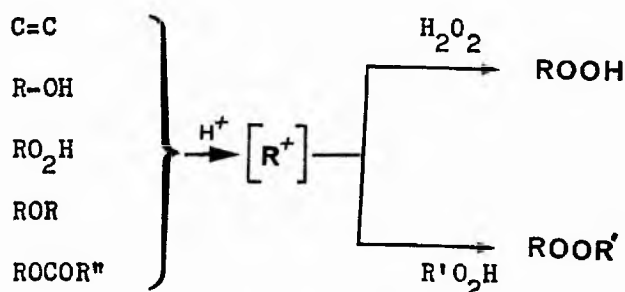


SCHEME 2

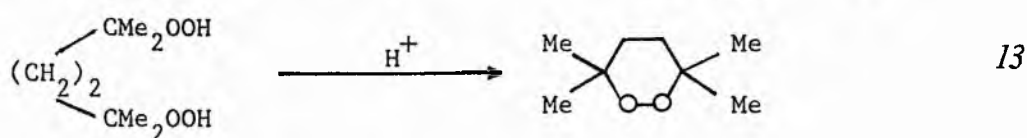
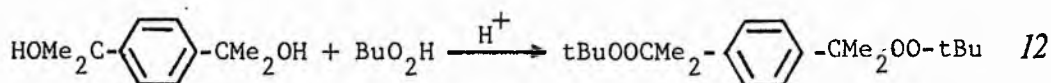
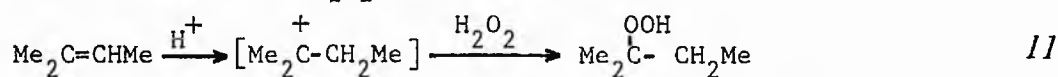
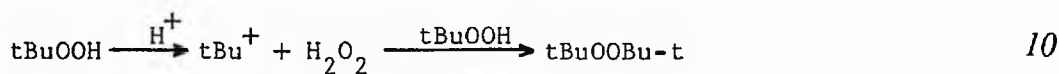
Literature results suggest that the method is excellent for making dialkyl, and (bi)cyclic peroxides but is less useful as a hydroperoxide synthesis. Porter *et al*^[32] used this approach for the synthesis of prostaglandin H_2 (12) in 17-24 % yield.

Alkylation by carbonium ions.

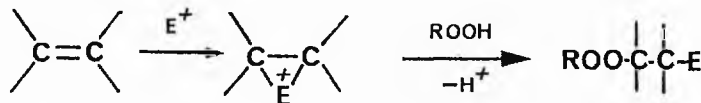
Tertiary or resonance-stabilised carbonium ions, produced by protonation of alkenes^[33], alcohols^[34], hydroperoxides^[34a,35], ethers^[36], or esters^[33a] alkylate hydrogen peroxide or alkyl hydroperoxides readily.



Thus *t*-butyl peroxides^[35b] and *t*-amyl hydroperoxide^[34d] have been prepared by this route (equation 10 and 11). Diperoxides may be obtained from diols and cyclic peroxides from suitably functionalised dihydroperoxides (equation 12 and 13).

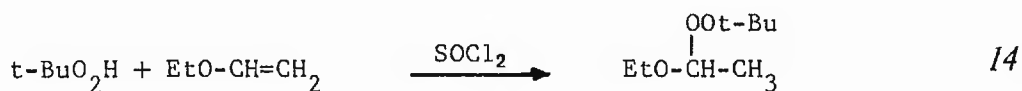


Although protonation of alkenes to generate carbonium ions to alkylate hydrogen peroxide (Scheme 3) has found application its scope as a synthetic route is limited. Other electrophiles have however met with more success.



SCHEME 3

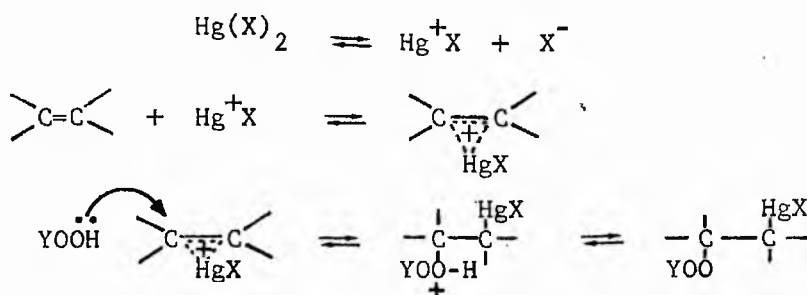
Positive halogen obtained from t-BuOCl^[38], Br₂^[39], N-chloroacetamide^[40], N-bromosuccinimide^[40] and 1,3-diiodo-5,5-dimethylhydantoin^[40] has been used to prepare β-halogenoalkyl hydroperoxides. Weissmermel and Lederer^[38] prepared β-chloroperoxides by substituting t-butyl or α-cumyl hydroperoxide for hydrogen peroxide. In an apparent free radical chain addition, using catalytic amounts of SOCl₂ or SO₂Cl₂ instead of equimolar amounts of t-BuOCl, they obtained non-halogenated hydroperoxides and peroxides from vinyl ethers (equation 14).



β-halogenoalkyl hydroperoxides are useful synthons for dioxetane synthesis.

The use of mercury (II) salts as an electrophilic source has been exploited extensively by Bloodworth and co-workers^[41]. The formation

of an intermediate 'mercurium ion' by electrophilic attack of cationic mercury on the olefin followed by nucleophilic attack of the peroxyreagent (Scheme 4) has been utilised to form a variety of β -mercurioalkyl peroxides including acyclic^[41], cyclic^[42], and bicyclic^[43] peroxides in high yields.

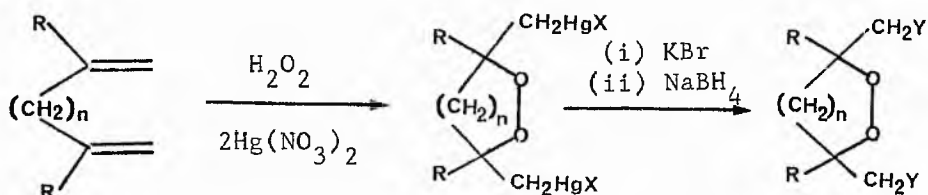


SCHEME 4

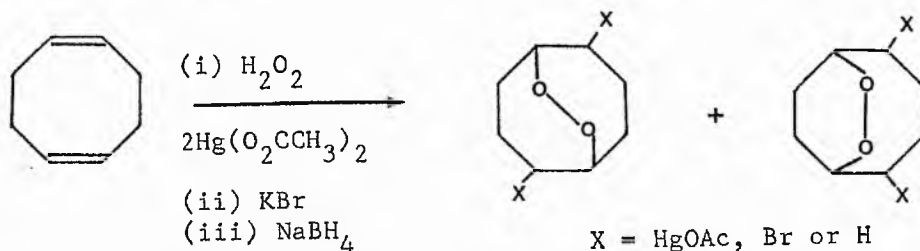
Sodium borohydride or halogeno demercuration of the peroxides (and more recently tributyltin hydride demercuration^[44]) generally occur without substantial cleavage of the O-O bond (although for some cyclic peroxides with exo-cyclic β -mercurio functionality, competitive $\text{S}_{\text{H}1}$ attack on the O-O bond occurs, the extent of which is intimately linked with the conformation of the ring (see section two of this chapter for a further discussion of this point). Thus secondary dialkyl peroxides^[41a,c,f], and β -halogeno alkyl peroxides^[41h] have been obtained in high yields (60-75 %). The procedure for t-butyl peroxymercuration and bromodemercuration has recently been improved by carrying out the peroxymercuration under conditions of equilibrium control induced by the presence of 20 mol % HClO_4 ^[45]. Under these conditions stereospecific trans-peroxymercuration of non-terminal olefins occurs with little if any competing reaction. Ten

diastereoisomerically pure bromo-peroxides were prepared by this method.

The reaction of acyclic dienes with mercury (II) nitrate and hydrogen peroxide has afforded good yields of cyclic peroxides whereas cyclic dienes give rise to bicyclic peroxides albeit in lower yields in general.



$n = 1$ or 2 , $X = Br, Cl$ or (NO_3) , $Y = H$ or Br

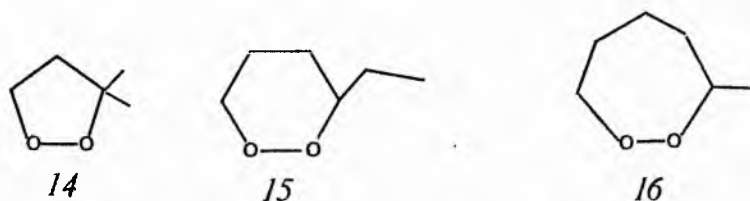


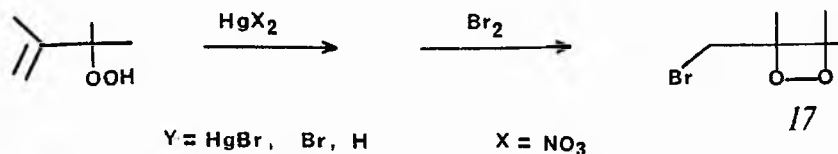
In these diene reactions the initial peroxymercuration generates an unsaturated hydroperoxide which then cyclises via a second intramolecular addition.

An alternative approach utilises cycloperoxymercuration (Scheme 5). Such reactions have provided synthesis of 4-7 membered peroxide rings (13-17) although yields were generally poor^[46,47].



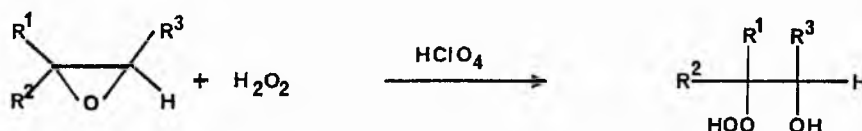
SCHEME 5



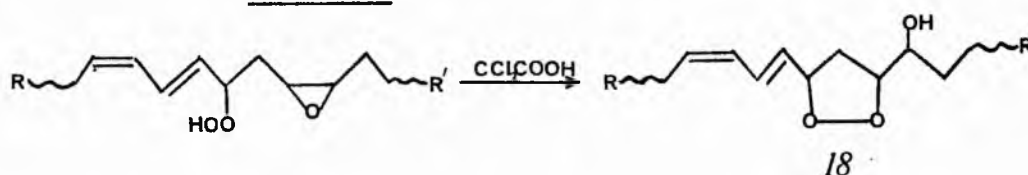


Alkylation by epoxides.

The perhydrolysis of epoxides under Lewis acid conditions has been utilised to prepare β -hydroxy alkyl hydroperoxides^[48,49] (Scheme 6). Porter *et al*^[50] used an intramolecular perhydrolysis reaction to afford good yields of cyclic peroxides including the fatty acid cyclic peroxide (18).

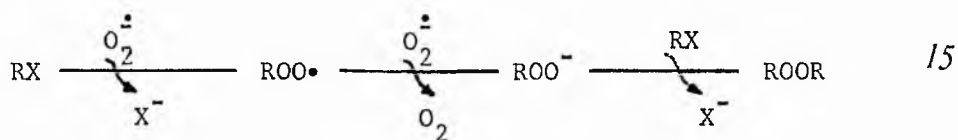


SCHEME 6

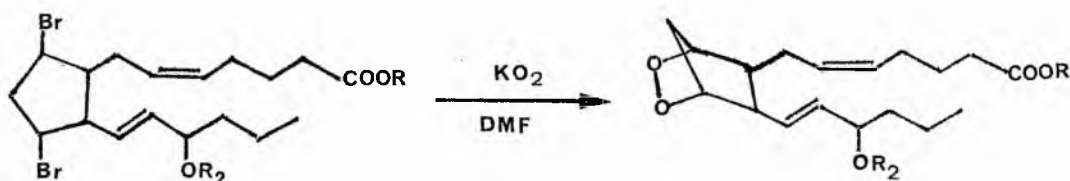


Alkylation of superoxide anion.

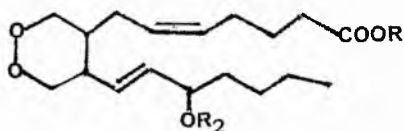
Johnson and co-workers^[51] of the UpJohn group have prepared dialkyl peroxides in yields of up to 72 % from primary and secondary alkyl bromides or sulphonates. Equation 15 describe the reaction pathway which proceeds with inversion of configuration.



Crown ethers are required to produce solutions of potassium superoxide in organic solvents. Using this approach PGH_2 was produced from the dibromide (19) in 3 % recovered yield using KO_2 in DMF. Similarly the 10-nor-9,11-secoprostaglandin H_2 (20) has recently been prepared in 69 % yield from the appropriate bis-tosylate.



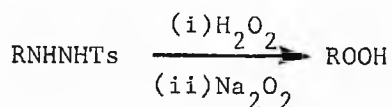
19



20

Some miscellaneous routes.

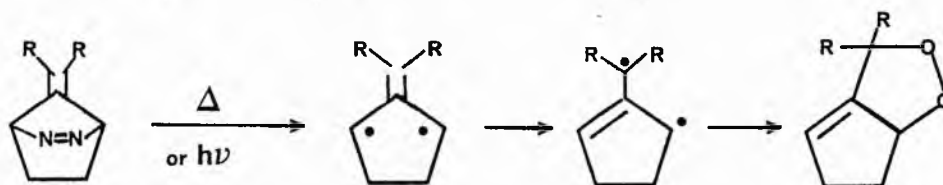
The oxidation of simple alkyl and steroidal N-alkyl-N'-tosyl hydrazines (equation 16) has been employed to prepare a variety of hydroperoxides [54].



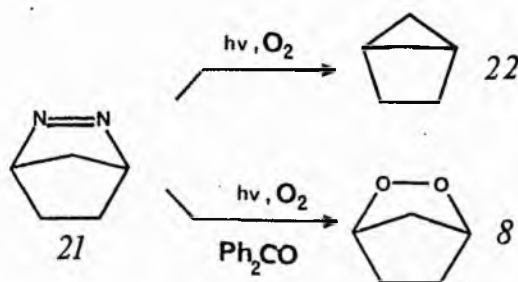
16

Yields for the reaction (determined by HPLC analysis) were excellent 87 % to quantitative and a notable advantage of the method is that it employs low strength H_2O_2 (30 %).

Wilson and Geiser^[55] prepared bicyclic peroxide by decomposition of azo compounds in the presence of oxygen. The biradicals formed either by thermolysis or photolysis can be trapped by oxygen to furnish the peroxides in 37-40 % yield (Scheme 7). The method was employed for the synthesis of 2,3-dioxabicyclo[2.2.1]heptane (8) from the azo compound (21). In this experiment however, the decomposition is brought about by benzophenone-sensitised photodecomposition by irradiation of benzophenone only, since direct photolysis of (21) gives rise to the singlet biradical which collapses to bicyclo[2.1.0]pentane (22) before it can be trapped with oxygen.



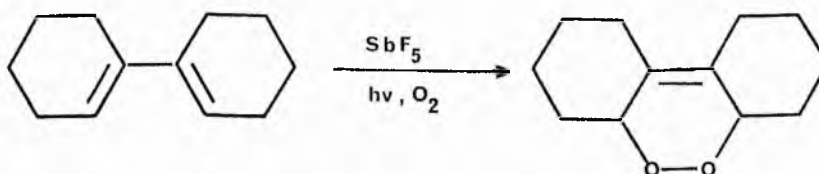
SCHEME 7



The same research group have prepared a variety of unusual peroxides by trapping other transient species with oxygen.^[56-59]

Another route involving triplet oxygen addition to 1,3-dienes, catalysed by Lewis acids and aminium radical cations (Scheme 8) has

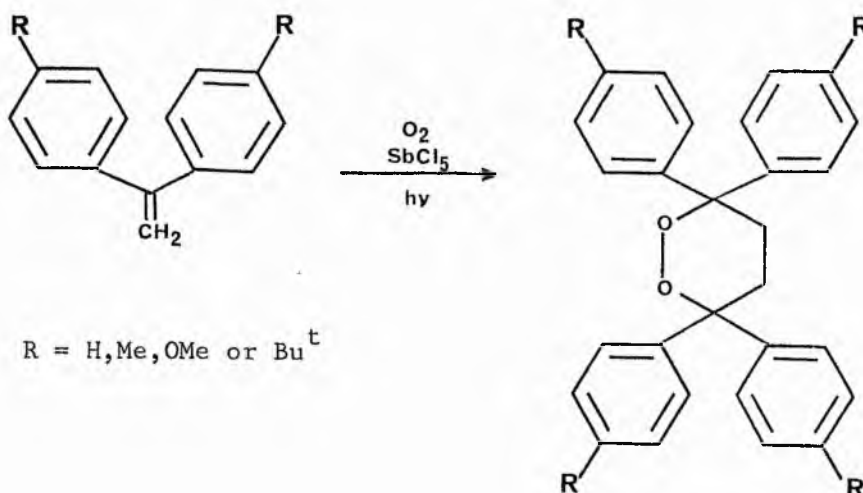
recently been reported.



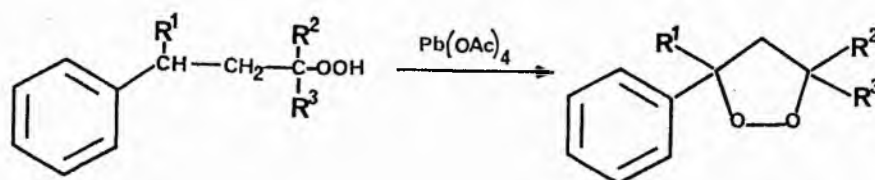
SCHEME 8

With some catalysts (BF_3 , SnCl_4 , SnBr_4 , SbF_5 , SnCl_5 , WF_6 , I_2 and Ph_3CBF_4) simultaneous irradiation is necessary for optimum yields whereas with others (VOCl_3 , FeCl_3 , MoCl_5 , WCl_6 and $(4\text{-BrC}_6\text{H}_4)_3\text{NBF}_4$) the reaction proceeds satisfactorily in the dark. The addition of ground-state triplet oxygen to conjugated dienes is spin forbidden. To rationalise the above reactions Barton and co-workers^[60-62] suggested that the catalyst forms an assembly with the 1,3-diene and oxygen, hence overcoming the spin barrier impeding cycloaddition. However, two more recent independent publications favour electron transfer from the alkene to the catalyst to generate intermediate radical cations^[63-65].

Haynes *et al*^[66] extended the procedure to form 3,3,6,6-tetraaryl-1,2-dioxans from 1,1-diarylethylenes in the presence of antimony (v) chloride in high yields.



Kropf and von Wallis^[67] have recently reported the formation of aryl substituted 1,2-dioxolanes via a Barton-type-cyclisation of alkyl hydroperoxides using lead tetraacetate.



Best yields were reported for $\text{R}^1 = \text{R}^2 = \text{R}^3 = \text{aryl}$ and replacement of one or all of these aryl groups by methyl gave successively poorer yields.

References.

1. D.G. Hendry in "Encyclopedia of Polymer Science and Technology", Vol. 9, Wiley and Sons, New York, 1968, p 807.
2. a) A. Rieche and R. Meister, Ber., 1932, 65, 1274.
b) A. Rieche, R. Meister and H. Sauthoff, Ann., 1942, 533, 187.
3. a) R. Hiatt in "Organic Peroxides" Vol 2, (Ed D. Swern), Wiley and Sons, New York, 1971, pp 799-931.
b) A.G. Davies, "Organic Peroxides", Butterworths, London, 1961, pp 63-71.
c) E.G.E. Hawkins, "Organic Peroxides", Van Nostrand, Princeton, N.J., 1961, pp 300-329.
d) A.V. Tobolsky and R.B. Mesrobian, "Organic Peroxides", Interscience, New York, 1954.
4. a) A.G. Davies in "Organic Peroxides" Vol 2 (Ed. D. Swern), Wiley and Sons, New York, 1971, pp 337-355.
b) G.A. Razuvaev, V.A. Shushunov, V.A. Dodonov and T.G. Brilkina in "Organic Peroxides" Vol 3 (Ed. D. Swern), Wiley and Sons, New York, 1972, pp 141-271.
5. D. Swern in "Organic Peroxides" Vol 2 (Ed. D. Swern), Wiley and Sons, New York, 1971, pp 355-535.
6. a) J. Bland, J. Chem. Ed., 1976, 53, 274.
b) N.I. Krinsky in "Singlet Oxygen" (Ed. H.H. Wasserman and R.W. Murray), Academic, New York, 1979, pp 597-641.
7. Ref 6b pp 606-609 and references therein.
8. a) T. Maugh, Science, 1975, 187, 154.
b) A.A. Lamola, T. Yamane and A.M. Trozzolo, Science, 1973, 179, 1131.
c) C. Rimington, J.A. Magnus, E.A. Ryan and D.J. Gripps. Quar. J. Med., 1967, 141, 29.

9. a) J.T. Chan and H.S. Black, Science, 1974, 186, 1216.
b) H.F. Blum, in "Photodynamic Action and Diseases Caused by Light", Reinhold, New York, 1941, pp 3-5.
10. a) R.W. Denny and A. Nickon, Org. Reactions, 1973, 20, 133.
b) K. Gollnick and G.O. Schenck in "1,4-Cycloaddition Reactions" (Ed J. Hamer), Academic, New York, 1967 pp 225.
c) W. Adam and A.J. Bloodworth, Annual Reports B, 1978, 342.
d) H.H. Wasserman and J.L. Ives, Tetrahedron, 1980, 37, 1825.
e) A.A. Frimer, Chem. Rev., 1979, 79, 359.
11. a) "Singlet Oxygen", Ed. H.H. Wasserman and R.W. Murray, Academic, New York, 1979.
b) "Singlet Oxygen. Reactions with Organic Compounds and Polymers", Ed. B. Ranby and J.F. Rabek, Wiley and Sons, New York, 1978.
c) P.A. Schaap in "Singlet Molecular Oxygen", Dowden, Hutchinsonson and Ross, Stroudsburg, Pennsylvania, 1976.
12. R.S. Mulliken, Rev. Mod. Phys., 1932, 4, 1 and references cited therein.
13. See M.K. Kasha and D.E. Brabham in "Singlet Oxygen" (Ed. H.H. Wasserman and R.W. Murray, Academic, New York, 1979, pp 1-33.
14. G. Herzberg, Nature, 1934, 133, 759. See also G. Herzberg "Molecular Spectra and Molecular Structure, J. Spectra of Diatomic Molecules, Van Nostrand-Reinhold, New York, 1950, pp 446.
15. W.H. Childs and R. Mecke, Nature, 1930, 125

16. The mechanism of the "ene" reaction is discussed in most of the references cited in footnotes 10 and 11. Additional references cited in this footnote deal only with the mechanism of the "ene" reaction.
- a) L.B. Harding and W.A. Goddard III, J. Amer. Chem. Soc., 1980, 102, 439, ibid 1977, 99, 4520.
 - b) M.J.S. Dewar, Chem. Brit., 1975, 11, 97 and 106.
 - c) M.J.S. Dewar, and W. Thiel, J. Amer. Chem. Soc., 1975, 97, 3978.
 - d) S. Inagaki, S. Yamabe, H. Fujimoto, and K. Fukui, Bull. Chem. Soc. Jpn., 1972, 45, 3510.
 - e) S. Inagaki and K. Fukui, J. Amer. Chem. Soc., 1975, 97, 7480.
 - f) S. Inagaki, H. Fujimoto and K. Fukui, Chem. Lett., 1976, 749.
 - g) R.D. Ashford and E.A. Ogryzlo, J. Amer. Chem. Soc., 1975, 97, 3604.
 - h) J.C. Carmier and X. Deglise, Bull. Soc. Chim. Fr., 1973, 868.
17. a) G.O. Schenck and K. Ziegler, Naturwissenschaften, 1944, 32, 157.
- b) G.O. Schenck and D.E. Dunlop, Angew Chem., 1956, 68, 248.
18. C.S. Foote, S. Wexler, W. Ando and R. Higgins, J. Amer. Chem. Soc., 1968, 90, 975.
19. a) W. Bergmann and M.J. McLean, Chem. Rev., 1941, 28, 367.
- b) C. Moreau, C. Dufraisse and P.M. Dean, Compt. Rend., 1926, 182, 1446.
 - c) H.H. Wasserman and J.R. Scheffer, J. Amer. Chem. Soc., 1967, 89, 3073.
 - d) H.H. Wasserman, J.R. Scheffer, and J.L. Cooper, J. Amer. Chem. Soc., 1972, 94, 4991.

20. K. Kondo and M. Matsumoto, J.C.S. Chem. Comm., 1972, 1332.
21. a) H.R. Williams and H.S. Mosher, J. Amer. Chem. Soc., 1954, 76, 2984 and 2987.
- b) S. Wawzonek, P.D. Klimstra and R.E. Gallio, J. Org. Chem., 1960, 25, 621.
- c) F.D. Gunstone, E.G. Hammond, H. Schuler, C.M. Scrimgeour and H.S. Vedanayagam, Chem. Phys. Lipids, 1975, 14, 81.
22. M.F. Salomon, R.G. Salomon and R.D. Gleim, J.O.C., 1976, 41, 3983.
23. M.F. Salomon and R.G. Salomon, J. Amer. Chem. Soc., 1977, 99, 3500.
24. M.F. Salomon and R.G. Salomon, J. Amer. Chem. Soc., 1979, 101, 4290.
25. T. Gramstad and R.N. Haszeldine, J.C.S., 1957, 4069.
26. R.G. Salomon and M.F. Salomon, J. Amer. Chem. Soc., 1977, 99, 3501.
27. a) P.G. Cookson, A.G. Davies and B.P. Roberts, J.C.S. Chem. Comm., 1976, 1022.
- b) A.A. Frimer, J.O.C., 1977, 42, 3194.
28. W. Adam, A. Birke, C. Cadiz, S. Diaz and A. Rodriguez, J.O.C., 1978, 43, 1154.
29. a) A.J. Bloodworth and B.P. Leddy, Tet. Lett., 1979, 729.
- b) A.J. Bloodworth and H.J. Eggelte, J.C.S. Perkin I, 1981, 1375.
- c) A.J. Bloodworth and H.J. Eggelte, J.C.S. Perkin I, 1981, 3272.
- d) A.J. Bloodworth and H.J. Eggelte, J.C.S. Chem. Comm., 1979, 741.
- e) A.J. Bloodworth and H.J. Eggelte, Tet. Lett., 1980, 2001.

30. N.A. Porter and D.W. Gilmore, J. Amer. Chem. Soc., 1977, 99, 3503.
31. K.R. Kopecky, J.E. Filby, C. Mumford, P.A. Lockwood and J.Y. Ding, Canad. J. Chem., 1975, 53.
32. N.A. Porter, J.D. Byers, R.C. Mebane, D.W. Gilmore and J.R. Nixon, J.O.C., 1978, 43, 2088.
33. a) A.G. Davies, R.V. Foster and A.M. White, J.C.S., 1954, 2200.
b) C.K. Ikeda, R.A. Braun and B.E. Sorenson, J.O.C., 1964, 29, 286.
c) M.S. Kharasch, A. Fono, W. Nudenburg and A.C. Poshkus, J.O.C., 1950, 15, 775.
34. a) M. Bassey, E. Buncl and A.G. Davies, J.C.S., 1955, 2550.
b) J.I.G. Cadogan, D.E. Hey and W.A. Sanderson, J.C.S., 1958, 4498.
ibid 1960, 3203.
ibid 1961, 5236.
c) M.S. Kharasch and J.G. Burt, J.O.C., 1951, 16, 150.
d) M.S. Kharasch, A. Fono and W. Nudenburg, J.O.C., 1950, 15, 753.
35. a) A.G. Davies, R.V. Foster and R. Nery, J.C.S., 1954, 2204.
b) J.O. Turner, Tet. Lett., 1971, 887.
36. A.G. Davies and R. Feld, J.C.S., 1956, 4669.
37. R. Criegee and G. Paulig, Ber., 1955, 88, 712.
38. W. Weissermel and M. Lederer, Ber., 1963, 96, 77.
39. a) A. Rieche, M. Schulz and K. Kirschke, Ber., 1966, 99, 3244.
b) M. Schulz, A. Rieche and K. Kirschke, Ber., 1967, 100, 370.
40. K. Kipecky, J. Van de Sande and C. Mumford, Can. J. Chem., 1968, 46, 25.
41. a) D.H. Ballard and A.J. Bloodworth, J. Chem. Soc. (C), 1971, 945.
b) A.J. Bloodworth and R.J. Bunce, J. Chem. Soc. (C), 1971, 1453.
c) A.J. Bloodworth and G.S. Bylina, J.C.S. Perkin I, 1972, 2433.

41. d) A.J. Bloodworth and R.J. Bunce, J. Organometallic Chem., 1973, 60, 11.
- e) A.J. Bloodworth and I.M. Griffin, J.C.S. Perkin I, 1974, 688.
- f) A.J. Bloodworth and I.M. Griffin, J.C.S. Perkin I, 1975, 195.
- g) A.J. Bloodworth and I.M. Griffin, J.C.S. Perkin II, 1975, 531.
- h) A.J. Bloodworth and I.M. Griffin, J.C.S. Perkin I, 1975, 695.
42. a) A.J. Bloodworth and M.E. Loveitt, J.C.S. Chem. Comm., 1976, 94.
- b) A.J. Bloodworth and M.E. Loveitt, J.C.S. Perkin I, 1978, 522.
- c) A.J. Bloodworth and J.A. Khan, J.C.S. Perkin I, 1980, 2450.
43. a) A.J. Bloodworth and J.A. Khan, Tet. Lett., 1978, 3075.
- b) A.J. Bloodworth, J.A. Khan and M.E. Loveitt, J.C.S. Perkin I, 1981, 621.
- c) A.J. Bloodworth and B.P. Leddy, Tet. Lett., 1979, 729.
44. A.J. Bloodworth and J.L. Courtneidge, J.C.S. Chem. Comm., 1981, 1117.
45. A.J. Bloodworth and J.L. Courtneidge, J.C.S. Perkin I, 1981, 3258.
46. J.R. Nixon, M.A. Cudd and N.A. Porter, J.O.C., 1978, 43, 4048.
47. W. Adam and K. Sakanishi, J. Amer. Chem. Soc., 1978, 100, 3935.
48. V. Subramanyam, C.L. Brizuela and A.H. Soloway, J.C.S. Chem. Comm., 1976, 508.
49. W. Adam and A. Rios, J.C.S. Chem. Comm., 1971, 822.
50. N.A. Porter, M.O. Funk, D. Gilmore, R. Isaac and J. Nixon, J. Amer. Chem. Soc., 1976, 98, 6000.
51. a) R.A. Johnson and E.G. Nidy, J.O.C., 1975, 40, 1680.
- b) R.A. Johnson, E.G. Nidy and M.V. Merritt, J. Amer. Chem. Soc., 1978, 100, 7960.
52. R.A. Johnson, E.G. Nidy, L. Baczynskyj and R.R. Gorman, J. Amer. Chem. Soc., 1977, 99, 7738.

53. C-H, Liu, D.L. Alexander, C.G. Chichester, R.R. Gorman and
R.A. Johnson, J. Amer. Chem. Soc., 1982, 104, 1621.
54. L. Caglioti, F. Gasparrini, D. Misiti and G. Palmieri,
Tetrahedron, 1978, 34, 135.
55. R.M. Wilson and F. Geiser, J. Amer. Chem. Soc., 1978, 100, 2225.
56. R.M. Wilson, E.J. Gardner, R.C. Elder, R.H. Squire and L.R. Florian,
J. Amer. Chem. Soc., 1974, 96, 2955.
57. R.M. Wilson and S.W. Wunderly, J.C.S. Chem. Comm., 1974, 461.
58. R.M. Wilson and S.W. Wunderly, J. Amer. Chem. Soc., 1974, 96, 7350.
59. R.M. Wilson, S.W. Wunderly, J.G. Kalmbacher and W. Brabender,
Ann. N.Y. Acad. Sci., 1976, 207, 201.
60. D.H.R. Barton, R.K. Haynes, P.D. Magnus and I.D. Menzies., J.C.S.
Chem. Comm., 1974, 511.
61. D.H.R. Barton, R.K. Haynes, G. Leclerc, P.D. Magnus and I.D. Menzies,
J.C.S. Perkin I, 1975, 2055.
62. D.H.R. Barton, G. Leclerc, P.D. Magnus and I.D. Menzies, J.C.S.
Chem. Comm., 1972, 447.
63. R.K. Haynes, Aust. J. Chem., 1978, 31, 121.
64. R.K. Haynes, Aust. J. Chem., 1978, 31, 131.
65. R. Tang, H.J. Yue, J.F. Wolf and F. Mares, J. Amer. Chem. Soc.,
1978, 100, 5248.
66. R.K. Haynes, Aust. J. Chem., 1978, 31, 1737.
67. H. Kropf and H. Von Wallis, Synthesis 1981, 237.

Section 1

**Synthesis, characterisation and transformations
of an unsaturated lipid peroxide**

Summary.

The photosensitised oxidation of the conjugated, diene ester methyl octadeca-9E,11E-dienoate gives an unsaturated cyclic peroxide (epidioxide) in high yield. ; This has been characterised spectroscopically. The 9,12-peroxide undergoes facile rearrangement to the 9,12-furanoid ester under a variety of reaction conditions. Catalytic reduction of the unsaturated peroxide cleaves the O-O bond. Bromination and epoxidation give dibromo and epoxy esters in high yield with the peroxide group still intact.

1 Introduction.

The role of singlet molecular oxygen(1O_2) in enzyme-mediated peroxidation reactions in vivo has aroused considerable interest^[1]. Singlet oxygen has been identified spectroscopically in the interaction of linoleic acid peroxy radicals in aqueous systems^[2]. Support for the generation of singlet oxygen in vivo is provided by the observation of chemiluminescence in NADPH-dependent microsomal lipoxygenation systems^[3,4], in microbiocidal systems of polynuclear leucocytes, and also from the evidence of numerous other reports^[5].

The products of photosensitised oxidation of methyl oleate and of methylene-interrupted polyene esters have been identified and quantified by a variety of techniques^[6-10]. Singlet oxygen reacts with alkyl substituted olefins in an ene type reaction to give allylic hydroperoxides with a shifted double bond^[11-15]. This may occur by a concerted mechanism^[16] or via a perepoxide intermediate^[17]. In contrast, reaction with conjugated dienes occurs by a 1,4 cyclo-addition and yields cyclic peroxides (epidioxides)^[18].

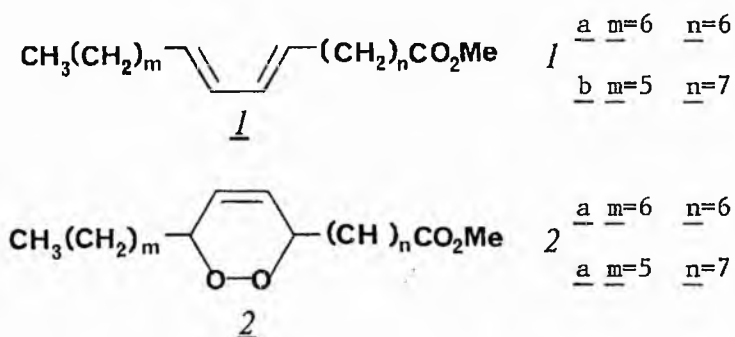
Growing interest in cyclic peroxides of unsaturated fatty acids is apparent in a number of reports on the isolation of hydroperoxy epidioxides from both enzymic^[19,20] and non-enzymic^[21-24] oxidation of polyene acids, and it has been suggested that singlet oxygen may be involved in the biosynthesis of prostaglandins^[25a,b] and of furano terpenes^[26a,b].

We now report the synthesis, reactions, and spectroscopic properties of an epidioxide produced by photo-oxidation of a long-chain conjugated dienoic ester.

2 Results and discussion

2.1 Preparation of the epoxide

In their study of long-chain furanoid acids Gunstone et al.^[27] converted the 8E,10E diene ester (1a) to the epoxide (2a) in a 5-day photo-oxidation in methanol using methylene blue as sensitiser.



We have now prepared the cyclic peroxide(2b) from the more readily available 9E,11E diene ester(1b) obtained from methyl 12-mesyloxyoleate (from ricinoleate) by a base-catalysed elimination reaction^[28].

The lifetime of singlet oxygen can vary about 1000 fold depending on the solvent in which it is generated. Merkel and Kearns^[29] correlated the lifetime of singlet oxygen with the infrared absorption of the solvent at about 8000cm^{-1} and suggested that direct conversion of the electronic energy from the $^1\Delta_g$ state to vibrational energy is predominant in the decay of singlet oxygen. Singlet oxygen has a lifetime of only $7\mu\text{s}$ in methanol but more than $600\mu\text{s}$ in carbon tetrachloride and Freon 11. We therefore used a mixture of carbon tetrachloride and methanol(95:5) as solvent and a reaction time of

only 16h compared with the 5 days used previously. Using methylene blue as the sensitiser and operating on a gram scale >80% yield of epidioxide (based on the content of E,E-diene in the starting material) was obtained after purification by column chromatography.

GLC analysis of the purified product showed a single peak of ECL 20.4 on a SP2300 column. This is the same value as that of the furanoid ester(10) and a sample of material recovered from the GLC eluate had the same $^1\text{Hnmr}$ spectrum as did the furanoid ester. As previously indicated by Demole et al^[30] for a related peroxide this change probably results from thermal dehydration on the column.

The cyclic peroxide can be stored at -20° for long periods. Chromatographic analysis of a sample kept for 12 months at -20° showed only traces (< 2 %) of more polar material.

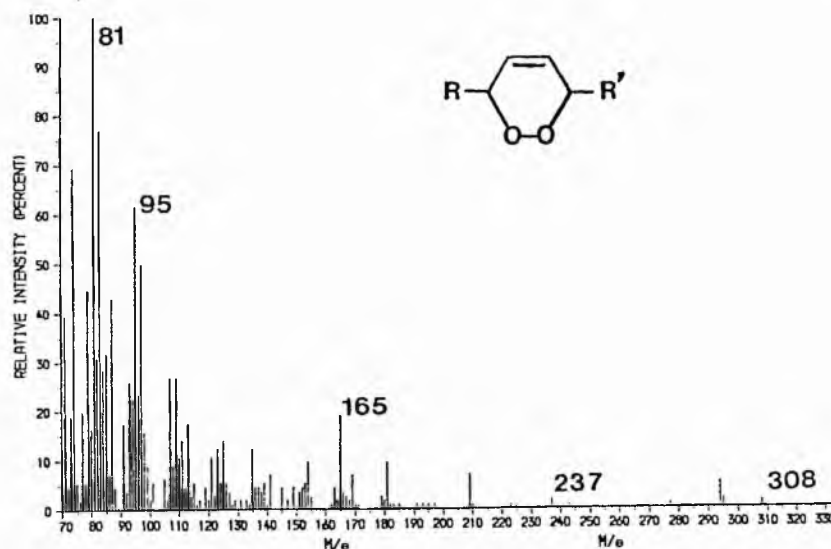
The infrared spectrum of the cyclic peroxide showed only the absorption expected of a long-chain ester including olefinic C-H stretching absorption at 3020cm^{-1} .

The $^1\text{Hnmr}$ spectrum showed three signals of special interest at 5.84δ (2H, $J=0.8\text{Hz}$, olefinic protons), 4.37δ (a broad multiplet, peroxy methines), and 1.47δ (broad signal, methylenes α to the peroxy methines). Decoupling the 5.84δ signal had no observable effect on the peak at 4.37δ but decoupling at 4.37δ collapsed the olefinic doublet to a sharp singlet and also made the broad signal at 1.47δ sharper. Decoupling at 1.47δ collapsed the peroxy methines into a broad singlet as expected since the coupling constant from the peroxy methines and the olefinic hydrogens is very small as a result of the dihedral angle (approx. 90°) between the two hydrogens.

The $^{13}\text{Cnmr}$ spectrum showed only one signal for the olefinic carbon atoms (127.65 ppm) and only one for the peroxidic carbon atoms

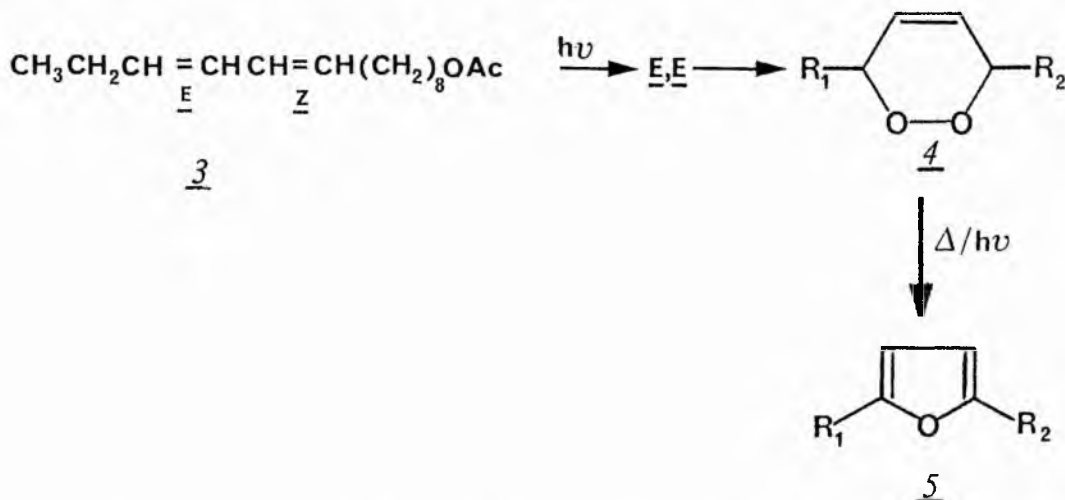
(78.35 ppm). No splitting of these signals was observed, even at -20°C .

Fig. 1



The mass spectrum [Fig 1] showed peaks characteristic of the corresponding furanoid ester and we assume that this change occurs under the conditions existing in the mass spectrometer.

It is of interest to note that Shani *et al* [31] concluded that photo-oxidation of tetradeca-9Z,11E-dienyl acetate (3) gave the furan (5) via the unstable peroxide (4) on the basis of GLC evidence.



The product furanoid compound was isolated by preparative GLC, TLC or HPLC isolation would presumably have given the cyclic peroxide which we believe should be no less stable than (2b).

2.2 Fe²⁺ induced decomposition

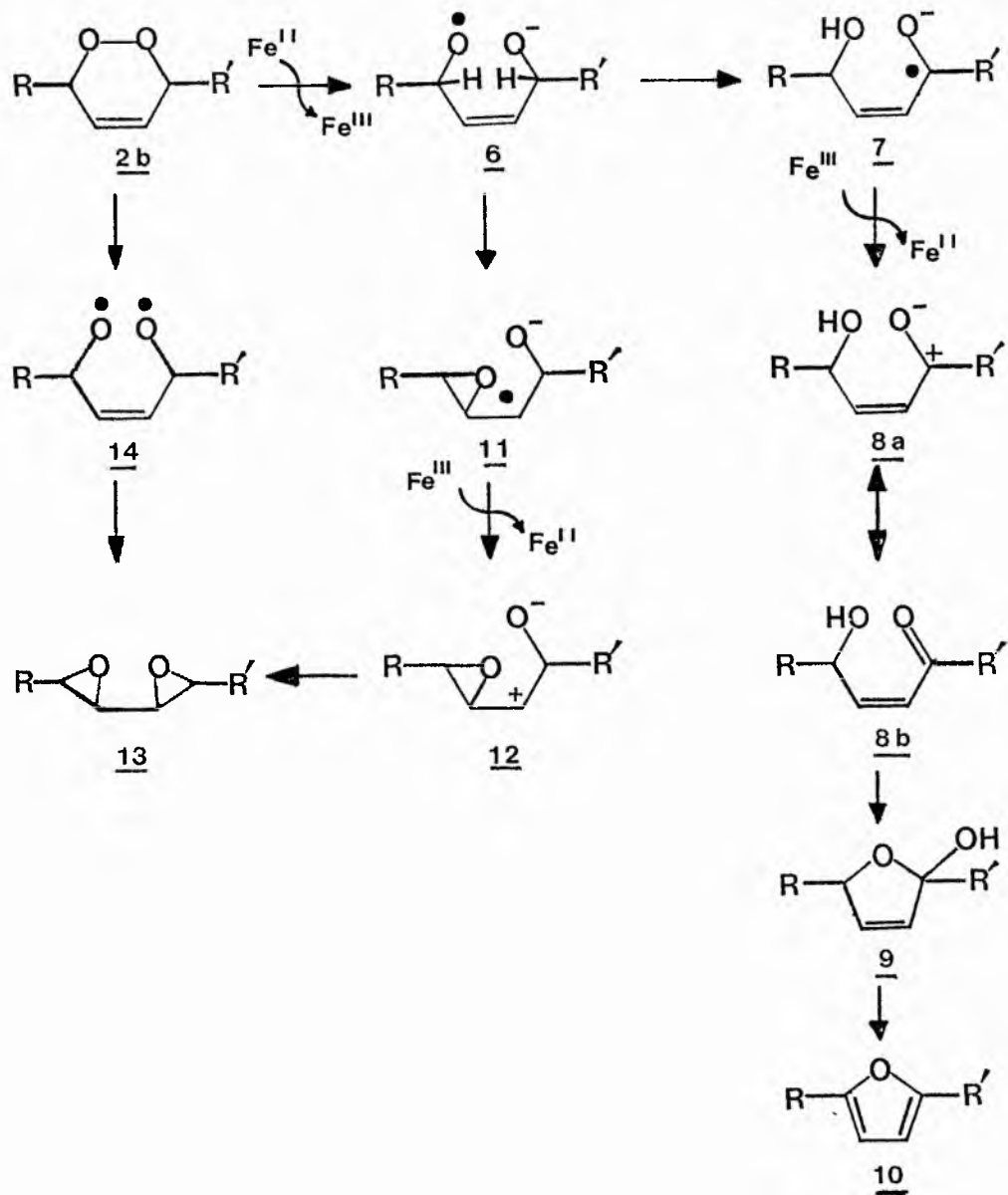
With ferrous ion in aqueous tetrahydrofuran solution the unsaturated cyclic peroxide (2b) is converted to the furanoid ester (10) and to two minor products identified as isomeric bis-epoxides (13) by infrared, mass, and ¹Hnmr spectroscopy.

The formation of the furanoid ester (10) probably follows the route shown by analogy with similar reactions in the phellandrene series^[32]. Cleavage of the O-O bond as a result of one electron transfer to Fe²⁺ gives the radical anion (6) which is converted to (7) by 1,5-hydrogen migration.

This furnishes the hydroxy ketone (8b) which forms the hemi ketal (9) and the furan (10). The dehydration is presumably catalysed either by the Lewis acid Fe³⁺ or by a proton within the system. The reaction is worked up by extraction of an ethereal solution of the product mixture with dilute acid to facilitate removal of Fe³⁺. However dehydration of (9) does not occur at this stage since TLC showed conversion prior to work up, confirming similar observations by Turner *et al*^[33].

The rearrangement of peroxide (2b) to bis-epoxides (13) may occur via the radical anion (6) and the monoepoxide intermediates (11) and

(12) or via the diradical (14) produced from (2b) by thermolysis.



We were unable to determine the exact stereochemistry of the bis-epoxides but a related study suggests that these have the trans configuration^[34].

2.3 Thermolysis.

Heating the peroxides (2b) in various solvents at reflux temperature or at 80° where this is lower than the boiling point sometimes gave an appreciable amount of the furan (10) and some unidentified minor products (<5%) (Table 1). Separate experiments showed that there was no significant decomposition of the peroxide in boiling toluene even after 24h and that longer reaction times in butanol gave >90% of the furanoid ester. Our results suggest that a solvent of high dielectric constant (E) is required before reaction occurs. This is in marked contrast to bicyclic peroxides which undergo thermolysis readily in toluene^[35].

Table 1 Conversion of peroxide (2b) to furan (10) by heating in various solvents for 5h.

Solvent	E Debye (°C)	%furan ^a
hexane	1.89(20)	none
toluene	2.38(25)	none
chloroform	4.38(20)	5
methanol	32.6 (25)	27
butan-1-ol	17.8 (20)	33
DMF		36

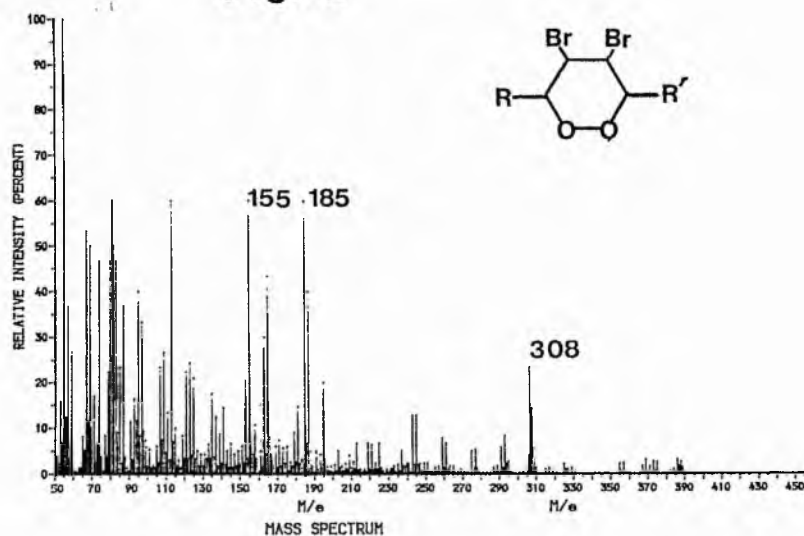
^a determined by ¹Hnmr.

2.4 Bromination.

Bromination of the unsaturated peroxide in dichloromethane solution in the dark gave good yields (85-90%) of the dibromide after 16h along with minor amounts of more polar material. However a $^1\text{Hnmr}$ study suggested that the reaction was complete within 5mins and almost quantitative yields of dibromide were obtained after this reaction time.

As expected the infrared spectrum showed the absence of absorption associated with O-H and C=O groups, the $^1\text{Hnmr}$ spectrum showed signals between 4.52 and 4.10 δ one of which results from the peroxidic methines, and a double doublet at 4.23 δ arising from the bromomethines. The $^{13}\text{Cnmr}$ spectrum showed peroxidic carbon resonances at 88.58 and 86.84 ppm and the bromo carbon resonances at 53.73 and 52.72 ppm. The mass spectrum is shown in Fig 2 and a possible explanation of many of its fragment ions is given in the Experimental.

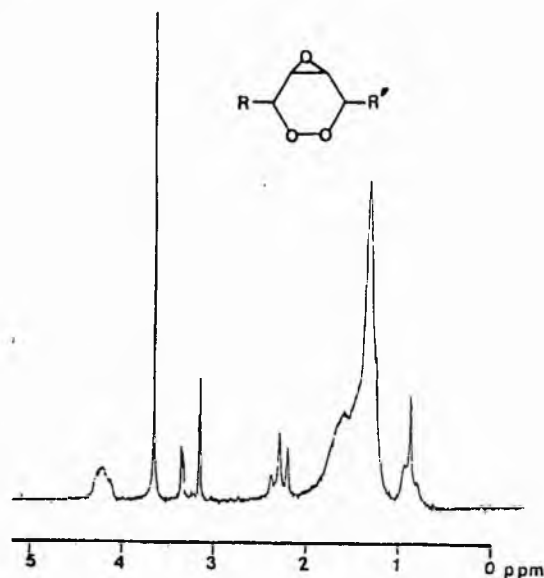
Fig. 2



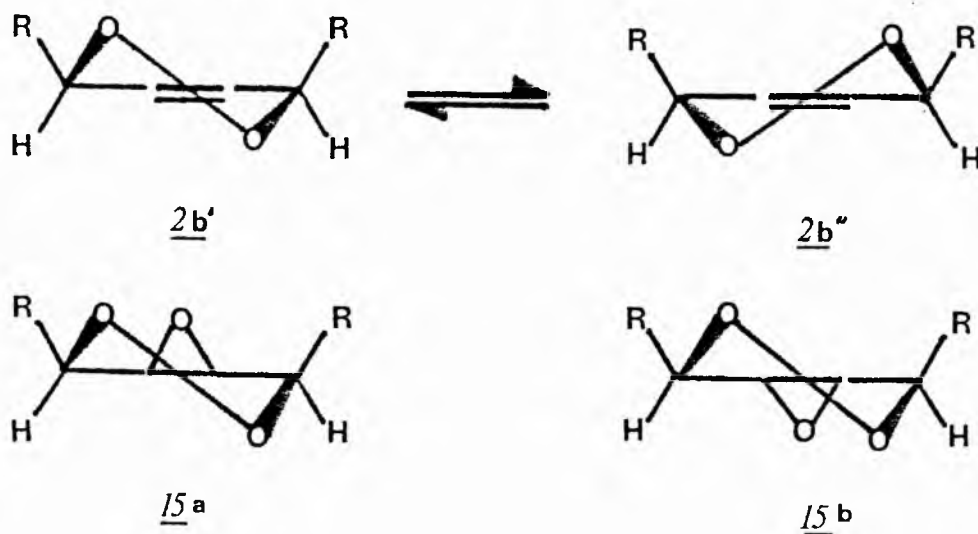
2.5 Epoxidation.

Using a two phase system of dichloromethane and aqueous sodium bicarbonate the unsaturated cyclic peroxide (2b) was epoxidised at room temperature

FIGURE 3



for 16h with 3-chloroperbenzoic acid and isolated in high yield by preparative TLC. The unsaturated cyclic peroxide can exist in two half-chair conformers 2b' and 2b''. Epoxidation can occur from either the exo or the



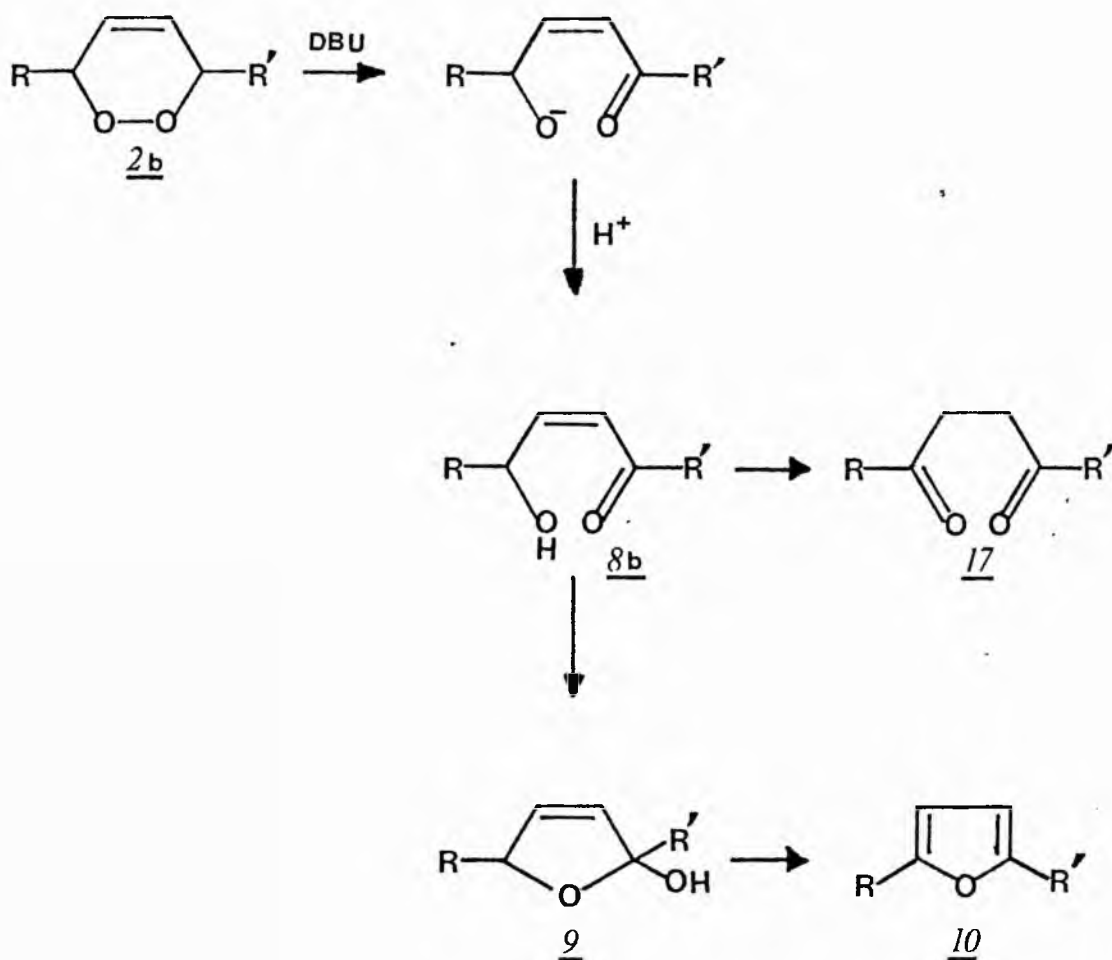
endo face of the ring, however molecular models suggest that endo attack will be less sterically hindered. If attack occurs from either face then (15a) and (15b) can be envisaged with each configurational isomer existing in two "half chair" conformers, giving a possible total of four isomers.

The $^1\text{Hnmr}$ [Fig 3] of the epoxy-cyclic peroxide showed a 2-proton multiplet at 4.22δ corresponding to the peroxide methines and two 1-proton multiplets at 3.35 and 3.16δ corresponding to epoxidic methines. Decoupling the 4.22δ signal collapsed both multiplets at 3.35 and 3.16δ to apparent singlets. Decoupling at 3.35δ partially collapsed the apparent triplet at 3.16δ to an unsymmetrical doublet. Decoupling at 3.16δ collapsed the apparent double doublet at 3.35δ to an apparent doublet. The $^{13}\text{Cnmr}$ showed only one resonance for the epoxide carbons at 52.25ppm . The proton-coupled spectrum split the resonance into a doublet ($J=38.25\text{Hz}$). Our results do not allow us to conclude whether both exo and endo epoxides are formed or whether endo epoxide formation is stereospecifically favoured.

The mass spectrum of (15) at 70eV was notably uninformative but more intense peaks were observed at lower ionising potentials (30eV). The most significant high mass fragments were observed at m/e 257 and 225 ($257-\text{MeOH}$) at 30eV . The infrared spectrum showed no hydroxyl or ketonic stretching as expected. The symmetrical stretching, or ring breathing frequency of the epoxy ring, is known to occur about 1250cm^{-1} . Although an absorption was observed it must be born in mind that methyl esters absorb near 1250 , 1205 and 1175cm^{-1} . Absorption at 835cm^{-1} however, the so called 12μ -band is more diagnostic for epoxides and was observed.

2.6 Reaction with DBU.

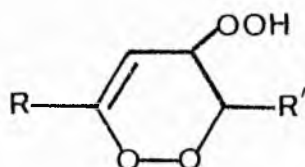
The cyclic peroxide (2b) is stable in dilute acid solution being recovered unchanged from a solution of methanolic sulphuric acid (2M) at room temperature after 36h. In contrast it undergoes a series of changes when stirred with 1,8-diazobicyclo[5.4.0]undec-7-ene (DBU) in hexane at room temperature. The product was separated into four



components by TLC, the furan ester (10, 4 %), methyl 9,12-dioxostearate (17, 19 %), methyl 9(12)-hydroxy-12(9)-oxo-octadec- 10Z-enoate (8b 74 %) and an unidentified polar product (3 %). These compounds were identified by spectroscopic procedures and are probably formed according to the sequence shown. The instability of the ketols complicates their recovery and identification. Thus their mass spectrum is similar to that of (10) into which they are probably converted in the mass spectrometer. On standing even at -20°C they rearranged in part to the furanoid (ca 20 %) and diketo esters (ca 5 %) and on gas chromatographic analysis they gave peaks of ECL 20.4 (70 %), 23.5 (20 %), and 24.4 (10 %) of which the first is that associated with the furanoid ester. On further standing with DBU the major product (80-85 %) was the dioxo ester (17). It is known that in an acidic solution the 1,4-dioxo and the furanoid ester are in equilibrium^[36]. Similar observations on bicyclic peroxides have been reported by Hagenbuch *et al*^[37].

2.7 Attempted further oxidation with singlet oxygen.

An attempt to oxidise the unsaturated peroxide (2b) to hydroperoxy peroxides such as (18) by further reaction with singlet oxygen gave only unchanged starting material after 5 days.



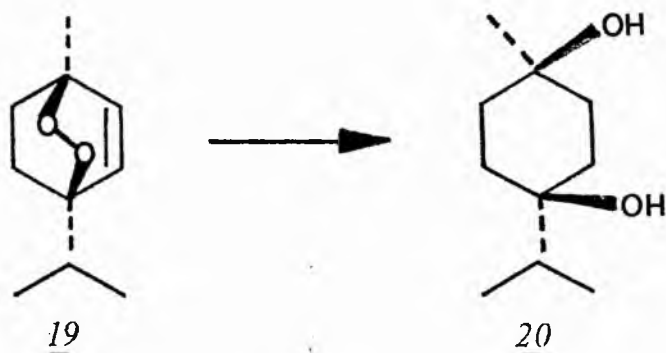
2.8 Attempted reduction with sodium borohydride.

Attempts to reduce the cyclic peroxide with sodium borohydride were unsuccessful under two sets of experimental conditions. The stability of the dialkyl peroxide to this reduction is in contrast to that of the hydroperoxide which is smoothly reduced to the corresponding hydroxy derivative.

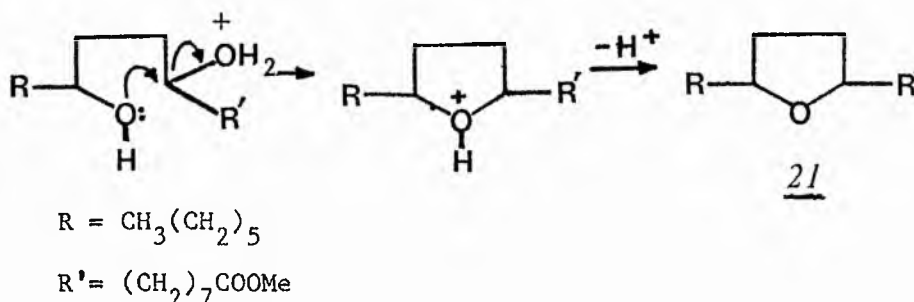
2.9 Catalytic hydrogenation.

Catalytic hydrogenation of the cyclic peroxide over a 10% Pd/C catalyst in an atmosphere of hydrogen for approximately 90 min gave methyl 9,12-epoxystearate (21) as a mixture of cis and trans isomers (ECL's 20.5 and 20.7 resp.) as the major products together with methyl stearate, methyl 9-hydroxystearate, methyl 12-hydroxystearate, their corresponding keto derivatives, and small amounts of methyl 9,12-dihydroxystearate.

Analogous reductions of bicyclic peroxides gives dihydroxy derivatives almost exclusively as the major products as typified by the hydrogenation of ascaridole (19) to the diol (20)^[38].



We believe that the results are explained by the acidic nature of the catalyst support. The methyl 9,12-dihydroxystearate initially formed could undergo facile intramolecular displacement of one hydroxyl group (probably in a protonated form) by a second hydroxyl function acting as a nucleophile.



Support for the formation of the dihydroxystearate as an intermediate was obtained by catalytic hydrogenation of an authentic sample of methyl 9,12-dihydroxystearate, produced by oxymercuration of ricinoleate^[39]. Amongst the products were methyl 9,12 epoxystearate (21) as a mixture of cis and trans isomers. The formation of the fully saturated, mono hydroxy, and keto esters result from hydrogenolysis of the dihydroxystearate.

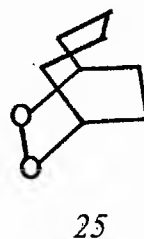
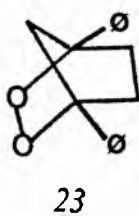
Shorter reduction times of (2b) resulted in a more complicated product distribution with greater amounts of the 9,12-dihydroxystearate and concomitant reduction of the epoxystearates.

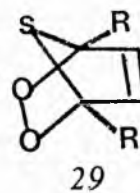
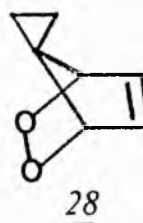
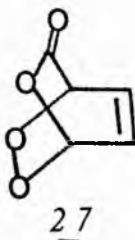
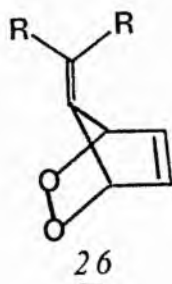
2.10 Attempted reduction with di-imide.

In certain cases, unsaturated bicyclic peroxides have been selectively reduced by catalytic hydrogenation to saturated bicyclic peroxides. Thus dihydroascaridole (22) is available from ascaridole by this method.^[40]



However complete reduction of unsaturated peroxides to saturated diols is generally found in most cases^[41] The discovery that di-imide^[42] reduces the double bond of singlet oxygen-diene adducts while leaving the peroxide linkage intact opened up a general route to saturated bicyclic peroxides^[42-44] (23-25). The reduction is usually effected in methanol solution using di-imide generated in situ from dipotassium azodicarboxylate and acetic acid. For the more labile compounds (26-29) it is desirable to use dichloromethane as solvent and to employ a little less than the required amount of acetic acid^[45-47].





Addition of hydrogen occurs stereospecifically cis-exo as a result of steric hindrance to endo attack due to the non-bonding electron pairs on oxygen, and also as a result of the unsymmetrical π -bond which has greater electron density on the exo-face.

Attempted reduction of (2b) with di-imide was unsuccessful in dry methanol or dichloromethane, even after repeated reduction using a 15-fold excess of dipotassium azodicarboxylate. Conducting the experiment under nitrogen or in air made no difference. No examples of di-imide reduction of monocyclic peroxides are to be found in the literature.

As the ring strain is reduced in the bicyclic ring systems, with increase in n , then di-imide reduction becomes increasingly more difficult (Table 2)

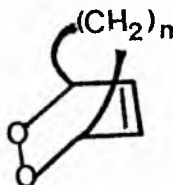
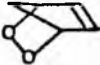





Table 2

cyclic peroxide	% reduction	Ref
	30	47
	40 - 48 ^a	43
	20 - 38 ^a	44
	19	44

^a We have obtained similar results for these two compounds.

However it is unlikely that ring strain is the overriding consideration since acyclic olefinic systems can be reduced. For example, methyl linoleate was reduced with a 2-fold excess of di-imide to a mixture of monoenoic (40.8 %) and fully saturated ester (11.4 %). Numerous other examples of acyclic reductions exist^[49]. A more likely explanation is that approach of di-imide to the cyclic peroxide (2b) is hindered as a result of unfavourable electronic interaction between di-imide and the non-bonded electron pairs on oxygen. In bicyclic systems with $n=1,2$ or 3 the preferred conformation of the six-membered ring is such that the C-O-O-C moiety is co-planar, ie in

the boat conformation. However in a non-strained system such as (2b) the preferred conformation of the six-membered ring will be the half-chair conformers (2b' and 2b'').



In the half-chair conformers electron repulsion will be experienced on approach of di-imide from either above or below the plane of the double bond. With larger values of n in bicyclic peroxides the conformation of the six-membered ring will tend to the half-chair conformation hence making reduction more difficult.

3 Experimental

3.1 General procedures.

Petroleum ether, hexane and diethyl ether were redistilled from calcium chloride. Petroleum ether refers to the fraction boiling between 40-55°C. Methanol, ethanol and dimethyl formamide(DMF) were purified by the method of Vogel^[50]. Butan-1-ol was twice redistilled after initially standing over calcium hydride for 24h. Carbon tetrachloride was redistilled from phosphorus pentoxide.

Thin layer chromatography (TLC) was carried out on thin layers of silica gel-G (0.5mm for preparative purposes, 0.25mm for analytical purposes). In certain cases the plates were pre-washed with diethyl ether and reactivated at 110°C. The developing solvent was petroleum mixed with diethyl ether and these mixtures are designated by symbols such as PE30 indicating a 70:30 mixture by volume of petroleum and diethyl ether. The chromatograms were rendered visual by spraying with an ethanolic solution of 2',7'-dichlorofluorescein (0.2%) and viewing under ultra violet light for preparative work, or by brief heating in an oven after spraying with phosphomolybdic acid (10%) in ethanol for analytical purposes. Peroxidic material was apparent after spraying with either a freshly prepared solution of 4-amino-N,N-dimethylaniline hydrochloride (2%) in methanol or a freshly decolourised solution of ammonium thiocyanate and ferric chloride in pentan-1-ol^[51].

Column chromatography was carried out with silica gel (sorbisil) using 20-25g per gram of material to be separated and eluting with petroleum ether containing increasing proportions of ether.

Separation was monitored by TLC and/or GLC.

Gas liquid chromatography (GLC) was carried out on a Pye series 104 chromatograph equipped with flame ionisation detector and fitted with a glass column (5'x1/4") packed with SP2300 (10%) as stationary phase on chromosorb WAW(100-120 mesh) operating at 220°C. Carrier gas (nitrogen) was used at a flow rate of 55-65ml/min. Quantitation was based on peak heights times retention times and retention characteristics are reported as ECL values using saturated esters as standards.

Infrared spectra were run on a Perkin Elmer 257 grating spectrophotometer using thin films between sodium chloride discs. Absorption frequencies normally associated with long chain esters are not quoted but only unusual absorptions of diagnostic value.

¹Hnmr spectra were recorded at 80MHz on a Bruker WP80 instrument, using dilute solutions in deuteriochloroform. Chemical shifts are given in ppm relative to the chloroform lock signal at 7.27δ. ¹³Cnmr spectra were recorded at 20 MHz on a Varian CFT-20 ¹³C-nmr instrument, using dilute (0.5-0.55M) solutions in deuteriochloroform.

Mass spectra were obtained following direct probe insertion of samples into the source of the mass spectrometer (AEI MS902). Source pressure was 2.7×10^{-5} Pa, source temperature 200°C, and the ionisation voltage 70eV unless otherwise stated.

3.2 Preparation of 12-hydroxy and 12-mesyloxy-oleate.

Methyl ricinoleate (methyl 12-hydroxyoctadec-9-enoate) was obtained from castor oil esters by chromatography on a column of silica using PE25 as developing solvent or by preparative HPLC using petroleum/iso-propanol (98.5:1.5) as eluent on normal phase chromatography (Rt 9 min). The chromatographed product was shown to be analytically pure by GLC and TLC (PE35; Rf 0.4). The hydroxy ester (4.5g, 14 mmol) was stirred by magnetic spin bar with redistilled methanesulphonyl chloride (4ml., 45 mmole) and pyridine (30ml) for 2h at 0°C, followed by a further 2h at 5-10°C. Ice-cold hydrochloric acid (150ml, 2M) was then added slowly with further cooling. Methyl 12-mesyloxyoleate (4.7g) was obtained as a straw-coloured oil by extraction with ether (3x50ml) and dried over anhydrous sodium sulphate.

¹Hnmr spectrum: 5.47δ(m, 2H, -CH=CH-), 4.67δ(m, 1H, -HC-OMs),
3.67δ(s, 3H, -CO₂Me), 3.00δ(s, 3H, SO₂Me)

plus peaks typical of long chain carboxylic esters.

infrared spectrum: absence of any O-H stretch, diagnostic absorptions at 1350cm⁻¹ and 1175cm⁻¹ arising from the asymmetric and symmetric SO₂ stretching respectively.

Methyl 12-mesyloxyoctadec-9-enoate (4.7g, 1.2 mmol), was placed in a round bottom flask (100ml) with toluene (20ml) and 1,8-diazobicyclo[5.4.0]undec-7-ene (8.0ml) added in that order. The solution was refluxed for 4h. When cool the resulting solution was neutralised with acetic acid, followed by the addition of water

(40ml). The product was extracted with diethyl ether (3x50ml) and the combined extracts washed with water (30ml), saturated sodium bicarbonate solution (30ml) and finally water (30ml). The organic extract was dried over sodium sulphate and the solvent removed on a rotary film evaporator at 5°C to yield a product (2.9g). GLC analysis showed three peaks ECL 18.7(9Z,12E.,6.4%), 19.7(9Z,11E.,73.0%) and 20.0(9E,11E.,20.6%).

Isomerisation of this mixture with a crystal of iodine in hexane (20ml) illuminated by a 100W tungsten lamp for 4-6h gave a product (2.9g) after washing with 0.1N sodium thiosulphate solution (50ml), drying over anhydrous sodium sulphate and evaporation of the solvent whose composition was determined by GLC as ECL 18.7(9Z,12E,6.4%), 19.7(9Z,11E.,22.0%) and 20.0(9E,11E.,71.6%).

3.3 Photosensitised oxidation of methyl octadeca-9E,11E-dienoate.

Conjugated diene (1.00g,3.3mmole) was placed in a photochemical reactor with an inner and outer cooling jacket. Methylene blue (50mg) dissolved in dry carbon tetrachloride/methanol (95:5 v/v.,250ml) was added and oxygen bubbled through the solution at flow rate of 50-60ml/min. The flask was illuminated with 3x150W tungsten light bulbs for 16h. The cyclic peroxide (2b) was isolated by column chromatography on a silica column (30g) eluting with a PE gradient from PE5 to PE20. Pure cyclic peroxide (560mg) was eluted after unreacted starting material.

¹Hnmr spectrum: 5.84δ(d, J=0.8Hz, 2H HC=CH), 4.37δ(m, 2H -HCO-)
3.62δ(s, 3H,-CO₂Me), 2.32δ(at, 2H, -CH₂CO₂Me), 1.60δ
(shoulder, 4H, C8 and C13 methylenes), 1.35δ(bs, 18H,

chain methylenes), and $0.8\delta(\text{at}, 3\text{H}, \text{CH}_3-)$.

infrared spectrum: absence of hydroxyl or ketone stretch. 3020cm^{-1}

(olefinic C-H stretch)

mass spectrum: 309 (0.3, $\text{M}^+ + 1$), 308 (3.0, M^+), 277 (1.0), 251 (0.3),
237 (3.7), 209 (0.3), 207 (0.3), 205 (0.3), 197 (0.3),
180 (0.3), 179 (4.3), 169 (1.7), 168 (1.0), 167 (1.7),
166 (7.0), 165 (47.0), 163 (3.3),

and below m/e 160 intense peaks at

155 (11.0), 152 (100.0), 143 (20.0), 138 (16.0), 129
(18.0), 128 (14.0), and 127 (17.0).

[see text for explanation of fragmentation pattern].

Table 3 gives accurate mass analysis for the significant cleavage fragments from (2b). The assignments are compatible with fragments a-e for the mass spectrum of the furanoid ester (10).

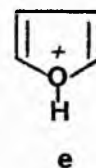
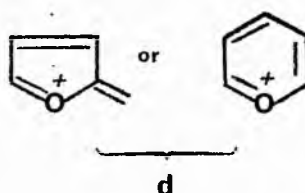
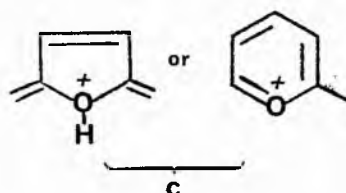
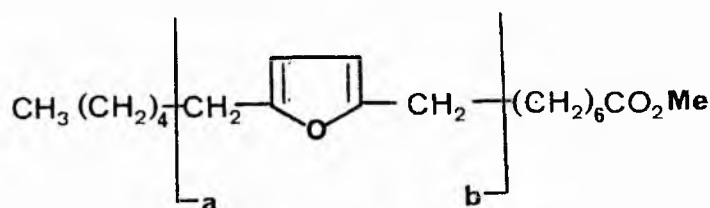


Table 3 Accurate mass analysis for significant cleavage fragments from (2b).

m/e	residual mass calculated	residual mass found	assignment
308	.235131	.234774	$C_{19}H_{32}O_3$ (M^+)
277	.216743	.217605	$C_{18}H_{29}O_2$ (M^+-31)
237	.149060	.148316	$C_{14}H_{21}O_3$ (a)
165	.127933	.127177	$C_{11}H_{17}O$ (b)
95	.048916	.049687	C_6H_7O (c)
81	.033884	.034037	C_5H_5O (d)

^{13}C nmr spectrum: 174.16 (C1), 127.65 (C10,11), 78.35 (C9,12),
51.37 (COOMe), 34.08 (C2), 33.04 (C8,13), 31.74
(C16), 29.10 (C4-6, C15), 25.38 (C7,14),
24.94 (C3), 22.58 (C17) and 14.05 (C18).

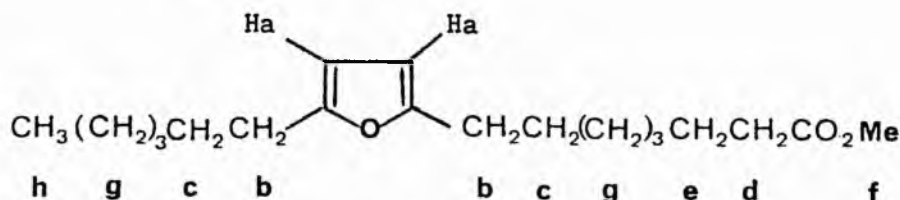
3.4 Reaction with ferrous sulphate.

A solution of ferrous sulphate (40mg) in distilled water (0.6ml) was added all at once to a solution of (2b) (40mg) in redistilled THF (0.6ml) and stirred by magnetic spin bar at room temperature for 5h. After removal of the THF on a rotoevaporator at $10^{\circ}C$, the mixture was diluted with distilled water (10ml), acidified with 2M HCl (to facilitate removal of the ferric sulphate) and extracted with diethyl ether (3x15ml). Drying over sodium sulphate and removal of the solvent gave an organic product (36.4mg). GLC analysis showed only one peak (ECL 20.4) and prep TLC gave five bands A-E on elution with

PE20:

Band A (16.8mg (50 %), ECL 20.4, R_f 0.71 in PE20) was identified as methyl 9,12-epoxyoctadeca-9,11-dienoate on the basis of the following spectroscopic data.

$^1\text{Hnmr}$ spectrum: $5.83\delta(\underline{s}, 2\text{H}, \text{Ha})$, $3.68\delta(\underline{s}, 3\text{H}, \text{Hf})$, $2.58\delta(\underline{at}, 4\text{H}, \text{Hb})$, $J=7.0\text{ Hz}$, $2.30\delta(\underline{at}, 2\text{H}, \text{Hd}, J=7.0\text{Hz})$, $1.63\delta(\underline{bm}, 6\text{H}, \text{Hc and He})$ and $1.20\delta(\underline{bs}, 12\text{H}, \text{Hg})$ and $0.88\delta(\underline{at}, 3\text{H}, J=6.2\text{Hz}, \text{Hh})$.

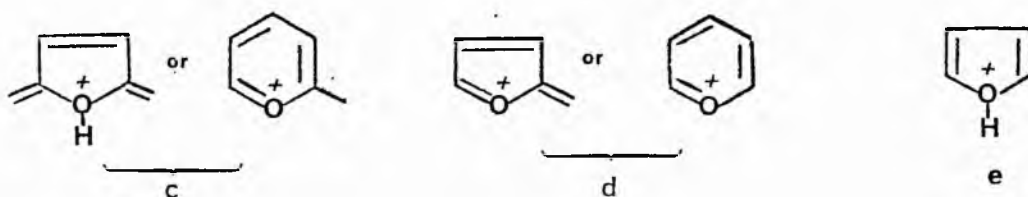
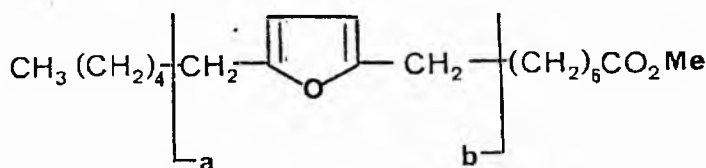


Ultraviolet spectrum: absorption at 224nm (pi-pi* transition)

Infrared spectrum: peaks at 3145 cm^{-1} ($\nu\text{ C-H}$ furan ring stretching), 1745 cm^{-1} ($\nu\text{ C=O}$, carbonyl stretching), 1683 cm^{-1} ($\nu\text{ C=C}$ in furan ring stretching), and 1012 cm^{-1} (ring breathing).

Mass spectrum 70eV: ions of m/e 308 (4%, M^+), 277 (2, M^+-31), 237 (5, \underline{a}), 205 (4, $\underline{a}-32$), 179 (6), 165 (66, \underline{b}), 149 (10, *), 135 (5), 109 (16) 107 (26), 97 (23), 95 (76, \underline{e}), 87 (25), 83 (29), 81 (69, \underline{d}), 79 (24,), 74 (44, McLafferty rearrangement), 71 (25,), 69 (48, \underline{e}) and 55 (base peak, C_4H_7^+).

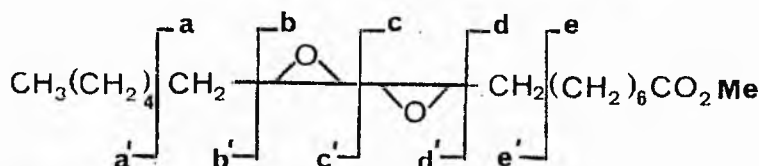
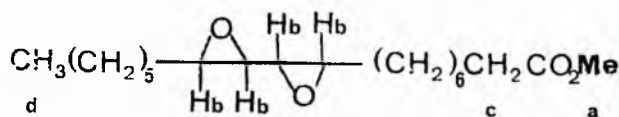
* possibly due to impurity.



Band B (4.6mg, 14%, ECL 20.4, Rf 0.56) was unreacted peroxide on the basis of its infrared and $^1\text{Hnmr}$ spectra.

Band C (4.3mg, 13%, no peak on GLC, Rf 0.29) was a mixture of diastereoisomeric methyl 9,10,11,12-diepoxyoctadecanoates.

$^1\text{Hnmr}$ spectrum: 3.68 δ (s, 3H, Ha), 2.85 and 2.60 δ (both m, 2H, Hb)
2.30 δ (at, 2H, Hc), 1.55 and 1.35 δ (chain methylenes)
and 0.88 δ (at, 3H, Hd).



mass spectrum:

241 (0.3,b), 225 (0.3,a-30), 223 (0.4,a-32), 209
(2,b-32), 181 (2,a-74), 169 (2,d'), 165 (1), 163 (1),
155 (22) and other peaks at 141, 140, 139, 135, 125,
123, 121, 111, 109, 107, 98, 97, 96, 95, 84, 83, 81,
74, 73, 71, 70, 69, 67, 59, 57, and 55 (base peak)

Band D (2.9mg, 9%, no peak on GLC, Rf 0.24) gave $^1\text{Hnmr}$ and mass spectra identical with those obtained for band C.

Band E (4.8mg, 14%, Rf <0.1) was not identified.

3.5 Thermolysis

(a) The peroxide (2b, 50mg, 0.15mmole) was dissolved in butanol (2ml) and heated to 80 $^{\circ}$ for 5h. After removal of the solvent under reduced

pressure (2mm Hg) the residue was analysed by GLC, TLC, and $^1\text{Hnmr}$. In some experiments with other solvents the reaction temperature was that of the refluxing solvent (Table 1). The product was a mixture of unreacted peroxide (2b), furan (10), and unidentified minor products (<5%).

(b) In a similar reaction peroxide (50mg) was refluxed with toluene for 24h. The product showed one major spot on TLC (>96%) and a single peak of ECL 20.4 on GLC. The spectroscopic properties were identical with those of the starting cyclic peroxide.

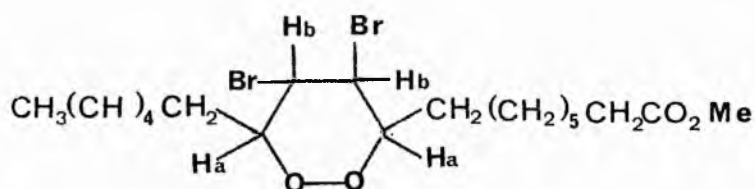
3.6 Bromination.

Bromine (60mg, 0.33mmole) was added to a solution of the peroxide (2b, 100mg, 0.3mmole) in dichloromethane (5ml) in a vial protected from the light and kept at 0°C. After 5min the solvent was removed under a stream of dry nitrogen and the residue was purified by prep TLC (Rf 0.80, PE10) to give methyl 10,11-dibromo-9,12-epidioxyoctadecanoate in almost quantitative yield. The following spectroscopic data was recorded.

Infrared spectrum: there is a loss of the absorption at 3020cm^{-1}

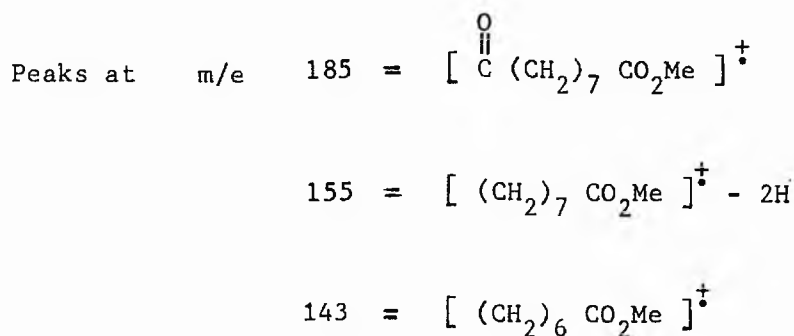
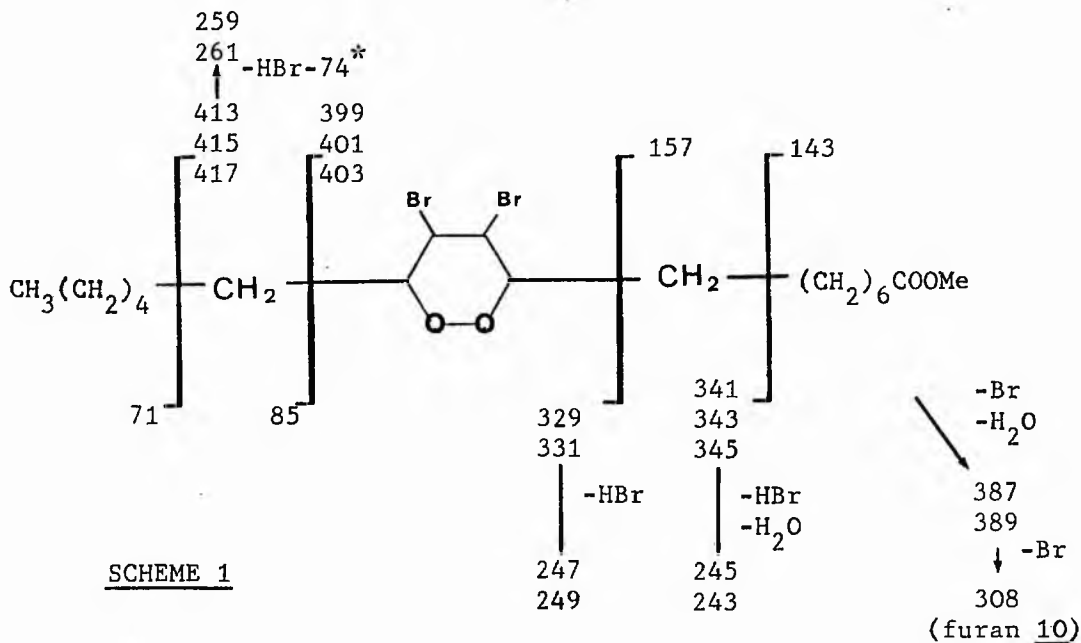
(C=C) present in the unsaturated peroxide and appearance of bands at 733 and 909cm^{-1} (C-Br_{equ} stretch)

¹Hnmr spectrum: $4.52-4.10\delta$ (m, 2H, Ha), 4.23δ (dd, 2H, Hb J=14.0 and 8.0 Hz, Hb), 3.64δ (s, 3H, Hc), 2.28δ (at, 2H, Hd), $1.50-1.25\delta$ (m, 4H, He), 1.30δ (bs, 18H, chain CH₂ groups), and 0.88δ (at, 3H, Hf).



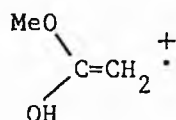
¹³Cnmr spectrum: 173.95 (C1), 86.84 and 88.58 (C9 and 12), 53.73 and 52.72 (C10 and 11), 51.15 (-COOMe), 33.81 (C2), 31.73 (C16), 31.46 and 31.33 (C8 and 13) 28.74, 26.74 (C4,5,6 and 15), 25.27, 25.09 (C14 and 7), 24.66 (C3), 22.32 (C17) and 13.79 (C18).

The mass spectrum of the dibromocyclic peroxide contained numerous intense peaks [Fig 2], but no molecular ion. Speculation as to the fragmentation pattern is depicted in scheme 1 .



Peaks at m/e 185, 155, 143 and 113 are common to 9,12-dioxygenated methyl esters.

* = m/e 74 = McLafferty rearrangement fragment.



Fragments at 277, 237, 209, 181 and 165 are derived from the furan fragment (10).

3.7 Epoxidation

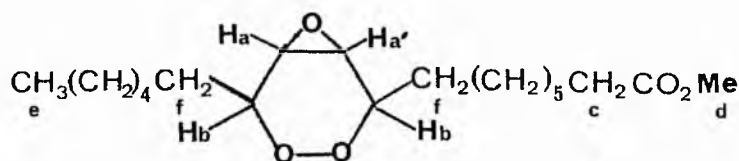
A mixture of the cyclic peroxide (95mg, 0.29mmole) in dichloromethane (2ml), 3-chloroperoxybenzoic acid (80%, 70mg, 0.32mmole) in the same solvent (3ml), and a saturated aqueous sodium bicarbonate solution (5ml) was stirred vigorously for 16h. The organic layer was separated and washed with sodium bicarbonate solution (2x5ml), brine (5ml), and water (3ml). All the aqueous washings were re-extracted with chloroform (2ml) and the organic layers were combined. Preparative TLC (PE25) gave three bands:

Band A (6mg, 7%, Rf 0.82, ECL 20.4) unreacted peroxide.

Band B (83mg, 90%, Rf 0.57) identified as methyl 9,12-epidioxy-10,11-epoxyoctadecanoate on the basis of the following spectroscopic evidence:

Infrared spectrum: showed the absence of O-H stretch and olefinic stretch, significant absorption at 813cm^{-1} (see text).

$^1\text{Hnmr}$ spectrum: 4.22δ (m, 2H, Hb), 3.63δ (s, 3H, Hd), 3.55δ (ap dd, 1H), 3.16δ (apt, 1H, see text), 2.30δ (at, $J=7.0\text{Hz}$, 2H, Hc), $1.80\text{--}1.50\delta$ (shoulder, 4H, Hf), 1.30δ (bs, chain CH_2 's), 0.88δ (at, $J=5.5\text{Hz}$, 3H, He).



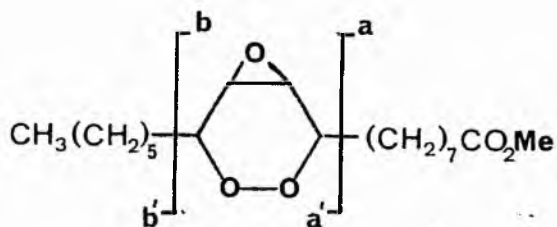
$^{13}\text{Cnmr}$ spectrum: 78.02 and 77.42 (C9 and C12), 52.25 (C10 and C11),

51.25 (COOCH_3), 33.91 (C2), 31.59 (C16), 30.19, 28.90
and , 25.06 (C4-7 and C12-15), 24.76 (C3), 22.38
(C17), 13.86 (C18).

Mass spectrum at 70eV: 223 (1.1), 185 (0.9), 167 (1.3), 155(0.7)
151 (2.8), 125 (6.0), 109 (10.0), 97 (17.0), 87
(21.0), 83 (28.0), 81 (23.0), 74 (32.0, McLafferty
rearrangement), 69 (37.0), 67 (33.0), 59 (29.0), 57
(29.0), 57 (39.0), 55 (100.0, C_4H_7).

Mass spectrum at 15eV: 225 (27.0,b-32), 197 (3.0), 185 (18.0),
156 (55.0), 155 (55.0, a-2), 125 (55.0), 113 (36.0),
111 (45.0), 109 (45.0), 97 (45.0), 87 (91.0), 86
(100.0), 83 (45.0), 81 (45.0), 74 (55.0,*), 71
(64.0), 67 (55.0), 55 (55.0, C_4H_7).

*= McLafferty rearrangement peak.



a = 157

a' = 185

b = 257

b' = 85

3.8 Reaction with DBU

1,8-Diazobicyclo[5.4.0]undec-7-ene (DBU, 25mg, 0.16mmol) was added to a solution of the peroxide (2b, 50mg, 0.15mmole) in hexane (3ml). The mixture was stirred at room temperature until TLC showed the complete consumption of the peroxide. After the removal of the solvent under a stream of dry nitrogen the residue was separated into four fractions (net recovery 36.1mg, 72%) by prep TLC (PE30).

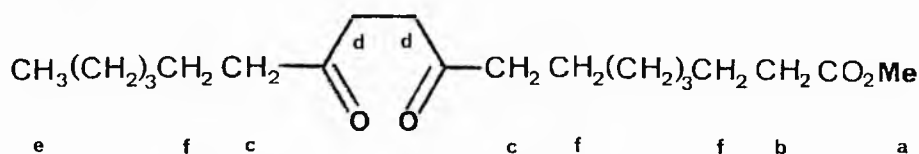
Band A (1.3mg, 4%, $R_f=0.7$ in PE20) gave a single peak of ECL 20.4 on GLC and was identified as the furanoid ester (10) by comparison with an authentic sample.

Band B (6.8mg, 18.8%, $R_f=0.52$ in PE30) was identified as methyl 9,12-dioxostearate on the following spectral evidence.

Infrared spectrum: showed an absence of O-H stretch, significant

absorption at 1740cm^{-1} (ester carbonyl stretch), and 1595cm^{-1} .

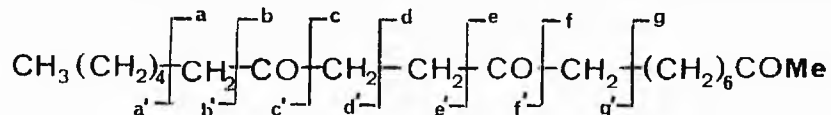
$^1\text{Hnmr}$ spectrum: $3.68\delta(\text{s}, 3\text{H}, \text{Ha})$, $2.65\delta(\text{s}, 4\text{H}, \text{Hd})$, $2.44\delta(\text{t}, j=7.0\text{Hz}, 4\text{H}, \text{Hc})$, $2.29\delta(\text{t}, j=7.0\text{Hz}, 2\text{H}, \text{Hb})$, $1.55-1.30\delta$ (shoulder, $6\text{H}, \text{Hf}$), $1.25\delta(\text{bs}, 12\text{H}, \text{chain } \text{CH}_2\text{'s})$ and $0.88(\text{at}, J = 5.4\text{Hz}, 3\text{H}, \text{He})$.



Mass spectrum: 326 (3.1, M^+), 309 (0.3,), 308 (0.5, M^+-18),

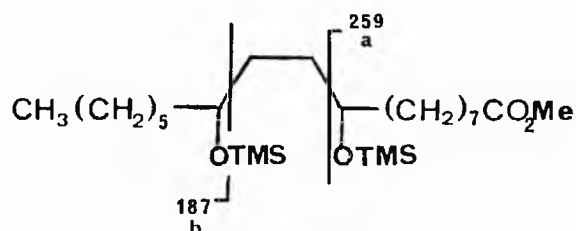
295 (1.0, M^+-31), 294 (0.9, M^+), 277 (0.8), 263 (0.8),

256 (10.0, $a+1$), 241 (1.3, b) 239 (1.1), 238 (6.2), 237



(2.3), 224 (3.0), 213 (6.9,c), 209 (17.8), 197 (8.5), 184 (17.8,g'+1), 183 (17.8,g'), 180 (22.3), 169 (20.0,f'), 153 (8.5), 149 (6.2), 141 (20.0,e'), 127 (18.5,d'), 125 (20.0), 114(37.7,c+1), 113 (36.9,c'), 111 (25.4), 109 (21.5), 97 (39.2), 95 (27.7), 85 (32.5,b'), 83 (45.4), 81 (33.9), 71 (48.5,a), 69 (53.5), 67 (30.8), 57 (73.0), 55(100.0).

Sodium borohydride reduction of band B followed by trimethylsilylation afforded methyl 9,12-bis-trimethylsilyloxystearate, identified by comparison with an authentic sample on GLC (ECL 20.6) and by its characteristic mass spectrum fragmentation pattern which showed peaks at:



429 (4.4), 383 (6.2), 311 (7.1), 310 (4.0), 309 (10.2), 299 (3.1), 281 (4.4), 279 (4.4), 271 (4.4), 259 (14.7,a), 236 (8.9), 227 (12.4,a-32 and/or c-90), 187 (26.7,b), 181 (10.2), 155 (15.1,a-104)**, 147 (11.6), and numerous peaks below m/e 140 (base peak m/e 57).

* 90=TMS-OH

** 104=TMS-OMe

Independent synthesis of 9,12-dioxostearic acid^[52] followed by esterification gave a product spectroscopically identical to band B.

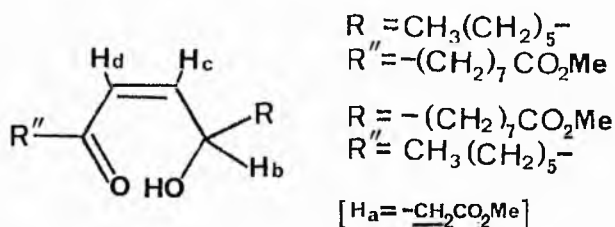
Band C (27mg, 75%, Rf=0.17 in PE30) was shown to be a mixture of the

ketols methyl 9(12)-hydroxy-12(9)-oxooctadec-10Z-enoate (8b) on the basis of the following spectroscopic results.

Infrared spectrum: absorption bands at 3600-3200 (O-H stretching), 1740 (C=O stretch), 1670, 1628, and 978cm^{-1} .

$^1\text{Hnmr}$ spectrum: $6.80\delta(\text{dd}, J_{dc}=16.0\text{Hz}, J_{db}=4.8\text{Hz}, 1\text{H}, \text{Hd})$,

$6.27\delta(\text{dd}, J_{cd}=16.0\text{Hz}, J_{cb}=1.4\text{Hz}, 1\text{H}, \text{Hc})$, $4.50-4.13\delta(\text{bm}, 1\text{H}, -\text{OH})$, $3.61\delta(\text{s}, 3\text{H}, \text{COOCH}_3)$, $2.50\delta(\text{at}, J=7.2\text{Hz}, 2\text{H}, \text{Ha})$, $2.25\delta(\text{at}, J=7.2\text{Hz}, 2\text{H}, \text{Ha})$, $1.77-1.40\delta(\text{shoulder})$, $1.27\delta(\text{bs}, \text{chain methylene groups})$, and $0.81\delta(\text{t}, J=5.5\text{Hz}, 3\text{H}, \text{Hf})$.



Mass spectrum: see text for explanation of the fragmentation pattern.,

308 (26.7), 295 (2.8), 277 (11.7), 265 (1.7), 255 (1.4), 251 (4.2), 249 (1.4), 237 (17.8), 223 (1.7), 221 (2.8), 209 (8.9), 207 (5.6), 197 (2.2), 191 (2.8), 185 (7.2), 181 (13.9), 179 (13.9), 166 (17.8), 165 (100.0), 141 (11.1), 139 (11.7), 121 (11.1), 113 (23.9), 111 (11.1), 109 (15.0), 108 (11.1), 107 (29.4), 97 (20.0), 95 (50.0), 94 (20.6), 87 (12.8), 85 (12.8), 83 (23.9), 81 (31.7), 79 (13.3), 74 (20.6), 71 (20.6), 69 (31.7), 67 (22.2), 59 (21.1), 57 (21.1), 55 (67.8).

Band D (1.0mg, 3%, $R_f=0.05-0.00$ in PE30) was not identified.

3.9 Reaction with methanolic sulphuric acid.

When the cyclic peroxide (2b, 20mg) was stirred with 10% methanolic sulphuric acid (5ml) for 36h at room temperature the starting material was recovered unchanged in quantitative yield.

3.10 Attempted further oxidation with singlet oxygen

Cyclic peroxide (2b, 100mg) and methyl palmitate (5mg) were placed in a photolytic cell with tetrachloromethane (238ml), methanol (12ml), and methylene blue (50mg) and irradiated (3x150W tungsten bulbs) for 5 days. Aliquots (ca 0.1ml) were withdrawn at 12h intervals and examined by GLC after removal of the solvent. There was no change in the relative size of the two peaks. TLC examination of the product after 5 days also indicated that the peroxide was unchanged.

3.11 Attempted reduction with sodium borohydride.

A solution of sodium borohydride (20mg) in dimethylformamide (0.3ml) was added to cyclic peroxide (2b) in the same solvent (1ml) and stirred for 1h. After addition of water (2ml) and extraction with ether (3x5ml) the product (18.5mg) was shown to be unchanged starting material on the basis of its GLC (single peak at 20.49) and TLC behaviour. A similar result was obtained when the reaction was attempted in water-tetrahydrofuran (1:1) solution.

3.12 Attempted reduction with di-imide.

A mixture of peroxide (2b, 100mg, 0.3 mmole) and dipotassium azodicarboxylate (870mg, 4.5 mmole) in superdry methanol (10ml) was added at 0°C during the dropwise addition over 30min of a 30% solution of acetic acid in methanol (5ml). After 3-5h the solvent was evaporated at room temperature and the residue, dissolved in water (20ml), was extracted with petroleum ether (2x25ml). After washing with saturated sodium bicarbonate solution (2x15ml), and drying over sodium sulphate, followed by rotoevaporation of the solvent at room temperature the product was examined by ¹Hnmr to determine the ratio of the size of the signals at 5.84δ(olefinic hydrogens) and 4.37δ(peroxy methines) as an indication of the extent of reduction. No reduction was observed from 5 separate experiments.

The experiment was repeated without success (i) using dichloromethane as solvent in place of methanol, (ii) using a nitrogen atmosphere and each of the solvents used above, and (iii) repeating the reduction procedure three times on the same sample.

3.13 Catalytic hydrogenation.

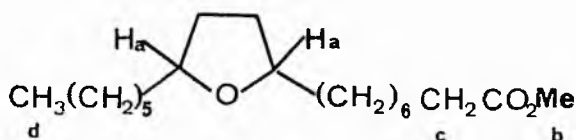
To a round bottom flask with magnetic spinbar was charged 10%-palladium/charcoal (20mg), methanol (5ml), and cyclic peroxide (20mg) and the mixture stirred at room temperature for 90 min under a hydrogen atmosphere. The charcoal was filtered off and washed with two further aliquots of methanol (5ml). The combined washings being evaporated at room temperature to remove the solvent and furnish an organic product (16mg). Preparative TLC (PE 30) furnished seven bands A-G.

Band A (ECL 18.0, Rf 0.63 in PE20) was identified as methyl stearate

from its ECL, Rf values and mass spectrograph comparison with authentic material.

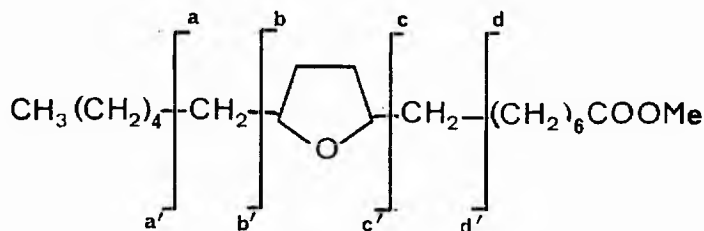
Band B (ECL 20.5 and 20.7 , 65 % and 35 % respectively, Rf 0.5 in PE20) was identified as a mixture of cis and trans methyl-9,12-epoxy octadecanoates on the following spectral evidence.

¹Hnmr spectrum: 3.80δ(b_a, 2H, Ha), 3.68δ(a, 3H, Hb), 2.30δ(a_t, 2H, Hc), 1.30δ(b_a, H, chain CH₂'s), 0.88δ(a_t, 3H, Hd)



infrared spectrum: showed only absorptions typical of a long chain aliphatic ester.

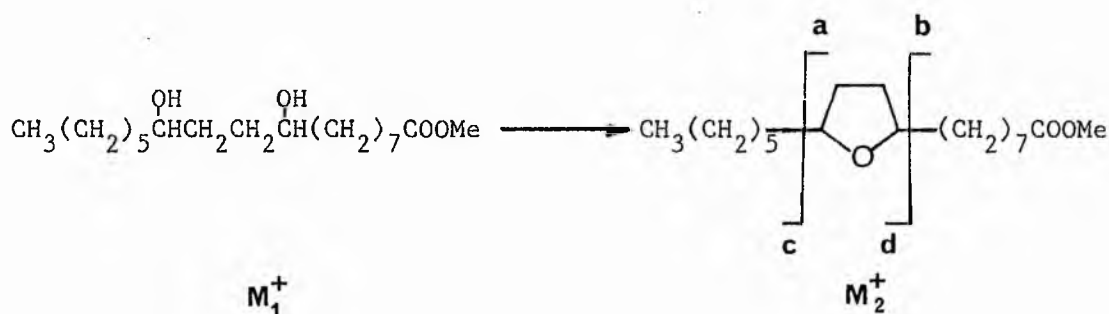
mass spectrum: significant peaks at m/e 313 (1, M⁺+1), 312 (1.3, M⁺), 294 (0.8, M⁺-18), 281 (1.6, M⁺-31), 263 (2.0), 242 (0.8), 227 (48.0, b), 209 (15.0, b-18), 195 (51.0, b-32), 177 (14.0, b-18-32), 159 (8.0), 156 (8.0), 155 (100, c' and/or c-2) 149 (16.0), 137 (55.0, a-18), 123 (9.0), 95 (70.0), 81 (80.0), 69 (48.0) 67 (52.0), 55 (88.0, C₄ H₇⁺).



Bands D-F were identified as 9- and 12-hydroxystearates and 9- and 12-oxostearates by GLC and mass spectroscopic comparison with authentic material.

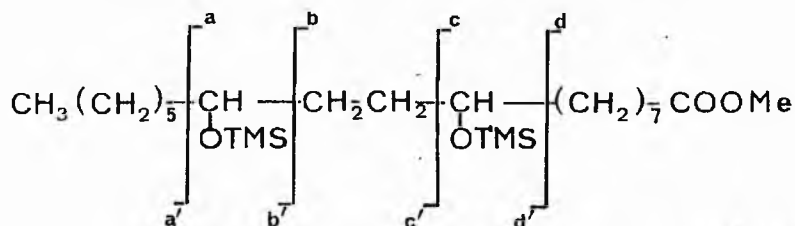
Band G: was identified as methyl 9,12-dihydroxystearate on the following spectral evidence.

mass spectrum: significant peaks at m/e 313 (0.9), 312 (1.0, M_2^+), 282 (2.0), 279 (2.0), 250 (10.0), 227 (27.0, a), 223 (13.7), 209 (8.7, -18), 195 (33.3, 227-18), 187 (31), 185 (11.7), 177 (11.3, 209-32), 166 (14.3), 155 (100, d and/or b-2), 151 (60.0), 137 (30.0, d-18), 111 (30.0), 109 (30.0), 97 (53.3), 95 (50.0), 85 (33.3, c), 83 (60.0), 81 (56.7), 74 (27.7), 71 (47.7, $C_5H_{11}^+$), 69 (73.3), 67 (43.3), 57 (83.3), 55 (100, $C_4H_7^+$).



The mass spectrum of the bis-trimethylsilyl ether showed the following significant peaks: 369 (10.8, a-30), 312 (17.1), 299 (11.3),

283 (8.3, a-104), 259 (13.3, c), 239 (9.6), 236 (10.4), 227 (12.7, c-32), 204 (8.3), 187 (13.3, b'), 185 (8.7), 178 (8.3), 176 (12.5), 155 (10.4, c-104 and/or d-2), 149 (8.8), 147 (12.9), 145 (8.8), 137



(10.0), 135 (11.3), 133 (13.3), 129 (22.9), and numerous peaks below m/e 128 (base peak 57).

References

1. For recent reviews see
 - a) N.I. Krinsky in "Singlet Oxygen", (Ed. H.H. Wasserman and R.W. Murray), Chap 12, Academic Press, New York, 1979 pp 597.
 - b) J. Bland, J. Chem. Ed., 1976, 53, 274.
2. M. Nakano, K. Takayama, Y. Shimizu, Y. Tsuji, H. Inaba and T. Migata, J. Amer. Chem. Soc., 1976, 98, 1974.
3. R.M. Howes and R.H. Steele, Res. Commun. Chem. Path. Pharmacol., 1972, 3, 349.
4. M. Nakano, T. Noguchi, K. Sugioki, H. Fukuymama, M. Sato, Y. Shimizu, Y. Tsuji and H. Inaba, J. Biol. Chem., 1975, 250, 2404.
5.
 - a) R. Yamauchi and S. Matsushita, Agric. Biol. Chem., 1979, 43, 2157.
 - b) E.K. Lai, K-L Fong and P.B. McCay, Biochim. Biophys. Acta, 1978, 528, 497.
 - c) M.M. King, E.K. Lai and P.B. McCay, J. Biol. Chem., 1974, 249, 6496.
6. H.W-S. Chan, J. Amer. Chem. Soc., 1977, 54, 100.
7. D. Cobern, J.S. Hobbs, R.A. Lucas and D.J. Mackenzie, J. Chem. Soc., (C), 1966, 1897.
8. J. Terao and S. Matsushita, J. Amer. Oil Chem. Soc., 1977, 54, 234.
9. E.N. Frankel, W.E. Neff and T.R. Bessler, Lipids 1979, 54, 234.
10. E.N. Frankel in "Autoxidation in Foods and Biological Systems", (Ed. M.G. Simic and K. Marcus), Plenum Press, New York, 1980, pp 141.

11. R.W. Denny and A. Nickon., Org. React., 1973, 20, 133.
12. C.S. Foote, Acc. Chem. Res., 1968, 1, 104.
13. K. Gollnick, Adv. Photochem., 1968, 6, 1.
14. D.R. Kearns, Chem. Rev., 1971, 71, 395.
15. K. Gollnick and H.J. Kuhn in "Singlet Oxygen", (Ed. H.H. Wasserman and R.W. Murray), Academic Press, New York, 1979, pp 287.
16. See A.A. Frimer, Chem. Rev., 1979, 79, 359 and references cited therein.
17. See D.B. Sharp, Abst. 138th Meet., Amer. Chem. Soc., 1960, 79P, 359.
18. K. Gollnick and G.O. Schenck, "1,4-Cycloaddition Reactions" (Ed. J. Frimer), Academic Press, New York, 1967, pp 255.
19. P. Haverkamp Bergemann, W.J. Woesterburg and S. Leer, J. Agric. Food. Chem., 1968, 1679.
20. M. Roza and A. Francke, Biochem. Biophys. Acta, 1978, 528, 119.
21. D.T. Coxon, K.R. Price and H.W-S. Chan., Chem. Phys. Lipids, 1981, 28, 365.
22. H.W-S. Chan, J.A. Mathew and D.T. Coxon, J. Chem. Soc. Chem. Comm., 1980, 235.
23. W.E. Neff, E.N. Frankel and D. Weisleder, Lipids, 1981, 16, 439.
24. E.D. Mihelich, J. Amer. Chem. Soc., 1980, 102, 7141.
25. a) J.A. Turner and W. Herz, J. Org. Chem., 1977, 42, 1900.
b) A. Rahimtula and P.J. O'Brien, Biochim. Biophys. Res. Commun., 1976, 70, 898.
26. a) K. Kondo and M. Matsumoto, Tet. Lett., 1976, 4363.
b) M. Matsumoto and K. Kondo., J. Org. Chem., 1975, 40, 2259.
27. F.D. Gunstone and R.C. Wijesundera, Chem. Phys. Lipids, 1979, 24, 193.

28. F.D. Gunstone and A.I. Said, Chem. Phys. Lipids, 1971, 7, 21.
29. P.B. Merkel and D.R. Kearns, J. Amer. Chem. Soc., 1972, 94,
1029 and 7244.
30. E. Demole, C. Demole and D. Berlhét, Helv. Chim. Acta, 1973,
56, 265.
31. A. Shani and J.T. Klug, Tet. Lett., 1980, 21, 1563.
32. J.A. Turner and W. Herz., J. Org. Chem., 1977, 42, 1895.
33. J.A. Turner and W. Herz., J. Org. Chem., 1977, 42, 1900.
34. J.P. Hagenbuch and P. Vogel, Tet. Lett., 1979, 561.
35. W. Adam and M. Balci., Angew. Chem. Int. Ed. Engl., 1980, 19, 48.
36. M.S.F. Lie Ken Jie and S. Sinha, Chem. Phys. Lipids, 1981, 28, 99.
37. J.P. Hagenbuch and P. Vogel, J. Chem. Soc. Chem. Comm., 1980,
1062.
38. O. Wallach, Ann., 1912, 392, 49.
39. F.D. Gunstone and R.P. Inglis., Chem. Phys. Lipids, 1973, 10, 89.
40. H. Paget, J. Chem. Soc., 1938, 829.
41. W. Adam and M. Balci, J. Amer. Chem. Soc., 1979, 101, 7542.
42. D.J. Coughlin and R.G. Salomon, J. Amer. Chem. Soc., 1977, 99,
655.
43. W. Adam and H.J. Eggelte, Angew. Chem. Int. Ed. Engl., 1977, 16,
713.
44. W. Adam, A.J. Bloodworth, H.J. Eggelte and M.E. Loveitt, Angew.
Chem. Int. Ed. Engl., 1978, 17, 209.
45. a) W. Adam and I. Erden, Angew. Chem. Int. Ed. Engl., 1978,
17, 210 and 211.
b) W. Adam and I. Erden, J. Org. Chem., 1978, 43, 2737.
46. W. Adam and H.J. Eggelte, Angew. Chem. Int. Ed. Engl., 1978, 17,
765.

47. W. Adam and H.J. Eggelte, J. Org. Chem., 1977, 42, 3987.
48. W. Adam and M. Balci, J. Amer. Chem. Soc., 1979, 101, 7537.
49. For a review on hydrogenation with di-imide see C.E. Miller,
J. Chem. Ed., 1965, 42, 254.
50. Vogel's textbook of practical organic chemistry, 4th Ed.,
Longman, New York, 1978.
51. J.C. Touchstone and M.F. Dobbins in "Practice of Thin Layer
Chromatography", Wiley, New York, 1978, pp 199.
52. G.G. Abbot, F.D. Gunstone and S.D. Hoyes, Chem. Phys. Lipids,
1970, 4, 351.

Section 2

**Synthesis of cyclic peroxides from
methyl oleate**

Summary.

Methyl 9(10)-hydroperoxyoctadec-10(8)E-enoates (3a,b), produced by photosensitised oxidation of methyl oleate are suitable substrates for the synthesis of substituted dioxolanes. Peroxymercuration of (3) affords on hydrogenodemercuration methyl 8,10- and 9,11-epdioxyoctadecanoates (5a,b) in good yield (45-70%). Bromodemercuration yields the corresponding bromo substituted cyclic peroxides (9a,b) in higher yield (95%). Direct bromination of the allylic hydroperoxides (3a,b) also affords the bromo substituted cyclic peroxides (9a,b) in almost quantitative yield, presumably via a bromonium ion intermediate.

1 Introduction.

THE primary oxidation products of unsaturated lipids are mono hydroperoxides formed by either addition of ground state triplet oxygen to unsaturated fatty acids via a radical chain mechanism^[1] or by the addition of the low-lying singlet excited states of oxygen via a concerted ene-reaction or a perepoide intermediate^[2].

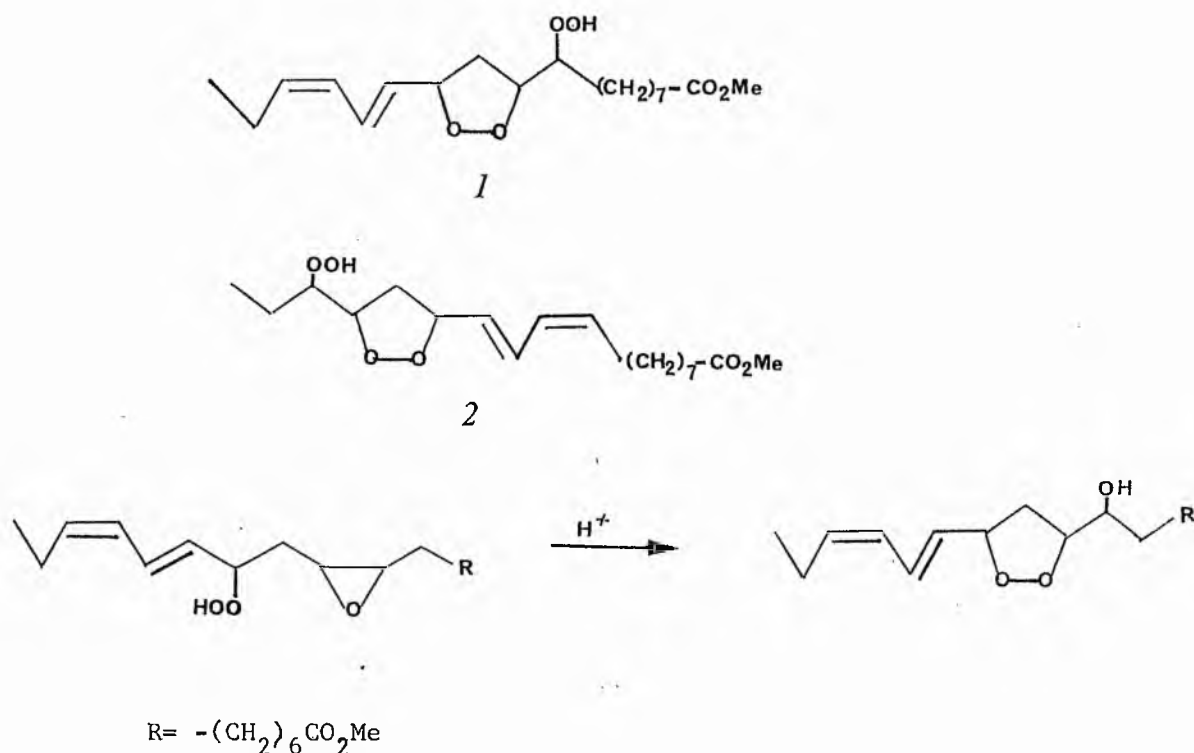
Further oxidation of the monohydroperoxides of unsaturated lipids containing more than two double bonds is known to give hydroperoxy cyclic peroxides as major products and dihydroperoxides as minor products^[3-10]. Roza and Franke^[6] isolated and identified compounds of structure (1) and (2) from the products of incubation of methyl linoleate with an aqueous extract of soybean flour at neutral pH. These findings were in close agreement with the cyclic peroxides isolated from autoxidised methyl linolenate by Haverkemp Begeman *et al*^[7]. These were considered to contain six-membered ring systems on the basis of inconclusive mass spectrometer data on minor rearrangement products, but five-membered rings were not ruled out by the authors.

More recently two independent reports on the HPLC separation of the isomeric hydroperoxy cyclic peroxides from autoxidised methyl linoleate appeared by Neff *et al*^[5] and Coxon *et al*^[4]. Both groups separated and characterised the isomeric products, their results being in good agreement.

These hydroperoxy cyclic peroxides have been suggested as intermediates for the TBA test giving rise to the malondialdehyde-TBA

complex^[11]. Porter *et al*^[12] have reported the synthesis of a hydroperoxy cyclic peroxide of methyl linolenate via cyclisation of a β -hydroperoxide onto an oxirane ring (Scheme 1). Frankel *et al*^[13] have isolated hydroperoxy cyclic peroxides by allowing the methanesulphonate of methyl ricinoleate to react with 90 % hydrogen peroxide in diethyl ether.

We now report that allylic hydroperoxides from methyl oleate can undergo cyclisation when an electron deficient site is created adjacent to the hydroperoxide functionality.



SCHEME 1

2 Results and discussion

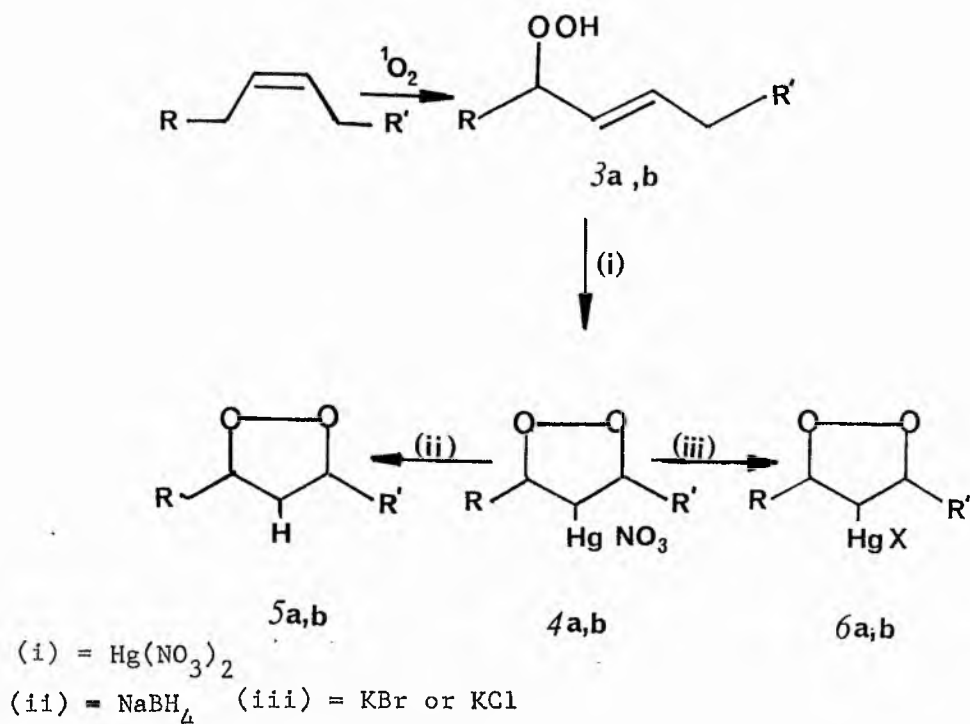
2.1 Preparation of allylic hydroperoxides.

Photosensitised oxidation of methyl oleate in carbon tetrachloride/methanol (95:5) using methylene blue as sensitiser gave the two isomeric trans unsaturated allylic hydroperoxides (3a) and (3b) in a clean reaction in 16h. Preparative HPLC separation of the isomeric hydroperoxides from the unreacted starting material gave the hydroperoxides in 80 % yield. Separation of the latter from the unreacted starting material was achieved in less than nine minutes, thus minimising on-column decomposition of the labile products. The reaction could be scaled up to nine grams with no modification of the procedure. The hydroperoxides were used immediately after removal of the solvent to minimize any possible isomerisation^[14].

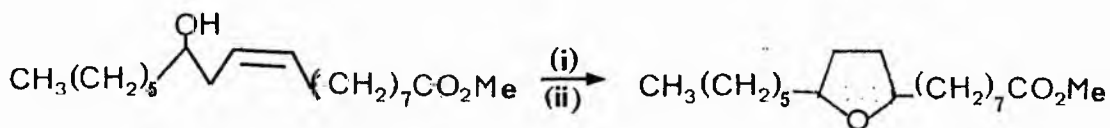
2.2 Peroxymercuration-hydrogenodemercuration.

The allylic hydroperoxides (3a,b) reacted with an excess of mercuric nitrate demi-hydrate in dry dichloromethane at ambient temperature to afford the organomercury nitrates (4a,b) which were not isolated, but reduced in situ by the addition of a three fold excess of aqueous sodium borohydride, to give the cyclic peroxides (5a,b) which were separated from the other products of reaction by TLC in yields varying from 45-70 % . Time course experiments showed that no significant improvement in the yield of cyclised product was obtained by increasing the reaction time beyond 24h. Similarly increasing the

amount of mercuric salt to a 2-3 fold excess had no effect.



The choice of mercury(II) salt was based on the success of this salt in the synthesis of model compounds by Bloodworth *et al.*^[15,16] and also by Porter *et al.*^[17]. Bloodworth's results suggested that an anion with low nucleophilicity was required and also that the products of intramolecular alkoxymercuration are far more stable towards strong acids than are acyclic oxymercurationals. Furthermore oxymercuration experiments with methyl ricinoleate only gave appreciable yields of cyclised products (Scheme 2) with mercuric nitrate. Mercuric acetate, chloride, trifluoroacetate and sulphate all being ineffective^[18,19].



(i) = HgX , [X = $(\text{NO}_3)_2$, $(\text{OAc})_2$, $(\text{OCOCF}_3)_2$, or SO_4]

(ii) = NaBH_4

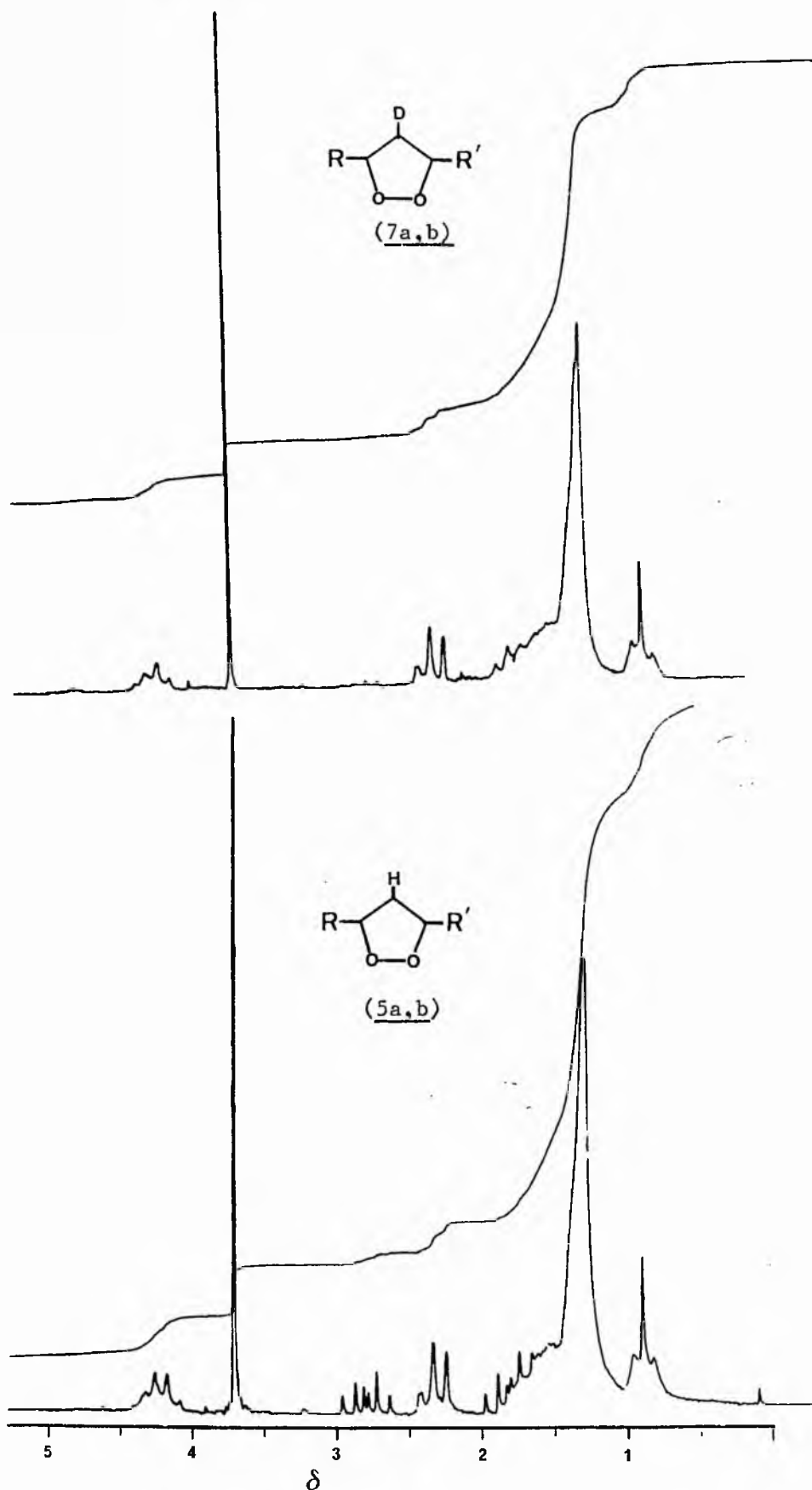


FIGURE 1 90 MHz ¹Hnmr spectra of the cyclic peroxide (5a,b) (bottom trace) and its deuterium derivative (7a,b) (upper trace.)

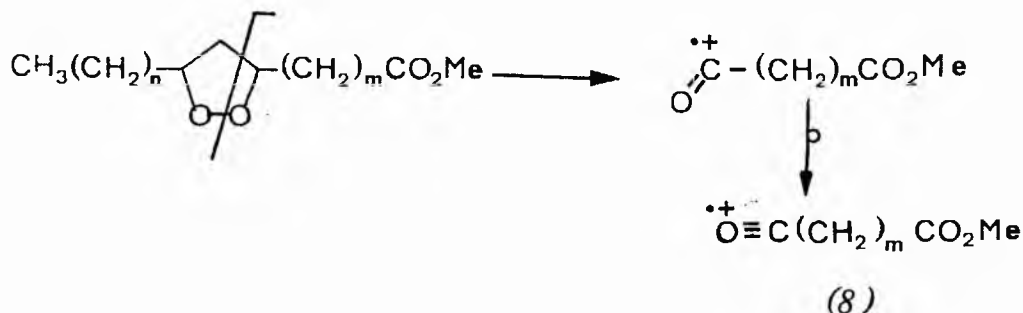
Dichloromethane was employed as solvent even though the mercuric salt has only a limited solubility in this solvent.

Other groups have successfully isolated the organomercuric chlorides for model compounds^[15-17], however the long chain fatty acid methyl ester mercuric chlorides (6a,b) were viscous tacky oils which were difficult to handle and isolate clean. The reaction is less troublesome by not attempting to isolate the mercury derivatives but to reduce the compound in situ with sodium borohydride.

The ¹Hnmr spectrum of the cyclic peroxide (5a,b) is shown in Figure 1. Decoupling at 1.7 δ altered the apparent quartet at 4.13 δ to a broad apparent doublet ($J=7.0\text{Hz}$). The 2.80 δ triplet part of the double triplet collapsed to a singlet at 2.88 δ and an asymmetric triplet at 2.75 δ . Decoupling of the peroxy methines at 4.13 δ collapsed the double triplets at 2.80-2.62 and 1.80 -1.55 δ to broad doublets ($J=12.0\text{ Hz}$). A shoulder at 1.5 δ became much sharper.

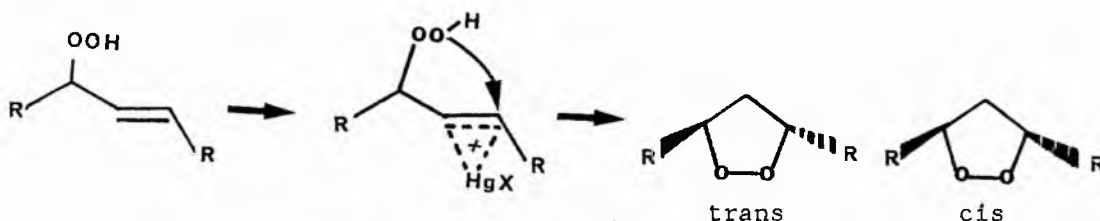
Reduction of the organomercury (II) nitrates (4a,b) with sodium borodeuteride gives the cyclic peroxides (7a,b) with an endocyclic deuterium substituent. The ¹Hnmr of (7a,b) is similar to that of (5a,b) apart from the absence of the double triplet at 2.80-2.62 δ , and an apparent triplet rather than a quartet at 4.13 δ . The double triplet at 1.80-1.55 δ was collapsed to a triplet ($J=6.8\text{ Hz}$).

The mass spectrum of (5a,b) was in accord with the expected spectrum based on data from model compounds^[15,16]. Several intense high mass peaks were observed resulting from cleavage α to the ring and also from cleavage of the ring as shown below. The fragment (8) locates the position of the peroxide linkage and is common to a wide number of oxygenated esters.

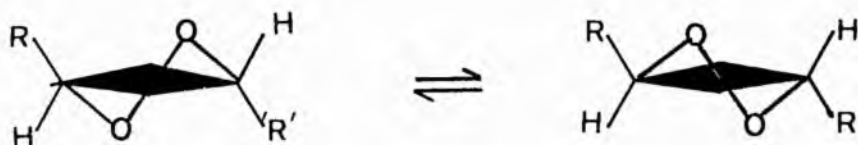


2.3 Diastereoisomerism, conformation and configuration.

The photosensitised oxidation of methyl oleate generates the allylic hydroperoxides as racemic mixtures of positional isomers. The subsequent intramolecular peroxymercuration can proceed via electrophilic attack on either face of the double bond thereby affording diastereoisomeric cyclic products from each enantiomeric and positional isomer of the hydroperoxides. Attack of one face in preference to the other may be favoured on grounds of steric hindrance, especially if the reaction is under thermodynamic control.



Bloodworth et al^[15b] briefly discussed the conformational aspects of 3,4-dimethyl-1,2-dioxacyclopentanes, concluding that the ring exists in two half-chair or envelope conformers (as illustrated for a trans isomer) with alkyl groups in pseudo-equatorial or axial positions.



Five-membered ring systems are pseudorotational systems with very low or no potential energy barriers^[20,21]. The introduction of bulky substituents and/or heteroatoms into the ring will be expected to raise the barrier above the pseudorotational energy levels and the ring will adopt either an envelope or half-chair form, whichever is the most stabilised^[20,21]. The replacement of two methylenes in cyclopentane with two oxygen atoms as in 1,2-dioxacyclopentanes will reduce Pitzer strain in these heterocyclic ring systems, and hence lead to a more planar structure than the corresponding carbocyclic system. Cis 1,3-dimethylcyclopentane is 0.6 kcal/mole lower in energy than its trans isomer^[22]. This difference arises from the fact that in the cis configuration the methyl groups can both assume pseudo-equatorial positions in the envelope conformer common to both isomers, while in the trans isomer one methyl must assume the unfavourable axial position. A MINDO/3 study on the conformation of the 3,5-dimethyl-1,2-dioxacyclopentanes gave an energy difference of 0.26 kcal between the cis and trans isomers with the trans being lower in energy. This value is consistent with the ring being more planar ie as the ring approaches planarity the pseudo axial and equatorial substituents become equivalent. The calculated geometry suggests that the ring is very nearly planar^[23].

The ring methylenes of the cis isomer are reported to give double triplets at 1.71 and 2.77 δ in the ¹Hmr spectrum while the trans isomer methylenes form a triplet at 2.19 δ . For (5a,b) double triplets were observed at 2.17 and 1.70 δ . Any triplet at 2.19 δ would be

obscured by the methylenes adjacent to the carboxyl group. The integral of the cis ring methylenes is difficult to evaluate since the 1.71 δ double triplet occurs on the edge of the signal from the methylenes of the alkyl chain. However from the integral of the 2.25 δ peak relative to the methyl ester peak at 3.6 δ the trans isomer if present must be <<10%. Thus the predominant isomer is the cis isomer which will exist as two half-chair or envelope conformers for each positional isomer, with the alkyl groups preferring pseudo equatorial positions.

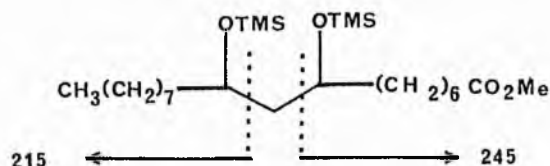
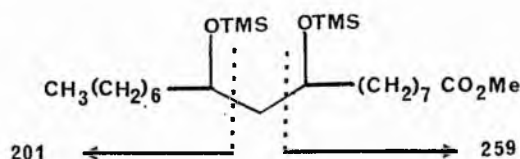


The presence of only one intense peroxy bearing carbon signal in the ^{13}C nmr spectrum at 81.04 ppm also supports the preferential formation of one configurational isomer. The presence of small amounts of the trans isomer cannot be precluded from the available spectral data however.

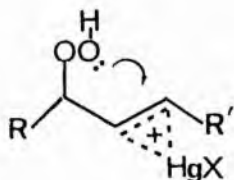
2.4 Catalytic hydrogenation.

The cyclic peroxides (5a,b) were catalytically reduced to the corresponding dihydroxystearates which were analysed after derivatisation to the trimethylsilyl ether, by mass spectrometry. Characteristic fragment ions at m/e 201 and 259 in the spectrum of the trimethylsilyl derivatives located the peroxide link at carbons 9 and 11, while fragment ions at m/e 215 and 245 locate the peroxide at

carbons 8 and 10.



The mode of cyclisation deserves mention. The predictions for cyclisation developed by Baldwin^[24] are not well defined for nucleophilic attack on 3-membered rings, but are said to lie between those for tetrahedral and trigonal systems, generally preferring exo-modes.



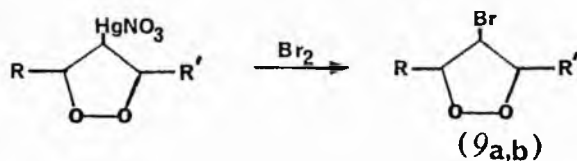
5-endo-tet ?
5-endo-trig

However, irrespective of whether the mercurium cation is considered to be a tetrahedral or trigonal system the mode of cyclisation would be predicted to be disfavoured. Other examples of disfavoured 5-endo-trigonal reactions have been reported^[25].

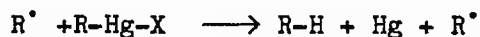
2.5 Bromodemercuration.

Bromodemercuration of model acyclic and cyclic peroxymercurials takes place under mild conditions and is generally a clean reaction^[15-17]. The bromodemercuration of (4a,b) was no exception and the reaction product gave essentially one spot on TLC analysis with only a minor amount (< 5 % in total) of by-products, from which (9a,b) were separated by simple preparative chromatography. The bromo cyclic peroxides (9a,b) were identified by ¹Hmr, ¹³Cmr, ir and mass spectroscopy and the major diastereoisomer was attributed to the cis dialkyl cyclic peroxide on the premise that it was the cis isomer that predominates in the hydrogenodemercuration. Confirmation of the proposed structure was also obtained by independent synthesis of (9a,b) by bromination of the allylic hydroperoxides and a detailed discussion of the diastereoisomerism and conformational aspects of the molecule will be found in section 2.7.

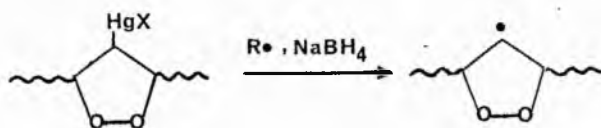
The cleanness of the reaction warrants a brief comment. Bromodemercuration is believed to involve a free radical chain mechanism^[26]. Such a chain mechanism requires that bromodemercuration proceeds through the same intermediate peroxy alkyl radicals involved in the hydrogenodemercuration which leads to competing reactions (see later) producing oxygenated by products. The formation of by products in the bromodemercuration is, however, almost negligible. This is accounted for by the fact that abstraction of a bromine atom by the alkyl radical is expected to be diffusion controlled, the rate constant being about 10³ fold greater than that for the most favoured ring closure^[28,29].



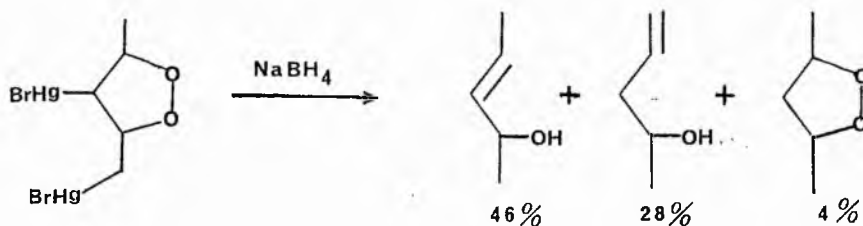
Alkyl-mercuric compounds react with sodium borohydride to yield the corresponding alkyl radical^[30,31]. The mechanism of radical production has been shown to involve an intermediate alkyl hydrido mercury compound $R-Hg-H$ ^[30]. Chain propagation occurs as shown below by radical attack on $R-Hg-H$.



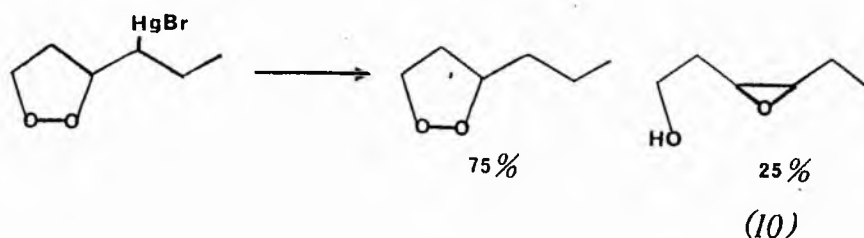
If this mechanism holds for the reduction of the peroxymercurated compound (4a,b) then an endocyclic β -peroxy radical can be envisaged.



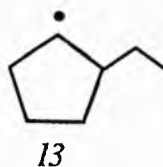
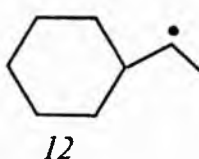
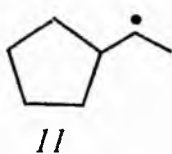
It has been reported that cycloperoxymercurials containing endocyclic mercurio-substituents have a strong tendency to deoxymercurate under reduction conditions^[16] and poor yields of peroxides can be expected, the major products being unsaturated alcohols.



This is in stark contrast to cycloperoxymercurials containing exo-cyclic mercurio-substituents, which on reduction generate an exo-cyclic β -peroxy radical. The expected products from such radicals are the cyclic peroxide resulting from H atom abstraction and the epoxy-alcohol (10) resulting from S_{Hi} radical attack on the peroxide linkage^[17,33].

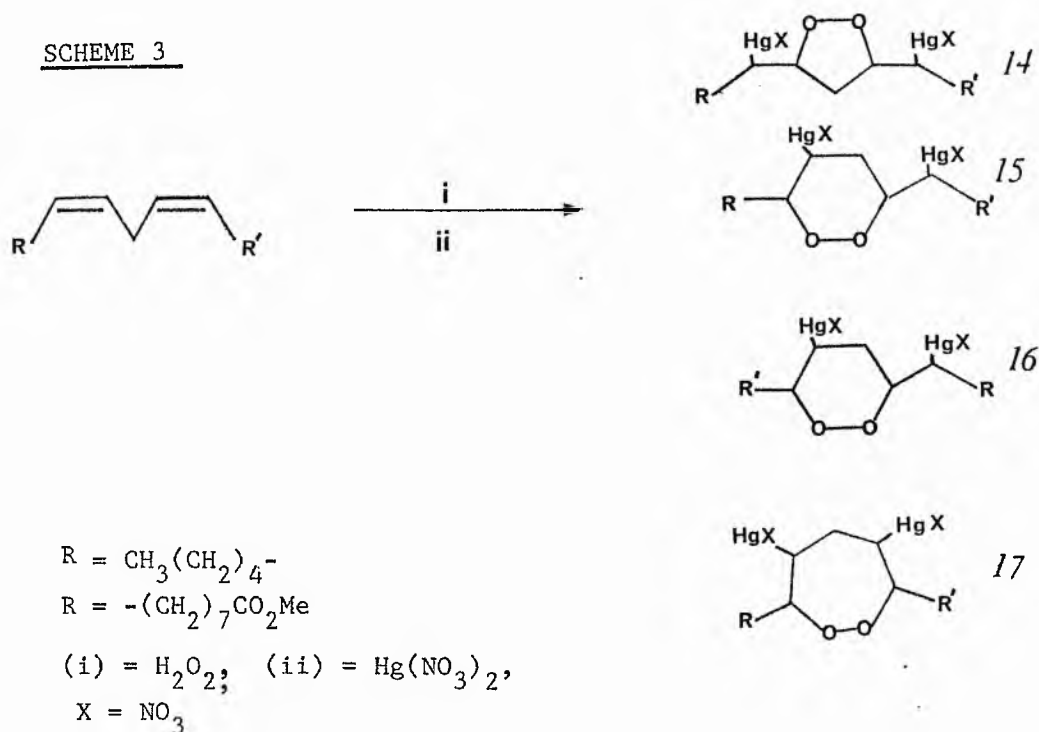


The relative amount of products resulting from H atom abstraction to S_{Hi} attack will be intimately dependent on the structure of the intermediate radical. Porter *et al*^[33] suggested that the critical geometric parameter for the S_{Hi} reaction is the dihedral angle θ , about the O-C bond between the attacking radical and the leaving oxygen. Maximum S_{Hi} reactivity occurring when this dihedral angle is 180° i.e. the peroxide linkage and the radical centre are co-linear. For the analogous radical derived from a five-membered ring ($n=1$) the O-C dihedral angle is substantially less than 180° having a maximum of approximately 165° in the most favourable conformation for S_{Hi} attack. Hence the amount of S_{Hi} product from radical (11) is substantially less than for the six-membered analogous radical (12), which can adopt a dihedral angle of 180° . It is impossible however for endocyclic radicals such as 13 to assume the required conformation



since the radical centre is located within the ring. As a consequence, no S_{H1} reaction is expected from such radicals.

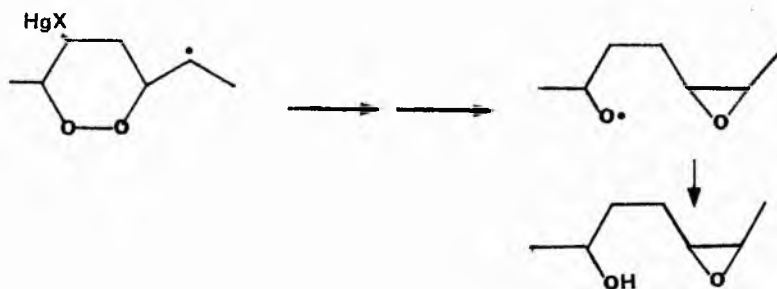
These observations are consistent with the products formed by the sodium borohydride reduction of (4a,b) no epoxy-alcohols being detected by TLC. This is in marked contrast to preliminary results obtained on the attempted peroxymercuration of methyl linoleate (Scheme 3).



Three possible ring sizes can be obtained, the six-membered ring being formed as two positional isomers 15 and 16.

The predictions for cyclisation developed by Baldwin^[24] are not well defined for nucleophilic attack on 3-membered rings as in the mercurium ion. However from molecular model studies and from results obtained by Porter *et al*^[17] it is apparent that exo-modes are likely to be favoured, while 6-endo cyclisation will be disfavoured.

Hence one would expect structures (14-16) to predominate. Sodium borohydride reduction of the peroxymercurials however, yielded a complex mixture of products from which unsaturated epoxides and epoxy-alcohols were identified as the major reaction products. Tentative evidence from ^1Hmr and mass spectra suggests that (15) and (16) may be formed as minor products. These results are consistent with the hypothesis that 6-membered rings containing exo-cyclic β -peroxy radicals are likely to undergo extensive S_{Hi} rearrangement to form epoxy alcohols.



Bromodemercuration of the peroxymercurials gave an isomeric mixture of dibromo cyclic peroxides (18a,b), which show parent peaks in the mass spectrum at m/e 484, 486 and 488 in the expected 1:2:1 ratio for dibromo peroxides. Also present were peaks resulting from β -cleavage to the ring for the dibromo peroxides of the type shown in Figure 2 (corresponding to products from 6-exo cyclisation).^[27]

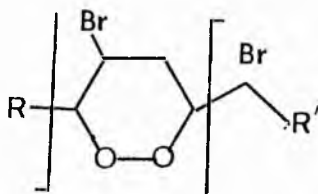


FIGURE 2

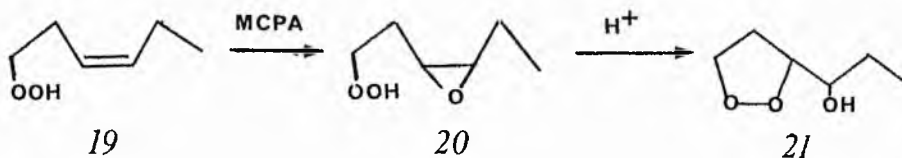
18 a,b

- a $R = -(CH_2)_7CO_2Me$ $R' = -(CH_2)_5CH_3$
 b $R = -(CH_2)_4CH_3$ $R' = -(CH_2)_8CO_2Me$

The ^{13}C nmr spectrum of the isomeric dibromoperoxides shows peaks in the region 80-82 ppm indicative of peroxy bearing carbons and peaks at 56-58 ppm for the bromo bearing carbons. The infrared spectrum showed no OOH absorption hence confirming the dialkyl nature of the peroxide. The 1H nmr showed two 2-proton signals in the region 4.0-4.6 δ indicative of 2-peroxy and 2-bromo bearing methines. No olefinic protons were observed. The fraction showed several spots on TLC analysis at R_f 0.65-0.70 in PE 20, but none of these were completely resolved and hence preparative TLC separation of the individual components was not attempted. It is presumed that we were separating positional and diastereoisomers of which there would be no less than 32 possibilities.

2.6 Epoxidation and attempted cyclisation of allylic hydroperoxides (3a,b)

Cyclisation of unsaturated hydroperoxides can be induced by generating an electron deficient site from the olefin functionality. For example the hydroperoxide (19) is converted to the β -hydroperoxy cyclic peroxide (21) via the oxirane hydroperoxide (20)^[12]. The β -hydroxy cyclic peroxides are reported to have interesting



pharmacological properties^[34].

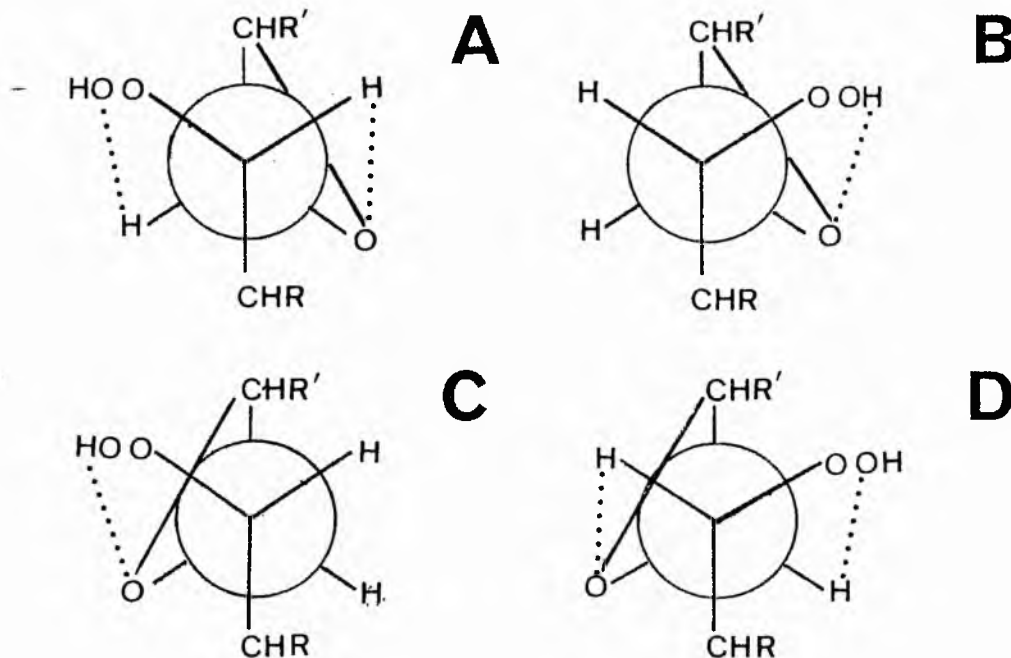
Epoxidation of the allylic hydroperoxides (3a,b) in dichloromethane/sodium bicarbonate solution with m-chloroperoxybenzoic acid (MCPA) furnished an organic product which on work up showed two broad spots on TLC, both of which gave a positive peroxide spray test. Repeated development chromatography suggested as with the cyclic peroxides (5a,b) that each spot contained at least two components.

The two bands were separated by preparative TLC on silica gel G. The ¹Hnmr spectrum of each fraction showed that both compounds were hydroperoxides (H-C-OOH at 9.45 and 8.97 δ for band 1 and 2 respectively). The less polar product showed two one proton multiplets between 3.10-2.83 δ whereas the more polar product showed only one multiplet at 2.86 δ .

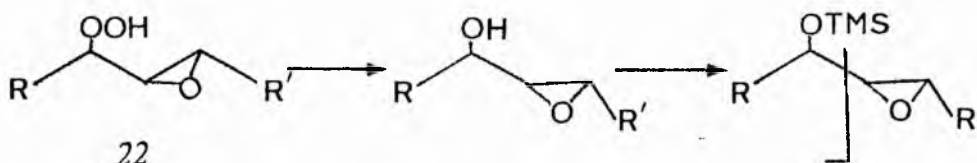
Epoxidation of (3a,b) can give rise to two diastereoisomers for each positional isomer. For two isomers there is hydrogen bonding between the hydroxyperoxy O-H and the oxirane oxygen. For the other isomers hydrogen bonding can be envisaged between the peroxy group and the oxirane methines as depicted (Figure 3). On the basis of these conformational preferences we consider the least polar of the two peroxidic fractions to be isomers A and D and the more polar band to be isomers B and C. In isomers A and D the ¹Hnmr shifts of the peroxy methine and of the oxirane methine β - to the peroxy group will both be downfield from the corresponding hydrogens in isomers B and C as a result of hydrogen bonding. Furthermore the hydrogen bonding in isomers B and C is between the hydroperoxy hydrogen atom and the oxirane oxygen and results in a broad OOH signal. The OOH signal for isomers A and D being much sharper. Each pair of diastereoisomers

will also be a mixture of positional isomers, and it is probably the positional isomers which show a slight separation after multiple development chromatography.

FIGURE 3 Diastereoisomers of the hydroperoxyoxiranes (22). The dotted lines indicate the possibility of hydrogen bonding.



The mass spectra of the sodium borohydride reduced products after conversion to the trimethylsilyl derivatives confirmed that each spot was a mixture of positional isomers since both mass spectra showed peaks characteristic of each positional isomer.



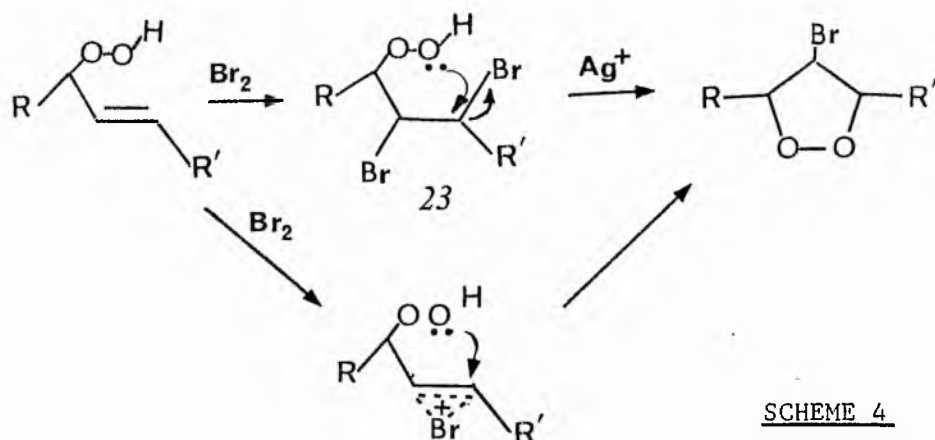
The most intense high mass peaks resulted from cleavage between the trimethylsilyl ether group and the epoxide ring as shown, and was the fragment containing the silyl group.

Attempted acid catalysed cyclisation of the hydroperoxy oxiranes was unsuccessful with either trichloro- or trifluoro- acetic acid^[33].

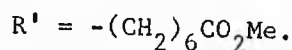
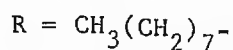
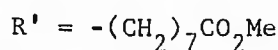
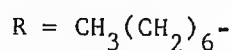
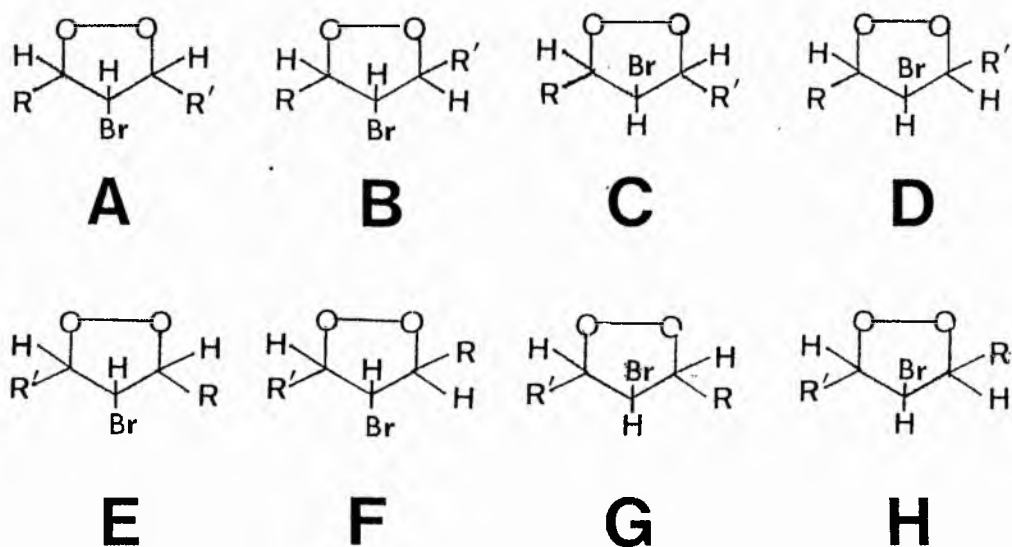
2.7 Bromination of the allylic hydroperoxides.

The allylic hydroperoxides (3a,b) react smoothly with bromine at 0-5°C in dry dichloromethane when protected from light. Two major bands were observed on TLC analysis which gave red spots when sprayed with peroxide detecting reagents. A further minor unidentified component was not peroxidic but very polar. The first band which is formed in 80-85 % yield as judged by TLC was identical with the product of the bromodemercuration of the peroxymercurials (4a,b). The other component (10-15 %) was identified as the dibromohydroperoxides (23a,b) by ¹Hnmr and infrared spectroscopy.

In preliminary experiments the product of bromination was not isolated per se since it was expected that the major product would be the dibromohydroperoxides (23a,b). Silver trifluoroacetate was added to the reaction mixture at room temperature for 1h. Although yields of bromo cyclic peroxide (9a,b) were good by this route it is evident from above that the majority of the cyclisation occurs unassisted prior to the addition of silver trifluoroacetate as shown in Scheme 4.

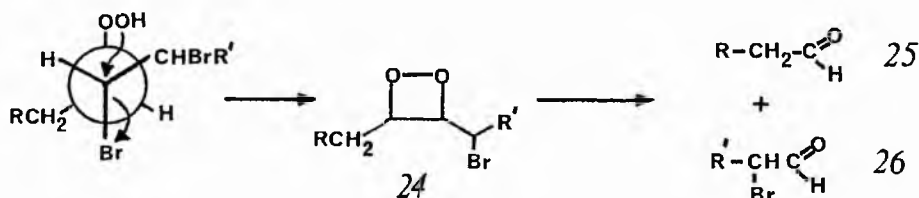


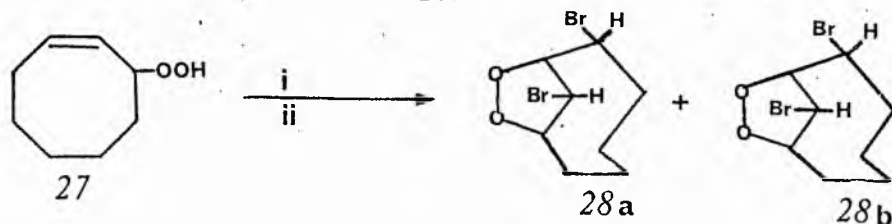
Eight diastereoisomers can be expected from the reaction (9 A-H) for each positional isomer, giving a total of 16 isomers in all. Eight of these isomers arise from different combinations of substitution of the alkyl chains on the 1 and 3 position of the dioxolane ring and the other 8 isomers arise from the relative spatial distribution of the bromo substituent to the 2 alkyl groups.



We were unable to separate these isomers chromatographically, if they are indeed all present. The ^{13}C Nmr spectrum for the bromo cyclic peroxides showed only one peroxidic carbon resonance (89.08ppm) and only one C-Br resonance (57.18ppm) however the spectral quality was such that <5 % of a second isomer would not easily be detected. The difference in ^{13}C chemical shifts reported for the peroxy bearing carbons of cis and trans isomers of 3,5-dialkyl-1,2-dioxacyclopentanes is less than 1.2 ppm^[15,16]; replacement of the methyl group by long chain alkyl groups may well decrease this difference and the signals observed could be a composite of one or more of the diastereoisomers.

The silver assisted intramolecular cyclisation of the dibromo-hydroperoxides (23a,b) will proceed via an $\text{S}_{\text{N}}2$ mechanism, with the hydroperoxy group and the β -bromine atom being in an antiperiplanar juxta position leading to an inversion of configuration at the site of displacement. The dibromo-hydroperoxides could conceivably undergo a 4-exo cyclisation to form the dioxetane (24) since the bromo bearing carbon adjacent to the hydroperoxide will be free to undergo rotation and hence adopt the trans 1,2-relationship required for cyclisation. precedence for this reaction has been reported^[36]. However under a variety of reaction conditions we found no evidence for dioxetane production or indeed its intermediacy since the dioxetan could readily undergo cleavage to yield the aldehyde (25) and the α -bromo aldehyde (26).





(i) = $\text{Hg}(\text{OCOCF}_3)_2$, (ii) = Br_2 .

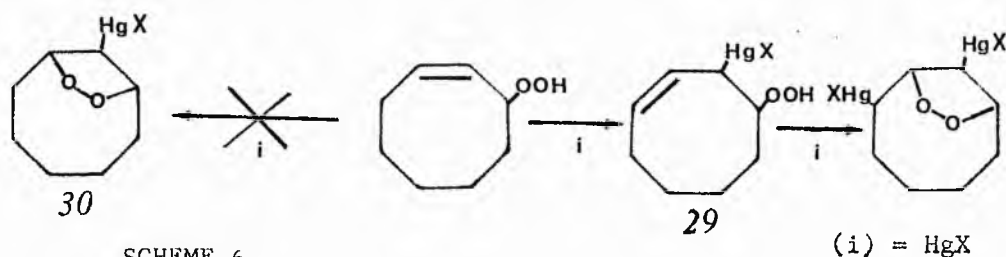
SCHEME 5

The bromo cyclic peroxides (9a,b) generated from bromodemercuration of the oxymercurials (4a,b) were spectroscopically and chromatographically identical. Bloodworth and Leddy^[37] reported that peroxymercuration/bromodemercuration of cycloalkenyl allylic hydroperoxides (27) gives rise to cyclic peroxides (28a) and (28b) in very poor yields (0.6 % and 2.7 % respectively). More importantly the cyclic peroxides contain two bromo substituents (Scheme 5).

To account for these products, Bloodworth *et al*^[37] concluded that allylic mercuration occurs to give (29), followed by 5-exo cyclisation in preference to the 5-endo cyclisation required for the formation of (30) (Scheme 6).

We have repeated the reaction for cyclohexenyl hydroperoxide using mercuric nitrate in place of mercuric trifluoroacetate as mercury salt and have arrived at essentially the same result, namely the formation of a cyclic peroxide with two mercury substituted sites.

Thus the cyclic alkenyl hydroperoxides prefer to undergo a 5-exo cyclisation in preference to the disfavoured 5-endo cyclisation, via allylic mercuration. The independent synthesis of (9a,b) by the silver trifluoroacetate method confirms that for the acyclic allylic hydroperoxides 5-endo cyclisation occurs exclusively with the exclusion of allylic mercuration. Furthermore the signal intensity

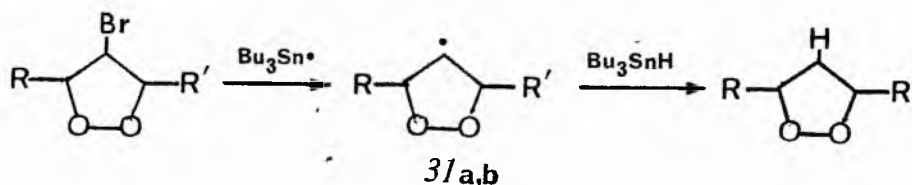


SCHEME 6

(i) = HgX

ratio for C-OO and C-Br in the ^{13}Cmr of these products supports this view allowing for the expected differences in the relaxation time of the two types of carbon. We are unable at present to rationalise the discrepancy between the two systems on a firm basis but steric constraints imposed by the small-medium ring sizes may be part of the answer.

The aim of the synthesis of these cyclic peroxides was to produce compounds which might be of pharmacologically active. To this end the bromo substituent is not an attractive substituent to have in the molecule. Tributyltin hydride reduction (Scheme 7) appeared to be a promising route for the replacement of bromine on the basis of independent work by Bloodworth *et al* [16] and Porter *et al* [33].



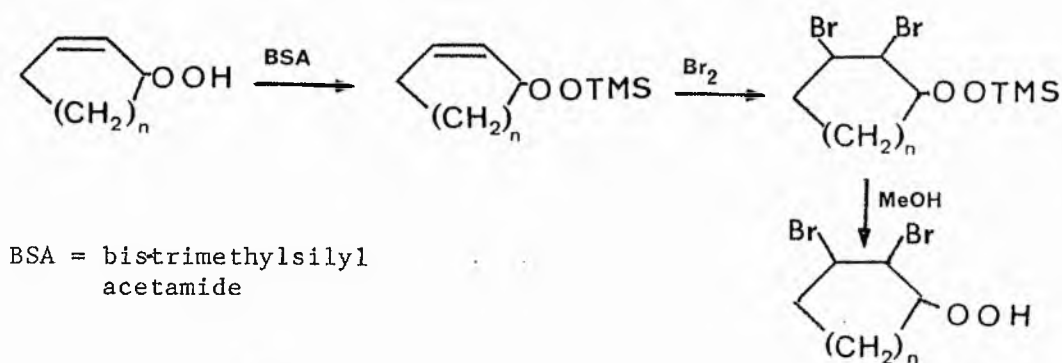
SCHEME 7

The reaction proceeds via a radical mechanism and involves the abstraction of the bromine atom by the trialkyltin radical. The transient radical (3/a,b) would then be converted to the cyclic peroxide (5/a,b) via reaction with the efficient hydrogen donor Bu_3SnH . The geometry of the intermediate radical (3/a,b) is such as to preclude intramolecular attack on the peroxide bond and hence β -scission to form epoxides should not compete seriously with the desired hydrogen abstraction.

Reaction between tributyltin hydride and the bromocyclic peroxide

furnished the desired cyclic peroxide (5a,b) in 75 % yield which was comparable with the best yields obtained from the hydrogenodemercuration reaction. Although the by products were not isolated in these experiments comparison of the reaction products on TLC with that of the hydrogenodemercuration experiment suggested a similar product distribution. The cyclic peroxide from this reaction was identified by TLC, ^1Hmr and infrared spectral comparison with authentic material. Attempts to compare mass spectra were unsuccessful due to contamination of the product with organic tin material, which we were unable to completely remove either by TLC chromatography or by repeated washing.^[38] This complication detracts from this route for preparative purposes.

Bloodworth *et al*^[35a] reported that trimethylsilylation of the hydroperoxides prior to bromination results in less cyclised product and enables isolation of the dibromo-hydroperoxide (Scheme 8).

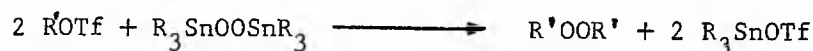


SCHEME 8

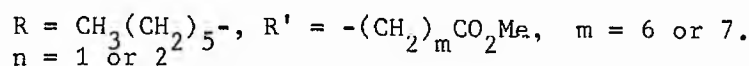
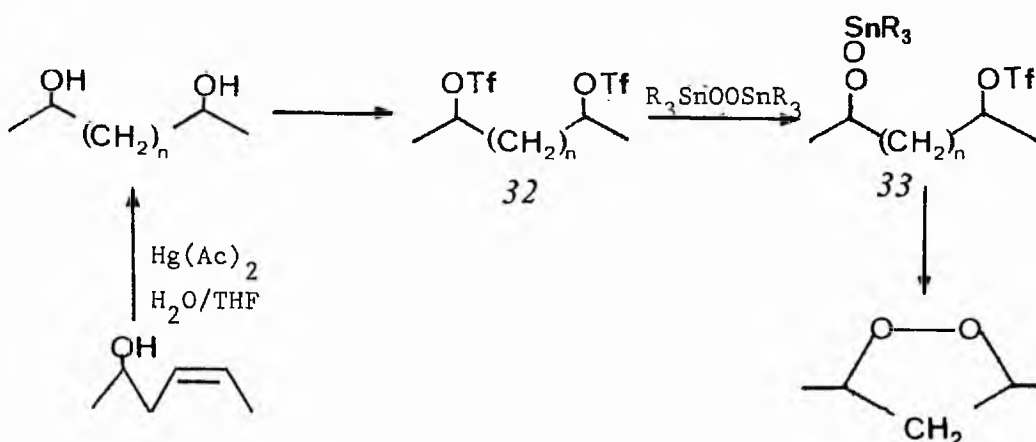
Attempted trimethylsilylation of (3a,b) was unsuccessful in our hands and we suspect that derivatisation had not occurred. The reaction was not pursued further since the primary objective *ie.* synthesis of the cyclic peroxide had been achieved.

2.8 Attempted synthesis of cyclic peroxides via the peroxide transfer reaction.

Peroxide transfer between tin peroxides and alkyl triflates or bistriflates to furnish dialkyl and cyclic peroxides has been used to prepare simple peroxides in fair to excellent yields^[39] by the route shown below.

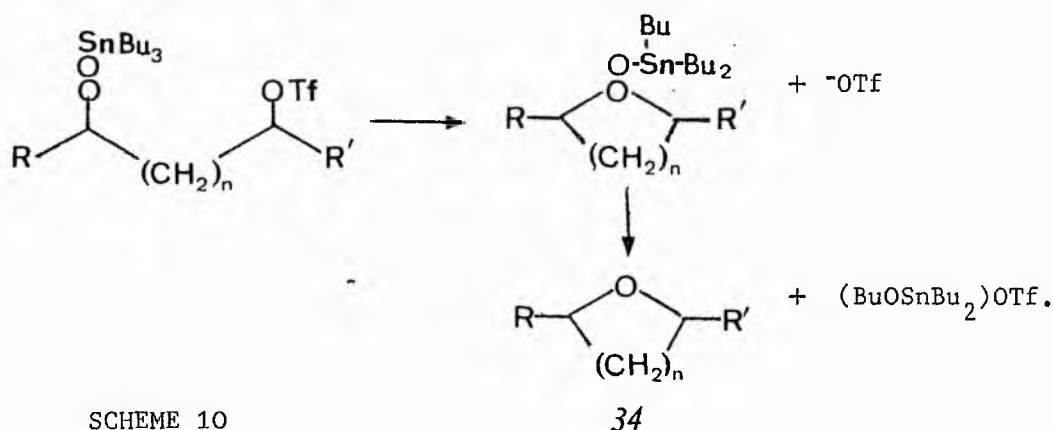


Attempts to extend the peroxide transfer reaction to the synthesis of fatty acid cyclic peroxides were unsuccessful in our hands. Methyl 9,12- and 10,12-dihydroxystearates were prepared by oxymercuration of methyl ricinoleate^[19], and the planned strategy for the synthesis of the product is outlined below.



SCHEME 9.

The procedure involves the initial formation of the mono transalkylated tin peroxide (33) followed by a second intramolecular transalkylation. Reaction of the bistriflates (32) however with di-*t*-butyl tin peroxide furnished only one non-polar product which was identified as the cyclic ether (34) by $^1\text{Hnmr}$, mass and infrared spectroscopy. The formation of the cyclic ether was not unexpected since Salomon *et al*^[39] also reported the concomitant formation of cyclic and acyclic ethers in their pioneering syntheses of dialkyl and cyclic peroxides. Their proposed mechanism is depicted in the following Scheme



SCHEME 10

The absence of the desired peroxidic products was disappointing, however the usefulness of this approach would have been questionable on a large scale even if the target molecule had been obtained since the organic tin by-products of reaction make chromatographic purification difficult (*vide supra*).

3 Experimental

Mercury (II) nitrate demihydrate and sodium borohydride were commercially obtained and protected from moisture by storing the closed bottle over silica gel in a desiccator. Hydrogen peroxide (85%) was kindly gifted by Laporte Industries Limited and was stored at 0°C; required amounts were measured by glass pipette assuming the density to be 1.33 gcm^{-3} . The peroxide content was checked periodically by the method of Vogel^[40].

3.1 Preparation of methyl 9(10)-hydroperoxyoctadec 10(8)-enoates.

Methyl oleate (99.9 %, 1g) was placed in a photochemical reactor with an inner and outer water cooling jacket as previously described. Methylene blue (50mg) dissolved in carbon tetrachloride/methanol (95:5) (250mls) was added and oxygen bubbled through the solution at a flow rate of 40-50mls/min. The flask was illuminated with 3 tungsten light bulbs (150W) for 16 h. Rotoevaporation of the solvent at 2 mmHg and 5°C gave a product containing methylene blue which was removed by passage through a short column of sorbsil eluting with dry diethyl ether. The pale yellow oil obtained showed only two spots on TLC. The least polar being unreacted starting material, and the most polar (R_f 0.41 in PE 30) giving a red colour when sprayed with peroxide detecting reagents. Preparative HPLC on a partisil column gave the pure hydroperoxide in yields of 75-83 % using petroleum ether/isopropanol (97.5:2.5) as eluting solvent. The reaction could be scaled up to 6g with no modification. The following spectroscopic data was recorded for the hydroperoxides (3a,b).

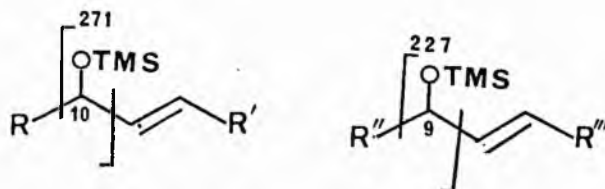
$J=5.6\text{ Hz}, 3\text{H}, \text{CH}_3).$ ^{13}C nmr spectrum:

δ /ppm	assignment	
	9-OOH	10-OOH
174.17	C1	C1
136.18, 135.79	C10,11	C8,9
128.87, 128.55		
86.50	C9	C10
33.78	C2	C2
32.26	C8	C11
32.09	C12	
31.94		C7
31.59	C16	C16
29.23, 28.83	C4,5,6, 13,14,15	C4,5,6, 13,14,15
24.98	C7	C12
24.61	C3	C3
22.38	C17	C17
13.78	C18	C18

infrared spectrum: 3480cm^{-1} (OO-H stretch), 973cm^{-1} ($\sim\text{CH}=\text{CH}-$, trans, stretch).

mass spectrum: the allylic alcohols produced by sodium borohydride

reduction of the hydroperoxides were examined as their trimethylsilyl ethers and showed intense m/e fragments at 227 and 271.



$R = \text{CH}_3(\text{CH}_2)_7-$, $R' = -(\text{CH}_2)_6\text{COOMe}$, $R'' = \text{CH}_3(\text{CH}_2)_8-$
 $R''' = -(\text{CH}_2)_5\text{COOMe}$

The intense fragments occur from cleavage α to the allylic ether with the charge being carried with the allylic system.

3.2 Peroxymercuration of (3a,b).

To a vigorously stirred suspension of mercury (II) nitrate demihydrate (370mg, 1.1mmol) in dry dichloromethane (15ml) was added the oleate hydroperoxides (3a,b) (320mg, 1mmol) in dry dichloromethane (5ml). The mixture was stirred for 24h at ambient temperature, and the solvent removed to furnish the crude organomercury nitrate (4a,b).

3.3 Hydrogenodemercuration.

To the crude organo mercury nitrate was added sodium borohydride (138mg, 3.5mmol) in distilled water/tetrahydrofuran (50:50, 10ml) over 35 min maintaining the temperature of the solution below 0°C . The mixture was stirred vigorously for a further 30min, allowed to warm

slowly to room temperature before adding ether (10ml). The organic phase was isolated and the aqueous phase washed with two further aliquots (10ml) of ether. The combined ether fractions were dried over sodium sulphate before removing the solvent on a rotary film evaporator at 5°C. Analytical TLC showed 5 spots when developed with PE 25 at R_f 0.71, 0.51, 0.41, 0.25, 0.20 and 0.1-0.0.

The spot at R_f 0.41 gave a positive peroxide spray test. No other peroxidic material was observed. Each band was isolated by preparative TLC. The following spectroscopic data was recorded and the quoted yields represent the range from seven experiments.

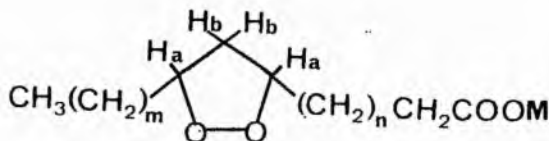
Band A (16-19mg, 5-6 %, R_f 0.51 in PE30)

$^1\text{Hnmr}$ spectrum: 5.37 δ (m, 2H, olefinic H), 3.65 δ (s, 3H, -CO₂Me), 2.30 δ (at, 2H, -CH₂CO₂Me), 2.00 δ (m, 2H, allylic CH₂'s), 1.61 δ (shoulder), 1.25 δ (bs, chain CH₂'s) and 0.86 δ (at, 3H, CH₃-).

infrared spectrum: absence of O-H or C=O stretch

Band B (144-200mg, 45-70 %, R_f 0.41) was identified as a mixture of methyl 8,10- and 9,11-epidioxyoctadecanoates (5a,b).

$^1\text{Hnmr}$ spectrum: 4.11 δ (bq, 2H, Ha), 3.65 δ (s, 3H, -CO₂Me), 2.74 δ (dt, J_{ab} =6.0, $J_{bb'}$ =12.0Hz, 1H, Hb), 2.25 δ (at, J =7.4Hz, 2H, -CH₂CO₂Me), 1.74 δ (dt, J_{ab} =6.0, $J_{bb'}$ =12.0Hz, 1H, Hb), 1.50 δ (bs, chain CH₂'s) and 0.90 δ (at, J =5.7Hz, 3H, CH₃-).



$m = 7$
 $m = 6$

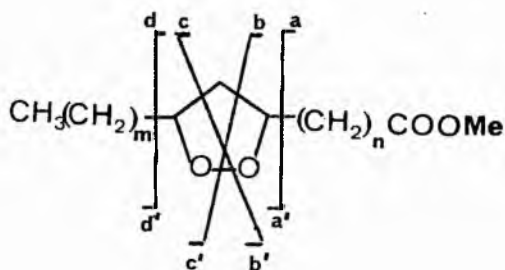
$n = 6$
 $n = 7$

$^{13}\text{C}_{\text{nmr}}$ spectrum:

δ /ppm	assignment	
	9,11 epidioxide	8,10 epidioxide
174.06	C1	C1
81.04	C9,11	C8,10
51.27	$-\text{CO}_2\text{Me}$	$-\text{CO}_2\text{Me}$
46.27	C10	C9
33.81	C2,8,12	C2,7,11
31.72	C16	C16
29.38	C4,5,6	C4,5,13
29.02		
26.21	C7,13	C6,12
24.77	C3	C3
22.52	C17	C17
13.93	C18	C18

infrared spectrum: absence of O-H and $-\text{HC}=\text{CH}-$ (trans) stretch.

mass spectrum:



$$\begin{array}{ll} m = 7 & n = 6 \\ m = 6 & n = 7 \end{array}$$

high mass peaks at

m/e (rel. %)	isomer	
	9,11	8,10
240 (0.1)		
229 (0.4)	d	
215 (0.7)		d
197 (7.4)		
185 (10.4)	b-H ⁺	a'
183 (10.0)		
171 (19.6)	a'	b'-H ⁺
155 (7.8)	a-2H ⁺	
143 (4.3)		a
141 (9.6)		a-2H ⁺

and below m/e 140 intense peaks at m/e 129 (8.7), 125 (13.0), 113 (11.3) 111 (28.3), 109 (15.2), 101 (8.3), 97 (27.8), 95 (22.6), 93 (9.1), 87 (47.8), 83 (54.3), 74 (39.1), 71 (32.6), 67 (34.8), 59 (29.6) and 55 (100).

Band C (25-56, 8-18 %, R_f 0.25 in PE30) was identified as a mixture of allylic alcohols.

¹Hnmr spectrum: 5.50δ(m, 2H, olefinic H), 4.02δ(aq, 1H, -HCOH-), 3.60δ(s, 3H, CO₂Me), 2.32δ(at, 2H, J=7.4Hz, -CH₂CO₂Me), 2.00δ(aq, 2H, allylic CH₂), 1.32δ(bs, chain CH₂'s) and 0.87δ(at, J=5.6Hz, 3H, CH₃).

infrared and mass spectra were in accord with those produced from sodium borohydride reduction of the allylic hydroperoxides.

Band D (14-35mg, 4-10%, R_f 0.20 in PE30)

¹Hnmr spectrum: 8.15δ(bs), 5.50δ(m, olefinic H), 3.73δ(s, 3H, -CO₂Me), 2.37δ(at, J=7.4Hz, -CH₂CO₂Me), 2.07δ(aq, 2H, allylic CH₂), 1.65δ(shoulder), 1.32δ(bs, chain CH₂'s) and 0.97δ(at, J=5.6Hz, CH₃-).

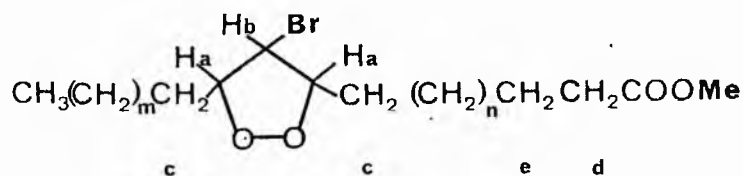
infrared spectrum: 3500-2900cm⁻¹ (O-H stretch), 1760cm⁻¹ (ester C=O stretch) 1720cm⁻¹ (C=O stretch) and 840cm⁻¹.

Band E (35-50mg, 10-15%, R_f 0.1-0.0) was unidentified.

3.4 Bromodemercuration.

Bromine (180mg, 1.13mmol) in dry dichloromethane (10ml) was added to a vigorously stirred suspension of the organomercury nitrate (2a,b) in dichloromethane (5ml) at 0°C. The mixture was stirred for 12h in the dark, filtered through a short column of sorbsil to remove the precipitate of Hg₂Br₂^[41] and the solvent removed under a stream of dry nitrogen to furnish a pale yellow/brown oil. Analytical TLC showed predominantly one product (>95 %) at R_f 0.79 in PE 30 together with a slight tail and traces (ca 4-5 %) of more polar unidentified material. The major product was isolated by preparative TLC and identified as an isomeric mixture of methyl 10-bromo,9,11-epidioxyoctadecanoate and methyl 9-bromo,8,10-epidioxyoctadecanoate on the basis of the following spectroscopic data.

¹Hnmr spectrum: 4.75 δ(q, J=6.0 Hz, 2H, Ha), 4.29 δ(at, J=5.6 Hz, 1H, Hb) 3.60 δ(s, 3H, -COOMe), 2.25 δ(at, J=7.0 Hz, 2H, Hd) 1.55 δ(shoulder, 6H, Hc and He), 1.25δ(bs, chain CH₂'s) and 0.81 δ(at, J=5.6 Hz, 3H, CH₃-).



^{13}C nmr spectrum:

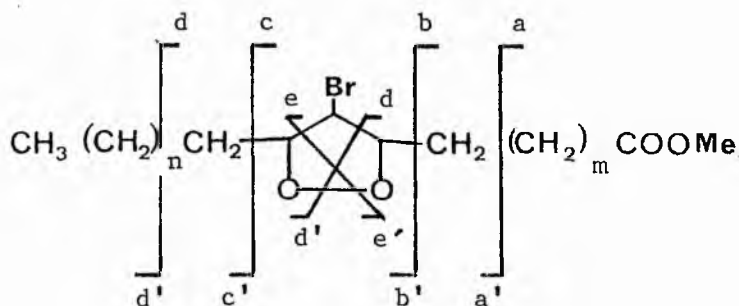
δ /ppm	assignment	
	8,10 epidioxide	9,11 epidioxide
89.08	C8,10	C9,11
57.18	C9	C10
51.21	C0 ₂ Me	C0 ₂ Me
33.85	C7,11	C8,12
31.54	C16	C16
29.21 29.02 28.84	C4,5,13,14,15	C4,5,6,14,15
25.71	C6,12	C7,13
24.68	C3	C3
22.44	C17	C17
13.87	C18	C18

infrared spectrum: absence of O-H stretch and -HC=CH- stretch.

1553cm^{-1} , 820cm^{-1} (C-O ring breathing) and

714cm^{-1} (C-Br stretch).

mass spectrum:



n = 5 m = 6
n = 6 m = 5

high mass peaks at (intense peaks only)

m/e (%)	9,11 isomer.	8,10 isomer.
359(0.5), 357(0.5)	$M^+ - 31 - H_2O$	$M^+ - 31 - H_2O$
329(0.3), 327(0.3)		
311(1.8), 309(2.0)		
293(2.3)	$M^+ - Br - H_2O_2$	$M^+ - Br - H_2O_2$
277(1.7), 279(2.0)	$e - H^+$ and/or a'	
263(1.4), 265(1.4)		$e - H^+$ and/or b', a'
249(6.7), 251(6.0)	b'	
235(1.7), 233(1.7)		
219(1.4), 217(1.4)		
213(1.4), 211(1.7)		
199(2.3), 197(2.0)		
187(21.0), 185(21.0)	$d + H^+, d - H^+$	
173(13.3), 175(9.3)		$d + H^+, d - H^+$
155(50.0)	$b - 2H^+$	
143(11.3)		
141(40.0)		$b - 2H^+$

3.5 Epoxidation of (3a,b).

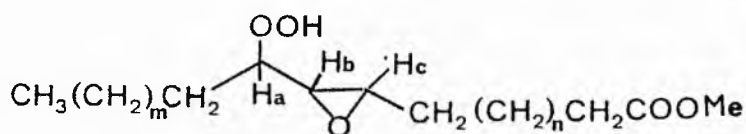
A solution of m-chloroperbenzoic acid (85 %, 260mg, 1.1mmol) in anhydrous dichloromethane (5ml) was added to a stirred solution of the allylic hydroperoxides (3a,b), (320mg, 1mmol) in dichloromethane/saturated sodium bicarbonate (50:50, 20ml). The reaction mixture was stirred at room temperature for 16h and the aqueous phase then separated. The organic layer was washed with saturated sodium bicarbonate solution (2 x 10 ml), brine (2 x 10 ml) and finally distilled water (10 ml). The aqueous washings were extracted with a small volume of dichloromethane (10 ml), the organic phases combined and dried over sodium sulphate before removal of the solvent at 5°C on a rotoevaporator. Analytical TLC showed two major

spots at R_f 0.42-0.36 and 0.24-0.20 in PE40, together with minor amounts of unidentified polar material (ca 5-8 %). Both spots gave a red colour when sprayed with peroxide detecting sprays. Preparative TLC afforded pure fractions of each component.

Band A (138mg, 41 %, R_f 0.42-0.36 in PE40) see text for assignment The following spectroscopic data was recorded.

$^1\text{Hnmr}$ spectrum: 9.45 δ (appd, 1H, -OOH), 3.98 δ (m, 1H, Ha)

3.65 δ (s, 3H, -CO₂Me), 3.10 δ (m, 1H, Hc), 2.83 δ (dd, 1H, Hb), 2.28 δ (at, 2H, -CH₂CO₂Me), 1.43 δ (shoulder, 2H, Hd), 1.27 δ (bs, chain CH₂'s), and 0.86 δ (at, 3H, CH₃-).



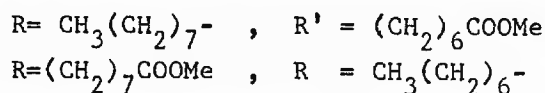
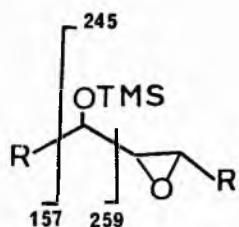
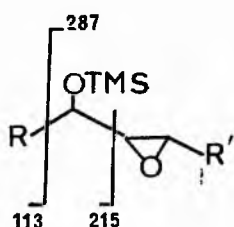
m = 5 n = 6
m = 6 n = 5

$^{13}\text{Cnmr}$ spectrum:

δ /ppm	assignments	
	9-OOH	10-OOH
174.12	C1	C1
82.51	C9	C10
60.27	C10	C9
56.52	C11	C8
51.28	-CO ₂ Me	-CO ₂ Me
33.88	C2	C2
31.62	C16	C16
31.46	C12	C12

29.90	29.43	}	C4,5,6,8,14,15	C4,5,11,13,14,15
29.16	29.03			
28.82				
25.75	25.58	}	C7,12	C12,6
25.30	25.22			
24.69			C3	C3
22.48			C17	C17
13.89			C18	C18

mass spectrum:



The hydroperoxides were reduced to the hydroxy derivatives with sodium borohydride and analysed as the TMS-ether derivatives^[42].

Significant/intense high mass peaks were observed at m/e

385($\text{M}^+ - \text{Me}$), 370($\text{M}^+ - 2\text{Me}$), 369($\text{M}^+ - \text{Me} - \text{MeOH}$), 311($\text{M}^+ - \text{OTMS}$),
259, 245(287-32), 227(259-32) and 215 plus numerous peaks
below m/e 180.

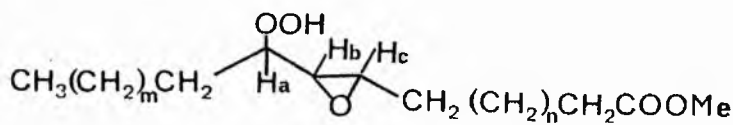
infrared spectrum: 3330 cm^{-1} (OO-H stretch), 890 cm^{-1} (C-O ring breathing)

Band B (131 mg, 39 %, R_f 0.24-0.20 in PE40) see text for assignment.

The following spectroscopic data was recorded

¹Hnmr spectrum: 8.97 δ (bs, 1H, -OO-H), 3.65 δ (s, 3H, -CO₂Me),
3.8-3.5 δ (m, 1H, Ha), 2.86 δ (ad, J=5.0Hz, 2H, Hb, Hc),

2.29 δ (at, 2H, $-\text{CH}_2\text{CO}_2\text{Me}$), 1.30 δ (bs, chain CH_2 's) and 0.86 δ (at, 3H, CH_3 -).



m = 5 n = 6

m = 6 n = 5

^{13}C nmr spectrum:

δ/ppm	assignments	
	9-OOH	10-OOH
174.09	C1	C1
85.23	C9	C10
59.66	C10	C9
55.91	C11	C8
51.27	$-\text{CO}_2\text{Me}$	$-\text{CO}_2\text{Me}$
33.87	C2	C2
31.62	C16	C16
29.46, 29.03, 28.83	C4,5,6,8,14,15	C4,5,11,13,14,15
25.74, 25.57, 25.22	C7,13	C12,6
24.68	C3	C3
22.45	C17	C17
13.87	C18	C18

mass and infrared spectra were identical with those from band A

3.6 Bromination of methyl 9(10)-hydroperoxyoctadec-10(8)-enoate (3a,b).

To a solution of (3a,b) (320 mg, 1mmol) in dry dichloromethane at 0°C was added bromine (180 mg, 1.13mmol). The solution was stirred and protected from the light, for 45min. Rotoevaporation of the solvent gave a red/brown oil which showed three spots on analytical TLC at R_f 0.77, 0.67 and 0.57 in PE30. A $^1\text{Hnmr}$ spectrum of the reaction product showed signals at 4.50-4.10 (m, 2H), 4.29 (t, 1H), 3.60 (s, 3H), 2.25 (at, 2H), 1.55 (shoulder), 1.24 (bs) and 0.81 δ (at, 3H). An infrared spectrum of the crude product showed an O-H stretching absorption at 3430cm^{-1} of medium/weak intensity. Preparative TLC afforded two major bands A and B, together with a minor unidentified trail (5mg).

Band A (342 mg, 85 %, R_f 0.77 in PE30) was identified by comparison of $^1\text{Hnmr}$, $^{13}\text{Cnmr}$, infrared and mass spectra with the product from experiment 3.4.

Band B (53 mg, 11 %, R_f 0.67 and 0.57 in PE30) was identified as an isomeric mixture of methyl 9(10)-hydroperoxy-10,12(8,9)-dibromooctadecanoates (23a,b). The following spectroscopic data was recorded.

$^1\text{Hnmr}$ spectrum: 4.23 δ (at, $J=6.0\text{Hz}$, 3H, Ha), 3.60 δ (s, 3H, $-\text{CO}_2\text{Me}$), 2.25 δ (at, $J=7.1\text{Hz}$, 2H, $-\text{CH}_2\text{CO}_2\text{Me}$), 1.55 δ (shoulder, 4H, Hd, He), 1.25 δ (bs, chain CH_2 's) and 0.81 δ (at, $J=5.7\text{Hz}$, CH_3).

infrared spectrum: 3420cm^{-1} (O-H stretch), 815cm^{-1} C-O stretch), and 712cm^{-1} (C-Br stretch).

3.7 Attempted silver trifluoroacetate induced cyclisation.

To the crude reaction product from experiment 3. was added silver trifluoroacetate in situ (1.5mmol) all at once and with vigorous stirring for 25min. The reaction was quenched by the addition of ether (50ml) and the organic solution washed with saturated brine (20ml) and finally distilled water (20ml). The organic fraction was dried over sodium sulphate. Filtration and removal of the solvent at 5°C gave a product whose TLC analysis showed a major band (>95 %) at R_f 0.77 in PE30 with small amounts of more polar material. Preparative TLC gave the major product pure to TLC. The spectroscopic and chromatographic properties were identical to the bromo cyclic peroxide (9a,b).

3.8 Tin hydride reduction of the bromo-cyclic peroxides.

To the bromo-cyclic peroxide (9a,b) (50mg, 0.13mmol) in dry hexane (5ml) was added tri-n-butyl tin hydride (0.3mmol) via microsyringe. The mixture was stirred at room temperature for 4h before washing with water (2 x 5 ml), saturated brine (5 ml) and finally water (5 ml). Isolation of the organic product in the usual manner gave a colourless oil. TLC showed a product distribution similar to that for sodium borohydride reduction of (2a,b). The major component was isolated by preparative TLC in 75 % yield and was shown to be identical with the cyclic peroxide (5a,b) by TLC, $^1\text{Hnmr}$ and infrared spectroscopy.

3.9 Catalytic hydrogenation of 5a,b).

To a round bottom flask with magnetic spinbar was added 10 % palladium/charcoal (10mg), methanol (1ml) and (3a,b) (20mg) and the mixture stirred for 30min at room temperature. The charcoal was filtered off and washed with two further aliquots of methanol (5 ml). The combined washings were rotoevaporated to give an organic product. Trimethylsilylation of the reaction product gave a product which showed only one peak on GLC analysis.

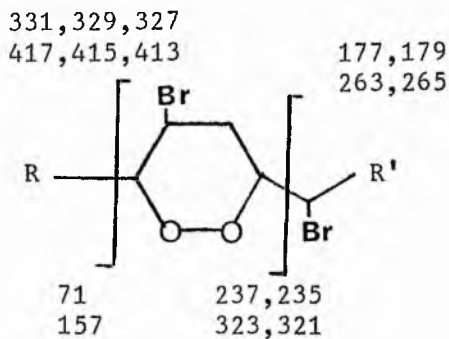
3.10 Peroxymercuration bromodemercuration of methyl linoleate.

To a vigorously stirred suspension of mercury (II) nitrate monohydrate (370mg, 1.1mmol) in dry dichloromethane was added methyl linoleate (300mg, 1mmol) in dry dichloromethane (5ml). The mixture was stirred for 24h at ambient temperature and the solvent removed on a rotary film evaporator.

Bromine (180mg, 1mmol) in dry dichloromethane (10ml) was added to a vigorously stirred suspension of the crude peroxymercurial in dichloromethane (5ml) at 0°C for 12h. Work up as described in 3.4 gave a pale yellow oil. Analytical TLC showed a broad non-polar band in PE 25 at Rf 0.75-0.65. together with more polar material. The non-polar band gave a positive peroxide test with peroxide detecting spray. Isolation of the peroxidic material by preparative TLC gave a pale yellow oil (179mg, 40 %) which is tentatively assigned as a mixture of dibromo cyclic peroxides (18a,b) on the basis of the following spectroscopic data.

¹Hnmr spectrum: 4.38 δ (m, 2H, -CHOO), 4.00 δ (m, 2H, -CHBr),
3.65 δ (s, 3H, ?CO₂Me), 3.0-2.5 δ (m),
2.27 δ (at, J=7.4Hz, 2H, -CH₂CO₂Me), 1.60 δ
(bs, chain CH₂'s) and 0.87 δ (at, J=5.4Hz, CH₃-).

Mass spectrum:



high mass peaks at 323 (1.3), 321 (1.3)
307 (4.3), 293 (6.3), 291 (11.3), 289 (11.7)
249 (5), 247 (5), 237 (3.3), 235 (3.3), 221
(3.3), 219 (3.6), 209 (10), 199 (6), 195
(5), 193 (7.3), 187 (8.3), 185 (13), 181
(7), 177 (24.3), 171 (6.6), 157 (12), 155
(40.0).

References.

1. See a) E.N. Frankel in "Fatty Acids" (Ed. E.H. Pryde),
Amer. Oil Chem. Soc., Champaign, Ill. 1979, Ch. 17, pp 343-378.
b) V. Karnojitzky, Russ. Chem. Rev., 1972, 41, 630
2. For recent reviews see a) E.N. Frankel., Progr. Lipid Res., 1980, 19, 1
b) S. Matsushita and J. Terao in "Autoxidation in Food and
Biological Systems" (Ed. M.G. Simic and M. Karel), Plenum,
New York, 1980, pp 27-44.
see also c) D. Cobern, J.S. Hobbs, R.A. Lucas and D.J. Mackenzie,
J. Chem. Soc., (C)., 1966, 1897.
d) E. Federi, G. Gamurati and G. Jacini, J. Amer. Oil Chem. Soc.,
1973, 48, 787.
e) H.W.S. Chan, J. Amer. Oil Chem. Soc., 1977, 54, 100.
f) J. Terao and S. Matsushita, J. Amer. Oil Chem. Soc., 1977, 54, 234.
g) E.N. Frankel, W.E. Neff and T.R. Bessler, Lipids., 1979, 14, 961.
h) B.A. Svingen, F.O. O'Neal and S.D. Aust, Photochem. Photobiol.,
1978, 28, 803.
3. J. Terao and S. Matsushita, Agric. Biol. Chem., 1975, 39, 2027.
4. D.T. Coxon, K.R. Price and H.W.S. Chan., Chem. Phys. Lipids, 1981, 28, 365.
5. W.E. Neff., E.N. Frankel and D. Weisleder, Lipids 1981, 16, 439.
6. M. Roza and A. Francke., Biochem. Biophys. Acta., 1978, 528, 119.
7. P. Haverkamp Begemann, W.J. Woesterburg and S. Leer.,
J. Agric. Food Chem., 1968, 16, 679.
8. D.E. O'Connor., E.D. Mihelich and M.C. Coleman.,
J. Amer. Chem. Soc., 1981, 103, 223.
9. H.W.S. Chan, J.A. Matthew and D.T. Coxon, J.C.S. Chem. Comm., 1980, 235.
10. E.D. Mihelich, J. Amer. Chem. Soc., 1980, 102, 7141.
11. N.A. Porter, J. Nixon and R. Isaac, Biochem. Biophys. Acta
1976, 441, 506.

12. N.A. Porter, M.O. Funk, D. Gilmore, R. Isaac and J. Nixon.,
J. Amer. Chem. Soc., 1976, 98, 6000.
13. E.N. Frankel, D. Weisleder and W.E. Neff,
J.C.S. Chem. Comm., 1981, 766.
- 14a) W.F. Brill., J. Amer. Chem. Soc., 1965, 87, 3286.
b) G.O. Schenck, O.A. Neumuller and W. Elsfeld,
Justus Liebigs Ann. Chem., 1958, 618, 262.
- 15a) A.J. Bloodworth and M.E. Loviett, J.C.S. Chem. Comm., 1976, 94.
b) A.J. Bloodworth and M.E. Loviett, J.C.S. Perkin 1., 1978, 522.
16. A.J. Bloodworth and J.A. Khan, J.C.S. Perkin 1., 1980, 2456.
17. J.R. Nixon, M.A. Cudd and N.A. Porter, J. Org. Chem., 1978, 43, 4048.
18. E. Bascetta and F.D. Gunstone, unpublished results.
19. F.D. Gunstone and R.P. Inglis, Chem. Phys. Lipids, 1973, 10, 73 and 89.
- 20a) F.V. Brutcher, Jr., T. Roberts, S.J. Barr, and N. Pearson.,
J. Amer. Chem. Soc., 1959, 81, 4915.
b) F.V. Brutcher, Jr., and W. Bauer, Jr., Science 1960, 132, 1489.
c) F.V. Brutcher, Jr., and W. Bauer, Jr., J. Amer. Chem. Soc., 1962, 84,
2233 and 2236.
21. J.P. McCullough, D.R. Douslin, W.N. Hubbard, S.S. Todd,
J.F. Messerly, I.A. Hossenlopp, F.R. Frow, J.P. Dawson and
G. Waddington, J. Amer. Chem. Soc., 1959, 81, 5884
and references therein.
22. M. Hancock in "Conformational Theory", Academic Press, New York,
1965, pp 77.
23. E. Bascetta, J.R. Ball and F.D. Gunstone., to be published
(see Chapter 6).

24. J.E. Baldwin, J.C.S. Chem. Comm., 1976, 734.
25. J.E. Baldwin, J. Cutting, W. Dupont, L. Kruse, L. Silberman and R.C. Thomas, J.C.S. Chem. Comm., 1976, 736.
26. A.J. Bloodworth and I.M. Griffin, J.C.S. Perkin 1 1975, 696 and references cited therein.
27. Although we have interpreted the mass spectrum in terms of the six-membered cyclic peroxides, the presence of five and/or seven membered rings cannot be discounted from our available data.
28. L. Batt and F.R. Cruickshank, J. Phys. Chem., 1967, 71, 1836.
29. A.J. Bloodworth, A.G. Davies, I.M. Griffin, B. Nuggleton and B.P. Roberts., J. Amer. Chem. Soc., 1974, 96, 7599.
30. A.J. Bloodworth and G.S. Bylina, J.C.S. Perkin 1, 1972, 2433.
31. R.P. Quirk and R.E. Lea., J. Amer. Chem. Soc., 1976, 98, 5973.
32. C.C. Hill and G.M. Whitesides, J. Amer. Chem. Soc., 1976, 98, 5973.
33. N.A. Porter and J.R. Nixon, J. Amer. Chem. Soc., 1978, 100, 7116.
34. N.A. Porter, M.O. Funk, D.W. Gilmore, S.R. Isaac, D.B. Menzel, J.R. Menzel, J.R. Nixon and J.H. Roycroft, in "Biochemical Aspects of Prostaglandins and Thromboxanes" (Ed. N. Kharasch and J. Fried). Academic, New York, 1977, pp39.
- 35a) A.J. Bloodworth and H.J. Eggette, J.C.S. Perkin 1, 1981, 1375.
- b) A.J. Bloodworth and H.J. Eggette, J.C.S. Perkin 1, 1981, 3272.
- c) N.A. Porter and D.W. Gilmore, J. Amer. Chem. Soc., 1977, 99, 3503.
- d) W. Adam, A. Birke, C. Cadiz, S. Diaz and A. Rodriguez, J. Org. Chem., 1978, 43, 1154.
- e) P.G. Cookson, A.G. Davies and B.P. Roberts., J.C.S. Chem. Comm., 1976, 1022.

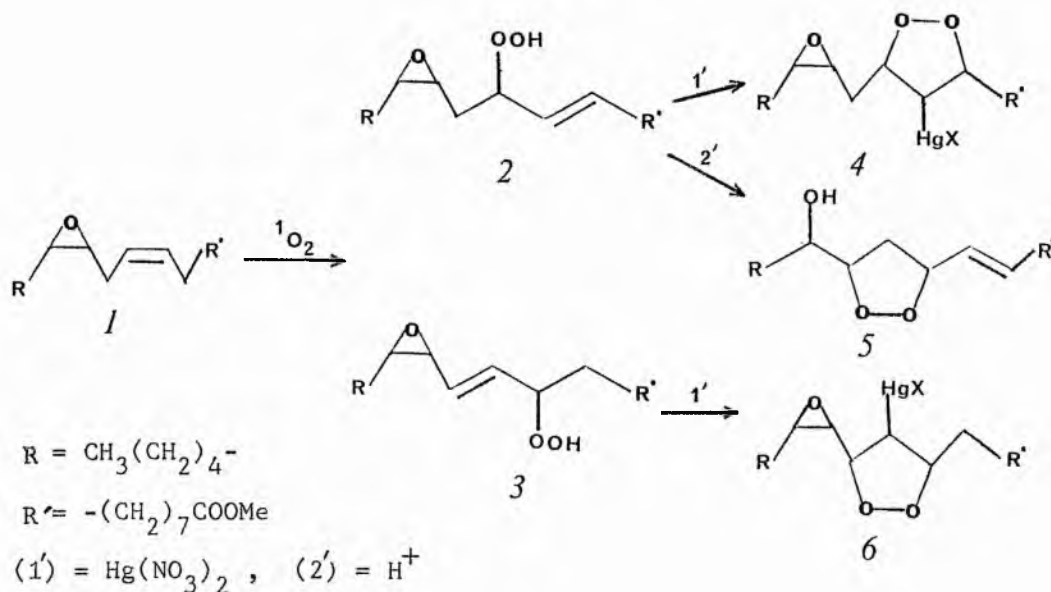
36. K.R. Kopecky, J.E. Filby, C. Mumford, P.A. Lockwood and J.Y. Ding, Canad. J. Chem., 1975, 53, 1103.
37. A.J. Bloodworth and B.P. Leddy, Tet. Lett., 1979, 729.
- 38a) D. Milstein and J.K. Stille, J. Org. Chem., 1979, 44, 1613.
- b) J.E. Leibner and J. Jacobus, J. Org. Chem., 1979, 44, 449.
- 39a) M.F. Salomon and R.G. Salomon., J. Amer. Chem. Soc., 1977, 99, 3500.
- b) M.F. Salomon and R.G. Salomon., J. Amer. Chem. Soc., 1979, 101, 4290.
40. Vogel's textbook of Practical Organic Chemistry, 4th Ed., Longman Press, New York, 1978.

Section 3

**Photosensitised oxidation of oxygenated
fatty acid esters.**

2 Results and discussion.

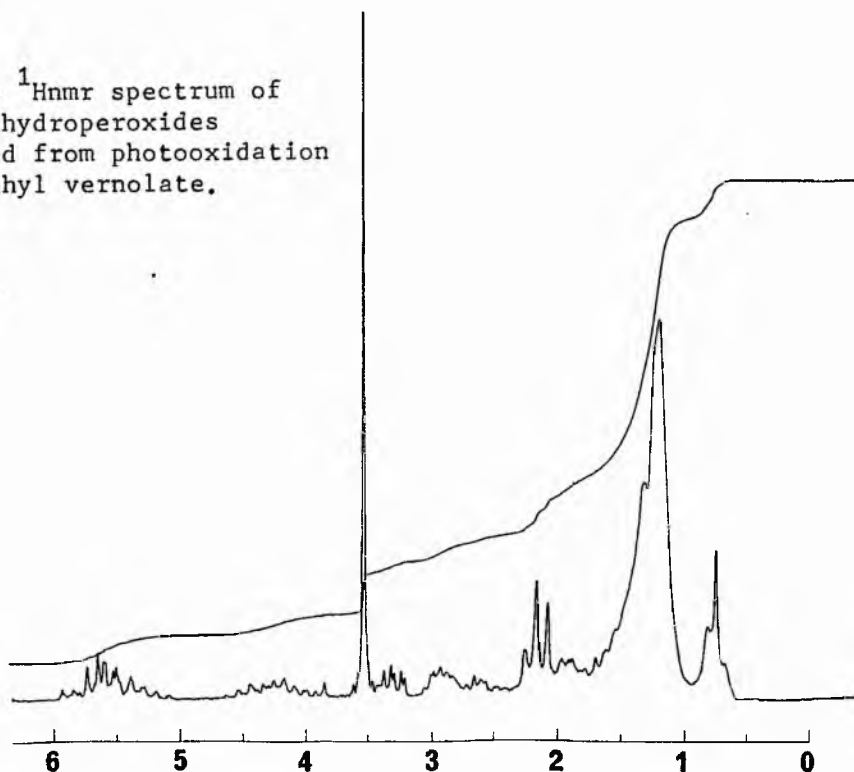
The photosensitised oxidation of methyl vernolate (1) should give rise to two positional isomeric hydroperoxides (2 and 3) in which the double bond has undergone a shift in position by one carbon atom as required by an ene-type reaction^[13]. Both of the hydroperoxy-oxiranes would be interesting synthons for the target molecules (4-6). The β -hydroperoxy-oxirane (2) could conceivably undergo acid catalysed cyclisation via a 5-endo process to give (5). The hydroperoxide (3) on the other hand cannot undergo a similar reaction since this would involve the incorporation of a trans double bond in a six membered (via 6-exo cyclisation) or a seven membered (via 7-endo cyclisation) ring.



Both hydroperoxides (2) and (3) could undergo an intermolecular peroxymercuration as described in section 2 of this chapter via a 5-endo cyclisation onto the intermediate mercurium cation to give the mercury adducts (4) and (6).

The photosensitised oxidation of methyl vernolate in carbon tetrachloride/methanol (95:5) solution for 36 hr at ambient temperature gave only one new product on TLC analysis. The new product accounted for 80 % of the reaction mixture and was shown to be peroxidic by spraying with 4-amino-N,N-dimethylaniline hydrochloride (2 %) in methanol. The photooxidation takes place with first-order kinetics and under the conditions described in the experimental, the first-order rate constant was $7.8 \times 10^{-6} \text{ s}^{-1}$. The pure peroxidic product, isolated by prep. TLC on prewashed plates of silica gel G, was very labile and decomposed rapidly at ambient temperature (estimated $t_{1/2}$ from TLC analysis of 16-24 hr).

FIGURE 1. 90 MHz ^1H nmr spectrum of epoxy hydroperoxides derived from photooxidation of methyl vernolate.



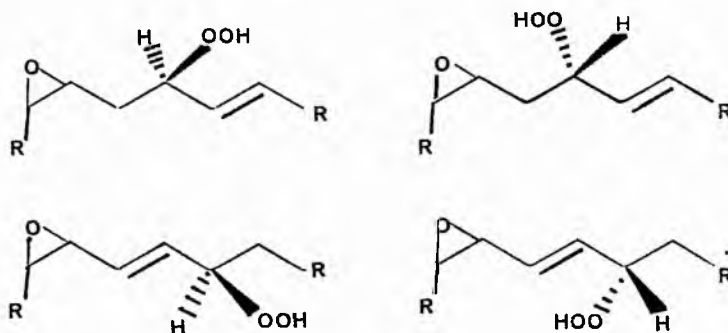
The ¹Hnmr spectrum of the product (Figure 1) was very complex, and extensive decoupling experiments were required for its interpretation. It was anticipated that the spectrum of (2) would be distinct from that of (3) by virtue of the methylene group at C11 in (2).

Decoupling of the olefinic protons at 5.6 δ collapsed the 3.5-3.2 δ multiplet, the 1.93 δ doublet and also affected the 2.60 δ multiplet, but had no effect on the 2.90 δ complex multiplet. Decoupling the peroxy methines at 4.3 δ affected the olefinic signals, as expected for an allylic peroxy methine. The 2.60 δ multiplet collapsed into an apparent doublet ($J=5.0$ Hz). Decoupling the signal at 3.3 δ altered the olefinic hydrogen signal only, whereas decoupling at 2.9 δ had no apparent effect on the spectrum although the adjacent signal at 2.6 δ was obscured as a result of the applied decoupling power. Finally decoupling the 2.9 δ signal had no effect on the olefinic proton signals or the signal at 3.3 δ . The peroxy methines signal was altered however and once again the adjacent signal, at 2.6 δ was lost as a result of the applied decoupling power and may or may not have been affected.

On the basis of the decoupling experiments the signal at 3.5-3.2 δ (apparent double doublet) can be unambiguously assigned to the epoxy protons of (3), the signal at 2.90 δ to the epoxy protons of (2) and the signal at 2.60 δ to the C11 methylene group of hydroperoxide (2). From the ratio of the epoxy signal integrals (aa 1:1) we estimate that both isomers are formed in equal amounts.

Each hydroperoxide has three chiral centres, two of which, the

epoxy carbons are of known absolute configuration (12S,13R)^[14,15]. Hence two diastereoisomers will be formed for each positional isomer, these are depicted below, the product however will be a racemic mixture of all the diastereoisomers.

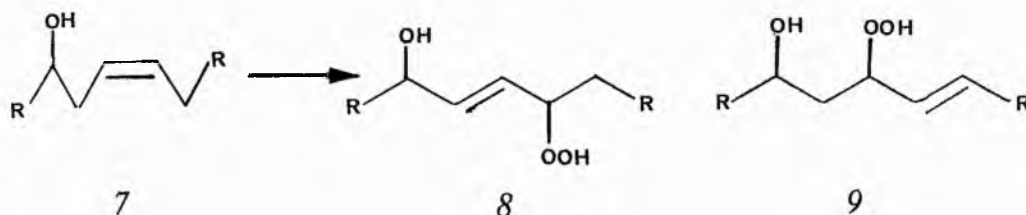


Double and continuous development TLC experiments suggested that two bands were barely resolvable on an analytical scale. Possibly analytical or semi-preparative HPLC would be more successful

The lability of the products to thermal decomposition made attempted further transformations as outlined earlier difficult. Peroxymercuration-demercuration resulted in numerous products being formed with none predominating. Similarly attempted acid catalysed cyclisation resulted in a host of products. Neither reaction was examined further.

2.2 Photosensitised oxidation of methyl ricinoleate.

The photosensitised oxidation of methyl ricinoleate (7) can lead to two positional isomeric hydroperoxy alcohols (8 and 9).



Further transformations of these products is likely to be more complex than the corresponding vernolate derivative since the hydroxyl group may compete with the hydroperoxy group in any attempted cyclisation.

Photosensitised oxidation of methyl ricinoleate for 36 hr gave three major products on analytical TLC analysis together with a fourth minor fraction. Figure 2 shows a typical chromatogram after approximately 75 % consumption of the starting hydroxy ester. Isolation of each of the individual components by preparative TLC at 0°C was difficult as a consequence of the poor separation of the bands and their intrinsic instability. Even when stored at -20° considerable decomposition of the products was observed within 16 hr. All the bands gave a positive test when sprayed with peroxide detecting reagents. Pure fractions were obtained by repeated development chromatography and taking only the central portion of each band, thus minimising contamination from adjacent bands.

The three major bands labelled B-D gave $^1\text{Hnmr}$ spectra which were

readily interpretable after extensive decoupling experiments. The $^1\text{Hnmr}$ spectra of band B and D are shown in Figure 3. The $^1\text{Hnmr}$ of band C was similar to that shown for band D except that the -OOH absorption was so broad as to be unobservable. The spectra for bands B and D are readily distinguishable, band B gives rise to two well resolved methine signals, at 4.52 and at 3.75 δ . Band D shows a composite multiplet corresponding to the two methines. Band B has been assigned to isomer (9) since its spectrum clearly shows the C11 methylene protons at 1.67 δ , decoupling of which collapses the peroxy-methine quartet at 4.5 δ to a broad doublet ($J=7.0$ Hz) and the hydroxy methine at 3.75 δ to a broad apparent singlet. The allylic methylenes at C7 are also observed at 2.03 δ and the signal is collapsed to a poorly resolved broad signal on decoupling the olefinic signal.

Band D shows a simpler olefinic proton splitting as a result of the similarity of substitution at the allylic sites. The hydroxy and hydroperoxy allylic methines overlap to some extent, both having a double triplet structure, which appears as an apparent quartet splitting. Decoupling of the olefinic protons collapses both methine signals to triplets ($J=4.0$ Hz).

The infrared spectra of all three isomers confirmed the trans nature of the double bond (970 cm^{-1}) as required by the ene-mechanism^[13]. $^{13}\text{Cnmr}$ spectra were obtained for bands B and D only. The ^{13}C chemical shifts of the important functionalised carbons between C9 and C12 are given in Table 1.

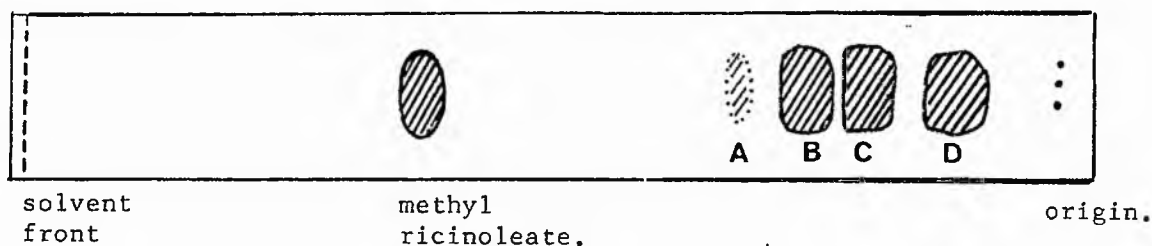


FIGURE 2. Thin layer chromatogram of the products of photosensitized oxidation of methyl ricinoleate. Solvent: petroleum ether diethyl ether (40/60 v/v).

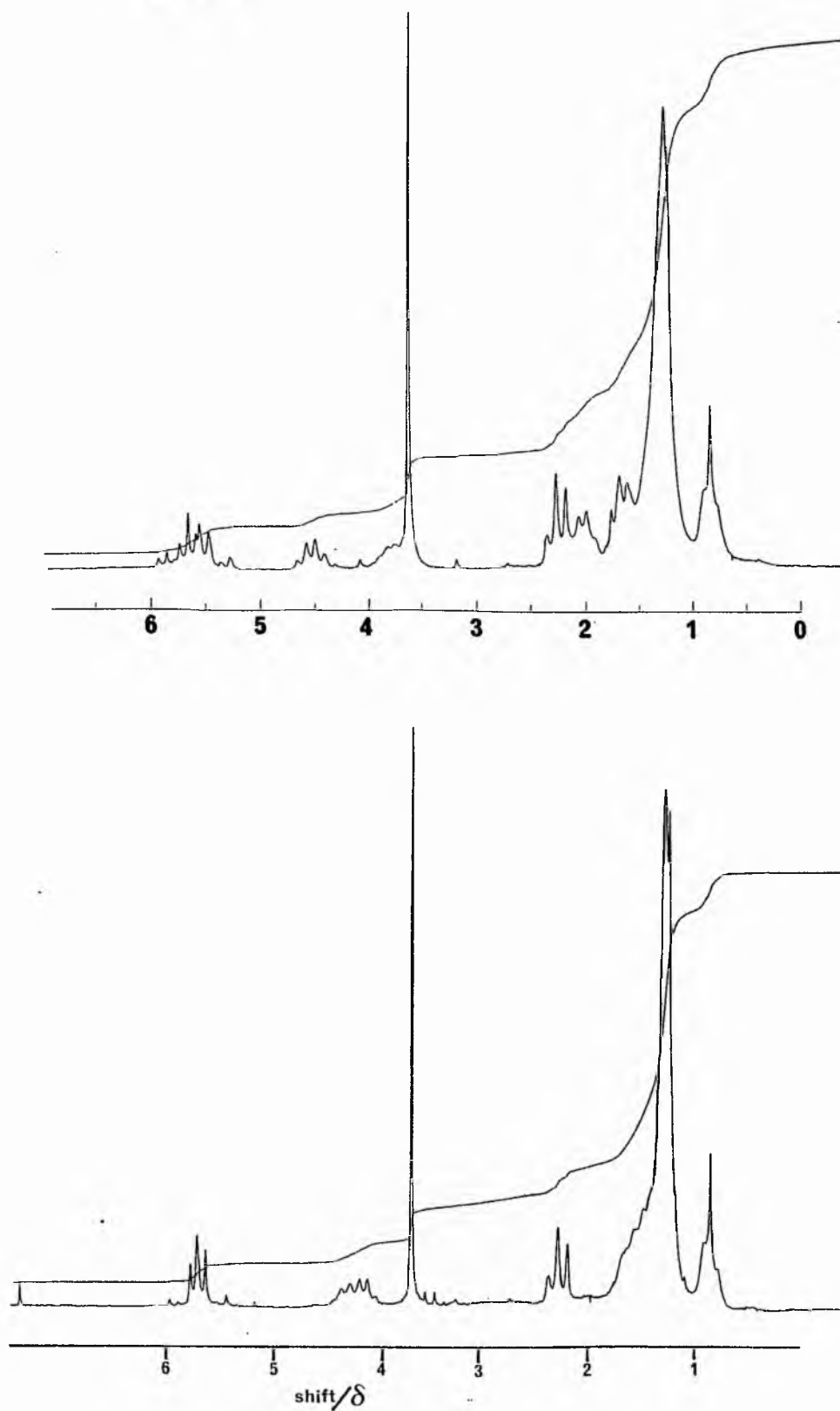
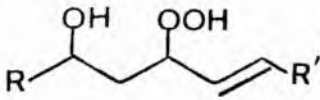
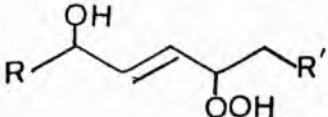


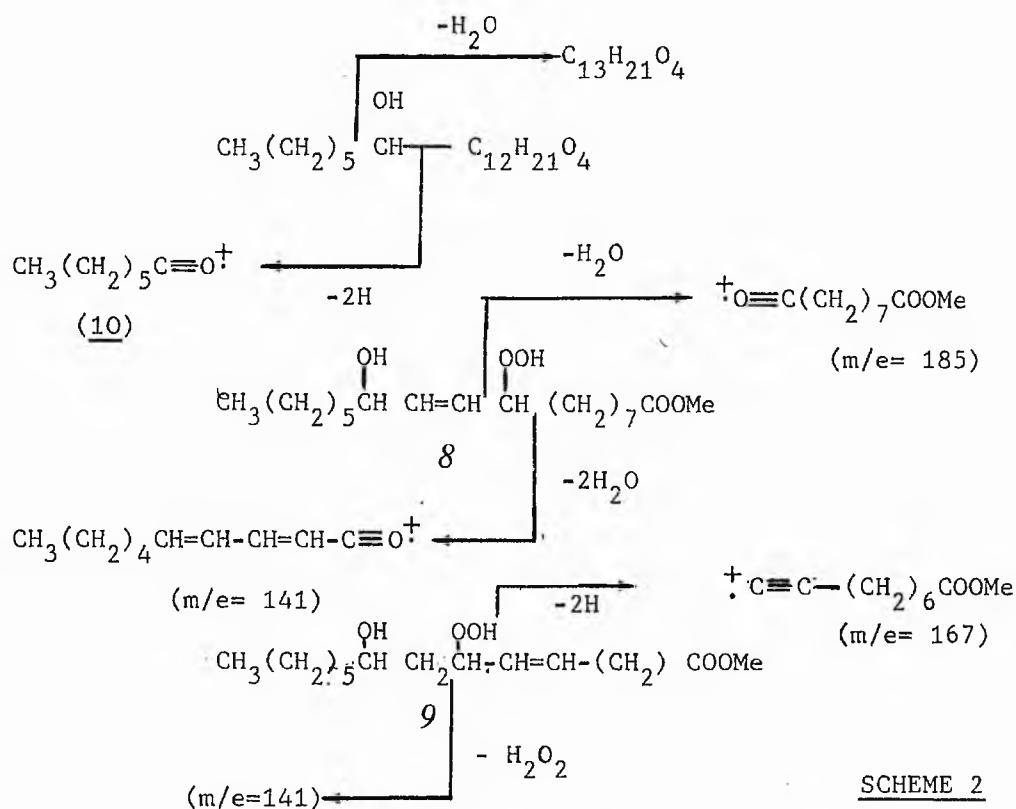
FIGURE 3. 90 MHz ^1H nmr spectrum of hydroxy hydroperoxides derived from photooxidation of methyl ricinoleate.
Top. Methyl 12-hydroxy-10-hydroperoxyoctadec-8E-enoate.
Bottom. Methyl 12-hydroxy-9-hydroperoxyoctadec-10E-enoate.

Table 1 Selected ^{13}C chemical shifts for (8) and (9).

	C=C	C-OH	C-OOH	CHOH-CH ₂ -CHOOH
	135.65 128.31	68.30	83.33	40.32
	137.89 129.85	72.38	86.02	—

In general mass spectral fragmentation patterns of hydroperoxides are weak, lacking characteristic high mass fragment ions. The mass spectra of B, C and D showed few intense peaks above m/e 100 but those that were observed could readily be assigned on the basis of the proposed structure. In particular, cleavage between the C12-C13 bond (β to the OH group) gives a fragment which readily losses H_2O to give a fragment of m/e 241. β -Cleavage at the C11-C12 bond gives a fragment ion which readily losses 2H^+ to give the fragment ion (10). Likewise, β -cleavage to the hydroperoxide in (9) with subsequent loss of 2H or H_2O_2 gives fragment ions at m/e 167 and 141 respectively which are amongst the most intense of the high mass peaks.

β -Cleavage to the hydroperoxide in isomers of (8) after loss of H_2O gives fragment ions at m/e 185 and 141. The cleavages are shown schematically in Scheme 2.

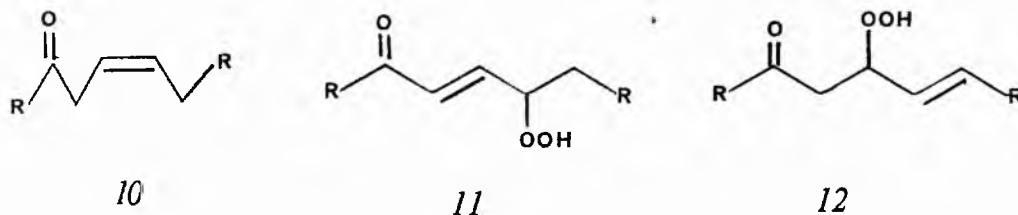


SCHEME 2

2.3 Photosensitised oxidation of methyl 12-oxooleate.

Methyl 12-oxooleate was prepared in good yield by chromic acid oxidation of methyl ricinoleate^[16]. As for methyl vernolate photosensitised oxidation of the keto ester gave only one new spot on TLC analysis after 75 % conversion (determined by GLC). The product was shown to be peroxidic by spraying with 4-amino-N,N-dimethylaniline hydrochloride (2 %) in methanol and hydroperoxidic by reduction of the reaction mixture which gave a non-peroxidic product. The hydroperoxides were isolated by simple preparative TLC at $0^\circ C$ on

prewashed silica plates in high yield. The isolated product appeared slightly more stable than the corresponding vernolate or ricinoleate hydroperoxides, although it too decomposed readily at ambient temperatures. Two keto hydroperoxides can be envisaged from the photosensitised oxidation of the keto ester.



The $^1\text{Hnmr}$ spectrum of the isolated product is shown in Figure 4. The two types of peroxy methines have different chemical shifts occurring at 4.35 (isomer 11) and 4.62 δ (isomer 12). Decoupling of the 4.35 δ signal collapsed the 6.0-6.9 δ multiplet into a double doublet.

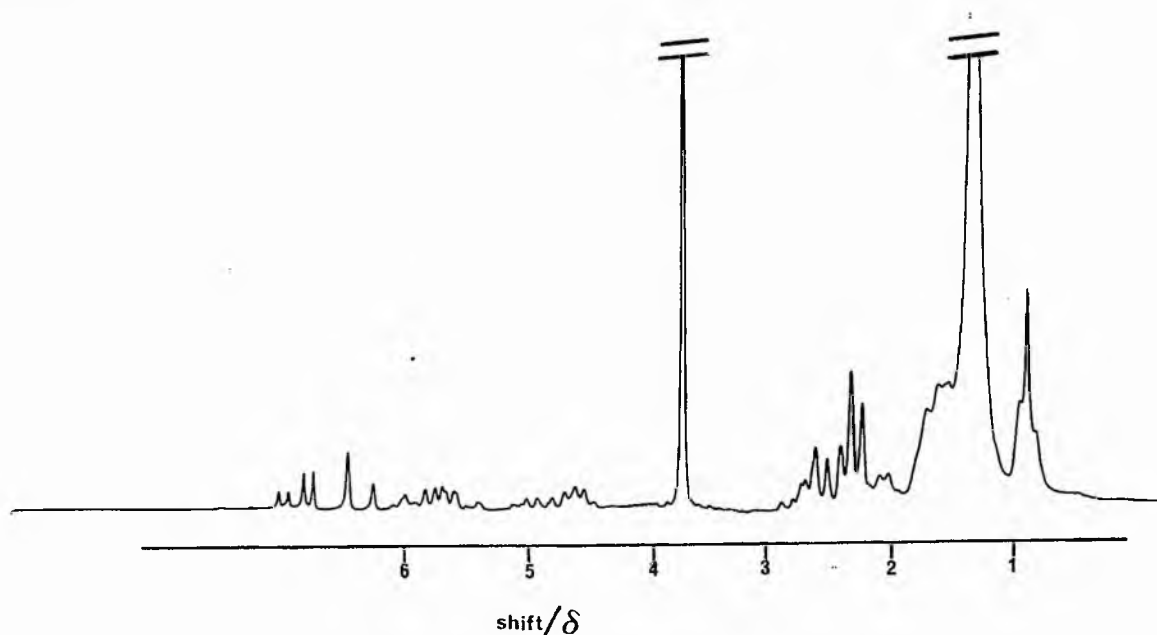
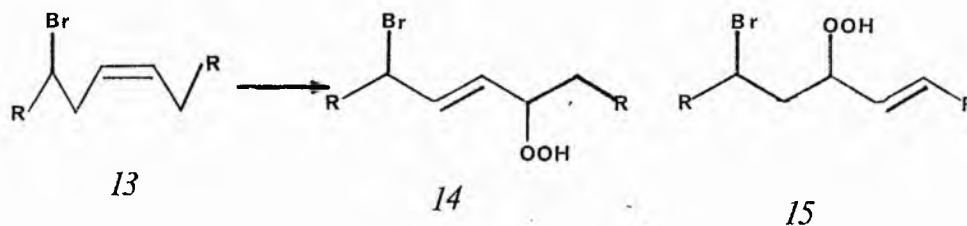


FIGURE 4. 90 MHz $^1\text{Hnmr}$ spectrum of hydroperoxy ketones (11 and 12) derived from photooxidation of methyl 12-oxooctadec-9Z-enoate.

The infrared spectrum shows three strong absorptions in the carbonyl region. The most intense of these is the ester carbonyl stretch, the absorption at 1660cm^{-1} has been assigned to the keto stretch frequency for isomer 12 and the absorption at 1630cm^{-1} to isomer 11 on the basis that extended conjugation lowers the stretching frequency.

2.4 Photosensitised oxidation of methyl 12-bromooleate.

As with the other three compounds studied in this work, singlet oxidation of methyl 12-bromooleate (13) can lead to two positional isomeric hydroperoxides (14 and 15).



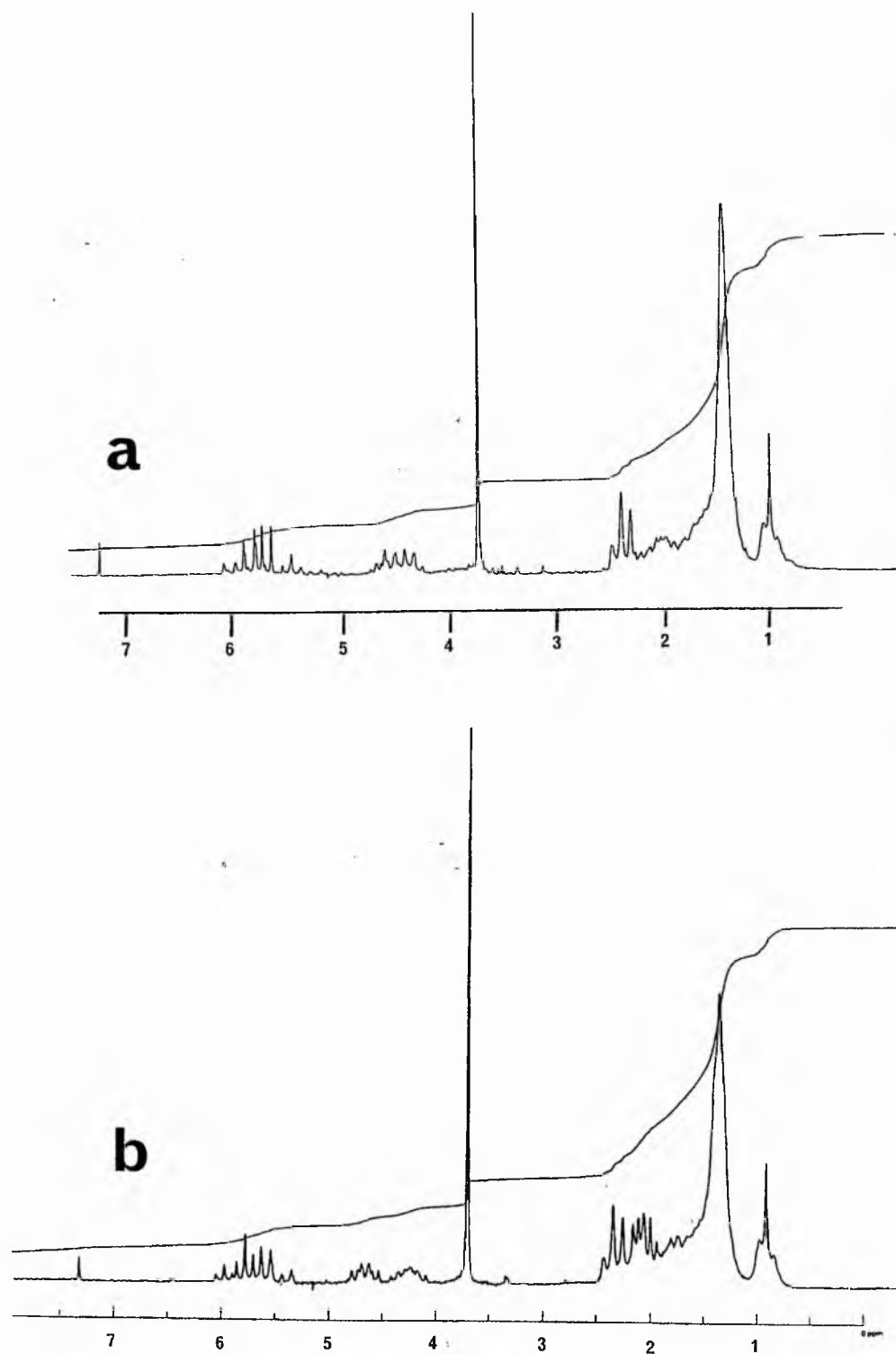
Photosensitised oxidation of methyl 12-bromooleate (13) for 33h at ambient temperature gave two major and one minor products on analytical TLC analysis. The two major products which were both peroxidic were isolated pure in small amounts by preparative TLC at 0°C . The third minor component was also isolated but was not

completely identified.

The least polar band (R_f 0.48 in PE35) has been unambiguously identified as the 9-hydroperoxy isomer (14) on the basis of its $^1\text{Hnmr}$ spectrum (Figure 5a). The signals for the peroxy methine and the bromo methine partially overlap (4.25-4.75 δ). Decoupling either of the overlapping quartets collapsed the olefinic signal and also the signal at 1.45 δ (methylenes α to the bromo and hydroxy bearing carbons). Decoupling of the olefinic protons collapses both of the overlapping quartets at 4.25-4.75 δ to triplets.

The more polar of the two major bands was identified as the 10-hydroperoxy isomer. Once again the $^1\text{Hnmr}$ spectrum (Figure 5b) was definitive for the identification. In this case the signals for the peroxy and bromo methines are completely resolved from one another. This type of behaviour was also observed for the hydroperoxides derived from methyl ricinoleate. The methylene at C11 is clearly present at 2.10 δ as a double doublet ($J=8.0\text{Hz}$, $J=4.0\text{Hz}$). The infrared spectra showed the expected O-O-H stretching signal and also confirmed the trans stereochemistry of the olefinic bond for both isomers.

FIGURE 5. 90 MHz ^1H nmr spectrum of hydroperoxy-bromides derived from photooxidation of methyl 12-bromo-octadec-9Z-enoate.
a) methyl 12-bromo-9-hydroperoxyoctadec-10E-enoate.
b) methyl 12-bromo-10-hydroperoxyoctadec-8E-enoate.



3 Experimental.

3.1 General procedures.

Methyl vernolate and ricinoleate were prepared by either reported procedures^[17] or by preparative HPLC separation from methyl esters of *Vernonia anthelmintica* seed oil and castor oil respectively.

3.1 Preparation of methyl 12-oxooctadeca-9Z-enoate.

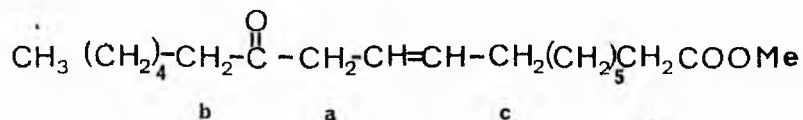
Sodium dichromate (3.25g) in distilled water (5ml), acetic acid (30ml), conc. H_2SO_4 (2ml) was quickly added to a vigorously stirred solution of methyl ricinoleate (5.00g, 1.67mmol) in acetic acid (50ml). After 30s iced-water (50ml) was added all at once and the mixture transferred to a separatory funnel and ether (50ml) added. The organic phase was extracted and washed with water (20ml), saturated sodium bicarbonate (2x20ml) and again with water (20ml). The ethereal layer was dried over sodium sulphate and the solvent removed at reduced pressure. Column chromatography on sorbsil, eluting with a PE gradient from PE 15-40 gave the 12-oxo ester (2.40g, 48 %) and unreacted methyl ricinoleate (0.83g, 17 %). The following spectral characteristics were recorded for methyl 12-oxooctadeca-9Z-enoate.

¹Hnmr spectrum: 5.37δ(t, J=5.0 Hz, 2H, olefinic H), 3.46δ(s, 3H, -COOMe).

2.95 δ(d, J=7.0 Hz, 2H, Ha), 2.23δ(at, J=7.4 Hz, 2H, -CH₂COOMe), 2.09δ(at, J=7.6 Hz, 2H, Hb), 1.83δ(m, 2H, He), 1.13δ(bs, chain CH 's) and 0.68δ(at,

$J=5.4$ Hz, 3H, CH_3 -).

the assignments were confirmed by extensive decoupling experiments.



^{13}C nmr spectrum: 210.18, 176.64, 136.26, 125.04, 54.34, 45.46, 44.87
37.23, 35.16, 32.56, 30.89, 28.36, 27.15, 25.98 and
17.35. ppm

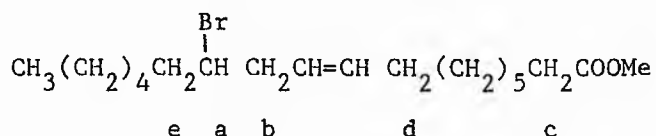
The free acid (4.2g, 84 %, mp $35-7^\circ\text{C}$) was prepared as above from ricinoleic acid. However considerable double bond migration was observed on attempted esterification.

3.3 Preparation of 12-bromooctadec-9Z-enoate.

Freshly redistilled phosphorous tribromide ($\text{Bp}_{1.5}$ $31-2^\circ\text{C}$, 3.42g) was added slowly to well stirred and cooled solution of methyl ricinoleate (4.42g, 14mmol) in anhydrous ether (15ml) and dry pyridine (1ml). The reaction mixture was refluxed for 18h. After cooling and the addition of distilled water (20ml), the product was extracted with ether (2x15ml), washed with brine (10ml), sodium bicarbonate solution (10ml) and finally distilled water (10ml). TLC (PE 30) showed a major (R_f 0.84) and a minor (R_f 0.31) product. Column chromatography, eluting with PE 10, gave methyl 12-bromooctadeca-9Z-enoate (4.8g, 87 %, R 0.84). The following spectroscopic properties were

recorded.

$^1\text{Hnmr}$ spectrum: $5.48\delta(\underline{\text{cm}}, 2\text{H}, \text{olefinic H})$, $4.00\delta(\underline{\text{qu}}, J=6.1\text{Hz}, 1\text{H}, \text{Ha})$
 $3.65\delta(\underline{\text{s}}, 3\text{H}, -\text{COOMe})$, $2.60\delta(\underline{\text{at}}, J=7.0\text{Hz}, 2\text{H}, \text{Hb})$,
 $2.27\delta(\underline{\text{at}}, J=7.4\text{Hz}, 2\text{H}, \text{Hc})$, $2.00\delta(\underline{\text{d}}, J=6.0\text{Hz}, \text{Hd})$,
 $1.70\delta(\underline{\text{m}}, 2\text{H}, \text{He})$, $1.26\delta(\underline{\text{bs}}, \text{chain } \text{CH}_2 \text{ 's})$ and
 $0.85\delta(\underline{\text{at}}, J=5.4\text{Hz}, \text{CH}_3-)$.



$^{13}\text{Cnmr}$ spectrum: 174.01, 132.48, 125.60, 57.09, 51.19, 38.34, 36.74,
 33.91, 31.52, 29.23, 28.94, 28.53, 27.40, 24.77, 22.40
 and 13.84.

Infrared spectrum: showed an absence of O-H stretch.

3.4 General procedure for photooxidation.

Methyl ester (750mg) was dissolved in carbon tetrachloride/methanol (95:5 v/v) solution containing methylene blue (50mg). The solution was illuminated in a photooxidation apparatus with 3x150W tungsten lamps for approximately 38h. The progress of the reaction was monitored by TLC.

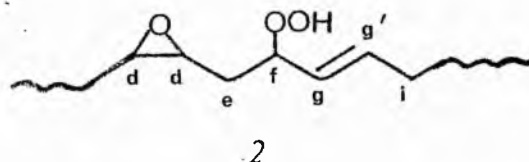
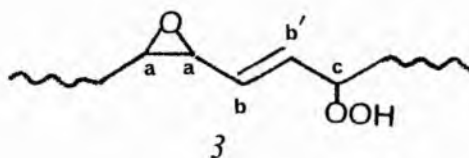
3.5 Photosensitised oxidation of methyl vernolate (3).

TLC of the reaction product showed only one spot in addition to the starting material, at lower R_f value. Preparative TLC at 0°C with PE 30 gave bands A and B.

Band A (R_f 0.71 in PE 30., 92mg., 12 %, ECL=23.4) was identified as unreacted starting material by $^1\text{Hnmr}$, ir, GLC, and TLC comparison with authentic material.

Band B (R_f 0.23 in PE 30, 584mg, 78 %) was identified as a mixture of hydroperoxy-oxiranes (2 and 3) on the basis of the following spectroscopic evidence.

$^1\text{Hnmr}$ spectrum 9.43 δ (s, 1H, -OOH), 5.95-5.05 δ (cm, 2H, olefinic H Hb, b', g, g'), 4.05-3.80 δ (cm, 1H, -CH-OOH) 3.50-3.20 δ (dd, $J=4.4$ Hz, $J=6.0$ Hz, 1H, Haa') 2.90 δ (cm, 1H, Hdd'), 2.60 δ (m, 2H, He), 2.19 δ (at, 2H, -CH₂-CO₂Me), 1.93 δ (ad, 1H, Hi), 1.18 δ (bs, 18H, chain CH₂), 0.775 δ (at, 3H, CH₃-).

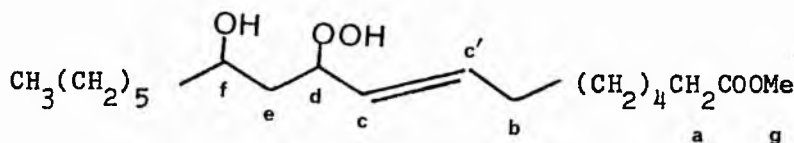


3.6 Photooxidation of methyl ricinoleate.

TLC of the reaction product on prewashed plates of silica gel G at 0°C gave four spots at R_f 0.34, 0.28, 0.22, and 0.14 in addition to the unreacted starting material. The three major bands were isolated, pure by preparative TLC using repetitive and continuous development techniques. Recovered yields were poor as a result of attempting to obtain pure material. From the charring density on analytical TLC analysis it was estimated that the major bands B-D are formed in roughly equal amounts. The minor band A constituted approximately 3-4 % of the total oxidation products.

Band B (R_f 0.28, 125mg, 16.7 %) was identified as methyl 10-hydroperoxy,12-hydroxyoctadec-9E-enoate on the basis of the following spectroscopic data;

$^1\text{Hnmr}$ spectrum: 9.40 δ (bs, 1H, OOH), 6.00-5.25 δ (m, 2H, $\text{H}_{\text{C}'}_{\text{C}}$), 4.52 δ (dt, $J=7.0$ Hz, 1H, H_d), 3.75 δ (m, 1H, H_f), 3.62 δ (s, 3H, -COOMe), 2.27 δ (at, $J=7.0$ Hz, 2H, H_a), 2.01 δ (aq, $J=6.0$ Hz, 2H, H_b), 1.67 δ (t, $J=6.0$ Hz, 2H, H_e), 1.28 δ (bs, chain CH_2 's) and 0.83 δ (at, $J=5.0$ Hz, 3H, H_g).



/ppm	assignment
174.21	C1
135.67	C8,9
128.31	
83.33	C10
68.30	C12
51.29	-CO ₂ Me
39.98	C11
37.39	C13
33.88	C2
32.01	?
31.65	C16
29.09	C4,5,6,15
28.53	
25.40	C14,7*
25.30	
24.69	C3
22.40	C17
13.86	C18

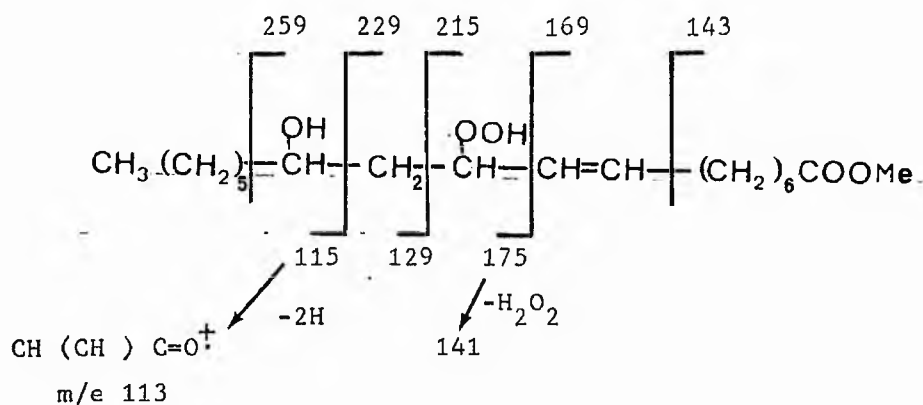
* tentative assignment.

infrared spectrum: 3480-3360cm⁻¹ (OO-H and O-H stretching) 972cm⁻¹

(trans HC=CH bending).

mass spectrum: m/e (rel %, assignment)

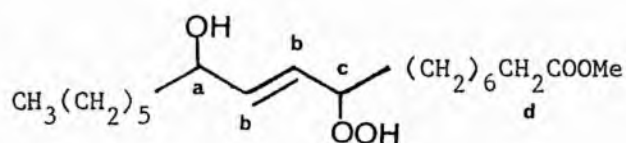
241 (0.6, 259-H₂O), 219 (1.0), 211 (0.6, 229-H₂O), 209
(0.4, 241-MeOH), 207 (0.2, 241-H₂O₂), 196 (0.7), 198
(0.4), 197 (2.1, 215-H₂O), 196 (0.7), 195 (0.2), 194
(0.2), 193 (0.4), 191 (0.3),



below m/e 190 relatively intense peaks were observed at 180 (2.1), 169 (2.0), 167 (4.2), 165 (2.4), 164 (2.1), 141 (3.5, 175-H₂O₂), 139 (3.5), 137 (8.4) 129 (2.1), 123 (3.5), 122 (3.5), 121 (3.5), 113 (8.5), 109 (6.3) and below m/e 100 intense peaks at 97, 95, 87, 84, 83, 74, 71, 70, 69, 68, 67, 59, and 55 (100, C₄H₇⁺).

Band C (R_f 0.22, 63mg, 8.4 %), was identified as methyl 9-hydroperoxy, 12-hydroxy-octadec-9E-enoate on the basis of the following spectroscopic data

¹Hnmr spectrum: 5.73 δ (dd, J=5.6Hz, 2H, Hbb'), 4.25 δ (aq, J=6.0Hz, 1H Hc), 4.08 δ (aq, J=6.0Hz, 1H, Ha), 3.60 δ (s, 3H, -COOMe), 2.30 δ (at, J=7.2Hz, 2H, Hd), 1.30 δ (bs, chain CH₂'s), and 0.88 δ (at, J=5.4Hz, 3H, CH₃-).



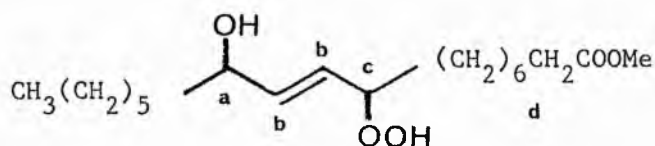
infrared spectrum: $3500-3360\text{ cm}^{-1}$ (OO-H and O-H stretch) and 972 cm^{-1} (C=C, trans C-H stretch).

mass spectrum: see band D for explanation of fragments

305 (0.1), 280 (1.0), 279 (0.2), 242 (0.4), 241 (0.4), 237 (0.4), 225 (0.6), 219 (0.6), 211 (1.0), 209 (1.0), 197 (1.0), 193 (1.0), below m/e 190 intense peaks were observed at 185 (1.8), 181 (2.0), 171 (1.4), 167 (1.4), 165 (3.2), 155 (1.0), 149 (1.0), 141 (2.0), 137 (2.0), 135 (1.6), 127 (2.9), 125 (3.6), 123 (4.3), 121 (2.8), 113 (23.6), 111 (5.0), 109 (6.8), 107 (4.3), 101 (3.9), 97 (15.7), 95 (15.0), 87 (20.7), 85 (15.7), 83 (22.1), 81 (22.9), 74 (40.4), 69 (32.1), 59 (23.9), 57 (57.1), 55 (100.0).

Band D (R_f 0.14, 105mg, 14 %), was identified as methyl 9-hydroperoxy, 12-hydroxyoctadec-9E-enoate on the basis of the following spectroscopic data;

$^1\text{Hnmr}$ spectrum: 9.20δ (bs, 1H, OO-H), 5.73δ (dd, $J=5.6\text{Hz}$, 2H, Hbb'), 4.25δ (aq, $J=6.0\text{Hz}$, 1H, Hc), 4.08δ (aq, $J=6.0\text{Hz}$, 1H, Ha), 3.60δ (s, 3H, -COOMe), 2.30δ (at, $J=7.2\text{Hz}$, 2H, Hd), 1.30δ (bs, chain CH_2 's) and 0.88δ (at, $J=5.6\text{Hz}$, 3H, CH_3 -).

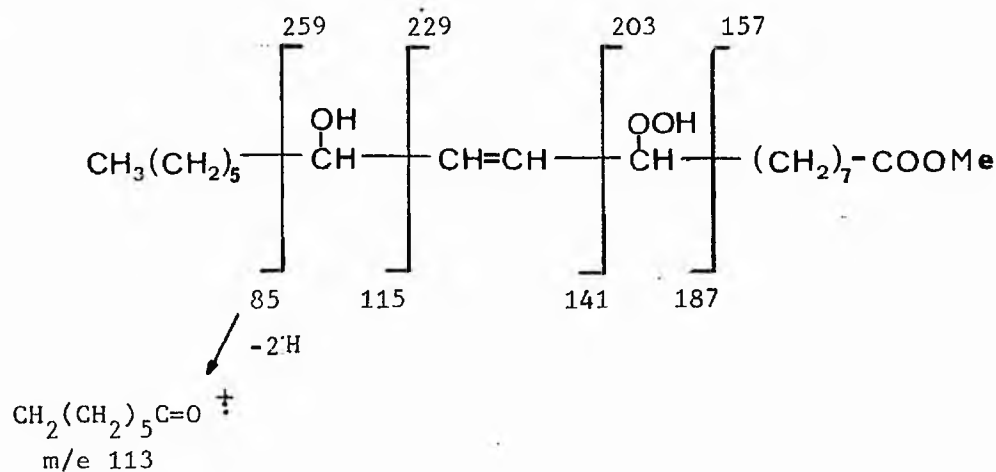


infrared spectrum: $3500-3360\text{ cm}^{-1}$ (OO-H and O-H stretch) and 972 cm^{-1}
(C=C, trans, C-H stretch).

^{13}C nmr spectrum:

shift/ppm	assignment
174.31	C1
137.89	} C10,11
129.85	
86.02	C9
72.38	C12
51.31	-CO ₂ Me
37.04	C13
33.94	C2
32.29	C8
31.67	C16
29.57	} C4,5,6,15
29.06	
28.87	
25.21	} C7,14
25.07	
24.74	C3
22.46	C17
13.91	C18

mass spectrum (70eV):

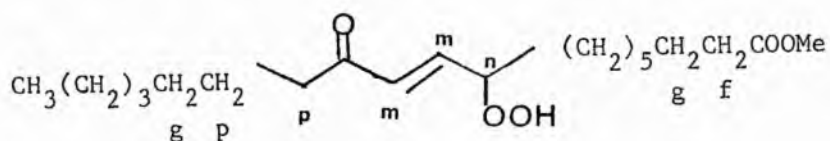
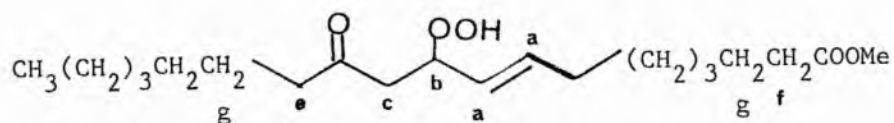


308(0.6, $M^+ - 2H_2O$), 279 (0.9), 277 (0.4), 265 (0.2)
 242 (0.2, 259-OH), 241 (0.4, 259- H_2O), 238 (0.4),
 237 (1.2), 225 (0.8, 259- H_2O_2), 223(0.2), 221 (0.2),
 213 (0.8), 212 (0.4), 211 (3.9, 229- H_2O), 210 (0.2),
 209 (5.8), 207 (0.2), 199 (0.2), 198 (0.2), 197 (0.4),
 193 (0.8, 229- $2H_2O$),
 below m/e 190 intense peaks observed at m/e
 185 (4.7, 203- H_2O), 181 (5.1), 171 (2.0)
 167 (3.0), 165 (8.5), 155 (4.1, 185-HCOH),
 149 (3.0), 141 (7.2, 177- $2H_2O$), 127 (6.8),
 125 (7.2), 123 (7.4), 121 (7.0), 113 (33),
 111 (10.0), 109 (12.8), 107 (7.2), 101 (6.0),
 98 (17.5), 97 (21.7), 95 (23.4), 87 (40.4),
 85 (26.4), 83 (32.2), 81 (38.3), 71 (27.3),
 69 (36.1), 67 (31.1), 57 (68.0), 55 (100.0).

3.7 Photooxidation of methyl 12-oxooctadeca-9E-enoate.

TLC of the reaction product on prewashed plates at 0°C, eluting with PE 40, gave only one spot besides unreacted starting material. The purified product (R_f 0.29 in PE 40) was identified as a mixture of methyl 9-hydroperoxy,12-oxooctadec-10E-enoate and methyl 10-hydroperoxy,12-oxooctadec-8E-enoate. The following spectroscopic properties were recorded.

¹Hnmr spectrum: 6.8-6.0δ (cm, H_{mm'}), 5.9-5.1δ (cm, H_{aa'}), 4.62δ (q, J=7.0Hz, H_b), 4.35δ (qu, J=6.0Hz, H_n), 3.50δ (s, 3H, -COOMe), 2.42δ (at, J=7.2Hz, H_{e,p} and c), 2.15δ (at, J=7.4Hz, H_f), 1.85δ (aq, H_d), 1.43δ (shoulder, H_g), 1.16δ (bs, chain CH₂'s), and 0.70δ (at, J=5.4Hz, CH₃-).



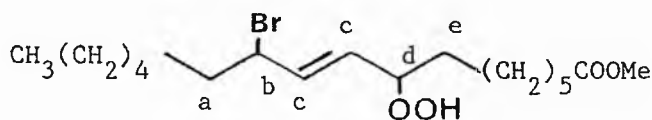
infrared spectrum: 3400 cm⁻¹ (OO-H stretch), 1745 cm⁻¹ (-CO₂Me carbonyl stretch), 1660 cm⁻¹ (C=O stretch isomer 12), 1630 cm⁻¹ (C=O stretch isomer 11) and 978 cm⁻¹ (trans HC=CH bending).

3.8 Photosensitised oxidation of methyl 12-bromooctadec-9Z-enoate.

Singlet oxidation of methyl 12-bromooctadec-9Z-enoate for 33h at room temperature gave three bands A-C on analytical TLC analysis at R_f 0.48, 0.42 and 0.35 in PE 35. Peroxide detecting sprays gave red spots for bands A and B only. Preparative TLC at 0°C on prewashed silica plates gave bands A-C after repetitive development. The following spectroscopic data was recorded.

Band A (R_f 0.48 in PE 35) was identified as methyl 12-bromo-9-hydroperoxyoctadec-10E-enoate.

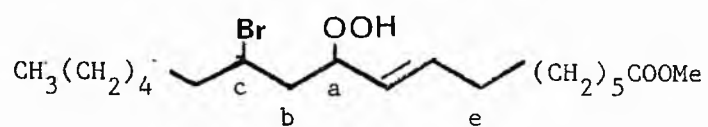
$^1\text{Hnmr}$ spectrum: 8.2 δ (bs , 1H, OO-H), 6.25-5.5 δ (m , olefin H_c)
 4.55 δ (q , $J=6.2\text{Hz}$, 1H, H_b), 4.32 δ (q , $J=6.2\text{Hz}$
 3.75 δ (s , 3H, -COOMe), 2.30 δ (at , $J=7.4\text{Hz}$, 2H,
 -CH₂CO₂Me), 1.92 δ (m , 4H, H_a and H_e), 1.40 δ
 (bs , chain CH₂'s) and 0.90 δ (at , $J=5.5\text{Hz}$, CH₃-).



infrared spectrum: 3420 cm^{-1} (OO-H stretch) and 749 cm^{-1} (C-Br stretch).

Band B (R_f 0.42 in PE 35) was identified as methyl 12-bromo-10-hydroperoxyoctadec-8E-enoate.

$^1\text{Hnmr}$ spectrum: 8.4 δ (bs , 1H, OO-H), 6.05-5.4 δ (m , 2H, olefinic H),
 4.65 δ (q , $J=6.8\text{Hz}$, 1H, H_a), 4.25 δ (m , 1H, H_a), 3.70
 3.70 δ (bs , 3H, -COOMe), 2.29 δ (at , $J=7.4\text{Hz}$, 2H,
 -CH₂CO₂Me), 2.07 δ (dd , $J=4.0\text{Hz}$, $J=8.0\text{Hz}$, 4H, H_b),
 1.50 δ (q , $J=6.0\text{Hz}$, 2H, H_e), 1.35 δ (bs , chain CH₂'s)
 and 0.90 δ (at , $J=5.4\text{Hz}$, 3H, CH₃-).



infrared spectrum: 3425 cm^{-1} (OO-H stretch) and 749 cm^{-1}
(C-Br stretch).

References

1. a) J. Bland, J. Chem. Ed., 1978, 55, 151.
b) J. Bland, J. Chem. Ed., 1976, 53, 274.
2. a) S. Epstein in "Dermatoses Due to Environmental and Physical Factors" (Ed. R.B. Rees), Thomas, Springfield, 111, 1962, pp 119.
b) C.S. Foote, Science 1968, 162, 963.
c) I.D. Spikes and R. Straight, Ann. Rev. Phys. Chem., 1967, 18, 409.
3. a) T. Maugh, Science, 1975, 187, 154.
b) C. Rimington, J.A. Magnus, E.A. Ryan and D.J. Gripps, Quar. J. Med., 1967, 141, 29.
c) A.A. Lamola, T. Yamane and A.M. Trozzolo, Science 1973, 179, 1131.
4. a) J.T. Chan and H.S. Black, Science 1974, 186, 1216.
b) H.F. Blum., in "Photodynamic Action and Diseases Caused by Light", Reinhold, New York, 1941, pp 3-5.
5. M.M. Oliga, F. Oliveira, D.L. Sanlioto and G. Cilento, Biochem. Biophys. Res. Comm., 1962, 7, 276.
6. See N.I. Krinsky in "Singlet Oxygen" (Ed. H.H. Wasserman, and R.W. Murray), Academic, New York, 1979, pp 606-609.
7. a) G.I. Dmitrienko, V. Snieckus and T. Viswanatha, Biorg. Chem., 1977, 6, 421.
b) H.W. Orf and D. Dolphin, Proc. Nat. Acad. Sci. U.S.A., 1974, 71, 2646.
8. a) J. Terao and S. Matsushita, J. Amer. Oil Chem. Soc., 1977, 54, 234.
b) S. Matsushita and J. Terao in "Autoxidation in Food and Biological Systems". (Ed. M.G. Simic and M. Karel) Plenum, New York, Ch 3, pp 27.

9. a) M.J. Thomas and W.A. Pryor, Lipids 1980, 15, 544.
b) E.N. Frankel, W.E. Neff, E. Selke and D. Weisleder, Lipids 1982, 17, 11.
c) J. Terao and S. Matsuishia, J. Food Process. Preserv., 1980, 3, 329.
d) E.D. Mihelich, J. Amer. Chem. Soc., 1980, 102, 741.
10. a) E.N. Frankel, W.E. Neff and D. Weisleder, J.C.S. Chem. Comm., 1982, 599.
b) W.E. Neff, E.N. Frankel and D. Weisleder, Lipids 1981, 16, 439.
c) Ref. 8a
11. a) J. Teroa and S. Matsushita, Lipids 1981, 16, 98.
b) J. Teroa and S. Matsushita, Agric. Biol. Chem. (Tokyo), 1981, 45.
12. See E.N. Frankel, Progr. Lipid Res., 1980, 19, 1 and in "Fatty Acids", Ed. E.H. Pryde, Amer. Oil Chem. Soc., Champaign, Ill, Ch 17 pp 343-378.
13. a) R.W. Denny and A. Nickon., Org. React., 1973, 20, 133.
b) C.S. Foote, Acc. Chem. Res., 1968, 1, 104.
c) D.R. Kearns, Chem. Rev., 1971, 71, 395.
d) K. Gollnick and H.J. Kuhn in "Singlet Oxygen". (Ed. H.H. Wasserman and R.W. Murray), Academic, New York, 1979, pp 287-427.
14. L.J. Morris and D.M. Wharry, Lipids, 1966, 1, 41.
15. R.G. Powell, C.R. Smith and I.A. Wolff, Lipids 1967, 2, 172.
16. G.G. Abbot, F.D. Gunstone and S.D. Hoyes, Chem. Phys. Lipids, 1970, 4, 351.

Section 4

**On the attempted synthesis of methyl
12-hydroperoxy oleate and stearate.**

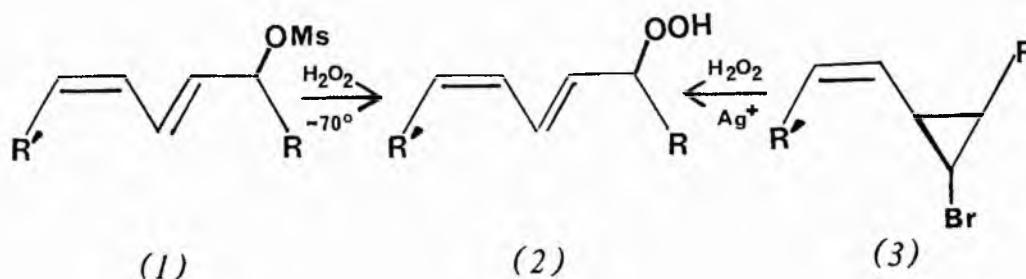
Summary

The silver trifluoroacetate assisted reaction of alkyl halides with hydrogen peroxide has been investigated. Reaction with methyl 12-bromostearate has furnished for the first time methyl 12-hydroperoxystearate in 34 % isolated yield. Reaction with methyl 12-bromocleate, however, is more complicated and leads to the formation of cyclopropane hydroperoxides via a homoallylic cation rearrangement, and to hydroperoxy-epidioxides presumably via methyl 12-hydroperoxyoleate which we were unable to isolate. Methyl 12-t-butylperoxyoleate has been produced by reaction of methyl 12-bromocleate with t-butylhydroperoxide in the presence of silver trifluoroacetate. None of these transformations occur if the silver salt is replaced by silver acetate.

1 Introduction.

The full spectrum of biological activity associated with fatty acid hydroperoxides has still to be fully elucidated, but it has already been shown that 5-hydroperoxyeicosatetraenoic acid, a catabolite of arachidonic acid, plays an important role in the allergic response^[1]. The synthesis of fatty acid hydroperoxides is commonly achieved by either singlet oxidation^[2] or by autoxidation^[3] and results in a number of positional and stereochemical isomers^[4]. Chromatographic methods have been developed for the purification of fatty acid hydroperoxides produced by either method^[5-7].

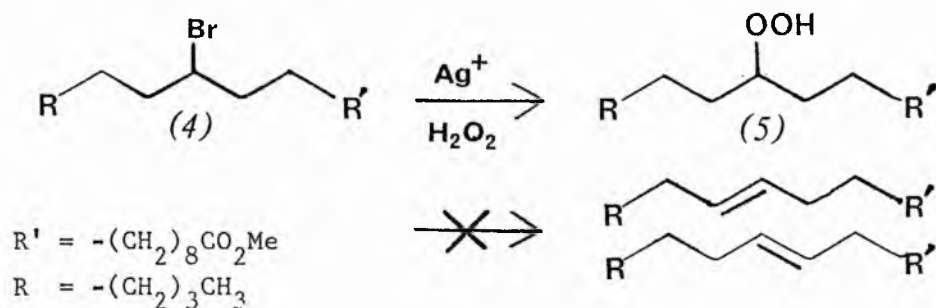
Approaches to the synthesis of an individual fatty acid hydroperoxide have only recently received attention. Corey *et al*^[8] have prepared allylic hydroperoxides from the corresponding diene mesylate by nucleophilic displacement (1-2). Porter *et al* have used silver ion displacement of halides for the preparation of prostaglandin endoperoxides^[9] and allylic hydroperoxides^[10] with considerable success. The same group applied the same silver ion / hydrogen peroxide methodology to the ring opening of vinyl cyclopropyl bromides (3-2) which is accomplished with complete stereochemical control.^[11]



Silver assisted intermolecular alkylation of hydrogen peroxide has been used to produce primary hydroperoxides from 1-bromooctane through octadecane in fair yield (see section 5). Some of these products have been prepared previously via base catalysed alkylation of hydrogen peroxide with the corresponding alkyl mesylates in yields which decreased with increasing chain length. Previous workers from this group have attempted the synthesis of secondary hydroperoxides from 12-mesyloxy stearate and oleate without success^[12].

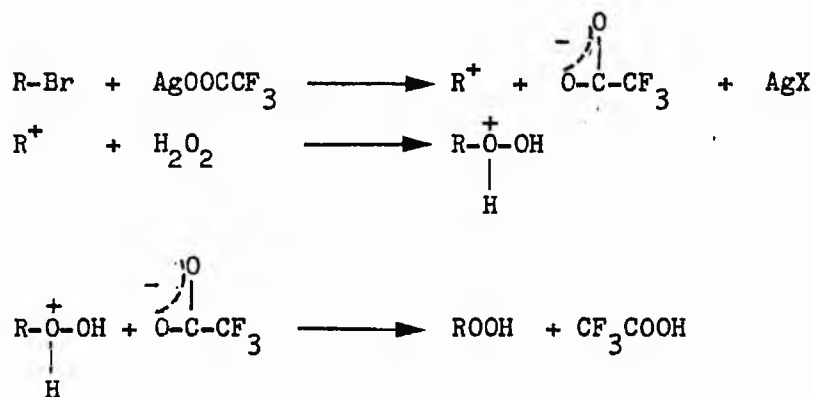
Reaction of 12-bromostearate (4), prepared by bromination of methyl 12-hydroxystearate via the corresponding mesylate, with hydrogen peroxide in the presence of a large excess of silver trifluoroacetate for 45 min gave methyl 12-hydroperoxystearate (5) in 34 % yield after isolation by preparative thin layer chromatography. The only other product isolated was unreacted starting material (58 %) which was identified by ¹Hnmr, mass, and ir spectroscopy. This suggests that dehydrohalogenation, which is a known competing reaction for tertiary bromides,^[13] had not occurred.

Scheme 1

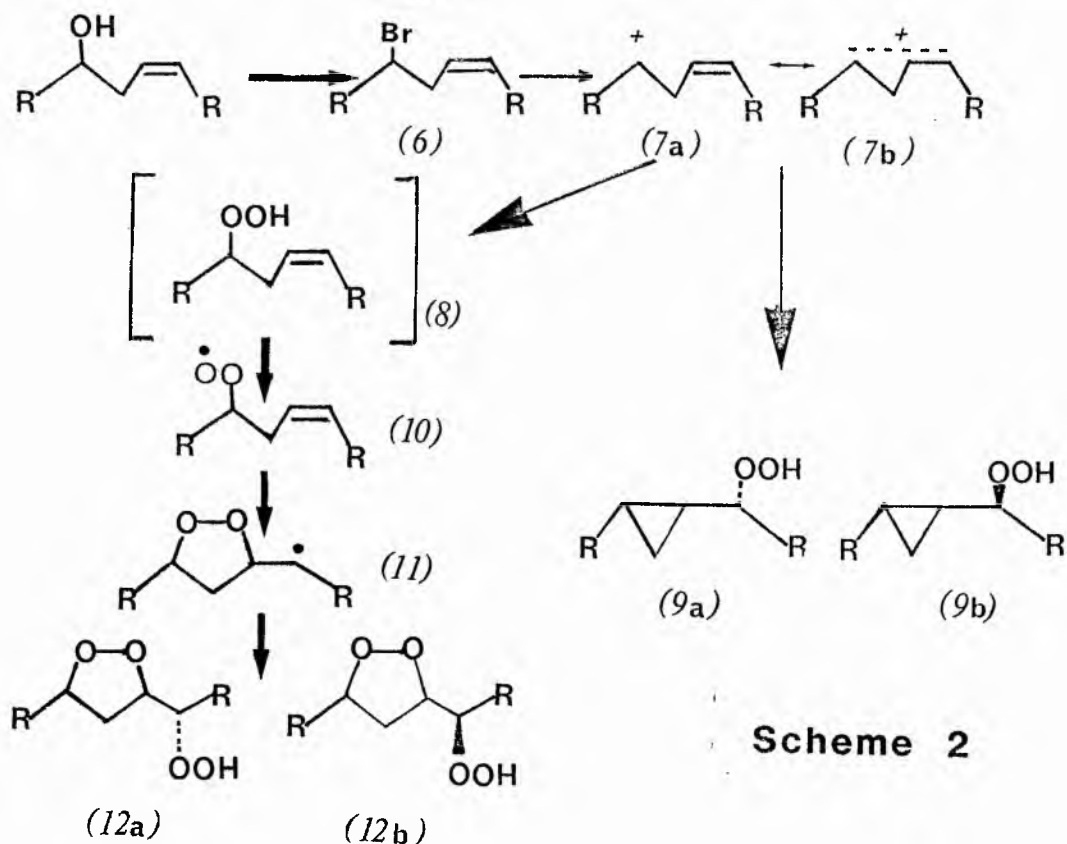


The ^{13}C nmr and ^1H nmr spectra were definitive for the identification of the product. The hydroperoxy bearing carbon (C12) having a ^{13}C shift of 85.53 ppm, some 13.9 ppm downfield from the corresponding alcohol. Similarly the peroxy methine in the ^1H nmr of the peroxide is downfield by 0.6 δ from the hydroxy methine in the alcohol. The mass spectrum of the hydroperoxide was extremely weak with no intense peaks above m/e 100.

The mechanism of the reaction is believed to involve oxonium ion intermediates as shown



Methyl 12-bromooleate (6) prepared from methyl ricinoleate, gave a more complicated product mixture on reaction with hydrogen peroxide in the presence of silver trifluoroacetate. The major isolable products were cyclopropane hydroperoxide esters and hydroperoxy-epidioxide esters.



Scheme 2

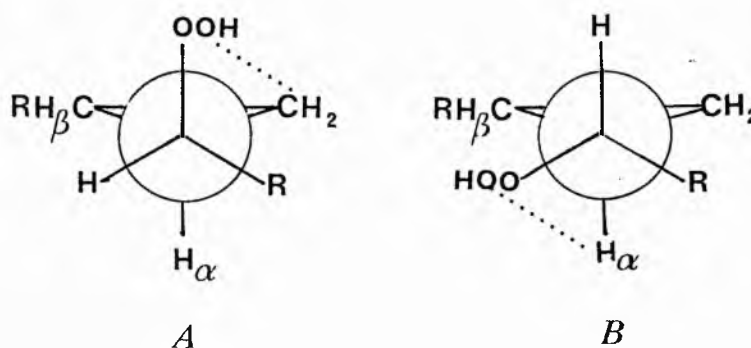
The silver assisted displacement of the bromine atom via a S_N1 process will furnish the homoallylic carbonium ion (7) which can be considered as having its charge delocalised over carbons C12, C10 and C9. Nucleophilic addition can then occur at either C12 or C9 to furnish the homoallylic hydroperoxide (8) and/or the cyclopropane hydroperoxide (9) respectively. Under our conditions the reaction will be under thermodynamic control and the 9-hydroperoxy cyclopropane ester (9) formed via the more stable carbonium ion (7b), is marginally the major product.

It has been argued that under acidic conditions the cyclopropane ester is formed reversibly and that the major products in the case of reaction of (7) with MeOH, AcOH or H_2O are the corresponding methoxy-, acetoxy- and hydroxy- octadec-9-enoates in which the configuration of the double bond can be either cis or trans, with the latter

predominating^[14]. However, attempts at buffering the reaction mixture for the reaction of (6) with trifluoroacetic acid (up to 1.0 M) gave no alteration in the product distribution. Reasons for the discrepancy between the two sets of results are not clear.

The structure of the two cyclopropane esters is based on chemical and spectroscopic evidence. The esters were shown to be peroxidic by spraying with 4-amino-N,N-dimethylaniline hydrochloride (2 %) in methanol and were shown to be hydroperoxidic since sodium borohydride reduction of the esters gave a product which was not peroxidic (hence excluding the possibility of a cyclic peroxide). More definitive evidence was obtained from the infrared spectrum which showed bands associated with the cyclopropane C-H stretching (3020 cm^{-1}), the cyclopropane CH_2 scissoring vibration (1432 cm^{-1}), and cyclopropane skeletal stretch (1020 cm^{-1}). An O-O-H stretching absorption was also observed (3450 cm^{-1}). The $^1\text{Hnmr}$ spectrum showed the absence of olefinic hydrogens and signals in the region 0-0.85 indicative of a cyclopropane substituent. As noted above the cyclopropane esters were resolved by T.L.C. into two components which differed in chromatographic behaviour and their $^1\text{Hnmr}$ spectra. Figure 1 shows two diastereoisomeric perspectives of the 9-hydroperoxy cyclopropanes in energetically preferred antiperiplanar conformations.

Figure 1

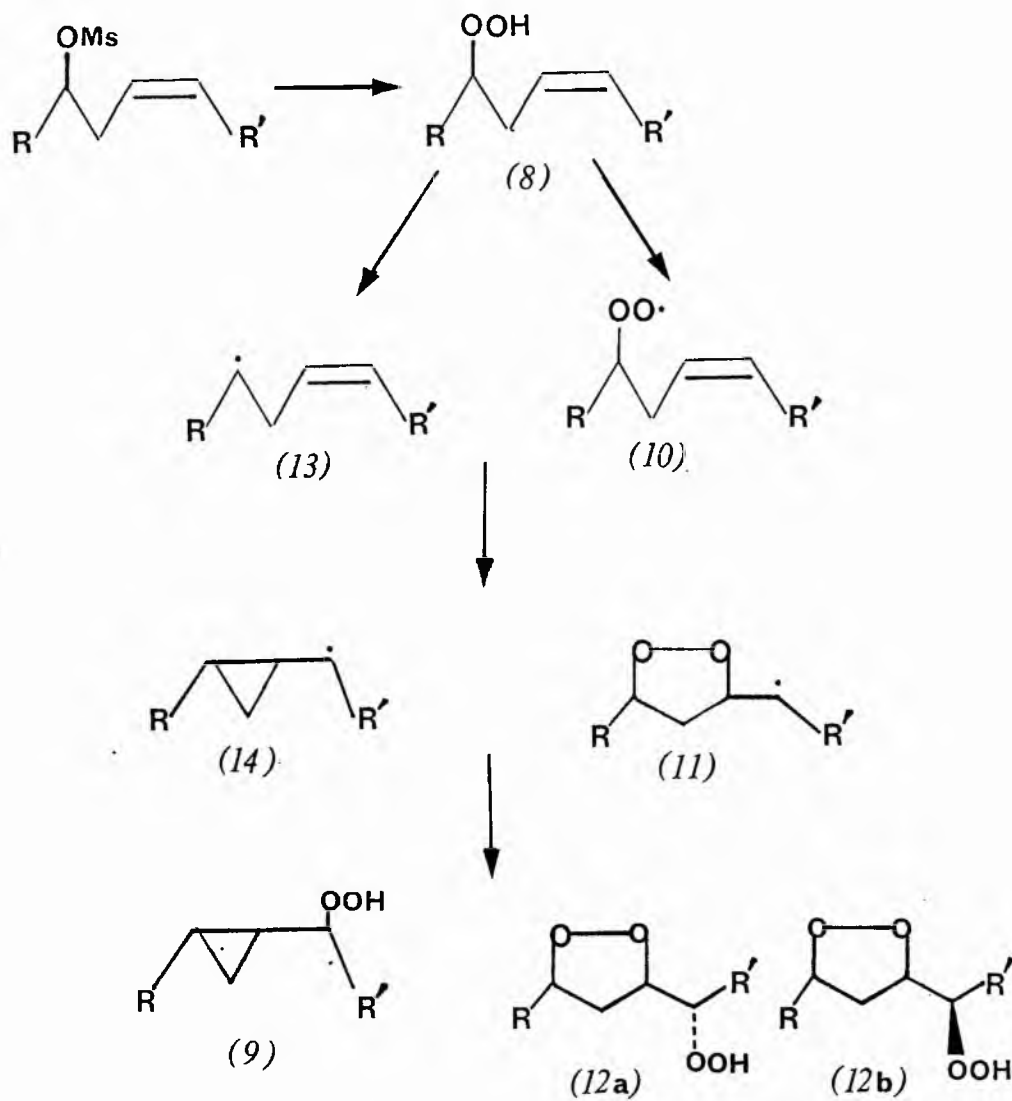


Diastereoisomer A can have a hydrogen bonding interaction with the cyclopropane methylene group only (since H_{α} will be across the ring), whereas diastereoisomer B has hydrogen bonding possibilities with the vicinal cyclopropane methine H_{α} . On the premise that hydrogen bonding will lead to a downfield $^1\text{Hnmr}$ shift we have tentatively identified the less polar of the two cyclopropane esters as diastereoisomer A, on the basis of the downfield shift of the ring methylene from its usual shift value of $0.2-0.16\delta$ and the more polar cyclopropane ester to diastereoisomer B since in this case it is the ring methines which are shifted downfield.

The formation of the hydroperoxy-epidioxides will proceed via the 12-hydroperoxyoleate which we were unable to detect. Formation of the peroxy-radical (10) with subsequent cyclisation via a 5-endo mode, furnishes the cyclic peroxide radical intermediate (11) which on further oxidation will produce the saturated hydroperoxy-epidioxides (12a,b), in approximately equal amounts (ca 14 %). We have assigned the stereochemistry of the cyclic peroxides on the basis of n.m.r. studies and comparison of the saturated trihydroxystearates, obtained by hydrogenation with authentic (9S,10R,12R)- and (9R,10R,12R)-standards as reported by Mihelich^[15] and more recently by Frankel et al^[16]. Our assignments are based on their chromatographic data.

Frankel et al^[16] have recently reported the formation of hydroperoxy-epidioxides and cyclopropane hydroperoxides in a similar reaction in which 12-mesyloxyoleate was allowed to react with 90 % H_2O_2 in anhydrous diethyl ether at -70°C and their proposed mechanism is shown in scheme 3. In this case however, the hydroperoxy-epidioxides (12a,b) were the major products arising from free radical cyclisation and further oxidation of the peroxy radical

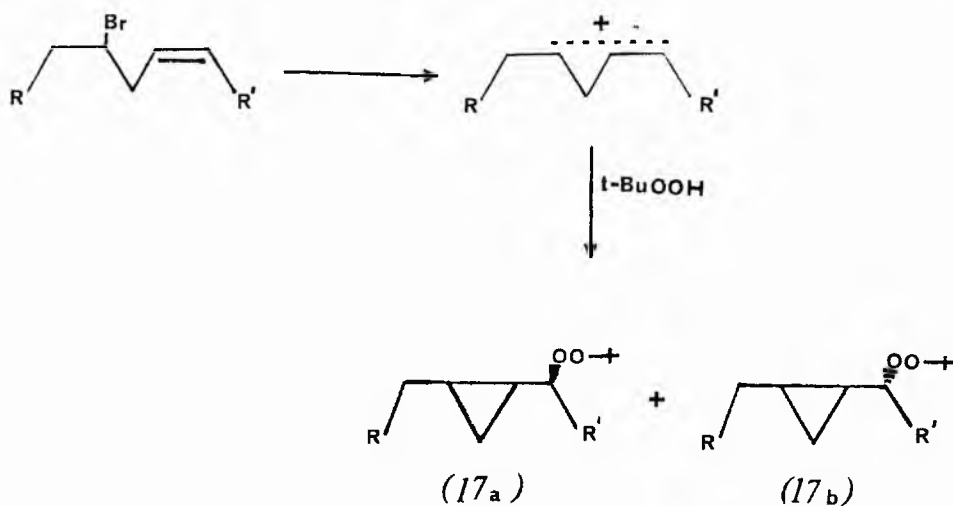
(11). Only one cyclopropane hydroperoxide was reported, in contrast to the two diastereoisomers formed from the silver trifluoroacetate reaction.



Scheme 3

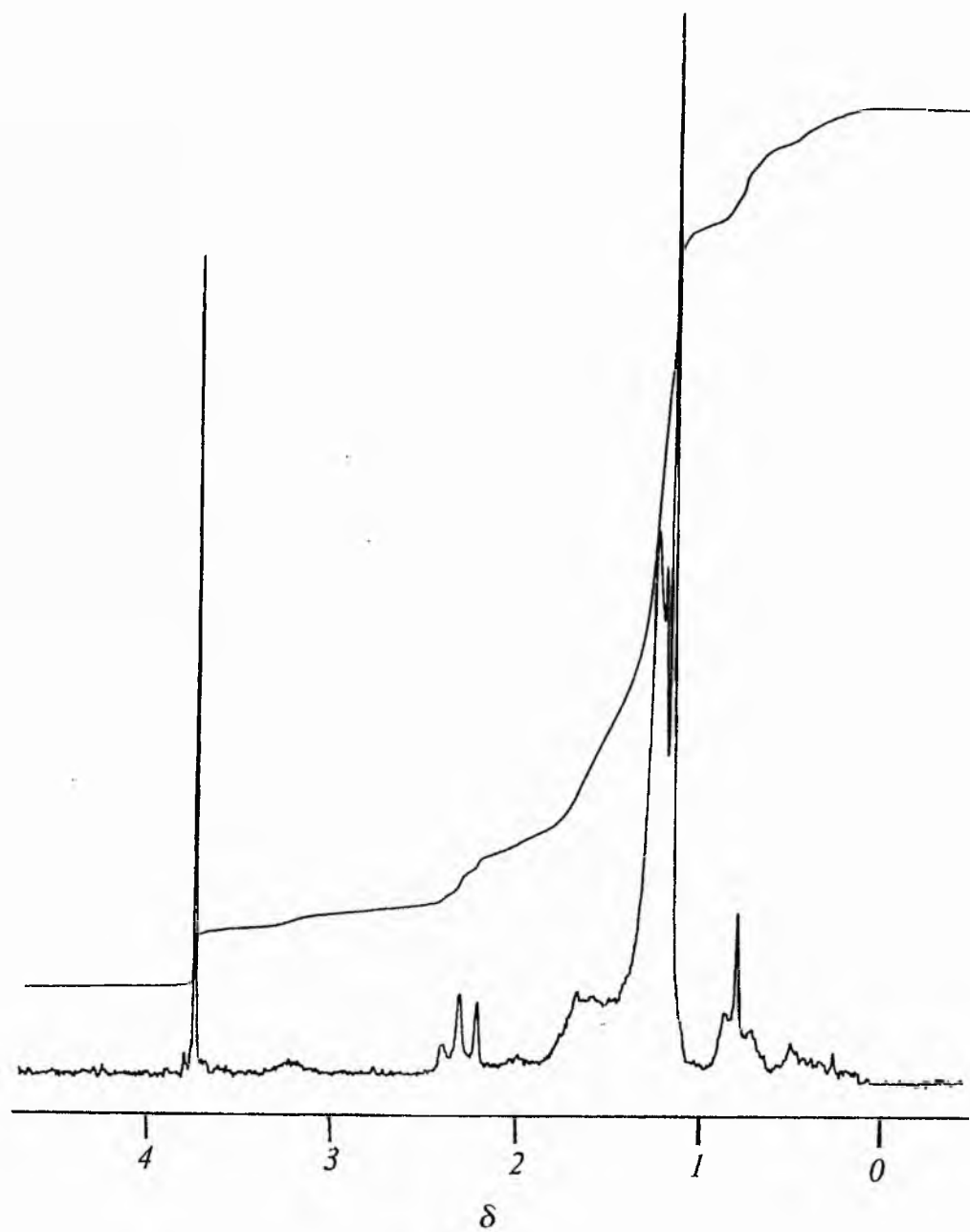
R = $-(CH_2)_5CH_3$

R' = $-(CH_2)_7COOMe$



Although the unsaturated β -bromides led almost exclusively to rearrangement products and none of the desired 12-hydroperoxy- or 12-t-butylperoxy-oleates were isolated the general methodology appears promising for the formation of lipid secondary hydroperoxides and alkyl peroxides.

FIGURE 2 ^1H nmr spectrum of methyl 12-t-butylperoxyoleate



3 Experimental

General experimental procedures have been reported elsewhere. Methyl ricinoleate was obtained from castor oil methyl esters by either chromatography on a column of silica followed by preparative T.L.C. using PE30 as developing solvent, or by HPLC as described in Chapter 3. Methyl 12-bromooleate was prepared as described in section 3 of this chapter.

3.1 Synthesis of methyl 12-hydroxystearate.

To methyl ricinoleate (> 99 %, 10g) in superdry methanol (100ml) was added Pd/C (10 %, 400mg) catalyst. Hydrogenation was carried out in a conventional hydrogenator. The reduction took 45min in which time 750 mls of hydrogen were taken up (theoretical volume required = 740 ml). GLC analysis of the reduced products showed peaks at ECL 18.0 (16 %) and 23.4 (84 %) corresponding to methyl stearate and methyl 12-hydroxystearate respectively.

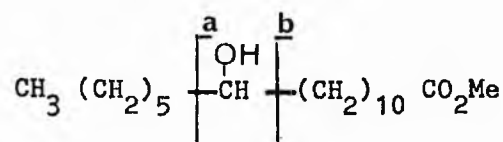
Preparative HPLC purification of the reaction product obtained after removal of the catalyst and solvent gave methyl 12-hydroxystearate as an analytically (GLC and TLC) pure product. The following spectral characteristics were recorded.

¹Hnmr spectrum: 3.57δ(bm, 1H, -HCOH-), 3.57δ(s, 3H, -COOMe),
2.20δ(at, J=7.0 Hz, 2H, -CH₂CO₂Me), 1.98δ(bs, 1H,

-OH), 1.25 δ (bs, chain CH₂'s), 0.76 δ (at, J=5.4 Hz, 3H, CH₃-).

infrared spectrum: 3345cm⁻¹ (O-H stretch), absence of C=C stretch.

mass spectrum: showed intense peaks at m/e 297 (M⁺-H₂O), 229 (a), 201 (a-CO), 197 (b-2), 157 (b-(CO-CH₂)), plus peaks associated with the sequential loss of methylenes.



3.2 Preparation of methyl 12-bromostearate (4).

To an ice-cold solution of methyl 12-hydroxystearate (4.5g, 1.5mmol) in dry methylene chloride (10ml) was added methanesulphonyl chloride (4ml) and pyridine (5ml) and the mixture stirred for 4h at 0-5°C. Ice-cold 2M hydrochloric acid (20ml) was added slowly, not allowing the temperature to rise above 10°C. Separation of the organic phase, drying over sodium sulphate and removal of the solvent in the usual manner gave methyl 12-mesyloxystearate. The purity of which was determined from its ¹Hnmr spectrum (from the integral ratio of COOMe to SO₂Me) was > 96 %. TLC showed only one spot.

¹Hnmr spectrum: 3.60 δ (s, 3H, -COOMe), 3.55 δ (bm, 1H, -CHOSO₂Me)
2.97 δ (s, 3H, -OSO₂Me), 2.23 δ (at, J=7.1 Hz, 2H, -CH₂COOMe), 1.20 δ (bs, chain CH₂'s), and 0.89 δ (at, J=5.4 Hz, 3H, CH₃-).

infrared spectrum: showed an absence of O-H stretch. Diagnostic absorptions at 1356cm⁻¹ and 1178cm⁻¹ arising from the

asymmetric and symmetric SO_2 stretching frequency.

To a solution of 12-mesyloxystearate (5.25g, 1.4 mmol) in dry acetone (20ml) was added a solution of lithium bromide (15g) in dry acetone (50ml). The solution was refluxed for 16h during which time a precipitate of lithium mesylate appeared. On cooling the solution was filtered and the solvent removed on a rotoevaporator at 5°C . The organic product was taken up in ether (20ml), washed with brine (2 x 15ml), aqueous sodium bicarbonate solution (20ml) and finally with distilled water (20ml). The ethereal layer was dried over sodium sulphate and rotoevaporated at 5°C . The crude product was judged to be > 95 % pure by TLC. Column chromatography eluting with PE5 gave the desired methyl 12-bromostearate free of more polar by-products. The following spectroscopic data was recorded.

$^1\text{Hnmr}$ spectrum: 4.10δ (qu, 1H, $-\text{HCBR}-$), 3.60δ (s, 3H, $-\text{CO}_2\text{Me}$),
 2.25δ (at, $J=7.0$ Hz, 2H, $-\text{CH}_2\text{CO}_2\text{Me}$), 1.25δ (bs, chain CH_2 's), and 0.85δ (at, $J=5.4$ Hz, 3H, CH_3).

infrared spectrum: showed an absence of O-H stretch.

3.3 Reaction of methyl 12-bromostearate with hydrogen peroxide and silver trifluoroacetate.

To methyl 12-bromostearate (380mg, 1mmol) in sodium dried ether (20ml) was added hydrogen peroxide (85 %, 1ml). The mixture was added dropwise with vigorous shaking to silver trifluoroacetate (1.0g, 4.6mmol) in a 50ml conical flask over a period of 5 min. The mixture was gently shaken for a further 10 min before adding saturated sodium chloride solution (20ml). The resulting cream precipitate of silver

chloride and silver bromide was filtered off to give a clear solution. The organic phase was isolated and the aqueous phase extracted with two further aliquots of ether. The combined organic extracts were dried over sodium sulphate and rotoevaporated at 5°C to furnish the crude product of reaction. TLC analysis showed only two bands A and B in PE 5.

Band A (220mg, 58 %) was identified as unreacted starting material by TLC, $^1\text{Hnmr}$, mass and infrared spectroscopy.

Band B (112mg, 34 %, Rf 0.42 in PE 30) was identified as methyl 12-hydroperoxyoctadecanoate on the basis of the following spectral evidence.

$^1\text{Hnmr}$ spectrum: 7.95δ (bs, 1H, $-\text{OOH}$), 4.20δ (bm, 1H, $-\text{HCOOH}$), 3.58δ (s, 3H, $-\text{CO}_2\text{Me}$), 2.22δ (at, $J=7.2\text{ Hz}$, 2H, $-\text{CH}_2\text{CO}_2\text{Me}$) 1.25 (bs, chain CH_2 's) and 0.86δ (at, $J=5.4\text{ Hz}$, 3H, CH_3 -).

$^{13}\text{Cnmr}$ spectrum: 162.91 (C1), 85.53 (C12), 34.00 (C2), 31.96 (C11,13), 31.69 (C16), 29.61, 29.34 and 29.07 (C4,5,6,7,8,9,15), 25.27 (C10,14) 24.83 (C3), 22.49 (C7), 13.93 (C18).

infrared spectrum: 3420 cm^{-1} (OO-H stretch) and absorptions typical of a long chain ester.

The mass spectrum showed no intense peaks above m/e 120 and peaks below m/e 120 were of general formula $\text{C}_n\text{H}_{2n-1}$ and $\text{C}_n\text{H}_{2n+1}$ corresponding to alkyl fragments. The base peak was m/e 55 (C_4H_7^+).

3.4 Reaction of methyl 12-bromooleate with hydrogen peroxide and silver trifluoroacetate.

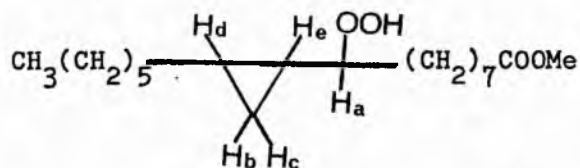
To methyl 12-bromooleate (380mg, 1mmol) in sodium dried ether (20ml) was added hydrogen peroxide (85 %, 1ml). The mixture was added dropwise with vigorous shaking to silver trifluoroacetate (1.0g, 4.6mmol) over a period of 5 min. Work up as above gave an organic product which showed seven bands A-G in PE-50 on analytical TLC analysis.

Band A (78mg, 21 %, $R_f = 0.73$ in PE 40) was identified as unreacted starting material on the basis of $^1\text{Hnmr}$ and infrared spectral comparison with authentic material.

Band B (15mg, 4 %, $R_f = 0.70$ in PE 40) was unidentified.

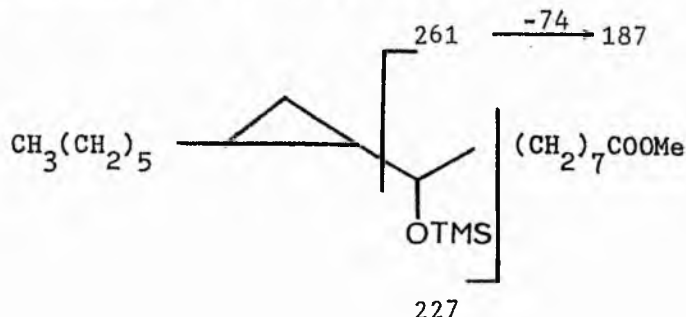
Band C (78mg, 24 %, $R_f = 0.60$ in PE 40) was identified as the cyclopropane hydroperoxide (9A) on the basis of the following spectroscopic evidence.

$^1\text{Hnmr}$ spectrum: 7.90δ (bs, 1H, OO-H), 3.65δ (s, 3H, -COOMe), 3.15δ (bm, 1H, Ha), 2.25δ (at, $J=7.2$ Hz, 2H, -CH₂COOMe), 1.28δ (bs, chain CH₂'s), 0.85δ (at, $J=5.4$ Hz, CH₃-) and $0.70-0.25\delta$ (bm, 4H, Hb,c,d,e).



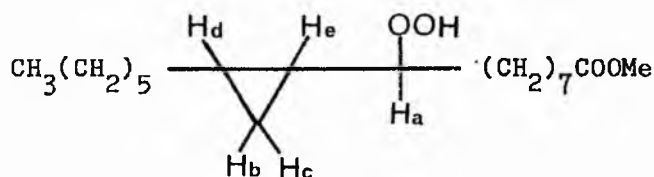
infrared spectrum: 3410cm^{-1} (OO-H stretch), 3050cm^{-1} (cyclopropane ring C-H stretch) and 1020cm^{-1} (ring C-C bond stretch).

mass spectrum: the hydroxycyclopropane ester produced by sodium borohydride reduction of the hydroperoxide was examined as its trimethylsilyl ether and showed intense m/e fragments at 227 (10 %), 187 (15 %), 129 (18 %) and a base peak at m/e 55 ($C_4H_7^+$).



Band D (70mg, 21 %, $R_f = 0.51$ in PE 40) was identified as the cyclopropane hydroperoxide (9B) on the basis of the following spectroscopic evidence

1H nmr spectrum: 7.80 δ (bs, 1H, OO-H), 3.65 δ (s, 3H, -COOMe), 2.85 δ (bm, 1H, Ha), 2.28 δ (at, $J=7.4$ Hz, 2H, -CH₂COOMe), 1.25 δ (bs, chain CH₂'s), 0.85 δ (at, $J=5.4$ Hz, 5H, CH₃- and Hd,e) and 0.27 δ (appd, $J=6.2$ Hz, Hb,c)

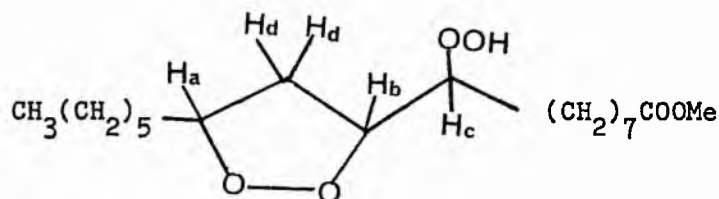


infrared spectrum: 3408cm^{-1} (OO-H stretch), 3050cm^{-1} (cyclopropane ring C-H stretch) and 1020cm^{-1} (cyclopropane ring C-C stretch).

mass spectrum: was identical with that obtained for band C.

Band E (45mg, 14 %, Rf = 0.41 in PE 40) was identified as 9(S)-hydroperoxy-10(R),12(R)-epidioxystearate on the basis of the following spectral evidence

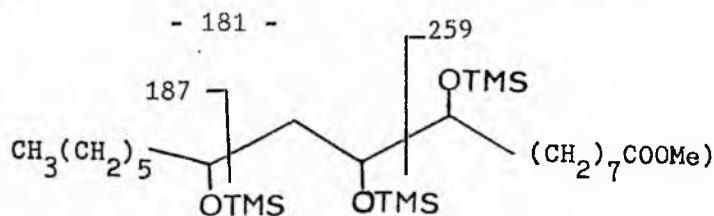
$^1\text{Hnmr}$ spectrum: 8.90δ (bs, 1H, OO-H), $4.50\text{--}3.90\delta$ (cm, 3H, Ha,b,c), 3.65δ (s, 3H, -COOMe), 2.56δ (m, 1H, Hd), 2.26δ (at, 3H, -CH₂COOMe and Hd*), 1.30δ (bs, chain CH₂'s) and 0.85δ (at, 3H, CH₃-).



(* The presence of Hd is inferred from the integral height although the signal to noise ratio was such as to preclude unequivocal identification of the splitting pattern for this signal and the other peroxy methine multiplets).

infrared spectrum: 3415cm^{-1} (OO-H stretch).

mass spectrum: the epoxide was catalytically reduced over Pd/C (10 %) to the corresponding trihydroxystearate and examined as its trimethylsilyl ether.



intense fragments observed at m/e 259 (4.5), 220 (3.2), 187 (5.5), 185 (5.0), 155 (8.5) and 147 (21.0) above m/e 100. Base peak m/e 74.

Band F (39mg, 12 %, R_f = 0.36 in PE 40) was identified as 9 (R)-hydroperoxy-10(R),12(R)-epidioxyoctadecanoate on the basis of the following spectral evidence.

$^1\text{Hnmr}$ spectrum: as for band E except Hd' at 2.00-1.90 δ (bm) instead of 2.26 δ .

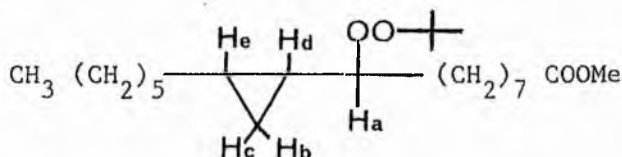
infrared and mass spectra were identical with those found for band E.

Band G (19mg, 5 %, R_f = 0.27 in PE 40) was unidentified.

3.5 Reaction of methyl 12-bromooleate with t-butylhydroperoxide and silver trifluoroacetate.

To methyl 12-bromooleate (380mg, 1mmol) in sodium dried ether (20 ml) was added t-butylhydroperoxide (85%, 1ml). The mixture was added dropwise with vigorous shaking to silver trifluoroacetate (1.0 g, 4.6 mmol) over a period of 5 min. Work up as above gave an organic product from which the t-butylperoxide was isolated as the major non-polar product by prep. TLC. (PE 5). The following spectroscopic data was recorded.

$^1\text{Hnmr}$ spectrum: 3.63 δ (s, 3H, -COOMe), 3.12 δ (bm, 1H, Ha), 2.26 δ (at, J = 7.4 Hz, 2H, -CH₂-COOMe), 1.77-1.17 δ (shoulder and bs, chain CH₂'s), 1.12 δ (s, 9H, t-Bu-), 0.82 (at, J =5.4Hz, 3H, CH₃-), and 0.90-0.15 (cm, 4H, Hd,e,b,c).



References.

1. P. Borgeat and B. Samuelsson, J. Biol. Chem., 1979, 254, 2463 and 7865.
- 2a) S. Matsushita and J. Terao in "Autoxidation in Food and Biological Systems" (Ed. M.G. Simic and M. Karel), Plenum Press, New York, 1980, pp 27-44.
- b) E.N. Frankel, Progr. Lipid Res., 1980, 19, 1.
3. E.N. Frankel in "Fatty Acids" (Ed. E.H. Pryde), Amer. Oil Chem. Soc., Champaign, Ill., Ch. 17 pp 343-378.
4. For example photosensitized oxidation of methyl oleate yields two isomeric hydroperoxides ($9 \Delta^{10}$, $10 \Delta^8$) while autoxidation yields four isomers ($8 \Delta^9$, $9 \Delta^{10}$, $10 \Delta^8$, $11 \Delta^9$).
5. N.A. Porter, J. Logan and V. Konitoyiannidou, J. Org. Chem., 1979, 44, 3177.
6. N.A. Porter, R.A. Wolf, E.M. Yarbrow, H. Weenen, Biochem. Biophys. Res. Commun., 1979, 89, 1058.
- 7a) M.O. Funk, R. Isaac and N.A. Porter, Lipids, 1976, 11, 113.
- b) H.W.-S. Chan and G. Levett., Lipids, 1977, 12, 99.
- 8a) E.J. Corey, A. Marfat, J.R. Falik, and J.O. Albright, J. Amer. Chem. Soc., 1980, 102, 1433.
- b) E.J. Corey, J.O. Albright, A.E. Barton and S.I. Hashimoto, J. Amer. Chem. Soc., 1980, 102, 1435.
9. N.A. Porter, J.D. Byers, K.M. Holden and D.B. Menzel, J. Amer. Chem. Soc., 1979, 101, 4319.
10. N.A. Porter, J.D. Byers, A.E. Ali and T.E. Eling J. Amer. Chem. Soc., 1980, 102, 1183.
11. N.A. Porter, D.H. Roberts and C.B. Ziegler Jr., J. Amer. Chem. Soc., 1980, 102, 5912.

12. F.D. Gunstone, E.G. Hammond, H. Schuler, C.M. Scrimgeour and
H. S. Vedanayagan, Chem. Phys. Lipids, 1975, 14, 81.
13. K.R. Kopecky, J.E. Filby, C. Mumford, P.A. Lockwood, and
J.Y. Ding, Canad. J. Chem., 1975, 53, 1103.
14. F.D. Gunstone and A.I. Said, Chem. Phys. Lipids, 1971, 7, 121.
15. E.D. Mihelich, J. Amer. Chem. Soc., 1980, 102, 7141
16. E.N. Frankel, D. Weisleder and W.E. Neff, J.C.S. Chem. Comm., 1981, 766.
17. K.L. Servis and J.D. Roberts, J. Amer. Chem. Soc., 1965, 87, 1331
and references cited therein.
18. T.A. Halgren, M.E.H. Howden, M.E. Medof and J.D. Roberts,
J. Amer. Chem. Soc., 1967, 89, 3050.
19. C.R. Warner, R.J. Strunk and H.G. Kuivila, J. Org. Chem.,
1966, 31, 3381.
20. E. Ucciani, A. Vantillard and M. Naudet,
Chem. Phys. Lipids, 1970, 4, 225.

SECTION 5

Synthesis of long-chain primary hydroperoxides

SUMMARY

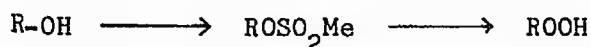
Seven primary alkyl long chain hydroperoxides have been prepared via the corresponding bromides. In our hands this procedure is superior to other published methods.

Hydroperoxides may be prepared from organic compounds by the action of molecular oxygen, ozone, or hydrogen peroxide^[1]. The use of molecular oxygen whether in the triplet ground state or the excited singlet state probably offers the greatest scope for synthesis, however isomeric mixtures can be expected in general^[2]. Reactions with ozone are limited to producing α -alkoxy hydroperoxides^[3]. However reaction of hydrogen peroxide at electrophilic carbon atoms provides the main route to many simple organic peroxides when a hydroperoxide of a particular constitution is desired as opposed to a mixture of isomers. Alkyl hydroperoxides have been obtained by S_N1 displacements at tertiary carbon atoms or S_N2 displacements at primary and secondary carbon atoms^[4]. Extremes of pH, elevated temperatures and long reaction times inevitably cause extensive decomposition of the desired product. Developments in methodology for hydroperoxide synthesis have been lucidely reviewed by Davies^[5], Hawkins^[6], Hiatt^[1] and more recently by Adam and Bloodworth^[4].

Baeyer and Villiger^[7] reported the first synthesis of a hydroperoxide in 1901 when they isolated ethyl hydroperoxide from the reaction of diethyl sulphate with dilute hydrogen peroxide in the presence of potassium hydroxide. The same method has also been applied to the preparation of methyl and propyl hydroperoxides^[8,9] albeit in low yields as a result of base-catalysed decomposition^[10].

Tertiary hydroperoxides have been prepared in 50-70% yields by the reaction of 30% hydrogen peroxide with alkyl hydrogen sulphates^[11,12]. The method has been adapted to produced dialkyl peroxides^[12].

A widely employed method for the synthesis of primary and secondary hydroperoxides involves the solvolysis of alkyl methane sulphonate esters in basic hydrogen peroxide solution^[13,14].



Williams and Mosher^[13,-15] prepared straight chain hydroperoxides from C3 to C10 and allyl hydroperoxide by the same method. Wawzonek et al^[16] prepared the C12, C14, C16 and C18 primary alkyl hydroperoxides by essentially the same technique. Gunstone et al^[17] reported higher yields of long-chain hydroperoxides (40-60%) by effecting the reaction in refluxing methanol with periodic addition of extra hydrogen peroxide. Radomsky and Gibian^[18] have drawn attention to the importance of pH in this reaction.

We now briefly report on the synthesis of seven primary long chain hydroperoxides prepared by the silver trifluoroacetate induced displacement of bromide from alkyl bromides in the presence of hydrogen peroxide^[19]. The procedure is compared with the alkyl mesylate method.

2 Results and discussion

The seven alkyl bromides used in this study, varying in chain length from C8 -C16, were cleanly converted to the corresponding alkyl hydroperoxides in yields of 37 - 47 %. No significant variation was observed with increasing chain length, which is an advantage over the the mesylate method of Williams and Mosher^[13,14] in which the yield of recovered hydroperoxide decreases sharply with increasing chain length^[16]. Gunstone et al^[17] previously reported higher yields by the mesylate method, but we have been unable to reproduce their reported yields, although they were marginally higher than those reported by Wazoneck et al^[16].

Two further advantages of the the reaction should also be noted. Firstly the reaction is essentially instantaneous and the procedure simple. Secondly the products of reaction are much simpler giving only unreacted starting material (43 - 50 %), the desired hydroperoxide (37 - 47 %) and small amounts of the corresponding alcohol (6 - 10 %). The mesylate method as applied by Gunstone et al^[17] gives rise to dialkyl peroxides, alkyl methyl ethers and alcohol. This makes chromatographic purification much simpler in the bromide method, and by recovering the unreacted bromide, the procedure can be repeated giving ultimately complete conversion to the hydroperoxide (> 75 %) and alcohol (13 -25 %).

¹Hnmr data for the alkyl hydroperoxides are reported in Table 2.1.

The hydroperoxy bearing methylenes are downfield from the corresponding hydrogens in primary alcohols by ~ 0.4 , with a marginally larger coupling constant. This is probably attributable to the greater electron withdrawing power of the hydroperoxide. The effect is transmitted to the α -methylenes which are 0.15 downfield from the corresponding signal in the alcohols. The hydroperoxy bearing bearing methine shows some variation in its chemical shift (7.80 - 7.97 δ) and its appearance, both of which probably result from concentration effects. Similar observations have been reported by Kropf et al^[20] and by Ward et al^[21].

3 Experimental.

3.1 Synthesis of primary alkyl hydroperoxides

General procedure.

The following procedure was carried out in all cases unless otherwise stated. To the freshly purified alkyl bromide (1 mmol) in dry diethyl ether (5ml) was added 85% hydrogen peroxide (1ml). The solution was then added dropwise over five minutes to silver trifluoroacetate (1.00g., 4.5 mmol) in a 50ml conical flask. The mixture was allowed to stand for a further 20 min before the addition of a saturated brine solution (15ml) and a further volume of ether (10ml). The organic layer was extracted and washed with saturated sodium bicarbonate solution (10ml) and finally with distilled water. Drying over anhydrous sodium sulphate before rotoevaporation at $<10^{\circ}\text{C}$ furnished the reaction product which was separated by preparative TLC. Yields, chromatographic and spectral data are reported in Table 3.1.

3.2 Preparation of primary alcohols from fatty acid esters.

The methyl esters or free fatty acids were converted to primary alcohols by reaction with excess lithium aluminium hydride in freshly prepared anhydrous diethyl ether. The following procedure is typical.

To a stirred suspension of lithium aluminium hydride (400mg) in dry ether (25ml) under dry nitrogen, was added dropwise a solution of the ester/acid (800mg) in dry ether (15ml). After stirring for 45min at room temperature excess lithium aluminium hydride was destroyed by

the cautious addition of "wet"^{*} ether (50ml) distilled water (20ml) and finally dilute H_2SO_4 (2M, 50ml). The product was extracted with ether (2 x 50ml) and dried over anhydrous sodium sulphate at 0°C. All the hydroxy alkenes were obtained in purities in excess of 95 % as judged by TLC, GLC and infrared and were not purified further unless otherwise stated. The 1H nmr data is reported in Table 3.2. The infrared spectra of all the alcohols showed O-H stretching absorptions at 3310-3300 cm^{-1} . The olefinic alcohols showed a -C=C- stretch at 3010-3000 cm^{-1} . A strong C-O absorption was observed at 1060-1055 cm^{-1} . Trans olefins gave an intense absorption at 965 cm^{-1} (olefinic C-H stretch). ^{13}C nmr spectral data are reported in Chapter 2 for these compounds.

* extracted from water.

Table 3.1 Yield (recovered %), R_f values, $^1\text{Hnmr}$ and i.r. spectral data^a for primary hydroperoxides of general formula $\text{CH}_3(\text{CH}_2)_n\text{CH}_2\text{OOH}$.

$^1\text{Hnmr}$ Chemical shifts.

n	Yield %	R_f	OO-H	$\text{CH}_2\text{-OOH}^a$	$\text{CH}_2\text{-CH}_2\text{-OOH}^b$	$(\text{CH}_2)^c_n$	CH_3^d	infrared OO-H (cm^{-1}).
6	38	0.43	7.90	4.06	1.65	1.29	0.88	3400
7	43	0.46	7.86	4.08	1.65	1.29	0.88	3450
8	45	0.40	7.90	4.06	1.65	1.28	0.89	3470
9	41	0.45	8.02	4.00	1.64	1.25	0.88	3465
10	40	0.43	7.95	4.03	1.66	1.28	0.89	3470
11	37	0.45	7.80	4.06	1.65	1.27	0.89	3460
14	34	0.45	7.92	4.13	1.65	1.27	0.89	3420
16	47	0.42	7.92	4.20	1.62	1.25	0.87	3450

a $^{13}\text{Cnmr}$ spectral data for these compounds are reported in Chapter 2.

b at, $J=6.4\text{Hz}$.

c quintet, $J=6.4\text{Hz}$.

d bs.

e at, $J=5.4\text{Hz}$.

Table 3.2 ¹Hnmr data for primary alcohols^e

alcohol	$\underline{\text{CH}}_2\text{-OH}^a$	$\underline{\text{CH}}_2\text{-CH}_2\text{-OH}^b$	$(\underline{\text{CH}}_2)_n^c$	$\underline{\text{CH}}_3^d$	$\underline{\text{CH}}=\underline{\text{CH}}$	allylic $\underline{\text{CH}}_2$
16:0	3.60	1.57	1.25	0.86		
18:0	3.61	1.59	1.25	0.86		
18:1(9c)	3.56	1.53	1.25	0.85	5.33	1.97
18:1(9t)	3.58	1.55	1.25	0.86	5.40	2.00
18:2(9c,12c)	3.44	1.50	1.28	0.85	5.30	2.00 ^f
18:1(3c)	3.65	2.30	1.27	0.87	5.45	2.08
18:1(4c)	3.58	2.05	1.23	0.83	5.42	2.05
10:1(4t)	3.62	1.65	1.23	0.84	5.42	1.97

^a at, J=6.2Hz unless otherwise stated.

^b quintet, J=6.4Hz unless otherwise stated.

^c bs.

^d at, J=5.4Hz.

^e assignments confirmed by extensive decoupling experiments.

^f also doubly allylic CH_2 at 2.72 (at, J=10Hz).

References

1. See R. Hiattin "Organic Peroxides" Vol 2 Ed. D. Swern Ch. 1,
Wiley and Sons, New York, 1971.
2. See K. Gollnick and H.J. Kuhn in "Singlet Oxygen", Ed. H.H. Wasserman
and R.W. Murray, Academic Press, New York, 1979, pp 287.
- 3a) P.S. Bailey., Chem. Rev. 1958, 58, 925.
- b) A.T. Menyailo and M.V. Pospelov., Russian Chem. Rev., 1967, 36, 284.
4. W. Adams and A.J. Bloodworth., Annual Reports B, 1978, 342.
5. A.G. Davies in "Organic Peroxides", Butterworths, London, 1961.
6. E.G.E. Hawkins, in "Organic Peroxides", Van Nostrand, Princeton,
New Jersey, 1961.
7. A. Baeyer and V. Villiger , Ber., 1901, 34, 738.
8. A. Rieche and F. Hitz, Ber., 1929, 62, 2473.
9. W. Eggergluss in "Organische Peroxyde", Angew. Monograph No. 61,
Verlag Chemie, Weinheim, 1951.
10. A.D. Kirk, Can. J. Chem., 1965, 43, 2236.
11. N.A. Milas and D.M. Surgenor , J. Amer. Chem. Soc., 1946, 68, 205 and 643.
12. N.A. Milas and L.H. Perry , J. Amer. Chem. Soc., 1946, 68, 1938.
13. H.R. Williams and H.S. Mosher, J. Amer. Chem. Soc., 1954, 76, 2984.
14. H.R. Williams and H.S. Mosher, J. Amer. Chem. Soc., 1954, 76, 2987.
15. D. Dykstra and H.S. Mosher, J. Amer. Chem. Soc., 1957, 79, 3474.
16. S. Wawzonek, P.D. Klimstra, and R.E. Gallio , J. Org. Chem.,
1960, 25, 621.
17. F.D. Gunstone, E.G. Hammond, H. Schuler, C.M. Scrimgeour and
H.S. Vedanayagam , Chem. Phys. Lipids, 1975, 14, 81.

18. N.A. Radomsky and M.J. Gibian., J. Amer. Chem. Soc., 1973, 95, 8713.
19. P.G. Cookson, A.G. Davies and B.P. Roberts, J.C.S. Chem. Comm.,
1976, 1022, and references cited therein.
20. H. Kropf and C.R. Bernet, Z. Anal. Chem., 1969, 248, 35.
21. G.A. Ward and R.D. Mair, Anal. Chem. 1969, 41, 538.

CHAPTER 2

A ^{13}C CHEMICAL SHIFT STUDY of OXYGENATED LONG CHAIN MOLECULES.

¹³C nmr chemical shifts are reported for a number of oxygenated long chain aliphatic compounds, including, epoxides alcohols, hydroperoxides and cyclic peroxides. The influence of the oxygenated functional groups on the chemical shifts of neighbouring carbons have been determined and a comprehensive set of chemical shift parameters derived. Results are discussed where applicable in terms of steric and electric field effects. The empirical equation $\Delta\delta_{AB} = A e^{-\zeta(2n+1)}$ is proposed to describe the non-equivalence of functionalised carbons.

Introduction

The phenomena of the chemical shift has been widely exploited since its first observation in 1950^[1,2]. Relying for the most part on empirically derived correlations the chemical shift has been used as a powerful and sensitive probe of molecular structure^[3]. Proton magnetic resonance spectroscopy has been a principle source of this type of data^[4]. However with molecules of large and/or complex structure, line broadening and spectral overlap tend to detract from the usefulness of this technique, although higher resolution instruments have gone some way to overcome the problem.

In such cases carbon-13 magnetic resonance (CMR) offers a potential advantage in the form of a greater dispersion of the chemical shifts and reduced line broadening resulting in considerably improved resolution^[5]. The low natural abundance (1.1%) and small gyromagnetic ratio of carbon-13 atoms compared with protons results in a signal to noise reduction of about 6000, these drawbacks are however overcome to a large extent by the use of pulse-Fourier transform techniques^[6].

The various factors contributing to the shielding of a ^{13}C nucleus generally combine in a complex manner^[7]. The nature and number of substituents on the carbon under consideration are the determining factors. The observation that substituent contributions are essentially additive^[8,9] is an outstanding feature of CMR chemical shifts and has resulted in a large body of structure-shift

relationships, which are generally based on linear-regression analysis of shift data as pioneered by Grant and co-workers^[10-13]. The resulting correlations are expressed as a set of additivity parameters from which the ^{13}C chemical shifts of carbons at the α , β , γ -positions etc can be predicted on the basis of the molecular geometry and the nature of the substituents.

1.1 Theoretical aspects of ^{13}C shielding.

The difference in chemical shift between carbon atoms in environment A and B, δ^{AB} may be expressed as a linear summation of local contributions as proposed by Saika and Slichter^[14], given by equations 1 and 2.

$$\delta^{AB} = \delta_{\text{el}}^{AB} + \sum_{i(\neq j)} \delta_{\text{anis}}^{AB} + \delta_{\text{inter}}^{AB} \quad (1)$$

$$\delta_{\text{el}}^{AB} = \delta_{\text{e}}^{AB} + \delta_{\text{ef}}^{AB} + \delta_{\text{st}}^{AB} + \delta_{\text{mis}}^{AB} \quad (2)$$

δ_{el}^{AB} and $\delta_{\text{inter}}^{AB}$ represent changes in diamagnetic and paramagnetic ring currents respectively on atoms A and B and $\sum \delta_{\text{anis}}^{AB}$ is the difference in the anisotropic screening term between atoms A and B which reflects the effect of electron currents on A and B from all other atoms in the molecule. McConnell^[15] and Pople^[16] have derived a simple expression for $\sum \delta_{\text{anis}}$ which is based on the assumption that these electronic currents may be approximated by point magnetic dipoles for which the magnetic susceptibilities χ_i can be defined. For the case where the susceptibility tensor χ_i is axially symmetric, the anisotropic term can be expressed as

$$\sum_{i(j)} \delta_{anis}^i = \sum (\Delta \chi_i) (1 - 3 \cos^2 \Theta_i) / 3 R_i^3$$

where $\Delta \chi_i = (\chi_i^{\parallel} - \chi_i^{\perp})$ is the anisotropy of the magnetic susceptibility of the i^{th} bond. R_i is the distance from atom j to bond i and Θ_i is the angle between the bond and the vector from j to i .

The electronic term δ_{el}^{AB} can conveniently be separated into four contributions given by equation 2 where δ_e^{AB} reflects the effect that changes in the electronic bonding framework may have on the local electronic distribution and shielding of the relevant nucleus. δ_{ef}^{AB} is an electric field term that is associated with differences in through-space influences that polarised regions of the two relevant species (A and B) can exert on the local electronic distribution and shielding of the nucleus. δ_{st}^{AB} is a steric term which is associated with perturbations of the local electronic distribution and shielding of the nucleus due to the effects of steric compression and δ_{mis}^{AB} is invoked to account for miscellaneous electronic effects not adequately covered by the other three terms.

Contributions to δ^{AB} are governed by inter- and intra-molecular electronic effects. These terms are often rationalised into terms familiar to chemists, the theoretical justification of which may be questionable, but nonetheless leads to a qualitative understanding of factors effecting ^{13}C chemical shifts. The most commonly identified contributions to ^{13}C chemical shifts arise from

- a) the state of hybridisation of the nucleus under consideration
- b) inductive effects of substituents

- c) van der Waals and steric effects
- d) electric fields originating from molecular dipoles
- e) hyperconjugation
- f) neighbouring anisotropic effects
- g) isotope effects
- i) mesomeric interactions in pi-electron systems.

Of these effects a-e are important in simple substituted hydrocarbon molecules of the type to be discussed and hence a brief insight into these is given below. For a more comprehensive discussion of these effects see text's by Levy and Nelson^[17], Strothers^[18], and by Wehrli and Wirthlin^[19].

Hybridisation.

The state of the observed carbon nucleus is a dominant factor in determining the chemical shift of that nucleus. This effect arises primarily from changes in the paramagnetic term δ_{inter}^{AB} . The general trend $\delta^{AB}(SP^3) > (SP) > (SP^2)$ parallels the order found in $^1H_{nmr}$ ^[19].

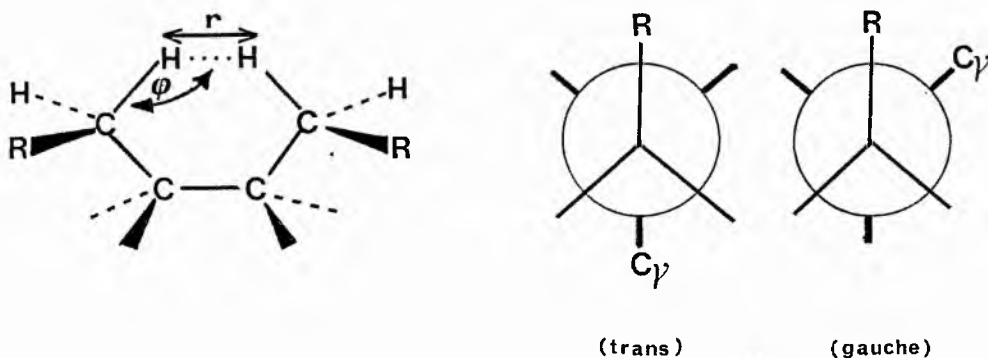
Inductive effects.

Satisfactory correlations of ^{13}C chemical shifts with electronegativity of the substituent(s) have been found for many series of compounds. The phenomena arises from removal of electron density from the carbon 2p orbitals by the electronegative substituent and is associated with a deshielding effect. Theoretical analysis^[20] predicts charge transfer to be propagated in an alternating effect along the carbon backbone, falling off with the inverse third power of

the distance. However other factors must be operative because no correlation of substituent electronegativity can be found for the β and γ carbons. This probably also implies that the α -shift is only contributed to in part by inductive effects.

Steric effects.

The steric interactions between closely neighbouring hydrogen atoms has been identified and rationalisation of the carbon shieldings in terms of geometrical parameters attempted. Grant and co-workers^[10-13,21] have interpreted the steric effect as a consequence of induced polarisation of C-H bonds. The steric perturbations of a C-H bond leads to a drift of charge along the C-H bond towards the carbon, resulting in orbital expansion and hence increased shielding. The upfield shift is operative when 1,4 carbons (γ -carbons) are in a gauche juxtaposition. Grant and Cheney^[21] proposed a semi-empirical formula to describe the γ -shift which has both angle and distance dependence as given below



$$\Delta \delta_{st} = K F_{HH}(r) \cdot \cos \phi$$

where the steric induced shift $\Delta\delta_{st}$ is related to the repulsive force between the interacting protons $E_{HH}(r)$ and the angle φ between the $H^{\cdots}H$ axis and the perturbed C-H bond, and k is an empirical constant.

Such so called γ -effects are manifest in conformationally rigid systems for which upfield shifts of approximately 6ppm have been recorded per $H^{\cdots}H$ interaction. In conformationally mobile systems, for example alicyclic hydrocarbons, the population of the gauche rotamer is about 30% resulting in steric shifts of the order of 2ppm. If the substituent is a heteroatom instead of CH_3 or CH_2 , the effect is slightly larger (1 to 3ppm).

A small but real downfield δ -substituent shift of 0.3ppm has also been observed for n-alkanes^[22]. Batchelor et al^[22] ascribed the shift to an increase of the trans rotamer brought about by any δ -substituent large enough to preclude g^+g^- conformers (Figure 1.1.1). The γ -shift at C_A resulted from a gauche conformation about C_B-C_C . Two possible gauche conformers exist about the C_C-C_D with the introduction of a δ -substituent (C_E). However of these two, one (the g^+g^-) is forbidden on grounds of orbital overlap, when both the C_B-C_C and C_C-C_D bond rotamers exist in a gauche form. Such perturbation leads to a relative decrease in gauche population with concomitant increase of the trans rotamer population. This change in rotamer population results in a decrease of the γ -substituent effect at C_A as a direct consequence of C_E (the δ -substituent).

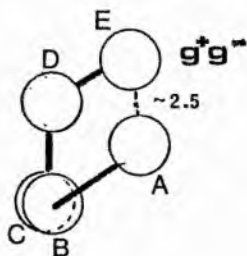


Figure 1.1.1

Electric field effects

The electric field effect has its origin in induced polarisation of the bonds between carbon and neighbouring atoms as a result of an electric field originating at a molecular dipole, point charge or other intra-or inter-molecular source^[23]. The induced polarisation can be represented as a summation of terms with linear and square dependence on the electric field vector E . The square dependence is important at short distances from the electric field source whereas the linear term becomes important at large distances.

The concomitant polarisation of the carbon bonds manifests itself as a change in electron density at the various carbons resulting in a chemical shift change. Such perturbations δ_q may be estimated by equation 3 ^[24]

$$\delta_q = \sum \frac{b E}{e l} \quad (3)$$

where b is the empirical longitudinal bond polarisability
 E is the electric field vector resolved parallel to
the bond
 l is the length of the bond under consideration
 e is the unit electronic charge
and the summation is of all the bonds to the carbon
atom

Electric field contributions to the spectra of polyunsaturated fatty acids are considerably complex, arising from contributions due to the polar head group and from bonds associated with other double bonds. The large longitudinal bond polarisabilities of the C=C and C≡C bond relative to the C-C and C-H bond polarisabilities means that the summation in equation 3 for an unsaturated carbon may be reduced to a single term for which the shift difference $\Delta\delta_{ef}$ is given by

$$\Delta\delta_{ef} = 2. (\delta/e) \frac{b E}{e r} \quad (4)$$

where δ/e is the shift per electron for the carbon in question. No such approximation can be made for saturated carbons for which the linear electric field effect is much smaller as a consequence of the low and nearly equal polarisabilities of C-C and C-H bonds.

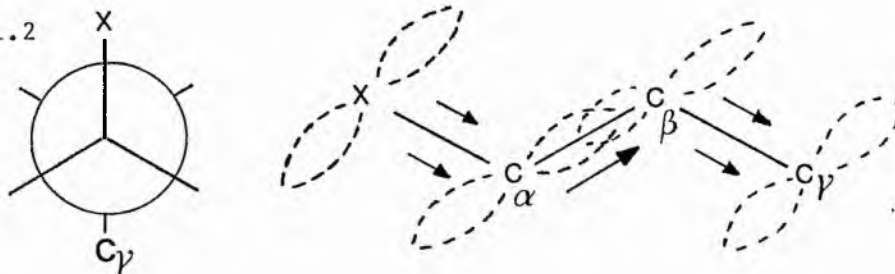
Theoretical treatments of electric fields on unsaturated carbons incorporating direction, magnitude and solvent effects are in accord with the experimental observations.

Hyperconjugative effects

Grant and coworkers^[24] have proposed hyperconjugation to account for upfield shifts caused by first-row heteroatoms located at the γ -position and antiperiplanar to the ^{13}C nucleus observed as shown in Figure 1.1.2. The C_γ resonance experiences an upfield shift of -2 to -6 ppm upon replacement of X=H or C by N, O or F. The hyperconjugation interaction of the lone pairs of X with the p-orbitals of the $\text{C}_\alpha\text{-C}_\beta$

bond proposal is in good agreement with the observed effects resulting in an increase of electron density at C_γ .

Figure 1.1.2



Finally a brief review of the relevant literature data pertaining to the interpretation of fatty acid CMR spectra in general and to oxygenated long chain molecules is warranted. Pioneering work on substituent shifts for alkanes by Grant and Paul^[10] was followed by more extensive data on branched paraffins by Linderman and Adams^[25]. Extensions to aliphatic alkenes, alkynes and allenes were reported by Friedal and Retcofsky^[26]. Dorman et al^[27] have reported on a systematic study of alkenes and alkynes, while de Haan and de Ven have reported on alkenes^[28].

Literature on fatty acids and their derivatives is more recent, and all post dates 1970. Early studies by Stoffel et al^[29] on saturated, mono- and polyenoic acids, phosphatidylcholines and spingosine bases, by Barton^[30] on a series of 1,2-dioctadec-cis-enoyl-sn-glycero- 3-phosphorylcholines and by Bus and Frost et al^[31] on the spectra of a limited number of cis and trans methyl octadecenoates did not unravel the more complex patterns of the ^{13}C chemical shifts due to the bulk methylenes, and some of these early assignments are in error.

Extensive assignments including the more complex regions of the spectra have been published by Tulloch and Mazurek et al^[32], who reported on specifically deuterated esters of stearate, oleate and

petroselinate, by Bus et al^[33,34] and independently by Gunstone et al^[35,36] on unsaturated acids and esters and by Batchelor et al^[23] on a variety of functionalised fatty acids.

CMR analysis of hydroxy fatty acids have been reported by Tulloch et al^[37] on a series of specifically deuterated monohydroxy octadecanoates and their oxo derivatives, and by Rakoff et al^[38] who made a limited study on the ¹³C chemical shifts of some diastereoisomeric dihydroxy acids. A comprehensive study on short chain alcohols was made by Roberts et al^[39].

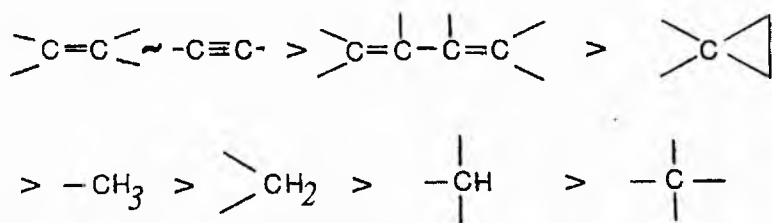
Literature on ¹³C chemical shift data for epoxides is limited to shorter chain and alicyclic compounds. Tori et al^[40] have studied the conformational effects in steroidal epoxides. Servis et al^[41] have investigated the conformational analysis of cycloheptane oxide by ¹³C spectroscopy and Anet et al^[42] have assigned additivity parameters to several classes of polyepoxides. Paulson et al^[43] and Davies et al^[44] independently published studies on simple epoxides in 1975. Paulson et al^[43] developed a set of additivity parameters which allows the calculation of the epoxide chemical shifts of the carbon atoms of the epoxide group, and these were in good agreement with those published by Davies et al^[44]. ¹³C chemical shift data on peroxides is even more scarce though Budinger et al^[45] have recently published a brief study on simple dialkyl peroxides and alkyl hydroperoxides.

Results & discussion

1.2.1 ^{13}C chemical shift data for saturated epoxy fatty acid methyl esters.

The chemical shifts of 26 methyl epoxyoctadecanoates are presented in Tables 1.2.1.1 and 1.2.1.2 for the cis and trans isomers respectively. Table 1.2.1.3 presents values of shielding parameters for both cis and trans epoxides. Tables 1.2.1.4 and 1.2.1.5 give values for carbons α , β , and γ to the epoxide ring which are unaffected by end groups.

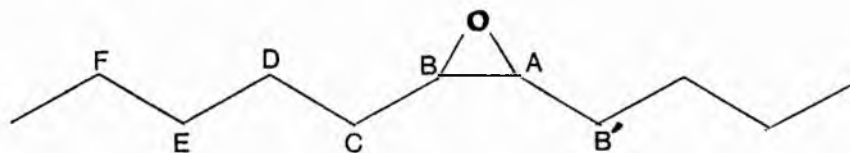
The two sets of data (cis and trans) can readily be distinguished by the chemical shift of the epoxidic carbons. The mean value for the cis epoxy carbons unaffected by perturbations from the end groups is 56.85 ± 0.05 ppm while the trans epoxy carbons resonate downfield at 58.51 ± 0.05 ppm. Figures 1.2.1.1 a and b show the systematic variation in the chemical shift difference between the two epoxy carbons as a function of the position along the C18 chain. The curves arise predominantly from inductive and electric field effects from the end groups. Comparison of this data with the corresponding alkenes or alkynes immediately suggests that electric field effects which are responsible for the source of non-equivalence in the central alkenes and alkynes have only a small effect on epoxy carbons. Batchelor et al^[22] have suggested the following order for the magnitudes of the linear electric field shifts for a variety of linkages.,



The factors determining the size of the induced shifts are the magnitude of the polarisabilities of adjoining bonds and δ/e (see equation 4). In general, linear electric fields shifts of methylenes are very small as a result of the very nearly equal polarisabilities of the C-C and C-H bonds. The unsaturated carbons have large linear electric field induced shifts because the highly polarisable unsaturated bond is adjacent to C-C and C-H bonds of much lower polarisability. This results in an increase or decrease of the electron density on the unsaturated carbon as a result of the electric field perturbation.

The difference between the chemical shifts of C6 and C7 in methyl octadecanoate is 0.15 ppm, this can be compared with 0.29 ppm for the Δ^6 cis epoxide. This implies a greater polarisability of the bonds in the epoxide ring compared with the C-C and C-H bonds. The chemical shift difference between C6 and C7 is also slightly larger than that obtained for a similar situated cyclopropane ring of 0.25 ppm. Hence epoxide bonds are marginally more polarisable than the skeletal bonds of cyclopropane rings, although the difference is very small and could result from solvent effects.

Steric induced shifts are also observed for some of the methylenes of the cis epoxy esters. A small δ -shift is apparent from the data in Tables 1.2.1.1 and 1.2.1.2. The carbon β to the oxirane ring (carbon D) experiences a δ -steric shift from the α - carbon across the ring (carbon B'), resulting in a shift difference of 1.2 ppm between the cis and trans isomers for the β -carbons.



The largest steric effects observed in the saturated epoxy fatty acid esters are those of the carbons α to the ring (carbons B' and C) which are in 1,4 or δ -juxta position with one another. The steric interaction results in the cis isomers α -carbons resonating some 4.05 ppm upfield from those of the trans isomer. Using Batchelor et al's^[22] value of 6.0 ppm for a 100% gauche γ interaction as opposed to Grants predicted value of 4.8 ppm^[21] gives rise to a gauche rotamer population of 68%. Higher values are calculated from the reported shift differences of cis and trans cyclopropane fatty acids of 5.8 ppm giving a 96.7% gauche rotamer population. Presumably the shorter C-O bonds in the oxirane ring will relieve the steric compression resulting from the interaction of the hydrogens on the α -methylenes (B' and C). A much smaller steric effect is observed for the methine ring carbons in the saturated epoxy esters. Trans epoxide methine carbons absorb approximately 1.7 ppm downfield from cis epoxide methine ring carbons. This value can be compared with 3.1 ppm for cyclopropane methines and with the 0.5 ppm difference observed between cis and trans olefinic carbons.

Figure 1.2.1.2 shows a logarithmic plot of the chemical shift difference between the epoxy methines $\Delta\delta$ against the distance from the carboxyl head group. A linear relationship is observed from the $\Delta 3$ to $\Delta 7$ epoxide. There are two significant features to the

correlation. First and foremost the quality of the fit is substantial and secondly the relationship appears to be independent of the stereochemistry of the epoxide ring. The empirical relationship of equation 5 is proposed for predicting the shift difference $\Delta\delta_{n,n+1}$.

$$\Delta\delta_{n,n+1} = 4.30 \left[e^{-0.43(2n+1)} \right] \quad (5)$$

where $\Delta\delta_{n,n+1}$ is the chemical shift difference between the epoxy methines and n and n+1 are the locations of the epoxy methines.

For the case when the epoxide approaches the ω -end of the chain a linear relationship with a slope of 4.3 is obtained. The quality of the fit is not as good, and the number of data points small, hence the correlation in this instance is at best tentative.

Table 1.2.1.3 Substituent shifts for epoxides.

Substituent position	shift/ppm	
	cis	trans
α	-1.55	+2.51
β	-2.77	-3.56
γ	-0.15	-0.34

TABLE 2.1.1

C M R data for long chain *cis* epoxides

comp.	carbon position																	
	1	2	3	4	5	6	7	8	9	10	11	12	13	14	15	16	17	18
5c	173.00	33.49	52.29	56.48	27.68	26.26	29.40	29.40	29.49	29.49	29.49	29.49	29.49	29.49	29.40	31.77	22.51	13.90
4c	173.10	30.80	23.25	55.72	57.17	27.56	26.36	29.14	29.49	29.49	29.49	29.42	29.42	29.42	29.42	31.71	22.45	13.84
6c	173.66	33.74	24.63	26.01	27.36	56.62	56.91	27.66	26.42	29.14	29.14	29.39	29.39	29.39	20.39	31.72	22.48	13.85
7c	173.66	33.60	24.54	28.72	26.04	27.38	56.62	56.75	27.55	26.30	29.02	29.26	29.26	29.26	29.26	31.60	22.34	13.74
8c	173.70	33.76	24.62	28.92	28.92	26.26	27.61	56.79	56.79	27.61	26.41	29.08	29.33	29.33	29.33	31.68	22.44	13.82
9c	173.69	33.63	24.54	28.85	29.18	28.85	26.25	27.48	56.67	56.67	27.48	26.25	28.85	29.18	29.18	31.51	22.29	13.66
10c	173.89	33.82	24.70	28.90	29.22	28.90	26.38	27.61	56.89	56.89	56.89	27.61	26.38	28.90	29.22	31.54	22.39	13.79
11c	173.89	33.82	24.70	28.97	29.23	29.23	28.97	26.36	27.61	27.61	56.88	56.88	27.61	26.36	28.97	31.54	22.35	13.78
13c	173.89	33.82	24.71	28.96	29.27	29.27	29.27	29.27	28.53	28.53	26.37	27.30	56.85	56.85	27.60	28.53	22.55	13.70
14c	173.96	33.87	24.74	28.95	29.02*	29.33	29.33	29.33	29.33	29.33*	28.95*	26.40	27.66	56.83	56.72	29.66	19.70	13.79
15c	173.90	33.87	24.74	28.96	29.34	29.34	29.34	29.24	29.34	29.34	29.34	28.96	26.40	27.51	57.05	58.08	20.89	10.34
16c	173.89	33.75	24.64	28.92	29.26	29.26	29.26	29.26	29.26	29.26	29.26	29.26	29.26	26.14	27.22	56.67	52.13	12.85
17c	173.87	33.85	24.73	28.95	29.02	29.37	29.37	29.37	29.37	29.37	29.37	29.37	29.02	28.95	25.72	32.36	51.08	46.71

TABLE 2.1.2

C M R data for long chain trans epoxides

comp.	c a r b o n p o s i t i o n																	
	1	2	3	4	5	6	7	8	9	10	11	12	13	14	15	16	17	18
3t	37.50	53.70	58.43	25.57	29.10	29.39	29.39	29.39	29.39	29.39	29.39	29.39	29.39	29.39	29.10	31.66	22.40	13.79
4t	173.11	30.14	27.22	57.30	58.72	31.79	25.80	29.48	29.48	29.48	29.48	29.48	29.48	29.48	29.48	31.79	22.52	13.90
5t	173.28	33.30	21.25	31.19	57.80	58.26	31.74	25.74	29.08	29.34	29.34	29.34	29.34	29.34	29.08	31.65	22.38	13.77
6t	173.38	33.67	24.50	25.38	31.54	58.48	58.15	31.84	25.79	29.10	29.35	29.35	29.35	29.35	29.10	31.67	22.43	13.81
7t	173.67	33.76	24.57	28.67	25.47	31.66	58.32	58.46	31.85	25.59	29.07	29.30	29.30	29.30	29.30	31.66	22.40	13.79
9t	173.84	33.82	24.68	28.98	28.98	25.80	31.89	58.54	58.54	58.54	31.89	25.80	28.98	29.26	29.26	31.63	22.42	13.81
10t	173.86	33.82	24.71	28.93	28.93	29.12	29.12	25.82	31.90	58.55	58.55	31.90	25.82	29.12	28.93	31.53	22.39	13.77
11t	173.87	33.79	24.67	28.86	28.86	29.15	29.15	29.15	25.77	31.87	58.52	58.52	31.87	25.77	28.86	31.50	22.27	13.73
12t	173.87	33.79	24.67	28.92	29.15	29.15	29.15	29.15	28.92	25.78	31.84	58.53	58.53	31.84	25.44	31.38	22.30	13.64
13t	173.84	33.81	24.70	28.97	28.97	29.26	29.26	29.26	29.26	28.90	25.80	31.89	58.51	58.51	31.57	27.95	22.26	13.68
14t	173.87	33.82	24.70	28.96	29.28	29.28	29.28	29.28	29.28	29.28	29.28	25.79	31.89	58.33	58.49	33.94	19.09	13.66
15t	173.92	33.87	24.74	28.99	29.34	29.34	29.34	29.34	29.34	29.34	29.34	29.34	25.83	31.88	58.32	59.61	24.95	9.62
16t	173.97	33.89	24.76	28.97	29.37	29.37	29.37	29.37	29.37	29.37	29.37	29.37	28.97	25.78	31.84	59.58	54.27	17.44

Table 1.2.1.4 Values for α , β , and γ carbon shifts^a for cis epoxyoctadecanoates.

epoxide position	α	β	γ
Δ 6	27.66	26.42	29.14
7	27.55	26.30	29.02
8	27.61	26.41	29.08
9	27.48	26.25	28.85
10	27.61	26.38	28.90
11	27.61	26.36	28.97
13	27.60	26.37	28.53
14	27.66	26.40	28.95
15	27.51	26.40	28.96
\bar{X}	27.60	26.38	29.00
$\bar{\sigma}$	± 0.04	± 0.04	± 0.23

Table 1.2.1.5 Values for α , β , and γ carbon shifts^a for trans epoxyoctadecanoates.

epoxide position	α	β	γ
Δ 6	31.84	25.79	29.10
7	31.85	25.79	29.07
9	31.89	25.80	28.98
10	31.90	25.82	29.12
11	31.87	25.77	29.15
12	31.84	25.78	28.92
13	31.89	25.80	28.90
14	31.89	25.79	28.96
15	31.88	25.83	
\bar{X}	31.87	25.80	29.02
$\bar{\sigma}$	± 0.02	± 0.02	± 0.09

^a shifts given in ppm downfield from TMS.

Figure 1.2.1.1 Systematic variation in the chemical shift difference between the two epoxy carbons as a function of the epoxide position along the C18 chain.

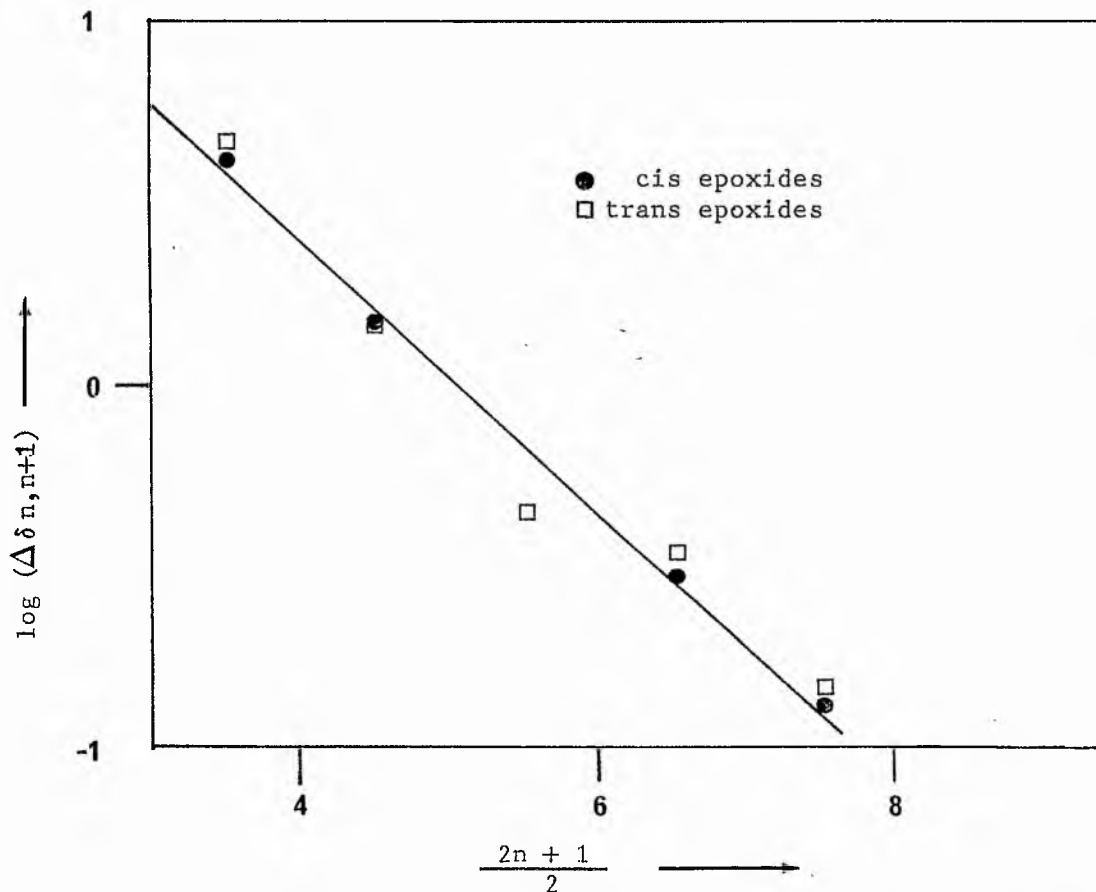
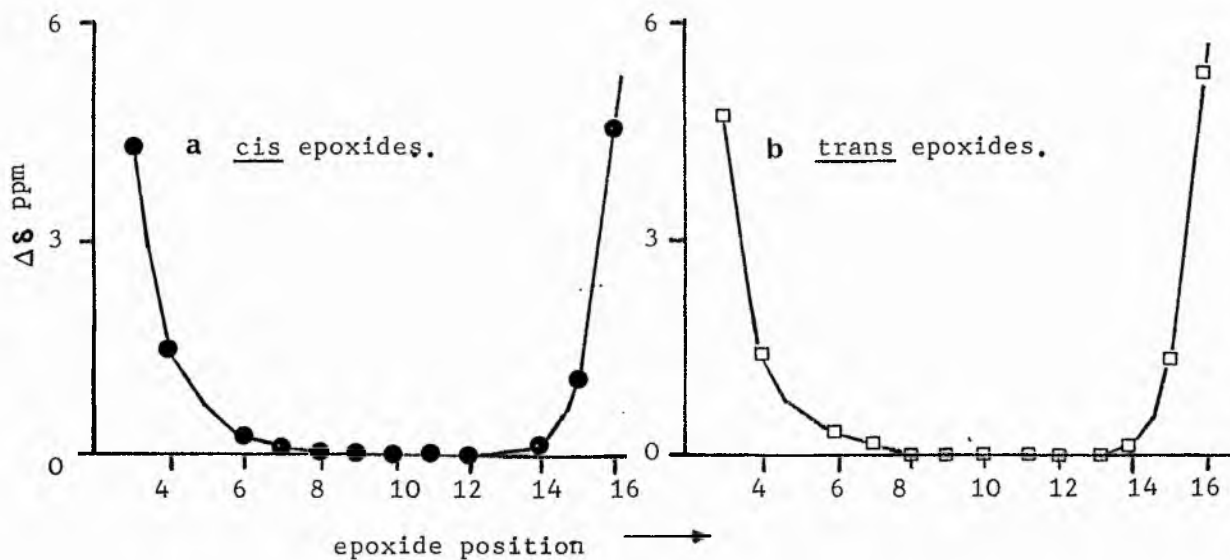


Figure 1.2.1.2 Plot of logarithm of the chemical shift difference between the epoxy methines $\Delta\delta_{n,n+1}$ against the mean distance from the carboxyl group $\left(\frac{2n+1}{2}\right)$.

Our substituent effects can be used to predict the CMR spectra for simple aliphatic epoxides. Davies and Whitham^[44] previously published data for a series of 1,2-epoxides, their assignments are shown in Table 1.2.1.5. However they are incorrect, primarily as a result of incorrect assignment of the α -3 carbon. We have reassigned their ^{13}C chemical shifts using our data from above and the corrected assignments are given in Table 1.2.1.6.

Table 1.2.1.5 ^{13}C Chemical shifts of terminal epoxides.
Incorrect data from Davies and Whitham^[44].

Oxide	C1	C2	C3	C4	C5	C6	C7	C8	C9	C10	C11	C12
Ethylene	40.8											
propene	47.8	48.0	18.1									
pentene	46.8	52.0	34.9	19.6	14.0							
hexene	46.8	52.2	32.5	28.4	22.8	14.1						
octene	46.8	52.2	32.8	32.1	29.4	26.2	22.8	14.2				
decene	46.8	52.2	32.8	32.1	29.8	29.8	29.5	26.3	22.9	14.2		
dodecene	47.0	52.3	32.7	32.1	29.8	29.8	29.8	29.8	29.6	26.2	22.9	14.2

Table 1.2.1.5 ^{13}C Chemical shifts of terminal epoxides.
Corrected data.

Oxide	C1	C2	C3	C4	C5	C6	C7	C8	C9	C10	C11	C12
Ethylene	40.8											
propene	47.8	48.0	18.1									
pentane	46.8	52.0	34.9	19.6	14.0							
hexene	46.8	52.2	32.5	28.4	22.8	14.1						
octane	46.8	52.2	32.8	26.2	29.4	32.1	22.8	14.2				
decene	46.8	52.2	32.8	26.3	29.5	29.8	29.8	32.1	22.9	14.2		
dodecene	47.0	52.3	32.7	26.2	29.6	29.8	29.8	29.8	29.8	32.1	22.9	14.2

1.2.2 ¹³Chemical shift data for unsaturated epoxy fatty acid methyl esters.

A limited number of cis-epoxy octadec-Z-enoates were available for CMR analysis. These epoxides are of interest since changes in steric and linear electric field effects will be expected as a result of replacing two methylene groups by an olefinic bond. For PUFA this leads to a breakdown of the assumed additivity of shielding and deshielding parameters and correction factors are required whose absolute magnitude increases concomitantly with the decrease in number of methylenes between the double bonds. Pollard et al^[46] found a linear logarithmic relationship for plots of correction factors versus the number of interposing methylene groups separating the double bonds (n) provided $n > 1$, suggesting that linear electric field contributions are important.

Table 1.2.2.1 lists the ¹³C chemical shifts for the cis-epoxy octadec-Z-enoates, in which the number of methylenes between the epoxide function and the double bond varies from 1 to 5. Table 1.2.2.2 lists the correction factors for the methylenes in between the functional groups. It is apparent that the correction terms for this class of compound are substantially less than those required for diene, diyne and higher PUFA systems. This is consistent with the predominant factor responsible for the observed shifts being perturbations from an induced polarisation brought about by the functional group. The epoxy group will create and be affected by a smaller linear electric field than would a similar situated olefinic or acetylenic site as a consequence of its reduced polarisability.

Thus for the examples studied a good correlation between experimental and predicted values is observed as shown below for methyl 8,9-cis-epoxyoctadec-12Z-enoate and methyl 6,7-cis-epoxyoctadec- 12Z-enoate for which the values are calculated using only the substituent parameters obtained in 1.2.1 and substituent parameters for cis-olefinic bonds^[35].

Comparison of experimental and calculated^{a,b} data

(1) methyl 6,7 epoxy octadec-12Z-enoate

C1	173.57	C10	28.86 (29.0)
C2	33.60 (33.5)	C11	26.54 (26.7)
C3	24.25 (24.3)	C12	129.28 (129.4) ^c
C4	25.80 (25.9)	C13	129.46 (129.5) ^c
C5	27.17 (27.2)	C14	26.73 (26.7)
C6	56.57 (56.5)	C15	28.86 (29.2)
C7	56.71 (56.7)	C16	31.46 (31.0)
C8	27.53 (27.5)	C17	22.24 (22.2)
C9	26.29 (26.0)	C18	13.69 (13.7)

(2) Methyl 8,9-epoxy octadec-12Z-enoate

C1	173.83	C10	24.07 (23.9)
C2	33.76 (33.5)	C11	27.59 (27.6)
C3	24.64 (24.6)	C12	128.26 (129.4) ^c
C4	28.76 (28.7)	C13	130.47 (129.5) ^c
C5	28.62 (28.7)	C14	26.86 (26.7)
C6	26.02 (26.4)	C15	29.16 (29.2)
C7	27.77 (27.7)	C16	31.46 (31.0)
C8	56.93 (56.3)	C17	22.32 (22.2)
C9	56.39 (56.4)	C18	13.67 (13.7)

^a data calculated without the use of the correction factors listed in Table 1.2.2.1

^b data calculated using parameters 129.50, 56.80 and 29.20 ppm for unperturbed olefinic, epoxidic and methylene groups respectively.

^c data are calculated without taking into account electric field effects from carboxyl head group.

Table 1.2.2.1 ^{13}C chemical shifts for epoxyoctadecenoates.


C	9,12 B	8,12 A	7,12 A	7,12 B	6,12 A	5,12 A	6,10 A
1	173.81	173.83	173.57	173.57	173.58		173.78
2	33.75	33.76	33.73	33.57	33.60	33.13	33.75
3	24.63	24.64	24.56	24.53	24.25	24.62	24.39
4	28.80	28.76	28.50	28.68	25.80	26.83*	26.43
5	28.80	28.62	26.00	29.06	27.17	56.86	27.71
6	28.80	26.02	27.52	26.38	56.57	56.86	57.03
7	29.20	27.59*	56.78	128.67	56.71	27.52	56.45
8	25.99	56.93	56.64	130.28	27.53	26.00	27.78
9	132.19	56.39	27.19	26.69	26.29	27.52*	24.18
10	123.78	24.07	26.42	26.00	28.86	28.89	128.72
11	25.99	27.77*	26.75	27.19	26.54	26.26	128.98
12	56.79	128.26	129.04	56.56	129.28	128.27	26.62
13	56.16	130.47	129.87	56.56	129.46	130.57	29.01
14	27.49	26.86	26.75	27.35	26.73	26.26	28.93
15	27.11	29.16	29.03	26.87	28.86	29.31	29.31
16	31.46	31.46	31.44	31.18	31.46	31.44	31.59
17	22.27	22.32	22.29	22.23	22.24	22.30	22.43
18	13.63	13.67	13.66	13.68	13.69	13.60	13.85
-COOMe	50.99	51.04	51.02	50.99	50.98	51.07	51.18

A refers to epoxide function at carboxyl end of m,n system.

B refers to epoxide function at methyl end of m,n system.

* some uncertainty exists.

Table 1.2.2.2 Correction factors for cis-epoxyoctadecenoates.

	C=C	correction factor/ ppm
12	9	$- \text{HC} = \text{CH} - \text{CH}_2 - \text{CH} \begin{array}{c} \diagup \text{O} \diagdown \\ \text{CH} \end{array} - \text{CH}_2$ $+2.8 \ +3.0 \ +0.8 \ +0.0 \ +0.2 \ +0.2$
8	12	$- \text{HC} \begin{array}{c} \diagup \text{O} \diagdown \\ \text{CH} \end{array} - \text{CH}_2 - \text{CH}_2 - \text{CH} = \text{CH} - \text{CH}_2 -$ $+0.2 \ +0.0 \ -0.2 \ +0.0 \ -1.1 \ +1.0 \ +0.2$
7	12	$- \text{HC} \begin{array}{c} \diagup \text{O} \diagdown \\ \text{CH} \end{array} - \text{CH}_2 - \text{CH}_2 - \text{CH}_2 - \text{CH} = \text{CH} -$ $0.0 \ 0.0 \ 0.0 \ 0.0 \ 0.2 \ -0.5 \ +0.4$
12	7	$- \text{HC} = \text{CH} - \text{CH}_2 - \text{CH}_2 - \text{CH}_2 - \text{HC} \begin{array}{c} \diagup \text{O} \diagdown \\ \text{CH} \end{array} -$ $-0.9 \ +0.8 \ 0.0 \ -0.3 \ +0.4 \ -0.2 \ -0.1$
6	12	$- \text{HC} \begin{array}{c} \diagup \text{O} \diagdown \\ \text{CH} \end{array} - \text{CH}_2 - \text{CH}_2 - \text{CH}_2 - \text{CH}_2 - \text{CH} = \text{CH} -$ $+0.1 \ 0.0 \ 0.0 \ -0.3 \ -0.1 \ -0.3 \ -0.2 \ 0.0$
5	12	$- \text{HC} \begin{array}{c} \diagup \text{O} \diagdown \\ \text{CH} \end{array} - \text{CH}_2 - \text{CH}_2 - \text{CH}_2 - \text{CH}_2 - \text{CH}_2 - \text{CH} = \text{CH} -$ $0.0 \ 0.0 \ 0.0 \ -0.2 \ -0.3 \ -0.3 \ -0.3 \ -0.7 \ +1.1$
6	10	$- \text{HC} \begin{array}{c} \diagup \text{O} \diagdown \\ \text{CH} \end{array} - \text{CH}_2 - \text{CH}_2 - \text{CH} = \text{CH} -$ $+0.6 \ 0.0 \ 0.2 \ -0.3 \ -0.6 \ -0.5$

correction expressed as $\delta_{\text{expt}} - \delta_{\text{predicted}}$.

1.2.3 ^{13}C chemical shift data for saturated cycloalkyl epoxides.

Table 1.2.3.1 presents ^{13}C chemical shift data for some cycloalkyl epoxides. The value of the epoxy carbons for cyclopentyl epoxide are very close to the values obtained for the aliphatic cis-epoxides. Cyclooctyl epoxide shows a small upfield shift of 1.4 ppm, but the largest upfield shift is observed for cyclohexyl epoxide whose epoxy carbons absorb at some 5 ppm upfield from the value obtained for the aliphatic epoxides.



Figure 1.2.3.1

Similar effects are observed in cycloalkenes, the olefinic carbons resonating at 130.6, 127.2, 133.3 and 130.7 ppm for cyclopentene^[47], cyclohexene^[47], cycloheptene^[48] and cyclooctene^[48] respectively. The trend is however different from that of the corresponding cycloalkenes^[17].

The observed chemical shifts will represent the weighted average of all the various conformations contributing to the ground state conformer population for each ring. For C5, C7 and C8 cycloalkanes, experimental evidence does not overwhelmingly distinguish between a single favoured conformation involved in a rapid pseudorotation itinerary or a mixture of preferred conformations. Hendrickson^[49] has calculated that the twist-chair conformation of cycloheptane

should be more stable than the chair, boat or twist boat conformers by more than 1.4 kcal/mole. Thus it is reasonable to presume that cycloheptane can be considered as a rapidly pseudorotating mixture of the various possible twist-chair conformers. For the cycloalkyl epoxides the perturbations to the geometry imposed by the epoxide ring will manifest itself primarily in steric effects by either increasing or decreasing steric shifts depending on the ring system under consideration.

As the ring size increases from C5-C8 the value of the C2 carbon fluctuates in a non-systematic manner, however for the least sterically strained cycloalkyl epoxide the shift for C2 (-1.43 ppm) is beginning to approach the α -substituent shift (-1.55 ppm) obtained for the aliphatic epoxides. For cyclopentyl epoxide the C2 shift is upfield by +0.29 ppm, which may result in part from the epoxide ring decreasing the population of the conformers which would relieve the steric interaction between the essentially eclipsed 1,2-methylenes, since cyclopentyl epoxide will be less 'flexible' than the corresponding cycloalkane. For cyclohexyl epoxide the downfield shift (-3.53 ppm) for C2 is larger than expected and probably results from a decrease in the 1,3-gauche steric interaction imposed by the half chair conformation (Figure 1.2.3.1) and by removal of a hydrogen at C1 (this latter effect although present for all the epoxides is more important for cyclohexyl epoxide since in the corresponding cycloalkane the gauche population is higher than in aliphatic or larger ring epoxides).

The C3 substituent shifts are all downfield and greater than expected on the basis of the substituent parameters for acyclic epoxides with the exception of cyclooctyl epoxide which is smaller

than expected. Anet and co-workers^[42] argued that the downfield shift in cyclohexyl epoxide was a result of the lone pair of electrons on the oxygen being spatially proximate to both the C3 carbons since ring flip is rapid at room temperature. Similar rationalisation can be evoked for C5 and C7 cycloalkyl epoxides as shown below (Figure 1.2.3.2). The conformations shown will contribute to the downfield C-3 shift but other more sterically favoured conformers with little or no interaction can be formulated.

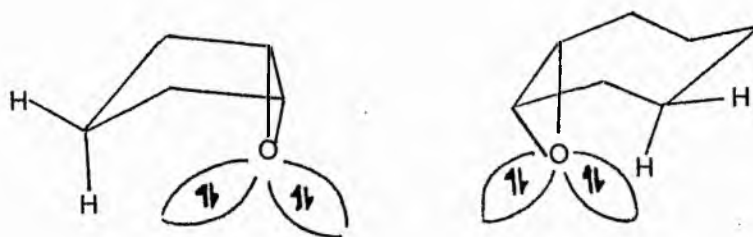
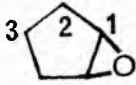
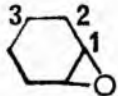
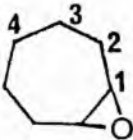
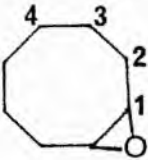


Figure 1.2.3.2 Possible conformations for cyclopentyl and cycloheptyl epoxides contributing to a downfield shift of the C-3 carbon as a result of steric perturbation from the oxygen lone pair.

Table 1.2.3.1^a ¹³C chemical shift parameters for cycloalkyl epoxides.

Epoxide	carbon			
	1	2	3	4
	56.67 (+30.17)	26.79 (+ 0.29)	17.88 (-8.62)	
	51.86 (+24.06)	24.27 (-3.53)	19.25 (-8.55)	
	55.5 (+26.1)	28.8 (-0.6)	24.2 (-5.2)	30.8 (+1.4)
	55.35 (+27.55)	26.37 (-1.43)	26.11 (-1.69)	25.40 (-2.4)

^a numbers in parentheses refer to shift differences between that carbon in the cycloalkyl epoxide and the corresponding cycloalkane [data from ref 18]

^b data from ref 44.

1.2.4 ^{13}C chemical shifts for saturated primary alcohols.

Table 1.2.4.1 presents the ^{13}C chemical shifts for a number of long chain saturated primary alcohols. The chemical shifts of the C1, C2, and C3 carbons are remarkably constant with mean values (+ S.D.) of 62.73 (+0.05) ppm, 32.64 (+0.04) ppm and 25.61 (+0.03) ppm respectively. All carbons give resolved signals up to nonanol, after which nine signals are observed. Three of which are unambiguously associated with the alcohol moiety and three with the terminal methyl group. As in other systems^[18] the carbon bearing the functional group experiences a pronounced downfield shift, while the C3 carbon has an upfield shift of a few parts per million. Longer range shieldings are only marginally outside experimental error, and could not be assigned with certainty.

Roberts et al^[39] have studied a comprehensive series of alcohols (36 examples) including short chain primary alcohols (C1-C10) and a number of secondary and alicyclic alcohols. They found a good linear relationship between carbon chemical shifts in alcohols and analogously constituted hydrocarbons, wherein the methyl group replaces the hydroxyl group as given by equation 6 .

$$\delta_{\text{c}}^{\text{ROH}}(\kappa) = m \delta_{\text{c}}^{\text{RCH}_3}(\kappa) - \text{constant}$$

where $\delta_{\text{m c}}^{\text{RCH}_3}(\kappa)$ is the shielding of the κ^{th} carbon. With the exception of the substituent bearing carbon ($m=1$), the deviation from unit

Table 1.2.4.1 ¹³C chemical shift data for primary alkanols.

Carbon	alcohol							
	C7	C8	C9	C10	C12	C14	C16	C18
1	62.69	62.66	62.72	62.71	62.70	62.79	62.77	62.81
2	32.60	32.58	32.63	32.62	32.62	32.68	32.65	32.71
3	25.55	25.60	25.61	25.61	25.59	25.65	25.65	25.64
4	28.92	29.10	29.09	29.11	29.15	29.52	29.24	28.71
5	31.64	29.23	29.31	29.30	29.44	29.52	29.33	29.55
6	22.60	31.65	29.41	29.43	29.44	29.52	29.54	29.55
7	13.80	22.40	31.71	29.43	29.44	29.52	29.54	29.55
8		13.80	22.48	31.71	29.44	29.52	29.54	29.55
9			13.84	22.44	29.27	29.52	29.54	29.55
10				13.82	31.72	29.52	29.54	29.55
11					22.46	29.52	29.54	29.55
12					13.83	31.78	29.54	29.55
13						22.52	29.54	29.55
14						13.89	31.78	29.55
15							22.53	29.55
16							13.89	31.80
17								22.55
18								13.92

gradient was explained by Roberts et al.^[39] in terms of polarisabilities of the substituents.

Table 1.2.4.1 Substituent shifts for primary alcohols.

Substituent position	shift/ppm
α	+3.15
β	-3.87

1.2.5 ¹³C chemical shifts for primary unsaturated alcohols.

Table 1.2.5.1 gives the ¹³C chemical shifts for a variety of long chain unsaturated primary alcohols with differing degrees of unsaturation. Many of the assignments are based on previous data on olefinic fatty acids and esters. As in the case of the unsaturated epoxides (section 1.2.2) the additivity parameters for primary alcohols and for the unsaturated centres require little adjustment. Maximum deviations were found for the allylic methylenes but in all cases were <0.3 ppm. These minor discrepancies did not hinder unambiguous assignments for any of the carbons. Table 1.2.4.1 lists the differences between experimental and calculated chemical shifts for entries where the olefinic group is in the proximity of the hydroxyl group.

Table 1.2.5.1. ^{13}C chemical shift data for unsaturated primary alcohols.

Carbon	10:1(4t)	13:1(4t)	11:1(4c)	18:1(3c)	18:1(4c)
1	62.24	62.33	61.97	61.95	62.02
2	30.60	32.40	32.41	30.59	32.45
3	32.24	28.76	23.34	124.87	23.40
4	128.99	129.22	128.62	132.71	128.64
5	129.21	131.09	130.33	27.15	130.38
6	32.34	32.40	26.94	29.15	27.01
7	29.08	29.41	29.43	29.15	29.17
8	31.22	29.13	29.00	29.48	29.50
9	22.33	29.35	31.52	29.48	29.50
10	13.81	29.13	22.36	29.48	29.50
11		31.76	13.72	29.48	29.50
12		22.51		29.48	29.50
13		13.90		29.48	29.50
14				29.48	29.50
15				29.48	29.50
16				31.72	31.75
17				22.45	22.47
18				13.79	13.82

Carbon	18:1(9c)	18:2(9c,12c)	18:3(6c,9c,12c)	19:3(7c,10c,13c)
1	62.64	62.27	62.61	62.68
2	25.60	25.49	25.22	25.48
3	32.57	32.57	32.44	32.57
4	29.12	29.19	29.13	28.90
5	29.12	29.39	27.00	29.14
6	29.30	29.19	129.80	27.02
7	29.57	29.39	127.76	129.97
8	27.01	27.07	25.45	127.66
9	129.60	129.82	127.99	25.48
10	129.68	178.82	128.14	128.06
11	27.01	25.72	25.45	128.14
12	29.57	127.82	127.45	25.48
13	29.30	129.82	130.19	127.48
14	29.12	27.07	27.00	130.19
15	29.30	29.55	29.22	27.27
16	31.72	31.39	31.33	29.43
17	22.47	22.43	22.34	31.33
18	13.84	13.84	13.80	22.36
19				13.81

A plot of the logarithm of $\Delta\delta_{n,n+1}$ (the shift difference between the unsaturated carbons) versus $2n+1/2$ as for the unsaturated epoxides gives a linear correlation. Figure 1.2.5.1 shows the data together with the data for the epoxides and data for unsaturated fatty acids (taken from Pollard etal^[35,34]). The quality of the fit is substantial in all cases and more importantly, although the gradients of the lines differ, the intercept on the $\log \Delta\delta_{n,n+1}$ axis is approximately constant. The lines can be adequately represented by the general equation

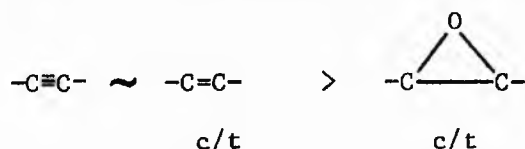
$$\Delta\delta_{n,n+1} = A e^{-\xi(2n+1)}$$

where A is a constant which is independant of the head group and of the polarisability of the site in question. Both of these two variables are incorporated in ξ . The intercept corresponds to $2n+1 = 0$ or alternatively $n = -1/2$. The physical interpretation of the intercept is that the functional group is located at carbon numbers $-1/2$ and $1/2$ ie directly on the head group. The value of the intercept corresponds to a shift difference of ca 100 ppm.

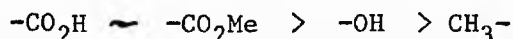
Table 1.2.5.2 presents values for A and ξ obtained from a least squares best fit line through the data points, with the exception of the data for the functional group at position 3 which appear to be smaller than predicted in all cases. The differences in the ξ -values between the isomeric olefins and the acetylenes are well within the experimental error and should be regarded as equivalent, suggesting that the polarisability of the three types of unsaturation are identical. As noted earlier, the isomeric epoxides also have

essentially the same polarisabilities.

A large difference of 1.2 fold is observed for the ξ -values when the carboxyl group is replaced by the hydroxyl group. The change represents the difference in magnitude of the head group dipole. Replacement of an unsaturated centre by an epoxide group also results in an increase in ξ , by a factor of 1.4 fold. The parameter ξ therefore is inversely related to the magnitude of the electric field effect. The values can be used to qualitatively compare polarisabilities and head group effects. Our data suggest the following order of polarisabilities of the functional groups



and the ability of the head group to induce polarisation is in the order.



Also included in Table 1.2.5.2 are A and ξ values for functional groups influenced by a terminal methyl group. These values may be compared with the polar head group values which are between 1.5-1.7 fold greater. However several reservations must be made before comparing these values. Firstly the number of data points is small, although their ξ -value suggests the extrapolation is valid. Secondly the ω -4 functionalised molecules consistently give shift differences which are smaller than expected from the plot. This anomaly presumably results from the 1,4-juxta position of the functional group with the methyl group resulting in a steric perturbation which will be

over and above the shift difference from any electric field effect.

Although the empirically derived relationship is useful for predicting the chemical shift difference between two adjacent functionalised carbons affected by a head group, and for giving relative magnitudes of electric field effects for the compounds investigated, the exponential fall off in $\Delta\delta$ is difficult to rationalise from a theoretical standpoint, involving dipole induced polarisation. Buckingham^[50] has formulated a general expression for electric field contributions to the rotationally averaged shielding constant of a nucleus in a molecular environment in terms of a power series in the electric field, E . The contribution to the chemical shift δ_{ei} is given by

$$\delta_{ei} = E_i \Phi_{ij} d\Psi_j + E_i E_j \Xi_{ijk} d\Psi_k$$

where E_i are components of the field vector

$d\Psi_k$ are components of a unit vector fixed in
the molecular framework.

and Φ_{ij} and Ξ_{ijk} are components of a second and
third rank tensors respectively.

The linear component may be ascribed to polarisation of the molecular bond by an electric field, while the second order term can be considered to arise from mixing of the excited states in the wave function. The second order term falls off rapidly with distance and at points well removed the polar group can be considered negligible. Furthermore the E^2 contributions to the shift difference will be in

the same direction for both carbons of the functional group, and by confining the discussion to the difference, $\Delta\delta_{el}$ between the shifts of a pair of functionalised carbons any residual effects of the E^2 term will be minimised further. With these assumptions in mind and suitable choice of coordinate system Batchelor et al^[23] derived an expression for the induced shift differences as

$$\Delta\delta_{el} = 2 E_z \Theta_{zz} \quad (5)$$

where E_z is the component of the electric field in the direction of the C-C bond of the functional group.

and Θ_{zz} is a linear electric field coefficient for one of the carbons under consideration.

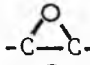
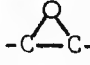
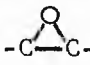

For any given chain conformation, the component of the field at carbon atom n, resolved along the functional group C-C bond will be given by

$$E_z(n) = \frac{3(\mu \cdot \Psi_n)(\Psi_n \cdot d\Psi)}{\Psi_n^5} - \frac{(\mu \cdot \Psi)}{\Psi_n^3}$$

where Ψ_n is the vector to the n^{th} carbon, and the unit vector along the bond from carbon n to n+1 is Ψ . μ is the dipole moment of the head group, assuming it to be a point source. Substituting the average field value $E_z(n + \frac{1}{2})$ into (5) gives

$$\Delta\delta_{el} = \frac{2 \mu \cdot d\Psi}{\Psi_{\frac{2n+1}{2}}^3} \Theta_{zz}$$

TABLE 1.2.5.2 Variation in A and ξ values with head group and functional group.

Head group	Functional group	A	ξ	corr. coef.	ref
-COOH	-C=C- (cis)	4.74	0.651	.994	35
	-C=C- (trans)	4.47	0.602	.998	35
	-C \equiv C-	4.30	0.588	.979	36
-COOMe	 (cis)	4.28	0.849	.994	this work
	 (trans)	4.30	0.852	.966	this work
-OH	-C=C- (cis)	4.50	0.764		this work
CH ₃ - ^a	-C=C- (cis)	4.3	1.1		35
	-C=C- (trans)	4.3	1.1		35
	-C \equiv C-	4.1	1.1		36
	 (cis)	4.3	1.4		this work
	 (trans)	4.3	1.4		this work

^a no corr. coef. are quoted for these parameters since only 2-3 points were used to generate the values.

Table
1.2.5.3

The effect of the methyl group on the ^{13}C chemical shift difference between the carbons of functionalised groups.

Position of functional groups.	cis ^a olefins	trans ^a olefins	acetylenes	cis epoxides	trans epoxides
ω -1	7.34	7.31	5.77	4.54	5.31
ω -2	2.16	2.40	1.96	1.03	1.29
ω -3	0.48	0.46	0.37	0.11	0.16

^a Data calculated from ref 36.

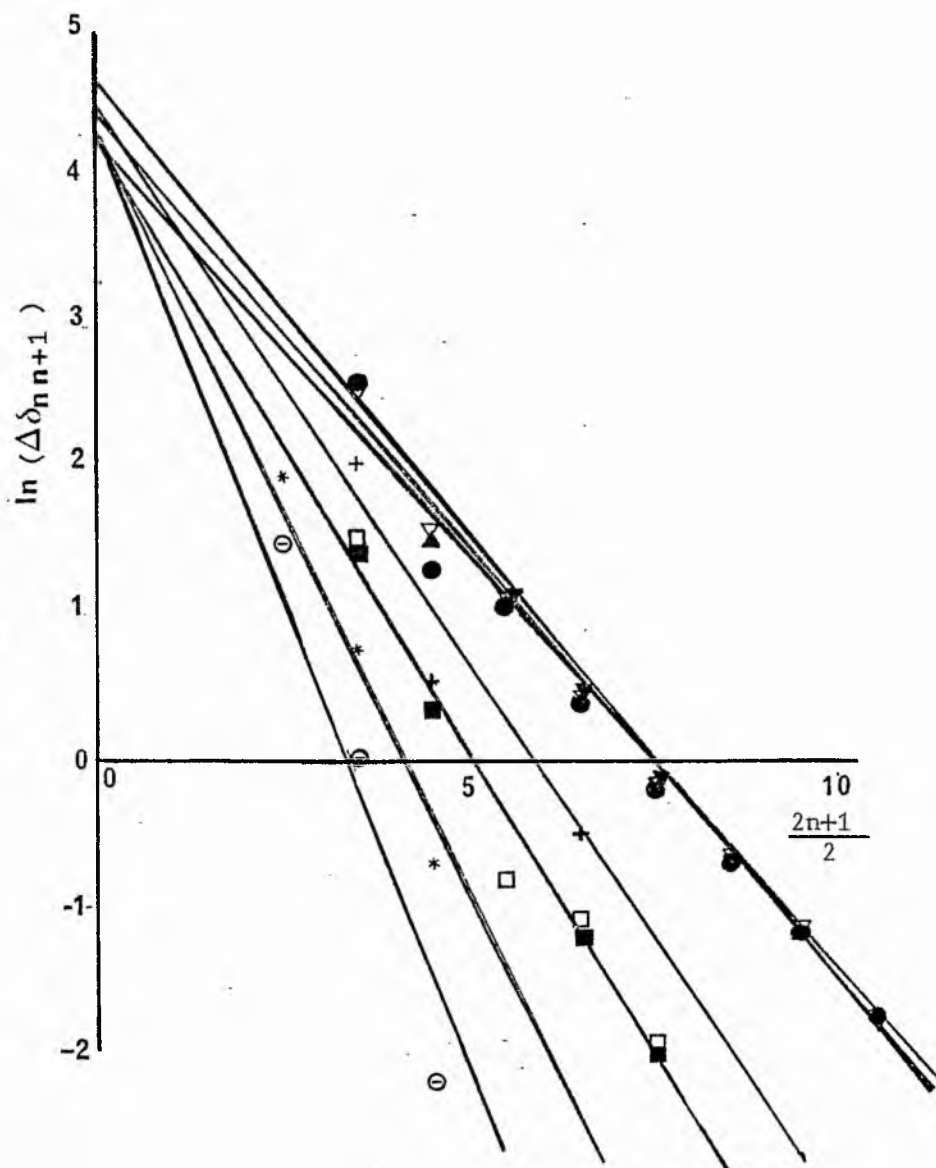
Table
1.2.5.4

The effect of the polar head group on the ^{13}C chemical shift difference between the carbons of functionalised groups.

Position of functional groups.	carboxylic acids. ^a			alcohols. cis olefins	methyl esters.		
	acet- ylenes	cis olefins	trans olefins		cis epoxides	trans epoxides	cis olefins.
Δ 3	13.90	14.12	14.18	7.84	4.19	4.73	12.40
4	3.72	4.89	4.92	1.74	1.45	1.42	4.01
5	2.91	3.23	3.26			0.46	2.76
6	1.46	1.30	1.64	0.81	0.29	0.33	1.58
7	0.80	0.85	0.92		0.13	0.14	0.73
8	0.499	0.50	0.54				0.45
9	0.30	0.26	0.30	0.08			0.24
10	0.17	0.16	0.16				
11	0	0.08	0.01				

^a Data calculated from ref 36

FIGURE 1.2.5.1 Plot of $\ln(\Delta\delta_{n,n+1})$ versus $2n+1/2$.



- ∇ cis olefinic carboxylic acids
- \blacktriangle trans olefinic carboxylic acids.
- \bullet acetylenic carboxylic acids.
- $+$ cis olefinic primary alcohols.
- \blacksquare cis epoxyoctadecanoates.
- \square trans epoxyoctadecanoates
- $*$ CH_3 - effect on cis olefins.
- \ominus CH_3 - effect on cis epoxyoctadecanoates.

assuming that the Ψ^{-5} term will be negligible at distances removed from the head group. If the chain were rigid, the orientation of the functional moiety relative to the dipole would remain fixed and only distance would contribute to Ψ , hence $\Delta\delta_{ei}$ would be proportional to n^{-3} . In fact Batchelor et al^[23] in a more sophisticated analysis showed that the fall off was proportional to the power -3.5 using a random walk model and weighting each conformation with respect to a Boltzmann factor, suggesting that the all-trans rigid chain model is a good approximation. Figure 1.2.5.2 shows the $\Delta\delta_{ei}$ data plotted as a function of n^{-3} . The correlation is sufficiently good to support the electric field interpretation.

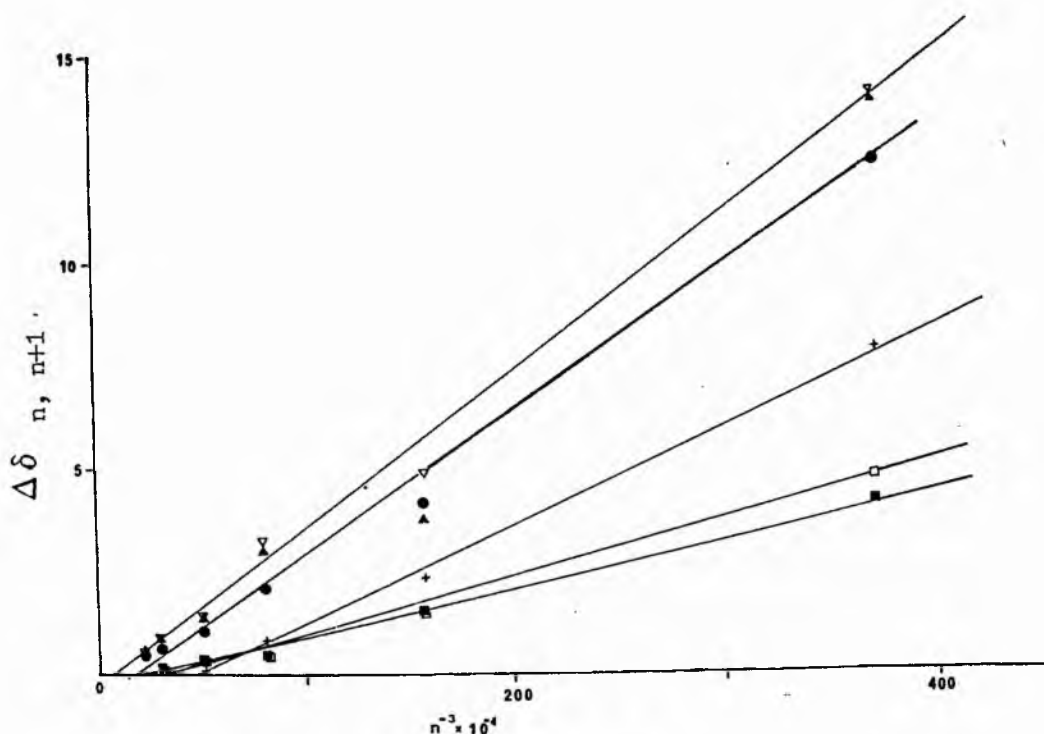


FIGURE 1.2.5.2

Plot of $\Delta\delta_{n, n+1}$ versus n^{-3} , where $\Delta\delta_{n, n+1}$ is the shift difference between olefinic or epoxy carbons. Symbols as in Figure 1.2.5.1

1.2.6 Vicinial diols

The vicinial diols methyl erythro- and threo-9,10-dihydroxy-stearates have been investigated by ^{13}C nmr spectroscopy⁽³⁸⁾.

A substantial difference between the chemical shifts for carbons 8 and 11 (adjacent to the hydroxyl bearing carbons at C11 and 12) between the two diastereoisomers was reported but no rationalisation of the data was attempted.

Two conformations can be drawn for each diastereoisomer, as depicted in Figure 1.2.6. In the gauche conformation both isomers may be stabilised by hydrogen bonding between the hydroxyl groups. In the trans conformation however no such stabilisation is possible.

The larger shift values for the threo isomer would suggest that a larger 1,4-steric perturbation is operative in the erythro diol, resulting in an upfield shift of C8 and C11 relative to the corresponding carbons in the threo diastereoisomer. Clearly from Figure 1.2.6.1 this implies that the hydroxyl groups will be gauche to each other, resulting in a decrease of the trans diol rotomer population.

In the threo isomers of cis and trans methyl 12,13-dihydroxy-octadec-9-enoate, C14 also appears at 33.7 ppm. In these two compounds C11 does not experience the same shift as a result of the adjacent double bond.

However application of the substituent parameters for olefinic carbons⁽³⁵⁾ suggests that in the 9E isomer the chemical shift of C11 in the absence of the double bond would be

$$31.8 - 2.51 = 34.5 \text{ ppm}$$

similarly for the 9Z isomer

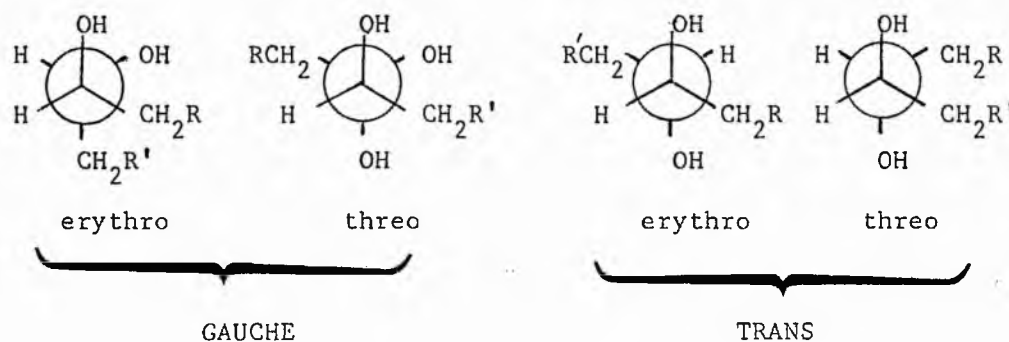
$$37.2 - 2.87 = 34.3 \text{ ppm}$$

The small difference between the calculated value and the value observed for C14 may result from electric field effects. Table 1.2.6.1 reproduces selected shifts for the compounds discussed taken from Rakoff *et al* [38].

Table 1.2.6.1 ^{13}C Chemical shifts for vicinial diols [38].

Carbon	threo 12,13-diOH 18:1(9Z)	threo 12,13-diOH 18:1(9E)	erythro 9,10-diOH 18:0	threo 9,10-diOH 18:0
15	25.4	25.5		
14	33.7	33.7		
13	73.9	73.8		
12	74.0	74.0	26.0	25.6
11	31.8	37.2	31.3	33.7
10	133.0	133.9	74.8	74.6
9	125.1	126.1	74.8	74.6
8	27.4	32.7	31.3	33.7
7			26.0	25.6

FIGURE 1.2.6.1



1.2.7 ¹³C Chemical shift data for primary alkyl hydroperoxides.

¹³C Chemical shift data for primary alkyl hydroperoxides have not been previously reported. Table 1.2.7.1 presents the chemical shift of long chain primary hydroperoxides. The shielding parameters are given in Table 1.2.7.2. The lower homologues show greater spectral detail, and for octyl and nonyl hydroperoxides a separate signal for each carbon is observed. Figure 1.2.7.1 shows the upfield region (32-13 ppm) for the alkyl hydroperoxides investigated. The C1 chemical shifts all fall within a very narrow range, 76.89-77.08 ppm.

The shift is further downfield than the corresponding carbon in primary alcohols, suggesting that the inductive effect is greater for the OOH linkage. Furthermore the direction of the α -shift is in the opposite sense to the corresponding alcohols. We have assigned the -3.76 ppm shift to the β -substituent shift on the basis that is of similar magnitude to the corresponding shift in primary alcohols and terminal epoxides. This may not be a valid extrapolation, but either way the α -shift will clearly be in the opposite direction to the α -shift for the hydroxy compounds.

Table 1.2.7.2 Substituent shifts for primary alkyl hydroperoxides.

Substituent position	δ /ppm
α	-2.06
β	-3.76

Table 1.2.7.1 ^{13}C chemical shifts for primary alkyl hydroperoxides.

Carbon	hydroperoxide							
	C8	C9	C10	C11	C13	C14	C16	C18
1	77.08	76.89	77.02	76.90	77.08	76.89	76.89	76.89
2	25.75	25.63	25.75	25.73	25.79	25.73	25.70	25.67
3	27.44	27.31	27.44	27.43	27.47	27.42	27.41	27.32
4	29.04	28.95	29.15	29.12	29.51	29.47	29.46	29.41
5	29.24	29.17	29.46	29.37	29.51	29.47	29.46	29.41
6	31.64	29.17	29.46	29.37	29.51	29.47	29.46	29.41
7	22.49	31.58	29.46	29.37	29.51	29.47	29.46	29.41
8	13.89	22.35	31.60	29.37	29.51	29.47	29.46	29.41
9		13.75	22.40	31.69	29.51	29.47	29.46	29.41
10			13.86	22.46	29.51	29.47	29.46	29.41
11				13.86	31.69	29.47	29.46	29.41
12					22.46	31.73	29.46	29.41
13					13.86	22.47	29.46	29.41
14						13.84	31.76	29.41
15							22.51	29.41
16							13.79	31.67
17								22.40
18								13.77

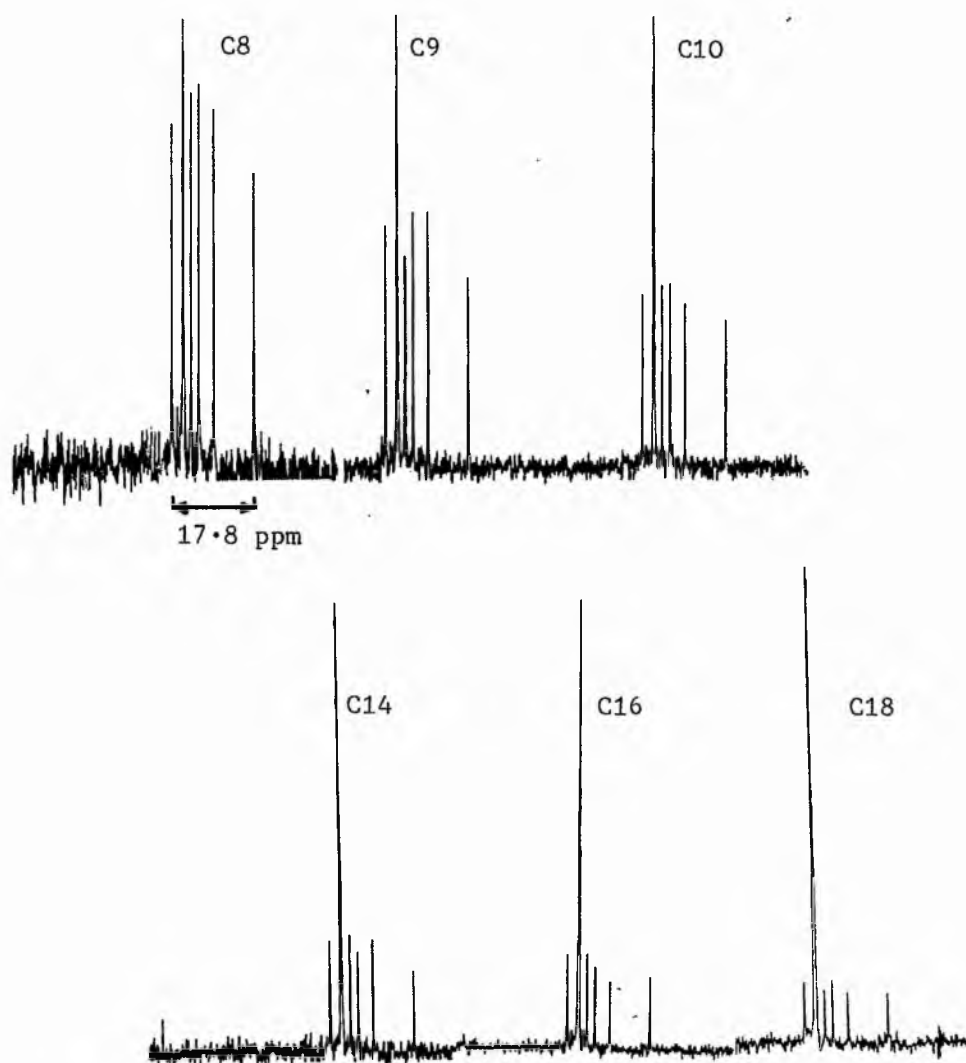
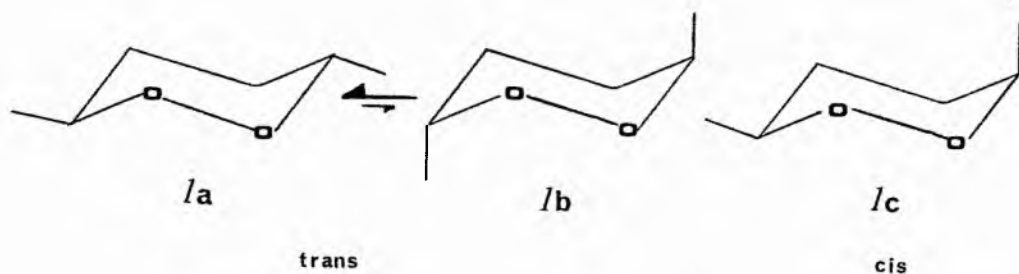


FIGURE 1.2.7.1 Upfield region of the ^{13}C NMR spectra of alkyl hydroperoxides.

1.2.8. Monocyclic peroxides.

Table 1.2.8.1 presents ^{13}C chemical shift data for a set of five and six membered cyclic peroxides reported by Bloodworth et al^[51,52]. The six-membered cyclic peroxide (1) exists in two diastereoisomeric forms in which the methyl groups are either cis or trans with respect to each other. By analogy with dimethylcyclohexane the trans isomer would be envisaged to exist for the most part in the diequatorial conformer on the basis that an equatorial methyl group results in a conformer with minimum steric strain while an axial methyl group creates a gauche steric interaction with the γ -carbon. Taking an estimate of 3.7 kJmole^{-1} for a gauche interaction^[53] then the diequatorial conformer (1a) should be approximately 7.4 KJmole^{-1} lower in energy than the diaxial conformer (1b).



This estimated difference in energy should preclude significant contributions to the CMR spectra of (1b) and the ^{13}C chemical shifts will therefore result from the predominant e,e form.

In the e,e trans isomer there will be no γ -gauche steric perturbations. In the cis isomer which of necessity has one of its methyl groups axial, a steric interaction between the axial

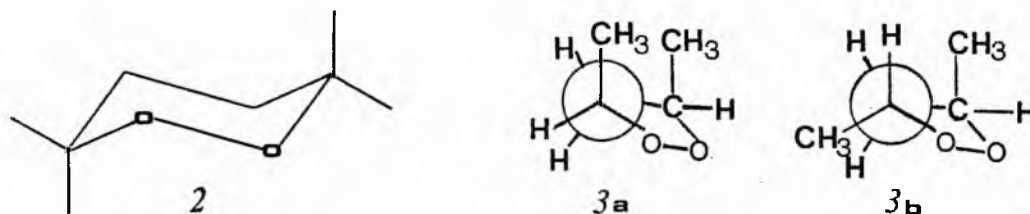
methyl group and the γ -carbon hydrogen can be expected to give rise to a γ -gauche steric shift. However the six-membered rings can readily undergo ring flip at room temperature and hence each methyl group for the cis isomer will experience 1/2 a full gauche steric interaction, as will each C2 carbon. The observed γ -steric shift for the cis C2 carbon is upfield by 4.54 ppm, giving the value 9.08 for a full γ -gauche steric effect in the 1,2-dioxacyclohexane. This may be compared with approximately 6.3 ppm for a full γ -gauche effect in methylcyclohexane^[53]. The higher value observed for the cyclic peroxide probably reflects a departure from an idealised chair conformation as a result of the shorter C-O and O-O bonds, which may decrease the distance between the interacting protons resulting in an increase in the polarisation. The shift difference between the methyl carbons is complementary to the shift difference of the C2 carbons. The value from methylcyclohexane for the γ -gauche effect on the methyl substituent is 1.98 ppm per full H''''H interaction. The observed value from methylcyclohexane for the cyclic peroxide is 1.22 ppm

The shift increments resulting from steric perturbations are listed in Table 1.2.8.2 along with values for analogous interactions in methyl substituted cyclohexanes.

For the tetramethyl substituted cyclic peroxide (2) a 'buttressing' effect^[53] will exist as a consequence of the geminal methyl substituents. Analysis of steric contributions is more difficult in this case since it is necessary to partition the effects between contributions transmitted through the electronic bonding framework (as a result of replacing -H with CH₃-), and electric fields effects from perturbations associated with steric compressions resulting from the geminal juxta position of the methyl groups. The

increment for the methyl groups compared with the cis dimethyl peroxide is downfield by 8.39 ppm. When the effect of a methyl group (-10.4 ppm)^[53] is substituted from the experimental value (and neglecting δ -substituent shifts of <0.1 ppm) a net upfield value of 2 ppm is observed per 1/2 gauche interaction giving a value for the full gauche interaction of 4 ppm. The corresponding value for the cyclohexane series is 4.18 ppm. The perturbation to the ring methylenes, after correction for β -axial, γ -equatorial methyls and γ -geminal methyl parameter shifts gives an upfield shift of 2.15 ppm. The corresponding shift in the cyclohexane system is 4.22 ppm.

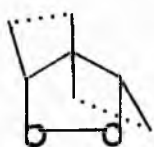
For the five-membered ring systems the situation is more complicated. For both cis and trans 3,5-dimethyl 1,2-dioxane (3a,b) the methyl groups are essentially eclipsed with the neighbouring hydrogens of the C4 methylene if the molecule is nearly planar. Even a substantial amount of puckering of the ring will still leave a large 1,2-interaction.



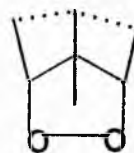
In the cis isomer a steric interaction will be observed across the ring between the two methyl groups (1,3-juxta position) although the interaction will be small since the methyl groups are not in fully axial but pseudo axial positions. The resulting shifts are +0.26 ppm and +0.85 ppm at the peroxy methine and at the methyl group respectively. The perturbation to the methylene group in the ring is

0.73 ppm. These shift increments are all downfield and hence in the opposite direction to the steric shifts incurred in the dioxacyclohexanes. The magnitudes of the shifts are small in comparison.

For the 3,4,4,5-tetramethyl 1,2-dioxacyclopentane isomers a large shift is observed for one of the methyl groups on C4.



(trans)



(cis)

For the symmetrical trans isomer both methyl groups on C4 resonate at 21.53 ppm while in the cis isomer one methyl group shift is observed at 21.77 ppm and the other at 14.44 ppm. This difference of 7.33 ppm probably reflects the magnitude of the 1,2-vicinal steric shift, although it appears that the increments are not additive after the first 1,2-interaction since a difference of only 0.24 ppm was observed between one (V_{α})(trans isomer) and two ($V_{\alpha\alpha}$)(cis isomer) 1,2-vicinal interactions. The incremental shifts are shown in Table 1.2.8.3.

Table 1.2.8.1 ^{13}C chemical shifts for cyclic peroxides.

Peroxide		carbon					
		1	2	3	4	5	6
	cis	77.30	49.34	19.25			
	trans	77.04	48.61	18.40			
		77.94	48.32	83.47	18.75	27.02	25.90
		83.64	58.56	26.47			
	cis	84.49	50.87	12.00	21.77	14.44	
	trans	85.38	50.80	12.92	21.53	21.53	
	cis	76.30	27.04	18.18			
	trans	77.08	31.58	18.79			
		77.00	31.10	27.18			

^a Data taken from refs 51 and 52.

TABLE 1.2.8.2

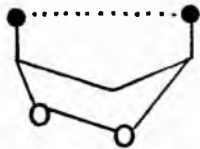
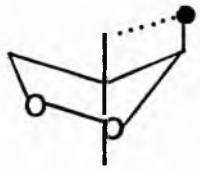
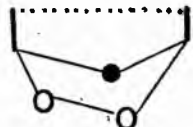
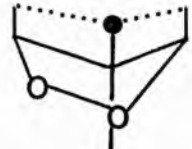
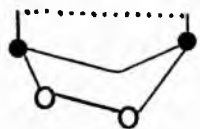
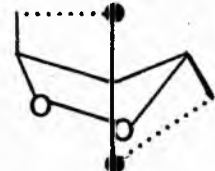
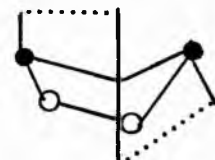
Observed ^{13}C chemical shift increments
resulting from steric interactions in
1,2-dioxacyclohexane derivatives.

Interaction	Fractional Shift per $\text{H}\cdots\text{H}$ interaction* (ppm)	Value for cyclohexane system ^a (ppm)
	-1 22	-1 98
	-9 08	-6 32
	-4.00	-4.18
	-2 19	-4 22

* shift at marked carbon(s), given in ppm.

a/data from Dalling, D.K. and Grant, D.M., J. Amer. Chem. Soc.
1972, 94, 5318.

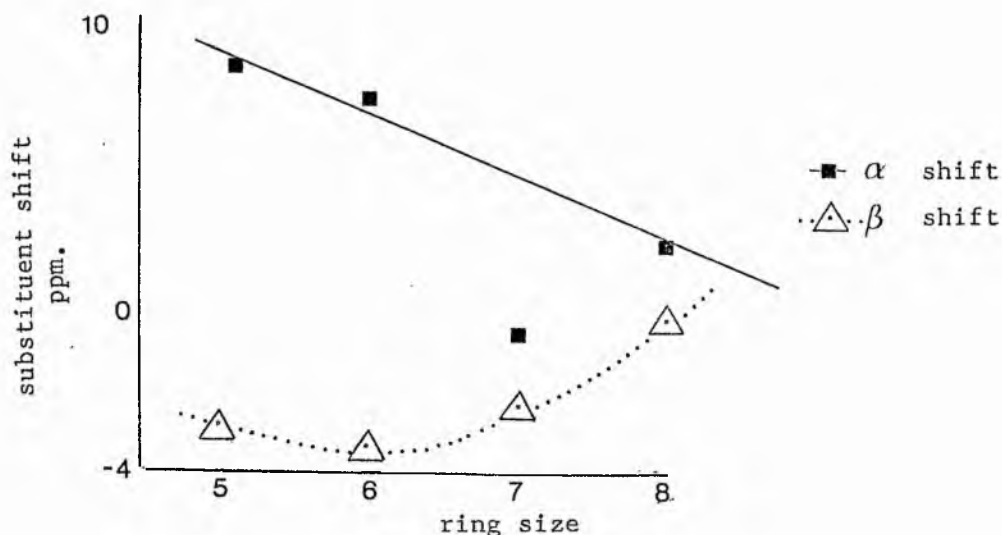
TABLE 1.2.8.3 Observed ^{13}C chemical shift increments resulting from steric interactions in substituted dioxolanes.

Interaction	Fractional shift* per steric interaction.		
	+ 0.85		+ 0.24
	+ 0.73		+ 7.33
	+ 0.26		+ 7.09
			+ 0.89

* shift at marked carbons(s), given in ppm.

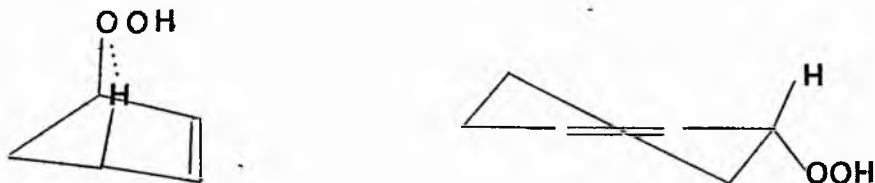
1.2.9 Cycloalkenyl hydroperoxides.

Table 1.2.9.1 presents ^{13}C chemical shifts for cycloalkenyl hydroperoxides, taken from this work and from Bloodworth *et al* [54]. Also shown in parenthesis are the corresponding shift differences for the carbons compared with their parent cycloalkene. Figure 1.2.9.1 shows a plot of the α -shifts and β -shifts for all six hydroperoxides. The β -shifts all lie on a smooth curve with a minimum at cyclohexenyl hydroperoxides. The α -shifts on the other hand lie on a straight line with the exception of cycloheptenyl hydroperoxide which appears to be anomalous.



From results on cyclic olefins [18] it would be expected that hydroperoxide bearing carbons will be subjected to two antagonistic effects, a deshielding influence from the adjacent double bond and a shielding effect from the cisoid configuration of the double bond. While the first of these factors should be independent of the ring size or conformation, clearly the steric factor will be intimately

linked with both. Comparison of the peroxy methine chemical shifts with the corresponding cycloalkanes amply demonstrates this fact. The induced shifts for cycloheptenyl and cyclooctenyl are very similar, differing by only 0.6 ppm. Cyclopentenyl hydroperoxide on the other hand is deshielded further by nearly 9 ppm as a result of 1,3 steric interaction.



Cyclohexenyl can effectively eliminate the 1,3 steric interaction by adopting the thermodynamically preferred half-chair conformer with the hydroperoxide in the pseudo equatorial position, and this manifests itself in an induced shift of only 51.0 ppm compared with the C7 and C8 analogues which will contain more pseudo axial conformers in their population distributions. This latter fact is very important in attempting to assign shift parameters to this set of compounds since subtle changes in the geometry of the ring systems will inevitably lead to an alteration of the conformer distribution, and since the observed chemical shifts at ambient temperature will be a weighted average of all the conformers the shift can be expected to change in general.

3 Experimental.

Natural abundance CMR spectra were obtained with a Varian CFT-20 spectrometer at 20MHz, with full proton noise decoupling (10^3 KHz band width). The spectra were scanned over a spectral width of 0-200 ppm (4000 Hz) with an acquisition time of 1.023 s and a pulse width of 7 μ s, at room temperature.

Samples (0.16 mmol) were dissolved in deuterochloroform (0.3 ml) in a standard ^1H nmr 5mm tube with a spherical bulb at the terminus of diameter 7mm. The deuterochloroform served as both the internal standard and as the field-frequency lock signal. The chemical shift values for the samples were then computed with respect to tetramethylsilane, using the known chemical shift of chloroform with respect to tertamethylsilane of 76.90 ppm.

Good spectra could be obtained with 14,000 data points (approx. 4 hr). This might be compared with the normal time required for a sample of 50 mg in a 10mm standard CMR tube in excess of 15 hr.

The samples were either commercially available, available from previous research programmes or were synthesised as described in Chapter 1 (sect 5).

References

1. W.C. Dickinson, Phys. Rev., 1950, 77, 736.
2. W.G. Proctor, Phys. Rev., 1950, 77, 716.
3. J.B. Strothers and N.K. Wilson, Top. Stereochem., 1974, 8, 1.
4. See L.M. Jackmann and S. Sternhill in "Applications of Nuclear Magnetic Resonance in Organic Chemistry", 2nd Ed, Oxford University Press, New York, 1969.
5. The total range of ^{13}C shieldings is more than 600 ppm. See
 - a) G.A. Olah and A.M. White, J. Amer. Chem. Soc., 1969, 91, 5801
 - b) O.W. Howarth and R.J. Lynch, Mol. Phys., 1968, 15, 431.
6. a) R.R. Ernst in "Advances in Magnetic Resonance", Ed J.S. Waugh, Vol 2, pp1, Academic Press, New York, 1966.
 - b) W. Horsley, H. Sternlicht and J.S. Cohen, J. Amer. Chem. Soc., 1969, 91, 7784.
7. Despite extensive theoretical investigation the origin of the chemical shift in large and/or complex molecules remains obscure¹⁴⁻¹⁶.
8. G.E. Macial, Top. Carbon-13 NMR Spectrosc. 1974, 1, 53.
9. G.L. Nelson and E.A. Williams, Prog. Org. Chem., 1976, 12, 229.
10. D.M. Grant and E.G. Paul, J. Amer. Chem. Soc., 1964, 86, 2984.
11. D.K. Dalling and D.M. Grant, J. Amer. Chem. Soc., 1967, 89, 6612.
12. W.M. Litchman and D.M. Grant, J. Amer. Chem. Soc., 1968, 90, 1400.
13. D.K. Dalling and D.M. Grant, J. Amer. Chem. Soc., 1973, 95, 3718.
14. A. Saika and C.P. Slichter, J. Chem. Phys., 1954, 22, 26.
15. H.M. McConnell, J. Chem. Phys., 1957, 27, 226.
16. J.A. Pople, Proc. Roy. Soc., 1957, A239, 550.
17. G.C. Levy and G.L. Nelson in "Carbon-13 Nuclear Magnetic Resonance for Organic Chemists", Wiley and Sons, New York, 1974.

18. J.B. Strothers in "Carbon-13 NMR Spectroscopy", Academic Press,
New York, 1972.
19. F. Wehrli and T. Wirthlin in "Interpretation of Carbon-13 NMR Spectra",
Heydon and Sons, New York, 1976.
20. J.A. Pople and M.S. Gordon, J. Amer. Chem. Soc., 1967, 89, 4253.
21. D.M. Grant and B.V. Cheney, J. Amer. Chem. Soc., 1967, 89, 5315.
22. J.G. Batchelor, R.J. Cushley and J.H. Prestegard, J. Org. Chem.,
1974, 39, 1698.
23. J.G. Batchelor, J.H. Prestegard, R.J. Cushley and S.R. Lipsky,
J. Amer. Chem. Soc., 1973, 95, 6358.
24. E.L. Eliel, W.F. Bailey, L.D. Kopp, R.L. Willer, D.M. Grant,
R. Bertrand, K.A. Christensen, D.K. Dalling, M.W. Duch, E. Wenkert,
F.M. Schell and D.W. Cochran, J. Amer. Chem. Soc., 1975, 97, 322.
25. L.P. Lindeman and J.Q. Adams, Anal. Chem., 1971, 43, 1245.
26. R.A. Friedel and H.L. Retcofsky, J. Amer. Chem. Soc., 1963, 85, 1300.
27. D.E. Dorman, M. Jautelet and J.D. Roberts, J. Org. Chem., 1973, 38, 1026.
28. J.W. de Haan and L.J.M. Van de Ven, Org. Magnetic Resonance, 1973, 5, 147.
29. W. Stoffel, O. Zierenberg and B.D. Tunggal, Z. Physiol. Chem., 1972,
354, 1962.
30. P.G. Barton, Chem. Phys. Lipids, 1975, 14, 336.
31. J. Bus and D.J. Frost, Recl. Trav. Chim. Pays-Bas, 1974, 93, 213.
32. A.P. Tulloch and M. Mazurek, Lipids, 1976, 11, 228.
33. J. Bus, I. Sies and M.S.F. Lie Ken Jie, Chem. Phys. Lipids, 1976, 17, 501.
34. J. Bus, I. Sies and M.S.F. Lie Ken Jie, Chem. Phys. Lipids, 1977, 18, 130.
35. F.D. Gunstone, M.R. Pollard, C.M. Scrimgeour, N.W. Gilman and
B.C. Holland, Chem. Phys. Lipids, 1976, 17, 1.
36. F.D. Gunstone, M.R. Pollard, C.M. Scrimgeour and H.S. Vedanayagam,
Chem. Phys. Lipids, 1977, 18, 130.

37. A.P. Tulloch and M. Mazurek, Lipids, 1976, 11, 228.
38. H. Rakoff, D. Weisleder and E.A. Emken, Lipids, 1979, 14, 81.
39. J.D. Roberts, F.J. Weigert, J.I. Kroschwitz and H.J. Reich,
J. Amer. Chem. Soc., 1970, 92, 1338.
40. K. Tori and T. Komeno, Tetrahedron Lett., 1974, 1157.
41. K.L. Servis, E.A. Noe, N.R. Easton, Jr. and F.A.L. Anet, J. Amer. Chem. Soc., 1974, 96, 4185.
42. N.R. Easton, Jr., F.A.L. Anet, P.A. Burns and C.S. Foote, J. Amer. Chem. Soc., 1974, 96, 3945.
43. D.R. Paulson, F.Y.N. Tang, G.F. Moran, A.S. Murray, B.P. Pelka, and Eva, M. Vasquez, J. Org. Chem., 1975, 40, 184.
44. S.G. Davies and G.H. Whitham, J.C.S. Perkin II, 1975, 861.
45. P.A. Budinger, J.R. Mooney, J.G. Grasselli, P.S. Fay and A.T. Guttman,
Anal. Chem., 1981, 53, 884.
46. M.R. Pollard, Unpublished results.
47. R.G. Parker and J.D. Roberts, J. Amer. Chem. Soc., 1970, 92, 743.
48. T. Pehk and E. Lippmaa, Eesti NSV Tead. Akad. Toim. Keem. Geol.
1968, 17, 291.
49. J.B. Hendrickson, J. Amer. Chem. Soc., 1967, 89, 7043.
50. A.D. Buckingham, Can. J. Chem., 1960, 38, 300.
51. A.J. Bloodworth and M.E. Loveitt, J.C.S. Perkin I, 1978, 522.
52. A.J. Bloodworth and J.A. Khan, J.C.S. Perkin I, 1980, 2451.
53. D.K. Dalling and D.M. Grant, J. Amer. Chem. Soc., 1972, 94, 5318.

CHAPTER 3

IMPROVED PROCEDURES FOR THE ISOLATION of FATTY ACIDS

Summary.

This chapter deals with the development of preparative high pressure liquid chromatography as a technique for the purification of lipids and compares this procedure with existing methodologies such as preparative thin layer chromatography, column chromatography and low temperature crystallisation. Effective procedures for obtaining methyl oleate, linoleate, α and γ -linolenate and ricinoleate are described.

1 Introduction.

The first scientist to recognise chromatography as an efficient method of separation was the Russian botanist Tswett^[1], who used a primitive form of liquid chromatography to isolate various plant pigments. Little further work was carried out until 1931 when Kuhn and Leder^[2] repeated some of Tswett's experiments, again using chromatography to separate plant pigments.

Elution chromatography was first effectively employed by Reichstien^[3] in the late 1930's and in the early 1940's Martin and Synge^[4] introduced liquid-liquid partition chromatography using silica gel loaded with water as a chromatographic stationary phase. About the same time, Tiselius^[5] developed frontal analysis and displacement analysis.

In 1939 Brown^[6] suggested that an adsorbent held between two glass plates, through which the mobile phase was allowed to percolate would be an effective chromatographic system. Maclean and Hall^[7] introduced the starch binder into an alumina absorbent, and in so doing introduced the first effective formal thin-layer chromatography. Thin layer chromatography, as it is presently known began to attract attention through the work of Kirchner and his associates^[8]. It was not until 1958 however, when Stahl^[9] described equipment and efficient sorbents for the preparation of plates that

the effectiveness of the new technique for separation was widely recognised.

The application of high pressure liquid chromatography (HPLC) to lipid analysis has begun to gather momentum after a slow start relative to many other classes of compounds. Aitzetmuller^[10], in a comprehensive review, concluded that the practice of HPLC of lipids is essentially different from that of normal lipid chromatography, in as much as it often involves adsorption rather than partition and may require multiple-solvent elution of classes of lipids of widely differing polarities rather than the isolation and detection of single species.

Differential refractometers or spectrometers (IR, UV and fluorescence) are the predominantly used detectors in modern HPLC. All are sensitive to concentration and their response factors are very dependent upon the nature of the substance. Furthermore in the case of lipid analysis the use of such detectors can impose severe restrictions.

The use of UV detectors has found application in the studies of oxidation^[11] where the oxidation products contain conjugated double bonds (λ_{max} ca 235nm). Alternatively lipids may be converted to UV-absorbing derivatives such as p-bromophenacyl esters^[12]. Unhydrolysed triacylglycerols have been characterised after iodination; the iodinated species absorb at 265nm and may be resolved into classes corresponding to the degree of original unsaturation^[13].

Lipids which do not absorb at longer wavelengths (and/or cannot be chemically modified) may be detected in the end absorption region between 195 and 215nm^[14]. This method has been extensively utilised

for semi-preparative HPLC of PUFA oxidation products by several groups^[15]. The practicability of this approach is severely limited since solvents must transmit at these low wavelengths; moreover severe interference may be encountered from traces of highly absorbing impurities either in the sample or in the solvent system.

Differential refractometers although less sensitive have been preferred to UV detection at 215nm by some groups^[16]. The differential refractometer however suffers from its limitation to isocratic elution. This severely restricts its range of application and also limits the efficiency of separations obtainable.

A detector with enormous potential for HPLC of lipids utilised the evaporation of the eluate on a moving wire or belt followed by continuous pyrolysis of the solute, conversion to methane and finally detection in the flame of an ionisation detector. Their reliability and performance were however not fully exploited and are unfortunately no longer commercially available. The detector with most promise for the future is the infrared detector which can either be tuned to monitor the C=O stretch, or the C-H stretch at 5.75 and 3.42 nm respectively provided the solvents are compatible^[17].

Reversed-phase HPLC has been applied to triacylglycerols^[18], fatty acids^[19], methyl esters^[20] and lecithins^[21]. Reversed-phase HPLC competes with GLC in that both separate lipids according to chain length and resolve geometrical isomers to some extent^[22]. The resolution may be enhanced if silver nitrate is dissolved in the eluting solvent^[23], or impregnated in the stationary phase^[24]. Reverse phase separations can produce complicated chromatograms since a double bond is almost equivalent to a shortening in chain-length of 2 carbons. Hence 18:1 and 16:0 acids show considerable overlap and 20:4 and 14:0 overlap completely.

2 Experimental parameters & procedures

2.1 Resolution, capacity, selectivity and efficiency [25,26]

The capacity factor (k') is defined as the ratio of the amount of compound on the adsorbent (stationary phase) to the amount of compound in the mobile phase during a chromatographic separation. The factor will only hold rigorously for a given set of conditions. The capacity factor can be expressed in terms of the retention volume of the compound and is simply a measure of its retention in terms of column volumes.

Capacity factor for compound i

$$k'_i = \frac{V_i - V_o}{V_o} \quad 1$$

The selectivity factor (α) is a measure of the degree of separation of the band centres between two components in a chromatographic run, and is given by

Selectivity factor for compounds i and j

$$\alpha_{i,j} = \frac{k_j}{k_i} = \frac{V_j - V_o}{V_i - V_o} \quad 2$$

The resolution of two components eluting from a chromatographic column can be defined in terms of the separation of the peak centres and the average peak width as in equation 3.

Resolution for compounds i and j

$$R_{i,j} = \frac{V_j - V_i}{1/2(W_j + W_i)} \quad 3$$

In order to effect the separation of two substances, the peaks of the two components must be moved apart during their passage through the column. However, having separated the peak widths should remain sufficiently small to allow the discrete elution of each peak. A measure of the efficiency of the column is given by the "theoretical plate number" N,

Theoretical plate number for compound i

$$= N = 16 \left[\frac{V}{W_i} \right]^2 \quad 4$$

Having determined N for a particular reference compound (preferably one which elutes within the range of compounds to be examined) under a given set of conditions the efficiency of the column can be used as an indication of the column aging. Clearly as N approaches a predetermined value the column will be no longer suitable for a particular type of separation.

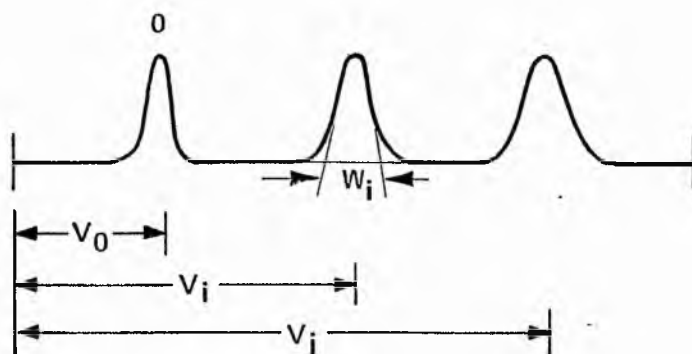


FIGURE 2.1.1

- V_0 = retention volume of an unretained compound
- V_i = retention volume of compound i
- V_j = retention volume of compound j
- W_i = peak width of compound i in terms of volume

2.2 Recycling and shaving.

The various parameters defining resolution, selectivity and efficiency have been discussed. For a preparative run we are concerned with how much material can be separated without sacrificing purity. A method for improving the separation of a particular pair of solutes that are poorly resolved on a preparative column is to use the technique of recycling.

Partially resolved components eluting from the column pass through the detector, and then instead of being collected they are directed back into the pump for subsequent passes through the columns and detector. By this method the effective column length is considerably increased. Theoretically the components could be

recycled an infinite number of times, practically however upper limits are in the range 8-12 depending on the substrates and eluents, since for rapidly eluting peaks peak broadening with each recycle may begin to cause overlap between the tail end of the peak and the front portion of the recycled peak. Recycling is an unattractive process for components with long retention times because of the long time required and the high solvent consumption.

Baseline resolution is not a prerequisite to recovering a pure sample from a preparative HPLC run. By "shaving off" parts of a poorly resolved set of peaks and recycling the remainder a large proportion of the components may be recovered pure. The following will illustrate the general principles of the technique.

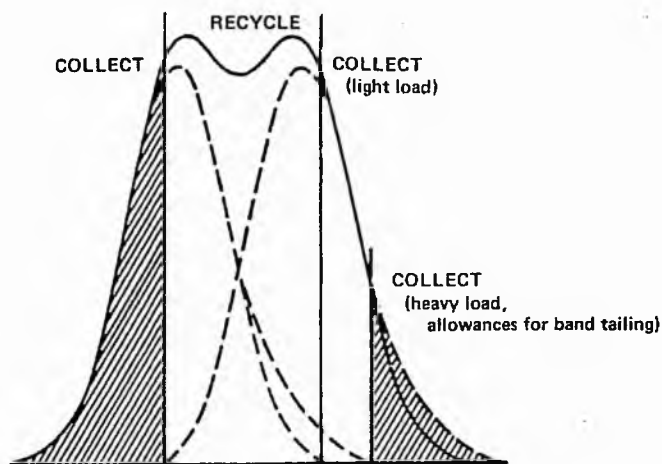


Figure 2.2.1

Consider two components X and Y present in a 1:1 ratio with a resolution of ca 0.7 on the first pass. As can be seen from Fig 2.2.1 pure X can be collected from the leading edge of the unresolved peaks and pure Y from the tail end of the peak. The intermediate portion can then be recycled and on its second pass the resolution will be

greater as a result of the smaller amount of sample and also the increased effective column length. Shaving can again be performed to collect pure X and pure Y. The process can be continued until the peaks have been completely resolved or sufficient material has been obtained.

2.3 Equilibration of the preparative LC column.

The continued passage of mobile phase over the stationary phase may modify the surface activity of the latter as one or more components of the solvent are reversibly adsorbed in varying amounts to the surface. Concomitantly the nature of the mobile phase is also modified as a result of depletion of one or more components of the eluent. These changes may result in variability in k' values. To minimise variations in k' , the column has to be equilibrated before a chromatographic run.

For example, consider a solvent system containing 1% isopropanol in hexane. If the solvent is applied to a virgin column then initially large amounts of the isopropanol will be adsorbed by the column, and hence the eluent will comprise of much less than 1% isopropanol. With continued passage of the mobile phase over the adsorbent the stationary phase will become "saturated" and no more isopropanol will be removed from the eluent and the composition of the solvent leaving the column will return to 1% isopropanol. The column is then said to be at equilibrium with the solvent and no changes in the value of k' will occur. In this condition the solvent composition as determined by the differential refractometer will remain constant and a baseline free of any appreciable drift will be obtained.

The volume of solvent required to reach equilibration will be in the region 20-60 litres depending on the solvent(s) and on the type of adsorbent. This quantity is of course undesirably high if the solvent is wasted. The recommended procedure to circumvent the problem is as follows., a) the column is initially purged with 500-1000 ml of solvent for every Prep PAK-500/silica cartridge being used b) the eluent line is transferred to the solvent reservoir and c) flow is resumed and the solvent allowed to recirculate until the base line on the refractometer ceases to drift.

2.4 Injection techniques.

For a solid sample to be injected onto the preparative column, it must of course be dissolved in a solvent. If the sample is readily soluble in the mobile phase a 10-50% solution is made and injected using the 10cc capacity gas-tight syringe.

In cases of low solubility smaller concentrations (down to 1%) may be injected in large volumes of solvent. Cases of severe insolubility (<1%) in the mobile phase may be handled by one of the following methods.

(a) The sample is dissolved in a solvent other than the mobile phase. In this situation the injection solvent may compete for the adsorption sites, resulting in displacement of the sample at the top of the column. Displacement will continue until the solvent is sufficiently dilute in the mobile phase solvent. This method frequently gives rise to lower values of k' .

(b) For very low-solubility samples the solute in a chromatographically weak solvent, is pumped onto the column via one of the solvent inlet ports of the instrument. The solute having a strong affinity for the adsorbent will be deposited at the top of the column. When the sample has been applied to the column the solvent is then changed, making use of the solvent selector valve, to the chromatographically stronger mobile phase. The solvent is thus eluted in a stepwise-gradient type process.

Although both (a) and (b) are well suited for systems employing a UV detector applications to RI detectors are limited to situations where two types of solvent have nearly equal RI's. Alternatively the preparative run may be conducted without using the detector and collecting aliquots at regular volume intervals. This procedure is, however, tedious since it then requires examination of all the fractions by TLC, GLC or analytical HPLC or a combination of these methods.

When dealing with liquid samples, as is the general case for fatty acids or triacylglycerols, the sample may be injected neat, or in the case of highly viscous oils the sample may be diluted. In general the sample is injected onto the column at about 15-20 ml/min. When injecting large volumes of solvent (>15 ml) the injection rate will probably decrease as it gets increasingly more difficult to displace large volumes of solvent from the column. The makers state that a volume up to 20% of the column volume may be injected.

However it must be realised that large sample volumes and sample mass will decrease resolution and capacity factors. Hence as small a volume of charge as possible should be employed in order to achieve maximum resolution. The majority of fatty acid methyl esters and oils can be injected neat.

3 Results and discussion

For the HPLC separations to be described solvent systems were chosen so as to be inexpensive, easy to purify and recover, and yet still give adequate separations in an acceptably short time.^[27] For normal phase chromatography of non-polar esters petroleum was generally employed. For reverse phase chromatography methanol was the solvent of choice. Although water increases the k' values for all the esters studied on reverse phase, and is undoubtedly the cheapest solvent, the fact that the separated material has to be extracted from the water for recovery detracts from its use. Hence the separations described do not represent the best separations obtainable with the system, but do represent the most convenient method for the rapid purification of useful quantities of commonly required methyl esters.

3.1 Methyl oleate from olive oil methyl esters.

Previous methodologies for the preparation of methyl oleate from olive oil have involved one or more of urea crystallisation, low temperature crystallisation and distillation. Schlenk and Holman^[28] reported a procedure for the preparation of methyl oleate (97-98 %) involving urea crystallisation to reduce the saturated content and a

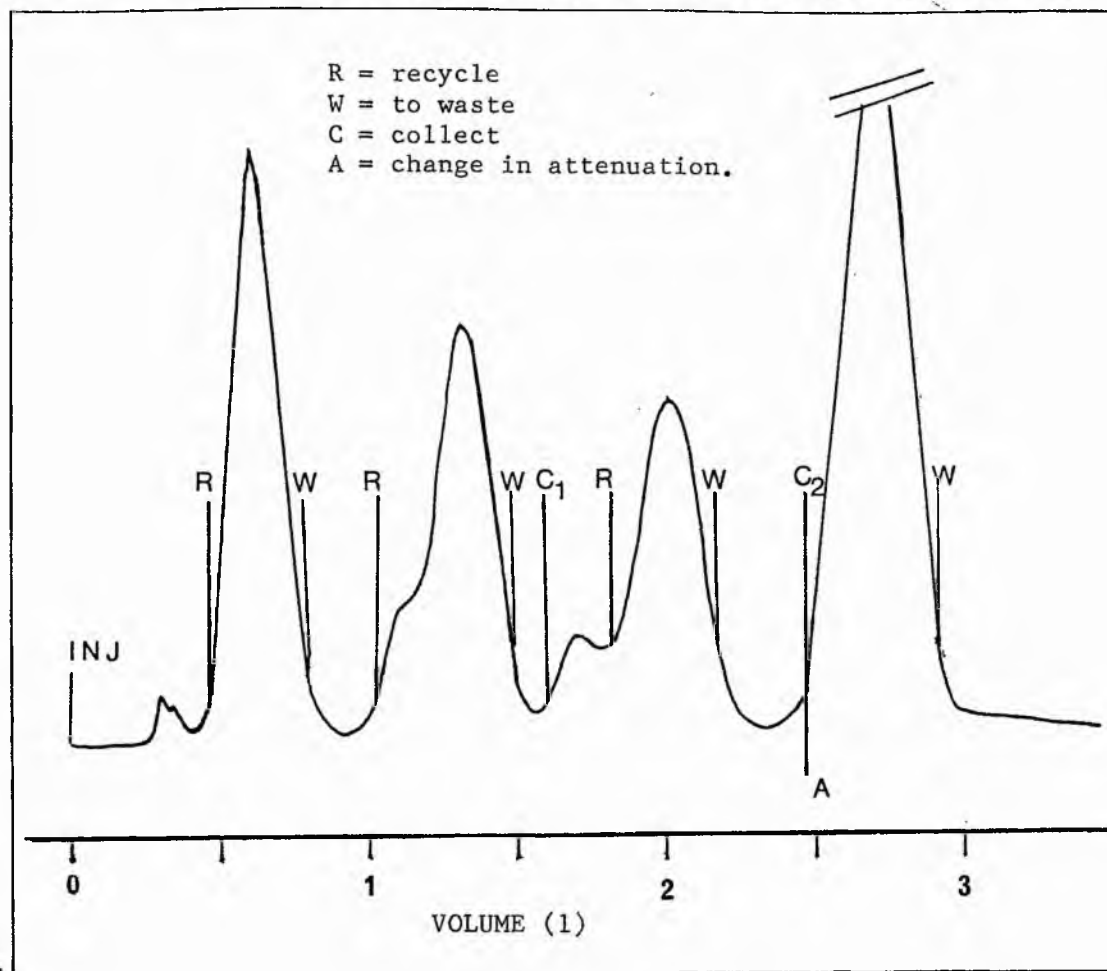
further urea crystallisation to complex the oleate followed by distillation and a final purification as a urea precipitate. Swern and Parker^[29] and Schlenk^[30] have both recommended urea crystallisation to remove the saturated esters followed by low temperature crystallisation and a final distillation to produce oleate in purity greater than 98 %. Keppler *et al.*^[31] described a large scale procedure to produce diene free oleic acid, involving repeated urea crystallisation and distillation followed by crystallisations with iodine and maleic anhydride. The method however leads to stereomutation of the double bond resulting in 5 % of the trans isomer.

This laboratory has previously recommended^[32] the following procedure (a) urea crystallisation of olive acids to reduce the saturated content to below 1 %, (b) low temperature crystallisation to bring the oleic acid up to > 99 % and (c) esterification followed by column chromatography to remove traces of coloured impurities and oxidised products.

We now use preparative HPLC to routinely prepare methyl oleate of purity > 99 % from olive oil methyl esters. As with the majority of the separations to be described it is advantageous to reduce the saturated content of the oil by preliminary urea fractionation since palmitate forms a critical pair with some of the C18 polyenes on the reverse phase column. Using such a pretreated oil in which the saturated content was below 5 % up to 15g of olive oil methyl esters could be chromatographed in a single run and pure methyl oleate obtained within 30 min operator time. Figure 3.1.1 shows a typical HPLC trace for a pretreated olive oil ester separation (7.5 g). After 3 recycles two distinct peaks are observed with resolution of 0.96 and

the majority of the linoleate (the major impurity) can be shaved off. Collection of the majority of the peak on the subsequent pass gives methyl oleate

Figure 3.1.1 Separation of methyl oleate from olive oil esters.



Column Prep PAK-500/C₁₈ cartridge (5.7x30 cm)
Solvent MeOH
Flow rate 250ml/min
Load 7.5g

contaminated only with palmitate (0.6%) and palmitoleate (0.2%).

The trace shown was obtained with a relatively new reversed-phase column using methanol as eluting solvent. However the price of reverse

phase columns is such that it becomes prohibitively expensive to replace the columns regularly. With this in mind we have examined the capability of "aged" columns to perform separations.

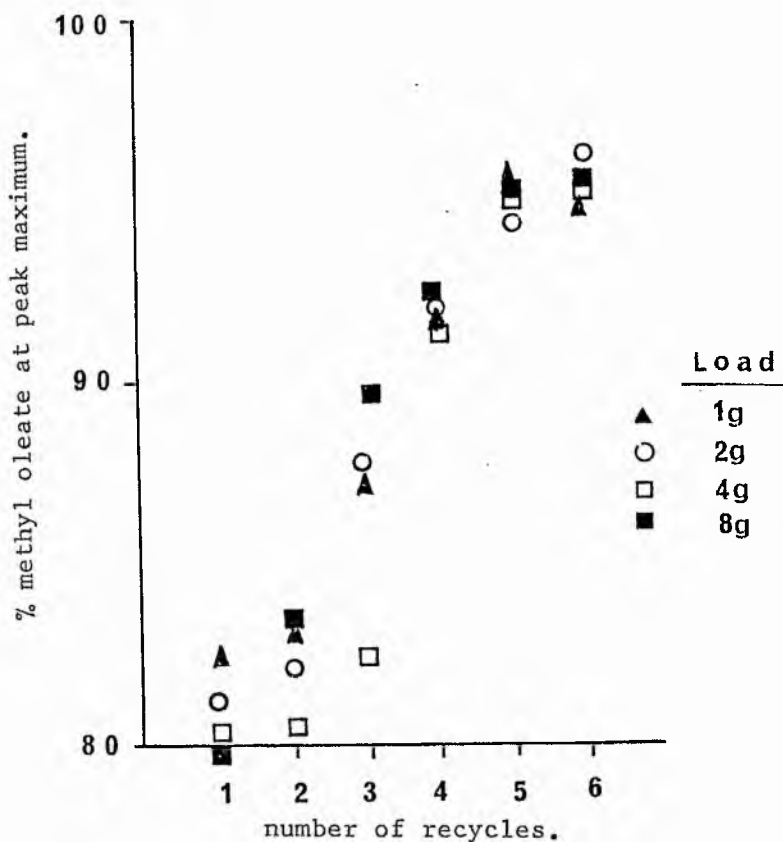
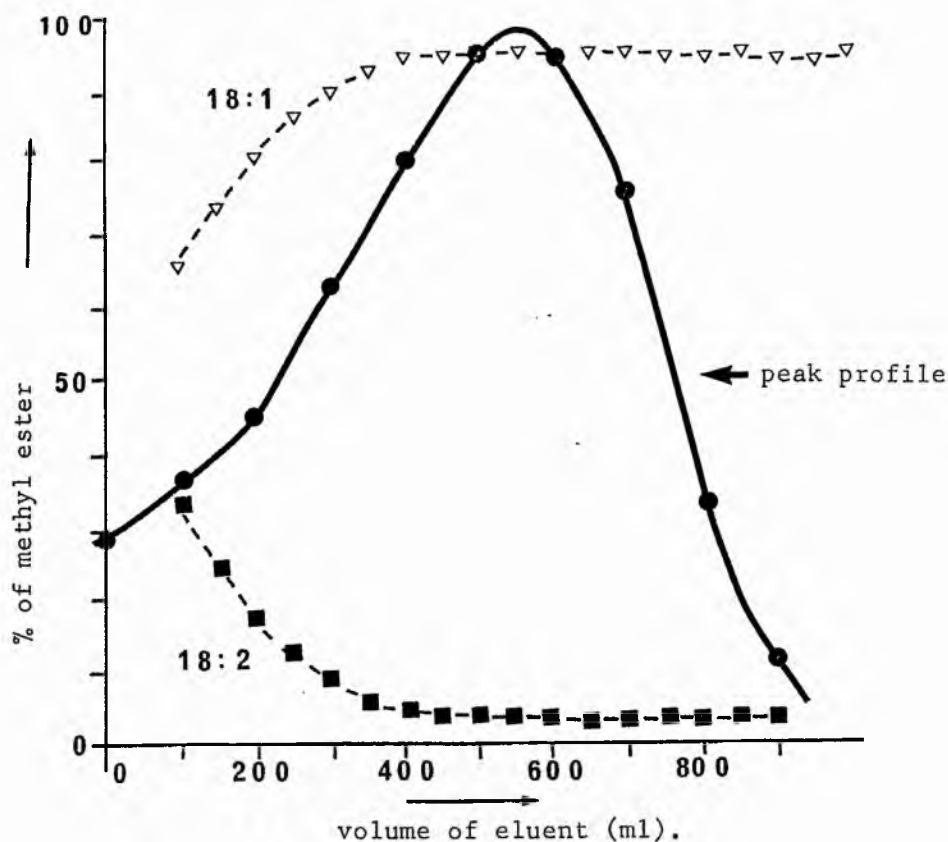


Figure 3.1.2 Plot of number of recycles against composition at peak maximum for olive oil methyl esters.

Figure 3.1.2 shows a plot of number of recycles against composition at the peak maximum for a series of loads from 1-8 g of olive oil methyl esters. The significant feature of the plot is that after the third recycle the composition at the peak centre is independent of the size of the load. Furthermore it allows one to accurately predict (within ± 0.5 %) the composition at each recycle.

Figure 3.1.3 Variation in composition of esters with peak profile.



As stated previously the essence of recycle-preparative HPLC relies on shaving the peaks to decrease the proportion of the unwanted component, and also decrease the load, both of which result in an increase of resolution in the subsequent pass. For peaks of resolution greater than 0.6-0.7 the cut off point is self evident. However with broad peaks when the resolution is less than 0.6 little if any insight into the progress of the chromatography is afforded and the optimum cut off points more difficult to ascertain. Figure 3.1.3 shows a typical composition variation across a peak. The data was obtained by collecting 50 ml fractions on the 6th recycle of a run on an 'aged' column during which no significant amount of shaving had taken place, and analysing each fraction by G.L.C. The Figure shows

that after ca 400 ml the composition profile is constant at an oleate level of 95.9 %, linoleate 2.7 % and the palmitate 1.4 % with standard deviation of <0.4 %.

3.2 Methyl linoleate from maize, sunflower and evening primrose oils.

Low-temperature crystallisation^[33] and urea crystallisation^[34,35] have been employed to purify the linoleic acid/ester (95-99 %) available in several seed oils. Other procedures which have been employed include solvent partition of mercury complexes^[36], liquid-liquid extraction^[37] and adsorption chromatography.^[38]

Gunstone *et al*^[32] isolated 300-320 g of pure methyl linoleate from one kilogram of evening primrose oil containing approximately 75 % of linoleic acid by a combination of low temperature crystallisation, urea fractionation and column chromatography.

We have isolated methyl linoleate from three linoleate rich oils namely maize, sunflower and evening primrose on a reverse phase column using methanol as eluting solvent. All three were equally facile to handle and yields of pure methyl linoleate (> 99 % purity) were in excess of 65 % of the theoretical yield in each case. Recycling was again employed, with shaving of the leading (to remove linolenates) and trailing edges (to remove monoenes and saturates). In general six recycles were required taking a total of 34min chromatographic time. Loads of up to 13.5 g were routinely handled.

As with olive oil we were interested in the capabilities of an 'aged' column to effect the separation. Unlike the olive oil situation however where we were able to recycle more than six times

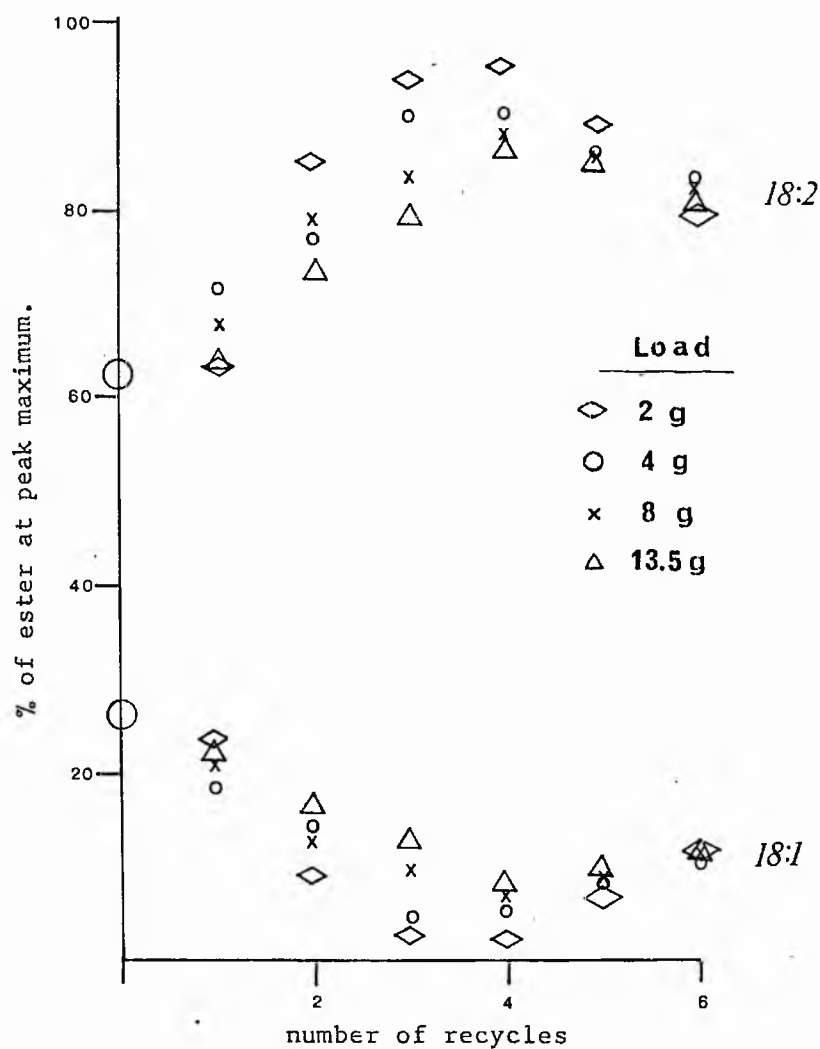


Figure 3.2.1 Plot of number of recycles against composition at peak maximum for maize oil methyl esters.

with increased separation on each pass without the use of a significant amount of shaving, purification of maize oil did require shaving to prevent overlap of components after more than three recycles. Figure 3.2.1 shows plots for four chromatographic runs with loads varying from 2-13.5 g. The plot was obtained by recycling the components and analysing the summit of each recycled peak. Shaving was kept to a minimum compatible with preventing observable overlapping of peaks. As can be seen after three to four recycles irrespective of yield, the separation has reached an optimum and in the absence of a significant amount of shaving the peaks begin to remerge with concomitant reduction in linoleate content at the peak summit. This plot demonstrates three important points. Firstly the separation of components after two or three recycles becomes independent of load, supporting similar observations for the olive oil separation. Secondly that shaving is often a prerequisite for separations involving several recycles, and thirdly that even without shaving linoleate can be upgraded to about 90 % within 17 min on an aged column. In fact we were able to obtain results comparable to those on relatively 'new' columns by shaving of both leading and trailing edges although recovered yields were somewhat poorer (50-55 %).

3.3 Methyl α -linolenate from linseed oil methyl esters.

The conventional techniques of low temperature and urea crystallisation do not readily furnish pure methyl α -linolenate because of the difficulty in separating linoleate from linolenate. Gunstone et al^[32] previously recommended (a) low temperature

crystallisation of linseed acids (55-60 %) from acetone at -75°C to raise the concentration of the linolenic acid to 65-75 %, (b) urea crystallisation to raise this further to 80-90 % and (c) purification by repeated column chromatography on silica after conversion of the acids to methyl esters. The method produces about 120 g of pure α -linolenic acid (>99 %) per kilogram of linseed oil.

Reverse phase preparative HPLC of linseed oil methyl esters containing only 48.1 % α -linolenate was performed in less than 28 min giving a colourless product of purity in excess of 96 %. In a typical run eight recycles were performed with continuous shaving of the trailing edge and collecting the first 70 % of the final recycle peak. The only contaminants being saturated and monounsaturated C16 fatty acid esters which are concentrated relative to the starting oil. However a preliminary urea fractionation to remove these minor components allows α -linolenate to be obtained in greater than 99.0 % purity. Approximately 7 - 8 g of linseed methyl esters can be conveniently handled per run with a net recovery of between 1.4-1.7g of pure α -linolenate.

3.4 Methyl γ -linolenate from pretreated evening primrose oil.

Evening primrose oil has been shown to be a particularly useful source of methyl linoleate as mentioned in 3.2. The initially small content of methyl γ -linolenate (7-9 %) can be upgraded to 60-70 % by collection of the waste fractions from the HPLC purification of linoleate from evening primrose oil methyl esters. HPLC of the upgraded γ -linolenate containing methyl linoleate (27.4 %) and methyl oleate (23.6 %) as impurities required only 28 min operator time and 4

FIGURE 3.4.1 a) HPLC chromatogram of the separation of γ -linolenate from recovered evening primrose oil methyl esters.

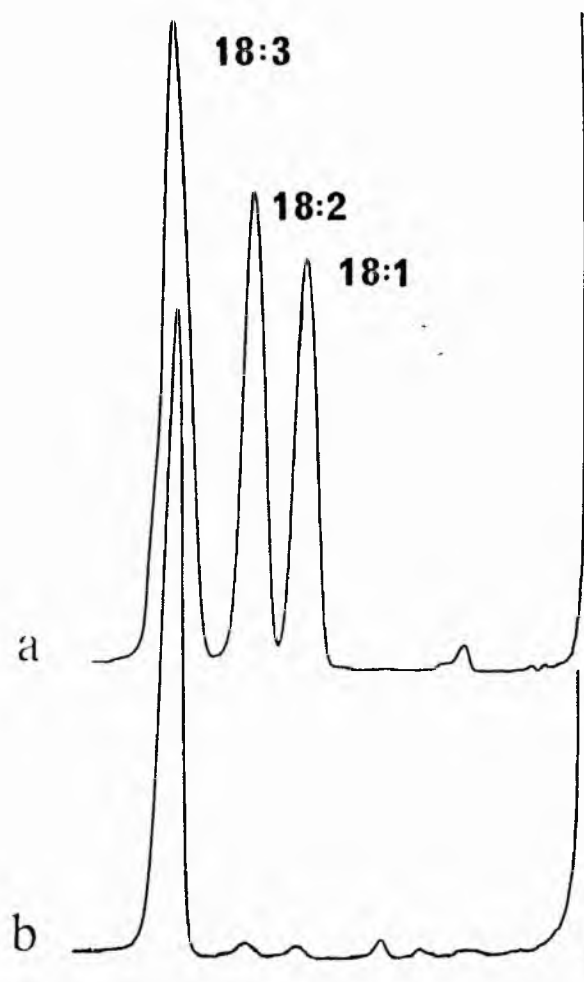
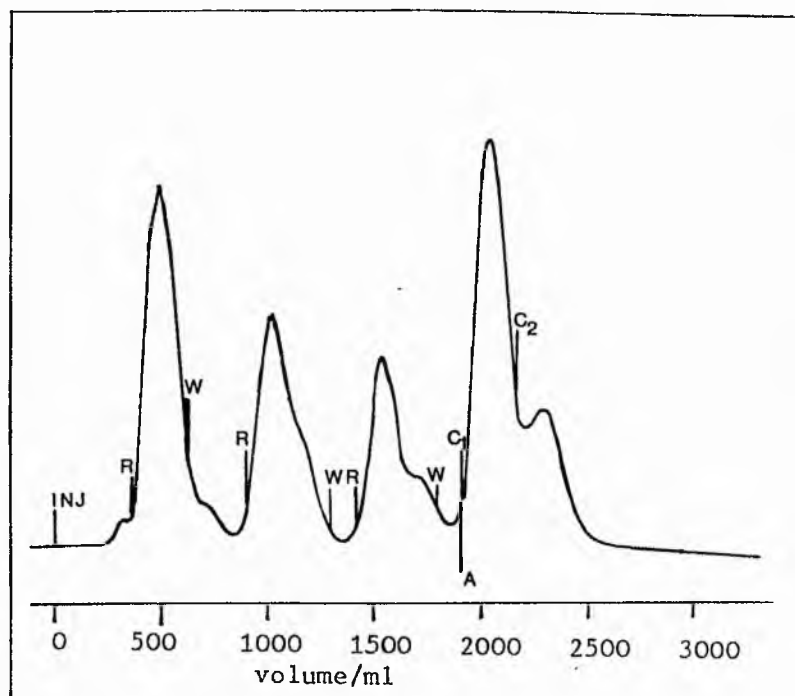


FIGURE 3.4.1 b)

GLC trace of
evening primrose
methyl esters
a) before
b) after
HPLC purification.

recycles to furnish linolenate of 97 % purity. The HPLC chromatogram and G.L.C. traces before and after purification are shown in Figure 3.4.1. Batches of linolenate purified to this level were then combined and rechromatographed 8 g at a time to give a final product of greater than 99.5 % purity within 20 min operator time.

As noted by other workers^[32] the separation of γ -linolenate from linoleate is a simpler procedure than purification of α -linolenate. This fact was evident in the HPLC separations described above, since after 4 recycles the resolution between γ -linolenate and linoleate was 0.78 whereas in the chromatogram from the linseed oil separation no resolution was observed even after 8 recycles.

3.5 Methyl ricinoleate from castor oil.

Methyl ricinoleate is the major component of castor oil methyl esters, constituting 90 % of the esters. The remaining components are saturated and unsaturated C18 esters together with a small amount of methyl palmitate. The isolation of methyl ricinoleate from castor oil methyl esters is a simple separation by either column chromatography or by thin layer chromatography, the more polar hydroxy ester being retained to a much greater extent than the less polar components.

Since the separation involved is dependant upon differences in polarity normal phase chromatography was routinely employed for the isolation of ricinoleate. Figure 3.5.1 shows a typical HPLC chromatogram obtained using a petroleum ether/diethyl ether (80:20) mixture as eluent. Loads up to 15 g can be tolerated and the separation can be accomplished within 15min operator time. Recycling

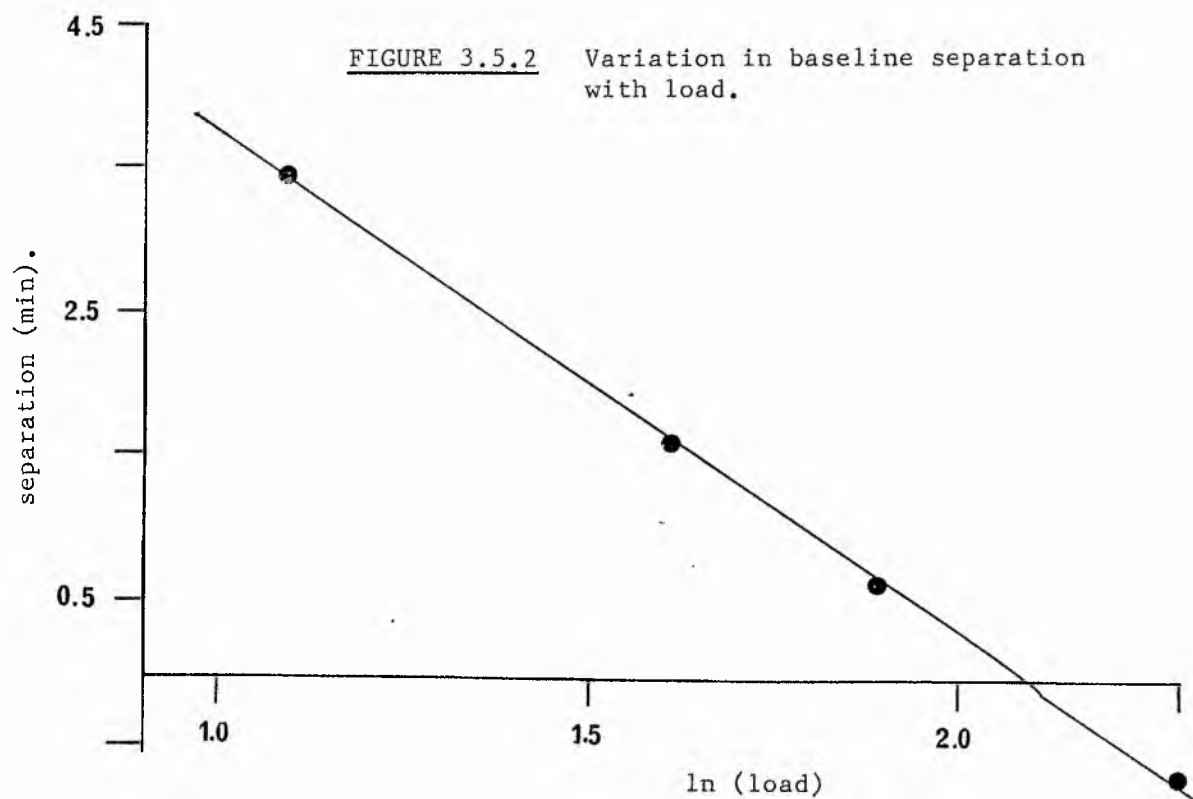
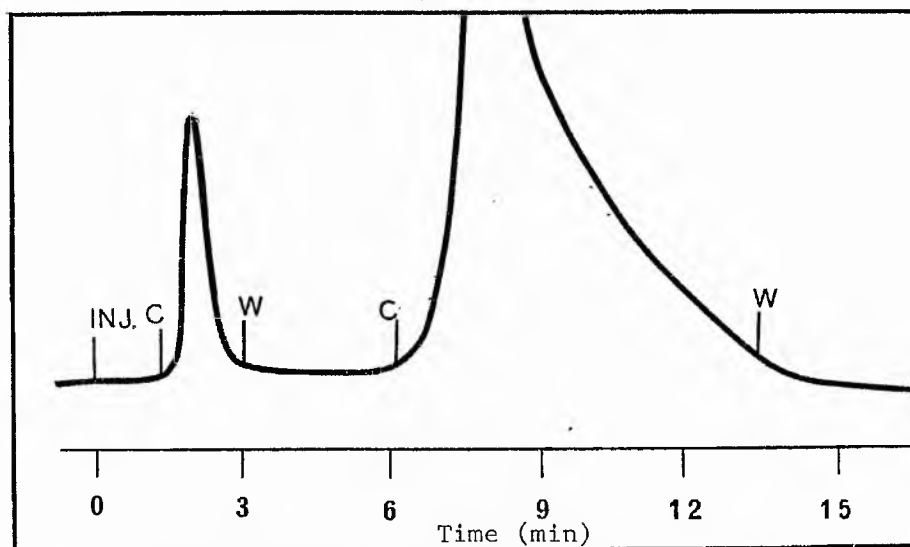


FIGURE 3.5.1 Separation of methyl ricinoleate from castor oil methyl esters.



Column Prep PAK-500 (5.7x30 cm)
Solvent petroleum ether/ diethyl ether (80:20)
Flow rate 250 ml/min.
Load 15.1 g

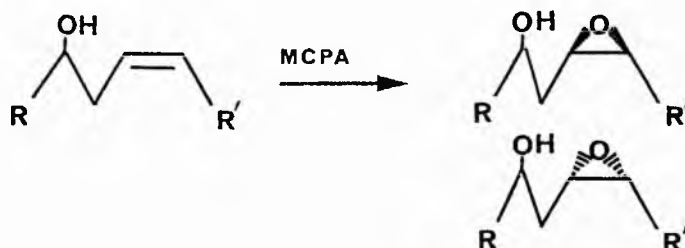
is not required since the peaks are well resolved up to 8 g. Even above this load the loss of material due to shaving off the earlier overlapping portion is minimal.

The variation in baseline separation with load is shown in Figure 3.5.2. For the petroleum ether/diethyl ether solvent system the predicted maximum load feasible to obtain base line separation is 8.2g. Above this load peak overlap occurs whereas below this load higher resolution is obtained at the expense of unnecessary solvent and operator time.

In all these separations using petroleum ether/diethyl ether as eluent, peak trailing is a severe problem and increases with increasing load. This can be circumvented by changing the solvent to petroleum/iso-propanol (99:1), which also has the added advantage that the petroleum can readily be recovered from the mixture.

3.6 Preparative separation of 12(R)-hydroxy-9(R),10(R) and 12(R)-hydroxy-9(S),10(S) stearates.

Peracid epoxidation of methyl 12-(R)-hydroxyoctadeca-9 \underline{Z} -enoate in a two phase system (dichloromethane/sodium bicarbonate) gives two diastereoisomeric hydroxy-epoxides arising from epoxidation from above or below the plane of the double bond (scheme 3.6.1). T.L.C. analysis even after double development showed no separation of the components. We were interested in extending the HPLC technique to the separation of diastereoisomers.



The ^{13}C Nmr of the diastereoisomeric mixture shows four epoxy carbon signals at 54.24, 55.14, 56.10 and 56.92 and two hydroxy bearing carbons at 69.98 and 70.67 ppm. HPLC on a normal phase column with petroleum ether/isopropanol (98.5:1.5 v/v) did not show any resolution of the two components even after four recycles. However shaving of the leading edge (fraction A) and the trailing edge (fraction B) gave two components whose ^{13}C Nmr each showed only two epoxy carbons and one hydroxy carbon. Fraction A had epoxy signals at 56.10 and 55.14 ppm and hydroxy bearing carbon signal at 70.67 ppm. Fraction B had epoxy signals at 56.92 and 54.27 ppm and hydroxy bearing carbon signal at 69.98 ppm. Although we were unable to quantify the diastereoisomeric purity of each fraction from the ^{13}C Nmr accurately we can put a lower limit of 94 % for each fraction, with both fractions probably being considerably higher.

3.7 Triacylglycerols.

Attempted purification of synthetic triacylglycerols was only partially successful by preparative HPLC. A sample of 1-lauroyl-2-myristoyl-3-stearoyl-rac-glycerol (LMS) contaminated with 1-lauroyl-2,3-distearoyl-rac-glycerol (LSS) (7 %) showed no significant improvement in purity with repetitive recrystallisation.

We were able to upgrade the LMS from 93.5 to 98.12 % using normal phase HPLC with methylene chloride as eluent. However, precipitation of the saturated triacylglycerol on the column was a serious problem. In a typical experiment 4-5 g of triacylglycerol were dissolved in

20-25 ml of dichloromethane and injected onto the column, but only 1.8-2.5 g of triacylglycerol were eluted off during the chromatographic run. The remainder being adsorbed to the column. Flushing of the column with large volumes of solvent to remove the adsorbed triacylglycerol, was then necessary before the column could be reused.

Analytical HPLC of triacylglycerols has been reported using acetonitrile as either solvent or co-solvent^[18]. However we found no significant improvement in solubility of LMS in acetonitrile/dichloromethane mixtures or neat acetonitrile. Similar results were obtained for 1-palmitoyl-2,3-dielaïdoyl-rac-glycerol.

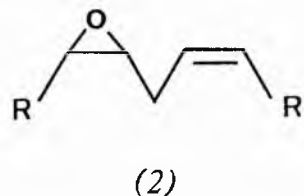
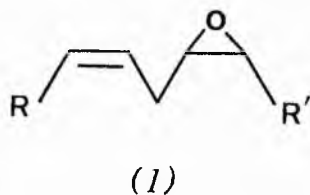
3.8 Failures.

Although we had achieved a high degree of success with the HPLC system for the separation of natural oils some separations were unsuccessful.

Attempted separation of a 40:60 mixture of cis and trans methyl octadeca-9-enoates was unsuccessful on either normal or reverse phase chromatography even after 8 recycles. No partial separation was achieved in the latter recycles since fractions from the leading and trailing edges were identical (capillary G.L.C. and silver ion T.L.C.). Similar results were obtained for cis,cis, cis,trans and trans,trans mixtures of methyl octadeca-9,12-dienoates. The use of silver impregnated columns may well provide the answer to the desired separation^[24], or alternatively incorporation of silver nitrate in the effluent as recommended by Heath et al^[23].

Attempts at separating the two isomeric epoxides (1) and (2)

obtained by peracid epoxidation of methyl linoleate was not very successful by HPLC on either normal or reversed phase columns. The two isomeric epoxides can be separated by double development T.L.C. but only small loads can be tolerated. HPLC of the epoxides furnished only ca 60-70 mg of each isomer (>93 %) from 1 g of starting material. No resolution of the components was observed on either reverse or normal phase chromatography. Larger amounts (250 mg) of poorer quality (> 85 %) fractions could be obtained by shaving off larger portions from the leading and trailing edges. Presumably careful chromatography involving a more suitable solvent system (such as water/methanol mixtures for reversed phase) would result in better separation^[39].

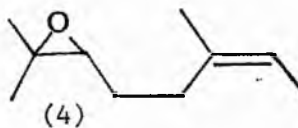
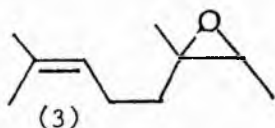


References.

1. M. Tswett, Compt. Rend., 1911, 152, 788.
2. R. Kuhn and E. Lederer, Z. Physiol. Chem. 1931, 200, 246.
3. See T. Reichstein and J. von Euw, Helv. Chim. Acta.,
1940, 23, 1114 and references cited therein.
4. A.J.P. Martin and R.L.M. Synge., Biochem. J., 1941, 35, 1358.
- 5a) A. Tiselius, Arkiv. Kemi, Mineral. Geol., 1943, 16A, No. 18.
b) A. Tiselius, Kolloid. Z. 1943, 105, 101.
6. W.G. Brown, Nature 1939, 143, 377.
7. R.P.W. Scott, "Contemporary Liquid Chromatography" (Ed. A. Weissenberger),
Wiley and Sons, New York, 1976.
- 8a) J.G. Kirchner, J.M. Miller and G.J. Keller, Anal. Chem., 1951, 23, 420.
b) J.M. Miller and J.G. Kirchner, Anal. Chem., 1952, 24, 1480.
c) J.M. Miller and J.G. Kirchner, Anal. Chem., 1954, 26, 2002.
d) J.G. Kirchner, 'Thin Layer Chromatography',
Wiley and Sons, New York, 1967.
- 9a) E. Stahl, Chemiker Ztg., 1958, 82, 323.
b) E. Stahl, (Ed) "Thin Layer Chromatography", Springer-Verlag,
New York, 1967.
10. K. Aitzetmuller, J. Chromatog., 1975, 113, 231.
- 11a) M.J. Thomas and W.A. Pryor, Lipids 1980, 15, 544.
b) H.W.S. Chan and G. Levett., Lipids 1977, 12, 99.
- 12a) R.F. Borch, Anal. Chem., 1975, 47, 2437.
b) H.W.S. Chan, and G. Levett, Chem. Ind., 1978, 578.
c) P.T.S. Pie, W.C. Kossa, S. Ramachandrai and R.S. Henly,
Lipids 1976, 11, 814.
13. A. Karleskind, Rev. Fr. Corps. Gras., 1977, 24, 419.

- 14a) W.M.A. Hax, and W.S.M. Geurts Van Kessel, J. Chromatog., 1977, 142, 735.
- b) T. Riisom and L. Hoffmajer, J. Amer. Oil Chem. Soc.,
1978, 55, 649.
15. W.E. Neff and E.N. Frankel, Lipids 1980, 15, 587.
16. N.A. Porter, R.A. Wolf and J.R. Nixon, Lipids 1979, 14, 20.
17. N.A. Parris, J. Chromatog., 1978, 149, 615.
- 18a) A.H. El-Hamdy and E.G. Perkins, J. Amer. Oil Chem. Soc., 1981, 58,
49 and 867.
- b) B. Herslof, O. Podlaha and B. Toregard, J. Amer. Oil Chem. Soc.,
1979, 56, 864.
- c) R.D. Plattner, J. Amer. Oil Chem. Soc., 1981, 58, 638.
- d) R.D. Plattner, G.F. Spencer and R. Kleiman, J. Amer. Oil Chem. Soc.,
1977, 54, 511.
- e) B. Petersson, O. Podlaha and B. Toregard, J. Amer. Oil Chem. Soc.,
1981, 58, 1005.
19. M.O. Funk, R. Isaac and N.A. Porter, Lipids 1976, 11, 113.
- 20a) C.R. Scholfield, Anal. Chem., 1975, 47, 1417.
- b) C.R. Scholfield, J. Amer. Oil Chem. Soc., 1975, 52, 36.
21. R.M. Carroll and L.L. Rudel, J. Lipid. Res., 1981, 22, 359.
22. J.D. Warthen, J. Amer. Oil Chem. Soc., 1975, 52, 15.
- 23a) R.R. Heath, J.D. Tumlinson and R.E. Doolittle,
J. Chromatogr. Sci., 1977, 15, 10.
- b) B. Vonach and G. Schomburg, J. Chromatogr., 1978, 149, 417.
- 24a) K.J. Aitzetmuller, J. Chromatogr. Sci., 1975, 13, 454.
- b) A.D. Jones, E.C. Smith and E.W. Hammond, J. Chromatogr., 1980, 188, 205.
- c) C.R. Scholfield and T.L. Mounts, J. Amer. Oil Chem. Soc., 1977,
54, 319.

25. G. Guiochonin, "High-Performance Liquid Chromatography",
(Ed. C.G. Horvath, Academic Press, New York, 1980, pp 1)
26. L.R. Snyder and J.J. Kirkland "Introduction to Modern Liquid
Chromatography", Wiley and Sons, New York, 1974.
27. An HPLC procedure for the preparative purification of phospholipids
has recently been described, see W.S.M. Geurts Van Kessel, M. Tieman
and R.A. Demel Lipids, 1981, 16, 58.
28. H. Schlenk and R.T. Holman, J. Amer. Chem. Soc., 1950, 72, 5001.
29. D. Swern and W.E. Parker, J. Amer. Oil Chem. Soc., 1952, 29, 431 and 614.
30. H. Schlenk, J. Amer. Oil Chem. Soc., 1961, 38, 728
31. J.G. Keppler, S. Sparreboom, J.B.A. Stroink and J.D.J. von Mikusch.,
J. Amer. Oil Chem. Soc., 1959, 36, 308.
32. F.D. Gunstone, J. McLaughlan, C.M. Scrimgeour and A.P. Watson,
J. Sci. Fd. Agric., 1976, 27, 675.
33. B. Sreenivarsan, J.B. Brown, E.P. Jones, V.L. Davison and
J. Nowakowska, J. Amer. Oil Chem. Soc., 1962, 39, 255.
34. A.R. Johnson, and G.M. Ali, J. Amer. Oil Chem. Soc., 1961, 38, 453.
35. D. Swern and W.E. Parker, J. Amer. Oil Chem. Soc., 1953, 30, 5.
36. E.M. Stearns, Jr., H.B. White Jr., and F.W. Quakenbush,
J. Amer. Oil Chem. Soc., 1962, 39, 61.
37. R.E. Beal and O.L. Brekke, J. Amer. Oil Chem. Soc., 1959, 36, 397.
38. R.W. Riemenschieder, S.F. Herb, and P.L. Nichols, Jr.,
J. Amer. Oil Chem. Soc., 1949, 26, 371.
39. The two isomeric epoxides (3) and (4)



are reported to be only partially separable under optimum

conditions on either normal or reverse phase HPLC. Small fractions of purity $> 94\%$ were obtained from 1g loads^[40].

40. N.J. Morrison, private communication.

Volume 2

CHAPTER 4

E.S.R. STUDIES on FATTY ACIDS and the role of VITAMINS E and C in LIPID PEROXIDATION



Th 9836

Since its discovery by Zavoiskii^[1] in 1945 the technique of electron spin resonance (E.S.R.) has provided detailed information on the environment of paramagnetic centres in organic and inorganic systems. Within 10 years the technique was being applied to biological samples and subsequently revolutionised free radical research in biology and medicine^[2], and despite the advent of other free radical spectroscopic techniques such as chemically induced dynamic nuclear polarisation (CIDNP)^[3], E.S.R. has remained the principle magnetic spectroscopic tool in free radical research.

In this study E.S.R. has been utilised to investigate lipid radicals. The aim of this introductory section is to provide a brief insight into some of the important fundamental concepts of the technique and to define and elucidate some of the terms used in the subsequent results and discussion sections.

Extensive reference has been made to texts^[4-10] rather than original literature to provide a more general overview of the concepts involved. Mathematical concepts have been kept to a minimum and for a more extensive mathematical description the reader is directed to excellent texts by Harriman^[5], Atherton^[8], Wertz and Bolton^[9] and Gordy^[11].

Aspects of E.S.R. spectrometer instrumentation and operation are considered outwith the scope of this introduction. Texts describing

practical aspects are available , in particular Knowles *et al*^[6], Borg^[4] are excellent and the interested reader is directed to these sources.

2 Fundamental Concepts.

Electron spin resonance (E.S.R.) is a branch of magnetic resonance spectroscopy dealing with molecules in which the net spin quantum number S is non-zero. The overwhelming majority of molecules exist in singlet states ($S=0$) and are therefore, unobservable by E.S.R. Although some stable organic molecules containing unpaired electrons ($S=0$) exist (of which oxygen and nitroxides are probably amongst the most well known) the majority of E.S.R. studies are based on highly reactive radicals which are invariably intermediates of a reaction pathway.

A molecule* with a non-zero electronic spin will have associated with the spin a magnetic moment. Quantum restrictions only allow two orientations of spin (and hence magnetic moment) relative to any axis or molecular reference (for $S=1/2$). If we define the two spin states as α and β , then in the absence of an external applied magnetic field the energy levels of the two allowed spin states are degenerate (ie. the free electron has no preference for either spin state). The application of an external magnetic field can lift the degeneracy since the electron can align itself parallel (ie. be of lower energy) or antiparallel (resulting in an increase in energy of the spin state) with the applied field. This results in two energy levels sometimes referred to as Zeeman levels, the separation of which varies directly with the strength of the applied magnetic field.

* the term molecule is used in a general sense relating to systems of interest to E.S.R.

Transitions between the two levels can be induced by an appropriately orientated, oscillating magnetic field of frequency ν , if the photon energy $h\nu$ matches the energy level separation (ΔE) as given below

$$h\nu = \Delta E = g\beta H \quad (1)$$

where β is the Bohr magneton (the value of the intrinsic magnetic moment associated with the spin of a free electron), H is the strength of the applied magnetic field and g is the proportionality constant (the g -factor).

For a free electron the value of g resulting from the electrons spin is very close to 2, the residual resulting from the relativistic velocity of the electrons unit negative charge^[12], giving a g -value of 2.002319278.

Initially the quantised particles will be thermally distributed among the different energy levels with the lower states having a greater population probability in accord with the Boltzmann distribution. The ratio of the number of spins in the excited (higher energy) and ground (lower energy) states is given by

$$n_2/n_1 = \exp[-(E_2 - E_1)/kT] \quad (2)$$

where k is the Boltzmann constant, T is the absolute temperature n_2 is the population in the excited state and n_1 the population of the ground state with energies E_2 and E_1 respectively. Irradiation with the oscillating electromagnetic radiation will result in transitions from the ground to excited states and non-radiative relaxation processes

will tend to maintain the Boltzmann distribution of the two states and normally prevent saturation of the excited state.

2.1.1 Anisotropic g-values.

In general the spin-orbit coupling is orientation-dependent, and hence will reflect the orientation of the molecule to the applied external field. If the radicals are orientated in a single crystal; the orientation-dependent spin-orbit components will behave as a crystal aligned ensemble, and the angular dependence of the g-value with respect to the external field can provide very detailed information pertaining to spatial environment of the paramagnetic centres^[13].

2.1.2 Isotropic g-values.

For free radicals of molecular weight <1000 the thermal or Brownian tumbling is sufficiently rapid to average out all of the components of the anisotropic g-values resulting in an orientationally independent g-value, particularly in solutions of low viscosity.

Clearly for free radicals centres in tissues and macromolecules the g-values will not be motionally averaged with resulting spectral broadening and frequently asymmetry of spectral lines resulting from anisotropic g-value components.

2.2 Nuclear Hyperfine Interactions.

Most radicals contain one or more atoms with magnetic nuclei. Interaction of the unpaired electron with the internal magnetic fields due to nuclear magnetic dipole moments as well as with the applied magnetic field is termed "the nuclear hyperfine interaction". This results in the splitting of resonance lines into two or more components, so-called hyperfine splittings (hfs), which can greatly enhance the informational content of an E.S.R. spectrum because the splittings may aid in the identification of the free radical(s). Furthermore careful analysis of the spectrum may permit accurate determination of the orbital distribution of unpaired electrons, and hence of reactivities, of spatial orientations, and of structural information. [4]

The nuclear moments result from intranuclear coupling of all the angular momenta of constituent nucleons. The nuclear spin moments are quantized and hence only discrete values of the nuclear spin quantum numbers are allowed. For a nucleus of spin I there are $(2I+1)$ possible nuclear spin states, each corresponding to quantum-allowed orientation of the magnetic moment to an external magnetic field. The quantum numbers, M_I , for the component of the magnetic moment parallel to the external field assume the values $-I, -I+1, \dots, I-1, I$. The local field generated by a nuclear moment will add vectorially to the external laboratory field to give the effective field sensed by the unpaired electron. [4,5,8,9,11,13]

$$H_{\text{EFF}} = H_{\text{EXT}} + H_{\text{LOCAL}} \quad (3)$$

With $(2I+1)$ possible values of M_I , $(2I+1)$ values of H_{LOCAL} must

be considered. Substitution of these $(2I+1)$ values of H_{LOCAL} in eqn 3 gives rise to $2I+1$ values of H_{EXT} and hence $2I+1$ resonance lines.

Since in "free space" all unpaired electrons would resonate at the same H_r , it is the perturbation caused by all the local fields that provide the identifying and descriptive information carried by an E.S.R. signal. In essence, the distribution of deviations of H_{EXT} (at resonance) from $H_r^\#$ provides a probe to measure the totality of local fields in a sample, which in turn, carries all spectroscopic information implied by an E.S.R. signal.

For most organic free radicals the unpaired electron will interact with more than one nuclear magnetic moment giving rise to a complicated spectral pattern. The quantum selection rules

$$\Delta M_s = \pm 1$$

$$\Delta M_I = 0$$

where ΔM_s represents the change in spin state of the electron under the E.S.R. conditions and $\Delta M_I = 0$ means that the nuclear spin does not change during E.S.R. In general for the case of n nuclei of the same spin that are also equivalent in terms of the strengths of their interactions with the unpaired electrons within a free radical, the number of hyperfine lines by which the spectrum will be split, N_{hfs} is given by

$$N_{hfs} = 2In+1 \quad (4)$$

Furthermore when $I = 1/2$ (as in the case of 1H) the intensities of the N_{hfs} lines will be proportional to the coefficients of the binomial expansion of order n as given in Table 2.2^[6]

$^\# H_r$ resonant magnetic field at the
centre of the signal

Table 2.2 Relative intensities of the hyperfine lines
from n equivalent nuclei.

n							
0				1			
1			1	1			
2			1	2	1		
3			1	3	3	1	
4			1	4	6	4	1
5		1	5	10	10	5	1
6	1	6	15	20	15	6	1

If the hfs for two or more sets of equivalent nuclei are not very different considerable overlap of lines will result and a spectrum of increased complexity will ensue as more nuclei interact with the unpaired electron. In each case the effect of an additional nuclear hfs pattern will be to split each line of the spectrum predicted by considering each of the preceding nuclear hfs interactions. The sum of the number of line centres in such an idealized spectrum aggregates rapidly in accordance with the following equation

$$N_{\text{hfs}} = \prod (2I_i n_i + 1) \quad (5)$$

Two major types of nuclear hyperfine interactions may be distinguished; directionally dependent (anisotropic interactions) and directionally independent (isotropic interactions).

2.2.1 Anisotropic interactions.

Anisotropic hfs arise from the fact that the fields of both the odd electron and of the magnetic nuclear dipoles have a directional dependence. The dipole-dipole interaction of the electron and nuclear spin dipoles are dependent upon the relative orientations and positions, the distance between them, and their strengths. The hyperfine local field parallel to the laboratory field resulting from the "classic" dipole-dipole components of hfs is given by

$$H_{\text{LOCAL}} = \mu_N (3\cos^2\theta - 1) / r^3 \quad (6)$$

where μ_N is the component of nuclear magnetic moment along the direction of H_{EXT} , θ is the angle between H_{EXT} and the axis joining electron and nucleus, and r is the electron-nucleus distance^[12]. For solutions in which the radical has limited mobility such as macromolecules, in viscous media or of powder spectra from tissues, the observed spectral envelope will be a superposition of the spectra from all the possible orientations, and in general spectral detail will be lost and the observed lines poorly resolved or broad. For free radicals in solution as the viscosity of the medium decreases molecular tumbling will become more rapid, hence all the molecular orientations will become equally probable and the hyperfine anisotropies will average to nearly zero (the average value of $\cos^2\theta$ is equal to 1/3 if all orientations have equal probability, hence H_{LOCAL} becomes equal to zero^[14]).

2.2.2 Isotropic interactions.

Isotropic hyperfine splitting results from interaction of the unpaired electron and a magnetic nucleus. This is occasionally referred to as the Fermi contact interaction. The isotropic interaction depends on there being a finite electron density at the same place as the magnetic nucleus under consideration. It might be expected to only be observable when the electron is in an s orbital, because other atomic orbitals have nodes at the nucleus. Since radicals manifest isotropic hfs, despite the fact that their unpaired electrons are delocalised primarily in carbon p-orbitals, there must be another mechanism for generating some s-character for the unpaired electron distribution.

The molecular orbital treatment, which leads to the assumption that the spin density at the carbon nucleus is zero, is not an adequate description because it neglects any interaction of the σ - and π - electrons. A more sophisticated approach introduces spin polarisation. Consider a $\text{>}\dot{\text{C}}\text{-H}$ fragment with the odd electron in a carbon p-orbital, electron pairs in the three bonds are polarised in such a manner that the carbon nucleus is more apt to be associated with spins of the same type as that of the unpaired electron in the p-orbital (Fig 1a) than with the spins of the opposite type (Fig 1b), resulting in some unpaired spin density



FIGURE 1 Spin polarisation in the two orbital representations of the C-H σ bond.

being induced in orbitals of s-character on both the carbon and hydrogen atoms. The carbon nucleus and the proton are thus associated with spins of the same and opposite signs respectively as that of the unpaired electron. This treatment of the spin polarisation leads to a net negative spin density in the s-orbital of the proton. The sign of the spin density, per se, cannot be determined from E.S.R. alone^[7], but can be determined from nmr^[15].

2.2.3 α -proton splittings.

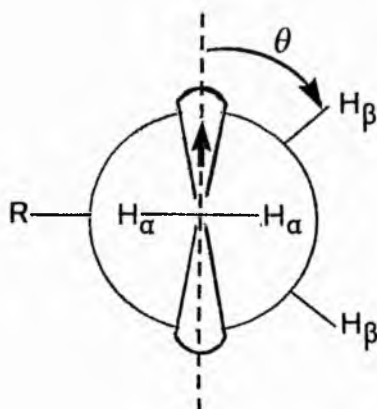
Although the sign of the spin density cannot be determined from the spectra, the hfs accurately reflect the distribution of the unpaired electron in the molecular fragment. McConnell^[16] has shown that for π -radicals the coupling constant, a_{H_i} , of a proton is directly proportional to the spin density, ρ_i , on the carbon atom i bearing that proton (eqn 7)

$$a_H = Q_H \cdot \rho_i \quad (7)$$

where Q_H is a proportionality factor with typical values between -2.00 and -3.00mT^[7]

2.2.4 β -proton splittings.

β -protons also produce very appreciable hyperfine splittings. An isotropic spin density at a nucleus can also result from hyperconjugative interactions between the odd electron in its p-orbital at an α -carbon atom and a bond to a β -substituent^[17]. This results in a direct spatial mixing of the β -proton orbitals with the odd electron bearing orbital, ie the proton is in the pi-electron cloud in which the unpaired electron is delocalised.



Fessenden and Schuler^[18] established that the hyperfine splitting constant for the protons of the β -methyl group, a_H^{Me} , in radicals of the type $\text{CH}_3\dot{\text{C}}\text{XY}$ is proportional to the spin density at the α -carbon atom.

$$a_H^{\text{Me}} = Q_H^{\text{Me}} \cdot \rho_\alpha \quad (8)$$

where Q_H^{Me} is a proportionality constant.

More interesting is the case when the β -carbon is asymmetrically substituted, in this situation the hfs, a_H , has been shown to depend on the dihedral angle θ , between the p-orbital containing the unpaired electron and the β -carbon-hydrogen bond and is given by the following eqn.,

$$a_H = (B_0 + B \cos^2 \theta) \cdot \rho_\alpha \quad (9)$$

where ρ_α is the electron-density at the α -carbon atom and B_0 and B are constants. The coupling constant with a β -proton is thus at a maximum when it is in the same plane as that of the p-orbital.

2.2.5 Other proton splittings.

Splittings by γ -protons in alkyl radicals are generally very small ($<0.1\text{mT}$) and are not always resolved. Larger splittings are observed when the spin density is transmitted across oxygen rather than methylene groups. Such splittings are believed to arise through hyperconjugation mechanisms.

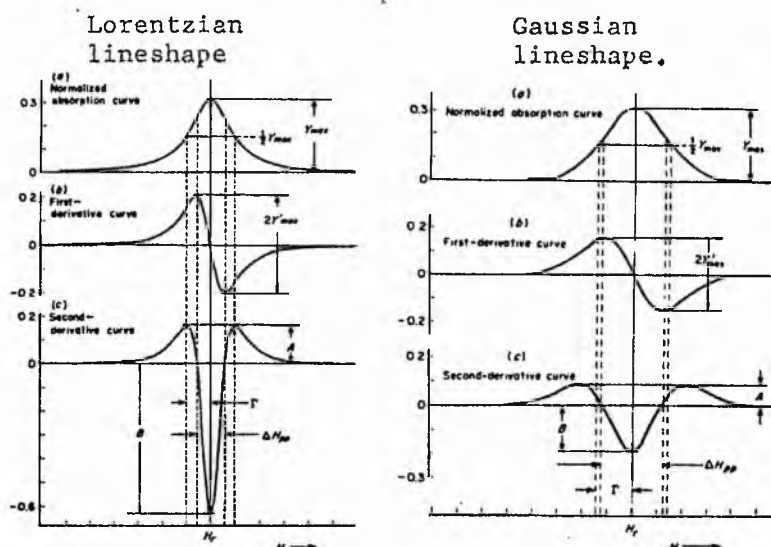
2.3 Lineshapes and linewidths.

The mechanisms giving rise to finite linewidths are said to be homogeneous and they usually reflect some kind of relaxation process that limits the lifetime of the spin states. The intrinsic shapes of homogeneously broadened lines closely approximate to Lorentzian curves, whose line shape can be defined by^[4].

$$Y = Y_{\max} (\Delta PP) / \left([\Delta PP]^2 + \frac{4}{3} [H_{\text{EXT}} - H_r]^2 \right)$$

where ΔPP is defined as the peak-to-peak amplitude of the first derivative curve.

Y is the signal intensity of the Lorentzian absorption curve (as opposed to the first derivative curve) corresponding to a given value of the independent variable, H_{EXT} .



As previously noted free radicals in low viscosity media tend to average out their anisotropic g-factor and hyperfine interactions as a result of rapid Brownian tumbling. However linewidth contributions are not completely eliminated and some homogeneous broadening persists. This results in Lorentzian line shapes when the lines are resolved, and for a given radical the peak-to-peak amplitude is a fundamental property of the resonance conditions, and can only be changed by altering the tumbling frequency via changes in temperature

or solvent viscosity.

2.3.1 Inhomogenous broadening.

In biological systems or large free radicals in viscous media each free radical will experience a slightly different field from its neighbour. This results in narrow intrinsic lines slightly displaced from the others at resonance and in general the distribution will be statistical leading to an absorption envelope whose shape appears to approach a Gaussian type curve.^[2] This type of broadening is commonly referred to as inhomogeneous.

2.3.2 Linewidths.

There are two major processes that can broaden E.S.R. lines, so-called "secular broadening" and "lifetime broadening". Secular broadening results from varying H_{LOCAL} , which implies that the energy difference ΔE between the two electron spin states will vary, resulting in a range of fields H_{EXT} , at which resonance occurs, hence generating a broad line. The variation in H_{LOCAL} may result from fluctuating local magnetic fields (vide supra). Alternatively the H_{LOCAL} variation may arise from varying H_{LOCAL} from one paramagnetic site to another but is constant in time for any given site; this is essentially the description of inhomogenous broadening described above.^[4]

Lifetime broadening intimately dependent upon relaxation phenomena whereby the unpaired electrons aligned by the external magnetic field in the higher energy spin state (antiparallel) can flip

to the more stable ground state in an attempt to reestablish the thermal or Boltzmann population distribution. The origin of relaxation time broadening can be rationalised in terms of the Heisenberg Uncertainty Principle, which implies that if a system exists in a certain energy state for only a short time then the energy of the state is not well defined and there is a limit on how accurately the energy of the quantised particle can be determined.

2.4 Quantification.

Where more than one type of radical is generated in an experiment the E.S.R. spectrum consists of a superposition of several signals. It is often desirable to be able to determine the relative amounts of each component present. The relative intensities of the different lines in a spectrum may be determined by one of the following methods.

(a) The definitive procedure for determining the intensity of a line is to calculate its area by integration of the full absorption curve ie. double integration of the first derivative representation. This procedure is time consuming and tedious if the spectrometer does not utilise a computerised data system and more importantly large errors can be obtained when peaks are of poor intensity.

(b) If the linewidths of the spectral components to be calculated are equal then peak-to-peak amplitudes of the derivative lines will, in fact, be directly proportional to their intensities. If linewidths are not the same the relative intensities can be computed by the following expression

$$I_{rel} \propto Y_{max} (\Delta PP)^2 \quad (11)$$

where Y_{\max} is the peak-to-peak derivative amplitude. This latter approximation only holds if the lineshapes are the same because of the different relationships of Lorentzian and Gaussian line intensities to $\Delta \overline{PP}$.

2.5 Sensitivity.

Characteristically free radicals are highly reactive species whose lifetime in chemical or biochemical reactions tend to be very short. Hence a common experimental problem in E.S.R. measurements is to develop methodology that will allow very short-lived radicals to be detected spectroscopically.

Radical concentrations of the order of $10^{-8}M$ are required for detection of a free radical by E.S.R. and at least a hundred fold greater to observe spectral detail with good signal to noise ratios. Theoretically, the sensitivity can be expressed in terms of the minimum number of detectable paramagnetic entities, N_{\min} . For a signal-to-noise ratio of one, equation 12 relates the various factors which contribute to either signal and/or noise levels

$$N_{\min} = \frac{3 k T_s \Delta \overline{PP}}{2 \pi Q_u \eta g^2 \beta^2 s(s+1) H_r} \left(\frac{3 F k T_d b}{P_0} \right)^{1/2} \quad (12)$$

where the parameters, their definition or description and typical values are given in Table 2.5

Table 2.5 Description and typical values of parameters
used in equation 12

Parameter	description	Typical values at Q band*
V_c	the cavity volume (see η below)	
V_s	the sample volume (see below)	0.008 cm ³
k	Boltzmann's constant (1.38×10^{16})	
T_s	sample temperature (absolute)	300 K
ΔPP	peak-to-peak width of the first derivative signal	0.05mT
F	a noise figure > 1 to account for noises sources other than detector thermal noise	50
T_d	detection temperature	300 K
b	bandwidth (in Hz) of the entire detection-amplification train,	1 sec ⁻¹
Q_u	effective unloaded Q-factor for the cavity [20]	5000
η	filling factor of the signal [21]	0.02
g	g factor of the signal	2
β	the Bohr magneton (92.7×10^{-21} erg gauss ⁻¹)	
S	spin quantum number for the para- magnetic centre ($S = 1/2$ for free radicals)	
H_r	resonant magnetic field at the centre of the signal	1250 mT
P_o	microwave power incident on the cavity	10 mW

Inserting typical values into equation 12 gives $N_{\min} = 2.8 \times 10^{10}$ spins or $5.8 \times 10^{-9} M$. If a spectrum is composed of many lines then a concomitant increase in radical concentration of R fold is required as given by

$$R = \sum_j I_j / I_k \quad (13)$$

with I_k the relative intensity of the central line and $\sum_j I_j$ the sum of relative intensities of all the lines in the spectrum.

References

1. E.K. Zavoiskii, Zh. Fiz. Khim., 1945, 9, 211 and 245.
2. B. Commoner, J. Townsend and G.E. Pake, Nature (London) 1954, 174, 689.
3. For a review on CIDNP, theory and application see S.H. Pine,
J. Chem. Educ., 1972, 49, 664.
4. D.C. Borg in "Free Radicals in Biology" Vol, Ch 3, pp 69,
Ed W.A. Pryor, Academic Press, New York, 1976.
5. J.E. Harriman in "Theoretical Foundations of Electron Spin Resonance",
Academic Press, New York, 1978.
6. P.F. Knowles, D. Marsh, and H.W.E. Rattle in "Magnetic Resonance of
Biomolecules", Wiley & Sons, London, 1976.
7. D.C. Nonhebel and J.C. Walton in "Free Radical Chemistry", Cambridge
Univ. Press, 1974.
8. N.M. Atherton in "Electron Spin Resonance", Wiley & Sons, New York, 1973.
9. J.E. Wertz and J.R. Bolton in "Electron Spin Resonance Elementary Theory
and Practical Applications", McGraw-Hill, New York, 1972.
10. M. Symons in "Chemical and Biochemical Aspects of Electron-Spin
Resonance Spectroscopy", Van Nostrand Reinhold, Berkshire, 1978.
11. W. Gordy in "Theory and Applications of Electron Spin Resonance",
Wiley & Sons, New York, 1980.
12. J.R. Bolton in "Biological Applications of Electron Spin Resonance"
Ed H.M. Swartz, J.R. Bolton and D.C. Bory, p 11, Wiley & Sons,
New York, 1977.
13. For an elegant example of the use of anisotropic g-values and hfs
see I.C.P. Smith, S. Schreier-Muccillo and D. Marsh in "Free
Radicals in Biology" Vol 1, Ch 4, pp 149, Ed W.A. Pryor,
Academic Press, New York, 1976.

14. H.R. Sands in "NMR and EPR Spectroscopy", Pergamon Press, Oxford, 1960.
15. E. de Boer and H. von Willigen, Progr. NMR Spectroscopy, 1967, 2, 111.
16. a) H.M. McConnell, J. Chem. Phys., 1956, 24, 632.
b) H.M. McConnell, J. Chem. Phys., 1956, 24, 764.
17. R.O.C. Norman and B.C. Gilbert, Adv. Phys. Org. Chem., 1967, 5, 53.
18. R.W. Fessenden and R.H. Schuler, J. Chem. Phys., 1963, 39, 2147.
19. R.W. Fessenden and R.H. Schuler, Advan. Radiat. Chem., 1970, 2, 1.
20. The factor 'unloaded cavity Q' is a measure of the ability of the microwave reflection cavity to increase the microwave radiation at the sample and is defined as

$$Q = \frac{2\pi (\text{maximum microwave energy stored in the cavity})}{\text{energy lost per cycle}}$$

see A.S. Brill, Phys. Tech. Biol. Res., 1969, 2(pt B), 136 and
C.P. Poole, Jr., "Electron Spin Resonance - A Comprehensive
Treatise on Experimental Techniques", Wiley & Sons, New York, 1967.

21. The filling factor of the cavity, η , depends upon the ratio of the microwave power dissipated in the sample to that dissipated in the cavity.

SECTION 1

An E.S.R. study of fatty acids.

**Part1. Hydrogen abstraction from
unsaturated long chain esters**

Summary.

The radicals generated from unsaturated fatty acid esters by hydrogen abstraction with photochemically formed *t*-butoxy radicals have been investigated by e.s.r. spectroscopy. The substituted allyl and pentadienyl radicals generated from monoenoic and dienoic esters were conformationally stable under the conditions of the experiments. The main species observed on H-abstraction from monoynoic esters were substituted propynyl radicals, and the same radical type was generated from diynoic esters with more than one methylene unit separating the triple bonds. Substituted penta-1,4-diynyl and penta-1,3-diynyl radicals were identified on H-abstraction from methylene-interrupted and conjugated diynoic esters. Hydrogen abstraction from triacylglycerols containing one or more double bonds was also examined. Most of the unsaturated esters also gave rise to secondary radicals produced by H-abstraction from the chain methylene groups. From the measured concentrations of the secondary and delocalised radicals the following relative rates of H-abstraction by *t*-butoxy radicals from the different sites were obtained; secondary : propynylic : allylic : bisallylic = 1 : 18 : 36 : 116 at 293 K.

1 Introduction.

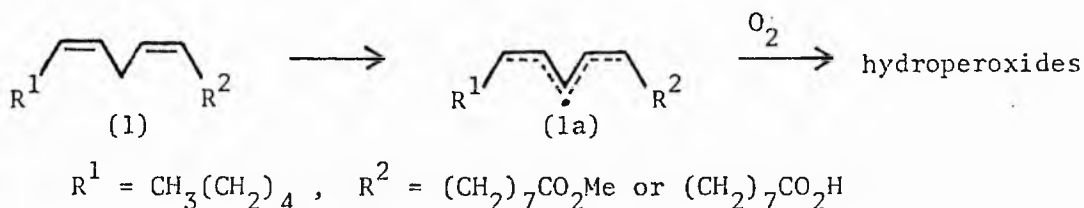
LIPID peroxidation may occur by a controlled enzymic oxidation leading to biologically important molecules^[1] whose physiological roles include blood pressure regulation^[2], inflammation^[3], platelet aggregation^[4], and anaphylaxis^[5]. Alternatively, lipid peroxides can be formed by random free radical reactions^[6]. The random free radical autoxidation of polyunsaturated fatty acids appears to be an important process *in vivo*^[7], as exemplified by the expiration of pentane and ethane by organisms under free radical-stress^[8].

In vivo lipid peroxidation has been identified as one of the major free radical deteriorative reactions associated with cell membranes^[9]. Among the pathological events associated with lipid peroxidation are oxidative damage to cells^[10] and lungs^[11] induced by atmospheric pollution^[11], certain phases of atherosclerosis^[12], chlorinated hydrocarbon hepatotoxicity^[13], oxygen toxicity^[14], ethanol induced liver injury^[15], cataract formation^[16], paraquat toxicity^[17], the aging process^[18] and cancer^[19]. Free radical damage to biological membranes and foodstuffs has been the subject of several reviews^[20].

Although the free radical nature of lipid autoxidation is undisputed, the evidence for this relies on indirect observations such as oxygen consumption^[21] and the formation of peroxides^[22] and conjugated dienes from polyene acids^[23,21b]. Much effort has been expended in trying to detect free radicals from fatty acids by E.S.R. spectroscopy^[24-31] and signals have been recorded from ozonised linoleic acid^[24], from γ -ray irradiated triacylglycerols^[28] and from the reaction of nitrogen dioxide with unsaturated fatty acids and

phospholipids^[29]. In all cases however the signals obtained were broad and without any resolved hyperfine splittings. Hence no structural or conformational information about the radical intermediates could be obtained.

Other research groups^[30-32] used the spin trap technique to obtain information about the environment of the unpaired electron. De Groot *et al.*^[30] studied the soybean lipoxygenase catalysed oxidation of linoleic acid in this way, and by the use of deuterium analogues, deduced that the main trapped species was the substituted pentadienyl radical (1a).



Similar observations were made for the oxidation of linoleic acid with potato lipoxygenase^[31]. Recently Chiba *et al.*^[32] observed spin adducts from UV-irradiated solutions of methyl linoleate in the presence of deuterated nitrosodurene as the spin trap.

We now report details of an E.S.R. spectral study of a variety of delocalised radicals obtained on hydrogen abstraction from methyl esters of long-chain acids with one or more double or triple bonds. The results provide insight into the mechanism of lipid autoxidation particularly with regard to the preferred sites of hydrogen abstraction.

2 Results and discussion

E.S.R spectra of the fatty ester radicals were obtained by photolysis of degassed solutions of the freshly purified ester and di-t-butyl peroxide in the cavity of the spectrometer. Hydrocarbon solvents could be used, particularly for low temperature work, but the most intense spectra were generally obtained with neat di-t-butyl peroxide and temperatures around ambient. Sample lifetimes were usually of the order of 15 minutes owing to the build of polymer on the walls of the tubes. In a few cases, where relatively large quantities of ester were available, a flow system was employed which increased the effective sample lifetime.

2.1 Monoenoic Fatty Acid Esters.

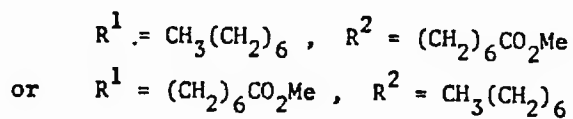
A series of isomeric methyl octadecenoates were studied in which the double bond varied from the $\Delta 2$ to the $\Delta 17$ positions. In most cases the spectra were very weak and/or poorly resolved and could not be analysed. The exceptions were methyl elaidate (18:1 $\Delta 9E$) and methyl oleate (18:1 $\Delta 9Z$). Hydrogen abstraction from the two allylic sites in methyl elaidate produced two isomeric transoid radicals (2b) but, as would be expected, these were spectroscopically indistinguishable, giving rise to the well resolved double septet spectrum shown in Figure 2. Methyl oleate, oleic acid and cis-octadec-9-ene (obtained by reduction of the carboxylate group) all gave identical spectra. These were readily analysed and the hyperfine splittings (hfs) were similar to those of allyl^[34,35] and alkyl

radicals^[35-38] and the assignments to specific hydrogens, made by comparison with these model compounds are in Table 1.

The spectrum obtained from methyl oleate (Figure 1) can be assigned to the cisoid allyl type radical (2a). On prolonged photolysis, especially at higher temperatures, i.e. ca 330 K, the spectra became more complex showing the presence of a second allyl radical; eventually the spectrum became identical to that obtained from methyl elaidate. On cooling the sample the spectrum of the transoid radical persisted, i.e. the change was irreversible. After photolysis the contents of the E.S.R. tube were analysed by capillary GLC and it was found that virtually all the remaining fatty acid ester had been converted to trans isomers. Capillary GLC showed peaks for 8Z (very small), 9Z (small) and 9E (very large) esters. This last peak may also contain the 8E, 10E, and 10Z isomers and we would expect the minor 8Z ester to be accompanied by a similar proportion of the 10Z ester^[39].

The initial observation of radical (2a) followed by (2b) on prolonged reaction might be explained by direct isomerisation of (2a) to (2b) via rotation about the partial double bond (see Scheme 1). However the process should then be reversible, i.e. on cooling the sample the spectrum of the cisoid radical (2a) should reappear, contrary to the experimental observations. Furthermore, the barriers to rotation about the partial double bonds in allyl (66 kJ mol^{-1})^[40] and substituted allyl radicals^[41] suggest that the direct isomerisation of the radicals would not occur at ambient temperatures. Alternatively, isomerisation could occur by reversible addition of t-butoxyl radicals to the oleate double bond (Scheme 1). The presence of methyl trans-octadecenoates after photolysis, though

substrate to give elaidate.



SCHEME 1

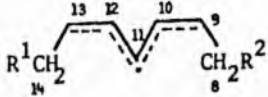
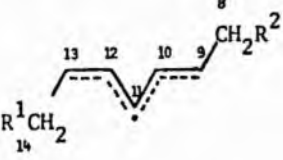
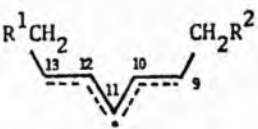
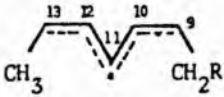
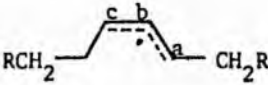
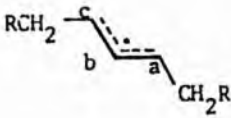
The conversion of (2a) to the transoid conformer (2b) has important implications for oleate autoxidation. The classical mechanism of oleate autoxidation involves allylic hydrogen abstraction to give (2a) followed by oxygen entrapment to give the corresponding peroxy radicals which subsequently give hydroperoxides on hydrogen abstraction^[39].

Experimentally it is found that trans hydroperoxides predominate and that the proportion of trans product increases with temperature of autoxidation^[42-45]. Oxygen entrapment by conformer (2a) does not provide an adequate explanation for the uneven distribution observed for both geometrical and positional isomers of oleate hydroperoxides^[42-47]. The results clearly parallel our E.S.R. observations on the reaction of oleate with t-butoxyl radicals. The increase in relative concentration of trans- to cis- hydroperoxides with increasing temperature observed in the autoxidations can be explained by a similar argument, namely that radical (2a), which can give rise to both cis- and trans- hydroperoxides is converted to the transoid radical (2b) which leads exclusively to trans- hydroperoxides. Our results do not give a definite indication of whether this conversion occurs directly or by reversible oxygen addition^[48].

The small proportion of hydroperoxides with cis unsaturation at $\Delta 8$ and $\Delta 10$ imply that the radical (2a) must also participate^[39]. This radical was not detected in the E.S.R. experiments, but the signal to noise ratio was such that only the main radicals would be observed and the participation of minor amounts of (2a) is not excluded.

TABLE 1

E.s.r. Parameters of Substituted Allyl and Pentadienyl Radicals^a

Radical	Precursor Methyl Ester	Temp/K	a/mT
	18:2 (9Z,12Z)	290	H (10,12) 0.32 CH ₂ (8, 14 <i>endo</i>) 0.78 H ² (9, 13 <i>exo</i>) 0.98 H (11) 1.11
	18:2 (9E,12Z) ^b	315	H (10,12) 0.32 CH ₂ (<i>endo</i>) 0.78 CH ₂ (<i>exo</i>) 0.90 H ² (9 <i>endo</i>) 0.90 H (13 <i>exo</i>) 0.98 H (11) 1.11
	18:2 (9E,12E)	310	H (10,12) 0.31 2CH ₂ (<i>exo</i>) 0.90 H ² (9,13 <i>endo</i>) 0.90 H (11) 1.11
	14:2 (9Z,12Z)	270	H (10,12) 0.32 CH ₂ (8 <i>endo</i>) 0.78 H ² (9,13 <i>exo</i>) 0.98 H (11) 1.11 CH ₃ (14 <i>endo</i>) 0.90
	18:1 (9Z)	230	H (b) 0.39 2CH ₂ (<i>exo</i> , <i>endo</i>) 1.24 H ² (a <i>endo</i>) 1.24 H (c <i>exo</i>) 1.43
	18:1 (9E)	270	H (b) 0.37 H (a, c <i>endo</i>) 1.29 2CH ₂ (<i>exo</i>) 1.29

a All hfs were checked by computer simulation of the spectra.

b 18:2 (9Z,12E) also present in the sample examined gives an identical spectrum.

The E.S.R. spectra from both methyl oleate and methyl elaidate showed additional weak signals from secondary radicals produced by hydrogen abstraction from non-allylic chain methylenes. The inner lines of the secondary radicals were unobservable because of extensive overlap by the main spectrum of the allylic radicals, but the outer lines were clearly distinguishable. Very weak, but distinct, signals could also be observed for the radicals produced by hydrogen abstraction from the methylene adjacent to the terminal methyl group because of the extra β -hydrogen but these radicals were too weak for observation in the spectra from methyl elaidate. They were, however, observed on hydrogen abstraction from saturated fatty acids.

The relative concentration of allylic (A) and secondary (S) radicals was estimated by double integration of suitable peaks in the spectra. Accurate values were difficult to obtain in the static system because of poor signal intensities and the build-up of broad signals from secondary products. Spectra were also run using a flow system and a signal averager which gave higher accuracy. From the flow system data we find $[A]/[S] = 7.2 \pm 1.6$ at 293K. There are 4 allylic hydrogens in methyl elaidate and 20 chain methylene hydrogens (excluding the methylene groups adjacent to the carboxylate and terminal methyl groups which gave separate signals too weak to measure) hence the relative rate of allylic to secondary abstraction for t-butoxyl radicals is about $36 \pm 8:1$ on a per hydrogen basis (see Table 2). Small *et al.*^[49] measured the absolute rates of hydrogen abstraction from fatty acids by t-butoxyl radicals using a laser flash photolysis method and obtained a value of $k(\text{rel}) = 7.2$ with stearic and oleic acids. Our E.S.R. results thus indicate greater selectivity for t-butoxyl radicals and the reasons for this discrepancy are not

clear.

The calculation of $k(\text{rel})$ from the measured concentration of the two radical types in the E.S.R. method depends on the assumption of equal termination rates for the secondary and allylic radicals. The termination rates are likely to be very similar, because they will be diffusion controlled, but a somewhat greater termination rate for secondary radicals could account for part of the difference.

TABLE 2

Relative Rates of Hydrogen Abstraction from Unsaturated C₁₈ Esters
by t-Butoxy Radicals at Ambient Temperature

site	secondary H	propynylic H	allylic H	bisallylic H
$k(\text{rel})$ (298 K)	1.0	18 ± 5	36 ± 8	116 ± 25
$D(\text{C-H}) /$ kJ mol^{-1}	397	365^{a}	345^{b}	322^{c}

^a From $\text{CH}_3\text{CH}_2\text{C}\equiv\text{CCH}_3$, ref. 61

^b From $\text{CH}_3\text{CH}_2\text{CH}=\text{CH}_2$, ref. 62

^c From $\text{CH}_2=\text{CHCH}_2\text{CH}=\text{CH}_2$, refs. 62 and 63

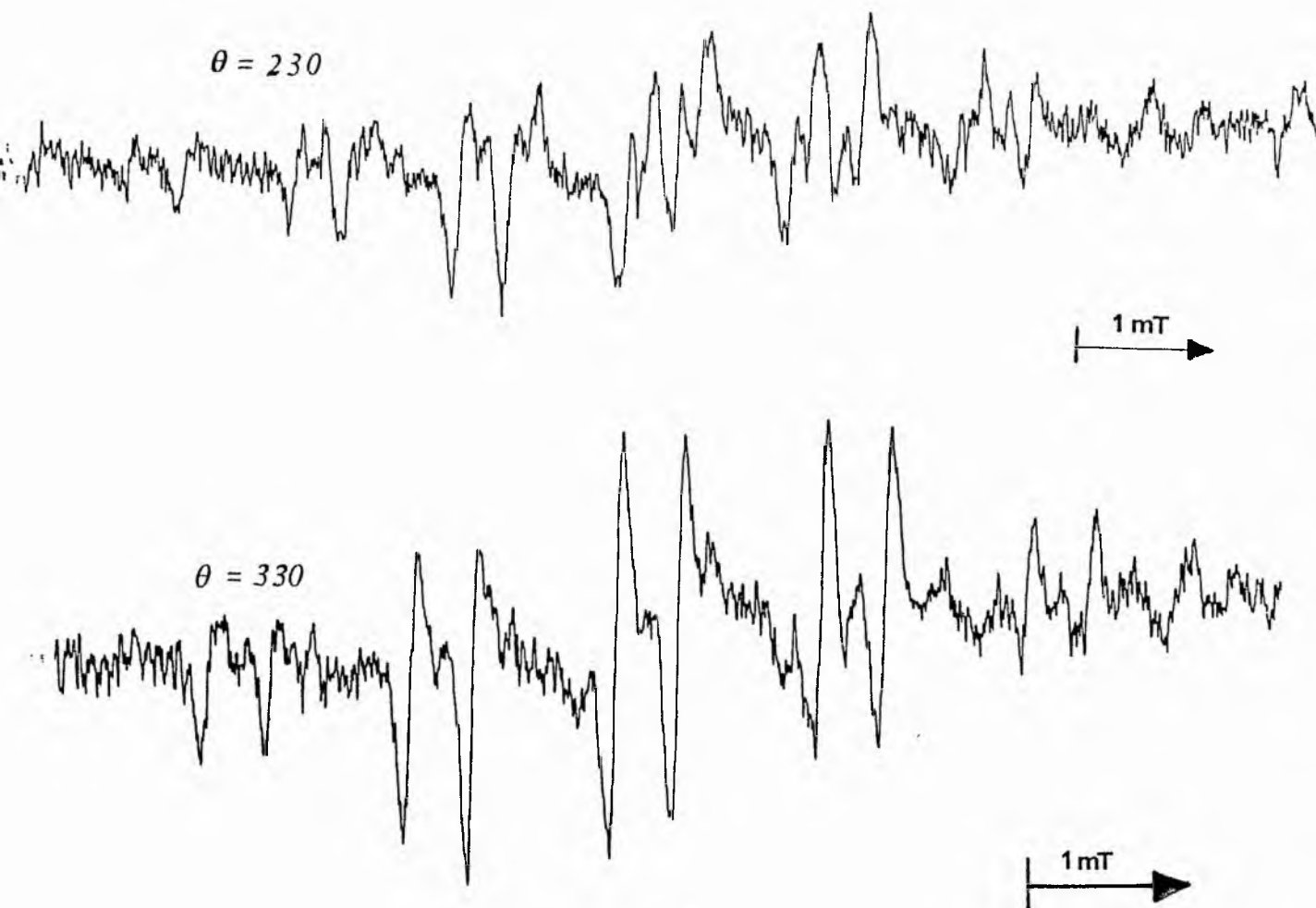


FIGURE 1

9.4 GHz E.S.R. spectra of the allyl radicals derived from methyl oleate.

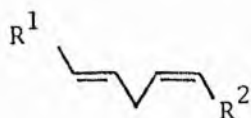
- TOP Spectrum obtained at 230 K. The predominant radical is the cisoid allyl type radical (2a)
- BOTTOM Spectrum obtained at 330 K. The predominant radical is the transoid allyl type radical (2b)

Our results, and those of Small et al.,^[49] show that hydrogen abstraction by t-butoxyl radicals from non-allylic positions in unsaturated acids/esters amounts to a significant proportion of the total. This contrasts with autoxidation studies where only hydroperoxides derived from attack on the allylic position are detected. In autoxidation reactions hydrogen is abstracted by peroxy radicals which may be more selective than t-butoxyl radicals, and this may account for the difference in the product distribution. The results with t-butoxyl radicals suggest however that minor amounts of hydroperoxides derived from attack at the non-allylic methylene groups should be formed in the autoxidation of unsaturated fatty acids. This could be more significant at higher temperatures because alkoxy radicals formed by thermal cleavage of hydroperoxides are present. Hydroperoxides attached to secondary carbon atoms are as yet undetected but their degradation products could be important in influencing the flavour and smell of stored fats and oils.

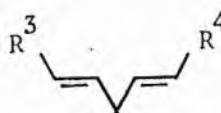
2.2 Di-, Tri-, and Tetra-enoic Fatty Acid Esters.

Hydrogen abstraction from methyl linoleate (1), the isomeric cis,trans mixture (3) and the trans,trans ester (4) gave rise to E.S.R spectra which were assigned to the pentadienyl radicals (1a), (3a), and (4a) respectively (Scheme 2). The three spectra were distinct from each other and the hfs were assigned to specific hydrogens by comparison with those of alkyl substituted pentadienyl radicals^[50-52] (Table 1). Pentadienyl radicals with E.S.R. parameters identical to those of (1a) were observed on hydrogen abstraction from the

hydrocarbon (octadeca-9 \underline{Z} ,12 \underline{Z} -diene) produced by reduction of the carboxylate group of (1).



(3)

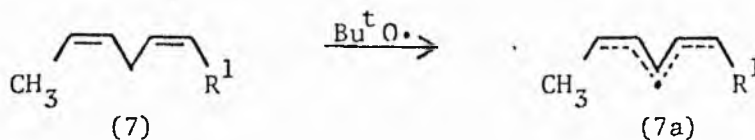


(4)

$R^1 = \text{CH}_3(\text{CH}_2)_4$, $R^2 = (\text{CH}_2)_7\text{CO}_2\text{Me}$, $R^3 = \text{CH}_3(\text{CH}_2)_4$, $R^4 = (\text{CH}_2)_7\text{CO}_2\text{Me}$
and $R^1 = \text{MeO}_2\text{C}(\text{CH}_2)_7$, $R^2 = (\text{CH}_2)_4\text{CH}_3$

It is seen that similarly sited hydrogens in the three radicals have identical hfs, e.g. all the endo hydrogens have the same hfs. This internal consistency which supports the assignments has also been reported for alkyl substituted pentadienyl radicals^[52]. Several conformations are conceivable for the radicals (1a), (3a) and (4a) but molecular models indicate that the conformations illustrated will be the most stable with least steric crowding and we assumed that other conformations are unimportant.

Photolysis of methyl tetradeca-9 \underline{Z} ,12 \underline{Z} -dienoate (7) in neat di-*t*-butyl peroxide gave the pentadienyl radical (7a). The hfs constants have been unequivocally assigned to the hydrogens of the pentadienyl system in the cis,cis conformation and are given in Table 1. The terminal methyl group has little effect on the hfs constants which are in excellent agreement with our parameters for methyl linoleate. The E.S.R. spectrum is shown in Figure 3.



$R^1 = (\text{CH}_2)_7\text{CO}_2\text{Me}$

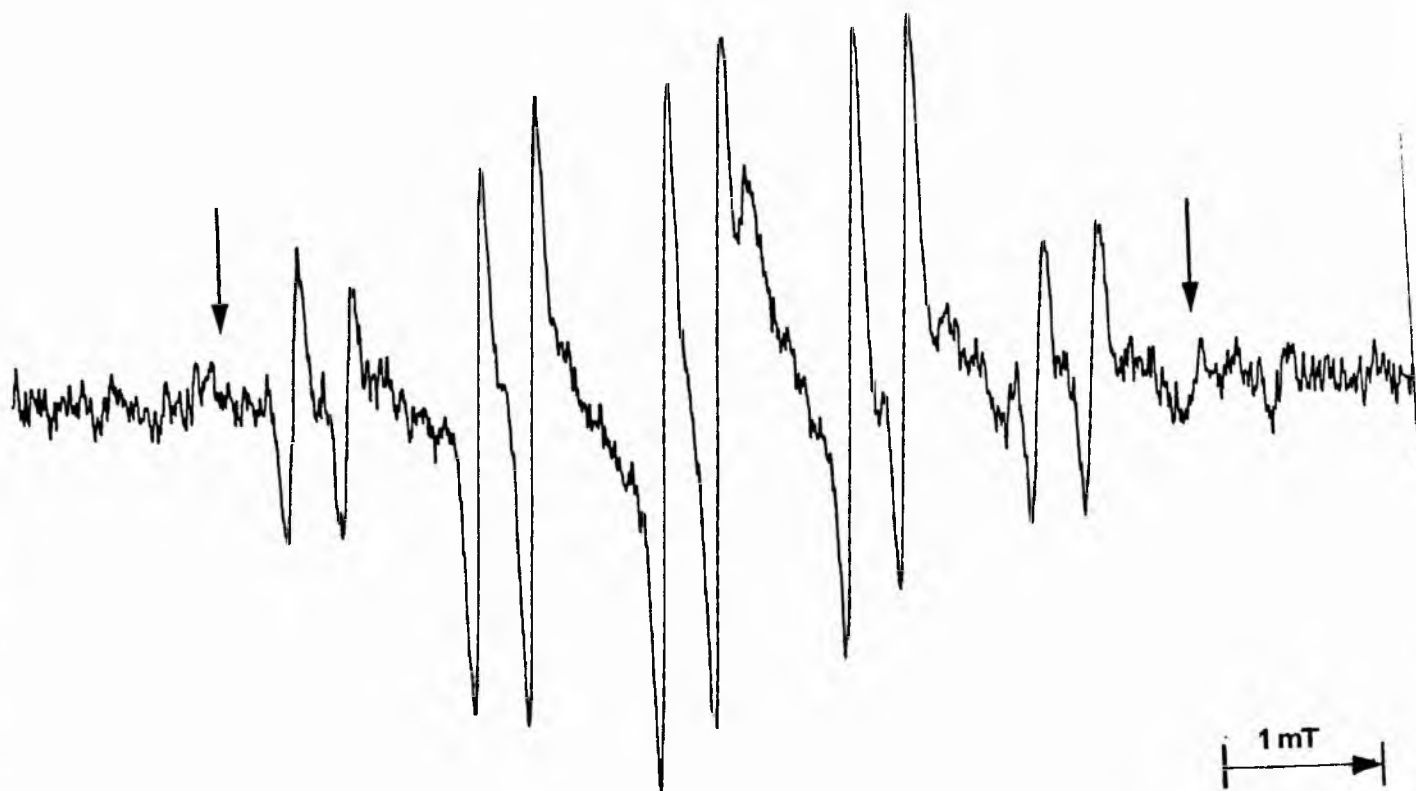


FIGURE 2 9.4 GHz E.S.R. spectrum of the allyl radical derived from methyl elaidate. Arrows indicate the main lines of the secondary radicals derived from H-abstraction at chain methylenes.

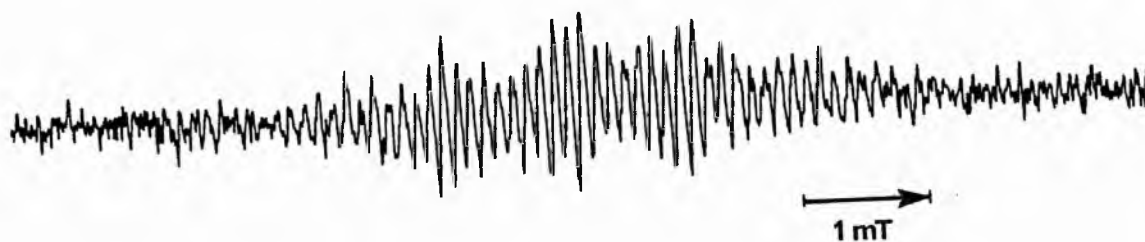


FIGURE 3 9.4 GHz E.S.R. spectrum of the pentadienyl radical (7a).

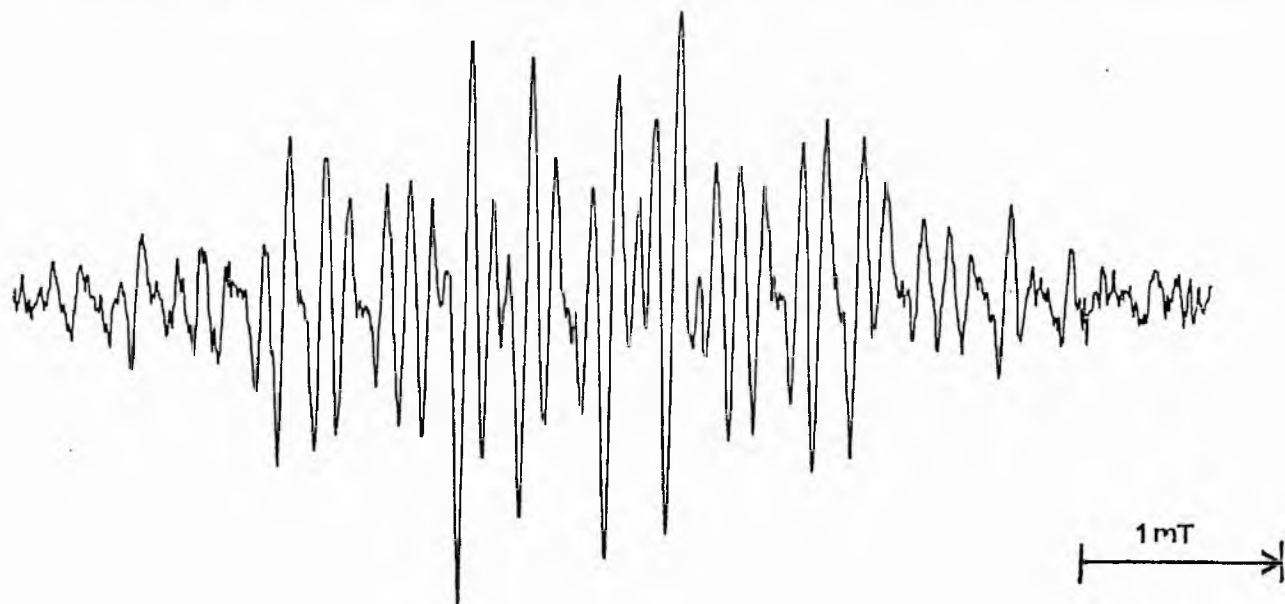


FIGURE 4

E.S.R. spectrum of pentadienyl radical (1a) at ambient temperature.

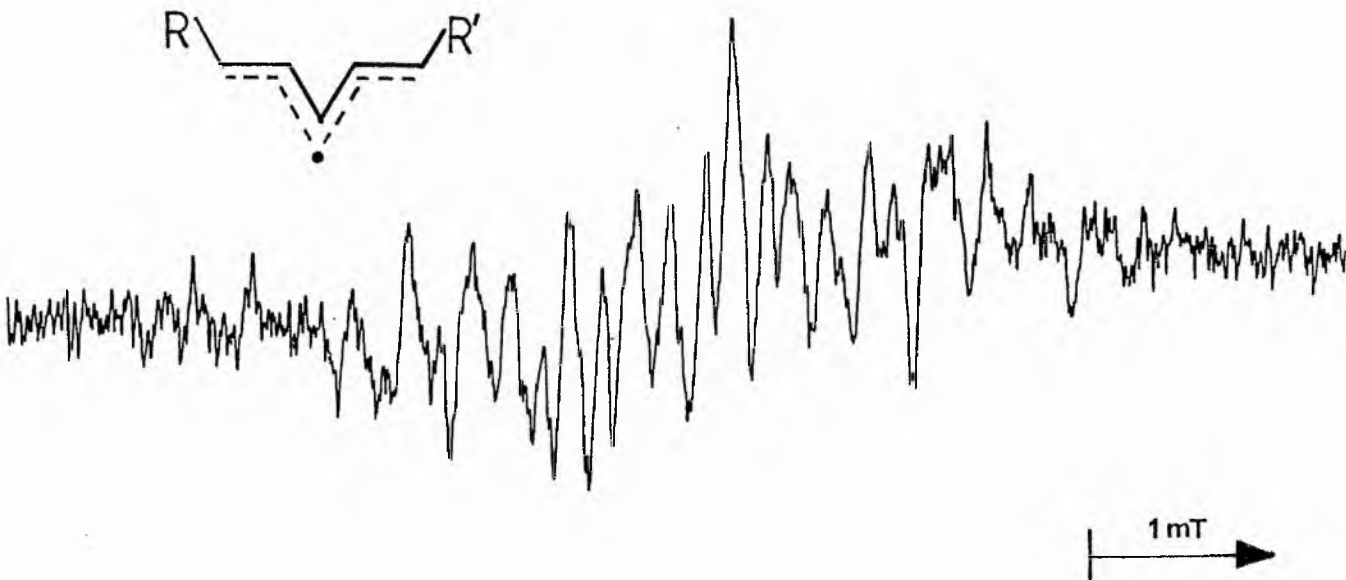


FIGURE 5

E.S.R. spectrum of pentadienyl radical (4a) at ambient temperature.

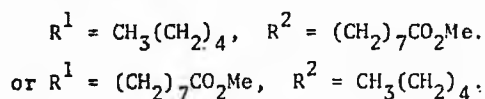
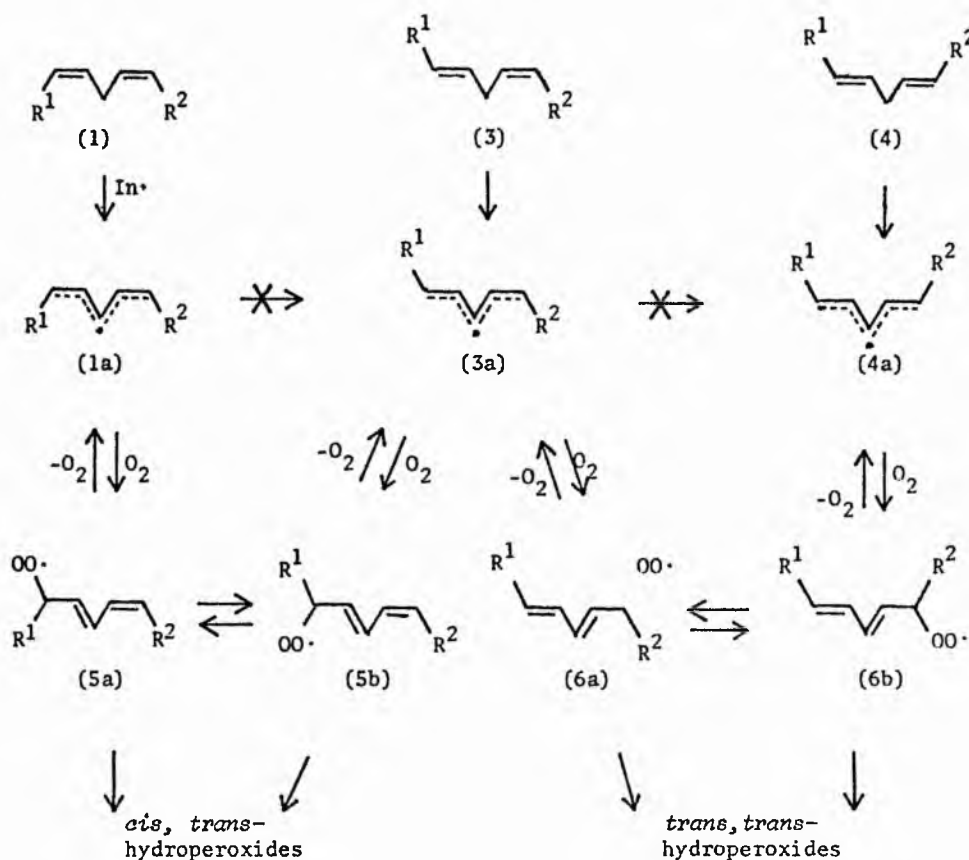
Neither secondary nor allyl radicals could be detected on the spectra obtained from methyl linoleate in static or flow systems. Secondary radicals were observable when mixtures of linoleic and methyl palmitate were examined and the relative concentrations of the bisallylic (BA) and secondary (S) radicals were measured. From the concentrations of the two radical types

[18:2]/[16:0]	0.069	0.347	0.442
[BA]/[S]	0.603	2.51	3.95
k(rel) (293 K)	109	104	135

the rate of abstraction of the bisallylic hydrogens relative to the rate of abstraction of secondary hydrogens on a per hydrogen basis [k(rel)] was calculated. Reasonable agreement in the k(rel) values was obtained for the three concentration ratios and the averages of three runs in each case are reported in Table 2

The spectrum of radical (1a) (Figure 4) generated from methyl linoleate did not change with time or temperature in the range 250 to 330 K, i.e. the cis,cis radicals do not convert to the trans,cis (3a) or trans,trans (4a) (Figure 5) conformers under the conditions of the E.S.R. experiments. It is generally accepted that autoxidation of methyl linoleate (1) proceeds by hydrogen abstraction at the bisallylic site [C(11)] to give the pentadienyl radical from (1a) and our direct E.S.R. identification of (1a) as the principle radical

from (1) confirms this assumption and agrees with the spin-trapping results of De Groot et al. [30]. Oxygen entrapment by (1a) gives the peroxy radicals (5a) and (5b) (Scheme 2) which can lead only to the formation of cis,trans-hydroperoxides. Experimentally it has been found that both cis,trans- and trans,trans-hydroperoxides are formed in this autoxidation.

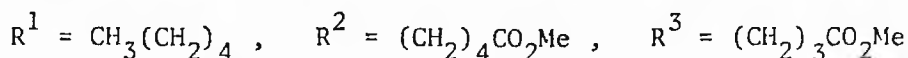
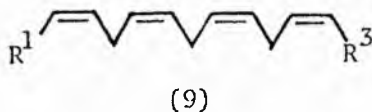
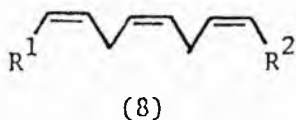


To account for this Porter^[53] and others^[46] proposed that the oxygen addition step must be reversible, so that the cis,trans radical (3a) can be generated from (1a) via (5a) and (5b). Oxygen addition to C(9) or C(13) in (3a) can then give peroxy radicals (6a) and hence (6b) which are responsible for trans,trans-hydroperoxides. The direct interconversion of (1a), (3a) and (4a) was discounted on energetic grounds and by analogy with the pentadienyl radical itself^[52]. Our E.S.R observations confirm that direct interconversion does not occur, and lend support to the indirect route.

We note with interest that the spin density at the central carbon of the pentadienyl system is higher than at C(9) and C(13). Experimentally, autoxidation of methyl linoleate has been reported to give exclusively conjugated diene hydroperoxides resulting from oxygen addition at C(9) and C(13). Oxygen entrapment at the central carbon of the pentadienyl system C(11) would give a non-conjugated hydroperoxide. However, if the product distribution is under thermodynamic control as opposed to kinetic control then the 11-hydroperoxide might rearrange, via reversible oxygen addition, to the thermodynamically more stable conjugated diene hydroperoxides. It is conceivable that at low temperatures the 11-hydroperoxide may be an isolable autoxidation product.

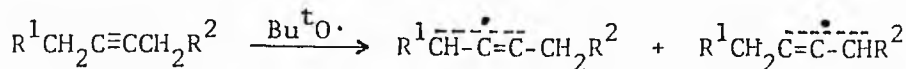
Hydrogen abstraction from the two bisallylic positions in methyl *p*-linolenate (8) would also be expected to produce pentadienyl radicals. We found that *t*-butoxyl radicals abstract hydrogen specifically from the bisallylic sites and that the two pentadienyl radicals are indistinguishable from each other and from (1a) by E.S.R. spectroscopy. Similarly, the pentadienyl radicals observed on

hydrogen abstraction from the three bisallylic methylenes of the tetraenoic ester (9) (methyl arachidonate) are indistinguishable. The E.S.R. parameters of these radicals are the same, within experimental error, as those for (1a) in Table 1.



2.3 Monoynoic Fatty Acid Esters.

A series of isomeric methyl octadecynoates in which the position of the triple bond varied from C(2) to C(17) was also studied. In contrast to the methyl octadecenoates well resolved spectra with good signal intensity were obtained for most of the isomers. The main radical in each case was readily identified as the corresponding substituted propynylic (allenic) radical. Similar spectra, consisting of a quartet of triplets, were obtained for the methyl octadec-4 through -13-ynoates; the spectrum from methyl octadec-8-ynoate is shown in Figure 6. The hfs were assigned to specific hydrogens by comparison with the parameters for propynyl^[54] and alkyl substituted propynyl radicals^[55], and the results are in Table 3. Two different propynyl radicals can be formed by hydrogen abstraction from the propynylic sites:



but for the 5-yne through -13-yne esters the two radicals were spectroscopically indistinguishable. Two propynylic radicals with different hfs but the same g-factor were observed for the 14-yne and 15-yne esters. For the 16-yne ester abstraction of the primary hydrogens of the terminal methyl group was not observed and only one propynyl radical was detected; in this and the single propynylic radical obtained from methyl octadec-17-ynoate triplet hyperfine splittings from methylene groups γ to the triple bonds were resolved. Two distinct propynylic radicals were expected for the 4-yne ester (by analogy with the 14-yne ester) but only one was detected. It is possible that the hydrogens α to the carboxylate group are deactivated so that the radical generated at this site is too weak for detection (see below).

Although the main radical from each ester was obtained by abstraction of the propynylic hydrogens, signals from secondary radicals generated by hydrogen abstraction from the chain methylenes were also observable in most of the spectra (see Figure 6). The acetylenic esters were not available in sufficient quantities to permit the use of the flow technique but the ratio of the concentrations of the propynylic (P) to secondary (S) radicals was determined from the intensities of the signals in static runs, for a number of isomers, and the results are given in Table 3. The methyl octadecynoates studied contained 4 propynylic hydrogens (except for the 14-yne isomer where the concentration ratio was calculated from only one of the two propynylic radicals) and 20 secondary hydrogens (excluding those adjacent to the terminal methyl and carboxylate groups) and the $k(\text{rel})$ values (Table 3) were calculated on this

assumption. The average $k(\text{rel})$ is given in Table 2 but the results for the 4-yne and 2-yne esters have been excluded. The lower $k(\text{rel})$ values obtained for these two isomers may be due to deactivation of the propynylic methylenes by the carboxylate group. Tedder and coworkers have shown that carboxylate and other electron withdrawing substituents deactivate both the α - and β -hydrogens to abstraction by halogen atom^[56]. In the case of the 4-yne ester one of the set of propynylic hydrogens is β - to the carboxylate group. The lower $k(\text{rel})$ for this isomer could be a consequence of similar deactivation towards hydrogen abstraction by t-butoxyl radicals. It is possible that the C(3) hydrogens in this isomer are sufficiently deactivated that the propynylic radical which would be generated by their abstraction is too weak to detect. This would explain the absence of the two distinct propynylic radicals in the spectra from this isomer (vide supra). Similarly, the deactivating effect of the electron-withdrawing carboxylate substituent would be transmitted by the triple bond in the 2-yne ester thus accounting for the lower rate of H-abstraction observed for the C(4) propynylic hydrogens of this ester.

The relative rates of hydrogen abstraction from the various sites in the fatty acid esters are collected in Table 2. The order of reactivity of the hydrogen bonds towards t-butoxyl radicals is bis-allylic > allylic > propynylic > secondary. This order is in agreement with the results of Small *et al.*^[49] but our E.S.R. data indicate a greater difference in selectivity between allylic and bis-allylic hydrogens. The overall rate constants for reaction of hydroxyl radicals with propane, propene, propyne and related molecules have been determined^[57-60]. The rate constants include addition to

the double bond as well as hydrogen abstraction, but they do suggest that the order of reactivity is the same for hydroxyl and t-butoxyl radicals. The C-H bond dissociation energies from model compounds are compared with the $k(\text{rel})$ values in Table 2, which shows that the rate of hydrogen abstraction increase monotonically with the decrease in $D(\text{C-H})$. The relative rates of abstraction of primary, secondary and tertiary hydrogen by t-butoxy radicals are 1:8:44. a plot of $\log[k(\text{rel})]$ against the bond dissociation energies is shown in Figure 7, where our data (Table 2) is combined with the relative rates for primary and tertiary hydrogens. For a closely related series of reactions the Evans-Polanyi relation ($E = [D(\text{C-H})] + C'$) predicts a

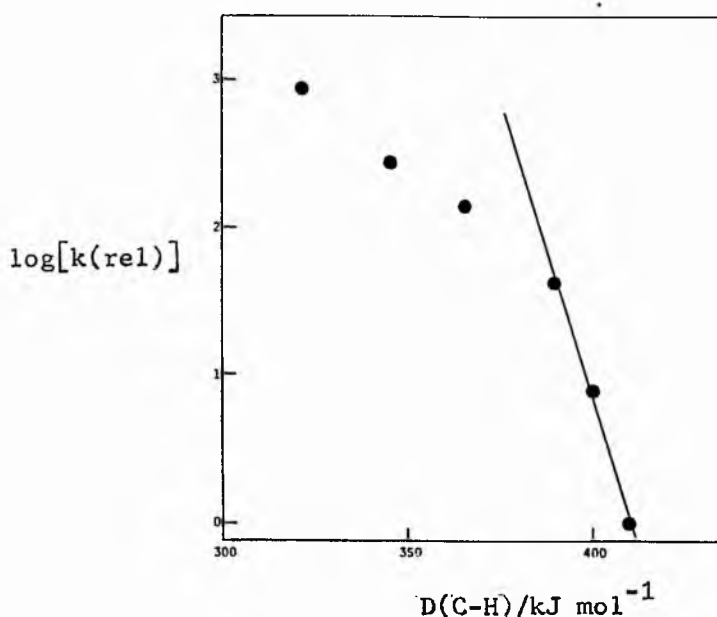


FIGURE 7 Plot of $\log[k(\text{rel})]$ against bond dissociation energies.

linear correlation of the activation energy of hydrogen abstraction with the strength of the C-H bond. If the A-factors do not change

TABLE 3

E.s.r. Parameters for Substituted Propynylic Radicals Derived from
Methyl Octadecynoates. Relative Rates of Hydrogen Abstraction by
Bu^tO• Radicals

Radical	Methyl Ester	Temp/K	hfs ^a /mT	[P]/[S]	k(rel) ^b
$\text{H} - \text{---} \overset{\cdot}{\text{C}} \text{---} \text{CH}_2\text{R}$ 18 17 16 15	17-yne	280	H(18) 1.12, CH ₂ (15) 1.80, H(16) 1.80, CH ₂ (14) 0.05	-	-
$\text{CH}_3 - \text{---} \overset{\cdot}{\text{C}} \text{---} \text{CH}_2\text{R}$ 17 16 15 14	16-yne	280	CH ₃ (18) 1.16, H(15) 1.74, CH ₂ (14) 1.74, CH ₂ (13) 0.05	-	-
$\text{Et} - \text{---} \overset{\cdot}{\text{C}} \text{---} \text{CH}_2\text{R}$ 16 15 14 13	15-yne	280	CH ₂ (17) 1.11, H(14) 1.77, CH ₂ (13) 1.77	-	-
$\text{CH}_3 - \text{---} \overset{\cdot}{\text{C}} \text{---} \text{CH}_2\text{R}$ 17 16 15 14	15-yne	280	CH ₂ (14) 1.21, H(17) 1.80, CH ₃ (18) 1.85	-	-
$\text{Et} - \text{---} \overset{\cdot}{\text{C}} \text{---} \text{CH}_2\text{R}$ 16 15 14 13	14-yne	295	CH ₂ (13) 1.11, H(16) 1.86, CH ₂ (17) 1.86	1.7 ± 0.5	17 ± 5
$\text{EtCH}_2 - \text{---} \overset{\cdot}{\text{C}} \text{---} \text{CH}_2\text{R}$ 15 14 13 12	14-yne	295	CH ₂ (16) 1.11, H(13) 1.69, CH ₂ (12) 1.69	-	-
$\text{RCH}_2 - \text{---} \overset{\cdot}{\text{C}} \text{---} \text{CH}_2\text{R}'$	13-yne ^c	270	(2H) 1.11, (3H) 1.77	3.6 ± 1	18 ± 5
"	12-yne ^c	270	(2H) 1.11, (3H) 1.77	3.7 ± 1	18.5 ± 5
"	9-yne ^c	280	(2H) 1.12, (3H) 1.77	-	-
"	8-yne ^c	280	(2H) 1.12, (3H) 1.77	3.8 ± 1	19 ± 5
"	6-yne ^c	280	(2H) 1.12, (3H) 1.77	-	-
"	5-yne ^c	270	(2H) 1.12, (3H) 1.79	3.6 ± 1	18 ± 5
$\text{RCH}_2 - \text{---} \overset{\cdot}{\text{C}} \text{---} \text{CH}_2\text{CH}_2\text{CO}_2\text{Me}$ 7 6 5 4 3 2	4-yne	295	H(6) 1.79, CH ₂ (7) 1.79, CH ₂ (3) 1.12	2.8 ± 1	14 ± 5
$\text{RCH}_2 - \text{---} \overset{\cdot}{\text{C}} \text{---} \text{C}(=\text{O})\text{OMe}$ 5 4 3 2 1	2-yne	290	H(4) 1.78, CH ₂ (5) 1.78	0.8 ± 1	12 ± 4

^aAll hfs checked by computer simulations.

^bRate of abstraction of propynylic hydrogens relative to secondary hydrogens on a per hydrogen basis, i.e. statistically corrected for the number of each type of hydrogen.

^cTwo indistinguishable radicals are present, see text.

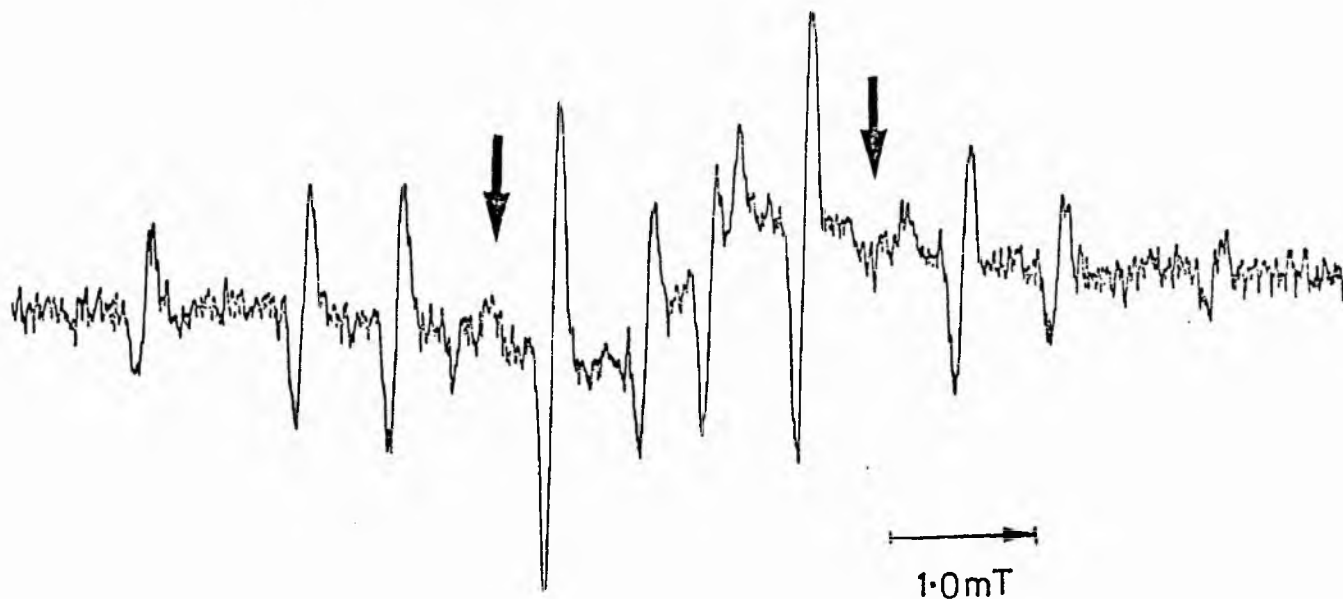


FIGURE 6 9.4 G Hz E.S.R. spectrum of the propynyl radical derived from methyl octadec-8-ynoate. Arrows indicate the main lines of the secondary radicals derived from H-abstraction at chain methylenes.

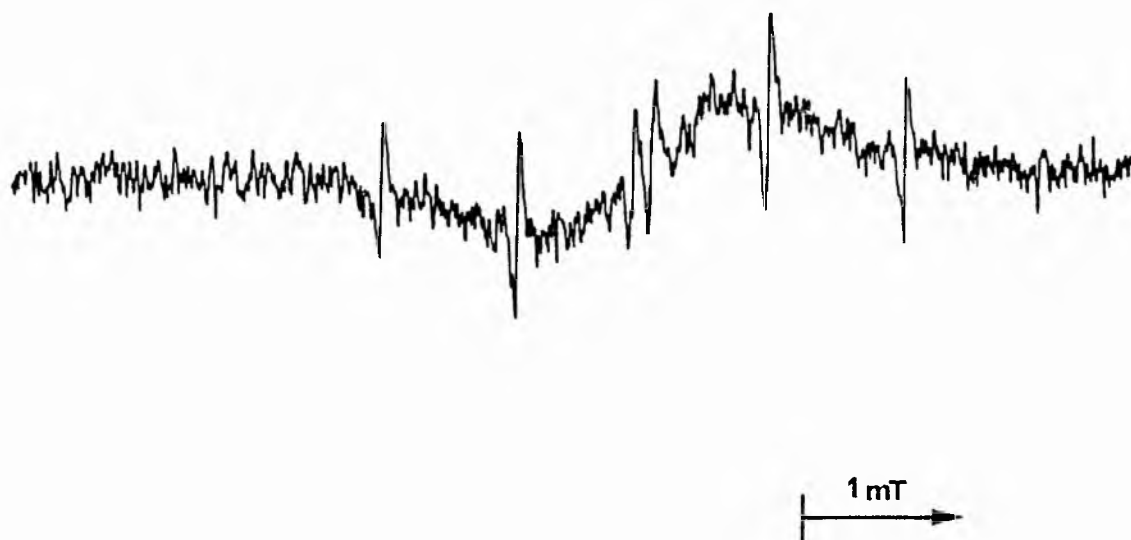
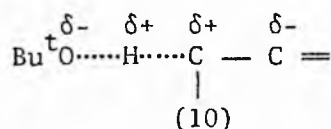


FIGURE 8 9.4 GHz E.S.R. spectrum of the penta-1,4-diynyl radical (11).

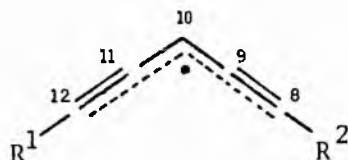
very much from one reaction to another, and often the changes are small for a series of similar abstractions, then $\log[k(\text{rel})]$ will be proportional to the activation energy. The points for primary, secondary and tertiary hydrogen abstraction lie on a straight line, but the remaining points for H-abstraction to one or more unsaturated bonds lie below this line. Thus, H-abstraction by t-butoxyl radicals from these sites is less rapid than would be expected on bond dissociation energy grounds alone. This may partly be explained by the presence of an unfavourable polar effect in the reactions adjacent to unsaturated bonds. Approach of the electron-attracting t-butoxy radical will be retarded by the electron-attracting multiple bond, i.e. there will be an unfavourable charge distribution in the transition state (10).



2.4 Divnoic and Enynoic Fatty Acid Esters.

The methylene interrupted diyne, methyl henicosa-8,11-diynoate, was difficult to purify because of rapid deterioration in air. The material was chromatographed and used immediately, after blowing off the solvent in a stream of dry nitrogen. The E.S.R spectrum (Figure 8) in neat di-t-butyl peroxide was very short lived due to polymer build up, but it consisted of a double quintet and the hfs are given in Table 4. The splitting pattern and the magnitude of the hfs, in comparison with those of unsubstituted penta-1,4-diynyl radicals^[65],

enabled the spectrum to be assigned to the substituted penta-1,4-diynyl radicals (11). The 1.64 mT hfs from H(10) in (11) is close to that of the analogous hydrogen in penta-1,4-diynyl (1.66) but is considerably larger than (H11) in pentadienyl radicals such as (1a), i.e. 1.11 mT (Table 1).

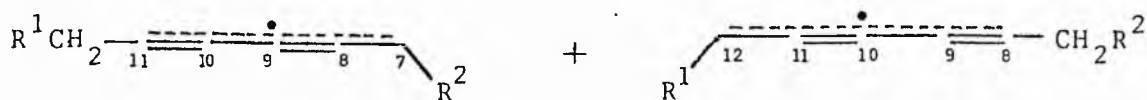


(11)



Similarly the hfs from the methylene hydrogens at the ends of the delocalised system in (11) are smaller than the hfs of the analogous hydrogens in pentadienyl radicals. This evidence corroborates the previous conclusion^[65] that triple bonds are less effective at delocalising spin density than double bonds. No other radicals were visible in the spectra from the diyne ester so we can estimate that the concentration of (11) must be at least three times that of the propynylic radicals which would be formed by hydrogen abstraction from C(7) or C(13), and also at least three times that of the secondary radicals generated by abstraction of the chain methylene hydrogens. Hydrogen abstraction from the conjugated diyne ester, methyl octadeca-8,10-diynoate, gave a radical with a spectrum consisting of a quartet of triplets; no other radicals were detectable. We attribute this spectrum to penta-1,3-diynyl radicals (12) formed by t-butoxy radical attack at the C(7) or C(12) methylenes. As expected, the two

radicals were spectroscopically indistinguishable. This type of delocalised radical has not been observed previously by E.S.R.

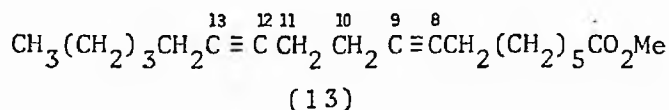


(12)



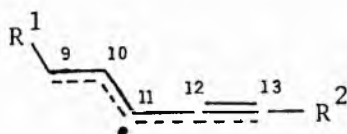
but comparison of the hfs of (12) (Table 4) with those of the propynyl radicals (Table 3) and penta-1,4-diynyl radicals strongly supports the identification.

Other methyl octadecadiynoates containing two to four methylene groups between the triple bonds were also examined. Intense spectra due to substituted propynylic radicals, similar to the spectra from mono-acetylenic esters, were obtained. In principle four different propynylic radicals can be formed by hydrogen abstraction from the four different sets of propynylic hydrogens. For the diacetylenic esters with more than two methylene groups between the triple bonds a single E.S.R. spectrum was obtained, i.e. the four radicals gave indistinguishable spectra. However, for methyl octadeca-8,12-diynoate (13) with only two methylene groups between the triple bonds two different spectra from two types of propynylic radical were obtained in approximately equal amounts. It is probable that the radicals formed by H-abstraction from the "outer" propynylic methylenes [C(7) and C(14)] are indistinguishable from each other and correspond to the spectrum identical to that obtained from the monoacetylenic esters. H-abstraction from the "inner" propynylic



methylenes [C(10) and C(11)] will give two radicals indistinguishable from each other, but different from the "outer" radicals because the hfs of the "inner" hydrogens will be perturbed by the proximity of the second triple bond (see Table 4). The spectrum obtained from methyl octadeca-7,12-diynoate was exceptionally intense and showed traces of secondary radicals generated from the chain methylenes. The ratio of the concentrations of the propynylic to secondary radicals was found to be 12 ± 3 . Since there are eight propynylic hydrogens and twelve hydrogens which can give radicals contributing to the secondary signal, the rate of abstraction of propynylic hydrogen relative to secondary hydrogen $k(\text{rel}) = 18 \pm 4$. This value is in good agreement with results from the mono-acetylenic esters (Table 3) and corroborates the average value used in Table 2.

The E.S.R spectrum obtained on H-abstraction from methyl octadeca-9E-en-12-ynoate is shown in Figure 9. H-Abstraction is expected to occur at the doubly activated site [C(11)] to give the substituted pent-1-en-4-ynyl radicals (14). The spectrum was analysed as shown in Table 4 and the computer simulation is also shown in Figure 9. The hfs are similar to those of pent-1-en-4-ynyl radicals^[65], which supports the assignment of the spectrum to radical (14).



(14)

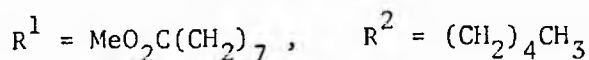


TABLE 4

E.s.r. Parameters for Radicals Generated from Diacetylenic Fatty Acid
Esters and Methyl Octadeca-9E-en-12-ynoate

Radical	Methyl Ester	Temp/K	hfs ^a /mT
(11)	8,11-diyne	300	H(10) 1.64, CH ₂ (7) 0.87 CH ₂ (13) 0.87
(12)	8,10-diyne ^b	270	(3H) 1.53, (2H) 0.64
$\begin{array}{l} \text{RCH}_2 - \text{C}\equiv\text{C} - \text{CH}_2\text{C}\equiv\text{CR}' \\ \text{RCH}_2 - \text{CH}=\text{C}\equiv\text{C} - (\text{CH}_2)_2\text{C}\equiv\text{CR}' \end{array}$	8,12-diyne ^c	290	(2H) 1.12, (1H) 1.78, (2H) 1.95 (2H) 1.12, (3H) 1.77
$\text{RCH}_2 - \text{CH}=\text{C}\equiv\text{C} - (\text{CH}_2)_3\text{C}\equiv\text{CR}'$	7,12-diyne	290	(2H) 1.12, (3H) 1.77
$\text{RCH}_2 - \text{CH}=\text{C}\equiv\text{C} - (\text{CH}_2)_4\text{C}\equiv\text{CR}'$	6,12-diyne	295	(2H) 1.12, (3H) 1.77
(14)	9E-en-12-yne	275	H(10) 0.36, H(11) 1.38, H(9) 1.01, CH ₂ (8) 1.01, CH ₂ (14) 0.74

^aAll hfs checked by computer simulations

^bTwo indistinguishable radicals are present

^cFour indistinguishable radicals are present

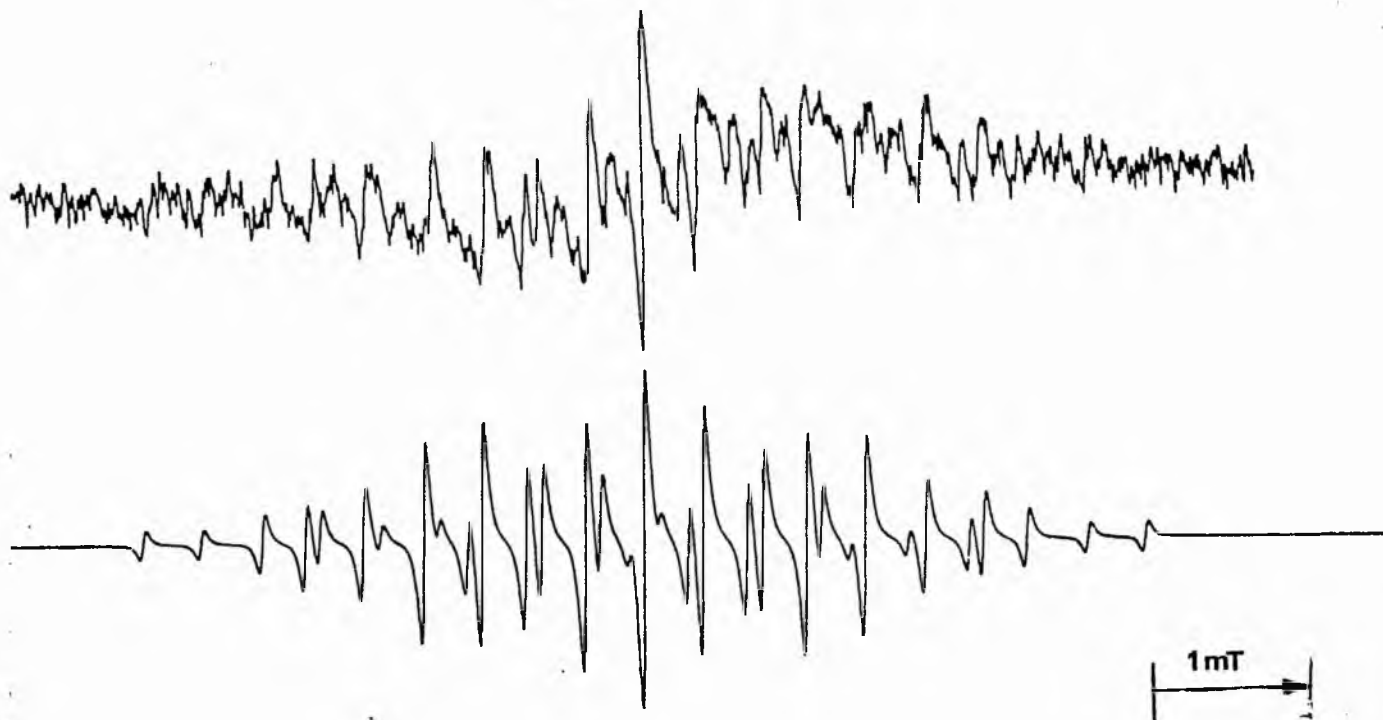


Fig. 9 9.4 G Hz e.s.r. spectrum of pent-1-en-4-ynyl radicals (14) in neat di-*t*-butyl peroxide. Upper trace, experimental spectrum; lower trace, computer simulation.

There are two possible conformations of radical (14), the transoid form as shown and the cisoid form which could be obtained by a 180° rotation about the C(10)-C(11) bond. For the unsubstituted pent-1-en-4-ynyl radicals both conformers were observed, but the transoid form predominated at temperatures above ambient. Radical (14) is probably mainly in the transoid conformation because this will be the least sterically hindered form. In addition, the hfs of H(11) (1.38 mT) is identical to the hfs of the analogous hydrogen in the transoid conformer of pent-1-en-4-ynyl radicals and significantly different from the hfs of the same hydrogen in the cisoid conformer. The quality of the spectrum was such that minor amounts of the cisoid conformer of (14) would not have been detectable (see Figure 9).

2.5 Triacylglycerols

E.S.R. spectra of allyl radicals derived from triacylglycerols were also observed on photolysis of mixtures containing di-t-butyl peroxide and a triacylglycerol having one or more oleate or elaidate units. The E.S.R. spectrum from 1-palmitoyl-2,3-dielaidoyl-rac-glycerol is similar to that obtained from methyl elaidate^[33], but, as expected, the proportion of hydrogen abstraction occurring from non-activated methylenes is larger, since one of the three fatty acids in the triacylglycerol has a fully saturated chain. Quantitative

determination of the relative amount of hydrogen abstraction from the allylic sites (A) to hydrogen abstraction from non-activated methylenes (S) gave a value of $[A]/[S] = 4.6 \pm 0.9$ [$k(\text{rel}) = 36.4 \pm 7$], in excellent agreement with that obtained from methyl elaidate.

The E.S.R. spectrum obtained from 1-palmitoyl-2-stearoyl-3-oleoyl-rac-glycerol showed signals due to the allyl radicals in the cisoid conformation and also signals due to the secondary radicals. Values of $[A]/[S]$ and $k(\text{rel})$ were 2.3 ± 0.5 and 40 ± 8 respectively.

The much larger triacylglycerol radicals tumble less efficiently than those from the fatty acids and line broadening is evident and probably arises from the incomplete averaging of the anisotropic dipolar coupling. It is unlikely that hydrogen abstraction from the glycerol backbone occurs to any significant extent since attempts to obtain an E.S.R. spectrum from a photolysed solution of triacetin in di-t-butyl peroxide were unsuccessful.

3 Experimental.

3.1 General

E.S.R. spectra were recorded with a Bruker ER200D spectrometer. Di-t-butyl peroxide was passed through a column of alumina and distilled under reduced pressure. Substrates dissolved in di-t-butyl peroxide (1:20) were placed in a quartz tube and degassed with at least three freeze-pump-thaw cycles. The samples were photolysed directly in the cavity of the spectrometer unless otherwise stated.

The flow cell used for some experiments consisted of a motor driven syringe which smoothly pumped the substrate in di-t-butyl peroxide through a quartz tube in the cavity of the spectrometer where it was photolysed. Flow rates were typically of the order 3-5 mls/min. In this case samples were de-aerated by purging the solution with nitrogen.

For determination of $k(\text{rel})$ for methyl linoleate, this ester was added to methyl palmitate in accurately known amounts. The mixture was then photolysed as described above and the spectra were accumulated using a signal averager. Values of $k(\text{rel})$ were corrected for the amount of methyl palmitate added.

General procedures were the same as those used previously^[66].

Methyl oleate, linoleate and γ -linolenate were isolated from Olive oil, Sunflower oil and Evening Primrose oil by reported procedures^[66]. Mono-acetylenic, diacetylenic and dienolic acids, available from previous research programmes^[67], were esterified using 2% MeOH/H₂SO₄. Methyl arachidonate was commercially available and had

a purity in excess of 99.9% by GLC. Great care was taken to ensure that no autoxidised product was present before the E.S.R. experiment was carried out and to this end all samples were subjected to column chromatography and used within 16 hr. Unless stated otherwise all samples had a GLC purity > 99.5% and were also judged pure by analytical TLC.

3.2 Methyl octadeca-9E,12E and octadeca-9E(Z),12Z(E)-dienoates

To methyl linoleate (99.5%, 5.0 g, 1.67 mmol) dissolved in ether (100 ml) was added an ice-cold mixture of aqueous sodium nitrate (2 M, 70 ml) and nitric acid (6 M, 45 ml), and the solution shaken vigorously for 20 min. The ethereal layer, separated from the aqueous phase and washed with aqueous sodium thiosulphate solution (5%, 2x 30 ml) and saturated brine (2x 30 ml), gave the isomerised product (4.8 g). As required this was separated by preparative silver ion TLC using PE 10 as eluent^[66], furnishing three bands at high R_f (A-C) together with a small amount of oxidised material at low R_f .

Band A, octadeca-9E,12E-dienoate, had ^1H , ^{13}C n.m.r., I.R. and mass spectral properties identical with previously published data^[69,70]. GLC analysis (SP2300) showed only one peak with a shorter retention time than either the cis,trans or cis,cis dienoate isomers. TLC showed one spot in 10% ether in petroleum (PE 10) R_f 0.83.

Band B was a mixture of octadeca-9E,12Z-- and octa-9z,12E-dienoates. ^1H , ^{13}C n.m.r., I.R. and mass spectral data were identical to those given in the literature^[69,70]. GLC showed two completely resolved peaks in approximately equal amounts. Their

retention times were longer than the trans,trans ester but shorter than the cis,cis ester. TLC showed only one spot in PE 10 R_f 0.83.

Band C was identified as unchanged methyl linoleate by comparison with authentic material.

3.3 Octadeca-9Z,12Z-diene

Methyl octadeca-9Z,12Z-dienoate (300 mg, 1 mmol) in dry diethyl ether (10 ml) was added dropwise to a vigorously stirred solution of lithium aluminium hydride (60 mg) in dry ether (25 ml) at such a rate as to maintain gentle reflux. This took 30 min. and the mixture was stirred for a further 30 min. before adding 'wet ether' (20 ml), water (20 ml), and finally dilute sulphuric acid (10%, 15 ml). Extraction of the organic phase gave octadeca-9Z,12Z-dien-1-ol, > 98.5% pure as judged by TLC and GLC.

$^1\text{Hnmr}$ spectrum: 5.31 δ (m, 4H, olefinic), 3.55 δ (t, $J=6.0$ Hz, 2H, $-\text{CH}_2\text{OH}$), 3.05 δ (bs, 1H, $-\text{OH}$), 2.72 δ (m, 2H, doubly allylic CH_2 's), 2.00 δ (m, 4H, allylic CH_2 's), 1.30 δ (bs, 20H, chain CH_2 's) and 0.88 δ (at, $J=5.4$ Hz, 3H, CH_3 -).

$^{13}\text{Cnmr}$ spectrum: 129.82 (C13), 128.66 (C9), 127.82 (C10), 126.66 (C12), 62.27 (C1), 32.57 (C3), 31.39 (C16), 29.55 (C15), 29.39 (C7, 5), 29.19 (C6, 4), 27.07 (C8, 14), 25.72 (C11), 25.49 (C2), 22.43 (C17), 13.84 (C18).

Infrared spectrum: 3300 cm^{-1} (O-H stretch), 3005 cm^{-1} (HC=CH, C-H stretch).

The mass spectrum showed no diagnostic fragments as expected from aliphatic polyene primary alcohols. Peaks of general formula $\text{C}_n\text{H}_{2n+1}$

and C_nH_{2n-1} predominated. The base peak was $m/e = 55$ ($C_4H_7^+$). The alcohol was stirred at $0^\circ C$ with dry pyridine (2 ml) and freshly distilled mesyl chloride (0.5 ml) for four 4 hours, after which time ice-cold 2 M HCL was added and the organic product extracted with hexane to give 1-mesyloxyoctadeca-9Z,12Z-diene (302 mg, 85%). The infrared spectrum showed loss of hydroxyl and new absorption bands at 1350 cm^{-1} , 1170 cm^{-1} and 940 cm^{-1} .

Lithium aluminium hydride reduction of the mesylate gave the desired octadeca-9Z,12Z-diene (200 mg, 79% for the three steps). $^1\text{Hnmr}$ spectrum: 5.33δ (m, 4H, olefinic), 2.72δ (m, 2H, doubly

allylic CH_2 's), 2.05δ (m, 4H, allylic CH_2 's), 1.30δ (bs, 20H, chain CH_2 's) and 0.88δ (at, $J=5.4\text{ Hz}$, 6H, CH_3 -).

Infrared spectrum: 3007 cm^{-1} ($\text{HC}=\text{CH}$, C-H stretch), absence of OH, $\text{C}=\text{O}$ and $\text{HC}=\text{CH}$ (trans) stretching or bending frequencies.

Mass spectrum showed an M^+-18 peak at 250 (10%) and peaks associated with sequential loss of methylene units.

3.4 Octadeca-9Z-ene

The procedure described for octadeca-9Z-diene was followed using methyl octadeca-9Z-enoate as a substrate to furnish the desired octadeca-9Z-ene (191mg, 76 % net yield).

The following spectral data was recorded for octadeca-9Z-en-1-ol;

$^1\text{Hnmr}$ spectrum: 5.33δ (appt, $J=4.6\text{ Hz}$, 2H, olefinic), 3.56δ (t, $J=6.0\text{ Hz}$, 2H, $-\text{CH}_2-\text{OH}$), 2.50δ (bs, 1H, $-\text{OH}$), 1.98δ (m, 4H, allylic CH_2 's), 1.25δ (bs, 24H, chain CH_2 's) and 0.85δ (at, $J=5.4\text{ Hz}$, 3H, CH -).

$^{13}\text{Cnmr}$ spectrum: 129.68 (C10), 129.6 (C9), 62.64 (C1), 32.57 (C3),
31.72 (C16), 29.57 (C7,12), 29.30 (C6, 13, 15)*, 29.12
(C4,5,14)*, 27.01 (C8,11), 25.60 (C2), 22.47 (C17),
13.84 (C18).

* Some uncertainty exists about these assignments.

Infrared spectrum: 3340 cm^{-1} (hydroxyl stretch), 3000 cm^{-1} (HC=CH,
C-H stretch).

The mass spectrum showed significant peaks at m/e 250 (M^+-18), 222
($250-\text{C}_2\text{H}_4$) and at 208 ($250-\text{C}_3\text{H}_8$), 194 ($250-\text{C}_4\text{H}_{10}$), 180 ($250-\text{C}_5\text{H}_{12}$),
166, 152 etc., due to the sequential loss of CH_2 units.

The following spectroscopic data was recorded for octadeca-9Z-ene.

$^1\text{Hnmr}$ spectrum: 5.37δ (app t , $J=4.6\text{ Hz}$, 2H, olefinic), 1.97δ
(m, 4 H, allylic CH_2 's), 1.25δ (bs, 24H, chain CH_2 's)
and 0.86δ (at, $J=5.4\text{ Hz}$, 6H, CH_3 -).

Infrared spectrum: 3005 cm^{-1} (HC=CH, C=H stretch), absence of O-H,
C=O and HC=CH (trans) absorptions. The mass spectrum
showed an M^+ peak at 252 (8.5 %).

3.5 Methyl elaidate from oleic acid.

The procedure described for the stereomutation of
octadeca-9Z,12Z-enoate was carried out on oleic acid to furnish a
mixture of elaidic and oleic acid (7:1 by capillary GLC). Four
recrystallisations from petroleum ether furnished pure elaidic acid

m.p. = 45-45.5 °C. The acid was transesterified using a 2% MeOH/H₂SO₄ to give methyl elaidate as a colourless oil.

Spectra were in agreement with the literature^[69,70].

3.6 Methyl octadeca-9,12-divynoate.

The free acid was available from a previous research programme^[68]. The acid was esterified with 2% MeOH/H₂SO₄. Column chromatography gave a product which still had a yellow taint and showed small amounts of polar material, presumably oxidation products. We were unable to obtain an analytically pure sample from even repeated chromatography. TLC was even less successful. Due to the materials extreme liability to autoxidation the ester was chromatographed, the solvent removed and the product used directly minimising air contact at all stages. GLC showed only one peak.

REFERENCES

1. a) B. Samuelsson, M. Goldyne, E. Granstrom, M. Hamberg, S. Hammarstrom and C. Malmsten, Ann. Rev. Biochem., 1978, 47, 997.
b) "Biochemical Aspects of Prostaglandins and Thromboxanes" ed. N. Kharasch and J. Fried, Academic Press, New York, 1977.
c) G. A. Veldink, J. F. G. Vliegthart and J. Boldingh, Prog. Chem. Fats Other Lipids, 1977, 15, 131.
2. a) M. Hamberg, P. Hedqvist, K. Strandberg, J. Svensson and B. Samuelsson, Life Sci., 1975, 16, 451.
b) J. Nakano in "Prostaglandins: Pharmacological and Therapeutic Advances", ed. M. F. Cuthbert, pp 41, Heinemann, London, 1973.
3. a) F. A. Kuehl, J. L. Humes, R. W. Egan, E. A. Ham, G. C. Beveridge and C. G. Van Arman, Nature, 1977, 265, 171.
b) J. R. Vane, Adv. Prost. Thrombox. Res., 1976, 2, 791.
c) F. A. Kuehl, R. W. Egan, J. L. Humes, G. C. Beveridge and C. G. Van Arman, in "Biochemical Aspects of Prostaglandins and Thromboxanes", ed. N. Kharasch and J. Fried, p 55, Academic Press, New York, 1977.
4. a) M. S. Hamberg, J. Svensson, T. Wakabayashi and B. Samuelsson, Proc. Natl. Acad. Sci. U.S.A., 1974, 71, 345.
b) S. Moncada, R. Gryglewski, S. Bunting and J. R. Vane, Nature, 1976, 263, 663.
c) M. Hamberg and B. Samuelsson, Proc. Natl. Acad. Sci. U.S.A., 1973, 70, 899.
d) M. Hamberg and B. Samuelsson, Proc. Natl. Acad. Sci. U.S.A., 1974, 71, 3400.
5. E. J. Corey, A. E. Barton and D.A. Clark, J. Am. Chem. Soc., 1980, 102.
6. J. F. Mead in "Free Radicals in Biology", Vol.1, ed. W. A. Pryor, pp 51, Academic Press, New York, 1976.
7. a) A. L. Tappel in "Free Radicals in Biology", Vol.4, ed. W. A. Pryor, pp 2, Academic, New York, 1980.
b) A. A. Barber and F. Bernheim in "Advances in Gerontological Research", Vol.2, ed. B. L. Strehler, pp 355, Academic Press, New York, 1967.

8. a) H. Frank, T. Hintze, D. Bimboes, H. Remmer, Toxicol. Appl. Pharmacol., 1980, 56, 337.
b) C.J. Dillard, M. Sagai and A. L. Tappel, Toxicol. Lett., 1980, 6, 251.
9. A. L. Tappel in 'Pathobiology of Cell Membranes', Vol. 1, ed. B. F. Trump and A. V. Arstila, pp.145, Academic Press, New York 1975.
10. a) D. B. Menzel in 'Free Radicals in Biology', Vol.2, pp.181, ed. W. A. Pryor, Academic Press, New York, 1976.
b) J. B. Mudd in 'Free Radicals in Biology', Vol.2, p.263, ed. W. A. Pryor, Academic Press, New York, 1976.
c) J. A. Kerr, J. G. Calvert and K. L. Demerjian in 'Free Radicals in Biology' Vol.2, p.159, ed. W. A. Pryor, Academic Press, New York, 1976.
11. a) A. Sevanian, J. F. Mead and R. A. Stein, Lipids, 1979, 14, 634.
b) H. V. Thomas, P. K. Mueller and R. L. Lyman, Science, 1968, 159, 532.
12. a) For a review see F. A. Kummerow, Chapt.31, pp.599 of reference 20a.
b) R. B. Wilson, CRC Crit. Rev. Food Sci. Nutr. 1976, 7, 325.
c) V. Z. Lankin, N. V. Kotelevtseva, A. K. Tikhaze, V. N. Titov and E. N. Gerasimova, Vopr. Med. Khim., 1976, 22, 513.
13. a) E. S. Reynolds, T. M. Moslen, R. J. Treinen in 'Oxygen and Oxy-Radicals in Chemistry and Biology', ed. M. A. J. Rodgers and E. L. Powers, pp.169, Academic Press, New York, 1981.
b) R. O. Recknagel, Pharmacol. Rev., 1967, 19, 145.
c) R. O. Recknagel, E. A. Glende, A. M. Hruszkewycz in 'Free Radicals in Biology', Vol.3, pp.97, ed. W. A. Pryor, Academic Press, New York, 1977.
d) R. O. Recknagel and E. A. Glende, Crit Rev. Toxicol., 1973, 2, 263.
14. a) I. Fridovich in 'Free Radicals in Biology', Vol.1, pp.239, ed. W. A. Pryor, Academic Press, New York, 1976.
b) N. Hauggaard, Physiol. Rev., 1968, 48, 311.

14. c) S. F. Gottlieb, Ann. Rev. Microbiol., 1971, 25, 111.
15. a) R. C. Reitz, Biochim. Biophys. Acta, 1975, 380, 145.
b) G. Cohen and A. E. Cedarbaum, Arch. Biochem. Biophys., 1980, 199, 438.
16. a) K. C. Bhuyan, D. K. Bhuyan and S. M. Podos, IRCS Medical Science Library Compendium, 1981, 9, 126.
b) D. K. Bhuyan and K. C. Bhuyan, in 'Biochemical and Clinical Aspects of Oxygen', pp.785 and 797, ed. W. S. Caughey, Academic Press, New York, 1979.
17. a) D. J. Kornbrust and R. D. Mavis, Toxicol. Appl. Pharmacol., 1980, 53, 323.
b) J. S. Bus, S. D. Aust, and J. E. Gibson, Res. Commun. Chem. Pathol. Pharmacol., 1975, 11, 31.
18. a) D. Harman, J. Gerontol., 1971, 26, 451.
b) D. Harman, S. Hendricks, D. Eddy and J. Seiboid, J. Amer. Geriatr. Soc., 1976, 24, 307.
c) W. R. Bidlack and A. L. Tappel, Lipids, 1973, 8, 203.
19. a) K. K. Carroll and H. T. Khor, Cancer Res., 1970, 30, 2260.
b) K. K. Carroll and H. T. Khor, Lipids, 1971, 6, 415.
c) G. J. Hopkins, C. E. West and G. C. Hard, Lipids, 1976, 11, 328.
d) B. S. Drasar and D. Irving, Br. J. Cancer, 1973, 27, 167.
e) R. J. Shambergerer, T. L. Andreone and C. E. Willis, J. Natl. Cancer Inst., 1974, 53, 1771.
f) R. J. Shambergerer, C. L. Corlett, K. D. Beaman and B. L. Koslen Mutaden Res., 1979, 66, 349.
20. a) See 'Autoxidation in Food and Biological Systems', ed. M. G. Simic and M. Karel, Plenum, New York, 1980.
b) 'Oxygen and Oxyradicals in Chemistry and Biology', ed. M. A. J. Rodgers and E. L. Powers, Academic Press, New York, 1981.
21. a) W. L. Porter, L. A. Levasseur and A. S. Henick, Lipids, 1972 7, 699.
b) W. L. Porter, L. A. Levasseur, J. I. Jeffers and A. S. Henick, Lipids, 1971, 6, 16.

22. See E. N. Frankel in 'Symposium on Foods: Lipids and their Oxidation', p.51, ed. H. W. Schultz, E. A. Day and R. O. Sinnhuber, Avi Publishing, Westport, CN, 1962.
23. G. E. Hall and D. G. Roberts, J. Chem. Soc. (B), 1966, 1109.
24. B. D. Goldstain, O. J. Balchum, H. B. Demopoulos and P. S. Duke, Arch. Environ. Health, 1968, 17, 46.
25. M. Haydar and D. Hadziyer, J. Amer. Oil Chem. Soc., 1974, 50, 171.
26. G. G. Odinkova, O. A. Azizova, A. G. Kotov, A. N. Remizov, and D. I. Roshchupkin, 'Ultraviolet Izluch. Ego Primen. Biol., Mater Vses. Sovershch., 10th', 1973, pp.62, ed. G. M. Frank, CA 1975, 82, 69469.
27. C. U. Deffner, H. Luck, and R. Kohn, Z. Lebensm. Unters. Forsch., 1964, 125, 281.
28. H. Luck, C. U. Deffner and R. Kohn, Z. Lebensm. Unters. Forsch., 1963, 123, 200.
29. R. M. Estefan, E. M. Gause and J. R. Roulands, Environ. Res., 1970, 3, 62.
30. J. J. M. C. De Groot, G. J. Garssen, J. F. G. Vligenthart and J. Boldingh, Biochim. Biophys. Acta, 1973, 326, 279.
31. H. Aoshima, T. Kayiwara, A. Hatanaka, and H. Hatano, J. Biochem., 1977, 82, 1559.
32. T. Chiba, K. Fujimoto, T. Kaneda, S. Kubota and Y. Ikegami, J. Amer. Oil Chem. Soc., 1981, 58, 587.
33. E. Bascetta, F. D. Gunstone, C. M. Scrimgeour and J. C. Walton, J. C. S. Chem. Comm., 1982, 110.
34. R. W. Fessenden and R. H. Schuler, J. Chem. Phys., 1963, 39, 2147.
35. J. K. Kochi and P. J. Krusic, J. Am. Chem. Soc., 1968, 90, 7157.
36. P. J. Krusic, P. Meakin and B. E. Smart, J. Am. Chem. Soc., 1974, 96, 6211.
37. D. J. Edge and J. K. Kochi, J. Am. Chem. Soc., 1973, 95, 2635.
38. T. Kawamura, P. Meakin and J. K. Kochi, J. Am. Chem. Soc., 1972, 94, 8065.
39. E. N. Frankel in 'Fatty Acids', pp.353, ed. E. H. Pryde, Amer. Oil Chem. Soc. Monograph 7, Champaign, Ill, 1970.

40. H. G. Korth, H. Trill and R. Sustmann, J. Am. Chem. Soc., 1980, 103, 4483.
41. A. L. J. Beckwith and K. U. Ingold in 'Rearrangements in Ground and Excited States', Vol.1, p.161, ed. P. de Mayo, Academic Press, New York, 1980.
42. M. W. Piretti, P. Capella and V. Pallotta, Riv. Ital. Sostanze Grasse 1969, 46, 652.
43. P. Capella, M. V. Piretti and A. Stroochi, Riv. Ital. Sostanze Grasse 1969, 46, 659.
44. M. V. Piretti, P. Capella and G. Bonaga, J. Chromatogr. 1973, 92, 196 .
45. R. F. Garwood, B. P. S. Khambay, B. C. L. Weedon and E. N. Frankel, J.C.S. Chem. Comm., 1977, 364
46. H. W-S. Chan and G. Levett, Chem. Ind., 1977, 692.
47. E. N. Frankel, W. E. Neff, W. K. Rohwedder, B. P. S. Khambay, R. F. Garwood and B. C. L. Weedon, Lipids, 1977, 12, 901.
48. H. W-S. Chan, G. Levett and J. A. Matthew, J.C.S. Chem. Comm., 1978, 756.
49. R. D. Small, L. K. Patterson and J. C. Scaiano, Photochem. Photobiol., 1979, 29, 49.
50. D. Griller, K. U. Ingold and J. C. Walton, J. Am. Chem. Soc., 1979, 95, 758.
51. R. Sustmann and H. Schmidt, Chem. Ber., 1979, 112, 1440.
52. A. G. Davies, D. Griller, K. U. Ingold, D. A. Lindsay and J. C. Walton, J.C.S. Perkin Trans.II, 1981, 633.
53. N. A. Porter, B. A. Weber, H. Weenen and J.A. Khan, J. Am. Chem. Soc., 1980, 102, 5597.
54. P. J. Krusic and J. K. Kochi, J. Am. Chem. Soc., 1968, 90, 7155.
55. J. K. Kochi and P. J. Krusic, J. Am. Chem. Soc., 1970, 92, 4110;
J. K. Bennet and J. A. Howard, Chem. Phys. Letts., 1971, 9, 460.
56. J. M. Tedder, Tetrahedron, 1982, 38, 313; and papers cited therein.
57. R. A. Goise and D. H. Volman, J. Photochem., 1974, 3, 115.
58. R. Atkinson, S. M. Aschmann, A. M. Winer and J. N. Pitts, Int. J. Chem. Kinet., 1982, 14, 507.

59. J. N. Bradley, W. Hack, K. Hoyerman and H. G. Wagner, J.C.S. Faraday I, 1973, 69, 1889.
60. S. Gordon and W. A. Mulac, Int. J. Chem. Kinet., Symposium 1, 1975, 289.
61. K. D. King and T. T. Nguyen, Int. J. Chem. Kinet., 1981, 13, 255.
62. D. M. Golden and S. W. Benson, Chem. Rev., 1969, 69, 125.
63. a) H. M. Frey and A. Krantz, J. Chem. Soc. (A), 1969, 1159.
b) K. W. Egger and M. Jola, Int. J. Chem. Kinet., 1970, 2, 265.
64. C. Walling and B. B. Jacknow, J. Am. Chem. Soc., 1960, 82, 6108.
65. C. Roberts and J. C. Walton, J.C.S. Perkin II, 1981, 553.
66. F. D. Gunstone and R. C. Wijesundera, Chem. Phys. Lipids, 1979, 24, 193.
67. F. D. Gunstone, J. McLaughlan, C. M. Scrimgeour and A. P. Watson, J. Sci. Fd. Agric., 1976, 27, 675.
68. F. D. Gunstone and M. S. F. Lie Ken Jie, Chem. Phys. Lipids, 1970, 4, 1; and references cited therein.
69. F. D. Gunstone, M. R. Pollard, C. M. Scrimgeour and H. S. Vedanayagam, Chem. Phys. Lipids, 1977, 18, 115.
70. D. J. Frost and F. D. Gunstone, Chem. Phys. Lipids, 1975, 15, 53.

SECTION 2

An E.S.R. study of fatty acids.

**Part II. Hydrogen abstraction from
saturated acids and related derivatives**

The radicals generated from saturated fatty acids and their derivatives by hydrogen abstraction with photochemically formed t-butoxyl radicals have been investigated by e.s.r spectroscopy. The main species observed from propionic and butyric acids arose from hydrogen abstraction α to the carboxyl group. The proportion of radicals arising from hydrogen abstraction from in chain secondary radicals increases concomitantly with chain length. Radicals arising from hydrogen abstraction of the ω -1 methylene were observed for all the acids investigated. From the measured concentrations of the α -carboxyl : in chain secondary : ω -1 radicals the following approximate rates of hydrogen abstraction by t-butoxyl radicals from the different sites were obtained 2.3 : 1 : 2.3.

Hydrogen abstraction by t-butoxyl radicals from propyl chloride and butyrl nitrile also occurs predominantly α to the head group.

1 Introduction.

The reaction between saturated fatty acids and esters with ground state molecular oxygen proceeds at a rate which is slow compared with their unsaturated counterparts. Stirton *et al*^[1] reported an 11-fold difference in rate of autoxidation between stearate and oleate. More recently Small *et al*^[2] have determined the reactivities of methyl oleate and stearate to t-butoxyl radicals and obtained a relative reactivity of 1.65.

The autoxidation of saturated fatty acids and their methyl esters has been studied at high temperatures (150-200°C)^[3-8] and under catalysed conditions^[9-12]. Not surprisingly under such adverse conditions complex mixtures of products have frequently been reported including carbonyl, hydroxyl and carboxylic compounds.

Several groups have postulated that thermal oxidation of saturated fatty acids proceeds with dehydrogenation as the initial step^[4,5,6]. The resulting unsaturated molecules subsequently autoxidising in accord with the more classical theories put forward for methyl oleate^[13]. Other groups have supplied evidence that hydroperoxides are the primary oxidation products.

The determination of the site of attack has also been fraught with controversy. Zvidema^[14] postulated that the oxidation of paraffins at 100-200°C took place predominantly at the β -carbon atom with an additional attack on the γ -atom. The primary product of the

reaction being the hydroperoxide which then decomposed to yield a β -ketone and water.

E.S.R. studies on saturated fatty acids have been reported previously^[16-23]. Several of these studies utilised a $\text{Ti}/\text{H}_2\text{O}_2$ flow system to generate hydroxyl radicals as the abstracting species.^[16-20,23] Other detailed studies have been made of the oxidation of acids and their anions by radiolysis^[21,22].

We have recently reported^[26,27] that hydrogen abstraction from mono -enoic and -ynoic fatty esters gave rise to E.S.R. spectra in which signals were observed which were attributed to secondary radicals (non-activated) from the alkyl backbone. Very weak, but distinct, signals could also be observed for the radicals produced by hydrogen abstraction from the methylene adjacent to the terminal methyl group because of the extra β -hydrogen.

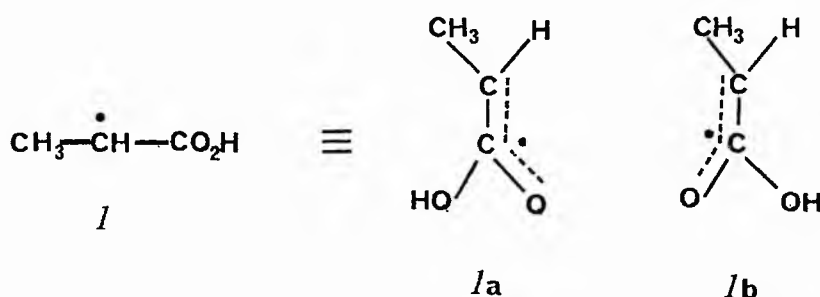
We now report details of an E.S.R. spectral study of a variety of secondary radicals obtained on hydrogen abstraction from saturated fatty acids and derivatives thereof. The results provide insight into the regioselectivity of hydrogen abstraction in saturated fatty acids by alkoxyl radicals. Such species may play an important role in the autoxidation of saturated fatty acids at elevated temperatures^[3-8] or catalysed conditions^[9-12].

2 Results.

E.S.R. spectra of the fatty acid radicals were obtained by photolysis of degassed solutions of the freshly purified acid or derivative thereof and neat di-*t*-butyl peroxide in the cavity of the spectrometer. Intense spectra were obtained for most of the samples but the sample lifetime of the higher homologues was short due to rapid build up of polymer on the walls of the tube.

2.1 Propionic acid and anhydride.

The predominant radical observed from photolysis of propionic acid and di-*t*-butyl peroxide results from hydrogen abstraction α -to the carboxyl group to give radical (1). Two configurations of the radical in which the O-C₁-C₂-C₃ skeleton is planar can be envisaged (1a and 1b), where the isomerism arises from the juxta position of the methyl group relative to the hydroxyl group, but only one set of signals was observed over the temperature range 250-305 K.



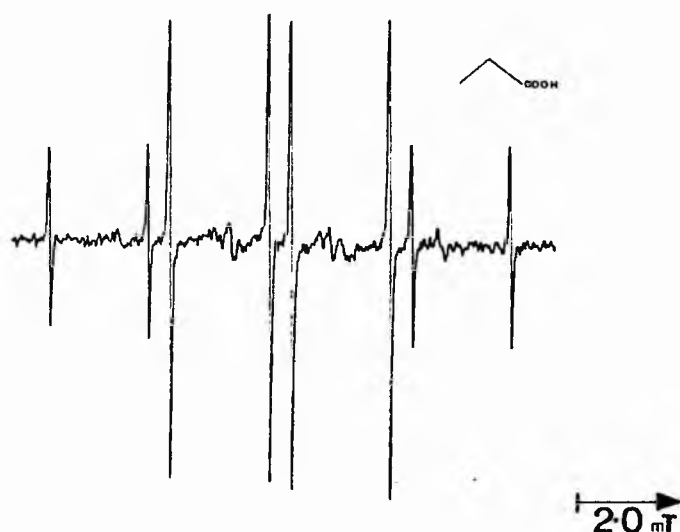


Figure 2.1.1 E.S.R. spectrum of the alkyl radical derived from propionic acid

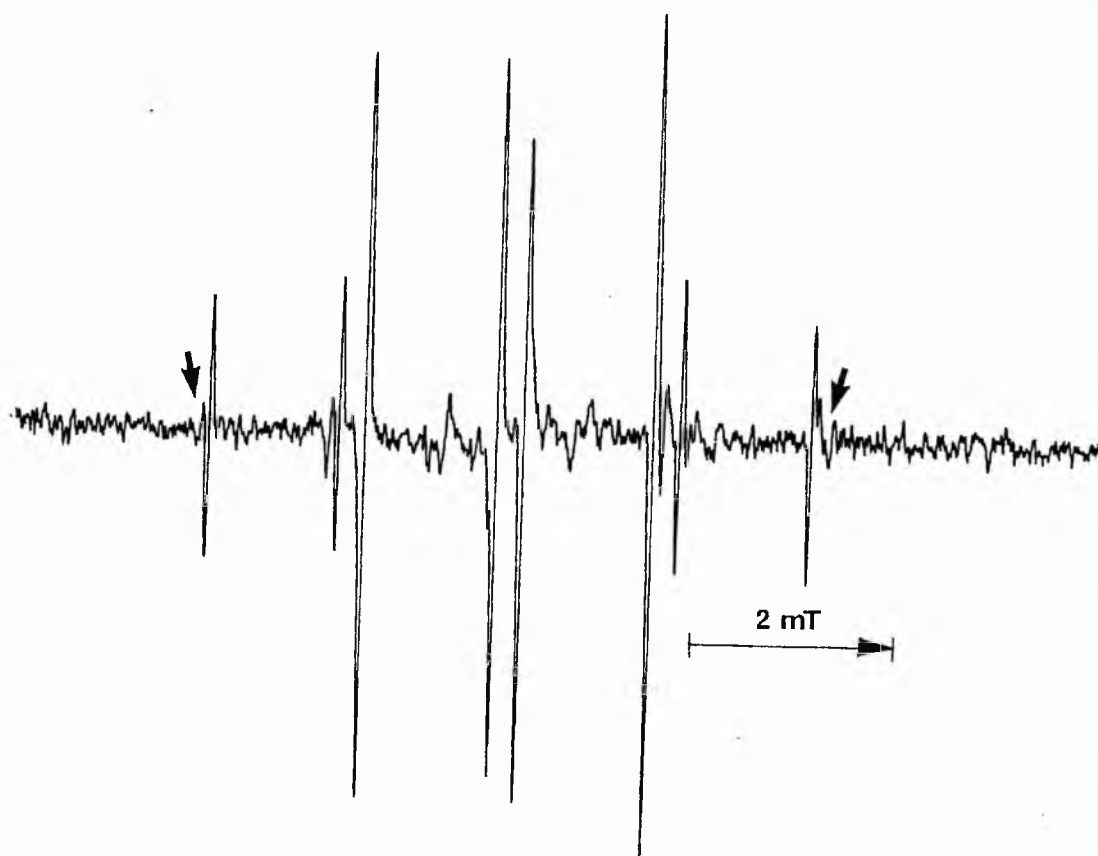
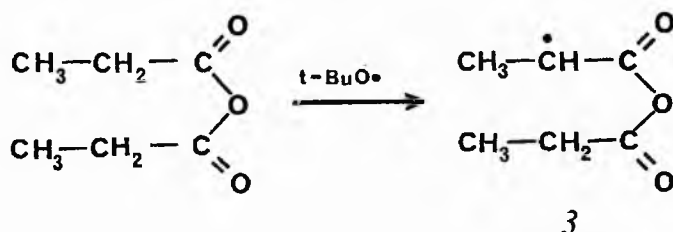


Figure 2.1.2 E.S.R. spectrum of alkyl radicals derived from propionic anhydride. Arrows indicate outer lines of minor α -radical.

The hyperfine splitting constants (hfs) of the double quartet spectrum (Figure 2.1.1) have been unequivocally assigned to specific hydrogens and are in excellent agreement with those previously reported^[16,19,24].

Hydrogen abstraction from propionic anhydride gave rise to two radicals each with a double quartet pattern. The minor radical (ca. 25 % at 250 K) had hfs similar to those of radical (1b) and the major radical (ca. 75 % at 250 K) had a smaller β -hfs (Figure 2.1.2).



2.2 Butyric acid, anhydride and methyl ester.

Hydrogen abstraction from n-butyric acid can lead to three distinct radicals (4-6). On photolysis of a solution of n-butyric acid in di-t-butyl peroxide at 250 K an intense spectrum (Figure 2.2.1) was obtained from which signals arising from radicals (4) and (5) could readily be observed and assigned. The assignments of the hfs to specific hydrogens are given in Table 2.2.1 along with the relative proportions of each radical, estimated by double integration of appropriate signals. The assignment for the primary radical (6) is tentative since considerable overlap of the lines occurs. However the hfs are in excellent agreement with those of structurally related primary radicals^[16,19,24].

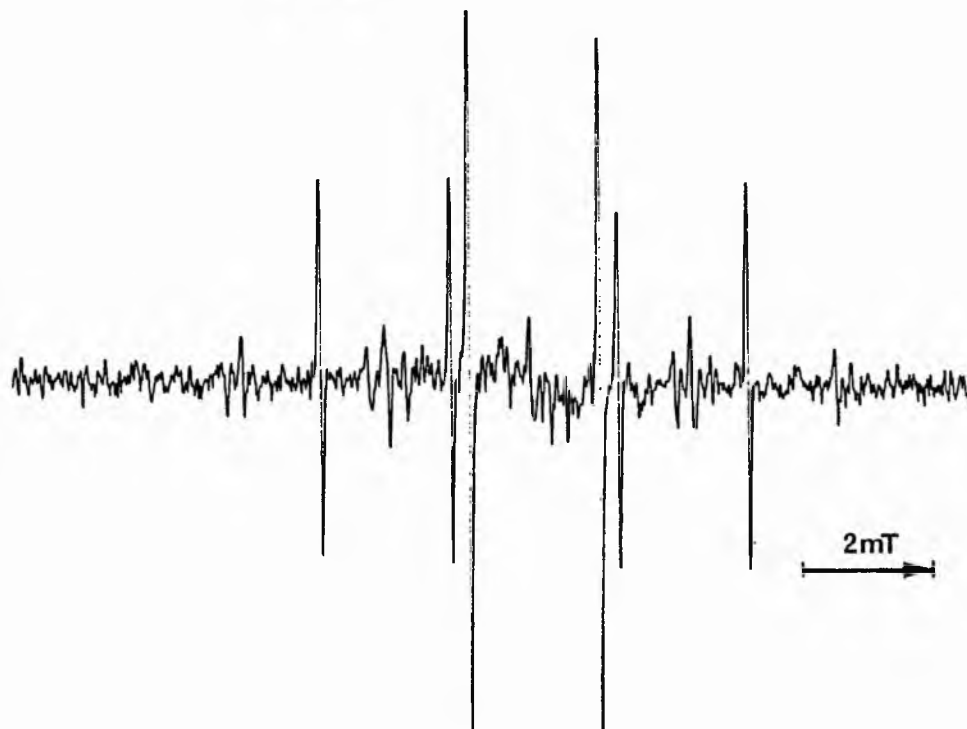


Figure 2.2.1 E.S.R. spectrum of alkyl radicals derived from butyric acid



Figure 2.2.2 E.S.R. spectrum of alkyl radicals derived from methyl butyrate

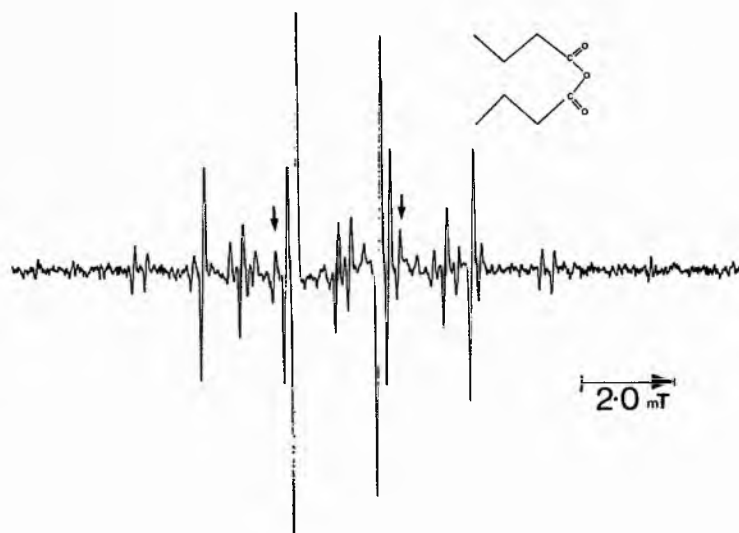
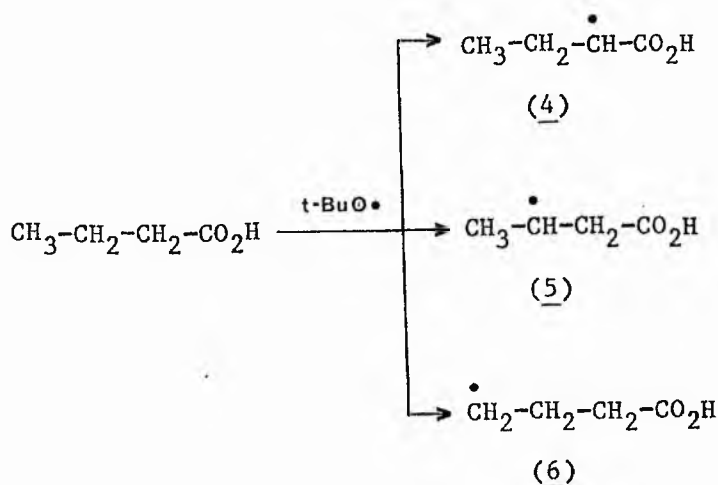


Figure 2.2.3 E.S.R. spectrum of alkyl radicals derived from butyric anhydride. Arrows indicate inner lines of the minor isomer resulting from H-abstraction of the α -methylene

Table 2.2.2 Variation of relative intensities of major (Ma) and minor (Mi) conformers of the α -radical from butyric anhydride with temperature.

Temp / K	$\frac{Ma}{Mi}$	% Major
250	4.46	81.7
260	4.68	82.4
270	4.44	81.6
285	4.16	80.6
300	5.00	83.3



As found for propionic acid hydrogen abstraction occurs overwhelmingly α -to the carboxyl group (> 77 %). The relative concentration of the primary radical could not be determined accurately, but an upper limit of ca. 3 % was estimated.

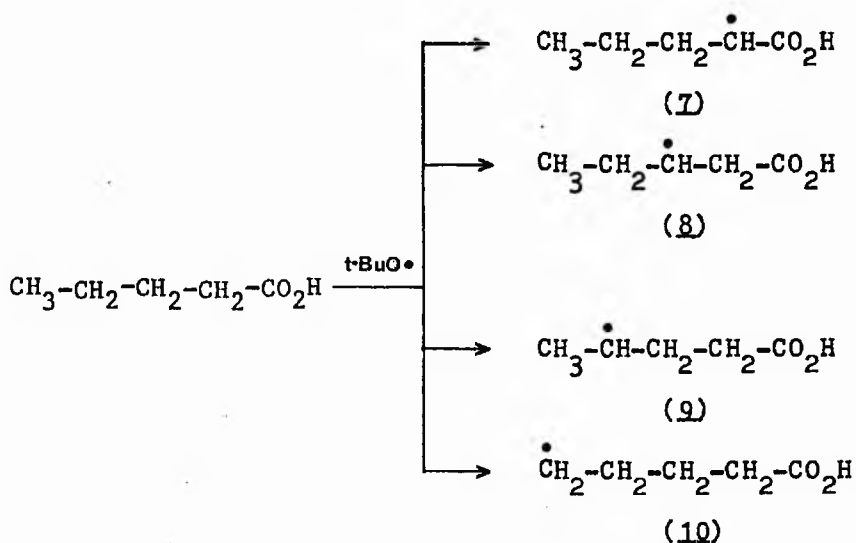
The E.S.R. spectrum obtained on H-abstraction from methyl butyrate (Figure 2.2.2) shows a much more complicated pattern than the acid. The increased complexity arises from coupling of the hydrogens of the ester group with the unpaired electron giving rise to an extra quartet splitting. The replacement of the carboxylic O-H by OMe has an effect on the relative ease of abstractability of the different hydrogens. The relative amount of the primary radical was increased considerably at the expense of the α -to the carboxyl radical. However, the latter species is still by far the most predominant radical formed.

As in the case of propionic anhydride two sets of E.S.R. signals resulting from hydrogen abstraction α -to the carboxyl group can be observed on photolysis of butyric anhydride and di-t-butyl peroxide

(Figure 2.2.3). The predominant radical having a smaller β -hfs than the minor one. The ratio of the concentrations of the two radicals shows no significant variation with temperature (Table 2.2.2) and has a mean value of $4.6 \pm 0.3: 1$. As for the acid and methyl ester hydrogen abstraction occurs predominantly α -to the carboxyl group and appears to be insensitive to temperature variation over the narrow range investigated.

2.3 Valeric, hexanoic and heptanoic acids.

For n-butyric acid two distinct types of secondary carbon atoms exist. In the case of the homologue, valeric acid, three distinct secondary carbons are present and hydrogen abstraction could give rise to four different radicals.



The predominant radicals observed in the E.S.R. spectra are the ω -1 radical (> 47 %) and the α -radical (> 41 %). The secondary radical arising from hydrogen abstraction at C3 was also observed but was difficult to quantify accurately due to its low relative concentration. The estimated upper limit for the amount of this radical is 12 %.

Hydrogen abstraction from hexanoic acid gave rise to an E.S.R. spectrum in which the ω -1 radical, α -to the carboxyl and in chain secondary (hereafter referred to as just secondary) radicals were clearly observed. The two radicals resulting from hydrogen abstraction from C3 and C4 are spectroscopically equivalent, inductive and electric field effects producing no observable perturbation on the spin density distribution at these sites. The experimental and simulated spectrum are shown in Figure 2.3.1. The relative amounts of each of the radicals observed and their respective hfs are reported in Table 2.3.1. Small triplet γ -hfs were resolvable in the secondary radicals derived from pentanoic and hexanoic acids, but could not be observed for higher homologues.

For heptanoic acid the spectrum obtained on photolysis of a solution of the acid in di-*t*-butyl peroxide gave rise to a spectrum in which the signals from the secondary radicals (the three possible secondary radicals are spectroscopically equivalent) predominates. The hfs of the three observable radicals in the spectrum are similar to those obtained from the spectra of valeric and hexanoic acids. It is worth noting that the splitting pattern for the ω -1 radical is distinct in the spectra from these three and higher acids from that of the same radical in butyric acid and its derivatives. In the longer

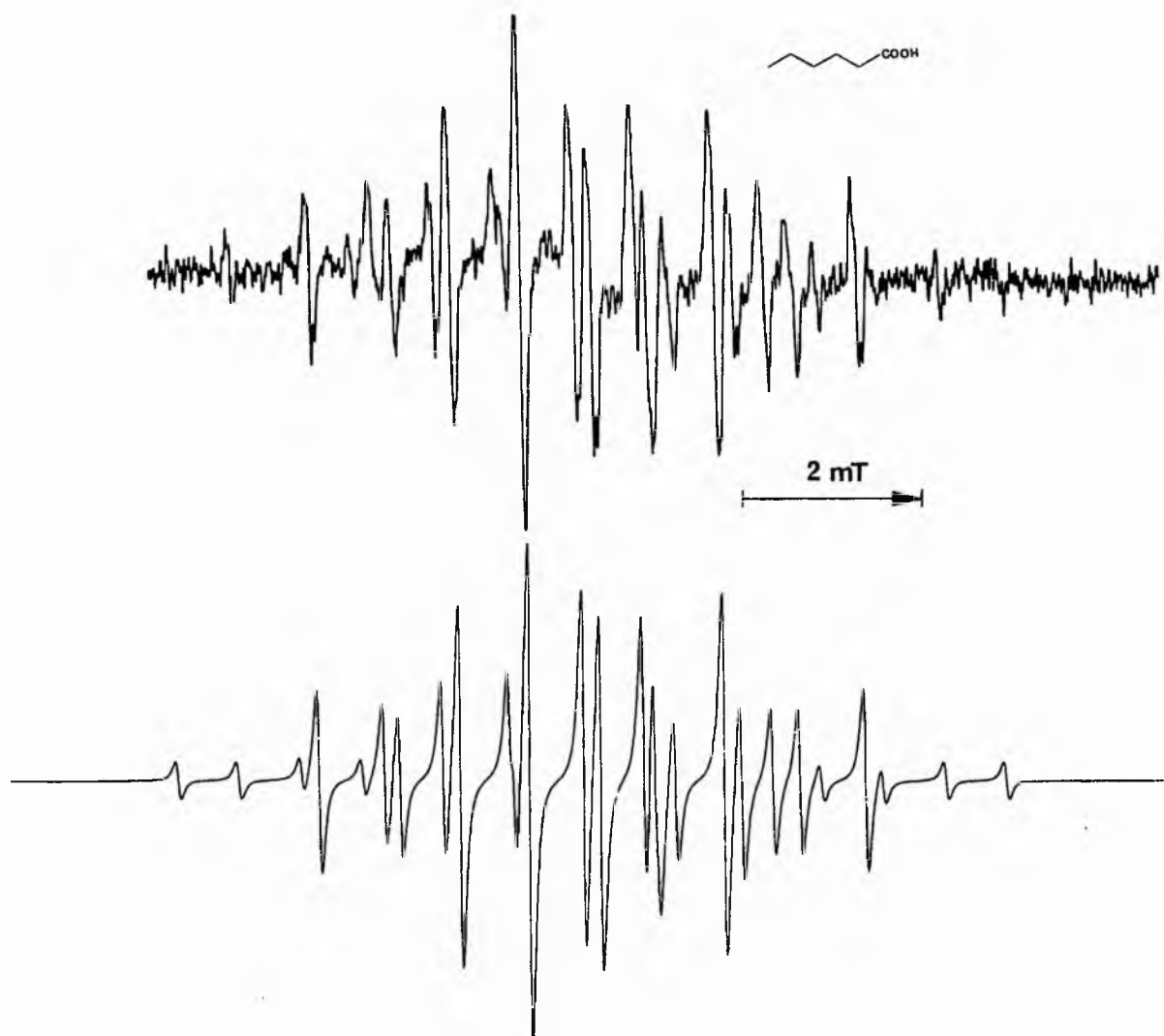


Figure 2.3.1 E.S.R. spectrum of alkyl radicals derived from hexanoic acid. Upper trace experimental spectrum; lower trace computer simulation

chain acids the hydrogens of the terminal methyl group have the same hfs as the hydrogens ω -2 methylene group. In the ω -1 radicals from butyric acid the hfs of the ω -2 methylene group are perturbed (reduced) because they are also α -to the carboxylic group i.e. the change results from the head group effect at C2.

2.4 Octanoic and higher homologues.

The E.S.R. spectra obtained on hydrogen abstraction from the higher homologues (C8-C18) are basically very similar to each other and contain three sets of signals resulting from hydrogen abstraction α -to the carboxyl group, at the ω -1 carbon and from the remaining secondary methylenes. Minor differences in hfs of the secondary methylenes (some of which are in the vicinity of the head groups) are not resolved and hence the signal from these radicals is an envelope of all the slightly different signals. This manifests itself in a larger linewidth for the secondary radicals and the line shape deviates from purely Lorentzian to Gaussian.

Figure 2.4.1 shows the variation of the relative concentrations of the three observable radicals (11-13) with increasing chain length of the aliphatic acid and the values are reported in Table 2.4.1. The steady increase in the relative concentration of secondary radical with concomitant decrease in concentration of the α - and ω -1 radicals with increasing carbon number is as expected on a purely statistical basis. Correction of each signal intensity for the number of hydrogens available suggests that hydrogen abstraction occurs more than twice as readily from the methylenes α -to the carboxyl and from the ω -1 carbon than from an inner-chain secondary (Figure 2.4.2).

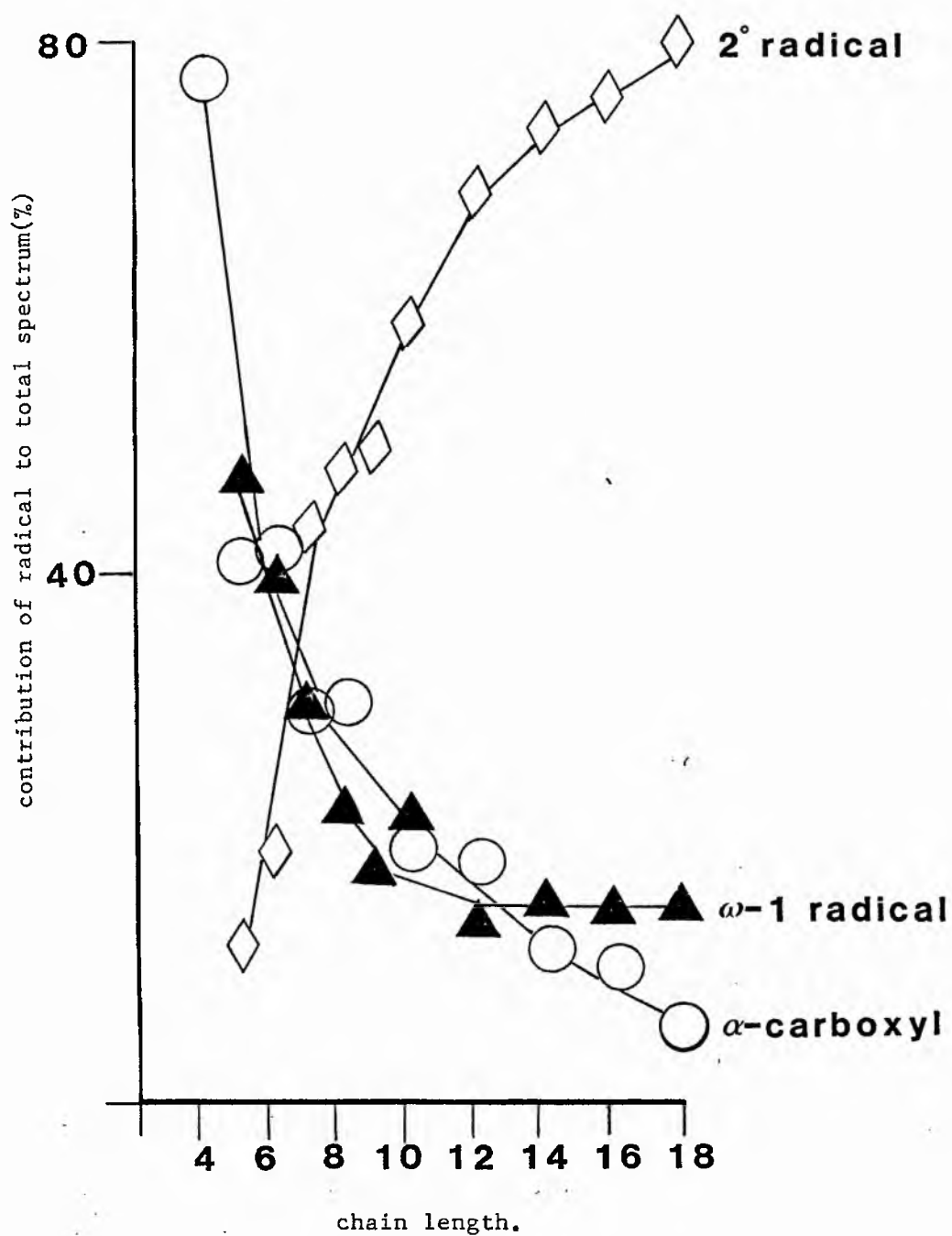
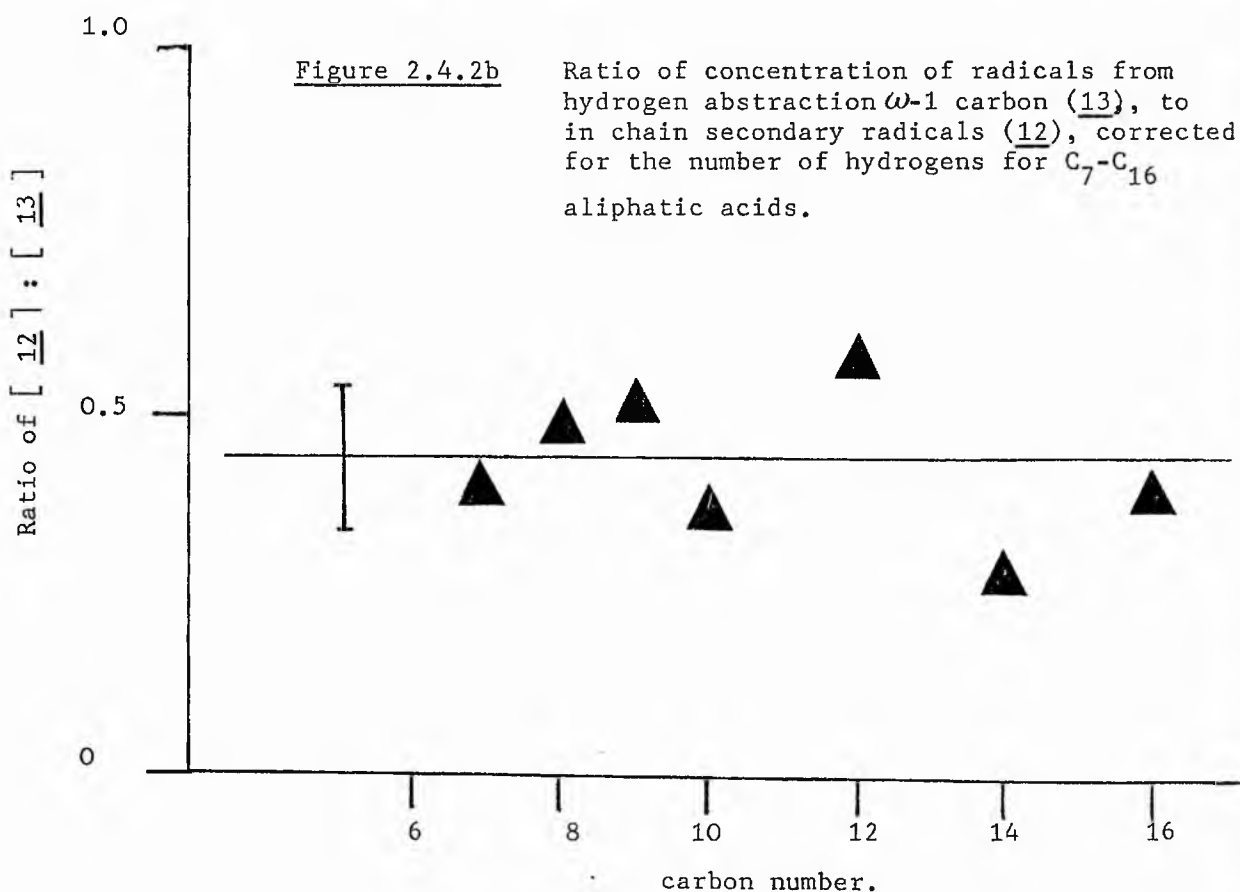
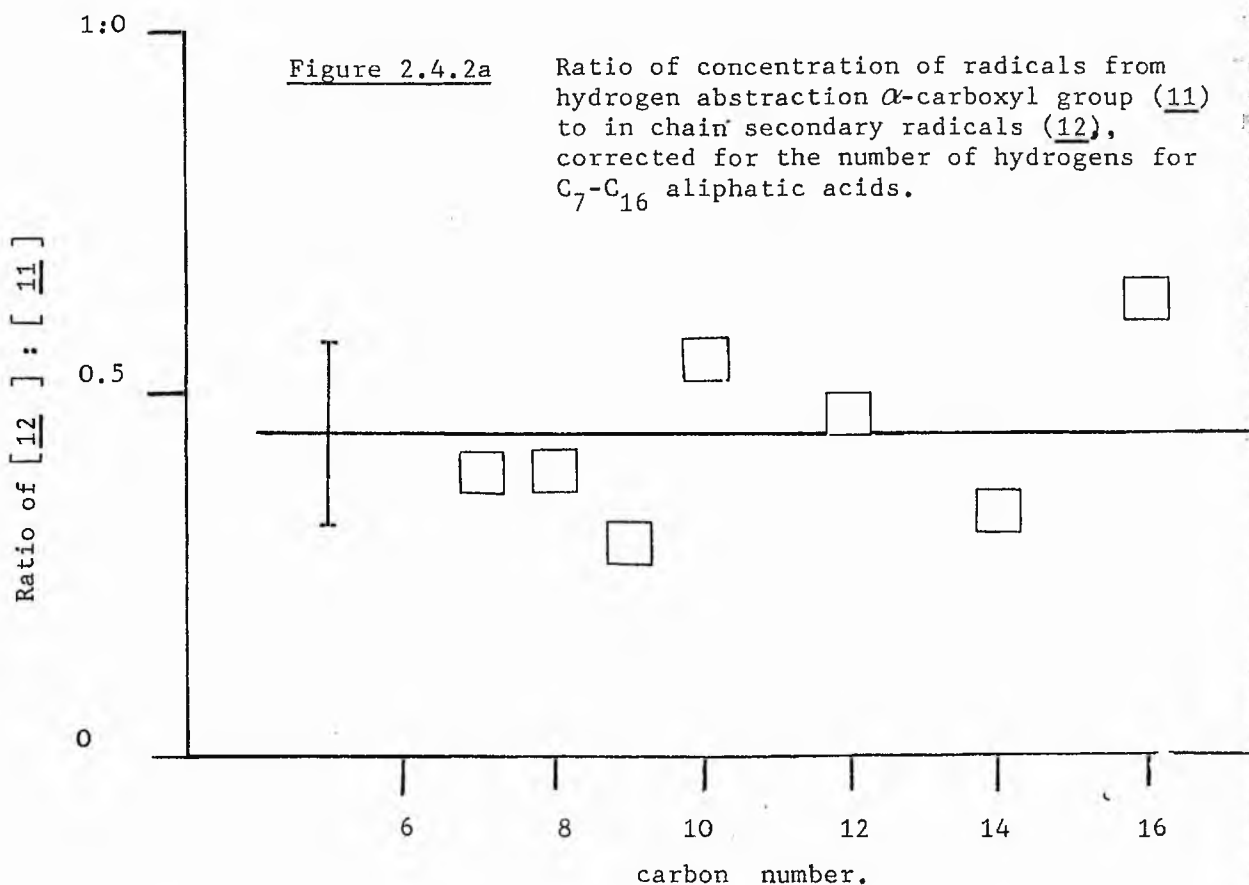


Figure 2.4.1 Plot of relative contributions of α -carboxyl, secondary and $\omega-1$ radicals derived from long chain carboxylic acids to the total radical population.



This gives krel for α -carboxyl: ω -1 carbon:secondary to be approximately 2.2 : 2.0 : 1. These values can be added to those obtained from our previous study on allylic, allenic and pentadienyl radicals forming a set of relative reactivities of the various sites in long chain aliphatic acids and esters to attack by t-butoxyl radicals.

2.5 Butyl acetate, trifluoroacetate and trichloroacetate.

Figure 2.5.1 shows the spectrum obtained on hydrogen abstraction from n-butyl trifluoroacetate. As in the case of valeric acid four distinct radicals could be observed. The spectrum was complicated as a result of the large number of overlapping lines. All four component radicals (14-17) were identified and their hfs are reported in Table 2.5.1. The g-value for radical (14) was less than that for (15-17).

As a result of the extensive overlapping of lines reliable quantification of the relative concentrations of each radical was extremely difficult. However, the approximate values of the relative ease of hydrogen abstraction from the α , β and γ sites were 1.5-2 : 3-4 : 1.

All of the lines for the α -radical (14) overlap extensively with other signals and hence we were unable to ascertain the relative amount of this radical.

The E.S.R. spectrum obtained on hydrogen abstraction from butyl trichloroacetate was distinct from that of the trifluoroacetate, but still showed a large number of overlapping lines, giving rise to a very complicated non-centrosymmetric spectrum. Although signals attributed to the α , β , and γ radicals could be observed in the

spectrum a large number of lines were unaccounted for, which could not be assigned to the expected signals for the α -radical, even by invoking γ -splitting.

Hydrogen abstraction from butyl acetate gave an E.S.R. spectrum which was rather simpler to interpret than those for the trifluoro- and trichloro- derivatives, although once again the central region of the spectrum contained a considerable number of overlapping lines. The relative amounts of each of the four radicals contributing to the spectrum has been determined, and although the experimental error is large the values are probably more accurate than those for the trifluoro- and trichloroacetates. One notable difference is the larger proportion of the α -radical compared to the other two analogues although once again the site appears to be slightly deactivated to relative to the β -site. The $\omega-1$ site was however activated which is consistent not only with the other results from this study but also with those from other groups. The hfs and the relative amounts of each radical in the E.S.R. spectrum are given in Table 2.5.1.

2.6 Propyl chloride.

The E.S.R. spectrum obtained from photolysis of a mixture of propyl chloride and di-*t*-butyl peroxide is shown in Figure 2.6.1. Three radicals were unambiguously identified in the spectrum resulting from hydrogen abstraction from each of the distinct sites in the three carbon backbone. The radical arising from hydrogen abstraction of an α -methylene (C1) gave a double triplet with a further smaller γ splitting. The spectrum was satisfactorily simulated using the

parameters given in Table 2.6.1. The hfs were unequivocally assigned to specific hydrogens by comparison with those of similar radicals in this study and the literature^[28].

Hydrogen abstraction occurs overwhelmingly from the α -site. Accurate quantification was not possible due to the large number of overlapping lines and the low signal-to-noise ratio for all but the radical from the α -site. Nonetheless a 'lower' limit of approximately 4.6 has been computed for the ratio of the relative amounts of hydrogen abstraction from the α to β sites. We were unable to estimate the amount of hydrogen abstraction from the terminal methyl group with any precision due to its low intensity; but it is probably more than an order of magnitude less than from the α -site.

Table 2.6.1 E.S.R. parameters for radicals derived from propyl chloride.

Radical	$a_{\alpha-H}$	$a_{\beta-H}$	$a_{\gamma-H}$	Rel conc.
$\text{CH}_3\text{-}\dot{\text{C}}\text{H}_2\text{-CH-Cl}$	1.38 (1H)	2.00 (2H)	1.60 (3H)	0.82
$\text{CH}_3\text{-}\dot{\text{C}}\text{H-CH}_2\text{-Cl}$	2.20 (1H)	2.20 (2H) 2.40 (3H)		0.18
$\dot{\text{C}}\text{H}_2\text{-CH}_2\text{-CH}_2\text{-Cl}$	2.13 (2H)	2.69 (2H)		n.d

all hfs checked by computer simulation.
n.d = not determined.

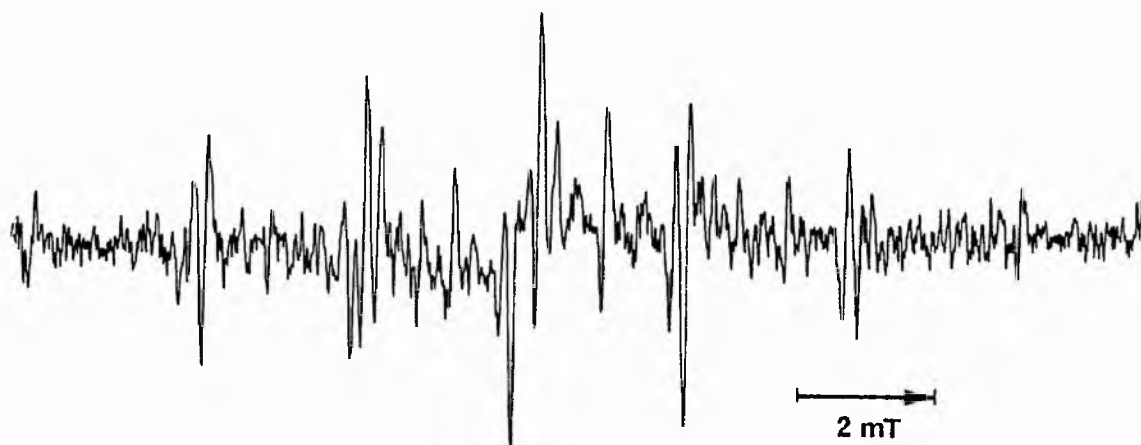


Figure 2.5.1 E.S.R. spectrum of radicals derived from butyl trifluoroacetate in di-t-butyl peroxide

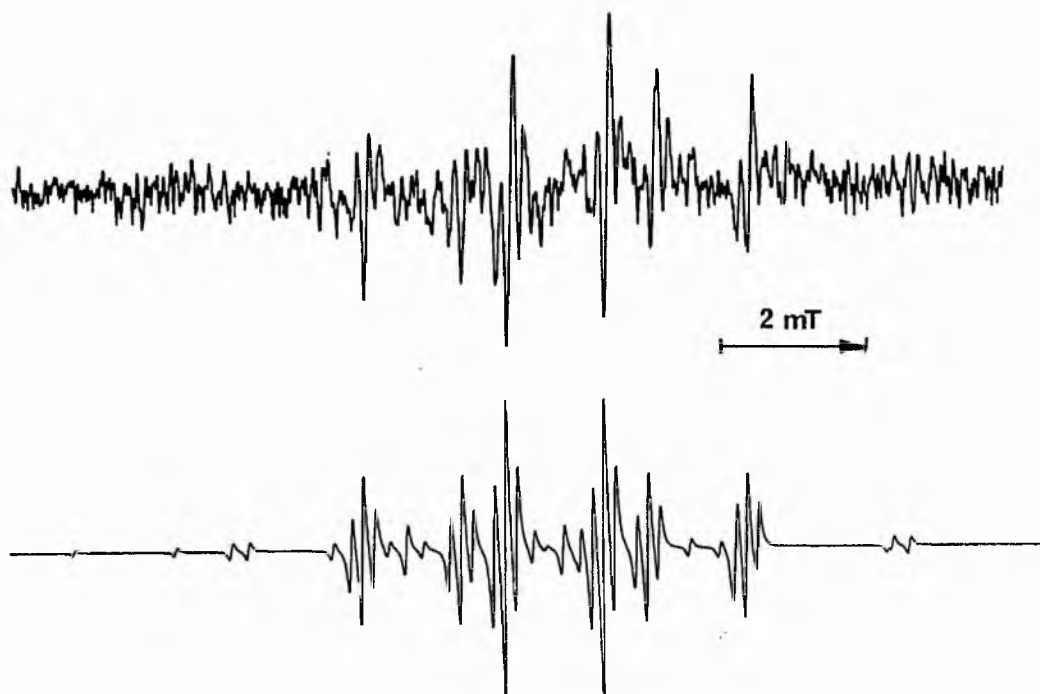
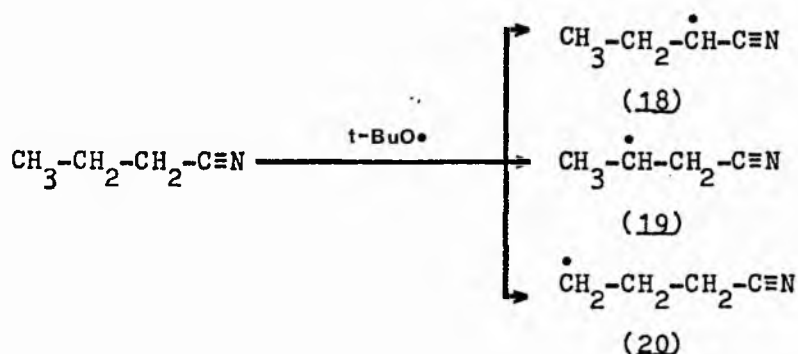


Figure 2.6.1 E.S.R. spectrum of alkyl radicals derived from propyl chloride. Upper trace, experimental spectrum; lower trace, computer simulation.

2.7 Butyryl nitrile.

The E.S.R. spectrum obtained on photolysis of a solution of butyryl nitrile and di-*t*-butyl peroxide is shown in Figure 2.7.1. As with the carboxylic acids *t*-butoxyl radicals preferentially hydrogen abstract at the α -site. The ω -1 and ω radical were observable but were very weak. The relative amounts of each radical and their respective hfs are reported in Table 2.7.1.



The relative proportions given in Table 2.7.1 are lower limits for hydrogen abstraction from the α -site, the relative amounts of ω -1 and ω radicals being upper limits each case. It is apparent however that there is an even greater activation of the α -site for the nitrile than the carboxylic acids.

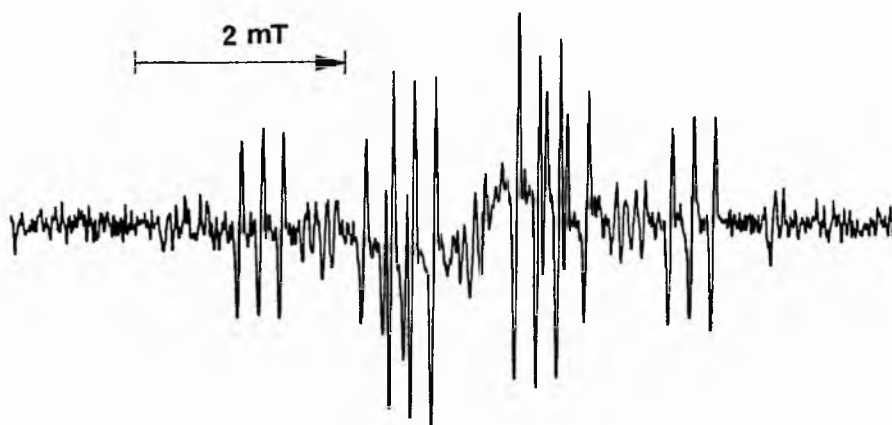


Figure 2.7.1 E.S.R. spectrum of alkyl radicals derived from butyryl nitrile.

Table 2.7.1 E.S.R. parameters for radicals derived from butyryl nitrile.^a

Radical	^a _{α-H}	^a _{β-H}	^a _{β-H}	Rel conc.
$\text{CH}_3\text{-CH}_2\text{-}\dot{\text{C}}\text{H}\equiv\text{CN}$	1.93 (1H)	2.38 (2H)	3.4	> 0.91
$\text{CH}_3\text{-}\dot{\text{C}}\text{H-CH}_2\equiv\text{CN}$	2.30 (1H)	2.30 (2H)		< 0.06
		2.50 (3H)		
$\dot{\text{C}}\text{H}_2\text{-CH}_2\text{-CH}_2\equiv\text{CN}$	2.20 (2H)	2.60 (2H) ^b		< 0.03

^a all hfs checked by computer simulation.

^b tentative assignment.

2.8 Dicarboxylic acids.

Hydrogen abstraction from a dibasic acid of general formula $\text{HO}_2\text{C}(\text{CH}_2)_n\text{CO}_2\text{H}$ should give rise to a simpler E.S.R. spectrum than the corresponding monobasic acid by virtue of there being no terminal methyl group and consequently no ω-1 methylene. Attempts to observe fatty acid radicals from such acids were however unsuccessful. The E.S.R. spectra from several different dibasic acids all contained a

prominent quartet ($a(3H) = 2.30$ mT) together with a complicated, 'less intense pattern of one or more other radicals. The coupling constant for the quartet is in good agreement with literature values for the methyl radical^[29].

2.9 Triacylglycerols.

An E.S.R. spectrum which contained the signals of radicals derived from hydrogen abstraction at the α -site, $\omega-1$ site, and the remaining secondary sites was obtained on photolysis of mixture of di-*t*-butyl peroxide and 1-lauroyl-2-myristoyl-3-palmitoyl-rac-glycerol (LMP) at 300 K. The spectrum was similar to that obtained on hydrogen abstraction from the long chain saturated acids. However, estimates of the relative concentrations of each type of radical indicated an increased amount of $\omega-1$ radical compared to the expected amount calculated from the summation of the spectra for C12, C14 and C16 saturated acids. The expected and calculated values are shown in Table 2.9.1.

This may tentatively be attributed to increased steric hindrance to hydrogen abstraction of methylenes towards the carboxyl end of each chain in the bulky triacylglycerols. No signals were observed which could be attributed to hydrogen abstraction from the glycerol moiety itself.

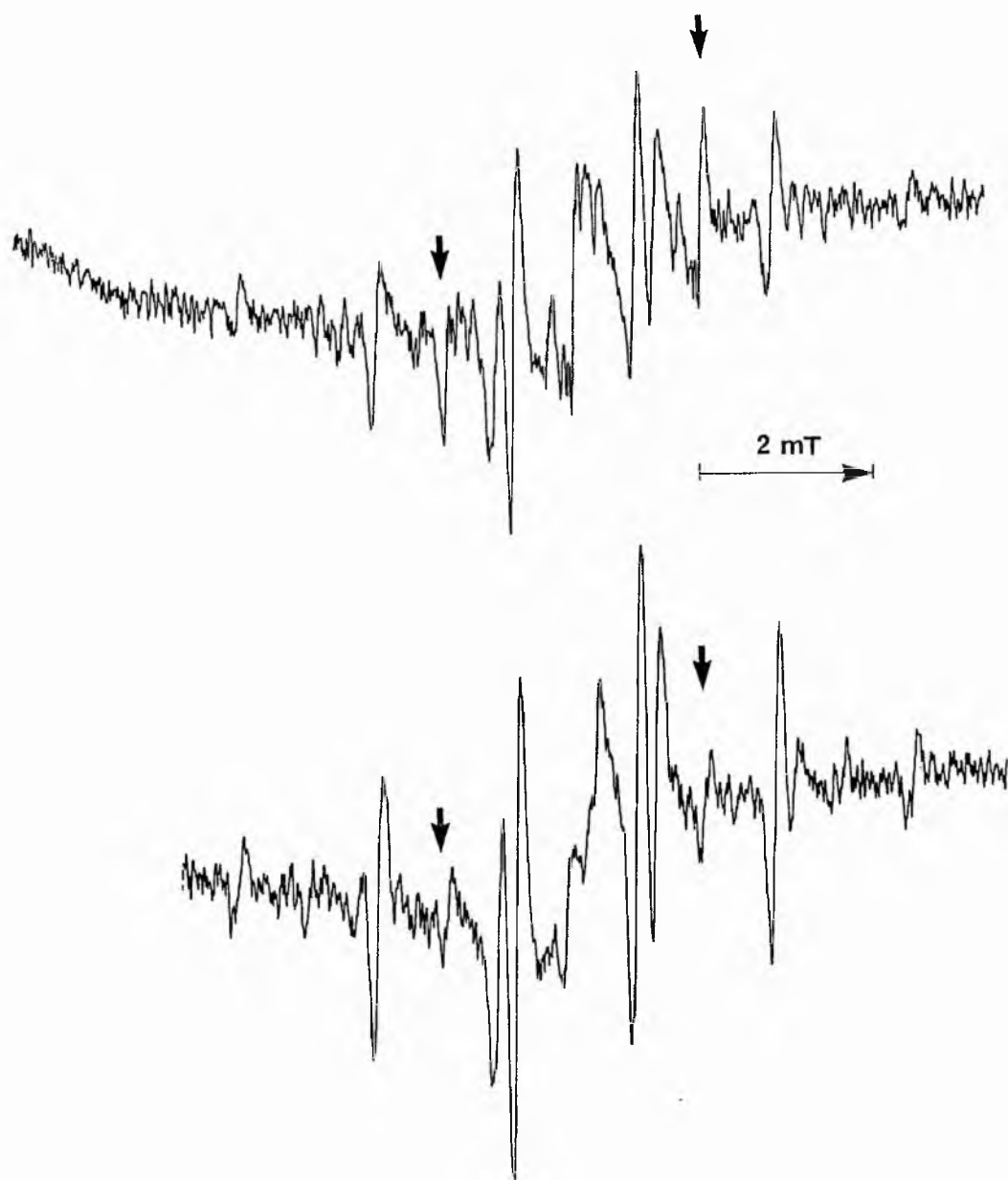


Figure 2.9.1

Top. E.S.R. spectrum obtained on photolysis of a solution of 1-lauroyl-2-myristoyl-3-palmitoyl-rac-glycerol and di-t-butyl peroxide at 300K.

Bottom. E.S.R. spectrum obtained on photolysis of a solution of palmitic acid and di-t-butyl peroxide. Outer lines of the radical arising from H-abstraction from the $\omega-1$ methylene are indicated.

Table 2.9.1 Experimental and calculated concentrations
of radicals from LMP.

Radical	%	
	Found	Calculated ^a
α -carboxyl	0.10	0.13
secondary	0.48	0.71
ω -1 radical	0.43	0.14

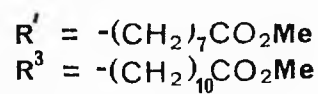
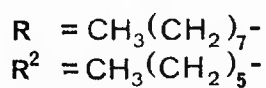
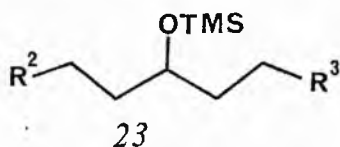
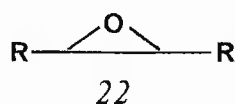
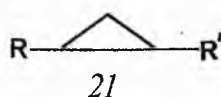
^a calculated from Table 2.4.1.

2.10 Short chain acid chlorides and aldehydes.

Attempts to observe the E.S.R. spectra from hydrogen abstraction from butyryl and valeryl chlorides and butan-al were unsuccessful in each case.

2.11 Long chain cyclopropane, epoxy and trimethylsilylether fatty acid esters.

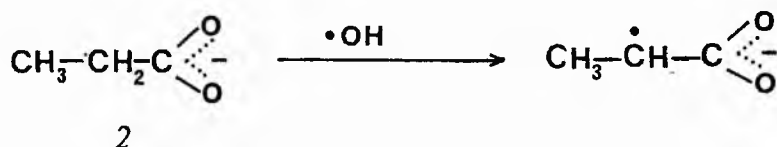
Hydrogen abstraction from long chain cyclopropane (24), epoxy (22) and 12-trimethylsilylether (23) derivatives of methyl stearate gave E.S.R. spectra which were indistinguishable from methyl stearate in each case.



This suggests that the distinct new sites for hydrogen abstraction introduced by the functional group are not significantly activated with respect to the other possible sites of attack.

3 Discussion.

The observation of (1) as the predominant radical species on hydrogen abstraction from propionic acid is in stark contrast to studies with other abstracting radicals. Tanaguchi *et al*^[19] using a flow technique to measure the relative ease of abstractability of the various types of C-H bonds towards hydroxyl radicals, generated by a H_2O_2/Ti^{4+} system, found that hydrogen abstraction occurred preferentially at the terminal methyl group (ca 70 %). Hewgill *et al*^[16] also using hydroxyl radicals in an aqueous system observed hydrogen abstraction at the methyl group (50 %) in acid solution, but in basic solution hydrogen abstraction occurred preferentially at the α -site for the anion (2) although the difference was small.

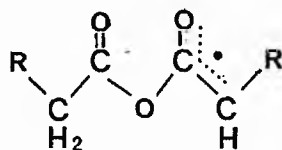


Radical (1) has also been observed by halogen abstraction from α -halopropionic acids by Anbar and Neta^[25] and independently by Beckwith and Norman^[24]. A MINDO/3 semiempirical calculation on the two possible isomeric α -radicals, the *cisoid* and *transoid* configurations, indicated that the *transoid* configuration is

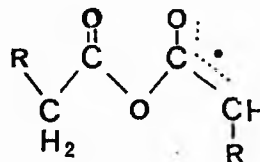
marginally lower in energy than the cisoid configuration, as would be expected. The barrier to rotation about the C1-C2 bond for conversion of cis to trans isomers was calculated to be 6.7 kJmol^{-1} .

This value is probably an underestimate because MINDO/3, despite predicting barriers to rotation about double bonds^[30] with reliability, often underestimates barriers to rotation about delocalised bonds^[30]. Nonetheless the relative stabilities are generally well reproduced by MINDO/3 which supports the intuitive expectation that the ground state rotamer population of the delocalised radical should be predominantly transoid.

For hydrogen abstraction from propionic and butyric anhydride two sets of signals were observed differing only in their β -hfs. The two radicals may well be cisoid and transoid conformers as shown below.



cisoid



transoid

The minor radical has been assigned to the transoid isomer on the basis of its β -hfs being the same as that for the α -radical from the parent acids which we believe to be transoid. The major radical therefore being the cisoid isomer. We tentatively interpret the drop-off in the amount of the transoid radical (in comparison with parent acids) to an increased conformational preference of the

anhydride for the extended zig-zag conformation. This would parallel n.m.r. data by Butcher and Wilson^[31] for propionaldehyde, a reasonable analogy, in which the cis rotamer is approximately 4.2KJmol^{-1} more stable than the trans form with a barrier to rotation of 10KJmol^{-1} . Further support for the assignment comes from the relative magnitudes of the β -hfs which are in accord with the β -hfs constants for cis and trans methallyl radicals^[32].

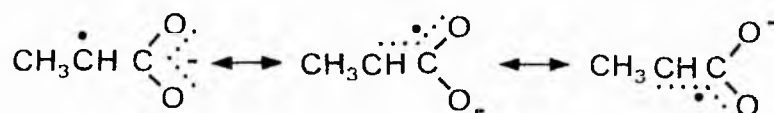
From the results on the carboxylic acids, esters, anhydrides and nitrile we find that there is preferential attack at the α -methylene group and at the $\omega-1$ methylene. The relative reactivities being independent of chain length length (within experimental error). This apparent activation at the α -site is, (vide supra) contrary to expectation^[33] and contrary to results obtained with hydroxyl radicals in aqueous solution^[16-19].

Tedder and co-workers^[33] have studied free radical substitution reactions in aliphatic acids and esters in both the gas phase and the solvent phase. The free radical substitutions were either with chlorine or bromine atoms. In the gas phase they found a marked deactivation of the α position and a somewhat smaller deactivation of the β -position, but the effect was not transmitted further, save an apparent consistent activation of the $\omega-1$ position. Similar results were found in solution, with the difference that the carboxyl group has a deactivating effect beyond the β -position; the results from heptanoyl chloride results suggesting that deactivation occurs up to the 6-position.

The results of Tanaguchi et al^[19] for relative reactivities towards hydroxyl radicals in aqueous solution are in good accord with the above work. They found an activation at the $\omega-1$ site and a

deactivation at the α -site. Effects transmitted further than the α -position would not be observable by E.S.R. unless they resulted in a change of the hfs constants for the secondary radicals as they became more remote from the carboxyl group, this evidently was not the case.

The increase in reactivity of the α -site for the carboxylic anions (2)^[16] was attributed to the increased possibility of the incipient radical being stabilised to some extent by resonance.



However there is also evidence that the free acid or its ester may also be resonance stabilised, although the delocalisation is spread over only one oxygen atom in this case.^[34]



Our present results for t-butoxyl radicals agree with all other studies in indicating activation of the ω -1 methylene group relative to the rest of the chain methylenes but they differ from the hydroxyl radical and halogen atom studies in showing activation of the α -methylene group. Two independent product studies on the reaction of t-butoxyl radicals with saturated fatty acids showed that the dimers produced were predominantly α -linked^[35,36], therefore the difference in regioselectivity of the abstracting species appears to be real. Non polar radicals (eg. CH_3^\bullet) also show a different regioselectivity towards carboxylic acids than halogens or hydroxyl radicals. Alkyl radicals attack carboxylic acids (or acid chlorides) preferentially α -to the carboxyl group^[37].

Tedder^[38] has discussed in detail the factors controlling the rates of hydrogen abstraction from aliphatic compounds. The differences in rates have been attributed to differences in activation energies of the various reactions, which in turn are dependent upon four main factors; the strength of the bond which is being broken, the strength of the bond being formed, the repulsion between the incoming radical and the molecule being formed, and finally the repulsion between the new radical and the new molecule. Table 2.12.1 lists the bond dissociation energies for t-butanol, water, hydrogen chloride, hydrogen bromide and methane. The strength of the bonds being broken from the aliphatic carboxylic acids is independent of the attacking radical species. Furthermore in Table 2.12.1, there is no significant difference in the strengths of the bonds being formed ie. X-H for X = Cl, OBU-t or CH.

Table 2.12.1

Bond dissociation energies of some radical-H bonds.

$H-X$	$D(X-H)/KJmole^{-1}$
H-Br	365.6
H-Cl	431.0
H-OBu ^t	439.3
H-OH	497.9
H-CH ₃	422.6

The differences between the $D(X-H)$ for $X=Br$, Cl and OH obviously cannot be of paramount importance in determining the activation energy since all three of these radicals have similar (to a first approximation) regioselectivities. It would appear therefore that the critical factor in determining the site of attack is the nature of the polar forces which will exist in the transition state.

Hydrogen abstraction by methyl radicals will furnish methane, which is essentially non-polar and hence polar forces in the transition state should be minimal. The methyl radicals will then preferentially abstract from the weakest carbon-hydrogen bond (which will be α -carboxyl group due to resonance stabilisation of the incipient radical, followed by the $\omega-1$ carbon hydrogen bond which is

stabilised due to hyperconjugation with the terminal methyl group). This is in accord with observations^[37]. With atomic halogenation and attack by hydroxyl radicals at the α -position the new molecule will be highly polar. This will lead to an increase in the repulsion between the new α - radical and the new molecule hence resulting in an increase in the activation energy. Furthermore in the case of the hydroxyl radical the incoming radical will also be polar and result in a further increment in the activation energy for attack at the α -position. In the case of non-polar X-H bonds there will be no repulsive polar force in the transition state for attack at the α -site. Hence the observed regioselectivity can be ascribed to the less polar nature of the t-butyl alcohol formed relative to the halogen acids and water.

An alternative explanation for the deactivation of the α -site to hydrogen abstraction by hydroxyl radicals generated from the $\text{TiCl}_3/\text{H}_2\text{O}_2$ system is noted. Hewgill *et al*^[18] have demonstrated that carboxylic acids can be coordinated to the titanium via the carboxyl group. In this situation cyclic transition states become possible if a chain methylene is transferred to titanium (see Figure 2.12.1). A six membered transition state is likely to be the most favoured, resulting in hydrogen transfer from the C_β -hydrogen. This is in accord with the preferential abstraction from the β -carbon observed for hydroxyl radicals^[16-19]. Clearly a five membered transition state will be unlikely in this case since the α -methylene is directed away from the titanium as a result of coordination involving the carboxyl group, giving rise to an apparent deactivation of the α -site. There is, however evidence that the reactive species in $\text{TiCl}_3/\text{H}_2\text{O}_2$ oxidations is the same as that in radiolysis, namely free

radicals. Differences in regioselectivity between these two systems has been ascribed to preferential reaction of some radicals with either the metal ions or hydrogen peroxide^[39-41]. The reported regioselectivities of hydroxyl radicals generated in such a manner should be treated with caution.

The results presented in this work suggest that hydrogen abstraction from saturated carboxylic acids by t-butoxyl radicals is essentially a random process, with the exception of slight activation at the α - and ω -1 sites. This may be contrasted with the regioselectivities observed towards polyunsaturated carboxylic acids^[26,27] where hydrogen abstraction occurs predominantly from the doubly allylic methylenes. The data presented in this and the previous paper^[26,27] may provide insight into the relative ease by which autoxidation processes may be triggered and sustained, although the overall mechanism involves complex chain propagation and termination steps which will undoubtedly be of paramount importance in any quantitative comparison^[2].

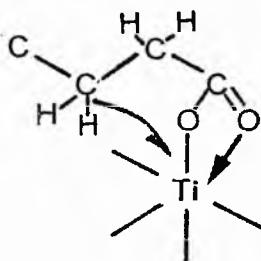


FIGURE 2.12.1

4 Experimental.

All of the saturated fatty acids were commercially obtained and were the best grades available. All the liquids were redistilled before use. The solids (from C10 upwards) were recrystallised from petroleum ether (40/60). The purity of the acids (in excess of 99.0 %) was checked before use by capillary G.L.C.

Methyl esters were prepared by acid catalysed esterification by standard procedures, and after distillation or recrystallisation were analytically pure by capillary G.L.C. and where applicable T.L.C.

Propionic and butyric anhydride, butyrl nitrile, n-butyl acetate, butan-ol and propyl chloride were all commercially available and redistilled prior to use.

3.1 Preparation of n-butyl trifluoroacetate.

To butan-1-ol (37g, 46ml, 0.5mol) was added trifluoroacetic acid (114g, 74ml, 1.0ml) in a round bottom flask. Conc. sulphuric acid (1ml) was added dropwise. A reflux condenser was attached and the mixture refluxed for 16h. Water was then added (200ml) and the upper layer was then washed with distilled water (50ml) and saturated sodium bicarbonate solution (2 x 25ml). The crude ester was dried over anhydrous sodium sulphate, filtered and carefully fractionally

distilled. The pure n-butyl trifluoroacetate being collected at bp_{18.5} 121-123°C in 78 % yield (66.5g).

¹Hnmr spectrum: 4.32δ(t, J=6.4Hz, 2H, -CH₂-O-)

1.66δ(sextet, J=6.4Hz, 2H, CH₃-CH₂-CH₂-)

1.33δ(quintet, J=6.4Hz, 2H, -CH₂-CH₂-CH₂-)

0.90δ(t, J=6.8Hz, 3H, CH₃-)

¹³Cnmr spectrum: 67.88 (C1), 30.02 (C2), 18.67 (C3) and 13.30 (C4)

mass spectrum showed intense peaks at m/e 141 (1, M⁺-Et), 99 (4),

69 (31, CF₃⁺), 57 (34, C₄H₉⁺), 56 (100, C₄H₈⁺), 44

(26, CO₂), 43 (44, C₃H₇⁺), 41 (80, C₃H₅⁺), 32 (70)

and 31 (37, CF⁺).

3.2 Preparation of n-butyl trichloroacetate.

To butan-1-ol (37g, 46ml, 0.5mol) was added trichloroacetic acid (170g, 1.0ml) in a round bottom flask. Conc sulphuric acid (1ml) was added dropwise. A reflux condenser was attached and the mixture refluxed for 16h. Work up as above gave crude ester which was distilled to give pure n-butyl trichloroacetate bp₂₀ 100-1°C in 80 % yield (87.5g).

¹Hnmr spectrum: 4.30δ(t, J=6.4Hz, 2H, -CH₂-O-)

1.65δ(sextet, J=6.4Hz, 2H, CH₃-CH₂-CH₂-)

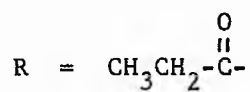
1.33δ(quintet, J=6.4Hz, 2H, -CH₂-CH₂-CH₂-)

0.91δ(t, J=6.8Hz, 3H, CH₃-)

¹³Cnmr spectrum: 69.09 (C1), 30.08 (C2), 18.70 (C3) and 13.35 (C4).

Table 2.1.1 E.S.R. parameters^a for radicals generated from propionic acid and anhydride

Radical	θ/κ	$a_{\alpha-H}$	$a_{\beta-H}$	relative concn
$\text{CH}_3\dot{\text{C}}\text{HCO}_2\text{H}$	250	2.00(1H)	2.44(3H)	1
$\cdot\text{CH}_2\text{CH}_2\text{CO}_2\text{H}$	250	nd	nd	0
$\text{CH}_3-\dot{\text{C}}\text{H}-\text{C}\begin{smallmatrix} \text{O} \\ \parallel \\ \text{OR} \end{smallmatrix}$ <u>cisoid</u>	250	1.92(1H)	2.28(3H)	0.75
$\text{CH}_3\dot{\text{C}}\text{H}-\text{C}\begin{smallmatrix} \text{O} \\ \parallel \\ \text{OR} \end{smallmatrix}$ <u>transoid</u>	250	1.92(1H)	2.48(3H)	0.25
$\cdot\text{CH}_2\text{CH}_2-\text{C}\begin{smallmatrix} \text{O} \\ \parallel \\ \text{OR} \end{smallmatrix}$	250	nd	nd	0



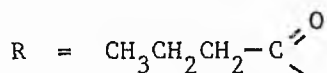
nd = not detected

^a all hfs checked by computer simulation

Table 2.2.1 E.S.R. parameters^a for radicals generated from
Butyric acid, methyl ester and anhydride

Radical	^a _{α-H}	^a _{β-H}	^a _{γ-H}	Rel conc.
CH ₃ CH ₂ $\dot{\text{C}}$ HCO ₂ H	1.97(1H)	2.28(2H)		0.77
CH ₃ $\dot{\text{C}}$ HCH ₂ CO ₂ H	2.20(1H)	2.20(2H)		0.23
		2.44(3H)		
$\dot{\text{C}}$ HCH ₂ CH ₂ CO ₂ H	2.20(2H)	2.58(2H) ^b		n.d.
CH ₃ CH ₂ $\dot{\text{C}}$ HCO ₂ Me	2.00(1H)	2.28(2H)	1.45(2H)	0.46
CH ₃ $\dot{\text{C}}$ HCH ₂ CO ₂ Me	2.23(1H)	2.23(2H)		0.31
		2.51(3H)		
$\dot{\text{C}}$ HCH ₂ CH ₂ CO ₂ Me	2.20(2H)	2.58(2H)		0.23
CH ₃ CH ₂ $\dot{\text{C}}$ HCO ₂ R (<u>cisoid</u>)	1.92(1H)	2.19(2H)		0.55
CH ₃ CH ₂ $\dot{\text{C}}$ HCO ₂ R (<u>transoid</u>)	1.92(1H)	2.34(2H)		0.12
CH ₃ $\dot{\text{C}}$ HCH ₂ CO ₂ R	2.20(1H)	2.20(2H)		0.28
		2.46(3H)		
$\dot{\text{C}}$ HCH ₂ CH ₂ CO ₂ R	2.20(2H)	2.58(2H)		0.04

nd = not determined but probably <<<25% of total



^a all hfs checked by computer simulation

^b tentative assignment only

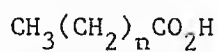
Table 2.3.1 E.S.R. parameters^a for radicals generated from pentanoic, hexanoic and heptanoic acids

Radical	$a_{\alpha-H}$	$a_{\beta-H}$	$a_{\gamma-H}$	Rel. Conc.
$CH_3CH_2CH_2\dot{C}HCO_2H$	1.96(1H)	2.22(2H)	0.05(2H)	0.41
$CH_3CH_2\dot{C}HCH_2CO_2H$	2.13(1H)	2.50(4H)	-	0.12
$CH_3\dot{C}HCH_2CH_2CO_2H$	2.12	2.42(5H)		0.47
$\cdot CH_2CH_2CH_2CH_2CO_2H$	n.d.			0.0
$CH_3CH_2CH_2CH_2\dot{C}HCO_2H$	1.96(1H)	2.22(2H)	0.10 (2H)	0.42
$CH_3CH_2CH_2\dot{C}HCH_2CO_2H$	2.13(1H)	2.50(4H)		0.19
$CH_3CH_2\dot{C}HCH_2CH_2CO_2H$				
$CH_3\dot{C}HCH_2CH_2CH_2CO_2H$	2.12(1H)	2.42(5H)		0.40
$\cdot CH_2CH_2CH_2CH_2CH_2CO_2H$	n.d.			0.0
$CH_3CH_2CH_2CH_2CH_2\dot{C}HCO_2H$	1.96(1H)	2.22(2H)		0.28
$CH_3CH_2CH_2CH_2\dot{C}HCH_2CO_2H$	2.13(1H)	2.49(4H)		0.44
$CH_3CH_2CH_2\dot{C}HCH_2CH_2CO_2H$				
$CH_3CH_2\dot{C}HCH_2CH_2CH_2CO_2H$				
$CH_3\dot{C}HCH_2CH_2CH_2CH_2CO_2H$	2.12(1H)	2.42(5H)		0.29
$\cdot CH_2CH_2CH_2CH_2CH_2CH_2CO_2H$	n.d.			0.0

nd = not detected

^a all hfs checked by computer simulation.

Table 2.4.1 E.S.R. parameters^a for radicals generated from long chain aliphatic carboxylic acids of general formula



Acid	n	radical	$a_{\alpha\text{-H}}$	$a_{\beta\text{-H}}$	Rel. concn ^b
octanoic	6	α	1.96(1H)	2.24(2H)	0.31
		secondary	2.10(1H)	2.48(4H)	0.48
		ω -1	2.12(1H)	2.42(5H)	0.22
nonanoic	7	α	1.96(1H)	2.24(2H)	0.33
		secondary	2.10(1H)	2.45(4H)	0.49
		ω -1	2.12(1H)	2.42(5H)	0.18
decanoic (caproic)	8	α	1.96(1H)	2.24(2H)	0.18
		secondary	2.10(1H)	2.40(4H)	0.60
		ω -1	2.12(1H)	2.42(5H)	0.22
dodecanoic (lauric)	10	α	1.96(1H)	2.24(2H)	0.18
		secondary	2.10(1H)	2.40(4H)	0.69
		ω -1	2.12(1H)	2.42(5H)	0.13
tetradecanoic (myristic)	12	α	1.96(1H)	2.24(2H)	0.12
		secondary	2.10(1H)	2.40(4H)	0.74
		ω -1	2.12(1H)	2.42(5H)	0.15
hexadecanoic (palmitic)	14	α	1.96(1H)	2.24(2H)	0.10
		secondary	2.10(1H)	2.40(4H)	0.76
		ω -1	2.12(1H)	2.42(5H)	0.15
octadecanoic (stearic)	16	α	1.96(1H)	2.24(2H)	0.06
		secondary	2.10(1H)	2.40(4H)	0.80
		ω -1	2.12(1H)	2.42(5H)	0.15

^a all hfs constants checked by computer simulation

^b deviation from $\Sigma = 1.00$ represent rounding off error.

Table 2.5.1 E.S.R. parameters^a for radicals generated from butyl trifluoro- and butyl acetate

Radical	^a _{α-H}	^a _{β-H}	Rel. concn.
CH ₃ CH ₂ CH ₂ $\dot{\text{C}}\text{H}$ -OCOCF ₃ (14)	2.10* (1H)	2.50 (2H)	not determined
CH ₃ CH ₂ $\dot{\text{C}}\text{HCH}_2$ -OCOCF ₃ (15)	2.20(1H)	2.50(4H)	1.5-2
CH ₃ $\dot{\text{C}}\text{HCH}_2\text{CH}_2$ -OCOCF ₃ (16)	2.30(1H)	2.50(CH ₃) 2.30(CH ₂)	3-4
$\dot{\text{C}}\text{H}_2\text{CH}_2\text{CH}_2\text{CH}_2$ -OCOCF ₃ (17)	2.13(2H)	2.60(2H)	1
CH ₃ CH ₂ CH ₂ $\dot{\text{C}}\text{H}$ -OCOCH ₃	2.12	2.61	1.2-1.3
CH ₃ CH ₂ $\dot{\text{C}}\text{HCH}_2$ -OCOCH ₃	2.12	2.40	1.6-2.0
CH ₃ $\dot{\text{C}}\text{HCH}_2\text{CH}_2$ -OCOCH ₃	2.30(1H)	2.50(CH ₃) 2.30(CH ₂)	2.5-3.0
$\cdot\text{CH}_2\text{CH}_2\text{CH}_2\text{CH}_2$ -OCOCH ₃	2.13(2H)	2.60(2H)	1

* tentative assignment

^a all hfs confirmed by computer simulator

References

1. A.J. Stirton, J. Turer and R.W. Riemenschneider, Oil and Soap, 1945, 22, 81.
2. R.D. Small, J.C. Sciano and L.K. Patterson, Photochem. Photobiol., 1979, 29, 49.
3. A. Crossley, T.D. Heyes, and B.J.F. Hundson, J. Amer. Oil Chem. Soc., 1962, 39, 9..
4. J.G. Endres, V.R. Bhalerao, and F.A. Kummerow, J. Amer. Oil Chem. Soc., 1962, 39, 118.
5. J.G. Endres, V.R. Bhalerao, and F.A. Kummerow, J. Amer. Oil Chem. Soc., 1962, 39, 159.
6. V. Ramanathan, T. Sakuragi, and F.A. Kummerow, J. Amer. Oil Chem. Soc., 1959, 36, 244.
7. M.H. Brodnitz, W.W. Nawar, and I.S. Fagerson, Lipids, 1968, 3, 59.
8. M.H. Brodnitz, W.W. Nower, and I.S. Fagerson, Lipids, 1968, 3, 65.
13. E.H. Farmer, Trans. Faraday Soc., 1942, 38, 340.
14. H.H. Zvidema, Chem. Rev., 1946, 38, 197.
15. G.H. Twigg, Special Suppl. to Chem. Eng. Sci., 1954, 3, 5.
16. F.R. Hewgill, and G.M. Proudfoot, Aust. J. Chem., 1976, 29, 637.
17. F.R. Hewgill, and G.M. Proudfoot, Aust. J. Chem., 1977, 30, 695.
18. F.R. Hewgill, and G.M. Proudfoot, Aust. J. Chem., 1981, 34, 335.
19. H. Taniguchi, K. Fukui, S. Ohnishi, H. Hatano, H. Hasegawa and T. Muruyama, J. Phys. Chem., 1968, 72, 1926.
20. W.T. Dixon, R.O.C. Norman and A.L. Buley, J. Chem. Soc., 1964, 3625.
21. G.P. Laroff and R.W. Fessenden, J. Chem. Phys., 1971, 55, 5000.
22. K. Giben and R.W. Fessenden, J. Phys. Chem., 1971, 75, 1186.

23. A.J. Dobbs, B.C. Gilbert and R.O.C. Norman, J.C.S. Perkin II, 1972, 2053.
24. A.L.J. Beckwith and R.O.C. Norman, J. Chem. Soc. B., 1969, 400.
25. M. Anbar and P. Neta, J. Chem. Soc. A., 1967, 834.
26. E. Bascetta, F.D. Gunstone and J.C. Walton, J.C.S. Perkin II in press.
27. E. Bascetta, F.D. Gunstone, C.M. Scrimgeour and J.C. Walton, J.C.S. Chem. Comm., 1982, 110.
28. a) K.S. Chen, I.H. Elson and J.K. Kochi, J. Amer. Chem. Soc., 1973, 95, 5341.
b) I.H. Elson, K.S. Chen and J.K. Kochi, Chem. Phys. Letts., 1973, 21, 72.
29. a) R.W. Fessenden, J. Phys. Chem., 1967, 71, 74.
b) K.S. Chen, J.P. Battioni and J.K. Kochi, J. Amer. Chem. Soc., 1973, 95, 4439.
c) J.K. Kochi and P.J. Krusic, J. Amer. Chem. Soc., 1969, 91, 3940.
30. A. Veillard in "Quantum Mechanics of Molecular Conformations", (Ed. B. Pullman), Wiley and Sons, New York, Ch 1, pp 1-116.
31. S.S. Butcher and E.B. Wilson, Jr., J. Chem. Phys., 1964, 40, 1671.
32. J.K. Kochi and D.J. Krusic, J. Amer. Chem. Soc., 1968, 90, 7157.
33. See H. Singh and J.M. Tedder, J. Chem. Soc., B, 1966, 605 and references cited therein.
34. C. Walling in "Free Radicals in Solution", John Wiley & Sons, New York, 1957, pp 363.
35. a) S.A. Harrison, L.E. Peterson and D.H. Wheeler, J. Amer. Oil Chem. Soc., 1965, 42, 2.
b) S.A. Harrison, K.E. McCaleb and D.H. Wheeler. Paper presented at the 28th annual fall meeting of the AOCS, October 1954.
c) S.A. Harrison and D.H. Wheeler, J. Amer. Oil Chem. Soc., 1954, 76, 2379.

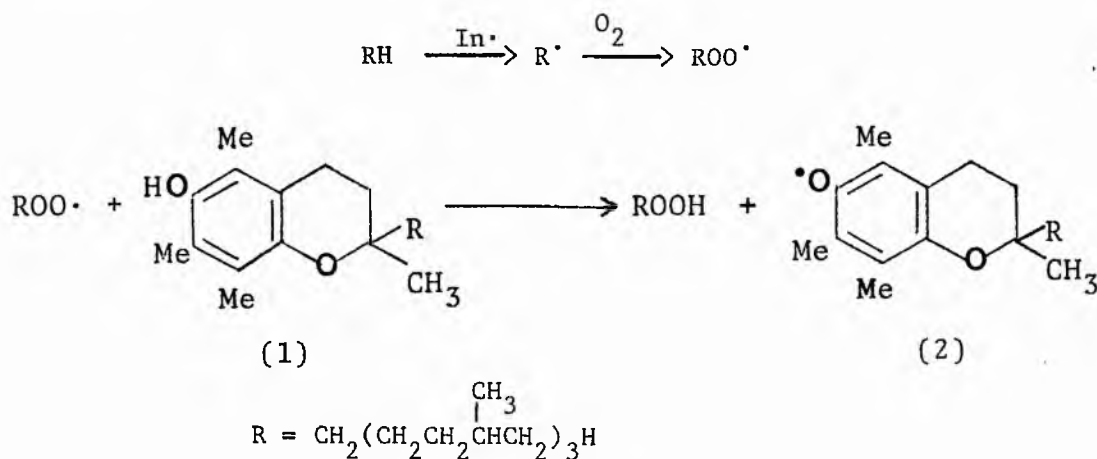
36. A.L. Clingman and D.A. Sutton, J. Amer. Oil Chem. Soc., 1953, 30, 53.
37. a) C.C. Price and H. Morita, J. Amer. Chem. Soc., 1953, 75, 3686.
b) M.S. Kharasch and M.T. Gladstone, J. Amer. Chem. Soc., 1943, 65, 15.
38. a) J.M. Tedder, Tetrahedron, 1982, 38, 313.
39. B.C. Gilbert and A.J. Dobbs in "Organic Peroxides", (Ed. D. Swern)
Vol 3, Interscience, New York, 1972, pp 271.
40. R.O.C. Norman and P.R. West, J. Chem. Soc., B. 1969, 389.
41. D. Behar, A. Samuri and R.W. Fessenden, J. Phys. Chem., 1973, 77, 2055.

Summary

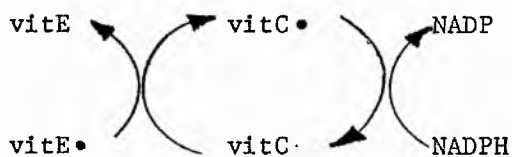
The neutral α -tocoperoxyl radicals, generated in monolayers on silica gel containing α -tocopherol and partly autoxidised methyl linoleate at 90 °C, were detected and identified by E.S.R. spectroscopy. Addition of ascorbic acid to the monolayer resulted in the complete quenching of the α -tocoperoxyl radical spectrum. This lends support to the view that ascorbate transfers hydrogen to α -tocoperoxyl radicals thus regenerating α -tocopherol.

Results and discussion

It is generally accepted that α -tocopherol (1), the major constituent of vitamin E, functions as an inhibitor of fatty acid (RH) autoxidation by transferring a hydrogen atom to the chain carrying peroxy radicals (ROO^\bullet), thus giving rise to neutral phenoxyl radicals (2) [1-4]:



It was proposed by Tappel that in vivo α -tocopheroxyl radicals abstract hydrogen from vitamin C, so regenerating α -tocopherol [5]. The vitamin C radical produced in this way may then be reduced back to vitamin C by NADPH:



Packer et al. provided some support for this mechanism by their pulse radiolysis study of α -tocopheroxyl radicals generated in a water-isopropanol-acetone solution containing carbon tetrachloride^[6]. The decay of the absorption spectrum of the α -tocopheroxyl radicals was shown to be much more rapid in the presence of vitamin C; thus indicating a fast reaction between radical (2) and vitamin C.

We have studied the effect of vitamin C on the α -tocopheroxyl radical in a model membrane system using E.S.R. detection. In solution radicals (2) have a characteristic E.S.R. spectrum with a large number of narrow hyperfine lines, and have been observed by several groups of workers^[7-9]. We found that the half-life of radicals (2) in hydrocarbon solutions at ambient temperature was of the order of 10s. This suggested that these radicals should be sufficiently long lived for E.S.R. detection when generated thermally in a monolayer coated on silica gel. Methyl linoleate containing 5 % α -tocopherol was coated in a monolayer on silica gel^[10]. The coated silica gel was placed in a quartz E.S.R. tube, the air was removed by gentle pumping, and the tube was transferred to the cavity of the spectrometer. An E.S.R. signal appeared on raising the temperature and the strong spectrum shown in the Figure (b) was obtained at 90°C. The 7 line pattern of hyperfine splittings ($a = 0.5\text{mT}$) is more clearly distinguished with second derivative presentation(Figure (c)). It is clear that the main species present is the α -tocopheroxyl radical (2) even though the spectrum has broad lines and shows fewer hyperfine splittings than can be resolved in solution. It has the same spectral width and the same g -factor as radicals (2). Similarly, the same hyperfine splitting pattern of 7 lines can be observed from radicals (2) generated in toluene solution and observed with high

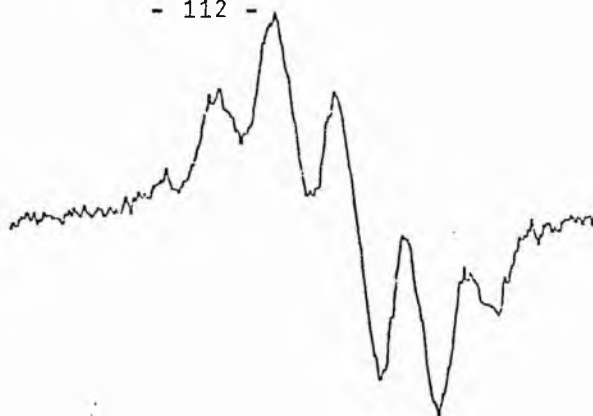
modulation; see Figure (a).

At 90°C the hydroperoxides in the autoxidising methyl linoleate decompose to give alkoxy and other radicals which abstract hydrogen from the α -tocopherol to produce α -tocoperoxyl radicals. A control experiment in which only methyl linoleate was coated as the monolayer on silica gel showed no well defined E.S.R. spectrum but only a broad featureless signal which was several orders of magnitude less intense than that shown in Figure (b) at 90°C. There were no observable signals when neat α -tocopherol was coated as a monolayer on silica gel and heated to 90°C in the spectrometer cavity.

When a monolayer containing vitamin C (3), and α -tocopherol (1) and methyl linoleate was coated on silica gel and examined under identical conditions the α -tocoperoxyl radical spectrum was completely quenched (Figure (d)). It is evident that the lifetime of the radicals (2) is greatly reduced by the presence of vitamin C, probably as a result of the hydrogen transfer reaction, and it becomes too weak for detection. The ascorbyl radicals generated on hydrogen abstraction from vitamin C were not detected; [11] they would be expected to decay too rapidly by combination and/or disproportionation reactions at 90°C.

The results show that in a model membrane, radicals generated from autoxidising methyl linoleate are scavenged by vitamin E to produce α -tocoperoxyl radicals which can be detected and identified by E.S.R. The quenching of the E.S.R. spectrum of these radicals by added vitamin C lends support to Tappel's suggestion that the radicals (2) abstract hydrogen from vitamin C thus regenerating vitamin E.

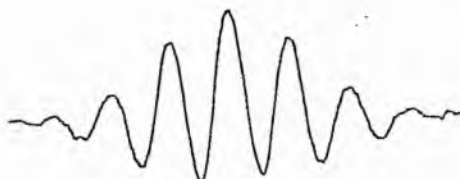
a



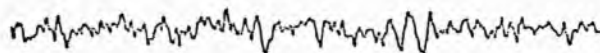
b



c



d



EFFECT OF VITAMIN C (ASCORBIC ACID) ON THE
LIFETIME OF α -TOCOPHEROXYL RADICALS ON A
MODEL MEMBRANE

- (a) 1st derivative e.s.r. spectrum of α -tocopherol in di-t-butyl peroxide and hexadecane solution obtained by photolysis at 320 K. Spectrum obtained with a gain of 2.5×10^4 and field modulation of 6.3 Gpp.
- (b) 1st derivative e.s.r. spectrum of a monolayer containing autoxidised linoleate and α -tocopherol only adsorbed on silica gel. Spectrum obtained at 363 K with a gain of 3.2×10^5 and modulation of 1.0 Gpp.
- (c) 2nd derivative representation of (b).
- (d) 1st derivative e.s.r. spectrum of a monolayer containing autoxidised linoleate, α -tocopherol and vitamin C adsorbed on silica gel. Spectrum obtained at 363 K with a gain of 10×10^5 and modulation of 1.0 Gpp.

REFERENCES

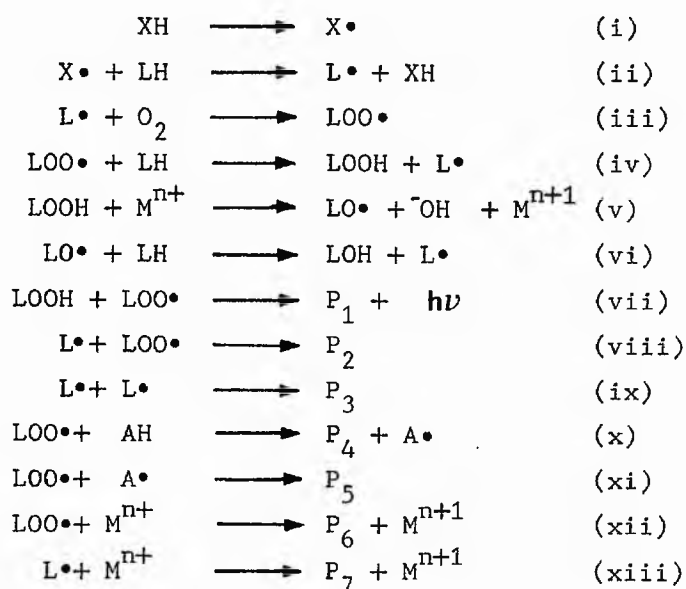
1. W.H. Sebrell, Jr., and R.S. Harris (Eds.) "The Vitamins", 2nd ed., Academic Press, New York, 1972, Vol.5, pp. 166-317.
2. C. De Duve and O. Hayaishi (Eds.) "Tocopherol, Oxygen and Bio-membranes", Elsevier, Amsterdam, 1978.
3. G.W. Burton and K.U. Ingold, J. Am. Chem. Soc., 103, 1981, 6472
4. L.A. Wittig in "Free Radicals in Biology", Academic Press, New York, 1980, Vol.4, pp. 295.
5. A. L. Tappel, Geriatrics, 23, 1968, 97.
6. J.E. Packer, T.F. Slater and R.L. Wilson, Nature, 278, 1979, 737.
7. T. Ozawa, A. Hanaki, S. Matsumoto and M. Mutsuo, Biochim. Biophys. Acta, 531, 1978, 72.
8. W. Boguth and H. Niemann, Biochim. Biophys. Acta, 248, 1971, 121.
9. K. Nukai, N. Tsuzuki, S. Auchi and K. Fukuzawa, Chem. Phys. Lipids, 29, 1981, 129.
10. W.L. Porter, L.A. Levasseur and A.S. Henick, Lipids, 6, 1971, 1.
11. Radicals from ascorbic acid have been observed in solution: see H.M. Swartz and N.J.F. Dodd in "Oxygen and Oxy-Radicals in Chemistry and Biology", N.A.J. Rodgers and E.L. Powers (Eds.), Academic Press, New York, 1981, pp. 161.

Summary.

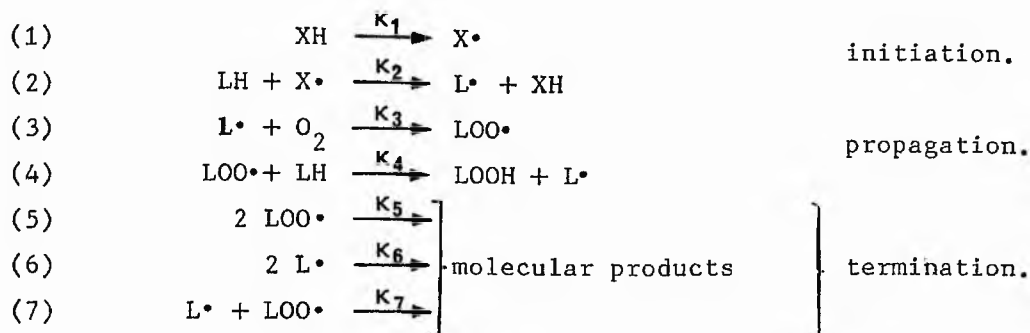
Autoxidation rates of polyunsaturated fatty acid methyl ester monolayers deposited on a silica gel surface at 70°C have been determined. First-order kinetics were observed for all the esters investigated, both as pure compounds or as mixtures of esters differing in degree of unsaturation. The relative rates of autoxidation of methyl oleate : linoleate : linolenate : arachidonate as pure compounds were 1 : 380 : 1140 : 1500. When examined as mixtures the relative rates were 1 : 5.6 : 10.3 : 17.3. The autoxidation rates on silica gel are compared with autoxidation rates of the methyl esters in dodecane at 70°C, for which autocatalytic kinetic profiles are observed. The kinetics of hydrogen abstraction from unsaturated fatty acid methyl esters by photochemically generated t-butoxyl radicals has also been investigated, both for pure compounds and mixtures. First-order kinetics were observed, with relative rates for hydrogen abstraction from oleate : linoleate : linolenate : arachidonate of 1 : 2.4 : 3.7 : 5.3 .

Introduction

Literature pertaining to the susceptibility of unsaturated lipids particularly those containing doubly allylic sites, to peroxidative damage is extensive and encompasses a wide variety of methodologies^[1]. The kinetic analysis of the reaction of the allylic sites with ground state oxygen (commonly referred to as autoxidation) is complex and susceptible to a large number of variables such as temperature, oxygen tension, presence of antioxidants and metal contaminants^[2]. Nonetheless the process may be described by the reaction pattern shown in equations i-xiii, which describe the autoxidation of a lipid (or more generally any olefinic hydrocarbon) in the presence of a radical initiator (XH), a radical inhibitor or antioxidant (AH) and metal catalyst (M^{n+}).



where P_1 - P_7 are molecular products not involved in further chain reactions.



In the absence of radical inhibitor and metal catalyst the scheme is simplified and can be adequately represented by equations 1-7 which can be subdivided into three kinetically distinct types of reaction namely initiation, propagation and termination. Bolland^[3] derived the kinetic rate expression

$$\text{overall rate} = k_2 k_4 k_5^{-1/2} [LH] \cdot \left[\frac{k_3 k_5^{1/2} [O_2]}{k_2 k_7^{1/2} [LH] + k_3 k_5^{1/2} [O_2]} \right]$$

assuming that $k_6^2 = k_5 \cdot k_7$ and that the chain length is long where the square brackets signify concentration terms. At higher oxygen tension when $k_3 \gg k_4$ and $[L\cdot] \ll [LO_2\cdot]$, termination can be assumed to occur entirely by reaction 5 and the equation reduces to

$$\text{rate}' = k_2^{1/2} k_4 k_5^{1/2} [LH]$$

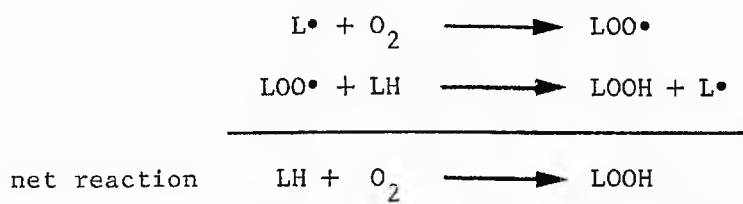
Initiation.

The primordial source of radicals in autoxidation processes has been the subject of speculation and controversy. There is neither sufficient energy nor the proper spin conservation in the reaction ${}^1\text{LH} + {}^3\text{O}_2 \longrightarrow \text{LOOH}$ to allow the reaction to take place^[4]. In vitro, the initiating radicals can be triggered by singlet oxygen^[5], excited states of photosensitisers^[6], radiation^[7] and environmental pollutants such as ozone^[8], nitrogen dioxide^[8a,9] and sulphur trioxide^[10]. In vivo the initiating radicals may have non-lipid origin such as hydroxyl radicals^[11], superoxide anion^[12], and xenobiotic metabolites such as $\text{CCl}_3\cdot$ ^[13]. Some of these radicals may be the intermediates in enzymatic pathways, while others may be formed by metal catalysts^[14].

Irrespective of the radical source the primary reaction of the chain autoxidation will be hydrogen abstraction from the lipid molecule to give the lipid radical $\text{L}\cdot$ which can then react with oxygen at diffusion rates^[15] to give the lipid peroxy radical $\text{LOO}\cdot$ in a spin allowed process. The essential role of the initiating step, is to provide reactive intermediates or chain carriers which then set in motion a series of self-perpetuating facile reactions, or propagation reactions.

Propagation.

The propagation sequence may best be described as a succession of recurring cycles of reactions, the net result of each cycle being to produce one molecule of the primary product (LOOH) and to reproduce the appropriate chain carrier (L^\bullet) for the next cycle, with the consumption of one molecule of lipid and one of oxygen as depicted by.,



The termination of the propagation reaction will be brought about by the intervention of reactions 5 - 7 which remove the chain carriers (L^\bullet and LOO^\bullet). The length of each chain (the number of propagating cycles per initiating radical) will depend upon the balance of the efficiencies of the propagation and termination reactions. Howard and Ingold^[16] have determined the propagation rate constants for the abstraction of a hydrogen atom from linoleate and linolenate to be 64 and $234 \text{ M}^{-1} \text{ s}^{-1}$ respectively at 30°C .

Termination. [17]

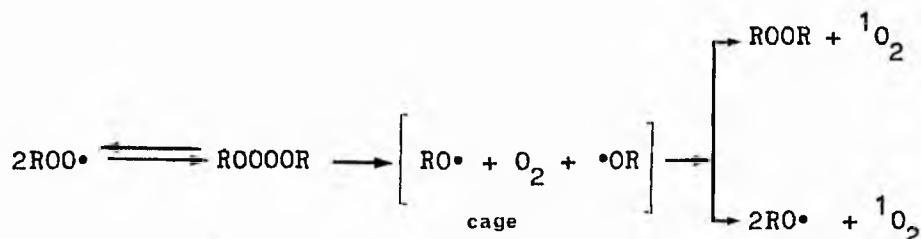
In the absence of metals and antioxidants reactions 5 - 7 describe the events removing chain carriers from the propagation sequence. Two of these are homo terminations while the other is cross termination. At high oxygen tension $[ROO^*] > [R^*]$ and the most important termination step is the self reaction of the peroxy radicals. At low oxygen tension $[R^*] > [ROO^*]$ and reaction 7 will be the principle termination process. At intermediate oxygen tension, the cross termination and at least one of the homo terminations will be important. The exact contribution of each reaction will be intimately linked to the structure of the incipient radicals, as amply demonstrated by Batemann et al. [18] for phytene, linoleate and 2,6-dimethylhepta-2,5-diene which show markedly different contribution profiles with variation in oxygen tension.

However, it is widely considered that under normal autoxidation conditions the self reaction of the peroxy radicals is predominant and this reaction has been extensively studied. The termination rate constants ($2k_t$) were found to be highly dependant on the structure of the radical as shown in Table 1.1 [17,19].

Table 1.1 Bimolecular termination rate constants for alkyl peroxy radicals.

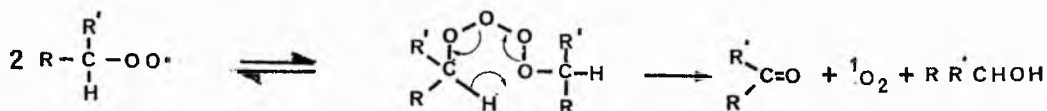
Radical type	$2k_t/M^{-1}s^{-1}$
primary ROO^*	$2-4 \times 10^{-8}$
secondary ROO^*	$4-10 \times 10^{-7}$
tertiary ROO^*	$5-10 \times 10^{-4}$

No alkyl peroxy radical terminates at rates even approaching the diffusion-controlled limit (ca. $2-8 \times 10^9 \text{ M}^{-1} \text{ s}^{-1}$). For tertiary peroxy radicals the slowness of the reaction has been accounted for on the basis of the reversible formation of a tetroxide intermediate^[20].



The formation of the tetroxide is exothermic by 9 Kcal/mole and has a negative entropy of formation (33-40 gibbs/mole). Diffusion out of the cage is 4-5 times as fast as combination. For peroxy radicals, 20% of the encounters are chain terminating.

In contrast essentially all encounters of secondary (and primary) alkyl peroxy radicals that lead to reaction are chain terminating events. Russell^[21] has suggested that an intermediate tetroxide decomposes via a cyclic transition state in which an α -hydrogen is transferred to give the observed products, ketone, alcohol and oxygen.



The mechanism provides an attractive explanation for the difference between secondary and tertiary alkyl peroxy radicals. Several workers have claimed to have identified ${}^1\text{O}_2$ from the self reactions of linoleate peroxy radicals^[22,23] although some of this work has been questioned^[24].

SECTION 1

Autoxidation of unsaturated fatty acids in a model membrane

2.1 Introduction

The autoxidation of hydrocarbon films of limited thickness on surfaces of high specific area have been studied by a few workers^[25-28] prior to 1950. Other workers have used films of lipids deposited on filter paper to study rancidity^[29,30]. Taufel^[31] studied autoxidation of lipids on chromatography paper, while Spruyt^[32] employed glass beads as a means of surface expansion. In 1961, Togashi *et al.*^[33] reported on the autoxidation of thin films of lipids deposited on glass and dried gelatin surfaces. In all of these cases however, layers were estimated to be greater than several hundred molecules in thickness.

Honn *et al.*^[34] correlated autoxidation rates with dispersion of soybean oil on the surface of highly porous silica gel. Maximum autoxidation rates were found at well defined oil/solid ratios characteristic of the specific surface area of the adsorbants. At these critical concentrations it was argued that the oil constituted a closely packed monomolecular layer. Leermakers and coworkers^[35,36] made an extensive study of the photochemical reactions of compounds bound to a silica gel surface.

Porter *et al.*^[37] refined the experimental of the previous work and studied the autoxidation of linoleic acid at 80°C. They showed that absorption of linoleic acid onto silica gel from petroleum ether solution conforms to a Langmuir isotherm^[38], consistent with the formation of a monolayer. The theoretical treatment of adsorption from solution at equilibrium is still only partly satisfactory, but Brooks^[39] has found that the Langmuir isotherm is well obeyed by long

chain fatty acid adsorption giving a value of the weight ratio for the theoretical saturated monolayer and for the equilibrium concentration of half-saturation.

Mead et al.^[40] in a more recent study developed the technique after initially studying the nature of the monolayer system with respect to the type of adsorption sites and the orientation of lipid molecules, to determine the systems suitability as a model for a biomembrane. The adsorption of linoleic acid was found to conform to a Langmuir^[38] isotherm showing a definite region of "limiting" adsorption characteristic of monolayer formation and exclusive of multilayer formation, confirming earlier results from Porter's^[37] and Brooks^[39] groups.

Estimates of the cross-sectional area of the fatty acids on the monolayers revealed this to be approximately 80 \AA^2 , considerably greater than the value found at an air-water interface^[40].

Having fully characterized the system Mead et al.^[41] studied the rates of autoxidation of linoleic, linoleic and oleic acid at 60°C . In the silica monolayer system for linoleic acid and its trans isomer, the autoxidation commences immediately without a detectable induction period. This is in clear contrast to the induction followed by an autocatalytic period which characterizes the sigmoid curve that is obtained as a plot of the rate of substrate disappearance in bulk phase autoxidations. This characteristic of monolayer oxidations extends to monolayers that do not saturate the silica gel surface. There is little doubt that the process involves free radicals because of the effectiveness of α -tocopherol and other natural and synthetic antioxidants in inhibiting the reaction.

The product distribution in monolayer oxidation points to other

significant differences from the bulk phase reaction. In the bulk phase autoxidation of linoleic acid, hydroperoxides accumulate as the major primary autoxidation product. In contrast monolayer autoxidation furnishes epoxides as the major isolable oxidation product. The epoxidation is stereospecific yielding cis epoxides from cis olefins and trans epoxides from trans olefins. The production of these compounds is rationalised as a direct result of the ordered arrangement of the unsaturated chains in which the peroxy radical on one chain transfers an oxygen to the double bond of a neighbouring chain (Figure 2.1.1). Any olefinic substance present in this monolayer is epoxidised during the reaction, including oleic acid, which does not form epoxides alone, and cholesterol, of which the α -5,6-epoxide is a known carcinogen.

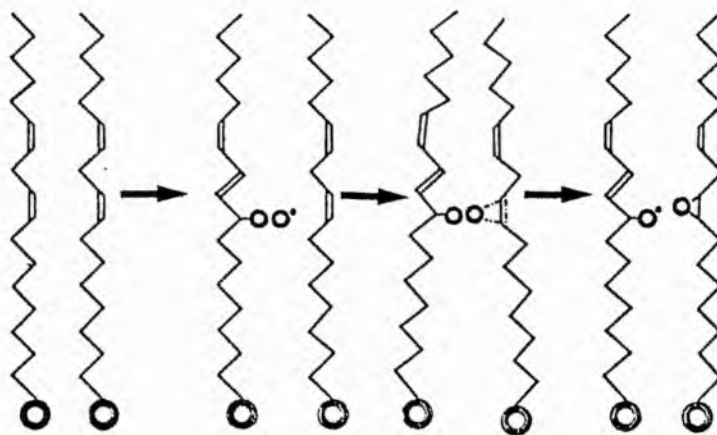


FIGURE 2.1.1 Schematic representation of formation of epoxyoctadecenoates.

At low linoleic surface coverage the product distribution again changes. No longer are epoxides of the type shown in Figure 2.1.1 the predominant product but a more polar product builds up. This product was found to be composed of the isomeric mixture of 11-hydroxy,

9,10-epoxyoctadec-12-enoate and 11-hydroxy-12,13-epoxyoctadec-9-enoate.

The hydroxyepoxides are free of isomeric compounds in which the epoxide and hydroxy groups are not adjacent. This is consistent with the unimolecular synchronous rearrangement depicted schematically in Figure 2.1.2 and is at variance with the suggested formation of an allyl free radical or ion in the rearrangement. The production of these compounds is attributed to the difficulty of intramolecular oxygen transfer under these conditions with the result that it is transferred intramolecularly. It is apparent, therefore that the rate of the reaction and the product distribution are markedly dependent on the spatial relationships between the membrane components^[42-44].

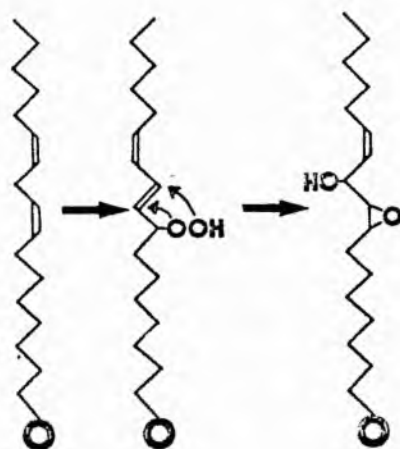


FIGURE 2.1.2 Schematic representation of formation of hydroxyepoxyoctadecenoates.

Instead of decreasing the concentration of linoleic acid by decreasing the surface coverage, the concentration can be decreased by diluting with relatively unreactive saturated fatty acids. The incorporation of saturated fatty acids decreases the apparent first order rate of autoxidation of linoleic acid in proportion to the

amount of saturated acid present^[42-44]. The maximum effectiveness of inhibiting the autoxidation of linoleic acid occurs when the terminal methyl end of the saturated acid extends to the vicinity of the methylene interrupted diene.

Cholesterol acetate, but not cholesterol incorporated into a linoleic acid monolayer acts as though it were a saturated fatty acid in that it decreases the rate of autoxidation of linoleic acid.

When α -tocopherol was included in the linoleic monolayer, an induction period resulted during which little oxidation of linoleic acid occurred. When the antioxidant had decreased to 10 % of its starting proportion, oxidation occurred at the same rate as if the antioxidant had not been there at all. α -Tocopherol produced a longer induction period but allowed a slow oxidation during this induction. A synthetic antioxidant, 3-[w-carboxynonyl]-4-methoxy-5-pentyl-phenol, represented a more extreme case of the same type of antioxidant action in that it produced a long induction period during which slow oxidation took place. It is interesting that tocopherol continues to protect the fatty acids from oxidation even at 10 % of the initial concentration of 0.04 mol %^[42-44].

2 Results and discussion

2.2.1 Characterisation of the monolayer.

Silica gel G was supplied by Camlab, and contained 13% calcium sulphate demi-hydrate as binder. Previous workers^[37,40,41-44] have pointed out the importance of the metal content of the support in autoxidation studies. Table 2.2.1.1 gives values of an atomic absorption analysis of the silica gel both prior to and after exhaustive washing with concentrated nitric and hydrochloric acid in distilled water (1:1:2 v/v, 3 x 100ml). Before the acid wash the predominant multivalent metals found, in order of decreasing amount were iron, zinc, chromium, nickel and copper. After acid wash treatment none of the metals could be detected over and above the blank value.

Table 2.2.1.1 Atomic absorption analysis of silica
gel prior to and after acid washing.^a

	iron	zinc	copper	cobalt	nickel	chromium
silica (untreated)	3.64	1.24	0.20	0.14	0.42	1.05
silica acid washed	0.70	0.22	0.13	0.14	0.18	0.71
acid blank	0.90	0.22	0.13	0.16	0.25	0.72

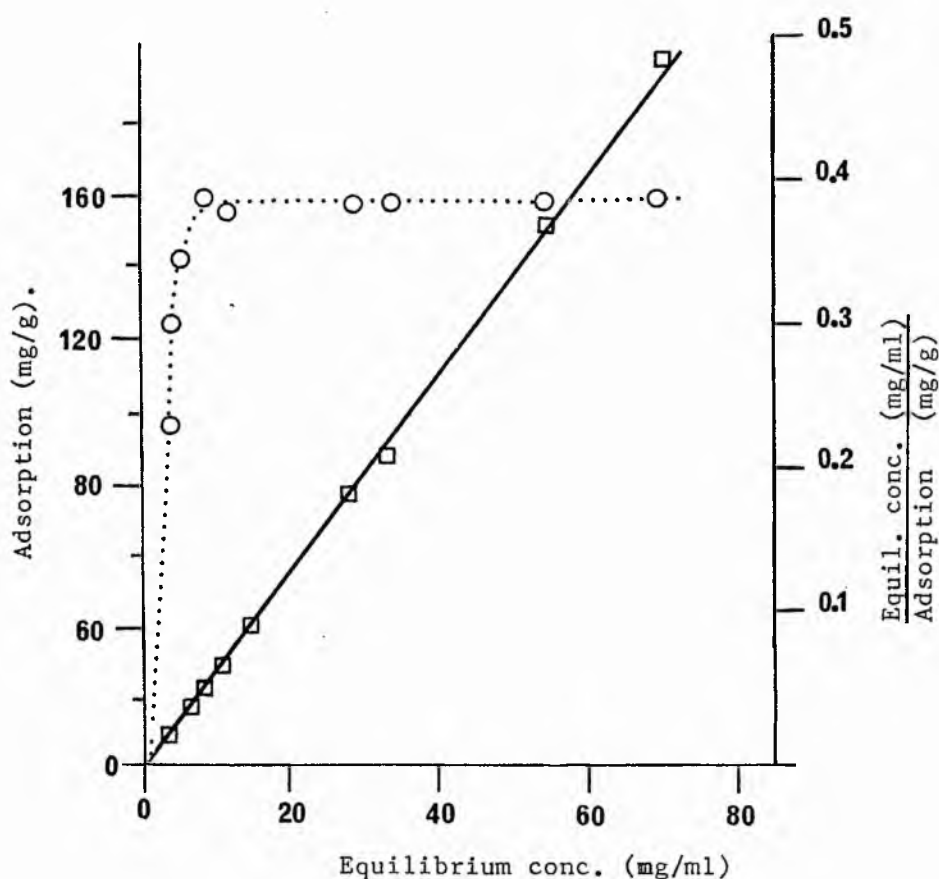
^a data given in ppm of the final acid solution.

When iron is determined in the presence of cobalt, copper and nickel the value may be depressed, similarly the mineral acids will also reduce the sensitivity to iron. Silicon is also known to depress the iron signal, but this can be overcome by the addition of 0.2 % calcium chloride. Presumably the calcium sulphate present as binder will have a similar effect. The presence of high concentrations of iron and chromium in the untreated silica gel may increase the nickel determination and hence this value is probably underestimated. Many of these interferences will be self-eliminating in the presence of a control reference. The main fact arising from the analysis is that after acid treatment no metals could be washed from the silica.

Since we intended to vary the type and degree of unsaturation of fatty acid methyl ester on the monolayer, it was important to establish the 'limiting' absorption characteristics for a representative of each type of unsaturation to be investigated. The results of limiting adsorption values determined from Langmuir isotherms are given in Table 2.2.1.2. The limiting values are in the range 156-165 mg ester per gram of silica irrespective of the nature of the ester. This observation supports similar findings by Mead et al^[40]. Our limiting value however, is lower by approximately 20 % than the value obtained in their work. This may possibly be due to differences in surface area of the silica, which we did not determine.

To ensure monolayer coverage we used slightly more than the calculated limiting value when forming the monolayer. However after removal of the solvent (see experimental) this will lead to a maximum

excess of 10 % on the monolayer. Although Mead *et al*^[41] coated their silica to within 85 % of the limiting absorption value to minimise multilayer formation, the results of Honn^[34] on the variation of rates of oxidation with surface coverage showed that within ± 15 % of the limiting true monolayer coverage, autoxidation rates were essentially constant.



Conventional (·O·) and Langmuir (-□-) plots of adsorption of methyl oleate on silica gel G at 25°C as a function of equilibrium concentration in hexane solution.

Table 2.2.1.2

Methyl ester	Limiting absorption value (mg ester/g silica)
stearate	1.65 \pm 0.09
oleate	1.59 \pm 0.08
linoleate	1.63 \pm 0.05
linolenate	1.68 \pm 0.10
ricinoleate	1.58 \pm 0.09
vernolate	1.61 \pm 0.11
stearolate	1.63 \pm 0.07

We chose to have a slightly larger value (at the risk of a small amount of multilayer formation <10 %) since preliminary screening experiments with methyl linoleate suggested that reproducibility from experiment to experiment was optimum under these conditions although no substantial difference in rates were observed either way.

2.2.2 Monounsaturated fatty acid esters.

Table 2.2.2.1 presents first order rate constants for monounsaturated fatty acid esters differing in position, type and stereochemistry of unsaturation. The autoxidation occurs slowly taking several months to obtain 50 % consumption of the starting material. As can be seen from the correlation coefficients the experimental scatter for this series of experiments was considerably larger than we had originally anticipated. Factors inherent to this experimental error were the small amounts of sample available, the length of time required to keep the standard solutions and probably more importantly variation in environmental factors such as relative humidity. It should be stressed however that in all the data the somewhat low correlation coefficients represents experimental scatter and not a deviation from first order kinetics (the acetylenes may be an exception as discussed below). Nonetheless several important facts arise from the data. No systematic trend was observed in the first order rate constants with variation of the position of unsaturation along the alkyl chain. All the olefinic esters autoxidised with rate constants in the range $3-20 \times 10^{-8} \text{ s}^{-1}$. We had originally hoped to be able to observe subtle differences in rates of autoxidation with varying position of unsaturation and also with the stereochemistry of the unsaturation. The position of the unsaturated centre in the alkyl chain will affect the conformation of the molecule. As the double bond approaches the carboxyl group the molecule adopts a more bent structure and hence can be expected to occupy a greater "effective molecular diameter" which may subsequently affect the ease of

intermolecular propagation in the monolayer system. Similar arguments can be expounded for cis and trans and also acetylenic unsaturation. The trans olefinic and acetylenic functions do not alter the conformation significantly from the conformation adopted by a saturated ester, whereas the introduction of a cis double bond into the C18 backbone has a much more pronounced effect and tends to bend the molecule at the site of unsaturation as shown by molecular models in Figure 2.2.2.1.

FIGURE 2.2.2.1

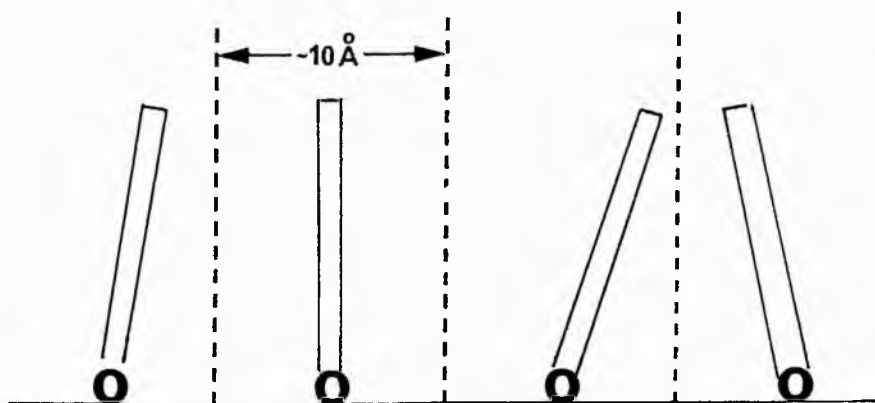
Molecular models of
a) oleic
b) elaidic and
c) stearoleic acids.



However in the silica gel monolayer model membrane the critical parameter defining the closeness of the packing will be the number of isolated hydroxyl groups on the silica surface available for hydrogen bonding with the fatty acid ester head group^[40]. Hence the adsorption limit, will be governed by the nature of the silica surface and not by the conformational or configurational preferences of the

fatty acid esters.

Mead et al have estimated the cross sectional area available per molecule for linoleic acid to be approximately 80 \AA^2 ^[40]. This value is considerably larger than experimental values for stearic acid at an air-water interface where the 'limiting' cross sectional area per molecule is $20\text{-}24 \text{ \AA}^2$ depending on the substrate pH^[45], and for oleic acid a somewhat larger value of $26\text{-}27 \text{ \AA}^2$ under the same conditions has been obtained. There have been reports postulating that the fatty acids adsorbed on silica are close-packed arrays with the hydrocarbon chains orientated parallel to the surface^[46]. However our results from Langmuir isotherm experiments indicate that the limiting adsorption is independent of the type or degree of unsaturation, confirming similar observations by Mead et al^[40]. This, together with an estimated cross sectional area of 80 \AA^2 per molecule suggests that the molecules cannot be close packed arrays parallel to the surface. Hence it is reasonable to assume that the esters are attached by hydrogen-bonding of the head group to the available silanol sites at distances considerably greater than the cross-sectional area of the molecule, giving the hydrocarbon chain an effective area in which it can adopt orientations to the surface. Thus visually the monolayer system may be regarded as hydrocarbon esters anchored at a site but free to sway within a cylindrical volume of surface area of 80 \AA^2 as depicted schematically below.



The large cross-sectional area available per molecule may well account for the lack of significant difference between the rates of autoxidation of the isomeric olefins, although the experimental scatter is undoubtedly a major contribution to this.

The acetylenic esters autoxidise with pseudo first order rate constants in the range $33-45 \times 10^{-8} \text{ s}^{-1}$, which is considerably faster than the rates for the corresponding olefins. However, the data presented in Table 2.2.2.1 for the acetylenes covers only 2 half-lives (approx. 75 % consumption) after which time the autoxidation appears to slow down considerably. For all the examples studied no significant decrease in the acetylenic ester concentration occurred after approximately 1400 h, although prior to this the acetylene is consumed in an exponential manner, giving a good fit to first-order analysis of the data with no significant curving of the semilog plot until this time is reached. Clearly factors other than autoxidation are inherent in this case. Furthermore comparison of the relative rates (k_{rel}) for the monoenes and the acetylenes gives a mean value of 2.8 which is in contradiction with our E.S.R. results for the relative rates of oleate and acetylenes. Although a direct comparison of this result is not really warranted since the radical species involved are different in the two systems the discrepancy is difficult to rationalise since the relative bond dissociation energies of the allylic methylenes and propargylic methylenes suggests that olefins should autoxidise quicker than acetylenes by virtue of an increase in k_2 and k_4 terms in equation 7* which are both hydrogen abstraction reactions from the reactive site in question.

* see introductory section 1.1.

$$\text{Rate} = k_2^{1/2} k_4 k_5^{-1/2} [\text{RH}]$$

Khan^[47] has also observed that acetylenic esters autoxidise faster than olefinic esters.

The method of analysis however, ie. observation of the rate of disappearance of the substrate will not discriminate between processes which remove the fatty ester other than autoxidation (as defined by the reaction sequence 1-7). The acetylenes may polymerise at rates significantly greater than olefinic esters ie. by reaction



Although no product analysis was made to substantiate this assumption, it would account for the increased rate of disappearance for the acetylenes.

Also included in Table 2.2.2.1 are rate constants for the autoxidation of methyl ricinoleate (12-hydroxyoleate) and vernolate (12,13-epoxyoleate). In both cases the oxygen functionality is β -to the double bond and some activation of the double bond may be anticipated, however both esters autoxidise at rates comparable to the non-oxygenated monoenoic esters.

Table 2.2.2.1 Pseudo first order rate constants for monounsaturated octadecanoate monolayers on silica gel at 70°C.

Ester	no. of 1/2 lives	First order constant ($\times 10^{-8} \text{ s}^{-1}$)	corr. coeff
Δ 5c	> 2	6.7	0.981
7c	> 2.5	20.0	0.869 ^a
9c	> 2	15.1	0.920
11c	> 2	3.0	0.979
5t	> 2.7	23.6	0.936
7t	> 1.8	16.1	0.963
9t	> 1.5	13.8	0.915
12t	> 2	11.3	0.951
5a	> 3	33.0	0.955
6a	> 3	41.0	0.974
7a	> 3	36.4	0.941
9a	> 2	34.3	0.973
12a	> 3	44.1	0.982
ricinoleate	> 2	3.2	0.928
vernolate	> 2	19.7	0.989

^a poor correlation coefficient represents experimental scatter and not a deviation from first order kinetics.

2.2.3 Dienes, diynes and higher polyenes.

Table 2.2.3.1 gives experimental values for the first-order rate constants for the autoxidation of fatty acids containing two or more unsaturated sites in the hydrocarbon chain^[48,49]. Methyl linoleate and its stereoisomers containing two methylene interrupted double bonds autoxidise at rates of the order of $4-7 \times 10^{-5} \text{ s}^{-1}$, which is greater than two orders of magnitude more than the rates of autoxidation of the monoenes or monoynes. This value is remarkable in view of reported relative rates for methyl oleate and linoleate in solution or bulk phase work, in which even the most generous values for k_{rel} are no greater than 30^[3,17,51].

The stereochemistry of the double bonds, as found for the monoenes, appears to have no significant effect on the rate of autoxidation although an apparent trend was consistently observed. The all trans isomer appeared to autoxidise consistently slower than the all cis isomer although the range of k values for both isomers overlap considerably, and consequently no real significance can be placed on the small difference. We note however, that Mead et al^[41] also noted that the all trans isomer autoxidised marginally slower than the all cis although no rate constants were calculated.

Dienes containing more than one methylene between the double bonds autoxidise at rates similar to the monoenes. On a purely statistical basis one would have anticipated the dienes to autoxidise approximately twice as fast as the monoenes provided the double bonds behave independently. The discrepancy probably arises from the large experimental scatter of the monoene data.

Only one methylene interrupted diyne was available for comparison with the methylene interrupted dienes. The value of k is reported in Table 2.2.3.1 and is approximately three fold smaller than the corresponding diene. This is in contrast to the situation for the monoenes and monoynes where the latter autoxidises faster by a factor of more than two. However as stated previously the data for the monoacetylenes appears anomalous and the value obtained for the methylene interrupted diyne relative to linoleate is more in accord with expectation, on the basis that hydrogen abstraction from the propynylic methylene will have a higher activation energy than hydrogen abstraction from an allylic methylene.

The two trienes α - and β -linolenate and the tetraene autoxidise with rates of the order $16-19 \times 10^{-5} \text{s}^{-1}$ and $22 \times 10^{-5} \text{s}^{-1}$ respectively at 70°C , which gives values of k_{rel} for oleate : linoleate : linolenate : arachidonate of approximately 1:382:1200:1507. Comparison of this data with previous data obtained from either solution or bulk phase work clearly shows either a marked deactivation (ie. protection) of the monoenes and dienes interrupted by more than one methylene group or conversely an activation of the methylene interrupted polyenes. Clearly conformational differences of the alkyl chains is not the overriding consideration since the dienes interrupted by more than one methylene are equally (if not more) distorted than the methylene interrupted polyenes. The relative rates for linoleate and the higher polyenes is in accord with expectation.

Table 2.2.3.1 Pseudo first order rate constants for
polyunsaturated methyl esters on silica
gel at 70°C.

Ester	no. of 1/2 lives	First order constant ($\times 10^{-5} \text{ s}^{-1}$)	corr. coeff
18:2 Δ 9c12c	> 4	5.73 \pm 1.3	0.993 ^a
9t12t	> 4	4.81	0.981
9c(t)12t(c)	> 4	5.21	0.977
8c12c	> 2	10.30 $\times 10^{-3}$	0.987
6c12c	> 1.5	14.16 $\times 10^{-3}$	0.975
5c12c	> 2	13.85 $\times 10^{-3}$	0.983
13:2 Δ 8c11c	> 4	7.27	0.972
21:2 Δ 8c11c	> 4	5.10	0.988
21:2 Δ 8a11a	> 3	1.70	0.981
18:3 Δ 6c9c12c	> 4	17.40 \pm 1.4	0.992 ^b
18:3 Δ 9c12c15c	> 3.5	16.80	0.995
20: 4 Δ 5c8c11c14c	> 4	22.62 \pm 1.7	0.998 ^c

^a mean corr. coeff. from 8 runs

^b mean corr. coeff. from 5 runs

^c mean corr. coeff. from 4 runs

2.2.4 Mixed monolayers.

In their pioneering work on the silica gel monolayer system Mead et al^[41-44] incorporated other biologically important constituents into the model membrane such as tocopherols, cholesterol and saturated fatty acids. They found that the rate of autoxidation of linoleic acid decreased with the increasing amount of saturated fatty acid incorporated into the monolayer and concluded that the saturated acid was effectively diluting the dienoic acid and hence affecting the chain propagation step. They also observed that the chain length of the saturated fatty acid had an influence on the effectiveness of the inhibition with dodecanoic acid having maximal effect.

We have extended our kinetics on pure fatty acids in which the model membrane can be considered to be homogeneous with respect to the fatty acid, to a system incorporating several fatty acids varying in degree of unsaturation. This situation is obviously more akin to in vivo systems such as biological membranes or seed oils in which a variety of fatty acids are found such as phospholipids and triglycerides respectively, within the system. Subtle variations in fatty acid compositions of membranes has been shown to have pronounced effects on critical functions as permeability and fluidity.

Table 2.2.4.1 gives the rate constants for each component of a variety of natural and synthetic mixtures together with the original composition of the mixture. In these experiments we have made use of the saturated ester present in the mixture as an internal standard and consequently the rate constants presented in Table 2.2.4.1 should be considered as relative rate constants, although we

have assumed that the the saturated esters do not autoxidise in the time scale of the experiment (generally less than 24h). This assumption has been verified in one of the experiments in which an external standard was incorporated and the results were in exact agreement with those obtained using the internal standard. In general the correlation coefficients are considerably superior to those for the monounsaturated homogeneous systems and the rate constants and correlation coefficients are based on the analysis of at least two and frequently three independent runs. No significant discrepancy in any two runs was observed for any of the mixtures analysed. The composition of the mixtures varies considerably, from a pretreated olive oil sample containing only oleate and linoleate to a synthetic mixture containing five unsaturated methyl esters ranging from palmitate to arachidonate.

The pretreated olive oil sample has the slowest rates of autoxidation for both methyl oleate and linoleate. The rate of autoxidation of methyl linoleate is slower than in the homogeneous autoxidation by a factor of 14. Conversely the rate of autoxidation of methyl oleate, is some 5.4 fold faster than in the homogeneous system. The difference becomes even greater when the oleate content of the mixture is decreased with concomitant increase in polyene content. The rate of oleate autoxidation in sunflower oil methyl esters containing a greater amount of linoleate, but no higher polyenes is $1.89 \times 10^{-6} \text{ s}^{-1}$ and the value increases to as high as $6.6 \times 10^{-6} \text{ s}^{-1}$ for mixture A5 (the mixture richest in higher polyenes), which is 44 times faster than in the homogeneous system. All of the higher polyenes autoxidise at rates slower than in their respective homogeneous systems with the exception of methyl linoleate in mixture

A5. We were unable to arrive at a simple relationship describing the relative rates of inhibition or acceleration in terms of bis-allylic and/or allylic methylene content, probably as a result of the non systematic variation in the compositions and the limited number of mixtures investigated. However, the relative rates of autoxidation with respect to methyl oleate (k_{rel}) appear to be only marginally affected by the composition and are reported in Table 2.2.4.2. The value of k_{rel} for methyl linoleate varies by a factor of 1.3 from olive oil to mixture A5, the mean value from all the samples investigated is 5.6 ± 0.6 . The variation in k_{rel} for methyl linolenate from six different mixtures is similar giving a mean value of 10.3 ± 0.9 . Only one mixture containing methyl arachidonate was investigated and a value of 17.3 was obtained. However, since the values of k_{rel} for linoleate and linolenate are in general agreement with the other entries this value can be expected to be reasonably accurate (± 1.0).

Figures 2.2.4.1-7 show the semi-logarithmic plots for the disappearance of each of the components in several of the mixtures investigated. Also shown along with each semi-logarithmic plot is a plot of the varying composition of the monolayers with extent of autoxidation. With the exception of the plot for olive oil methyl esters the compositions vary linearly with time.

Table 2.2.4.1 Pseudo first order rate constants for some natural and synthetic oil methyl esters autoxidising on silica gel G at 70°C.

Oil		16:0	18:0	18:1	18:2	18:3	18:3	20:4
Olive [*]	comp.(%) ₁			79.86	20.14			
	kx10 ⁻⁶ s ⁻¹			0.82	3.98			
	co.coeff.			.964	.993			
Linseed [*]	comp.(%) ₁	0.86	0.28	24.80	28.39	45.15		
	kx10 ⁻⁶ s ⁻¹			6.81	38.21	65.71		
	co.coeff.			.961	.968	.989		
Soybean	comp.(%) ₁	9.18	3.68	23.65	54.87	8.83		
	kx10 ⁻⁶ s ⁻¹			5.11	29.46	50.57		
	co.coeff.			.953	.996	.999		
Spanish seed ^a	comp.(%) ₁	5.41	1.62	13.07	71.40		8.63	
	kx10 ⁻⁶ s ⁻¹			7.01	40.22		72.12	
	co.coeff.			.971	.969		.989	
Sunflower	comp.(%) ₁	6.50	574.80	31.00	58.00			
	kx10 ⁻⁶ s ⁻¹			1.89	11.55			
	co.coeff.			.916	.995			
Evening primrose ^a	comp.(%) ₁	5.30	1.90	14.50	69.80		7.35	
	kx10 ⁻⁶ s ⁻¹			6.89	40.81		69.22	
	co.coeff.			.951	.985		.993	
A4	comp.(%) ₁	13.85		7.55	38.28		40.33	
	kx10 ⁻⁶ s ⁻¹			5.76	26.99		64.66	
	co.coeff.			.982	.979		.979	
A5	comp.(%) ₁	12.00		6.61	28.53		26.24	26.62
	kx10 ⁻⁶ s ⁻¹			6.62	41.75		76.31	114.5
	co.coeff.			.985	.998		.999	.999

^{*} designates pretreated oils
^a also 14:0 (1.2%)

Table 2.2.4.2 Relative rates of autoxidation of unsaturated methyl ester monolayers adsorbed on silica gel G at 70°C.

Oil	k(rel)			
	18:1	18:2	18:3	20:4
Olive	1	4.85	-	-
Linseed	1	5.61	9.65	-
Soybean	1	5.80	10.00	-
Spanish seed	1	5.15	9.23	-
Sunflower	1	6.11	-	-
Evening primrose	1	5.92	10.04	-
A4	1	4.68	11.23	-
A5	1	6.30	11.53	17.30

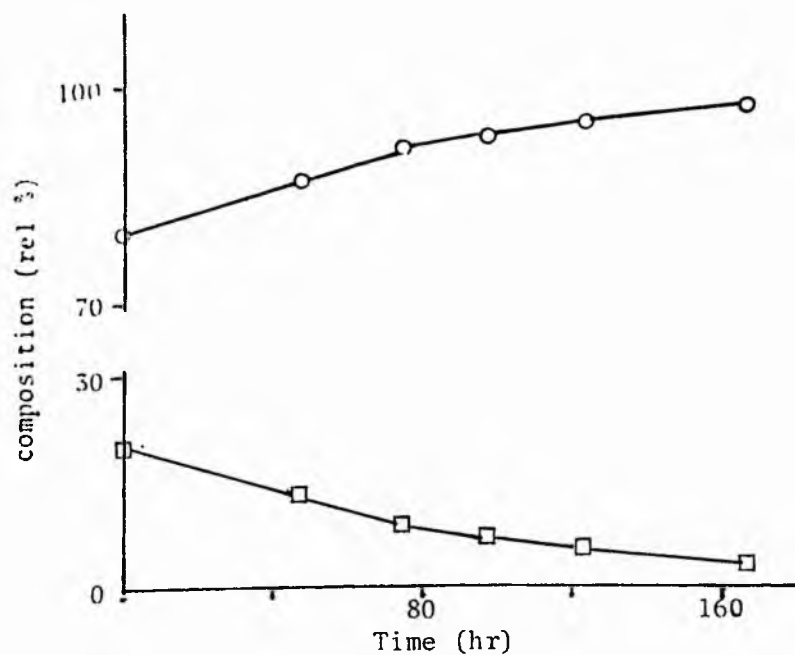
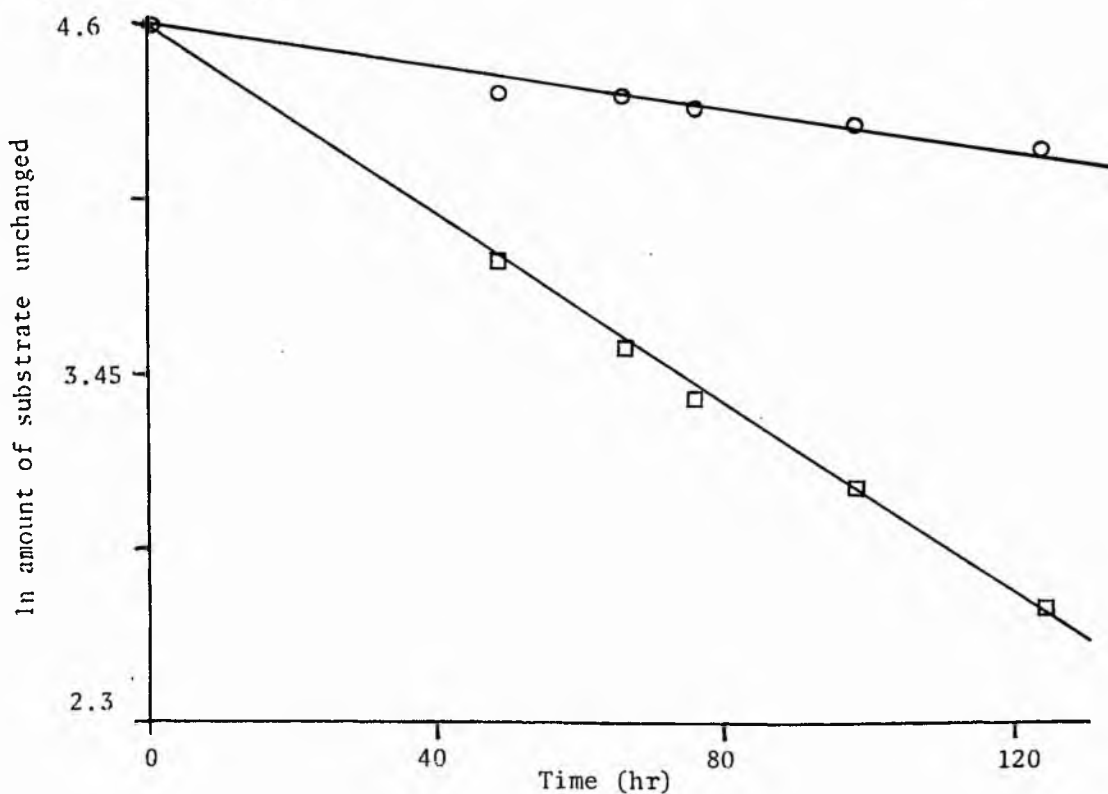


FIGURE 2.2.4.1 Plot of composition of olive oil methyl ester monolayers vs time (hr) autoxidising on silica gel at 70 °C.
-O- methyl oleate, -□- methyl linoleate.



Plot of logarithm of unchanged components of olive oil methyl ester monolayers vs time (hr) incubated at 70 °C.
-O- methyl oleate, -□- methyl linoleate.

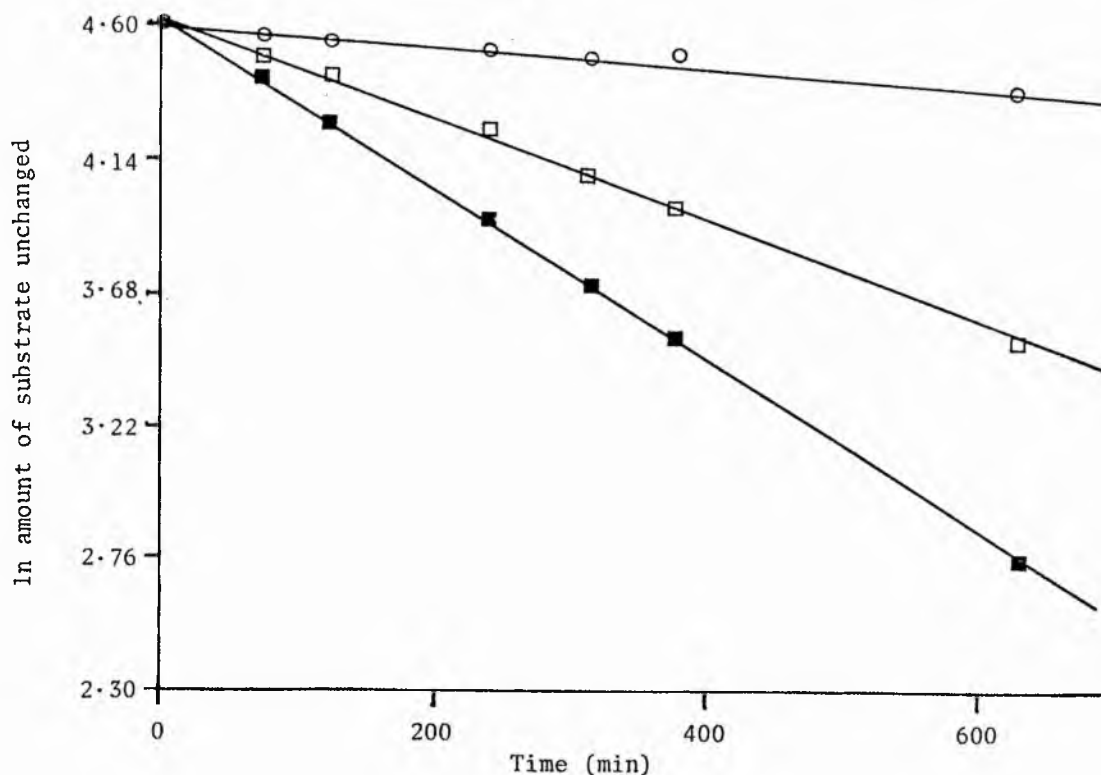
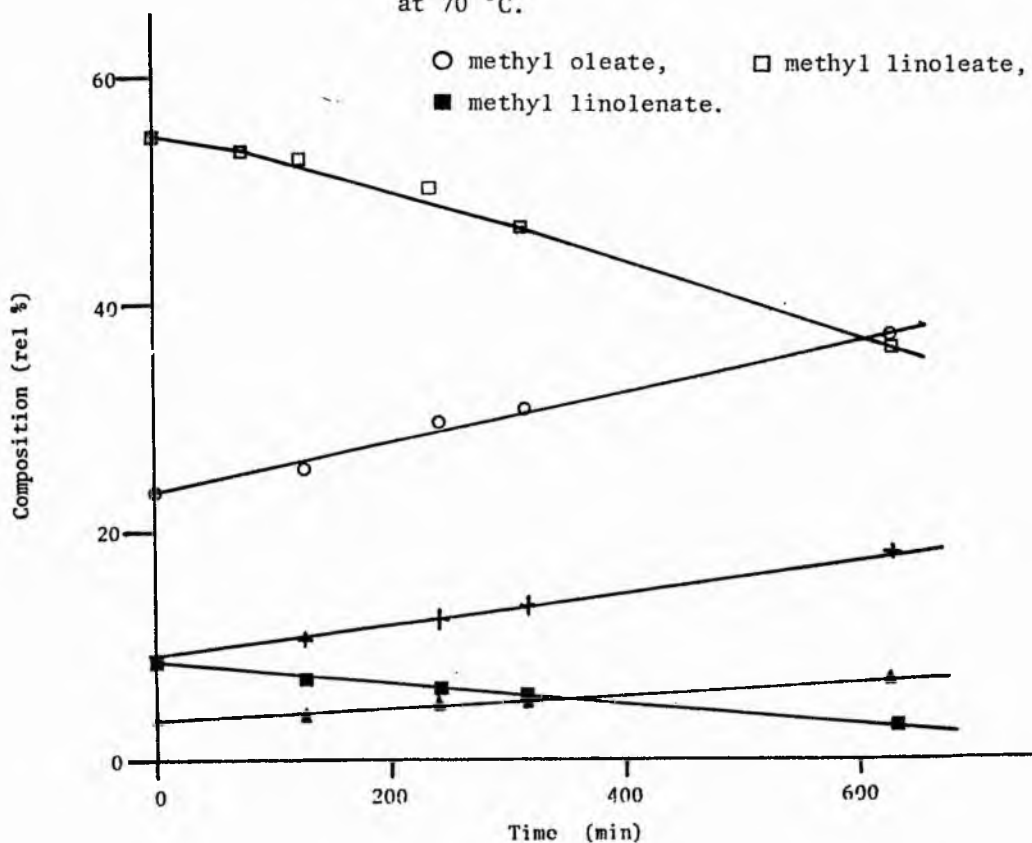


FIGURE 2.2.4.2

Plots of logarithm of unchanged components of soybean oil methyl ester monolayers vs time (min) incubated at 70 °C.



Plots of composition of soybean oil methyl ester vs time (min) incubated at 70 °C.

+ methyl palmitate, ▲ methyl stearate, ○ methyl oleate, □ methyl linoleate, ■ methyl α-linolenate.

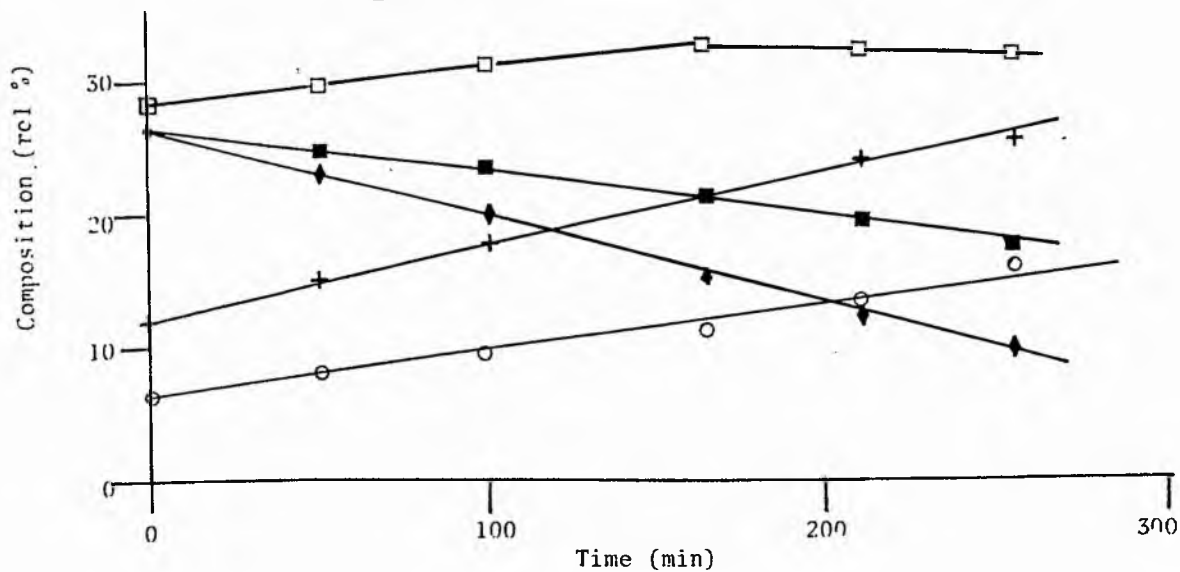
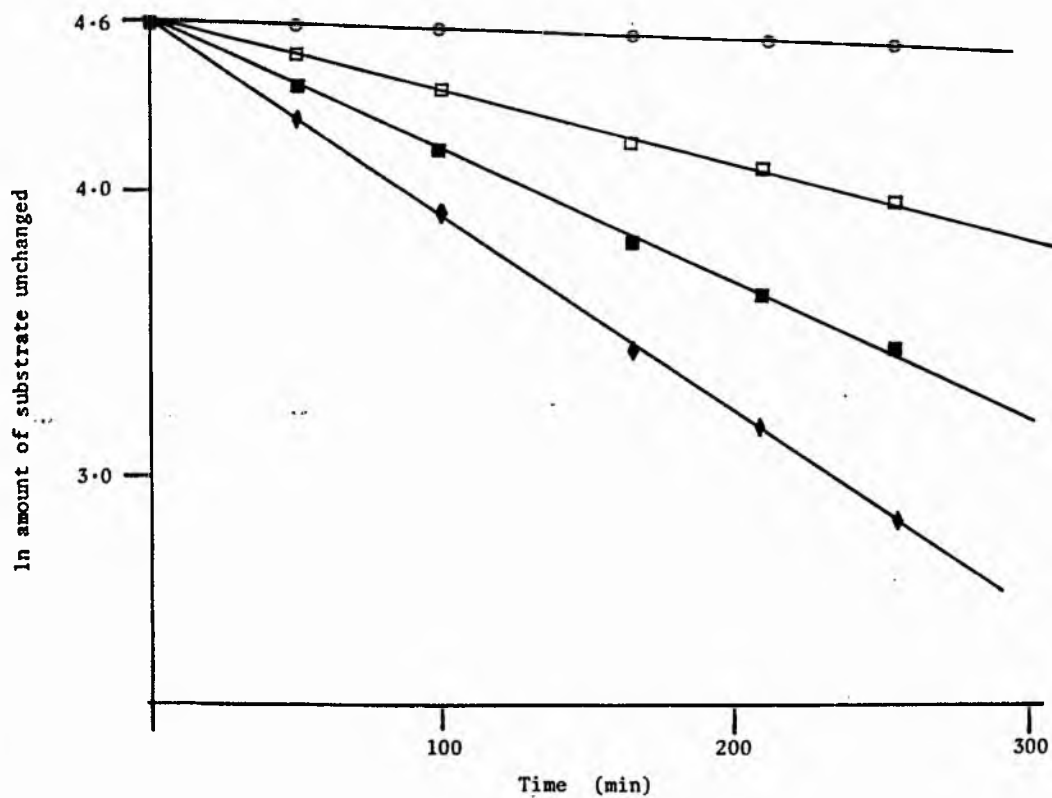


FIGURE 2.2.4.3

Plots of composition of mixture A₅ monolayer vs time (min) incubated at 70 °C.

+ methyl palmitate O methyl oleate
 □ methyl linoleate ■ methyl linolenate
 ◆ methyl arachidonate.



Plots of logarithm of unchanged components in mixture A₅ monolayers vs time (min) incubated at 70 °C.

O methyl oleate □ methyl linoleate
 ■ methyl p-linolenate ◆ methyl arachidonate.

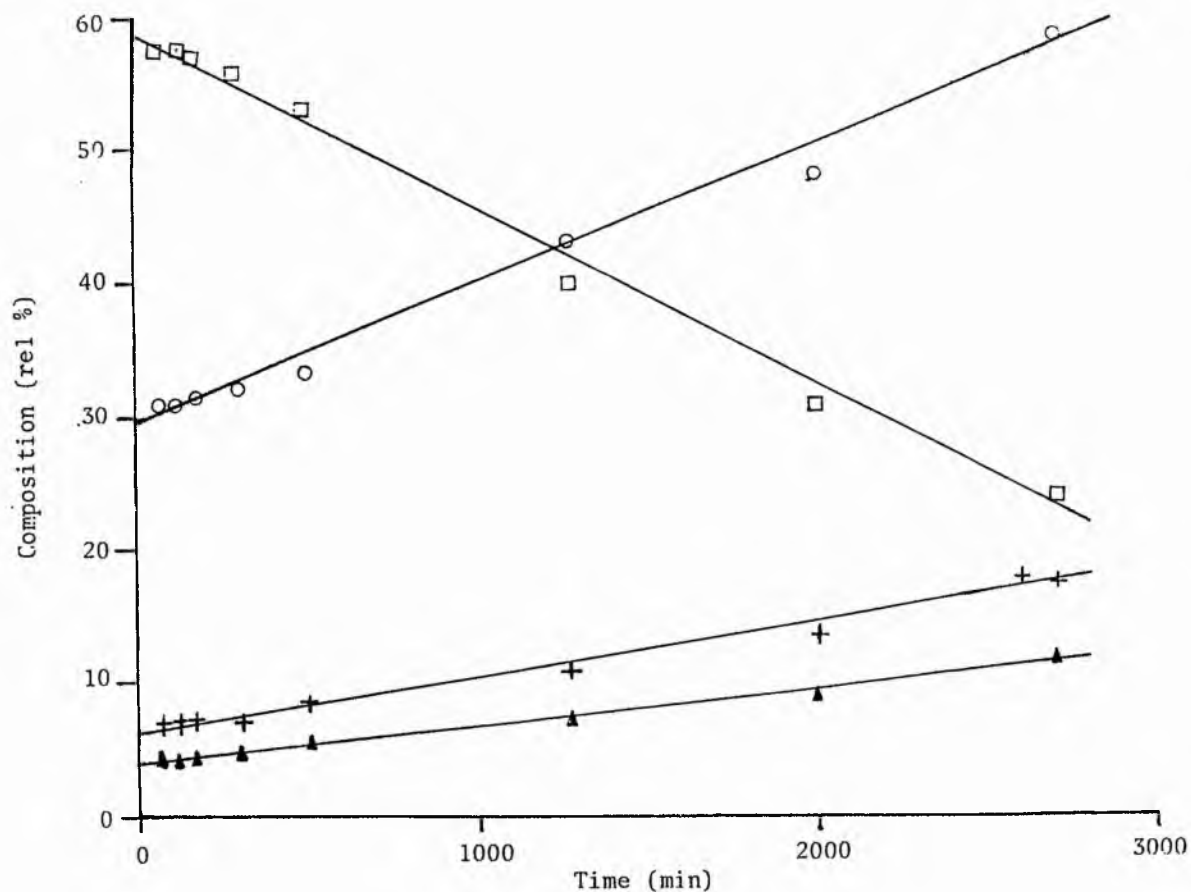
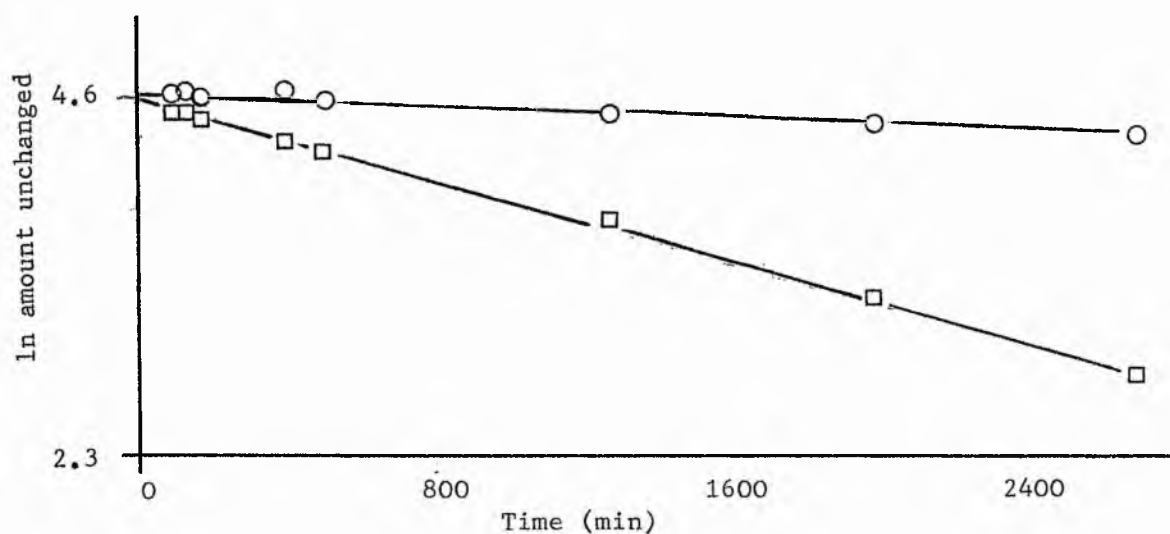


FIGURE 2.2.4.4

Plots of composition of sunflower oil methyl ester monolayers vs time (min) incubated at 70 °C.

+ methyl palmitate, ▲ methyl stearate,
○ methyl oleate, □ methyl linoleate



Plot of logarithm of unchanged components of sunflower oil methyl esters on silica gel vs time (min)

○ methyl oleate □ methyl linoleate

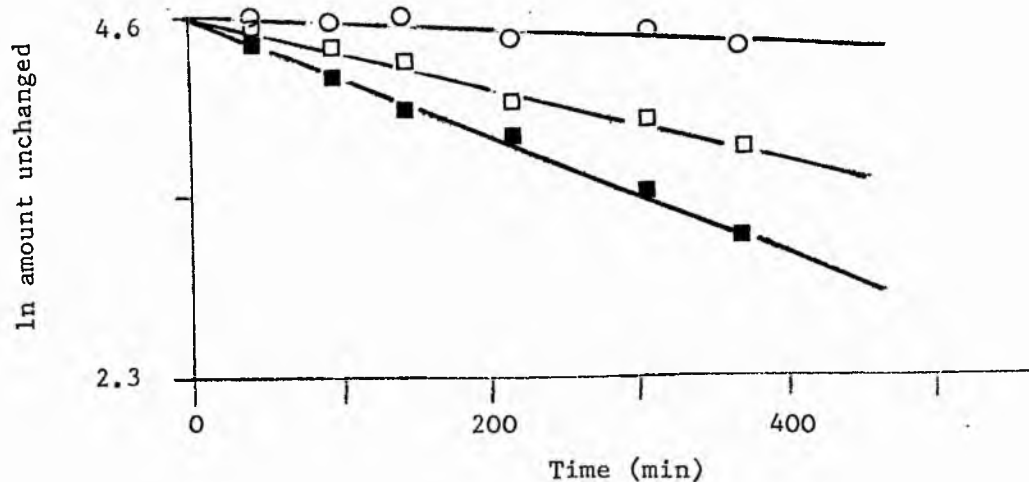


FIGURE 2.2.4.5 Plots of logarithm of unchanged components of linseed oil methyl esters vs time (min).

- methyl oleate
- methyl linoleate
- methyl α -linolenate.

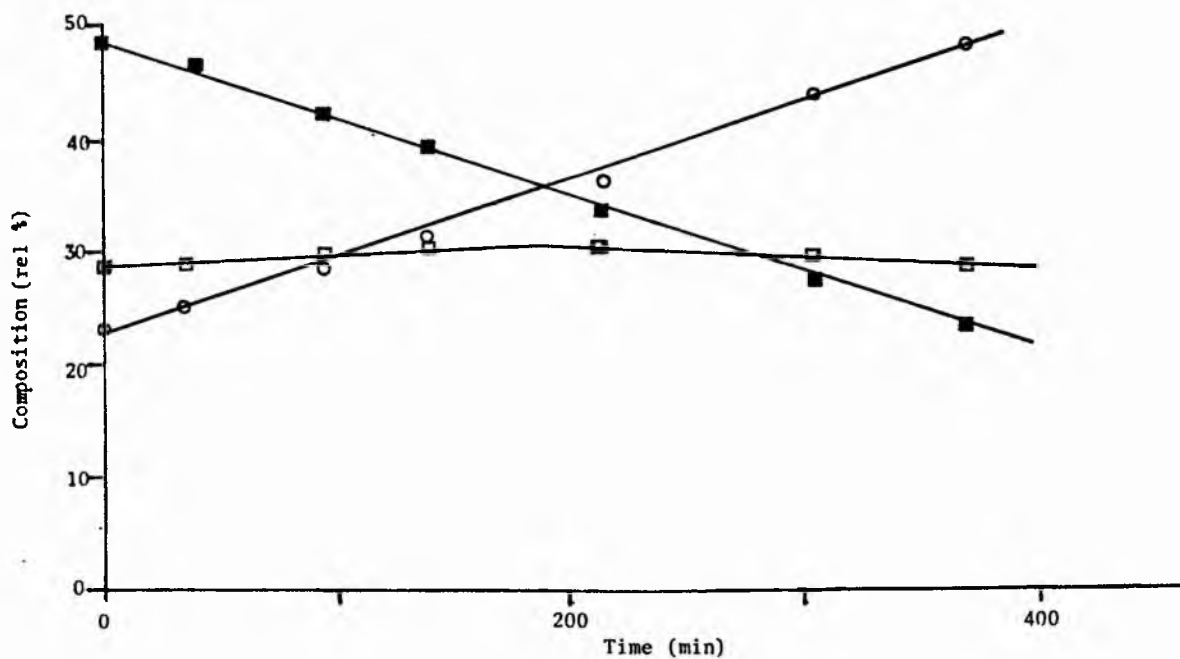


FIGURE Plots of composition of linseed oil methyl ester monolayers vs time (min) incubated at 70 °C. ■ methyl α -linolenate, □ methyl linoleate
○ methyl oleate.

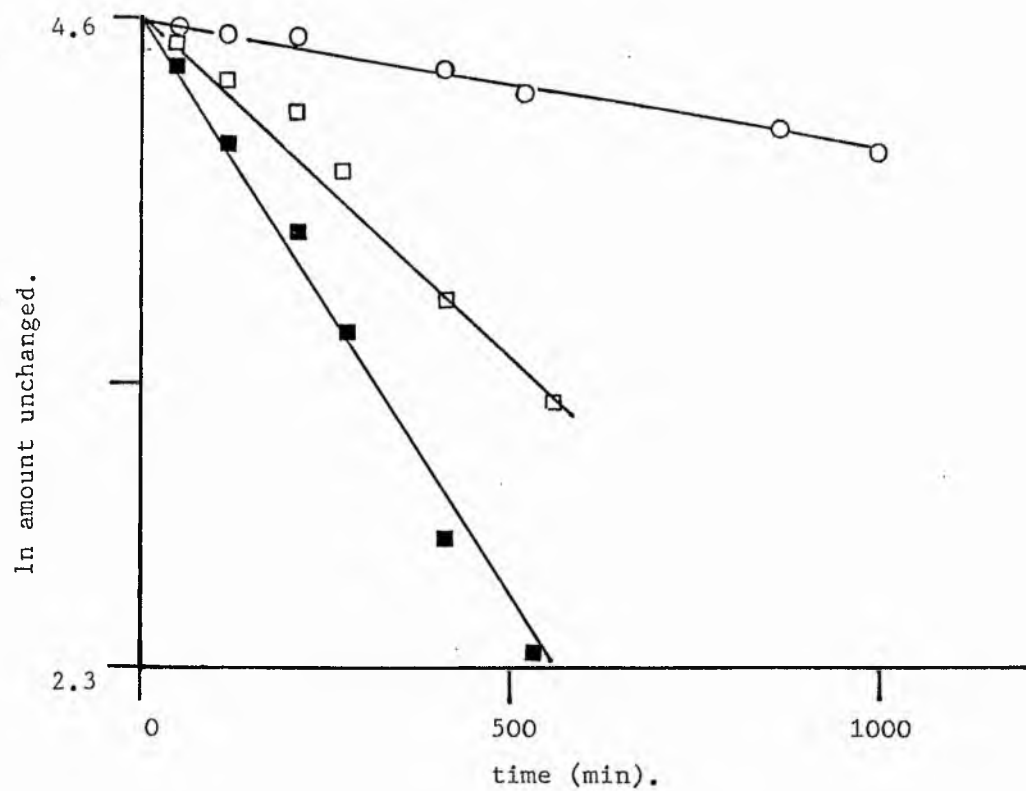


FIGURE 2.2.4.6 Plots of logarithm of unchanged components of spanish seed oil methyl esters on silica gel vs time (min) incubated at 70°C.

○ methyl oleate

□ methyl linoleate

■ methyl p-linolenate.

2.3 Experimental

2.3.1 Preparation of the silica.^[40]

Silica (500g) was stirred for 30min in a mixture of conc. hydrochloric, conc. nitric acids, and water (1:1:2 v/v). The mixture was allowed to settle and the supernatant decanted. The procedure was repeated four times and the silica was then washed with distilled water exhaustively until the washings were neutral. Finally the silica was washed with ethanol (2x150ml) and benzene (2x100ml) before drying in an oven at 110°C.

For the determination of the metal content removable by acid wash, 10g of silica gel were stirred for 60min in 250ml of the acid solution. After which time 50ml of the supernatant was withdrawn and used for the analysis. Two controls were also obtained, one of which was unwashed silica and the other was the acid solution alone.

2.3.2 Determination of adsorption isotherms.

Various amounts (ranging from 10mg to 300mg) of methyl ester were added to 250mg of silica gel and 5ml of sodium dried hexane, in a 25ml Q/F flask. The flask was stoppered and incubated at 25°C for 45min after which time exactly 0.1 ml of this solution was withdrawn from the supernatant and added to an external standard. The relative amount of sample to standard was determined by G.L.C analysis. From the initial and final concentration the amount of methyl ester adsorbed per g of silica gel was calculated.

2.3.3 Adsorption of FAME's on silica gel.

Approximately 62.5 mg of freshly chromatographed methyl esters were accurately weighed in a flask, to which approximately 250mg of silica was added (weighed accurately) followed by the addition of dry redistilled hexane (2.50ml). The flask was sealed with a glass stopper fitted with a two way tap, and shaken for 40min at $25.0 \pm 0.1^{\circ}\text{C}$. After this time the silica was allowed to settle for 10 min, the supernatant was withdrawn as completely as possible by pasteur pipette and the remaining silica dried at room temperature on an oil pump ca 1 mmHg for 15 min. The dry silica was then transferred to a clean vessel to avoid an ester film on the inside of the original flask.

The vessel was then placed in a Pye 104 GLC oven maintained at $70.0 \pm 0.3^{\circ}\text{C}$. Aliquots (20-40mg) were removed after appropriate intervals, weighed accurately and transferred to a 6in glass disposable pasteur pipette. The methyl esters were extracted with 2.0ml of ether/methanol (9:1) added in 0.5 ml portions. An internal standard (methyl palmitate unless otherwise stated) was added and the methyl esters subjected to GLC analysis as soon as possible.

2.3.4 Extraction of the supernatant.

The reproducibility of this step was determined by recording the volume of supernatant extracted from 50 samples. The distribution curve was roughly Gaussian in shape, as expected with a mean value of 2.1 ml and standard deviation of 0.05 ml.

SECTION 2

**Autoxidation of unsaturated fatty acid
esters in dilute solution**

3.1 Introduction

IT has been reported that the autoxidation of methyl oleate exhibits a prolonged induction period before steady state kinetics are observed whereas higher polyenes such as linoleate and linolenate autoxidise with short induction periods^[51]. Gunstone et al^[51] have studied the effect of small amounts of linoleate on the induction period of oleate autoxidation and observed that as little as 0.2% of methyl linoleate significantly reduces the induction period and accelerates the overall rate of autoxidation at 50°C.

Under steady-state conditions the initiation rate is constant, and under high oxygen tension with the assumption of long chain lengths the autoxidation of unsaturated fatty acids can be described by

$$\text{Rate} = k_2^{1/2} k_4 k_5^{-1/2} [RH]$$

as described in the introduction. Much of the pioneering work on olefin autoxidation has been studied under such conditions of steady-state initiation by the use of either thermal or photochemical initiators such as α, α' -azo-bis-isobutyronitrile (AIBN) or benzoyl peroxide respectively^[52].

In this study we have investigated the autoxidation of a variety of unsaturated fatty acids in the absence of endogenous initiator. The autoxidations are carried out at 70° so as to be comparable with the autoxidation kinetics of the monolayer system described in section 2 of this chapter.

3.2 Results and discussion

Table 3.2.1 presents pseudo first order rate constants obtained for the autoxidation of a variety of unsaturated fatty acid methyl esters in dodecane at 70°. The autoxidations are carried out in the presence of an internal standard, either methyl palmitate or heptadecanoate, and we have assumed that these saturated esters are not significantly autoxidised during the experiment. Methyl oleate has been studied previously^[51] and was shown to have an induction period of ca 210 hr at 50°C. In most kinetic studies involving methyl oleate however the ester is isolated from natural sources and may contain "trace" levels of higher polyene material. Figure 3.2.1 shows the rate of disappearance of several unsaturated fatty acid esters with respect to time. Methyl oleate, stearylolate (18:1 Δ 9a) and the dienes interrupted by more than two methylene groups all show large induction periods of up to 1250 hr. This increase in induction period cf. earlier published work may be ascribed in part to the greater purity of the unsaturated esters at the onset of the experiment. The monoolefinic ester shows the largest induction period, followed by the diene, and although the rate of autoxidation of the acetylenic ester is slower than the diene its induction period is shorter. Figure 3.2.2 presents a semilog plot for these methyl esters and their respective pseudo first order constants quoted in Table 3.2.1 were obtained from the steady state autoxidation part of the plots. As can be seen an

excellent correlation is observed with each line representing data from at least two runs. The relative rates of autoxidation of these methyl esters are given in Table 3.2.2 where $k(\text{rel})$ is defined as $k_1 \text{ ester}/k_1 \text{ oleate}$.

The value of $k(\text{rel})$ obtained for 18:2 (6 ω ,12 ω) and 18:2 (5 ω ,12 ω) are only marginally greater than the predicted value of 2.0, if each double bond oxidised independently of the other. The data also suggest that the acetylene autoxidises ca 1.4 fold faster than the monoene, although this result is at variance with our E.S.R. results (chapter 4).

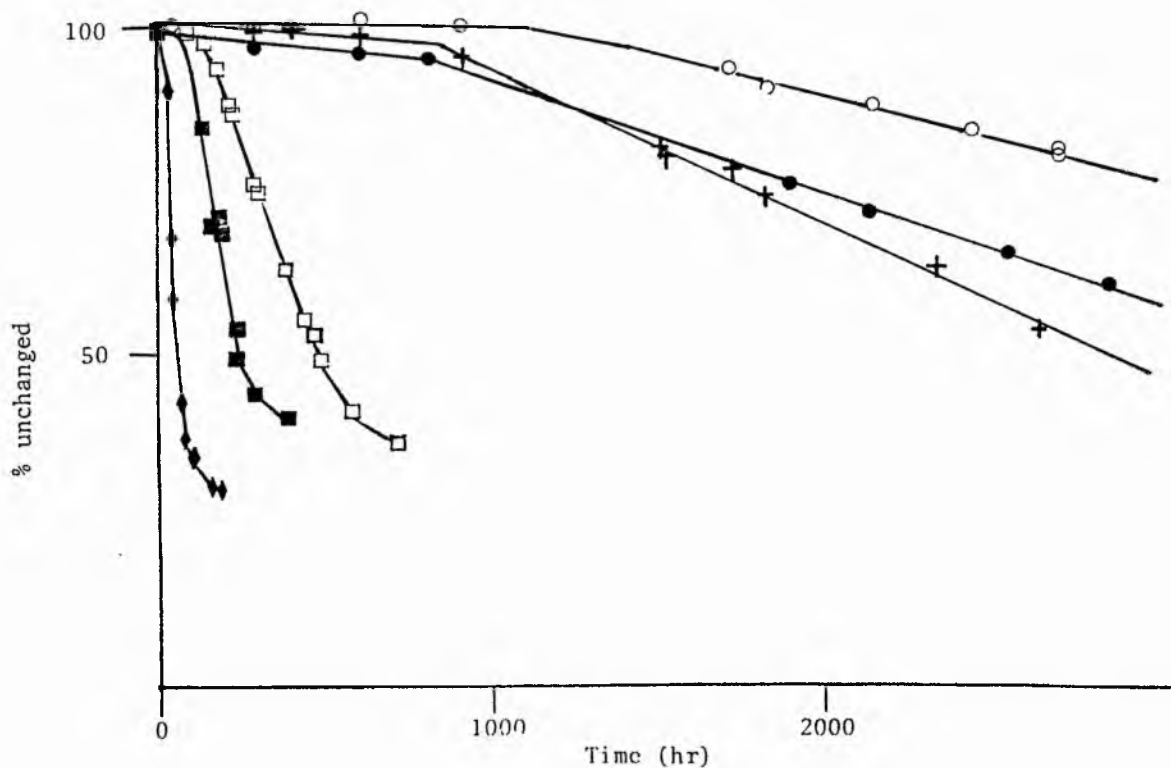


FIGURE 3.2.1

Plots of % of substrate unchanged vs time (hr)
in dodecane at 70 °C

- | | |
|--------------------------------|-----------------------|
| ○ methyl oleate | ● methyl stearolate |
| + methyl octadec-6,12-dienoate | |
| □ methyl linoleate | ■ methyl p-linolenate |
| ◆ methyl arachidonate. | |

Table 3.2.1 Pseudo first order rate constants for the autoxidation of unsaturated fatty acid methyl esters in dodecane at 70°C.

Substrate	conc.(Ml ⁻¹)	kx10 ⁻⁸ s ⁻¹	co.coeff.	t _i (h)
18:1(9c)*	0.0061	4.2	0.982	1250±20
18:1(9a)*	0.0060	5.8	0.971	875±17
18:2(6c12c)*	0.0061	9.0	0.991	1075±15
18:2(5c12c)*	0.0061	10.3	0.981	1090±21
18:2(9c12c)	0.0059	59.8	0.989	135±12
18:3(6c9c12c)	0.0061	158.6	0.992	112±5
20:4(5c8c11c14c)	0.0060	622.2	0.985	26±3

t_i induction period.

* denotes synthetic methyl esters.

Table 3.2.2 Relative rates (krel) for the autoxidation of unsaturated fatty acid methyl esters with respect to methyl 18:1(9c).

substrate	krel
18:1(9c)	1.00
18:1(9a)	1.38
18:2(6c12c)	2.14
18:2(5c12c)	2.45
18:2(9c12c)	14.19
18:3(6c9c12c)	37.76
20:4(5c8c11c14c)	148.09

3.3 Experimental

The samples of fatty acid methyl esters were obtained or synthesised and purified as described elsewhere. All glassware used in this experiment was washed in 1.0M EDTA solution and redistilled acetone before use to minimise metal ion catalysis. Dodecane was twice redistilled before use. 0.06 M fatty acid methyl ester in dodecane (2-5ml) was added to a 25ml Q/F test tube containing an internal standard. The flask was stoppered and placed in a PYE 104 g.l.c oven maintained at 70°C as described for section 2.3.3. Aliquots were periodically injected directly into a GLC and the relative proportions of the substrate and internal standard determined.

SECTION 3

**The reactivity of t-butoxyl radicals
towards fatty acid methyl esters**

4.1 Introduction

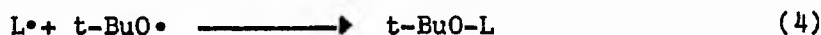
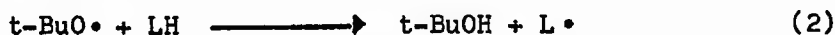
UNDER various conditions, the autoxidation of fatty acids either in vitro or in vivo may be governed by radicals other than peroxy radicals. In biological systems hydroxyl (OH^\bullet)^[11] and alkoxy (RO^\bullet)^[53] radicals may be formed. Likewise, the autoxidation of fatty acids at elevated temperatures or in the presence of metal catalysts may lead to significant amounts of hydroxyl and alkoxy radicals. These species can be expected to have differing specificities towards the various sites of attack in an unsaturated fatty acid molecule, both from each other and from peroxy radicals^[54]. For example, Patterson et al have recently shown that hydroxyl radicals exhibit very little selectivity toward the doubly allylic hydrogens from a linoleic acid anion, using a pulse radiolysis technique^[55]. Using a laser photolysis technique Small et al^[56] have determined the selectivity of t-butoxy radicals towards the possible sites of attack in polyunsaturated fatty acids in benzene solution in the absence of oxygen and obtained relative rates of hydrogen abstraction from secondary : allylic : doubly allylic methylenes to be 1:7:36. In chapter 4 we also determined this ratio using a direct observation E.S.R. technique and obtained values of 1:36:116. In this study we were able to correct the results for hydrogen abstraction from α -carboxyl group and from the ω -1 methylenes which the laser photolysis technique was unable to do. Nonetheless the discrepancy

between the two numerical sets of data is large. On the premise that accurate quantitative data for the selectivity exhibited toward various sites in unsaturated fatty acids by various radicals should contribute to a deeper understanding of lipid peroxidation we have reinvestigated this reaction using yet another technique.

In this section we report the kinetics of oxidation of a variety of fatty acids differing in type and degree of unsaturation in the presence of t-butoxyl radicals. The radicals were generated by photolysis of di-t-butyl peroxide in hexane in the presence of fatty acid ester substrate and in the absence of oxygen. At various time intervals the contents of the reaction were analysed by GLC after the addition of an internal standard and the rate of disappearance of the fatty acid determined.

4.2 Results and discussion

The kinetic equations describing the reactions taking place during the photolysis are given by



assuming that the $[\text{L} \cdot]$ is small relative to the $[\text{t-BuO} \cdot]$ and applying

steady state treatment gives

$$\frac{-d[\text{LH}]}{dt} = \frac{k_1 \cdot [\text{t-BuOOt-Bu}] \cdot [\text{LH}]}{k_5}$$

which in the presence of a vast excess of di-t-butyl peroxide reduces to the pseudo-first order rate equation

$$\frac{-d[\text{LH}]}{dt} = k[\text{LH}] \quad (6)$$

Table 4.2.1 summarises the pseudo-first order rate constants for fatty acid methyl esters at 27°C, and includes an enumeration of secondary, allylic and doubly allylic hydrogens for each ester. As in the study by Small *et al.* [56] we are unable to distinguish between attack at methylenes α -carboxyl, at the ω -1 carbon or the other non-activated sites in the carbon backbone and all these are included as secondary hydrogens.

Before discussing the quantitative details of the results, several qualitative details should be emphasised. The stereochemistry of the unsaturated bond has little or no effect on the reactivity of the site of attack implying that the approach of t-butoxyl radicals is not sterically hindered by conformational effects in the transition state. The kinetic analysis does not take into account the possibility of t-butoxyl radical addition to the double bond.

Although there is only limited data on the addition of alkoxy radicals to olefins^[57], the suggestions are that the extent of addition relative to hydrogen abstraction is very small and to a first approximation negligible. Precedence for a reversible addition stage in the reaction (scheme 4.2.1) is more common however, (we previously made reference to this type of reaction to explain the cis-trans isomerisation of methyl oleate in the presence of t-butoxyl radicals) but will not alter the kinetic treatment.



SCHEME 4.2.1

The relative value of the pseudo first-order rate constants for methyl stearate and oleate/elaidate is approximately $1:3.6 \pm 0.1$. This value may be compared with 1:1.6 obtained by Small et al.^[56] and with $1:5.2 \pm 1.2$ obtained in our E.S.R. study, using $k(\text{rel})$ secondary:allylic = $1:36 \pm 8$. However this latter value has taken into account differences in reactivity of other activated secondary sites besides allylic ones. Assuming that hydrogen abstraction from the methylenes α -carboxyl and at the $\omega-1$ carbon are 2.3 and 2 fold more reactive than non-activated methylenes; correction of the new kinetic data gives a value of $k(\text{rel})$ (oleate/stearate) of approximately 4.1 which is in good agreement with our E.S.R. results. Similar treatment of the data from Small et al.^[56] gives $k(\text{rel}) = 1.8$. The value of $k(\text{rel})$ for linoleate/oleate is 2.2 from the present study which is in excellent agreement with the value

obtained by our E.S.R technique and with the value obtained by Small et al. [56].

Table 4.2.2 presents pseudo-first order rate constants for some less common fatty acid methyl esters, including dienes interrupted by more than one methylene and acetylenic esters. The internal consistency of the results is very good. The monoolefins, dienes and trienes have rate constants of 1.55 ± 0.05 , 3.50 ± 0.1 and $5.65 \pm 0.05 \times 10^{-5} \text{ s}^{-1}$ respectively.

Following the formalism of Small et al. [56] the data may be used to determine $k(\text{rel})$ values for the various types of hydrogen atoms towards hydrogen abstraction by t-butoxyl radicals. Correction for the number of secondary hydrogens in methyl stearate gives a contribution of $0.14 \times 10^{-6} \text{ s}^{-1}$ per secondary hydrogen atom. Application of this value to methyl oleate and elaidate gives a mean value of $0.304 \times 10^{-5} \text{ s}^{-1}$ per allylic hydrogen. In turn these values allow the calculation of $k(\text{rel})$ for a doubly allylic hydrogen atom to be $1.02 \times 10^{-5} \text{ s}^{-1}$. The data may be used to determine the pseudo first-order rate constant for any unsaturated ester by application of equation 6 assuming that each contribution can be treated in an additive manner.

$$k' = 0.014 [H_{\text{sec}}] + 0.304 [H_{\text{allylic}}] + 1.02 [H_{\text{bis-allylic}}] 10^{-5} \text{ s}^{-1}$$

The data predicts values of 5.5 and $7.5 \times 10^{-5} \text{ s}^{-1}$ for linolenate and arachidonate respectively. Both values are within 6 % of the experimental values. A value of $2.7 \times 10^{-5} \text{ s}^{-1}$ is predicted for dienes interrupted by more than one methylene unit. The prediction underestimates the experimental value by 22 %. This is in accord with

the results obtained in dilute solution (section 2 of this chapter) where it was found that the same dienes autoxidised slightly quicker than expected. This may be due to some activation of the non-allylic methylenes in between the double bonds.










Once again the data for the acetylenes is difficult to rationalise. The diacetylenes have rate constants of similar magnitude to the monoacetylenes. Furthermore the rate constants for the monoacetylenes are larger than those for oleate, but the diacetylenes autoxidise slower than the corresponding dienes. This supports the hypothesis throughout this work that reactions other than hydrogen abstraction are contributing to the disappearance of the acetylenes.

Table 4.2.3 presents results obtained for two solutions, containing more than one type of ester. Solution A2 contains stearate, a monoacetylene and a diacetylene. Solution A4 contains stearate and unsaturated esters with 1-3 double bonds. The value of $k(\text{rel})$ with respect to methyl stearate from these mixed solutions are in excellent agreement with the values obtained from Table 4.2.1 and 4.2.2. The semi-log plots for solution A4 are shown in Figure 4.2.2.

The results obtained in this study are also in good agreement with those reported in our E.S.R. study. The relative reactivities providing insight into the degree of selectivity of alkoxy radicals towards the various sites of possible attack in fatty acid molecules.

Although the autoxidation of oils and fats in the absence of contaminants will take place predominantly via peroxy radicals as the chain propagating species, in the microenvironment of a lipid membrane other radicals such as hydroxyl and alkoxyl radicals may play a major role in lipid degradation.

Table 4.2.1 Pseudo first-order rate constants for the reaction of t-butoxyl radicals with fatty acid esters

Fatty Acid	Structure	sec.	allylic	doubly allylic	Rate ^a constant $\times 10^{-5} \text{ s}^{-1}$	Corr. Coeff.
Stearic		32	0	0	0.45	0.983
Oleic		24	4	0	1.5	0.997
Elaidic		24	4	0	1.6	0.993
Linoleic		18	4	2	3.6	0.992
Linolaidic		18	4	2	3.4	0.988
18:2 (c,t)		18	4	2	3.5	0.979
γ-linolenic		12	4	4	5.6	0.991
α-linolenic		12	4	4	5.7	0.988
Arachidonic		10	4	6	7.95	0.983

^a At $27^{\circ} \pm 1^{\circ}\text{C}$ as 0.1M solutions of fatty acid ester in hexane (250 μl) and di-t-butyl peroxide (100 μl)

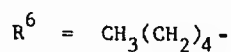
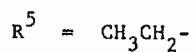
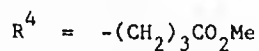
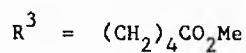
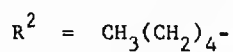
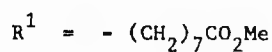


Table 4.2.2

Ester	Pseudo first order rate constant $\times 10^{-5}$	corr. coeff.
18:1 (8a)	2.1	0.986
18:2 (6c,12c)	3.3	0.988
(5c,12c)	3.2	0.981
(8a,12a)	2.0	0.997
(7a,12a)	2.0	0.986

Table 4.2.3

Mixture	composition	%of component	k $/(10^{-6})s^{-1}$	correlation coefficient
A2	18:0	30.7	0.7	0.987
	18:1	33.3	3.7	0.978
	18:2	36.0	3.7	0.988
A4	18:0	24.16	2.0	0.977
	18:1	20.26	8.3	0.992
	18:2	27.82	20.0	0.993
	18:3	27.77	31.0	0.993

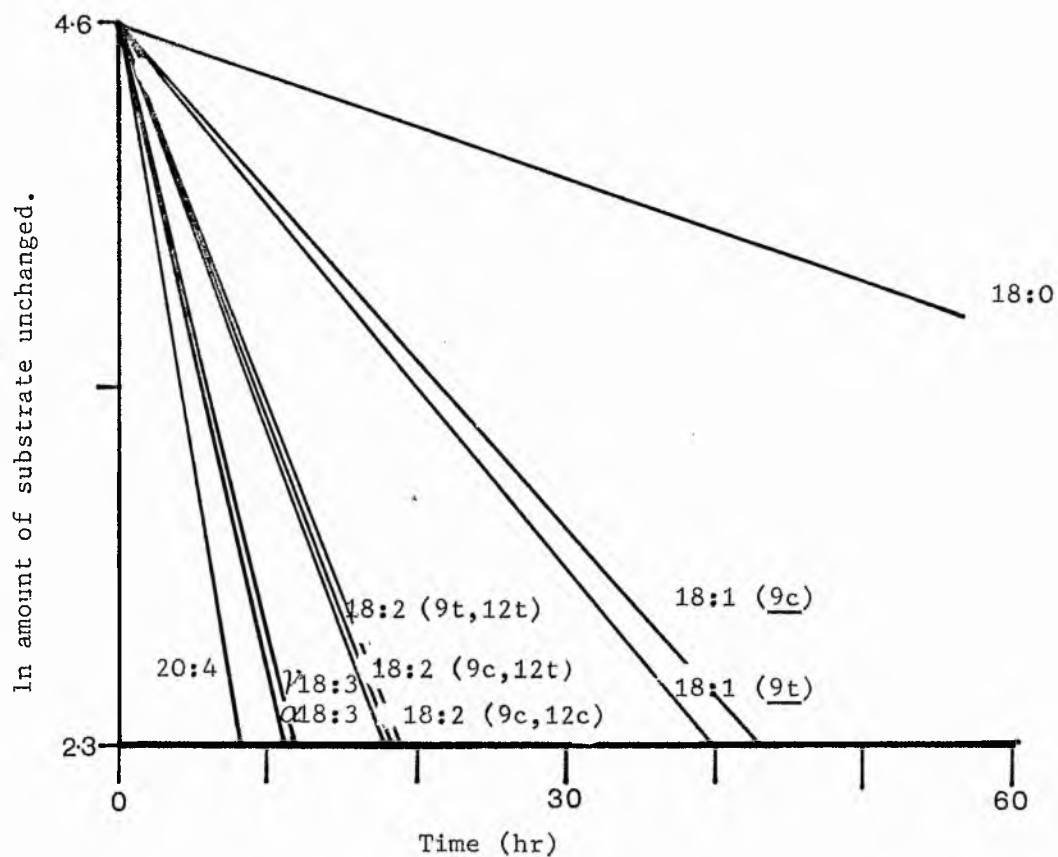


FIGURE 4.2.1

Plots of logarithm of amount of fatty acid methyl ester remaining after photolysis in the presence of di-*t*-butyl peroxide. vs time (hr).

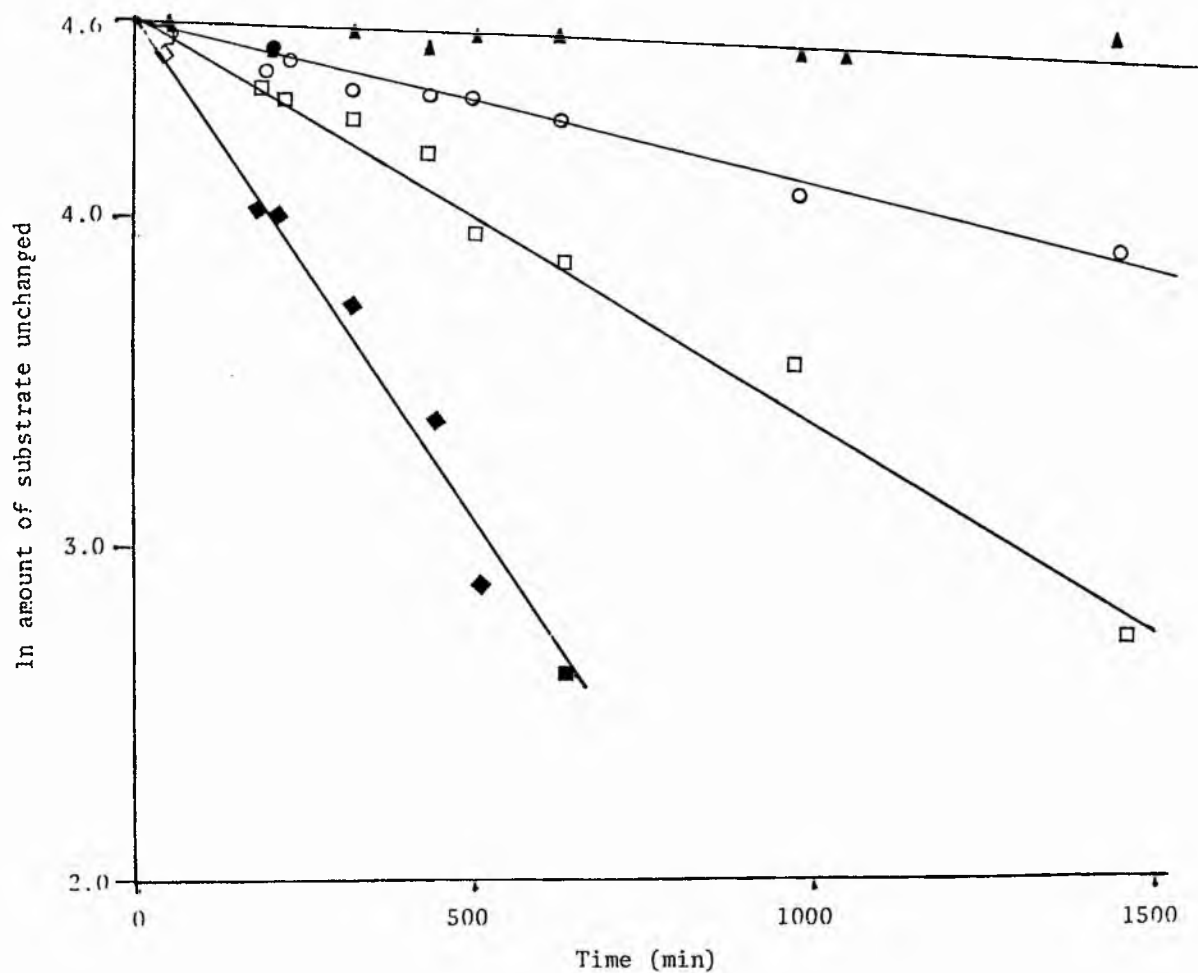


Figure 4.2.2

Plots of logarithm of unchanged components in mixture A4 vs time (min) for reaction with $t\text{-BuO}\cdot$. Symbol designations

- ▲ methyl palmitate
○ methyl oleate □ methyl linolate
■ methyl γ -linolenate

4.3 Experimental

The samples of fatty acid methyl esters were synthesised and purified as described elsewhere (Chapt.4). In all cases purity was in excess of 99% and the esters were free of peroxidic material as judged by TLC (charring and peroxide spray). Solutions were made up to 0.1M in hexane (unless otherwise stated). 250 μ l of this solution was transferred to a quartz tube and degassed by a minimum of three freeze-thaw-pump cycles. The tube was then placed in a photolytic quartz cell through which water at $27^{\circ} \pm 1^{\circ}\text{C}$ was passed. When the solution was considered equilibrated (10-12 min) the photolytic cell was placed in a light box at a preset distance from a Hanova medium pressure UV lamp. After irradiation for a time between 15 and 2,000 min the whole sample was transferred to a vial containing an external standard (either methyl palmitate or methyl heptadecanoate), the quartz tube rinsed with two small volumes of diethyl ether and the washings added to the vial. The disappearance of the methyl esters was determined with respect to the added external standard by either G.L.C. using packed columns (SP2300, SP2340 or EGGS-X as required) or by capillary G.L.C. using both a carbowax (20M) and OV-1 (30M) capillary columns.

5 Conclusions

In this study we have observed the rates of oxidation of several polyunsaturated fatty acid methyl esters either as single components or as mixtures in three diverse systems. Two of these systems proceed via peroxy radicals as the chain carrying species, while the third proceeds via alkoxy radicals. Table 5.1 summarises the relative rates of oxidation of the four common polyene esters with respect to methyl oleate obtained in this work and from the previous chapter on E.S.R. The Table also includes a limited amount of literature data, for a variety of different techniques and radical initiators.

Undoubtedly the most intriguing result in the Table is the large difference in k_{rel} for the monounsaturated fatty acid methyl esters compared with the high polyenes in the homogeneous monolayer autoxidations, and the observation that the relative rates approach the more 'normal' values in the mixed monolayer system.

The results obtained in the dilute solution autoxidations are in accord with those reported by Gunstone *et al.*^[51] in 1946, but are lower than the k_{rel} values reported by Bolland^[3], and by Howard and co-workers^[16,17]. Both of these latter groups use initiating radicals to alleviate the induction period and both used oxygen uptake as the method of monitoring the progress of oxidation. Gunstone *et al.*^[51] used peroxide values as an indicator of extent of autoxidation.

Results from the reaction of *t*-butoxyl radicals with fatty acids/esters under anearobic conditions from three different experimental techniques are more consistent. Small *et al.*'s^[56]

results for k_{rel} for linoleate, linolenate and arachidonate are in excellent agreement with our photolysis and E.S.R. results. The only discrepancies in this work is the value of k_{rel} for oleate and stearate. We have obtained reasonably consistent values for this parameter by both photolysis and E.S.R. techniques, but our value is substantially higher than the value reported by Small *et al*^[56]. The other inconsistency, the difference in k_{rel} for the acetylenes between the photolysis and the E.S.R. experiments has been ascribed to the interference of polymerisation reactions, and the E.S.R. results are believed to be the most accurate.

Also included in Table 5.1 are results from Hasegawa *et al*^[55] who used a pulse radiolysis technique to time resolve many of the individual reactions contributing to the oxidation profile. Their values of k_{rel} for linoleate are in accord with the results obtained in dilute solution in this work and in the bulk phase by Gunstone *et al*^[51]. Their k_{rel} linolenate values however are 1.5-2.0 fold smaller for both the hydroxyl radical and superoxide radical systems. However the relative rates of linoleate and linolenate are approximately 1:2 in the hydroxyl radical system which is in accord with the other autoxidation results. The same parameter for the superoxide radical anion is only 1:1.28 which is closer to the value obtained with the *t*-butoxyl radicals reactions under anearobic conditions, but the k_{rel} with respect to oleate is at variance.

In summary, it is apparent that the absolute and relative rates of oxidation of polyunsaturated fatty acids/esters are intimately dependant upon the initiating radical species, which manifest this difference through different selectivities towards the various sites of attack in the substrate. Furthermore careful evaluation of the

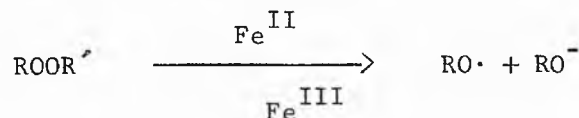
technique employed to monitor the oxidation reaction with respect to all other possible reactions occurring in the system under consideration is essential if misleading results are to be avoided.

The technique used throughout this chapter, namely following the rate of disappearance of substrate ester suffers from the fact that it cannot discriminate between the reactions involved in the oxidation pathway and other reactions such as polymerisation which may also remove substrate. Oxygen uptake experiments have been criticised by other workers^[57] since the apparent oxygen consumption may also include "oxygenation" as well as autoxidation. Furthermore at higher levels of oxidation secondary oxidation products^[58] may be formed, resulting in more than one oxygen molecule reacting per fatty acid substrate molecule. Monitoring reactions by peroxide value is limited to the early part of oxidation since other reactions may remove peroxidic material at higher levels of autoxidation. The laser technique as applied by Small *et al*^[56] and Scaiano *et al*^[59] suffers from similar problems to the GLC method.

Two important aspects of the monolayer autoxidations have not yet been discussed. Firstly the increased rate of autoxidation on the monolayer in comparison to the bulk and solution phase work, and secondly the change in kinetic profile from a typical autocatalytic profile, exhibiting an induction period to an "apparently" induction free first order process.

The increased rate of autoxidation for fatty esters on silica gel parallels similar observations for diacyl peroxide decomposition on the same surface^[50], in which an increase in rate of about 70 fold was observed. In this latter reaction the authors concluded that a larger fraction of the reaction was proceeding by an ionic mechanism on the silica gel than in hexane. This is not too surprising since in their work no attempt was made to reduce the metal content of the silica which contains significant amounts of variable valence transition metals which can catalyse peroxide decomposition by the

well known Fenton 1-electron transfer type reaction.



Comparison of the data in Tables 2.2.2.1 and 2.2.3.1 (monolayer data) with Table 3.2.1 (dilute solution data) shows that the monoenes autoxidise with the same order of magnitude in the two systems although the rates in the monolayer system are between 2-5 times greater than in the dilute solutions. For the dienes and higher polyenes however, the difference between the two systems is even greater, being between 60 and 100 fold greater in the monolayer system.

Although every effort to reduce the transition metal content of the silica was made, by acid washing, it is highly probable that the silica is not 'metal free'. Hence the monolayer autoxidations may be metal catalysed (particularly Fe^{II}). The change in kinetic profile of the reaction can be rationalised in terms of different contributions to the initiation, propagation and termination steps to the overall rate. If the initiation step is made more efficient on the silica surface, possibly as a result of metal catalysis, then the rate equation reduces to that for a steady state initiation rate process namely

$$\text{rate} \propto [\text{RH}]$$

Variable temperature work on methyl linoleate on silica also suggests that some thermal activation is necessary to maintain steady state initiation since an induction period was observed for autoxidations below 33°C.

Table 5.1

Relative rates of oxidation of pure (P) and mixtures (M)
of unsaturated fatty esters in the presence of various radicals.

Abstracting species	Method	Temp	18:1	18:2	18:3	20:4	Ref
			1	29.8	-	-	3
			1	23.3	43.3	-	Howard
	(P) bulk phase		1	12	25	-	16
	(P) dil. soln	70	1	14.2	37.8	148.1	This work
ROO·	(P) monolayer	70	1	380	1140	1500	This work
	(M) monolayer	70	1	5.6	10.3	17.3	This work
	(P) dil. soln	27	1	2.4	3.4		56
t-BuO·	(P) dil. soln	27	1	2.4	3.7	5.3	This work
(anaerobic)	(M) dil. soln	27	1	2.4	3.7		This work
	(P) e.s.r.		1	2.3	-	-	Chapt. 4
·OH ^a	(P) dil. soln		1	8.5	17.5	-	55
·O ₂ ⁻	(P) dil. soln		1	12.9	16.5	-	55

^a These values may reflect some contributions from ·OH and secondary growth.

(P) = pure esters

(M) = mixture of esters

References

1. For recent reviews see
 - a) E.N. Frankel in "Fatty Acids", (Ed. E.H. Pryde), Amer. Oil Chem. Soc., Champaign, Ill, 1979, Ch 17, pp 343-378.
 - b) V. Kamojitzky, Russ. Chem. Rev., 1972, 41, 630.
 - c) A.L. Tappel in "Free Radicals in Biology" (Ed. W.A. Pryor), Academic, New York, 1980, Vol 4, pp 2-48.
 - d) R.O. Recknagel, E.A. Glende, Jr, and A.M. Hruozkewycz in "Free Radicals in Biology" (Ed. W.A. Pryor), Academic, New York, 1977, Vol 3, 97-132.
 - e) J.F. Mead in "Free Radicals in Biology" (Ed. W.A. Pryor), Academic, New York, 1976, Vol 1, pp 51-68.
 - f) L.K. Patterson in "Oxygen and Oxy-Radicals in Chemistry and Biology" (Ed. M.A.J. Rodgers and E.L. Powers), Academic, New York, 1981, 89-96.
 - g) 'Autoxidation in Food and Biological Systems', (Ed. M.G. Simic and M. Karel), Plenum, New York, 1980.
2.
 - a) J.A. Howard in "Free Radicals" (Ed. J.K. Kochi), Wiley and Son, New York, 1973, Vol 2, pp3-56.
 - b) M.G. Simic, J. Chem. Ed., 1981, 58, 125.
3. J.L. Bolland, Quart. Rev., 1949, 3, 1.
4. E.P. Wigner, "Group Theory", Academic, New York, 1959.
5.
 - a) H.R. Rawls and P.J. Van Santen, J. Amer. Oil Chem. Soc., 1970, 47, 121.
 - b) J. Terao and S. Matsushita, J. Amer. Oil Chem. Soc., 1977, 54, 234.
 - c) E. Fedeli, F. Camurati and G. Jacini, J. Amer. Oil Chem. Soc., 1971, 48, 787.

- d) A.H. Clements, R.H. Van Den Engh, D.J. Frost, K. Hoogenhout and J.R. Nooi, J. Amer. Oil Chem. Soc., 1973, 50, 325.
- e) J. Terao, Y. Hirota, M. Kawakatsu and S. Matsushita, Lipids 1981, 16, 427.
- 6. a) H.W.S. Chan, J. Amer. Oil Chem. Soc. 1977, 54, 100
- b) K. Gollnick, Adv. Photochem., 1968, 6, 1.
- 7. a) A.W.T. Konings and S.K. Oosterloo, Radiat. Res., 1980, 81, 200.
- b) A.W.T. Konings, J. Damen and W.B. Trieling, Int. J. Radiat. Biol., 1979, 35, 343.
- c) B.H. Ershoff and C.W. Steers, Jr., Proc. Soc. Exp. Biol. Med., 1960, 104, 274.
- d) T.K. Mandal and S.N. Chatterjee, Radiat. Res., 1980, 83, 290.
- 8. a) D.B. Menzel in "Free Radicals in Biology" (Ed. W.A. Pryor), Academic, New York, 1976, Vol 2, 181-202.
- b) J.N. Roehm, J.G. Hadley and D.B. Menzel, Arch. Environ. Health, 1971, 23, 142.
- 9. a) M. Sagai, T. Ichinose, H. Oda and K. Kubota, Lipids 1981, 16, 64.
- b) H.V. Thomas, P.K. Mueller and R.L. Lyman, Science 1968, 159, 532.
- 10. a) H.C.C. Lizada and S.F. Yang, Lipids 1981, 16, 189.
- b) D. Kaplan, C. McJilton and D. Luchtel, Arch. Environ. Health 1975, 30, 507.
- 11. a) L.K. Patterson and K. Hasegawa, Radiat. Res., 1980,
- b) L.K. Patterson and K. Hasegawa, Ber. Bunsenges. Phys. Chem., 1978, 82, 951.
- 12. a) K. Brawn and I. Fridovich in "Autoxidation in Food and Biological Systems", (Ed. M.G. Simic and M. Karel), Plenum, New York, 1980, pp 429.
- b) T. Galeotti, G.M. Bartoli, S. Bartoli and E. Bartoli, Devel. Biochem., 1980, 118, 106.

13. a) E.S. Reynolds, M.T. Moslen and R.J. Treinen in "Oxygen and Oxy-Radicals in Chemistry and Biology" (Ed. M.A.J. Rodgers and E.L. Powers), Academic, New York, 1981, pp 169-176.
b) R.O. Recknagel and E.A. Glende, Jr, in "Intermediary Metabolism of the Liver" (Ed. H. Brown and D. Hardwick), Thomas, Springfield, Ill., 1973, pp 23.
c) T.F. Slater, "Free Radical Mechanisms in Tissue Injury". Pion, London, 1972.
14. a) G. Sandmann and P. Boeger, Plant Physiol., 1980, 66, 797.
b) N.H. Stacey, L.R. Cantilena, Jr, Klaassen, D. Curtis, Toxicol. Appl. Pharmacol., 1980, 53, 470.
c) N. Ikeda and K. Fukuzumi, J. Amer. Oil Chem. Soc., 1977, 54, 105.
15. S.W. Benson, "Thermochemical Kinetics", Wiley and Sons, New York, 1968, pp 167.
16. a) J.A. Howard and K.U. Ingold, Can. J. Chem., 1967, 45, 793.
17. J.A. Howard, Advan. Free Radical Chem., 1971, 4, 49.
18. L. Bateman and A.L. Morris, Trans. Faraday Soc., 1953, 49, 1026.
19. K.U. Ingold, Acc. Chem. Res., 1969, 2, 1.
20. K.U. Ingold in "Free Radicals", (Ed. J.K. Kochi), Wiley and Sons, New York, Vol 1, 1973, pp 59.
21. G.A. Russell, J. Amer. Chem. Soc., 1957, 79, 3871.
22. a) M. Nakano, K. Takayama, Y. Shimizu, Y. Tsuji, H. Inaba and T. Migita, J. Amer. Chem. Soc., 1976, 98, 1974.
b) K. Sugioka and M. Nakano, Biochim. Biophys. Acta. 1976, 423, 203.

23. E.K. Lai, K-L. Fong and P.B. McCay, Biochim. Biophys. Acta., 1978, 528, 497.
24. N.I. Krinsky in "Singlet Oxygen" (Ed. H.H. Wasserman and R.W. Murray), Academic, New York, 1979, pp 597-641.
25. G.W. Ellis, Biochem. J., 1932, 26, 791.
26. M.J. Nakamura, J. Soc. Chem. Ind. Jap. 1937, 40, 206B.
27. P. George, Trans. Faraday Soc., 1946, 42, 210.
28. D.J. Kreulen and F.G. Kreulen-van Selms., J. Inst. Petrol., 1948, 34, 930.
29. C.H. Lea., J.C.S., Chem. Ind., London, 1934, 53, 388T.
30. P. Dubouloz and J. Laurent, Oleagineux, 1948, 3, 255.
31. K. Taufel, Fette Seifen Anstrichm., 1952, 54, 619.
32. J.P. Spruyt, J. Amer. Oil. Chem. Soc., 1955, 32, 197.
33. H.J. Togashi, A.S. Henick and R.B. Koch, J. Food. Sci., 1961, 26, 186.
34. F.J. Honn, I.I. Berzman and B.F. Daubert, J. Amer. Oil Chem. Soc., 1951, 7, 699.
35. L.D. Weis, T.R. Evans and P.A. Leermakers, J. Amer. Chem. Soc., 1968, 90, 6109.
36. C.S. Irving and P.A. Leermakers, Photochem. Photobiol., 1968, 7, 665.
37. a) W.L. Porter, L.A. Laverseur and A.S. Henick, Lipids, 1972, 7, 699.
b) W.L. Porter, L.A. Laverseur and A.S. Henick, Lipids, 1971, 6, 1.
c) W.L. Porter, A.S. Henick and L.A. Laverseur, Lipids, 1973, 8, 31.
d) W.L. Porter, L.A. Laverseur, J.I. Jeffers and A.S. Henick, Lipids, 1971, 6, 16.

38. A.W. Adamson "Physical Chemistry of Surfaces", Wiley and Sons, New York, 1967.
39. C.S. Brooks,
J. Colloid. Sci., 1958, 13, 522.
40. G-S. Wu and J.F. Mead, Lipids, 1977, 12, 965.
41. G-S. Wu, R.A. Stein and J.F. Mead, Lipids 1977, 12, 971.
42. J.F. Mead, A. Sevanian, R.A. Stein and G-S. Wu in "Biochemical and Clinical Aspects of Oxygen". Academic Press, 1979, pp699-708.
43. J.F. Mead, J. Amer. Oil Chem. Soc., 1980, 57, 393.
44. J.F. Mead, R.A. Stein, G-S. Wu and A. Sevanian, in "Autoxidation in Food and Biological Systems" (Ed. M.G. Simic and M. Karel), Plenum, 1980, pp 413-428.
45. L.I. Burke, G.S. Patil, R.V. Panganamala, J.C. Geer and D.G. Cornwell, J. Lipid Res., 1973, 14, 9.
46. As shown in Table 2.2.1.2 the number of moles adsorbed per unit area of silica is independant of the number and isomerism of double bonds. This result is not compatible with hydrocarbon chains orientated parallel to the surface.
47. N.A. Khan, J.B. Brown and F.E. Deatherage,
J. Amer. Oil. Chem. Soc., 1951, 28, 105
48. Despite the large number of previous studies of autoxidation of unsaturated fatty acids on various surfaces, none of these have produced quantitative data⁴⁹.
49. For example see V. Slawson and J.F. Mead, J. Lipid Res., 1972, 13, 143.
50. J.E. Leffler and J.T. Barbas, J. Amer. Chem. Soc., 1981, 103, 7768.
51. a) F.D. Gunstone and T.P. Hilditch, J.C.S., 1945, 836.
b) F.D. Gunstone and T.P. Hilditch, J.C.S., 1946, 1022.

52. Invariably the rate of initiation has to be taken into account
in the overall rate equation.
53. See H.W. Gardner in reference 1g and references cited
therein.
54. G.A. Russell in "Free Radicals" (Ed. J.K. Kochi), Wiley and
Sons, New York, 1973, Vol 1, pp 275-332.
55. K. Hasegawa and L.K. Patterson, Photochem. Photobiol., 1978,
28, 817.
56. R.D. Small, Jr., J.C. Scaiano and L.K. Patterson, Photochem.
Photobiol., 1979, 29, 49.
57. I.M. Campbell, R.B. Caton and D.N. Crozier, Lipids 1974, 9, 916.
58. a) D.T. Coxon, K.R. Price and H.W-S. Chan, Chem. Phys. Lipids,
1981, 28, 365.
- b) W.E. Neff, E.N. Frankel and D. Weisleder, Lipids 1981, 16,
439.
- c) M. Roza and A. Francke, Biochim. Biophys. Acta., 1978, 528,
119.
- d) D.E. O'Connor, E.D. Mihelich and M.C. Coleman, J. Amer.
Soc., 1981, 103, 223.
59. For recent references see P.C. Wong, D. Griller and J.C. Scaiano,
J. Amer. Chem. Soc., 1982, 104, 5106, and V. Malatesta and
J.C. Scaiano, J. Org. Chem., 1982, 47, 1455.

CHAPTER 6

A THEORETICAL INVESTIGATION of the CONFORMATIONS of CYCLIC PEROXIDES

Summary.

Molecular structures and energies have been calculated in the MINDO/3 approximation for dioxirane, dioxetane, dioxolane, dioxane and their methyl derivatives. Potential surfaces have been calculated for dioxirane, dioxetane and dioxolane. The calculations predict planar geometries for dioxetane and dioxolane. Ab-initio calculations on the parent cyclic peroxides have been performed with STO-3G and 3-21G basis sets. Agreement between the semi-empirical and ab-initio approaches is good in all cases. Attempted calculations on the O-O bond cleavage of 2,3-dioxobicyclo[2.2.1]-heptane were however unsatisfactory, even with the inclusion of configurational interaction (CI) in the calculations.

1 Introduction

The application of quantum mechanical treatments for the prediction of molecular structure, ground and excited state properties and reactivity has been utilised extensively to predict inaccessible experimental data and to provide a theoretical basis for observed results.

The practical inability to solve the Schrodinger wave equation per se for polyatomic molecules forces approximations to be made to obtain a solution. By only considering differences in energy between related systems, the approximations may cancel, alternatively the introduction of adjustable parameters to upgrade the accuracy of the calculations may be made. These two approaches to the problem are commonly referred to as ab-initio and semi-empirical calculations respectively.

The majority of ab-initio studies are based on the formalism introduced independently by Roothan^[1] and Hall^[2] in which the orbitals are written as a linear combination of a given set (commonly referred to as basis set) of functions, usually Slater-Zener^[3] or Gaussian^[4] atomic orbitals. The results of ab-initio calculations can approach the theoretical limit (Hartree-Fock) set by the orbital approximation if the basis set is large and well chosen^[5]. However the neglect of electron correlation inherent to the approach can lead to unacceptably large errors when determining the molecular properties. The introduction of configurational interaction goes some way to amending the deficiency but the convergence is too slow^[6].

Other ab-initio methods have been suggested and applied with success although most if not all suffer from excessive cost and time required for calculation.^[7] Indeed even the Roothan-Hall (RH) calculations become prohibitively time and cost consuming for all but small molecules.

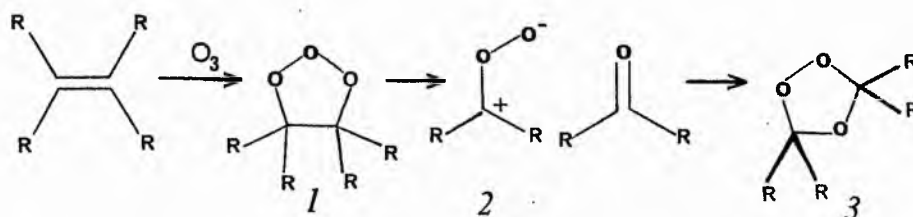
As a result of the need for calculations on molecules of wider interest rather than the somewhat limited application of ab-initio calculations to small molecules several workers derived semi-empirical methods applicable to the calculation of properties of reasonably complex and/or large molecules^[8-14]. Dewar and coworkers^[15] have developed a semi-empirical approach which has been shown to give better quantitative guides to chemical behaviour than even good RH calculations (ie. employing large basis sets) for a wide range of compounds.

In this chapter, the conformations of several cyclic peroxides have been investigated using MINDO/3 semi-empirical approach. More sophisticated ab-initio calculations have also been performed on selected molecules. The fundamental concepts of the MINDO/3 method will not be described here since they have been described by Dewar and collaborators^[15] and have been discussed in detail^[16].

The calculations to be described deal with the conformation of molecules in the gas phase. This is the most appropriate phase for studying conformational problems since only intramolecular forces contribute to the preferred molecular conformation. Although pure liquids or solutions in which competing intermolecular forces are also involved will clearly be the phase of most interest, these subtle effects can hardly be quantitatively described before the intramolecular forces in the free molecule are understood.

2.1 Dioxirane

The mechanistic and theoretical aspects of the reaction of ozone with olefinic bonds in aliphatic hydrocarbons has intrigued chemists since the early part of this century.^[17,18] The original mechanism proposed by Criegee^[19] has been supported by a large body of experimental data^[20-23], with only minor modifications^[24] (Scheme 2.1.1). The primary ozonide adduct (1) is unstable and decomposes readily into an aldehyde and the so called Criegee intermediate (2).

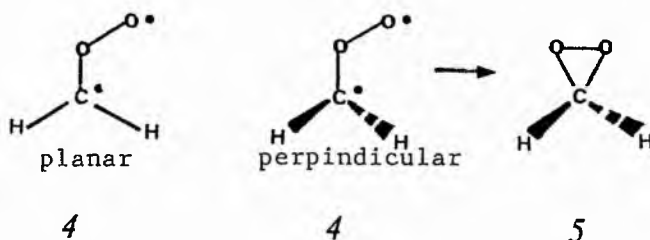


SCHEME 2.1.1

In the solution phase these two species recombine to form the ozonide (3). More recently the gas phase reaction has received considerable attention due to its importance in photochemical smog formation over built up areas.^[25-27]

The Criegee intermediate has been the subject of several recent ab-initio calculations.^[28-32] In particular attempts at determining the nature of the ground state molecule have led to controversy. Cremer^[30] has proposed that in the gas phase peroxymethylene (2; R=R'=H) is a superposition of a 1,3-singlet biradical (4) and a

zwitterion where the biradical character is predominant. Substituent and solvent effects can, however lead to a dominance of the zwitterion form.



SCHEME 2.1.2

Wadt and Goddard *et al.*^[29] and Cremer^[30] have concluded from their calculations that closure of the COO bond angle to obtain the ring state (Scheme 2.1.2) lowers the energy of the perpendicular^[29,30] form as previously proposed by Ha *et al.*^[31]. The discovery of (5) and its importance have now been reported^[33,34]. Lovas and Suenram^[34] detected (5) spectroscopically in the vapour phase reaction between ethylene and ozone at -150°C . They observed the same product from the reaction of ozone with other terminal olefins (propene, 1-butene, and vinyl fluoride), but were unable to observe substituted dioxiranes.

Tables 2.1.1 and 2.1.2 list the equilibrium molecular and geometric properties respectively of dioxirane (5) and methyl derivatives (6 and 7) calculated with complete optimisation of all bond lengths, angles and dihedrals by the MINDO/3 method. Tables 2.1.3 and 2.1.4 list equilibrium geometric properties of fluorinated derivatives of (5-7). Only the parent dioxirane (5) has been investigated theoretically previously [29,30,31,35].

Increasing methyl substitution decreases the calculated O-O bond lengths, while increased fluorination leads to an increase of the O-O distance. The O-O bond lengths can be expected to be systematically low as a result of the underestimate of the O-O repulsion integrals inherent in the MINDO/3 approximation. This is certainly born out by the only experimental value available for comparison^[34], that of the parent dioxirane (5) $r_{O-O} = 1.52$ Å. Nonetheless the systematic trends outlined can be expected to be correct. Glidewell^[36] has shown that MINDO/3 correctly predicts the order r_{O-O} bond lengths for a number of hydroperoxides, dialkyl peroxides and their fluoro derivatives.

Table 2.1.5 presents experimental geometrical parameters for some three-membered rings with successive replacement of CH_2 by an O atom. The introduction of heteroatoms into small strained rings will distort bond angles, lengths and strengths, through a combination of factors such as intrinsic hybridisation, electronic effects, non-bonded

interactions and magnitude of covalent radii. The two homonuclear species cyclopropane and the ring form of ozone have a purely equatorial triangle geometry of C_{3v} symmetry with the bond angle being precisely the theoretical 60° . The introduction of one oxygen atom for a methylene group in cyclopropane^[37] results in a shorter C-C interatomic distance while the replacement of an oxygen atom in ozone^[38] leads to an increase in the O-O bond distance. The trend can be rationalised in terms of formalism adopted for the bonding in transition metal-ethylene complexes^[39]. Figure 2.1.1 shows a schematic representation of the bonding in the cyclic species XY_2 . Donation of electrons from orbitals of proper symmetry from X into the π -antibonding orbital of Y would result in an increase of the Y-Y bond (Figure 2.1.1 a,b). Similarly donation of electrons from the π -bonding orbital of Y-Y to a suitable orbital of X will also result in a reduction of the Y-Y bond length. Using this simple approach the long O-O bond length in dioxirane can be rationalised in terms of donation of electrons from the π -orbitals of oxygen into a carbon d_{z^2} orbital. Back donation from a p_x or d_{xz} orbital into the π -antibonding orbital of oxygen will result in an increased O-O bond length, compared with ozone where the more electronegative O atom is less likely to participate in back donation. Similar rationalisation explains the shorter C-C bond length in oxirane^[40] compared with cyclopropane. The small back donation contribution from the O atom will result in a shorter C-C bond compared with the homonuclear species.

TABLE 2.1.1 Heats of formation, total energies, ionisation potentials and dipole moments of Dioxirane and its methyl derivatives


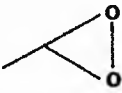

Compound	Entry	ΔH_f (kJ mole ⁻¹)	Total Energy (eV)	Vertical Ionisation Potential (eV)	Dipole Moment (Debye)
	1	-77.884	-776.490	11.8979	2.1453
	2	-144.968	-933.626	10.9299	2.6171
	3	-180.907	-1090.407	10.7248	2.8203

Table 2.1.2 Skeletal bond angles, lengths and dihedral angles for dioxirane and its methyl derivatives

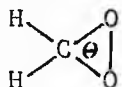
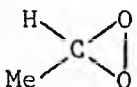
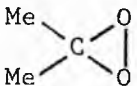
Compound	Entry	r O-O	r C-O	θ	ϕ_H	ϕ_{Me}
	1	1.457	1.342	136.3	111.9	-
	2	1.453	1.358	137.9	107.8	114.3
	3	1.448	1.378	143.0	-	108.5

Table 2.1.3 Heats of formation, total energies, ionisation potentials and dipole moments of fluoro-substituted dioxiranes

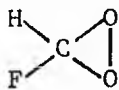
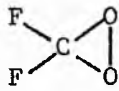
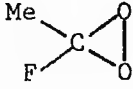
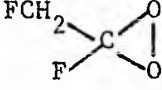
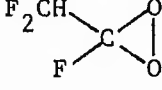
Compound	Entry	ΔH_f (kJ mole ⁻¹)	Total Energy (eV)	Vertical Ionisation Potential (eV)	Dipole Moment (Debye)
	4	-325.65	-1240.122	11.94	1.63
	5	-573.58	-1703.77	12.27	0.47
	6	-409.50	-1397.42	11.31	2.59
	7	-637.59	-1860.84	10.37	1.81
	8	-905.85	-2324.67	10.56	1.87

Table 2.1.4a Skeletal bond lengths of fluoro-substituted dioxiranes

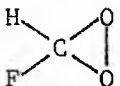
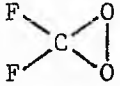
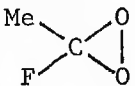
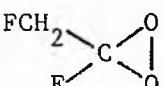
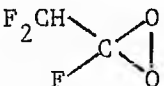
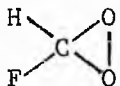
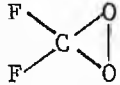
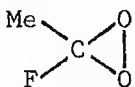
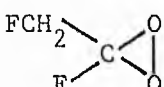
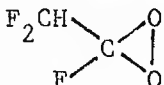
Compound	Entry	r O-O	r C-O	r C-H	r C-F	r C-C
	4	1.471	1.325	1.117	1.368	-
	5	1.481	1.317		1.341	
	6	1.462	1.328		1.388	1.474
	7	1.465	1.319		1.400	1.455
	8	1.467	1.311		1.483	1.529

Table 2.1.4b Skeletal bond and dihedral angles of fluoro-substituted dioxiranes

Compound	Entry	<HCO	<FCO	<CCO	<OOC	<HCOO	<FCOO	<CCOO
	4	124.3	124.5	-	56.2	242.8	117.4	-
	5	-	127.6	-	55.8	-	238.1	121.7
	6	-	122.6	130.2	57.1	-	246.1	122.6
	7	-	131.8	139.2	57.1	-	236.5	138.1
	8	-	120.1	148.7	57.1	-	245.2	171.1

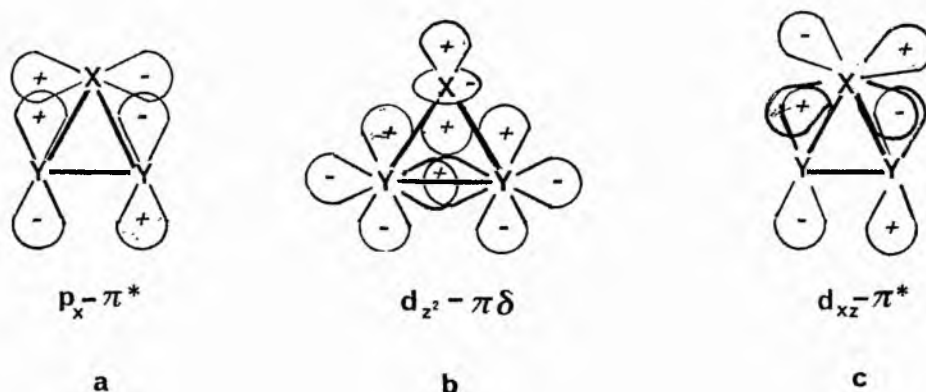
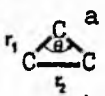
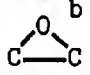
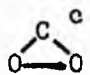
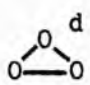


FIGURE 2.1.1 Schematic representation of the bonding in the cyclic species XYY.

Table 2.1.5 Comparison of experimental geometrical parameters in three membered rings.

ring	r_1/A	r_2/A	θ°
 a	1.510	1.510	60.0
 b	1.472	1.436	61.4
 c	1.52	1.34	66.2
 d	1.45	1.45	60.0

- a O.Bastiansen., F.N.Fritsch and K.Hedberg.
Acta Crystallogr. 1964, 17, 538
- b K.Pihlaja. and E.Taskinen in "Physical Methods in Heterocyclic Chemistry" (A.R.Katritzky., ed)., Vol 6, pp 199, Academic press, New York, 1974.
- c F.J.Lovas and R.D.Suenram.
Chem.Phys.Lett., 1977, 51, 453
- d P.J.Hay., T.H.Dunning and W.A.Goddard.
Chem.Phys.Lett., 1973, 23, 457

Table 2.1.6 Comparison of various theoretical structures obtained for dioxirane with observed experimental values.

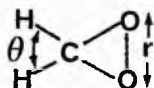
Method	rO-O	rC-O	rC-H	>HCH	>OCO	Ref.
HF [3s2p/2s]	1.48	1.44	1.09	116	61.8	31
MINDO/3 (2x2 CI)	1.46	1.34	1.12	107.4	65.7	35
GVD-CI [3s2p1d/2s] (1.46)	(1.46)	(1.44)	(1.09)	(116)	60.6	29
RSMP-STO-3G	1.49	1.46	1.11	115.1	61.2	30
RSMP [3s2p/2s]	1.645	1.47	1.09	117.4	68.1	30
RSMP [3s2p1d/2s]	1.53	1.40	1.09	116.6	66.3	30
MINDO/3	1.46	1.34	1.12	111.9	65.8	This work
Experimental	1.52	1.39	1.09	117.3	66.2	34

numbers in parenthesis are assumed structural parameters.

Table 2.1.6 contains a summary of the theoretical structures calculated for dioxirane by various methods and lists the experimentally determined parameters. The MINDO/3 calculations of Hull et al^[35] using 2x2 configurational interaction appear to be very similar to our MINDO/3 calculation without CI. However comparison of the data sets in Table 2.1.6 suggests that only ab-initio calculations with extensive basis sets, augmented by polarisation

functions, extensive correlation corrections and a complete optimisation of structural parameters are significantly better than the results obtained by MINDO/3. As mentioned earlier the low O-O bond distance calculated is to be expected for the MINDO/3 method, as a result of the underestimate of the repulsion integrals between adjacent atoms bearing non-bonded electrons. Only at RSMP ab-initio level calculation with large basis set (row 7) where additional charge is brought into the outer valence-shell regions of the O atoms, resulting in enhanced repulsion between the two oxygen atoms is this deficiency adequately corrected for.

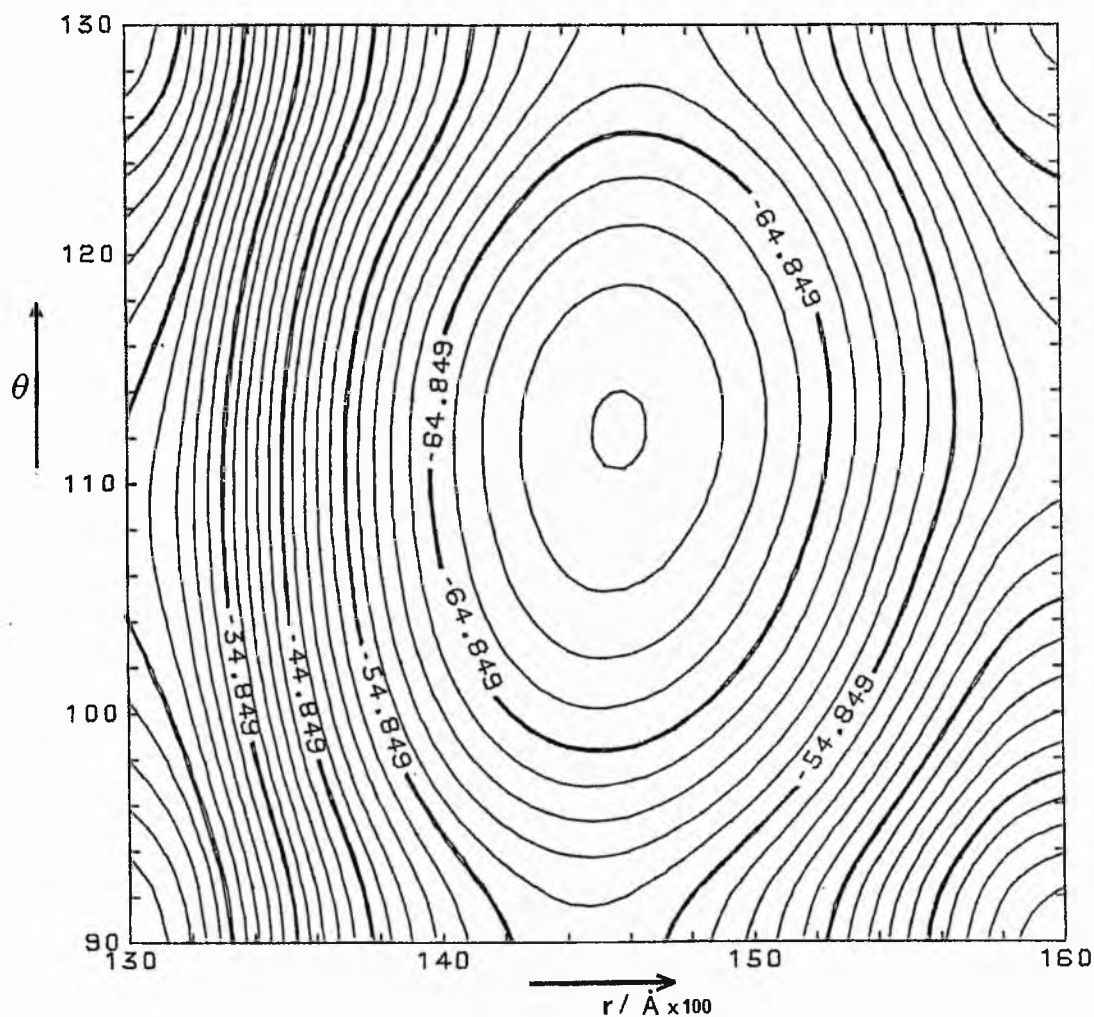
Figures 2.1.2 and 2.1.3 show the contour and transect diagrams of the potential energy surface for ring deformation as defined below. The surface was generated from 480 individual calculations, each calculation being fully optimised with the exception of the variables θ and r . The form of the potential surface suggests that the three membered ring is more sensitive to O-O bond deformation than to HCH bond angle deformation. As expected the calculations predict that O-O compression from the equilibrium bond length results in a larger energy change than corresponding O-O extension.



Although there is experimental data for the geometrical parameters for dioxirane no such data exists for the methyl substituted dioxiranes or the fluoro substituted dioxiranes. The difluorodioxirane (I) has however been identified (by its infrared

FIGURE 2.1.2

Contour map of the potential surface of dioxirane, according to MINDO/3 calculations. The innermost contour line corresponds to -72.849 KJ/mole. The vertical spacing of two equipotential curves is 2 KJ/mole.



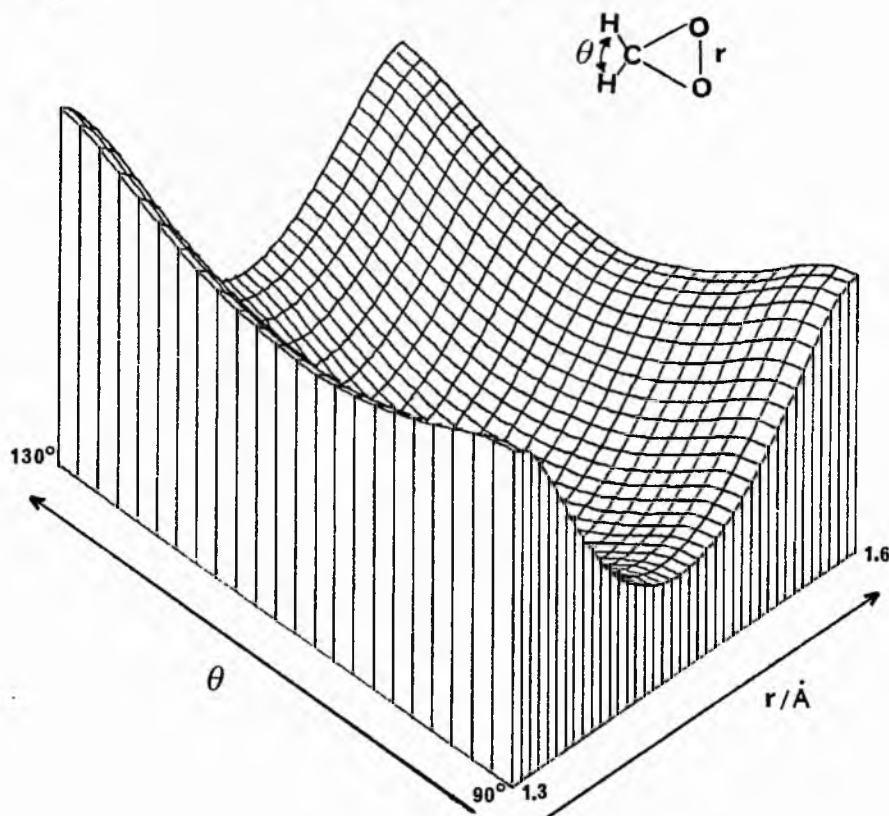
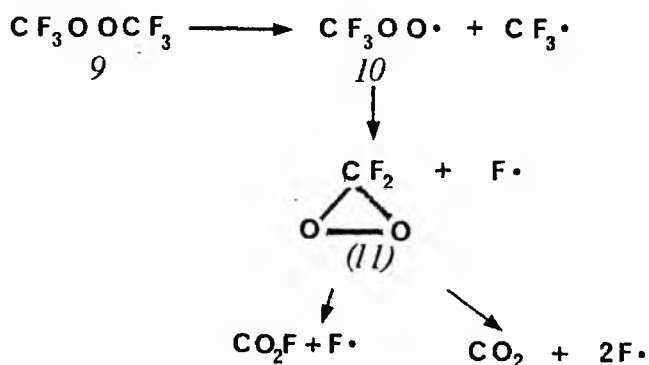


FIGURE 2.1.3 Transect diagram of the potential surface of dioxirane according to MINDO/3 calculations.

spectrum) as an intermediate in the gas phase pyrolysis or photolysis of the perfluoroperoxide (11) which gives mainly carbon dioxide and carbonyl fluoride^[42].

The MINDO/3 calculated geometries for the fluoro substituted dioxiranes suggest that increased fluorination results in a concomitant decrease in skeletal C-O distance and increased O-O distance. The first vertical ionisation potential also increases with increased fluorination of the dioxirane skeleton.



Barriers to free rotation in substituted dioxiranes.

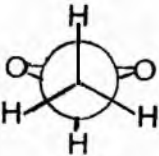
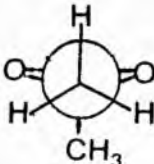
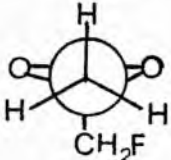
Molecular conformations correspond to the minima in a potential energy curve or surface of a molecule. The majority of large molecules will have more than one potential minima on its potential surface and consequently more than one stable molecular conformation. The barrier height to a particular motion (eg. rotation or inversion) will be given by the energy difference between the maximum and minimum along the minimum energy path interconnecting the minima under consideration. Calculation of the barrier heights requires a set of calculations for different conformations until the minima and maxima have been located on the potential surface. The computed barrier heights are then the differences between the maximum and minimum conformational energies.

Barrier heights to free rotation of the methyl groups in mono- and dimethyl- dioxane (2 and 3) respectively were calculated. All parameters except for the HCCO dihedral angle were fully optimised. The results are presented in 2.1.7. Rotational barriers around single bonds are consistently underestimated in the MINDO/3 approximation, although it gives good agreement for rotational barriers to π -bonds [15,16a]. The converse is true for ab-initio calculations. The potential function calculated for dimethyldioxirane (3) is shown in Figure 2.1.4

The optimised geometries calculated by the MINDO/3 method were used as parameters for minimal basis set ab-initio calculations. Several points around the MINDO/3 calculated minima and maxima were used to ensure that the ab-initio calculations agreed with the MINDO/3

calculation as to the location of the stationary points. The results are incorporated in Table 2.1.7. As can be seen the minimal basis set calculations give higher barriers to free rotation than the MINDO/3 calculations in both cases, as expected (*vide supra*).

Table 2.1.7 Calculated barrier heights to free rotation
in substituted dioxiranes.

Peroxide	Entry	MINDO/3	STO-3G
	2	3.12	8.12
	3	3.25	7.08
	12	2.80	

Attempted calculations of rotational barriers in the fluoro-substituted dioxiranes were unsuccessful with the exception of (12). In each case it was observed that a C-H bond stretch occurred concomitantly with rotation about the C-C bond. Attempted STO-3G basis set calculations using the geometric parameters calculated for (12) by MINDO/3 was unsuccessful, casting doubt on the validity of the MINDO/3 result.

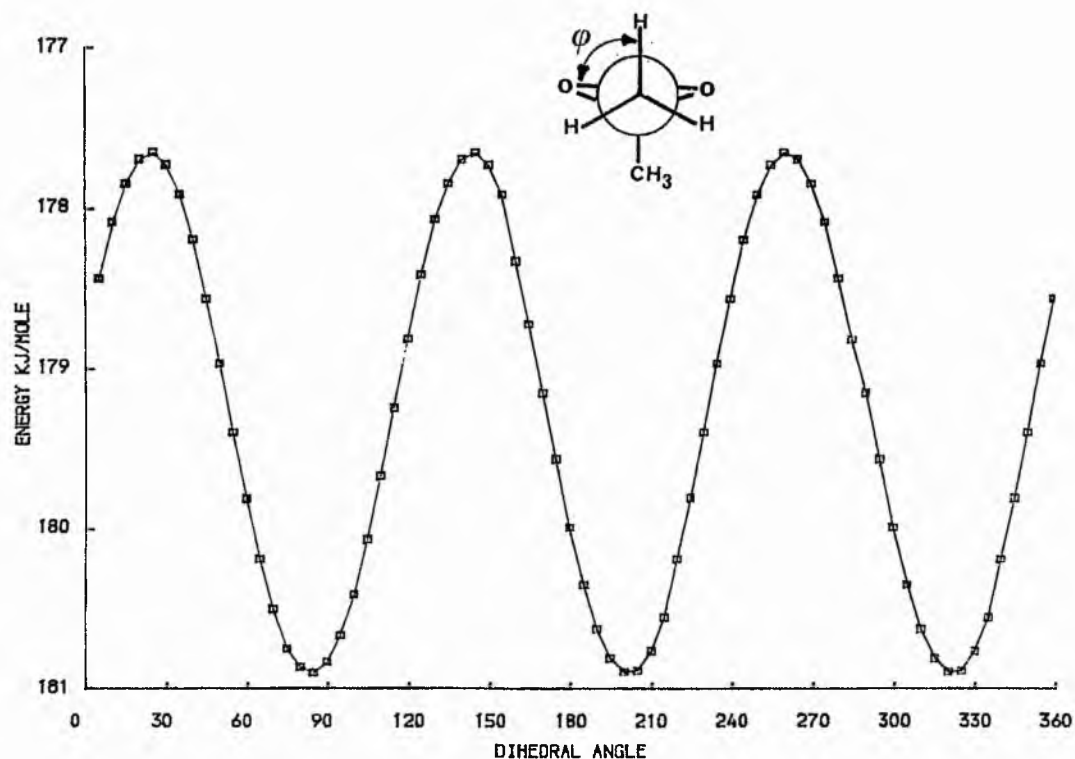


FIGURE 2.1.4

The potential energy function describing the barrier to rotation about the C-C bond in dimethyldioxirane (3) according to MINDO/3.

2.2 Dioxetanes^[44,45]

Dioxetane and its derivatives may be considered as cyclobutane analogues where two adjacent methylenes have been replaced by two oxygen atoms. There is growing evidence in the literature that cyclobutane preferentially adopts a non-planar structure from electron diffraction^[44,45], IR-Raman^[46-51] and NMR^[52,53] investigations. Theoretical studies at both ab initio (with large basis sets)^[54] and semi-empirical^[55] level support the experimental observation. Cyclobutane may be twisted by as much as 30° , to relieve Pitzer strain^[56a] inherent in a planar conformation (of D_{4h} symmetry) with four eclipsed methylene groups.

We have performed a MINDO/3 study for dioxetane (1) and all its methyl derivatives. The calculations were performed with complete optimisation of all bond lengths, angles and dihedral angles. The results, presented in Tables 2.2.1 and 2.2.2, suggest that dioxetane is very nearly planar with a twist angle of only 0.8° . (MINDO/3 calculations on cyclobutane^[56b] give a twist angle of 27° which is in good agreement with experimental observations). The departure from the twisted geometry for dioxetane is understandable on two accounts. Firstly, the replacement of two methylenes by two oxygen atoms in the four membered ring will result in the removal of 75% of the possible 1,2 interactions. Secondly, it has been shown for cyclobutane that 1,3 interactions^[55] are an underlying cause of the puckering of the ring. No 1,3 interactions are possible for dioxetane. The calculated structure is shown in Figure 2.2.1. The two methylene groups are completely eclipsed in the planar conformation, suggesting that ring

strain contributions, which will tend to keep the ring planar are greater than torsional strain contributions which would try to alleviate the eclipsing of adjacent methylene groups.

The 1,2-dimethyl isomers (4 and 5) show only a very small difference of 1.6° in their dihedral angle (O-O-C-C), with the cis-isomer adopting the more puckered conformation. In the cis-isomer (4), in a completely planar conformation the two methylene groups are fully eclipsed, hence the most favoured conformation would be expected to go some way to relieving the torsional strain at the expense of increased ring strain, by distorting the planar geometry. Clearly the very small deformation calculated suggests that the relief of torsional strain is very small compared with the increase in ring strain. To examine this effect in more detail we performed calculations on dioxetane (1) to determine the energy dependence on the dihedral angle. Figure 2.2.2 shows the energy profile with a twist angle of up to 30° . All other parameters were fully optimised

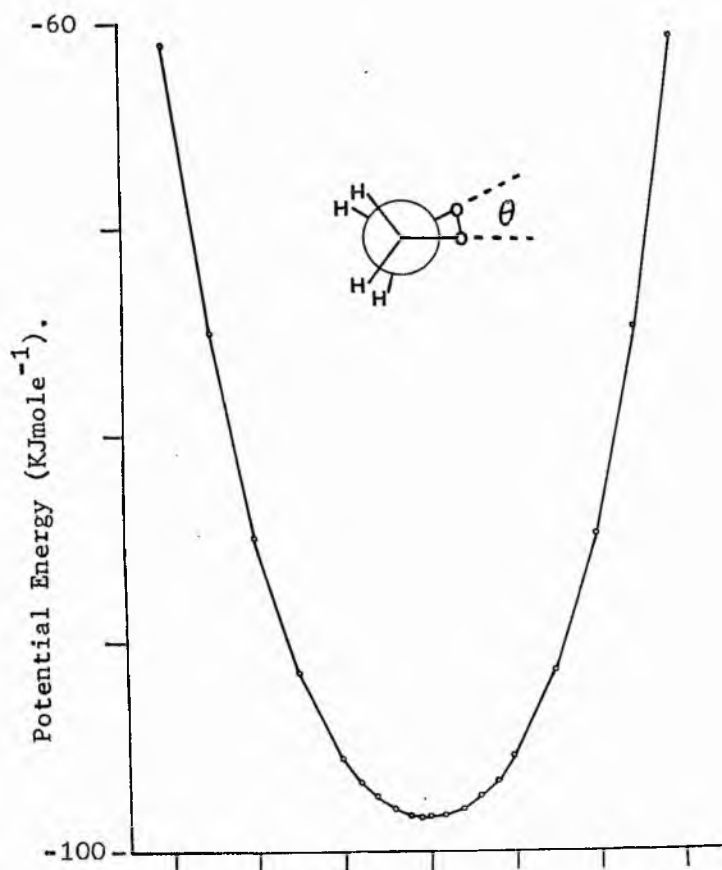
The potential well is fairly steep with a twist angle of only 20° increasing the energy by 14 KJmole^{-1} .

The substitution of a hydrogen with a methyl group in dioxetane leads to a decrease in the energy of ca 41 KJmole^{-1} . The replacement of a second hydrogen can occur at either of the three remaining sites to give either the 1,1 or the two 1,2 isomers. From the heats of formation the calculations suggest that 1,2 substitution is the more energetically favourable form with the slightly puckered cis-isomer being marginally preferred over the trans 1,2-isomer. Further methyl substitution leads to an increase in the heat of formation with the 1,1,2-trimethyl derivative (6) being slightly puckered (1.5°). The tetramethyl derivative (7) preferring the completely planar geometry.

With increasing methyl substitution the O-O bond length decreases with a concomitant increase in C-C bond length. The vertical ionisation potentials decreases steadily with increasing methyl substitution, detailed photoelectron spectral data for dioxetanes is scarce, however Brown^[57] has reported on the spectrum of the tetramethyl dioxetane (8). It exhibits a first ionisation potential at 8.98 eV which has been assigned to the removal of an electron from an antisymmetric π orbital. The second highest molecular orbital of (8) is described as an antisymmetric combination of C-O σ orbitals with a value of 10.94 eV. A linear relationship between the C-O-O-C dihedral angle and the splitting of the two highest occupied molecular orbitals (HOMO's) has been verified^[58]. The experimental value of the HOMO splitting from Browns' data suggests a dihedral angle very close to 0° for (8). Hence the experimental evidence available is in accord with the calculated geometries, although the calculated first ionisation potential is in poor agreement with the experimental observation (this will be discussed later).

FIGURE 2.2.2

Potential energy curve for dioxetane according to MINDO/3 calculations.



Dioxetane (1) has been the subject of previous MINDO/3 calculations concerning the possible mechanisms of formation^[78] and the thermolysis of dioxetane^[79]. No discussion or description of the ground state geometry was described in either paper. Table 2.2.3 presents ab-initio calculations on the dioxetane. The geometrical parameters calculated by MINDO/3 are included for comparison. As with the semi-empirical calculations the ab-initio calculations were completely optimised.

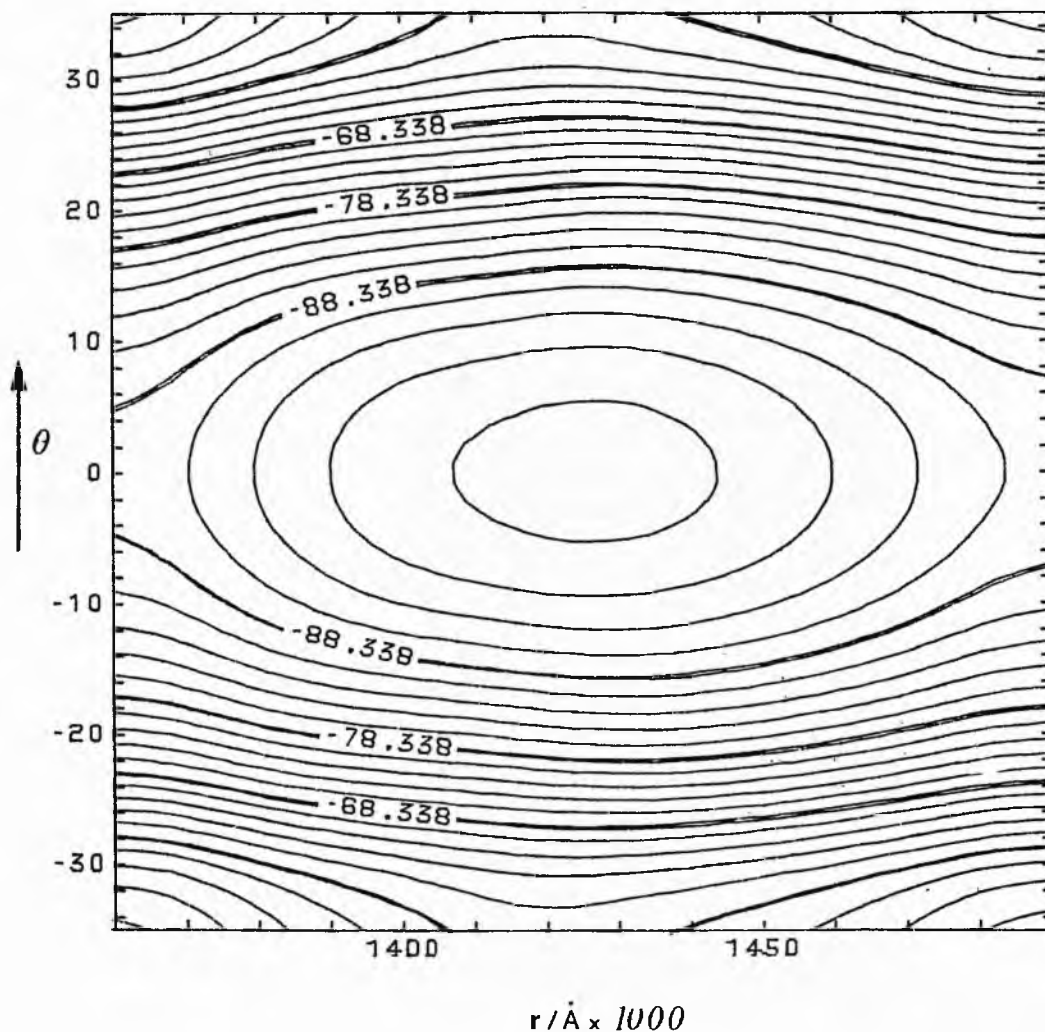
At STO-3G level the only significant discrepancy with the MINDO/3 calculations is the O-C bond length. The C-C and C-H bond length being slightly shorter and longer respectively in the MINDO/3 calculations as expected^[15]. At 3-21G level the O-O bond length increases considerably to 1.497Å cf 1.423 ± 0.001Å calculated by MINDO/3 and STO-3G basis set ab-initio calculation. The 3-21G basis sets also calculates a larger C-O bond length. All three levels of sophistication predict an essentially planar skeletal ring with the OCC bond angle being marginally below 90°.

The results suggest that MINDO/3 compares very favourably with STO-3G basis set calculations and the discrepancies with the 3-21G basis set are to be expected^[15,16]. A weakness of the MINDO/3 method however, is that unless symmetry restrictions are imposed on the calculation, bond lengths for equivalent substituents vary by as much as 0.003Å. Similar variations are observed for apparently equivalent bond angles.

Figures 2.2.3 and 2.2.4 presents the contour and transect diagrams of the potential energy surface for ring deformation as

FIGURE 2.2.3

Contour map of the potential surface of dioxetane according to MINDO/3 calculations. The innermost contour line corresponds to -96.34 KJ/mole. The vertical spacing of two successive equipotential curves is 2 KJ/mole.



defined below. The dihedral angle θ reflects the extent of ring puckering. The potential surface suggests that irrespective of the O-O bond length the potential well for ring puckering is deep. In contrast with dioxirane (section 2.1), the potential energy variation with O-O bond length is not very marked.

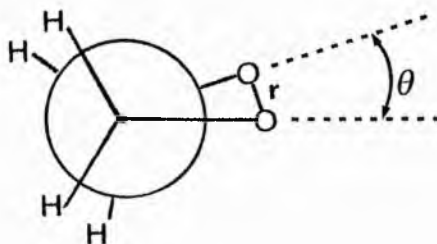
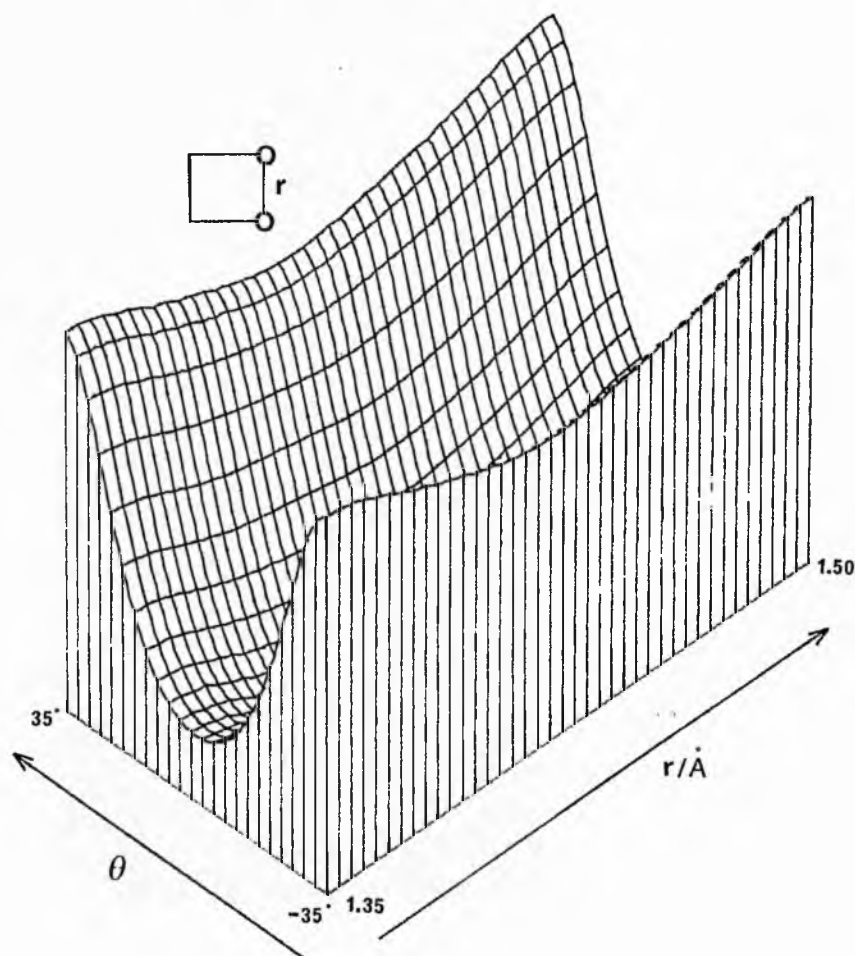


FIGURE 2.2.4

Transect diagram of the potential surface of dioxetane according to MINDO/3 calculations.

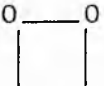
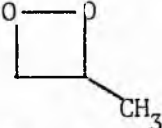
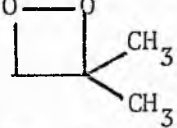
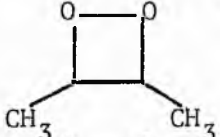
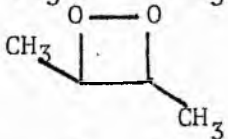
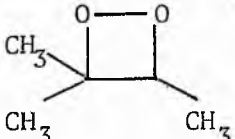
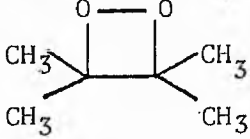


Tables 2.2.4 and 2.2.5 present MINDO/3 calculated equilibrium molecular and geometrical properties respectively for fluoro-substituted dioxetanes. The cis-1,2-disubstituted fluoro derivative is marginally more stable than the trans isomer, as found for the dimethyl dioxetanes (4 and 5). However, in contrast with the methyl substituted dioxetanes for the fluoro derivatives 1,1-substitution is energetically more favoured than 1,2-substitution. As with the methyl substituted dioxetanes the fluoro-substituted dioxetanes are essentially planar. A potential energy curve was calculated for the 1,1-difluorodioxetane (9), the results being qualitatively similar to that obtained for dioxetane (1). Selected values are listed in Table 2.2.6.

Table 2.2.6 Values of potential energies and dihedral angles for 1,1-difluorodioxetane

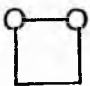
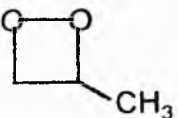
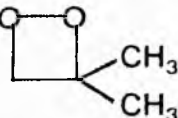
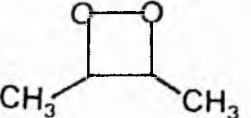
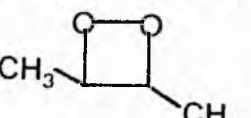
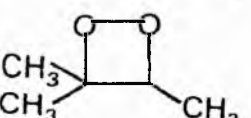
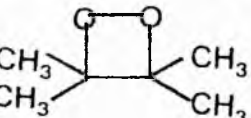
θ	$\Delta H_f / \text{KJmole}^{-1}$
35 and -35°	-542.85
25 and -25°	-576.09
15 and -15°	-592.72
8 and -8°	-598.18
4 and -4°	-599.66
0°	-600.15

Table 2.2.1 Heats of formation, total energies, ionisation potentials and dipole moments of Dioxetane and its methyl derivatives.

Compound	Entry	ΔH_f (kJ mole ⁻¹)	Total Energy (eV)	Vertical Ionisation Potential (eV)	Dipole Moment (Debye)
	1	-98.45	-933.14	10.00	2.42
	2	-139.49	-1089.98	9.86	2.64
	3	-140.39	-1246.40	9.73	2.79
	4	-178.91	-1246.80	9.72	2.80
	5	-174.72	-1246.75	9.69	2.85
	6	-171.60	-1403.13	9.58	2.94
	7	-153.19	-1559.35	9.43 (8.98) ^a	3.05

^a Brown, R.S. Can. J. Chem., 1975, 53, 3439.

Table 2.2.2 Skeletal bond lengths and dihedral angles^a for dioxetane and methyl derivatives

Compound	Entry	Twist Angle O-O-C-C	r C-C	r O-O	r C-O
	1	-0.78	1.50	1.42	1.38
	2	0.05	1.52	1.42	1.38
	3	0.53	1.55	1.42	1.38
	4	1.89	1.54	1.42	1.39
	5	-0.18	1.55	1.42	1.39
	6	1.52	1.57	1.41	1.39
	7	0.08	1.61	1.41	1.40

^a fully optimised

TABLE 2.2.3 Comparison of MINDO/3 and ab initio calculations
on dioxetane.^a

Parameter	MINDO/3	STO-3G	3-21G
rO-O	1.423	1.422	1.497
rO-C	1.382	1.464	1.486
rC-C	1.504	1.539	1.535
rC-H	1.125 ^b	1.094	1.076
< OCC	88.20	87.71	89.26
< OCH	114.42	112.76	111.19
<OCCO	0.78	0.00	0.00
<OOCH	238.10	242.59	242.54
<OOCH	120.15	117.41	117.46

^a all parameters were completely optimised.

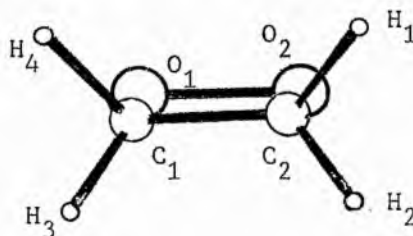


Figure 2.4.1 MINDO/3 calculated
structure for dioxetane.

Table 2.2.4 Heats of formation, total energies, ionisation potentials and dipole moments of fluoro-substituted dioxetanes.

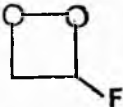
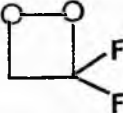
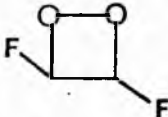
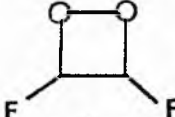
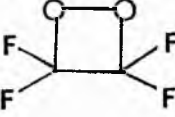
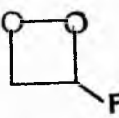
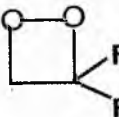
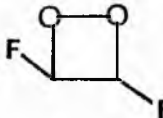
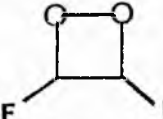
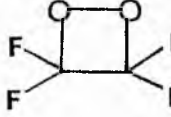
Compound	Entry	ΔH_f (KJ mole ⁻¹)	Vertical Ionisation Potential (eV)	Dipole Moment (Debye)
	8	-399.87	10.60	2.42
	9	-600.14	11.19	2.72
	10	-554.40	11.06	2.91
	11	-580.95	10.88	0.38
	12	-1054.29	12.09	1.53

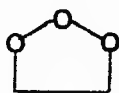
Table 2.2.5 Skeletal bond angles and lengths for fluoro-substituted dioxetones^a

Compound	Entry	Twist Angle O-O-C-C	r C-C	r O-O	r C-O
	8	0.53	1.497	1.422	1.388
	9	-0.25	1.494	1.420	1.392
	10	-0.52	1.505	1.420	1.365
	11	-2.93	1.488	1.420	1.363
	12	-0.05	1.507	1.412	1.356

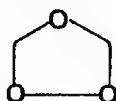
^a fully optimised

2.3 Dioxolanes

Interest in substituted dioxolanes has increased recently with the realisation that such structures have been isolated from oxidised polyene lipids via either free radical^[59], photosensitisation^[60] or enzymic^[61] pathways. No previous theoretical study of dioxolanes has been reported, although the trioxalanes (1) and (2) have been the subject of a very thorough ab-initio investigation by Cremer^[62] and of several semi-empirical studies^[63].

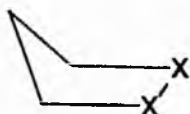


1

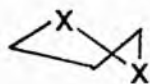


2

Following the approach outlined in sections 2.1 and 2.2 dioxolane may be considered as a cyclopentane ring in which two adjacent methylenes have been replaced by oxygen atoms. Cyclopentane and its derivatives have been the subjects of a large number of theoretical and spectroscopic studies^[64]. It is now widely accepted that cyclopentane systems are pseudorotational systems with very low or no potential barriers^[65]. The introduction of bulky substituents and/or heteroatoms into the ring will be expected to raise the barrier above the pseudorotational energy levels and the ring will adopt either an envelope or half-chair form, whichever is the most stabilised.



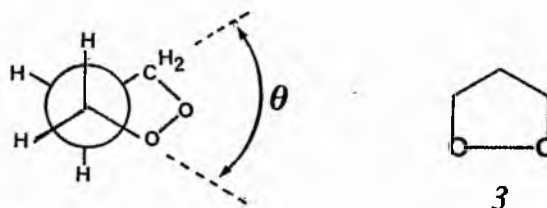
envelope.



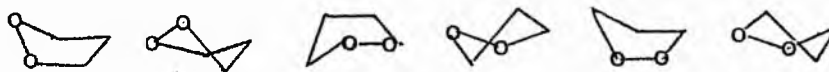
half-chair.

Cremer's ab-initio calculations on (1) and (2) predict the symmetrical envelope conformation and the symmetrical half-chair form respectively to represent the conformational minimum, in agreement with experimental data.

Tables 2.3.1 - 2.3.6 list the MINDO/3 calculated equilibrium molecular and geometric properties of dioxolane and a large number of mono- and poly- methyl derivatives thereof. Figure 2.3.1 presents a potential energy curve for a ring puckering mode of dioxolane (3) as defined below.



As can be clearly seen, the potential curve suggests that the conformational minimum occurs for the essentially planar ring form (3a).



Envelope and twist conformations along the pseudorotational itinerary of dioxolane.

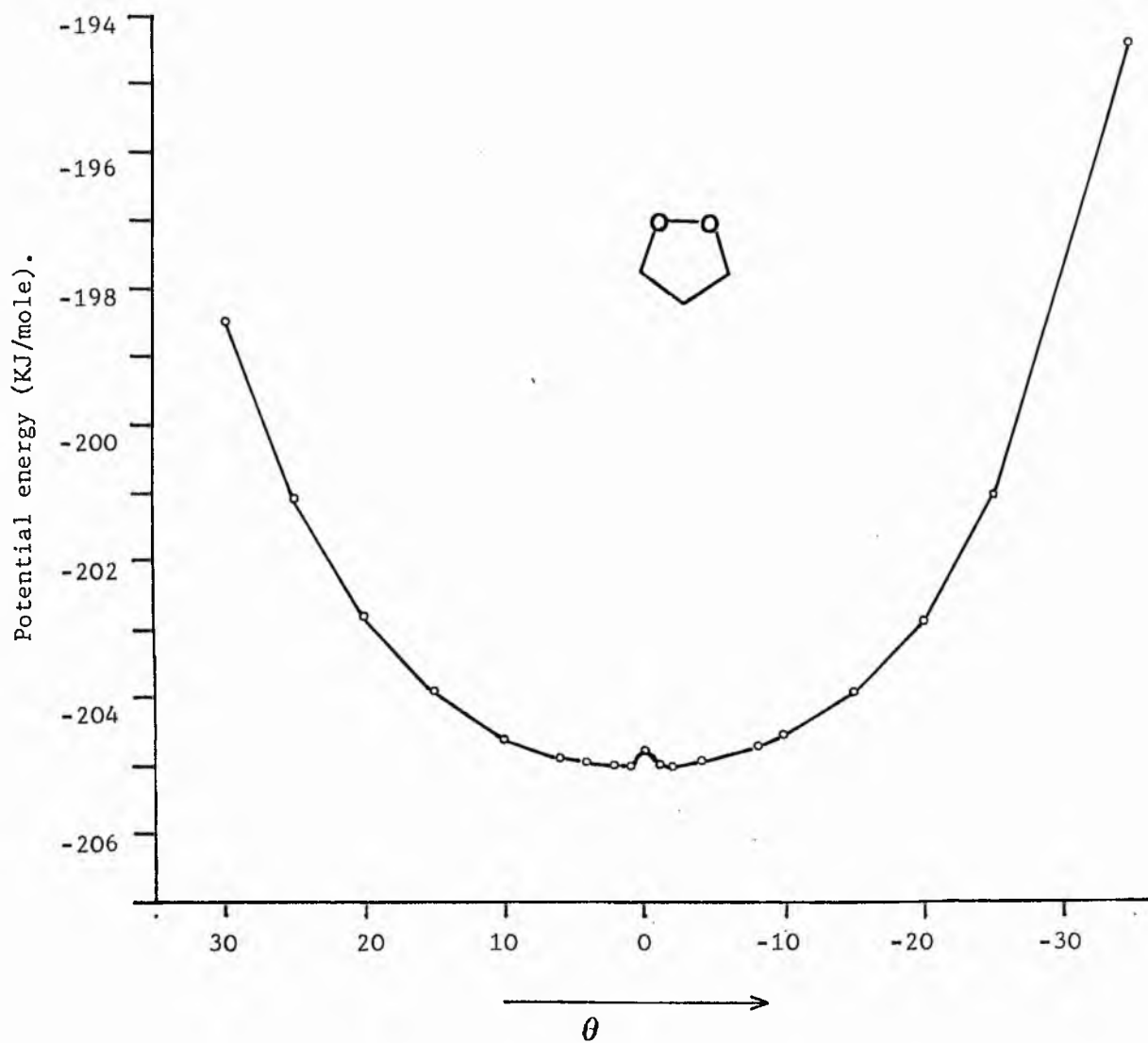


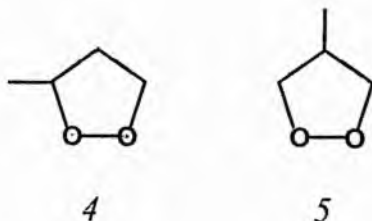
FIGURE 2.3.1

Potential energy curve for dioxolane
according to MINDO/3 calculations.

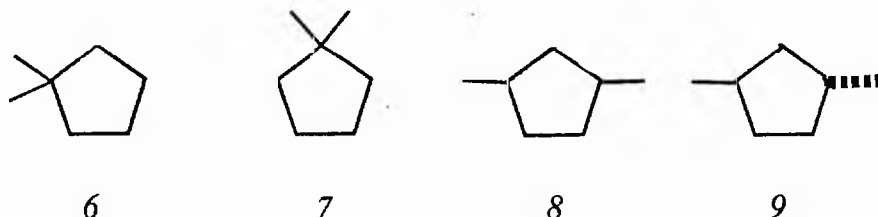
However, the barrier to ring puckering by as much as 20° is low. This is more clearly demonstrated by the contour and transect diagrams of the potential energy surface shown in Figures 2.3.2 and 2.3.3 respectively.

Cremer^[62] has argued that NDO methods would be unlikely to adequately describe the electronic features important in determining degree and mode of ring puckering. Indeed Cremer proposes that ab-initio calculations with large basis sets including polarisation functions have to be employed in the calculations of the various conformers. Table 2.3.7 presents a comparison of MINDO/3 and ab-initio calculations on dioxolane. At all levels of sophistication the calculations consistently predict a planar ring as the optimum geometry. With a STO-3G basis set the MINDO/3 calculations are in good agreement with the exception of the O-C bond length. Agreement with the larger basis set calculation is poor however for both MINDO/3 and STO-3G calculations. The discrepancies between the different approaches can be rationalised by the same argument applied to the dioxirane calculations (vide supra).

Substitution of a hydrogen by a methyl group can give rise to two positional isomers (4 and 5). The calculations suggest that 1-substitution is the thermodynamically favoured isomer by 34 KJmole^{-1} , with both isomers being essentially planar.



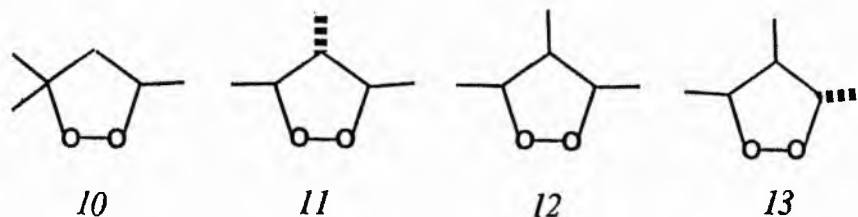
Four dimethyl isomers of dioxolane have been investigated. The 1,1-dimethyl isomer (6) is calculated to be 51 KJmole^{-1} more stable than the 2,2-dimethyl isomer (7), although both are less stable than the cis and trans 1,3-dimethyl isomers (8 and 9). The trans 1,3 isomer is calculated to be 1.1 KJmole^{-1} more stable than the cis isomer.



The latter fact is in contrast to the relative stabilities of 1,2-dimethylcyclopentanes^[64d] as determined from heats of formation in which the cis isomer is lower in energy than the trans isomer. For the dimethylcyclopentanes, the difference in stabilities arises from the fact that in the cis configuration the methyl groups can both assume pseudo-equatorial positions in the envelope conformer common to both isomers, while in the trans isomer one methyl group must assume the unfavourable axial position. As the ring tends to planarity the pseudo-axial and equatorial groups become equivalent. In the limiting case of a planar ring the predominant interactions determining the relative energies of the two isomers will be 1,3-steric perturbations. For trans 1,3-dimethyldioxolane no 1,2-steric interactions between the methyl groups are present resulting in a lower energy than its cis isomer.

The equilibrium properties of three 1,2,3-trimethyldioxolanes

(11-13) and 1,1,3-trimethyldioxolane (10) have also been calculated. The 1,1,3-trimethyl isomer (10) is determined to be less stable than the two 1,2,3-trimethyl isomers with two methyl groups on the same side of the ring, but more stable than isomer (12) in



which all the substituted groups are on the same side of the ring. The relative energies of isomers (11-13) suggests that 1,2-steric perturbations are more important than 1,3 interactions in determining the relative stabilities of substituted dioxolanes.

Five tetramethyldioxolanes have been investigated using MINDO/3. The relative enthalpies of formation of the isomers is in direct accord with the hypothesis put forward *vide supra*. The four 1,2 vicinial interactions in isomer (14) leading to a decrease in heat of formation by 91 kJmole^{-1} compared with isomer (15).



Isomers (17) and (18) are more than 26 kJmole^{-1} more stable than isomer (16) as a result of the fewer number of 1,2 interactions and fewer substituents in the 2 position. The number of 1,2 interactions also rationalises the 9 kJmole^{-1} difference in heats of formation of (17) and (18).

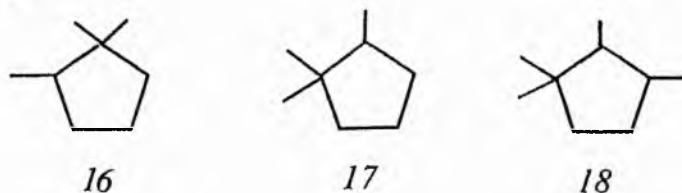


FIGURE 2.3.2 Contour map of the potential energy surface of dioxolane according to MINDO/3 calculations. The potential minimum of the (θ, φ) diagram is 205.0 KJ/mole.

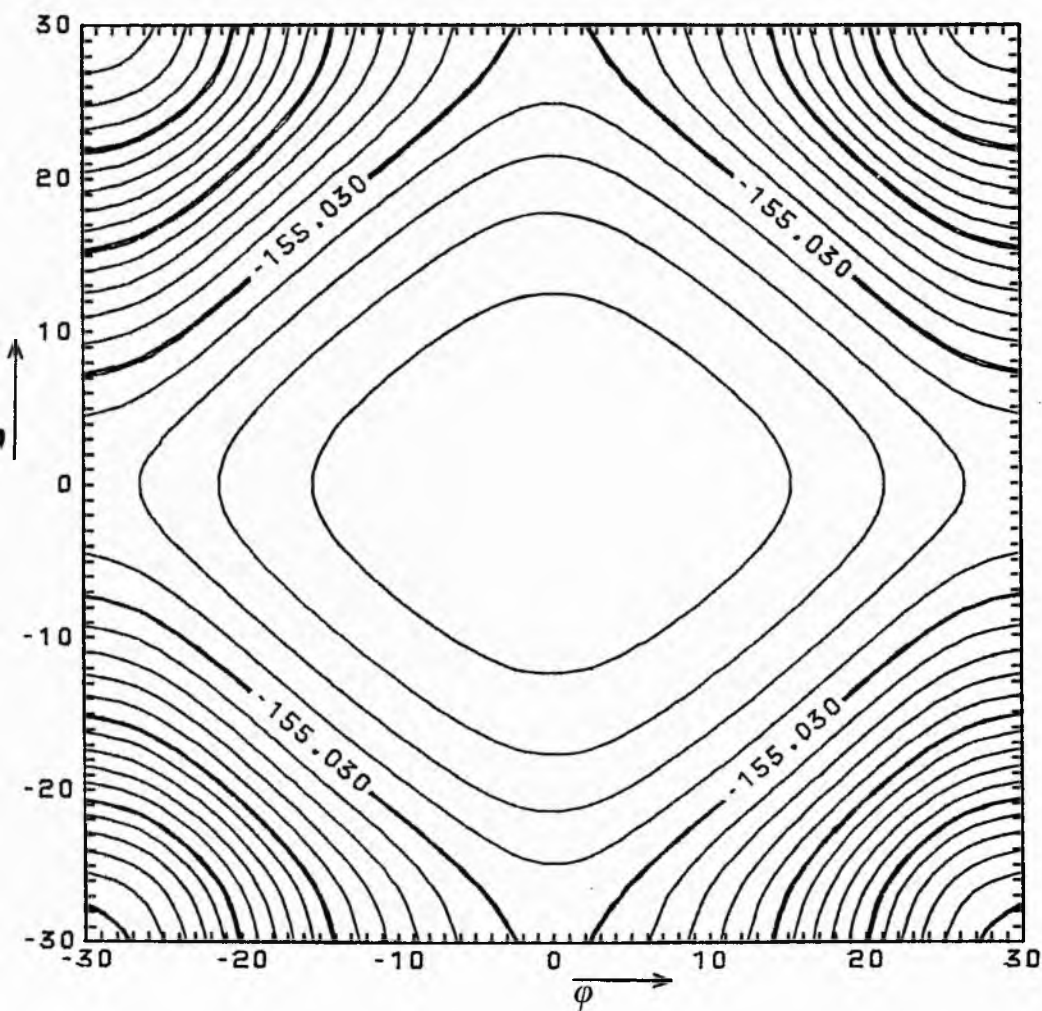
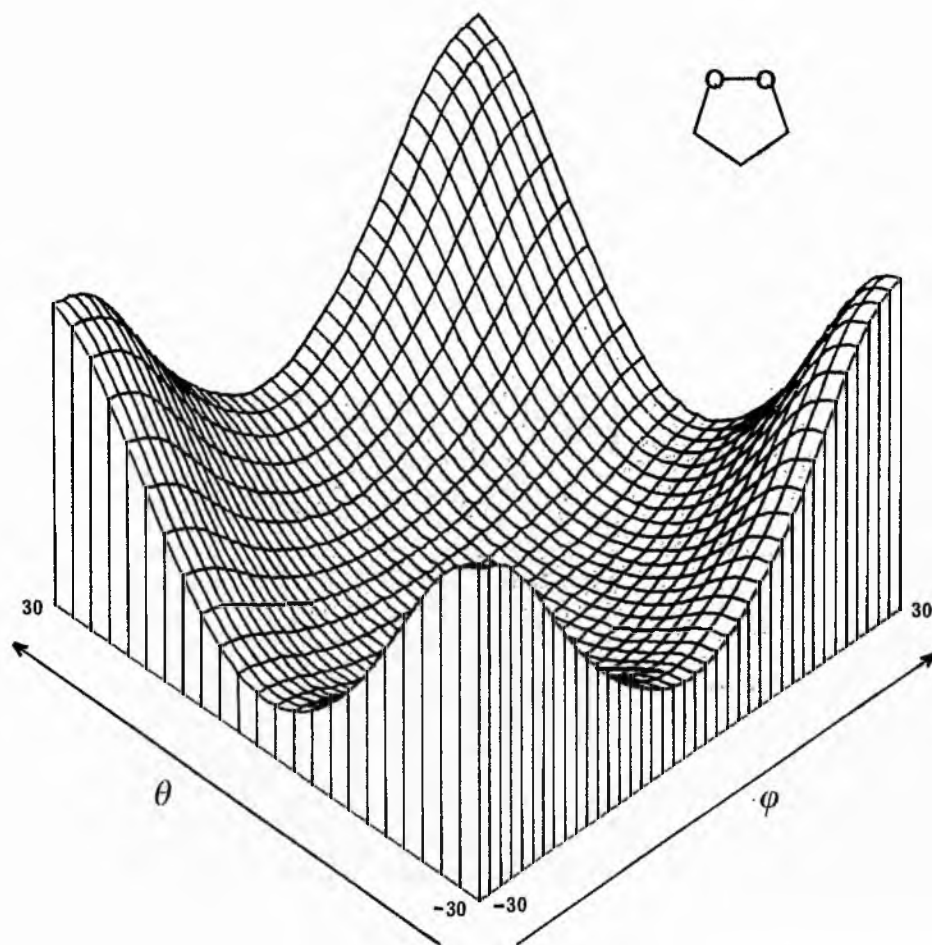


FIGURE 2.3.3 Transect diagram of the potential energy surface of dioxolane according to MINDO/3 calculations. The potential energy is -205.02 KJ/mole at the center of the (θ, φ) diagram and +48.45 KJ/mole at the summits.



As for the dioxetanes only a limited amount of photoelectron spectral data is available for the 1,3-dioxacyclopentanes. The agreement between 1,3-dioxocyclopentane (8) and experimental values is poor (9.67 of 9.86) however the tetramethyl isomer (15) agreement is excellent as show in Table2.3.4. A detailed calculation of the ionisation potentials should invoke both the ground and excited state geometries. The MINDO/3 values reported are calculated using only the ground state geometry and hence when the ground state geometry is different from the excited state the agreement between experimental and this naive theoretical approach cannot be expected. This is in accord with above calculations, the tetramethyl derivative (15) is likely to have a steeper potential well than (8) and hence should be expected to be essentially unchanged in the excited state.

Table 2.3.1 Equilibrium molecular properties for
dioxolane and mono- and dimethyl- derivatives.


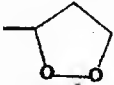
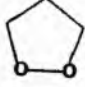

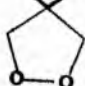
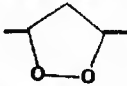
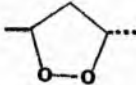
Peroxide	Entry	ΔH_f (KJ/mole)	Vertical Ionisation Potential (eV)	Dipole Moment (Debye)
	3	-205.02	9.672	2.727
	4	-235.96	9.575	2.789
	5	-201.96	9.663	2.688
	6	-224.68	9.440	2.862
	7	-173.89	9.649	2.632
	8	-265.82	9.436	2.832
	9	-266.90	9.523	2.760

Table 2.3.2 Equilibrium geometric properties for
dioxolane and mono- and dimethyl- derivatives.


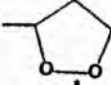
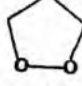

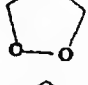
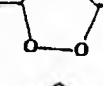

Peroxide	Entry	rO-O	rO-C1	rO-C3	rC1-C2	rC2-C3
	3	1.398	1.368	1.368	1.510	1.510
	4	1.398	1.380	1.368	1.528	1.509
	5	1.396	1.395	1.363	1.554	1.510
	6	1.395	1.395	1.363	1.554	1.510
	7	1.393	1.363	1.363	1.553	1.554
	8	1.394	1.380	1.380	1.528	1.528
	9	1.394	1.379	1.379	1.530	1.530

Table 2.3.3 Equilibrium geometric properties for
dioxane and mono- and dimethyl- derivatives.


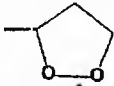


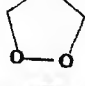
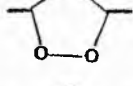
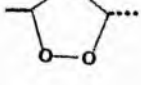
Peroxide	Entry	<CCC	<OCC	<OOC	<CCOO	<CCC03
	3	104.44	106.56	111.16		-0.19
	4	105.20	104.72	112.01	7.10	-4.54
	5	102.31	107.64	111.20	-0.33	0.45
	6	105.69	107.02	110.77	1.24	0.97
	7	100.27	108.51	111.29	-0.70	-0.12
	8	106.57	103.91	112.78	-1.12	4.36
	9	105.80	104.38	111.79	-9.75	0.81

Table 2.3.4 Equilibrium molecular properties for
polymethyldioxolanes

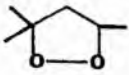
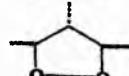
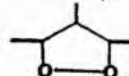
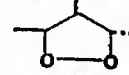
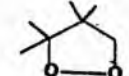
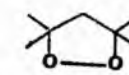
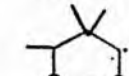
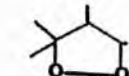
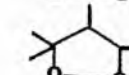
Peroxide	Entry	ΔH_f (KJ/mole)	Vertical Ionisation Potential (eV)	Dipole Moment (Debye)
	10	-254.51	9.339	2.867
	11	-265.79	9.437	2.765
	12	-251.78	9.414	2.711
	13	-260.39	9.520	2.679
	14	-152.10	9.383	2.754
	15	-241.29	9.236	2.921
	16	-207.08	9.958	2.541
	17	-242.13	9.317	2.799
	18	-233.95	9.285	2.802

Table 2.3.5 Equilibrium geometric properties for
polymethyldioxolanes


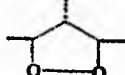
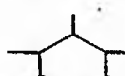
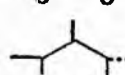
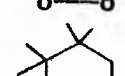
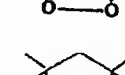
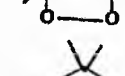
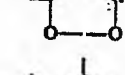
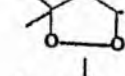
Peroxide	Entry	rO-O	rO-C1	rO-C3	rC1-C2	rC2-C3
	10	1.393	1.394	1.377	1.552	1.527
	11	1.392	1.375	1.376	1.552	1.550
	12	1.392	1.377	1.374	1.556	1.555
	13	1.391	1.374	1.380	1.553	1.554
	14	1.388	1.391	1.357	1.617	1.555
	15	1.391	1.392	1.392	1.552	1.552
	16	1.388	1.373	1.373	1.584	1.585
	17	1.388	1.394	1.372	1.580	1.553
	18	1.389	1.390	1.373	1.582	1.556

Table 2.3.6 Equilibrium geometric properties for
polymethyldioxolanes

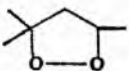
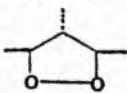
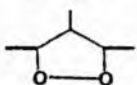
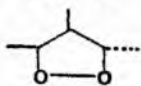
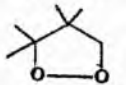
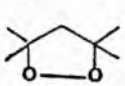
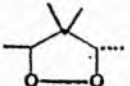
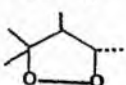
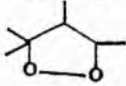
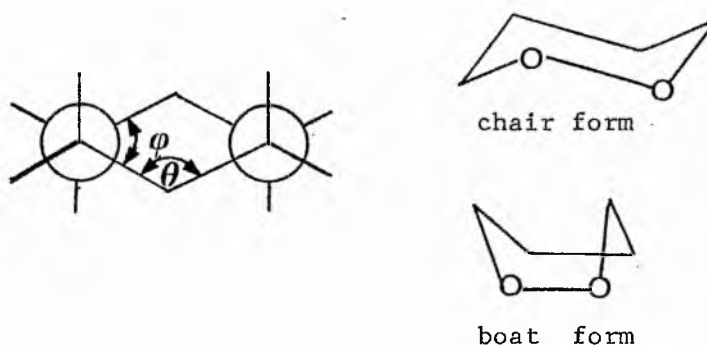
Peroxide	Entry	<CCC	<OCC	<OOC	<CCOO	<CCC03
	10	107.27	104.20	112.51	-4.82	3.75
	11	103.86	105.10	112.41	-8.63	9.53
	12	102.49	105.20	111.61	-15.96	17.04
	13	103.96	104.61	112.10	-12.72	3.40
	14	101.50	109.04	111.09	0.40	0.43
	15	107.95	102.32	113.69	0.36	0.08
	16	101.04	105.47	111.06	-20.36	7.61
	17	104.65	105.29	112.60	-7.48	7.66
	18	104.65	105.54	112.70	-0.37	-0.68

Table 2.3.7 Comparison of MINDO/3 and ab-initio calculations
on dioxolane.

Parameter	MINDO/3	STO-3G	3-21G
$r_{C_1-C_2}$	1.510	1.545	1.542
r_{O-C}	1.368	1.452	1.461
r_{O-O}	1.398	1.406	1.469
r_{C_1-H}	1.128	1.095	1.078
r_{C_2-H}	1.116	1.086	1.080
$\angle CCC$	104.44	103.02	104.71
$\angle OCC$	106.56	108.10	108.22
$\angle OOC$	111.16		
$\angle C_2C_1H$	113.77	111.34	111.69
$\angle C_1C_2H$	112.67	111.60	110.87
$\angle CCCO$	-0.19	0.00	0.00
$\angle CCCH$	237.98	240.61	241.86
$\angle CUCH$	120.94	119.39	118.14
$\angle OCCH$	240.02	240.60	240.42
$\angle OCCH$	124.93	119.39	119.58

oxygen atoms will be expected to flatten the ring relative to cyclohexane by virtue of the shorter C-O and O-O bond distances. In cyclohexane the optimum conformation is a balance between an ideal chair form, resulting in torsional angles (φ) of 60° and C-C-C bond angles (θ) of 109.3° and a chair form with idealised bond angles of 112.4° resulting in a torsional angle of 55.8° . The MINDO/3 calculations predict values of $58.48-62.64^\circ$ and $110.69-114.17^\circ$ for φ and θ respectively for the chair conformations of the dioxanes studied. For dioxane itself the calculated values of φ and θ are 58.48° and 114.17° respectively. The results suggest therefore that torsional strain predominates in determining the nature of the chair form at the expense of increased Baeyer strain.



The chair form of dioxane is calculated to be more stable than the boat form by 11 KJmol^{-1} . For cyclohexane the difference in energy between the chair and boat form is reported to be of the order of 30 KJmol^{-1} . Figure 2.4.1 shows the potential curve for variation of the torsional angle (φ) from one chair form to the other. As in previous calculations in this study all geometrical parameters were completely optimised at each point. The calculated barrier to inversion for the chair forms of dioxane is 13 KJmol^{-1} . The

potential well for the boat form was not located in this set of calculations. Presumably a more careful study around the maximum ($\phi = 0^\circ$) is required. However, the calculations do suggest that the potential well for the boat form must be shallow, with a very small barrier to change in conformation to the more stable chair form. This is not too surprising in view of the short C-O and O-O bond lengths in dioxane which will bring about adverse steric interaction of the hydrogens in the 3,6-position as the ring adopts the boat form. Hence one would intuitively predict a larger difference in potential energy between the chair and boat forms of dioxane than cyclohexane. This is not the case, suggesting that MINDO/3 underestimates the relative energies of conformers.

Two monosubstituted dioxanes have been investigated. The methyl substituent can assume either the axial or equatorial positions. Calculations have been performed on both the chair and boat forms of the axial and equatorial methyl dioxanes (3,4). For both (3) and (4) the chair forms are lower in energy than the boat form, with the substituent preferring to be in the equatorial position as expected on the basis of a reduced gauche interaction. The potential energies of all the 3-methyldioxanes are calculated to be lower than the 4-substituted dioxanes, irrespective of ring conformation by more than 14 KJmole^{-1} .

The substitution becomes a little more complicated with the introduction of a second methyl group in the dioxane ring. The introduction of the second substituent gives rise to the possibility of two diastereoisomeric forms a cis and trans compound. Five positional isomers are possible for dimethyldioxanes. We have investigated all the chair conformers and diastereoisomers of

3,4-dimethyldioxane (5) and the boat forms of 3,3-dimethyl- and 4,4-dimethyl- dioxanes (7 and 8). Two of the possible four 3,6-dimethyldioxanes have also been studied.

For the 3,4-isomers, the calculations predict that the e,e isomer is by far the most stable. This is in accord with the observed results for trans 1,2-dimethylcyclohexanes for which the molecule exists almost exclusively in the e,e form at ambient temperature. For dimethylcyclohexanes with cis-vicinial substituents the ring flip forms are equivalent. This is not the case for dimethyldioxane. The calculations suggest that for the cis-dimethyldioxanes the methyl group at C3 is preferred in the equatorial position. This is in accord with the relative energies of the monomethyl derivatives for which there is a larger difference in energy between equatorial and axial forms of the 3-methyl- than 4-methyl- dioxane. The calculations on the boat forms of geminal dimethyldioxanes (6 and 7) further support the conclusion that 3-substitution is preferred to 4-substitution.

For the 3,6-dimethyldioxane the e,e boat isomer is found to be lower in energy than the a,a chair isomer. The relative stabilities of the four positional isomer are $3,6 > 3,4 > 3,3 > 4,4$. The conformation of the e,e boat form of 3,6-dimethyldioxane is shown in Figure 2.4.2.

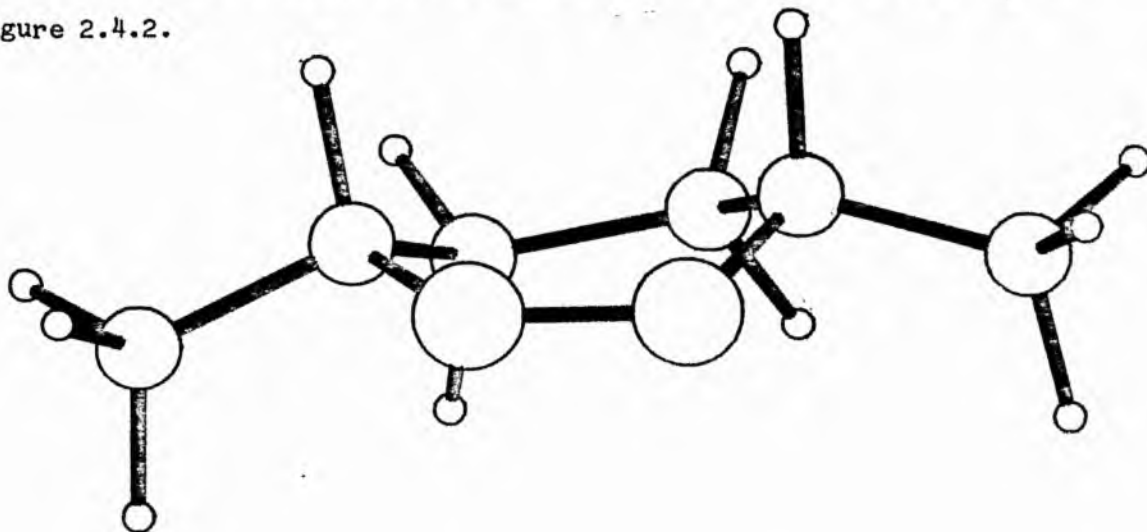


Figure 2.4.2 Conformation of e,e boat form of 3,6-dimethyldioxane.

Table 2.4.1 Heats of formation, ionisation potentials and dipole moments of dioxane and its monomethyl derivatives.


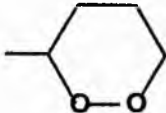
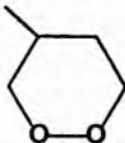
Peroxide	Conformation	ΔH_f KJmole ⁻¹	Ionisation Potential (eV)	Dipole Moment (debye)
	chair	-216.87	9.884	2.28
	boat	-203.94	9.449	2.57
	chair (ax)	-238.21	9.76	2.27
	(eq)	-245.65	9.82	2.22
	boat (ax)	-233.59	9.36	2.45
	(eq)	-225.07	9.34	2.60
	chair (ax)	-211.11	9.86	2.25
	(eq)	-214.03	9.88	2.27
	boat (ax)	-200.12	9.48	2.45
	(eq)	-200.28	9.44	2.54

Table 2.4.2 Heats of formation, ionisation potentials and dipole moments of dimethyldioxanes.

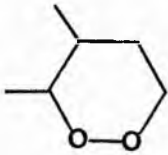
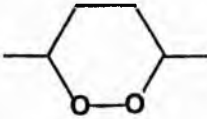
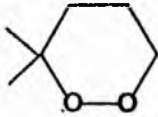
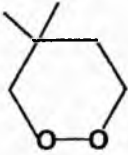
Peroxide	Conformation /isomer	ΔH_f KJmole ⁻¹	Ionisation Potential (eV)	Dipole Moment (debye)
	chair 1e2e	-236.35	9.79	2.18
	1e2a	-229.59	9.77	2.16
	1a2e	-225.17	9.74	2.26
	1a2a	-229.22	9.75	2.25
	chair a,a	-259.46	9.62	2.22
	boat e,e	-261.88	9.26	2.33
	boat	-211.68	9.25	2.57
	boat	-153.74	9.43	2.50

Table 2.4.3 Calculated bond lengths for dimethyldioxanes

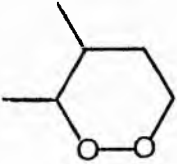

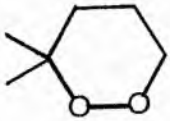
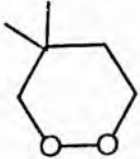
			rO-O	rC ₁ -O	rC ₄ -O	rC ₁ -C ₆	rC ₄ -C ₅	rC ₆ -C ₅
	1e2e		1.388	1.375	1.364	1.555	1.510	1.542
	1e2a		1.387	1.377	1.365	1.559	1.512	1.542
	1a2e		1.385	1.384	1.367	1.559	1.510	1.538
	1a2a		1.386	1.381	1.365	1.557	1.510	1.541
	chair	a a	1.386	1.383	1.385	1.533	1.528	1.516
	boat	e e	1.387	1.370	1.372	1.528	1.528	1.517
	boat		1.387	1.387	1.359	1.554	1.506	1.516
	boat		1.387	1.358	1.356	1.512	1.551	1.563

Table 2.4.4 Calculated bond lengths for dioxane and its monomethyl derivatives


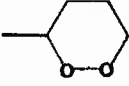
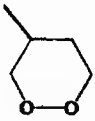
conf			rO-O	rC ₁ -O	rC ₄ -O	rC ₁ -C ₆	rC ₄ -C ₅	rC ₆ -C ₅
	chair		1.388	1.367	1.366	1.511	1.512	1.517
	boat		1.386	1.359	1.359	1.507	1.507	1.515
	chair	axial	1.386	1.380	1.366	1.532	1.509	1.518
		equ	1.388	1.378	1.364	1.532	1.511	1.517
	boat	axial	1.387	1.370	1.363	1.532	1.509	1.518
		equ	1.385	1.375	1.358	1.528	1.505	1.513
	chair	axial	1.388	1.365	1.364	1.535	1.510	1.540
		boat	1.388	1.365	1.365	1.532	1.511	1.538
	boat	axial	1.388	1.360	1.362	1.511	1.529	1.539
		equ	1.386	1.359	1.356	1.508	1.530	1.537

Table 2.4.5 Calculated bond and dihedral angles for dioxane and
its monomethyl derivatives


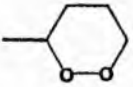
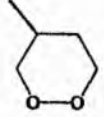
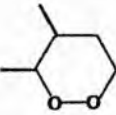
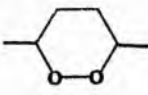
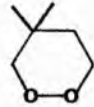
		$\angle \text{OOC}_1$	$\angle \text{OOC}_4$	$\angle \text{OC}_4\text{C}_5$	$\angle \text{C}_6\text{C}_5\text{C}_4$	$\angle \text{C}_4\text{OOC}_1$	$\angle \text{C}_5\text{C}_4\text{OO}$	$\angle \text{C}_6\text{C}_5\text{C}_4\text{O}_3$
	chair	116.11	116.28	114.17	115.20	58.48	312.05	30.64
	boat	123.19	121.77	116.05	115.42	1.85	331.69	33.19
	chair axial	117.16	115.76	113.72	115.73	61.90	311.56	28.80
	equ	117.16	115.79	114.18	115.30	60.57	312.76	30.69
	boat axial	122.28	120.49	115.45	115.03	-14.39	333.70	34.62
	equ	125.01	121.84	115.57	115.50	0.10	333.46	35.93
	chair axial	116.34	115.54	114.35	116.98	58.56	313.76	32.48
	equ	116.11	115.28	114.61	116.76	58.97	313.76	31.90
	boat axial	120.79	119.11	116.89	110.15	-20.90	335.11	43.82
	equ	122.24	121.46	115.68	109.48	0.14	326.06	45.64

Table 2.4.6 Calculated bond and dihedral angles for dimethyldioxanes

		$\angle \text{OOC}_1$	$\angle \text{OOC}_4$	$\angle \text{OC}_4\text{C}_5$	$\angle \text{C}_6\text{C}_5\text{C}_4$	$\angle \text{C}_4\text{OOC}_1$	$\angle \text{C}_5\text{C}_4\text{OO}$	$\angle \text{C}_6\text{C}_5\text{C}_4\text{O}$	
	chair	1e2e	118.18	114.41	113.87	117.08	61.51	312.33	33.31
		1e2a	116.82	115.44	113.88	116.89	60.69	315.38	34.01
		1a2e	117.11	115.47	113.76	116.97	62.07	314.57	31.84
		1a2a	117.02	115.25	114.01	117.51	62.64	313.73	29.23
	chair	aa	117.07	117.61	110.69	117.16	62.62	312.15	28.83
	boat	ee	121.85	121.70	112.77	115.53	-15.60	333.42	37.45
	boat		125.15	121.06	114.63	115.54	-6.22	329.99	36.19
	boat		120.68	121.41	117.92	106.87	-5.06	326.40	42.98

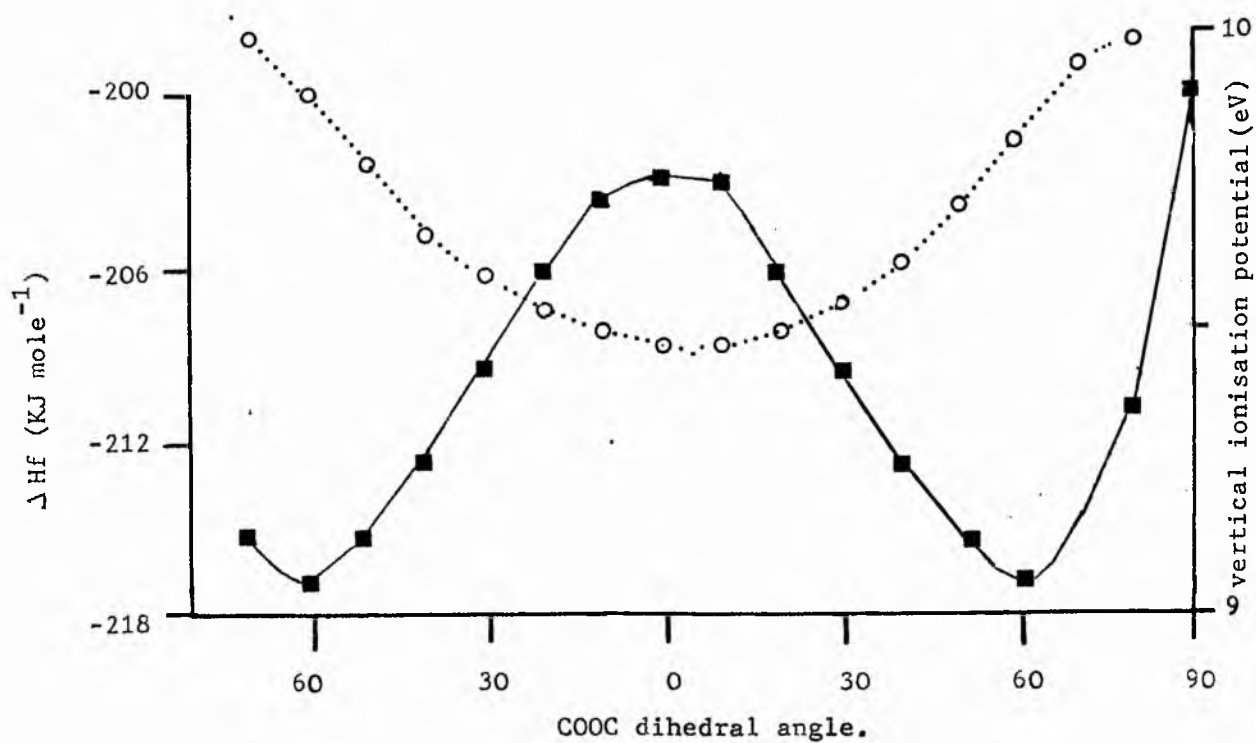
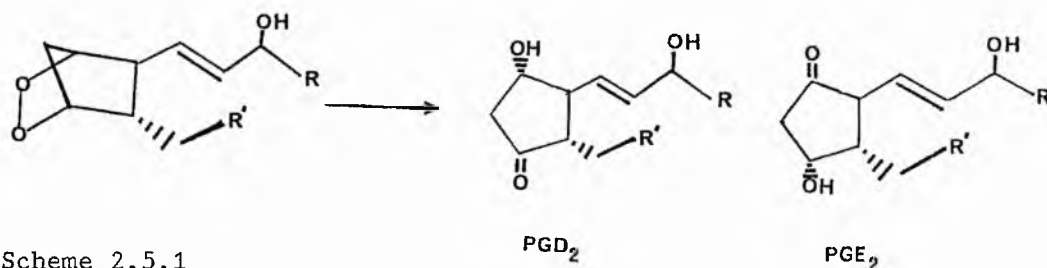


FIGURE 2.4.1 Potential curve for variation in the torsional angle COOC from one chair form to the other, for dioxane.

○ vertical ionisation potential.
 ■ heat of formation

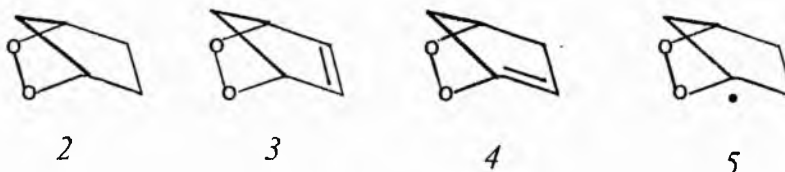
2.5 The decomposition of 2,3-dioxobicyclo[2.2.1]heptane and derivatives.

The breakdown of the peroxidic linkage of prostaglandin endoperoxides is a key step in the biosynthesis of potent bioregulators such as prostaglandins D and E (scheme 2.5.1).^[71]



The understanding of the complex biochemistry of prostaglandin endoperoxides is clearly of paramount importance. Coughlin and coworkers^[72,73] have studied the mechanism of decomposition of the prostaglandin nucleus 2,3-dioxobicyclo[2.2.1]heptane (2) under basic^[72] and non-polar^[73] conditions, while Wilson *et al.* have studied the decomposition of 1,5-dimethyl-6,7-dioxobicyclo[3.2.1]octane (4) under several conditions^[74].

We have investigated the O-O cleavage of the bicyclic peroxides 2-5 using MINDO/3. The reaction pathway should correspond to the gas phase ring opening of the peroxides which is clearly going to be analogous to the non-polar decomposition reaction. Compound (3) is well known and has been fully characterised and its chemistry

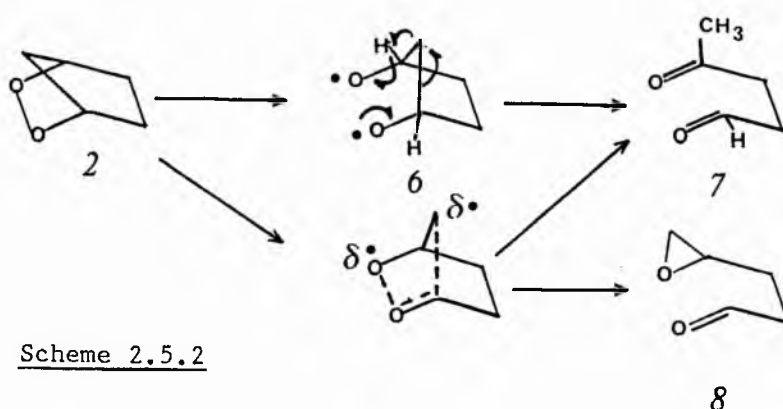


elucidated^[75]. Compound (4) on the other hand is a highly unlikely valence isomer of (3) since it contains a bridgehead double bond in the ring system and has not been reported. Species (5) could conceivably be the product of free radical hydrogen abstraction from (2).

Table 2.5.1 and 2.5.2 list the calculated molecular properties of the peroxides 2-5.

Figure 2.5.1 shows the calculated reaction co-ordinates for the O-O scission of the bicyclic peroxides. Geometries were completely optimised at each point and the calculations were performed using the single-configuration Hartree-Fock approximation. These optimised geometries were used as the starting geometries for further calculations as discussed below. The reaction product derived from the O-O cleavage of (2) is levulinaldehyde (7). The product found experimentally from the thermolysis of (2) is the epoxy aldehyde (8)^[73]. The formation of (7) from (2) has been observed under base-catalysed conditions^[72].

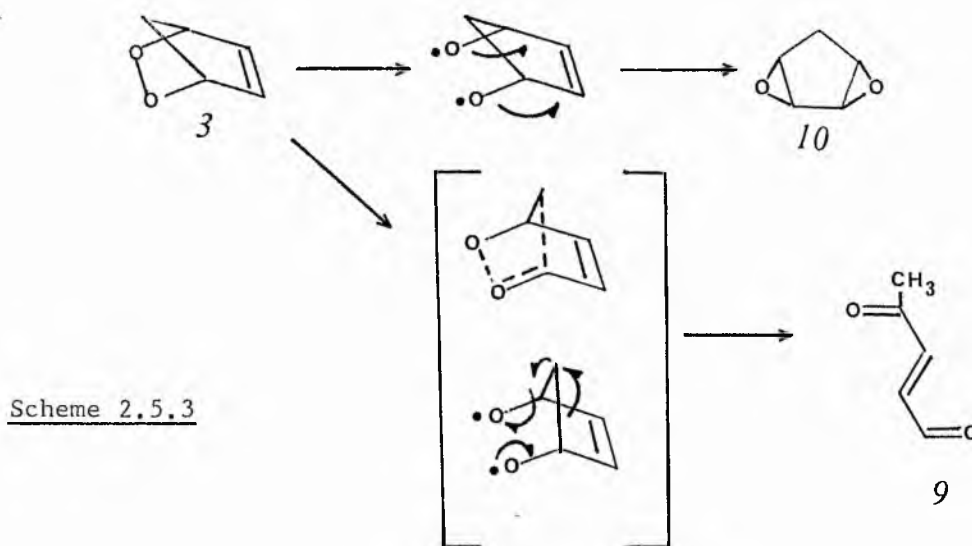
A plausible mechanism for the formation of levulinaldehyde (7) from (2) is shown in scheme 2.5.2.



The rearrangement could take place via the diradical or the

concerted pathway. The concerted β -scission pathway has been proposed^[73] to account for the formation of 4,5,-epoxypentanal (8) although the stepwise process could not be discounted.

The calculated product from cleavage of the O-O bond of (3) is the dialdehyde (9). Experimentally, however the bisepoxide (10) is found exclusively on thermolysis of (3).



The calculated energy profiles for the O-O cleavage of peroxides (2) and (3) seem unlikely. The energy rising steadily concomitantly with increasing O-O bond distance, then suddenly dropping to a value similar to that of the calculated product of reaction. The explanation for this strange result lies in the use of the single-configuration wave function inherent to the MINDO/3 method. Such wave-functions cannot satisfactorily describe the biradical or biradical type intermediates likely to be involved in a homolytic cleavage of a O-O bond.

The difficulty may be overcome by including configurational interaction (CI). In the calculations performed, using a single-configuration wave-function, the wave-function is represented by one Slater determinant built over 'occupied orbitals'. The configurational interaction wavefunction ψ , is a superposition of Slater determinants ψ_i

$$\psi = \sum_i c_i \psi_i$$

built from both sets of 'occupied' and 'virtual' orbitals. The leading term in the expansion will represent the Hartree-Fock single-configuration wave-function and the remaining terms will represent the configurations obtained by promoting electrons from the occupied orbitals to the virtual ones. The expansion coefficients c_i are determined by energy minimisation associated with this wavefunction. A drawback of the CI method is that it is only slowly convergent^[15,16].

Attempted calculations on (3) with CI using the geometries obtained (vide supra) as starting parameters did not however give satisfactory results. The single-configuration calculations overestimate the ionic contributions to the wavefunction, hence leading to a gross overestimation of the energies involved the homolysis. Calculations with CI should correct for this and lead variationally to a lower energy. However with the exception of the equilibrium geometry, higher energies were calculated with the inclusion of CI. The explanation for this is presumably a consequence of the poor description of the virtual orbitals in the MINDO/3 method. In fact MINDO/3 uses only one excited state configuration in its CI calculations along with the ground state configuration, and this excited state configuration corresponds to a double excitation (Figure 2.5.1). Although this may well be the most important excited state configuration for a singlet species, for biradicals the most

important excited state configurations are likely to result from a single excitation (Figure 2.5.1).

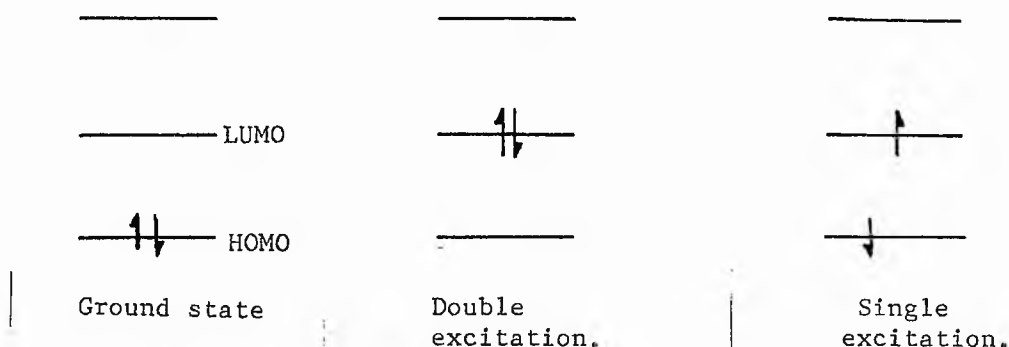


Figure 2.5.1

Furthermore the limitations of including only one excited state configuration in the CI wave-function may be unacceptable for biradicals, since the chosen unoccupied molecular orbital may not have a node between the two atoms of interest (in this case O-O). Indeed it would be fortuitous if the LUMO were of the correct symmetry. If this is so, then it would lead to a perpetuation of the errors manifested in the single-configuration treatment resulting in an increase in energy rather than a decrease and consequently giving a less accurate description of the molecule. This was indeed the case for the calculations described above.

Clearly the MINDO/3 method in its present form is unsuitable for these type of reaction coordinates. The unrestricted Hartree-Fock version of MINDO, UMINDO^[76] may well be a better alternative. Alternatively more sophisticated ab initio procedures involving a large number of configurations and allowing for single excitation may be used. Other methods of dealing with the problems of describing the wavefunction for a biradical type species exist. The 'Many Body Perturbation' method is such an alternative and calculations of this nature are currently in progress^[77].

Table 2.5.1 Heats of formation, total energies, ionisation potentials and dipole moments of bicyclic peroxides

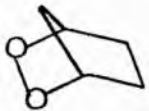

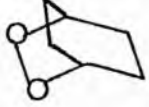
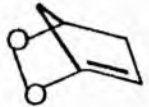


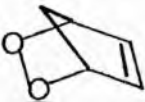

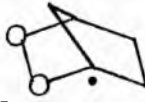
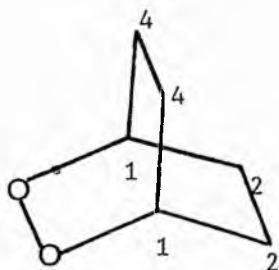
Compound	Entry	ΔH_f (KJmole ⁻¹)	Total Energy (eV)	Vertical Ionisation Potential (eV)	Dipole Moment (Debye)
	2	-114.76	-1373.01	9.240	2.812
	3	+22.38	-1342.06	9.150	2.837
	6	-183.67	-1530.13	9.060	2.694
	4	+126.15	-1340.99	8.318	3.142
	5	+ 33.37	-1356.71	4.247	2.994

Table 2.5.2 Equilibrium skeletal geometrical parameters for bicyclic peroxides

Parameter				
r O-O	1.411	1.406	1.423	1.430
r C ₁ -O	1.390	1.399	1.411	1.341
r C ₄ -O	1.390	1.406	1.396	1.396
r C ₁ -C ₂	1.546	1.522	1.508	1.522
r C ₂ -C ₃	1.537	1.358	1.523	1.549
r C ₃ -C ₄	1.547	1.522	1.549	1.554
r C ₁ -C ₇	1.543	1.549	1.536	1.528
r C ₄ -C ₇	1.546	1.548	1.555	1.549
< OOC ₄	106.48	106.06	98.80	109.92
< C ₇ C ₁ O	100.64	100.26	102.08	105.94
< C ₁ C ₂ C ₃	102.17	105.67	111.92	96.03
< O ₅ C ₄ C ₃	107.69	105.64	99.71	109.92
< C ₄ C ₃ C ₂ C ₁	1.97	-0.48	26.53	0.26
< O ₅ C ₄ C ₃ C ₂	66.95	68.20	55.83	66.59
< O ₆ O ₅ C ₄ C ₃	287.52	292.34	303.64	295.84
< C ₇ C ₁ O ₆ O ₅	-37.88	-36.67	1.01	-34.49



Bond lengths/ Å	bond angles	dihedral angles
r O-O 1.402	$\angle C_2 C_2 C_1$ 108.12	$\angle C_1 C_2 C_2 C_1$ 0.08
r O-C ₁ 1.386	$\angle O C_1 C_2$ 107.55	$\angle O C_1 C_2 C_3$ 57.25
r C ₁ -C ₂ 1.542	$\angle O O C_1$ 113.21	$\angle O O C_1 C_2$ 299.71
r C ₂ -C ₂ 1.529	$\angle O C_1 C_4$ 107.53	$\angle C_4 C_1 O O$ 299.71

FIGURE 2.5.2 Equilibrium skeletal geometrical parameters for
2,3-dioxobicyclo[2.2.2]octane.

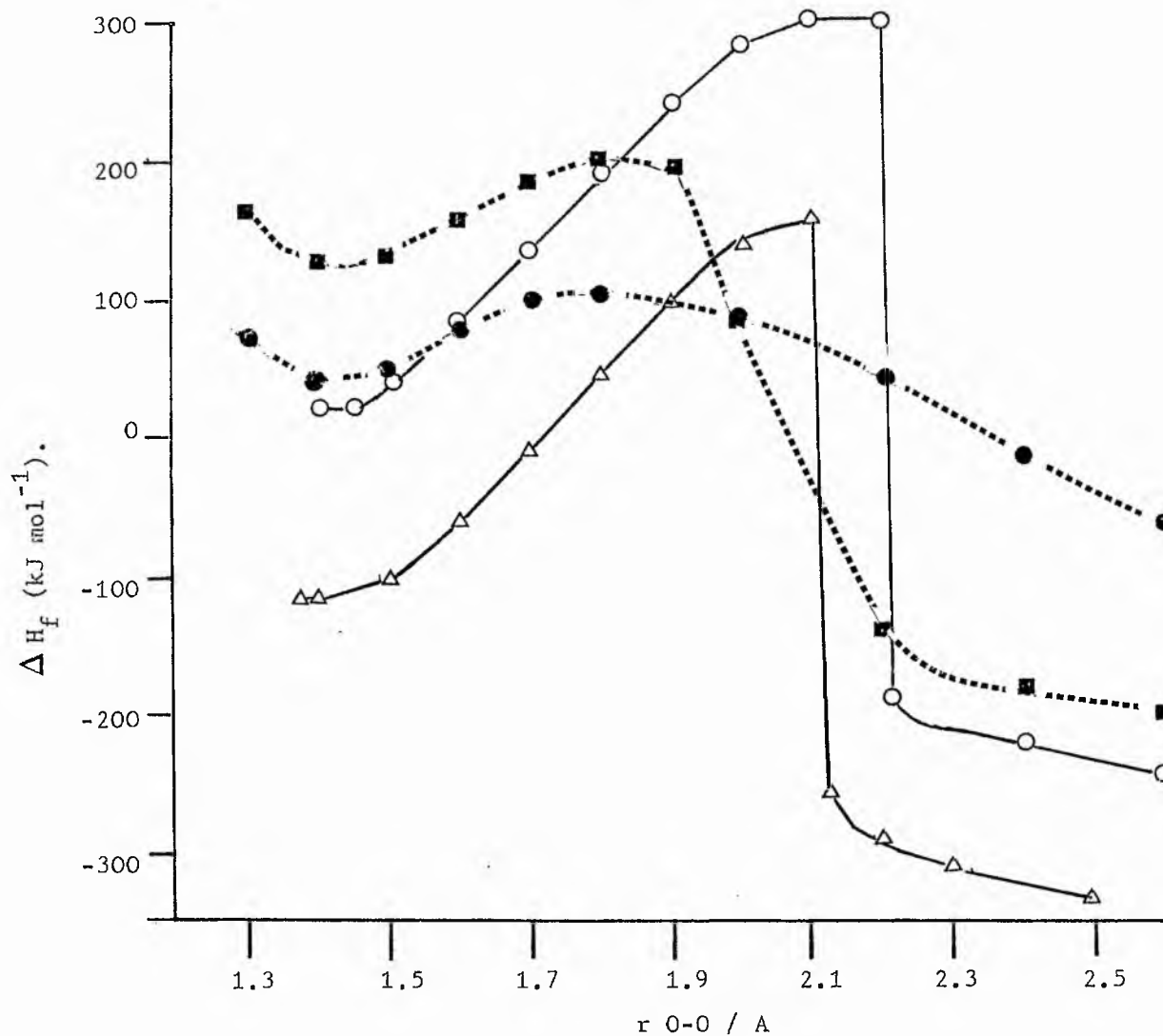


FIGURE 2.5.1

Potential energy curves for O-O bond stretching of the cyclic peroxides 2-5 according to MINDO/3.

Geometries were completely optimised for each point in the reaction co-ordinate.

Δ reaction co-ordinate for peroxide 2.

○ " " " 3.

● " " " 5.

■ " " " 4.

Theoretical procedures.

Semiempirical calculations were performed with the IBM version of MINDO/3^[80] implemented on a VAX 11/ 780 computer. No assumptions of any kind were made and the reported equilibrium properties of each molecule were obtained by energy minimisation with respect to all geometric variables simultaneously unless otherwise stated. Reaction co-ordinates were similarly obtained with full optimisation of all geometric variables, save those implicitly defined by the reaction co-ordinate.

Ab initio calculations described in this work were performed by Dr.J.R.Ball of the NFCR. The calculations were performed using the GAUSSIAN 80 system of programs^[81]. Two basis sets, STO-3G^[82] and 3-21G^[83] were routinely used.

The calculations used equilibrium geometries obtained by MINDO/3 (vide supra) as the starting parameters for a calculation. All variables were subsequently optimised with respect to force minimisation.

References

1. C.C.J. Roothaan, Rev. Mod. Phys., 1951, 23, 69.
2. G.G. Hall., Proc. Roy. Soc., Ser.A, 1951, 205, 541.
3. J.C. Slater, Phys. Rev., 1934, 46, 1002.
4. S.F. Boys, Proc. Roy. Soc., 1950, A200, 542.
5. See E. Clementi and J. Mehl in The Jerusalem Symposia on Quantum Chemistry and Biochemistry, Vol VI, 'Chemical and biochemical reactivity' (Ed. E.D. Bergmann and B. Pullman), Jerusalem. The Israel Academy of Sciences and Humanities, 1974, p 137.
6. Boys was the first to introduce C1 into RH calculations but abandoned this approach in 1958 as unpromising for chemical purposes. See S.F. Boys, G.B. Cook, C.M. Reeves and I. Shavitt., Nature 1956, 178, 1207; S.F. Boys and G.B. Cook, Rev. Mod. Phys., 1960, 32, 285.
7. a) S.F. Boys and N.C. Handy, Proc. Roy. Soc., Ser.A., 1969, 310, 43, 63.
b) W.A. Goddard III and R.C. Ladner., J. Amer. Chem. Soc., 1971, 93, 6750.
c) P.J. Hay, W.J. Hunt and W.A. Goddard III, ibid, 1972, 94, 638, 8293.
d) H. Conroy., J. Chem. Phys., 1964, 41, 1327, 1331, 1336 and 1341.
8. a) E. Huckel., Z. Physik., 1931, 70, 204.
b) E. Huckel., Z. Physik., 1932, 76, 628.
c) E. Huckel., Trans. Faraday. Soc., 1934, 30, 40.
9. a) R. Pariser and R.G. Parr., J. Chem. Phys., 1953, 21, 446, 767.
b) J.A. Pople., Trans. Faraday Soc., 1953, 49, 1375.

10. a) R.D. Brown and M.L. Heffernan., Aust. J. Chem., 1960, 13, 38, 49 and references cited therein.
b) R.D. Brown and R.D. Harcourt, Aust. J. Chem., 1963, 16, 737.
11. R. Hoffmann, J. Chem. Phys., 1963, 39, 1937.
12. J.A. Pople, D.P. Santry and G.A. Segal, J. Chem. Phys., 1965, 43, 5129
13. a) J.A. Pople, D.L. Beveridge and P.A. Dobosh.,
J. Chem. Phys., 1967, 47, 2026
b) R.N. Dixon., Mol. Phys., 1967, 12, 83.
14. a) S. Diner, J.P. Malrieu and P. Aavene, Theoret. Chim. Acta.,
1969, 13, 1.
b) S. Diner, J.P. Malrieu, F. Jordan and M. Gilbert,
Theoret. Chim. Acta, 1969, 15, 100
c) J.P. Malrieu, P. Claverie and S. Diner,
Theoret. Chim. Acta, 1969, 13, 18.
d) J.P. Malrieu, P. Claverie, S. Diner and M. Gilbert.,
Theoret. Chim. Acta, 1969, 15, 100.
15. a) R.C. Bingham, M.J.S. Dewar and D.H. Lo.,
J. Amer. Chem. Soc., 1975, 97, 1285.
b) R.C. Bingham, M.J.S. Dewar and D.H. Lo.,
J. Amer. Chem. Soc., 1975, 97, 1294.
c) R.C. Bingham, M.J.S. Dewar and D.H. Lo.,
J. Amer. Chem. Soc., 1975, 97, 1302.
d) R.C. Bingham, M.J.S. Dewar and D.H. Lo.,
J. Amer. Chem. Soc., 1975, 97, 1307.
e) M.J.S. Dewar, D.H. Lo and C.A. Ramsden.,
J. Amer. Chem. Soc., 1975, 97, 1311.

16. a) A. Veillard in "Quantum Mechanics of Molecular Conformations",
(Ed. B. Pullman), Wiley and Sons, New York, Ch 1, pp 1-116.
b) J.I. Fernández Alonso in "Quantum Mechanics of Molecular
Conformations", (Ed. B. Pullman), Wiley and Sons, New York,
Ch 2 pp 117-192.
17. C. Narries, Chem. Ber., 1903, 36, 1933.
18. H. Staudinger, Chem. Ber., 1925, 58, 1988.
19. R. Griegee, Rec. Chem. Prog., 1957, 18, 111.
See also R. Griegee, Angew. Chem. Internat. Edit., 1975, 14,
745.
20. P.S. Bailey, Chem. Rev., 1958, 58, 925.
21. R.W. Murray, Acc. Chem. Res., 1968, 1, 313.
22. L.A. Hall, I.C. Hisatsune and J. Heicklen., J. Amer. Chem. Soc.,
1972, 94, 4856.
23. C.W. Gillies and R.L. Kuczkowski, J. Amer. Chem. Soc., 1972, 94,
7609.
24. R.W. Murray and A. Suzui, J. Amer. Chem. Soc., 1973, 95, 3343.
25. P.A. Leighton in "Photochemistry of Air Pollution", Academic,
New York, 1961.
26. R. Atkinson, B.J. Finlayson and J.N. Pitts, J. Amer. Chem. Soc.,
1973, 95, 7592.
27. K.L. Demerjian, J.A. Kerr and J.G. Calvert, Adv. Environ. Sci.
Technol., 1974, 4, 1.
28. W.R. Wadt and W.A. Goddard III, J. Amer. Chem. Soc., 1975, 97,
3004.
29. L.B. Harding and W.A. Goddard III, J. Amer. Chem. Soc., 1978,
100, 7180.
30. D. Cremer, J. Amer. Chem. Soc., 1979, 101, 7199.

31. T. Ha, H. Kühne, S. Vaccani and H.H. Gunthard, Chem. Phys. Lett., 1974, 24, 172.
32. P.C. Hiberty, J. Amer. Chem. Soc., 1976, 98, 6088.
33. F.J. Lovas and R.D. Suenram, Chem. Phys. Lett., 1977, 51, 453.
34. R.D. Suenram and F.J. Lovas, J. Amer. Chem. Soc., 1978, 100, 5117.
35. L.A. Hull, J. Org. Chem., 1978, 43, 2780.
36. C. Clidewell, J. Mol. Struct., 1980, 67, 35.
37. O. Bastiansen, F.N. Fritsch and K. Hedberg, Acta. Crystallogr. 1964, 17, 538.
38. K. Pihlaya and E. Taskinen in "Physical Methods in Heterocyclic Chemistry" (Ed. A.R. Katritzky), Academic, New York, 1974, Vol 6, pp 199.
39. M.J.S. Dewar and A.P. Marchand, Annu. Rev. Phys. Chem., 1965, 16, 321 and references cited therein.
40. P.J. Hay, T.H. Dunning and W.A. Goddard III, Chem. Phys. Lett., 1973, 23, 457.
41. The dioxetane skeleton is found in biologically significant molecules such as α -peroxylactones⁴² which are active intermediates in firefly bioluminescence.
42. a) W. Adam, J. Chem. Educ., 1975, 51, 138.
b) J.W. Hastings and T. Wilson, Photochem. Photobiol., 1976, 23, 461.
43. For reviews on the synthesis of dioxetanes see W. Adam and A.J. Bloodworth, Annual Reports B, 1978, 342.
44. J.D. Dunitz and V. Shomaker, J. Chem. Phys., 1952, 20, 1703.
45. A. Almennigen, O. Bastiansen and P.N. Skancke, Acta Chem. Scand., 1961, 15, 711.

46. G.W. Rathjens, N.K. Freeman, W.D. Gwinn and K.S. Pitzer,
J. Amer. Chem. Soc., 1953, 75, 5634.
47. R.C. Lord and B.P. Stoicheff, Can. J. Phys., 1962, 40, 725.
48. D.A. Dows and N. Rich, J. Chem. Phys., 1968, 49, 470.
49. M.R. Stone and I.M. Mills, Mol. Phys., 1970, 18, 631.
50. F.A. Miller and R.J. Capwell, Spectrochim. Acta, Part A, 1971,
27a, 947.
51. F.A. Miller, R.J. Capwell, R.C. Lord and D.G. Rea, Spectrochim.
Acta, Part A, 1972, 28a, 603.
52. S. Meiboom and L.C. Snyder, J. Amer. Chem. Soc., 1967, 89, 1038.
53. S. Meiboom and L.C. Snyder, J. Chem. Phys., 1970, 52, 3857.
54. D. Cremer, J. Amer. Chem. Soc., 1977, 99, 1307.
55. N.L. Bauld and J. Cessac, J. Amer. Chem. Soc., 1977, 99, 942.
56. a) See J.B. Lambert and J.D. Roberts, J. Amer. Chem. Soc.,
1965, 87, 3884 and 3891.
b) Dewar et al [15b) report that MINDO/3 also correctly
predicts the puckered ring geometry, but this has been
refuted^[55].
57. R.S. Brown, Can. J. Chem., 1975, 53, 3439.
58. D.J. Coughlin, R.S. Brown and R.G. Salomon, J. Amer. Chem. Soc.,
1979, 101, 1533.
59. a) D.T. Coxon, K.R. Price and H.W-S. Chan, Chem. Phys. Lipids,
1981, 28, 365.
b) W.E. Neff, E.N. Frankel and D. Weisleder.
60. D.E. O'Connor, E.D. Mihelich and M.C. Coleman, J. Amer. Chem.
Soc., 1981, 103, 223.
61. M. Roza and A. Francke, Biochim. Biophys. Acta, 1978, 528, 119.

62. D. Cremer, J. Chem. Phys., 1979, 70, 1898.
63. a) J. Renard and S. Aiszár, J. Amer. Chem. Soc., 1970, 92, 2628.
b) R.A. Rouse, J. Amer. Chem. Soc., 1973, 95, 3460.
c) G. Klopman and P. Andreozzi, Bull. Soc. Chim. Belgium, 1977, 86, 481.
d) R.A. Rouse, Int. J. Quant. Chem., 1973, 57, 289.
64. a) K.S. Pitzer and W.E. Donath, J. Amer. Chem. Soc., 1959, 81, 3213.
b) F.V. Brutcher, Jr., T. Roberts, S.J. Barr and N. Pearson, J. Amer. Chem. Soc., 1959, 81, 4915.
c) F.V. Brutcher, Jr, and W. Bauer, Jr., J. Amer. Chem. Soc., 1962, 84, 2233 and 2236.
d) M.B. Epstein, G.M. Barrow, K.S. Pitzer and F.D. Rossini, J. Res. Natl. Bur. Stand., 1949, 43, 245.
e) N.C. Baird, Tetrahedron, 1970, 26, 2185.
f) R. Hoffmann, J. Chem. Phys., 1963, 39, 1937.
g) W.J. Adams, H.J. Geise and L.S. Bartell, J. Amer. Chem. Soc., 1970, 92, 5013.
65. a) J.P. McCullough, D.R. Douslin, W.N. Hubbard, S.S. Todd, J.F. Messerly, J.A. Hossenlopp, F.R. Frow, J.P. Dawson and G. Waddington, J. Amer. Chem. Soc., 1959, 81, 5884.
b) M. Hanack in "Conformational Theory", Academic Press, New York, 1965, pp 77.
66. a) H.D. Orloff, Chem. Rev., 1954, 54, 347.
b) W. Klyne, Progr. Stereochem., 1954, 1, Ch.2.
c) E.L. Eliel, J. Chem. Educ., 1960, 37, 126.
d) E.L. Eliel in "Stereochemistry of Carbon Compounds", McGraw-Hill, New York, 1962.
e) H.H. Lau, Angew. Chem., 1961, 73, 423.

67. a) F.R. Jensen, D.S. Noyce, C.H. Sederholm and A.J. Berlin, J. Amer. Chem. Soc., 1962, 84, 386.
- b) F.A. L. Anet, M. Ahmed and L.D. Hall, Proc. Chem. Soc., 1964, 145.
- c) R.K. Harris and N. Sheppard, Proc. Chem. Soc., 1961, 418.
68. J.R. Hoyland, J. Chem. Phys., 1968, 49, 2563, see also J.-M. Lehn, Org. Chem., 1971, 21, 129.
69. A. Komomicki and J.W. McIver, Jr, J. Amer. Chem. Soc., 1973, 95, 4512.
70. G. Claeson, G. Androes and M. Calvin, J. Amer. Chem. Soc., 1961, 83, 4357.
71. For recent reviews see "Essential Fatty Acids and Prostaglandins" (Ed. R.T. Holman), Prog. Lipid Res., 1982, Vol 20; "Chemistry, Biochemistry and Pharmacol Activity of Prostanoids", (Ed S.M. Roberts and F. Scheinmann), Pergamon, New York, 1979; "Prostaglandin Research". (Ed p. Crabbe), Academic, New York, 1977.
72. M.G. Zagorski and R.G. Salomon, J. Amer. Chem. Soc., 1980, 102, 2501.
73. D.J. Coughlin and R.G. Salomon, J. Amer. Chem. Soc., 1979, 101, 2761.
74. R.M. Wilson and J.W. Rekers, J. Amer. Chem. Soc., 1981, 103, 206.
75. a) R.G. Salomon and M.F. Salomon, J. Amer. Chem. Soc., 1977, 99, 3501.
- b) N.A. Porter and D.W. Gilmore, J. Amer. Chem. Soc., 1977, 99, 3503.
- c) W. Adam and H.J. Eggette, J. Org. Chem., 1977, 42, 3987.
- d) R.M. Wilson and F. Geiser, J. Amer. Chem. Soc., 1978, 100, 2225.
- e) R.G. Salomon, M.F. Salomon, and D.J. Coughlin, J. Amer. Chem. Soc., 1978, 100, 662.
76. W. Thiel, P. Wigner, J. Stewart and M.J.S. Stewart, QCPE 428, University of Indiana 1981.
77. For recent references see A. Banerjee, D. Mukherjee and J. Simons, J. Chem. Phys., 1982, 76, 1979 and references cited therein.

78. M.J.S. Dewar and W. Thiel, J. Amer. Chem. Soc., 1975, 97, 3978.
79. M.J.S. Dewar and S. Kirschner, J. Amer. Chem. Soc., 1975, 97, 7578.
80. The version of MINDO/3 used was a locally tailored version of QCPE 309,
the IBM version of MINDO/3.
81. J.S. Binkley, R.A. Whiteside, R. Krishman, R. Seeger, D.J. DeFrees,
H.B. Schlegel, S. Topiol, L.R. Kohn and J.A. Pople, QCPE, 1981,
13, 406.
82. J.A. Pople in "Modern Theoretical Chemistry", (Ed. H.F. Schaefer III),
Plenum Press, New York, Vol 4, 1977, pp 1-27.
83. J.S. Binkley, J.A. Pople and W.J. Hehre, J. Amer. Chem. Soc., 1980,
102, 939.